

P  
2mic

DEPARTMENT OF MECHANICAL AND INDUSTRIAL ENGINEERING  
LABORATORY FOR ERGONOMICS RESEARCH  
ENGINEERING EXPERIMENT STATION  
UNIVERSITY OF ILLINOIS AT URBANA - CHAMPAIGN  
URBANA, ILLINOIS 61801



485 p.

# Final Report of PHYSIOLOGICAL AND ENGINEERING STUDY OF ADVANCED THERMOREGULATORY SYSTEMS FOR EXTRAVEHICULAR SPACE SUITS

by

J. C. CHATO  
B. A. HERTIG

NASA-CR-130811)	PHYSIOLOGICAL AND	N74-14846
ENGINEERING STUDY OF ADVANCED		
THERMOREGULATORY SYSTEMS FOR		
EXTRAVEHICULAR SPACE SUITS (Illinois		Unclas
Univ.) — 485 p	CSCS 06K	G3/05 17228

483

Final Report No. M.E.-FR-400  
UIIU-ENG 72 4003  
August 1972

Reproduced by  
NATIONAL TECHNICAL  
INFORMATION SERVICE  
US Department of Commerce  
Springfield, VA. 22151

Supported by **PRICES SUBJECT TO CHANGE**  
National Aeronautics and Space Administration  
under  
Grant No. NGR-14-005-103

;

PHYSIOLOGICAL AND ENGINEERING STUDY OF  
ADVANCED THERMOREGULATORY SYSTEMS FOR  
EXTRAVEHICULAR SPACE SUITS

J. C. Chato

B. A. Hertig

Final Report No. ME-FR-400

UIIU-ENG 72 4003

August 1972

Supported by  
National Aeronautics and Space Administration  
under  
Grant No. NGR 14-005-103

## ACKNOWLEDGEMENTS

Among the number of people who contributed to the project, special thanks are due to the personnel of the Biotechnology Division of NASA Ames Research Center, Moffett Field, California. In particular, to Dr. John Billingham, E. G. Lyman, James Blackaby, and H. Vykukal who helped to initiate the project and to Drs. Alan Chambers and Bill Williams who contributed help and advice during the latter phases of the work. Professor Max Anliker of Stanford University was the coordinator of the NASA-ASEE Summer Faculty Fellowship Program that initiated one of the authors (Professor Chato) into the space program.

Thanks are due to the Department of Mechanical and Industrial Engineering, University of Illinois at Urbana-Champaign for material assistance in some phases of the work and also to the staff of the Publications Office of that department for their able help in preparation of the various manuscripts and reports.

Most of the numerical calculations were performed at the facilities of the Digital Computer Laboratory of the University of Illinois at Urbana-Champaign.

## SUMMARY

This final report on NASA Grant No. NGR-14-005-103 consists of three parts. Part I is a summary of the overall work; Part II consists of the major reports; Part III is a list of publications resulting from this work.

## TABLE OF CONTENTS

	Page
Part I	
SUMMARY OF THE PROGRAM . . . . .	I-1
INTRODUCTION . . . . .	I-2
REGIONALLY INDEPENDENT COOLING IN PROTECTIVE SUITS . . . . .	I-3
THE APPLICATION OF HEAT PIPES IN PROTECTIVE SUITS . . . . .	I-8
MODELING OF THE HUMAN THERMAL SYSTEM . . . . .	I-12
SUMMARY OF AUXILIARY STUDIES . . . . .	I-14
REFERENCES . . . . .	I-16
Part II	
MAJOR REPORTS . . . . .	II-1
Part III	
LIST OF PUBLICATIONS . . . . .	III-1
PUBLICATIONS . . . . .	III-2
THESES . . . . .	III-4

Part I  
SUMMARY  
OF THE PROGRAM

## INTRODUCTION

This study was initiated to explore various new aspects of thermoregulation in a protective garment, such as an extravehicular space suit. There were three main thrusts in the work with numerous minor investigations of the details. Two of the main efforts were concerned with hardware concepts while the third effort was an analysis and modeling of the human thermal system. In the following sections each of these three parts will be described after which a brief description of some of the results of the minor investigations will be given.

## REGIONALLY INDEPENDENT COOLING IN PROTECTIVE SUITS

In thermally hostile environments, such as in outer space, the human body needs a protective "micro-climate" in order to function properly. During the past decades the concept of water cooled garments has evolved into the practical designs of the Apollo extra-vehicular activity (EVA) space suits. In these units the excess heat of the body is removed by cooling water circulating through flexible tubes in direct contact with the skin. There is a single water supply with a single, manually controlled inlet temperature. Although these space suits performed well, they proved inadequate at the highest metabolic rates developed during explorations of the moon surface.

Preliminary studies with uniform cooling of the human body [1]\* indicated that one of the limits of such a system was the comfort sensation of the individual at the most sensitive part of the body. With some individuals, the lowest uniform coolant temperature tolerated proved to be inadequate to reduce the sweat rate to near the required minimum level. Thus, it became apparent that one way to improve the cooling capacity of a water cooled garment was to provide different coolant temperatures to different parts of the body depending on local need and tolerance levels. To this end a cooling garment with a cooling hood was constructed. The garment consisted of 16 individual pads made of Tygon tubes. These pads were grouped to provide an independent supply of cooling water to six separate regions of the body: head, upper torso, lower torso, arms, thighs, and lower legs. Experiments with the cooling garment were directed at exploring the characteristics of independent control of temperature and removal of excess heat from

---

\*Numbers in brackets refer to entries in REFERENCES.

separate regions of the body. Five activity schedules consisting of alternate sessions of standing and treadmill walking were used with five test subjects. Quasi-steady state and, to some extent, transient characteristics of the proposed scheme of independent regional cooling were studied.

The following results and conclusions were reached in this phase of the study [2]:

- (1) There are regions in the body that require more cooling during walking than others, e.g., thighs, head, and lower legs.
- (2) During standing, an almost uniform water inlet temperature was requested for all regions of the body by the test subjects. This situation changed significantly during exercise. Conclusions 1 and 2 indicate that independent regional cooling may be more efficient than the present scheme of uniform cooling.
- (3) Cooling of the head during exercise has a profound effect on comfort.
- (4) Transient times for reaching a thermal steady state from the onset of exercise are of the order of two hours. This transient time, however, includes a relatively slow active response of the human thermoregulatory system to changes in exercise rates, e.g., the shifting of the deep body temperature.
- (5) During exercise the thermal effectiveness of the cooling suit decreased as compared to the values obtained for standing.
- (6) Intermediate changes in the level of activity between an initial and a final level do not have a noticeable effect.

on the thermal state so long as sufficient time is allowed for reaching a steady state corresponding to the final level of activity.

- (7) Although the cooling suit increased the heat stress of the subjects, the heat strain seemed to be somewhat diminished as indicated by lower heart rates.
- (8) The regional order of preferred changes in water inlet temperatures from the onset of a change in the level of activity could not be determined. More experiments are required to identify the regions of the body that require faster cooling (or warming) than others.

Based on the comparative experiments with and without the cooling suit, the following observations were made:

- (1) Metabolic rates were, in most cases, higher during the experiments with the cooling suit indicating that a certain energy cost was associated with wearing the suit, i.e., the subject was under higher heat stress.
- (2) Ear canal temperatures were usually lower during the experiments without the cooling suit.
- (3) Heart rates seem to have been lower during the experiments with the cooling suit.
- (4) Weight losses were usually lower during the experiments with the cooling suit.

Thus, the cooling suit seems to have reduced the heat strain even though the heat stress was increased slightly.

Recommendations for future work were the following:

- (1) Application of optimization techniques to obtain design

guidelines for the construction of more efficient cooling suits,

- (2) Extensions of the model to include the local and temperature dependent variations of the physiological properties (this phase, however, should be delayed until more detailed physiological data become available),
- (3) Experimentation with various combinations of individual cooling pads, e.g., hood and thigh pad, to determine the local effects of cooling at various heat stresses and activities, and
- (4) Experimentation with cooling suits while exercising other parts of the body, e.g., arms, in order to determine preferred temperature patterns for the coolant.

In the next phase of the study the interaction between different types of individual cooling pads and the human body was investigated [3]. Three cooling pads with different cooling tube sizes and spacings were constructed and tested. These pads were equipped with thermocouples to measure the temperature profiles between adjacent tubes on the skin surface on the thigh of a male subject while he was performing various activity schedules on a bicycle ergometer. All pads were tested under identical experimental conditions. The pad with the highest tube density removed the greatest amounts of heat with the least temperature variations on the skin. Also, the transient times for this pad were the shortest.

The transient times associated with a change from a high metabolic rate of 1800 Btu/hr (528 w) to a low level of 300 Btu/hr (88 w) were found to be about 120 minutes. A change from 900 Btu/hr (264 w) to 300 Btu/hr (88 w) resulted in 90 to 100 minute transients. However, the

transient times for a change in metabolic rate in the opposite direction from 300 Btu/hr (88 w) to 1800 Btu/hr (528 w) were 40 to 60 minutes. When an intermediate step of 900 Btu/hr (264 w) was introduced between the last two metabolic rates, the transient times associated with the individual steps varied from 40 to 80 minutes. However, the overall transient times for each double step were approximately the same in either direction.

Some of the steady state experimental results were used for comparison with analytical predictions for the temperature distribution on the skin surface using both the cylindrical and rectangular models [2]. Agreement between measured and predicted temperature profiles was found to be fairly good. Improved techniques for measuring skin and, possibly, internal temperatures and physiological quantities, e.g., blood perfusion and metabolic heat generation rates, are required to render the comparison more reliable.

The results indicate clearly that both tube size and spacing have a noticeable effect on overall cooling efficiency. In order to optimize the relationship between these two parameters, the magnitude of the maximum expected metabolic rate should be established. Once obtained, a cooling pad can be designed that will remove heat from the body at any predetermined rate.

## THE APPLICATION OF HEAT PIPES IN PROTECTIVE SUITS

The final stage of heat rejection in the current Apollo EVA space suits occurs across sublimator plates in the back pack. Here, ice is sublimated into the ever present vacuum of outer space. Thus, the length of a mission is limited by the amount of water and ice that can be accommodated in the back pack. Any method that would provide additional cooling would increase either the length of the mission or the payload. The development of a new type of hard suit at NASA Ames Research Center [4] inspired the idea of incorporating the heat pipe concept into the available free surfaces of the suit. The idea was to utilize as much of the surface as possible to radiate heat to outer space. Since the astronauts moved about a great deal, it was imperative that the heat be transferred rapidly from one side to another as different parts of the suit became exposed to outer space. The heat pipe is essentially multi-directional; i.e., the direction of heat flow depends only on where heat is supplied and rejected. Thus, the application of the heat pipe concept to the hard suit was deemed feasible and was examined.

First a simple system was developed for determining the fluid transfer capabilities of various wick configurations without the need for a complete heat pipe or for any heat transfer [5]. Then a versatile heat pipe with variable dimensions was designed for the study of steady state and transient heat pipe performance using different fluids and wicking materials.

An open-ended dewar was designed and constructed for housing the heat pipe system. The maximum length of wicking materials was 82 cm; this distance was considered the maximum length of heat transfer required.

in future space suits. Distilled water was the transfer medium used in the wicking chamber.

The heat input to the dewar was supplied by electric heaters. Circulation of cool water was used to remove heat from the condenser end of the dewar. Approximately 45 thermocouples were used for measuring temperatures in the system.

The maximum heat transfer capability or wick "burn out" point was 10 watts with a wick length of 81.9 cm and operating temperatures of  $26.7^{\circ}\text{C}$  ( $80^{\circ}\text{F}$ )  $\pm 5^{\circ}\text{C}$ . For the Refrasil #C100-28 used, the 10 watt "burn out" point corresponds to 0.594 watts per cm width of the wick.

The required transport rate per  $\text{cm}^2$  area at "burn out" (10 watts) was  $0.361 \text{ cm}^3/\text{min}\text{-cm}^2$ . This value was well within the 0.299 to  $0.424 \text{ cm}^3/\text{min}\text{-cm}^2$  range predicted by horizontal wicking tests performed on the Refrasil #C100-28 using the simple system mentioned above.

Throughout the entire wicking chamber, a maximum temperature variation of  $\pm 0.5^{\circ}\text{C}$  was encountered during normal heat pipe operation. No transient temperature lag from one end of the wicking chamber to the other end was observed during heat input changes. Apparently the time constants of the heat input changes were much larger than the temperature equalizing time constant of the wicking chamber.

Further studies extended the capabilities of the simple wicking test [5] to allow the use of relatively volatile fluids [6]. The influence of a liquid filled gap between a wick and another surface was also investigated. It was found that such a gap increases the liquid transfer several fold. Consequently, it can be recommended that a wick should always be designed with an adjacent gap provided by either another layer of wicking or a suitable wall. The gap should be as narrow as possible since refilling a wide gap inside a sealed heat pipe could be practically impossible.

For the same reason, during the initial filling of the heat pipe, steps should be taken to insure complete filling of all such gaps with the working fluid. The results of Shaffer [7] indicate that gaps of any appreciable size tend to lose their liquid fill, i.e., if the wick is not touching the wall or the next layer forming the gap, particularly in an adverse gravity gradient.

In a wick limited heat pipe, the addition of water to alcohol does not improve the performance but tends to affect it adversely. A temperature difference, however, can be established across the heat pipe by the use of such mixtures. The property parameter,  $\rho h_{fg} \sigma / \mu^*$ , seems to give good qualitative predictions for the performance of mixtures in a wick limited heat pipe. If the heat pipe is vapor limited, however, the effect of higher vapor densities occurring with the mixtures could improve the heat transfer rates.

More specifically, in Part I, wicking material tests were performed on Refrasil #C100-28. The tests were run on 9-in. by 1-in. Refrasil strips. Displacement time curves were extrapolated for predicting the performance of a 21-3/4 in. (51 cm) heat pipe.

In Part II, heat pipe tests were run with a well defined wick length of 21-3/4-in. and a total width of 7 in. (17.8 cm). The same Refrasil was the wicking material. An open ended dewar housed the heat pipe system which consisted of heat input, mass transfer, and heat removal sections. Two electric heaters supplied heat input, while circulating water was used for heat removal.

The results showed water to be a much better operating fluid than ethyl alcohol or 50 percent ethyl alcohol by weight. Ethyl alcohol

---

\* $\rho$  = density,  $h_{fg}$  = latent heat of vaporization,  $\sigma$  = surface tension, and  $\mu$  = viscosity.

appeared to be only slightly better than the 50 percent mixture. At an angle of zero degrees, i.e., horizontally, the maximum heat transfer capacities were 15, 4, and 2 watts, respectively, for the three fluids. The predicted wattages from Part I were generally higher due to greater ease in saturating the wicking material with fluid.

A gap effect created by sewing two layers of wicking material together greatly enhanced the heat pipe performance. At an angle of zero degrees, water transferred over 80 watts, as compared to 15 watts previously.

While these studies were performed, the hard suit models at NASA Ames Research Laboratories underwent considerable change including the addition of bellows at several places. Some of these alterations substantially reduced the available free surfaces for heat pipes. In addition, studies conducted elsewhere indicated that the construction of a practical heat pipe system will be a very difficult manufacturing problem. Consequently, no further heat pipe studies were made.

## MODELING OF THE HUMAN THERMAL SYSTEM

The thermal system of homeotherms, particularly that of the human body, has long been of interest to many researchers. With the progress of scientific knowledge and methods, emphasis has shifted from mere observations of this system and its functions to more systematic studies including more and more analytical and numerical modeling techniques. These studies provide improved understanding of the mechanisms of thermoregulation as well as means for predicting the thermal performance of humans in various environments, e.g., space suits. Thus, parallel to experimental studies on space suits and cooling pads, analytical models of the human body were developed which included explicitly the effects of blood flow, local heat generation, conduction, and storage of heat as well as non-uniform cooling of the skin surface.

A second-order, partial differential equation, the "bio-heat" equation, was obtained for the model. The tissue was assumed to be isotropic and homogeneous and all properties were assumed to be constant. Transient, as well as steady-state, closed form, analytical solutions were obtained for cylindrical and rectangular geometries and for various parameters [2,3].

Based on the analysis, the following observations were made:

- (1) Because blood flow plays such a significant role in the transfer of heat inside the living tissue, models which do not include a separate blood flow term will generally be inadequate to describe properly the thermal effects in living systems.
- (2) Transient times for reaching a so-called "fully developed" temperature profile in the tissue were estimated to be of the order of 5-20 minutes with the shorter times associated with higher

final metabolic rates. These transient times were also found to be strongly dominated by a geometrical parameter.

- (3) At elevated metabolic rates, maximum temperature may occur in the muscle tissue rather than in the inner core.
- (4) Knowledge of the exact shape of the heat flux on the skin was found to be unimportant for the determination of the temperature distribution away from the skin surface.
- (5) Results obtained for the cylindrical and rectangular models were remarkably close for the practical range of variables. The rectangular geometry, however, was easier for computation.

The analysis was partially validated by measuring the temperature profiles on the skin of the thigh cooled by parallel tubes in contact with the skin as described in a previous section.

The transient models [2,8] can form a basis for systems modeling of the human body in combination with an environment. For example, the thermal control system of a space suit can be studied with one of the appropriate transient models of the human body serving as part of the overall model of the entire suit-body system.

On a supplementary grant, the steady-state analysis was applied to the problem of local, transcutaneous cooling of a blood vessel [9]. This study was undertaken as a result of experiments on localized cooling of the neck skin above the carotid artery which indicated a significant effect of this cooling on the thermal comfort sensation of the individual [10].

The results indicated that the optimum width of a cooling strip was approximately three times the depth to the centerline of the artery. The heat extracted from a typical carotid artery with such a strip was about  $0.9 \text{ w/m-}^\circ\text{C}$  which was too small to affect significantly the temperature of the blood flow through a main blood vessel such as the carotid artery.

## SUMMARY OF AUXILIARY STUDIES

There were a number of auxiliary studies performed, not all of which were directly supported by this grant. The most significant studies were as follows:

- (1) An experimental study was performed to determine the degree of essentially uniform, overall cooling necessary to suppress sweating. The results indicated that under some circumstances, and, in particular, with certain individuals, complete suppression of sweating is not feasible by uniform skin cooling alone [1].
- (2) A probe for the measurement of thermophysical properties of biological tissues "in vitro" and "in vivo" has been developed and used, e.g., [11].
- (3) A ventilated capsule system for quantitative measurement of sweat output from a local area was constructed. This technique was applied in a study to determine the influence of ingestions of water on sweating [1]. A drinking reflex which causes quick, transient increase of sweat rate was observed when the subjects drank either cold or body temperature water. The amount of liquid ingested had a very definite effect on sweat rate. A small amount (250 ml) fed through a stomach tube caused little or no increase in sweating; a larger amount introduced the same way caused a transitory increase in sweating. As longer lasting responses, hot water caused an increase in sweating, while cold water caused a decrease. These responses were attributed to the thermal effect of the ingested water on the alimentary tract.
- (4) The analytical work showed the frequent recurrence of a linear combination of modified Bessel functions for the cylindrical

models of the human thermal system. The behavior of these functions were examined and their values were tabulated for easy reference [12].

- (5) Preliminary analyses were performed to determine the feasibility of an "all-sweat" cooling scheme. The results indicated that the human body could be cooled by evaporation of water from the surface of the skin alone, provided that the moisture could be removed locally by the suit. One method may be the incorporation of porous sublimator plates into the space suit itself. The method could reduce the complexity of the system by eliminating the currently used water system and by utilizing the control system of the body [13].

## REFERENCES

1. Chato, J. C., Hertig, B. A., Gammon, N. A., Streckert, J. H., and Lechner, P., "Physiological and Engineering Study of Advanced Thermoregulatory Systems for Extravehicular Space Suits," Semiannual Status Report No. 2, NASA Grant No. NGR 14-005-103, June 15, 1968.
2. Shitzer, A., Chato, J. C., and Hertig, B. A., "A Study of the Thermal Behavior of Living Biological Tissue with Application to Thermal Control of Protective Suits," Report No. ME-TR-207, Department of Mechanical and Industrial Engineering, University of Illinois at Urbana-Champaign, January 1971.
3. Leo, R. J., Shitzer, A., Chato, J. C., and Hertig, B. A., "Steady State and Transient Temperature Distributions in the Human Thigh Covered with a Cooling Pad," Report No. ME-TR-286, Department of Mechanical and Industrial Engineering, University of Illinois at Urbana-Champaign, June 1971.
4. Vykukal, H., Billingham, J., Lyman, E., Blackaby, J., and others, NASA Ames Research Center, Moffett Field, California, Personal Communications, 1966.
5. Streckert, J. H. and Chato, J. C., "Development of a Versatile System for Detailed Studies on the Performance of Heat Pipes," Report No. ME-TR-64, Department of Mechanical and Industrial Engineering, University of Illinois at Urbana-Champaign, December 1968.
6. Hunsberger, D. L. and Chato, J. C., "Experimental Investigation of the Performance of Various Wick Configurations in Single- and Two-Fluid Heat Pipes Operating in the Gravitational Field," Report No. ME-TR-187, Department of Mechanical and Industrial Engineering, University of Illinois at Urbana-Champaign, October 1970.
7. Shaffer, J., "The Effects of the Proximity of a Wall on the Performance of a Wick," unpublished report, Department of Mechanical and Industrial Engineering, University of Illinois at Urbana-Champaign, 1969.
8. Shitzer, A. and Chato, J. C., "Analytical Solutions to the Problem of Transient Heat Transfer in Living Tissue," ASME Paper No. 71-WA/HT-36, 1971.
9. Chato, J. C. and Shitzer, A., "Analytical Prediction of the Heat Transfer from a Blood Vessel near the Skin Surface when Cooled by a Symmetrical Cooling Strip," Report No. ME-TR-344, Department of Mechanical and Industrial Engineering, University of Illinois at Urbana-Champaign, December 1971.
10. Williams, B. A. and Chambers, A. B., "The Effect of Neck Warming and Cooling on Thermal Comfort," 42nd Annual Sci. Meeting, Aerospace Med. Assoc., Houston, Texas, April 26-29, 1971. Also, Second Conference on Life Support Systems, NASA Ames Research Center, Moffett Field, California, May 1971, NASA SP-302, 1972.

11. Chato, J. C., "A Method for the Measurement of Thermal Properties of Biological Materials," Thermal Problems in Biotechnology, ASME Symposium Series, 1968, pp. 16-25.
12. Shitzer, A. and Chato, J. C., "A Linear Combination of Modified Bessel Functions," Technical Note No. ME-TN-310, Department of Mechanical and Industrial Engineering, University of Illinois at Urbana-Champaign, November 1971.
13. Chato, J. C., Hertig, B. A., et al., "Physiological and Engineering Study of Advanced Thermoregulatory Systems for Extravehicular Space Suits," Semiannual Status Report No. 4, on NASA Grant No. NGR 14-005-103, June 1969.

Part II

MAJOR REPORTS

DEVELOPMENT OF A VERSATILE SYSTEM FOR DETAILED  
STUDIES ON THE PERFORMANCE OF HEAT PIPES

J. H. Streckert

J. C. Chato

Technical Report No. ME-TR-64

December 1968

DEPARTMENT OF MECHANICAL AND INDUSTRIAL ENGINEERING  
PHYSICAL ENVIRONMENT UNIT  
ENGINEERING EXPERIMENT STATION  
UNIVERSITY OF ILLINOIS  
URBANA, ILLINOIS 61801



# DEVELOPMENT OF A VERSATILE SYSTEM FOR DETAILED STUDIES ON THE PERFORMANCE OF HEAT PIPES

by

J. H. STRECKERT

J. C. CHATO

Technical Report No. ME-TR-64

December 1968

Supported by

National Aeronautics and Space Administration

under

Grant No. NGR-14-005-103

I

24<

;

DEVELOPMENT OF A VERSATILE SYSTEM FOR DETAILED  
STUDIES OF THE PERFORMANCE OF HEAT PIPES

by

J.H. Streckert

J.C. Chato

Technical Report No. ME-TR-64

December 1968

Supported by  
National Aeronautics and Space Administration  
under  
Grant No. NGR-14-005-103

## ABSTRACT

A heat pipe with variable dimensions was designed for the study of steady state and transient heat pipe performance using different fluids and wicking materials.

An open ended dewar was designed and constructed for housing the heat pipe system. The maximum length of wicking material was 82 cm; this distance was considered the maximum length of heat transfer required in future space suits. Distilled water was the transfer medium used in the wicking chamber.

The heat input to the dewar was supplied by electric heaters. Circulation of cool water was used to remove heat from the condenser end of the dewar. Approximately 45 thermocouple points were used for measuring important temperatures in the system.

The maximum heat transfer capability or wick "burn out" point, was 10 watts with a wick length of 81.9 cm and operating temperatures of  $26.7^{\circ}\text{C}$  ( $80^{\circ}\text{F}$ )  $\pm 5^{\circ}\text{C}$ . For the Refrasil #C100-28 used, the 10 watt "burn out" point corresponds to 0.594 watts per cm width of the wick.

The required transport rate per  $\text{cm}^2$  area at "burn out" (10 watts) was  $0.361 \text{ cm}^3/\text{min}\text{-cm}^2$ . This value was well within the 0.299 to  $0.424 \text{ cm}^3/\text{min}\text{-cm}^2$  range predicted by horizontal wicking tests performed by the author on the Refrasil #C100-28.

Throughout the entire wicking chamber, a maximum temperature variation of  $\pm \frac{1}{2}^{\circ}\text{C}$ . was encountered during normal heat pipe operation. No transient temperature lag from one end of the wicking chamber to the other end was observed during heat input changes. Apparently the time constants of the heat input changes were much larger than the temperature equalizing time constant of the wicking chamber.

## TABLE OF CONTENTS

	Page
1. INTRODUCTION . . . . .	1
2. HEAT PIPE OPERATION . . . . .	3
3. GENERAL THEORY . . . . .	4
3.1 CAPILLARY PUMPING IN WICK . . . . .	5
3.2 VISCOUS LOSSES IN VAPOR . . . . .	5
3.3 VISCOUS LOSSES IN LIQUID . . . . .	6
3.4 GRAVITATIONAL FIELD EFFECTS . . . . .	6
3.5 MAXIMUM FLOW RATE IN THE WICK . . . . .	7
3.6 MAXIMUM HEAT TRANSFER RATE . . . . .	9
4. EXPERIMENTAL WORK . . . . .	11
4.1 HEAT PIPE DESIGN . . . . .	11
4.2 INITIAL TESTING PROCEDURE . . . . .	21
4.3 NORMAL TEST RUN . . . . .	22
4.4 WICKING MATERIAL TESTS . . . . .	24
5. DISCUSSION . . . . .	29
6. CONCLUSIONS . . . . .	33
7. RECOMMENDATIONS . . . . .	34
7.1 HEAT PIPE MODIFICATIONS . . . . .	34
7.2 WICKING MATERIAL TESTING . . . . .	35
7.3 FUTURE HEAT PIPE TESTS . . . . .	35
LIST OF REFERENCES . . . . .	37
LIST OF SYMBOLS . . . . .	38
APPENDIX A: SAMPLE CALCULATIONS . . . . .	40

## LIST OF FIGURES

Figure No.	Description	Page
1	General Heat Pipe Design . . . . .	5
2	Heat Pipe System . . . . .	13
3	Wicking Cage Assembly . . . . .	14
4	Heat Removal System . . . . .	16
5	Wicking Chamber Manifold . . . . .	18
6	Vacuum System . . . . .	19
7	Heat Pipe and Vacuum System . . . . .	20
8	Schematic of Test Arrangement for Measure- ment of Capillary Flow in Horizontal Wicks . . . . .	25
9	Wick Performance Graph . . . . .	27

## 1. INTRODUCTION

During future space exploration, astronauts will remain in outer space for extended periods of time. Extravehicular tasks will be performed by the astronauts and their only protection from the surrounding space will be a space suit.

A thermoregulatory system will, by necessity, be incorporated in the space suit. Its purpose will be to control the temperature of the atmosphere immediately surrounding the astronaut (the space between the astronaut's body and the inner layer of the space suit) and, in general, to provide a satisfactory thermal environment for him.

At present, liquid cooled undergarments are used for the temperature regulation. An intricate system of valves, pumps, and auxiliary equipment is required. Need for a more efficient, less complicated, and self-contained thermoregulatory system seems apparent.

A new system must be capable of rejecting heat from the space suit and of transferring heat from one part of the suit to another part. The heat rejection could be either by radiation to outer space or by heat exchange with a porous plate sublimator.

A heat pipe system for transferring heat has many advantages over the water-cooled undergarment. First, the heat pipe is a completely closed system and needs no recharging after initial assembly. Heat conducting capabilities of 100 to 1000 times that of the best conducting metals can be obtained using heat pipes. There exists no need for pumps, compressors, or auxiliary equipment during the operation of the heat pipe. If a temperature difference exists between the ends of the heat pipe, heat will be transferred down (evaporator to condenser) the pipe.

Regardless of the heat pipe orientation, relative to the gravitational field, the pipe will transfer heat in either direction as long as a wicking assembly is present to return the liquid to the heated end. The heat pipe is particularly suitable for "hard" suits now under consideration for future space exploration.

## 2. HEAT PIPE OPERATION

There are three distinct portions or sections to a heat pipe;

1. a heat input (evaporator) section,
2. a mass (vapor state) transfer and a mass (liquid state) return section, and
3. a heat rejection (condenser) section.

The heat input evaporates the liquid to the transfer section.

As a result of a very small pressure gradient, the vapor is forced down the pipe to the heat rejection section where the vapor is condensed. Either by capillary action or gravitational feed, the liquid is then carried back to the heat input section for recycling.

When capillary action is required for returning the liquid to the heat input section, some type of wicking material must be used. The wicking materials normally used are: fine wire screens, porous solid materials, and natural or synthetic cloths.

### 3. GENERAL THEORY

The heat pipe considered in this paper is shown in Fig. 1. The double open-ended dewar is assumed to be a perfect insulator in the radial direction. All heat added at the heat input section is transferred axially down the dewar. The major design consideration for the setup was to provide means for the evaluation of wick performance with a well defined transfer length within the heat pipe.

A temperature gradient of less than  $\frac{1}{2}^{\circ}\text{C}$  existed over the entire length of the mass transfer section. This nearly constant temperature existed because of the very small pressure gradient down the length of the transfer section.

The power transfer capability of a heat pipe depends on the following basic parameters:

- i. the capillary pumping head  $\Delta P_c$ ,
- ii. the vapor pressure drop  $\Delta P_v$ ,
- iii. the liquid viscous drag  $\Delta P_L$ , and
- iv. the gravity head  $\Delta P_g$  [1]\*.

There also is a pressure drop term caused by a momentum change in the flow of the returning liquid. This term, however, is negligible when compared to the other four terms [2]. From a pressure balance standpoint only, the equation for heat pipe operation is

$$\Delta P_c \geq \Delta P_v + \Delta P_L + \Delta P_g . \quad (1)$$

---

\*Numbers in brackets designate references.

Note : ● Represents Typical Thermocouple Locations  
 ○ Represents O-Ring Locations

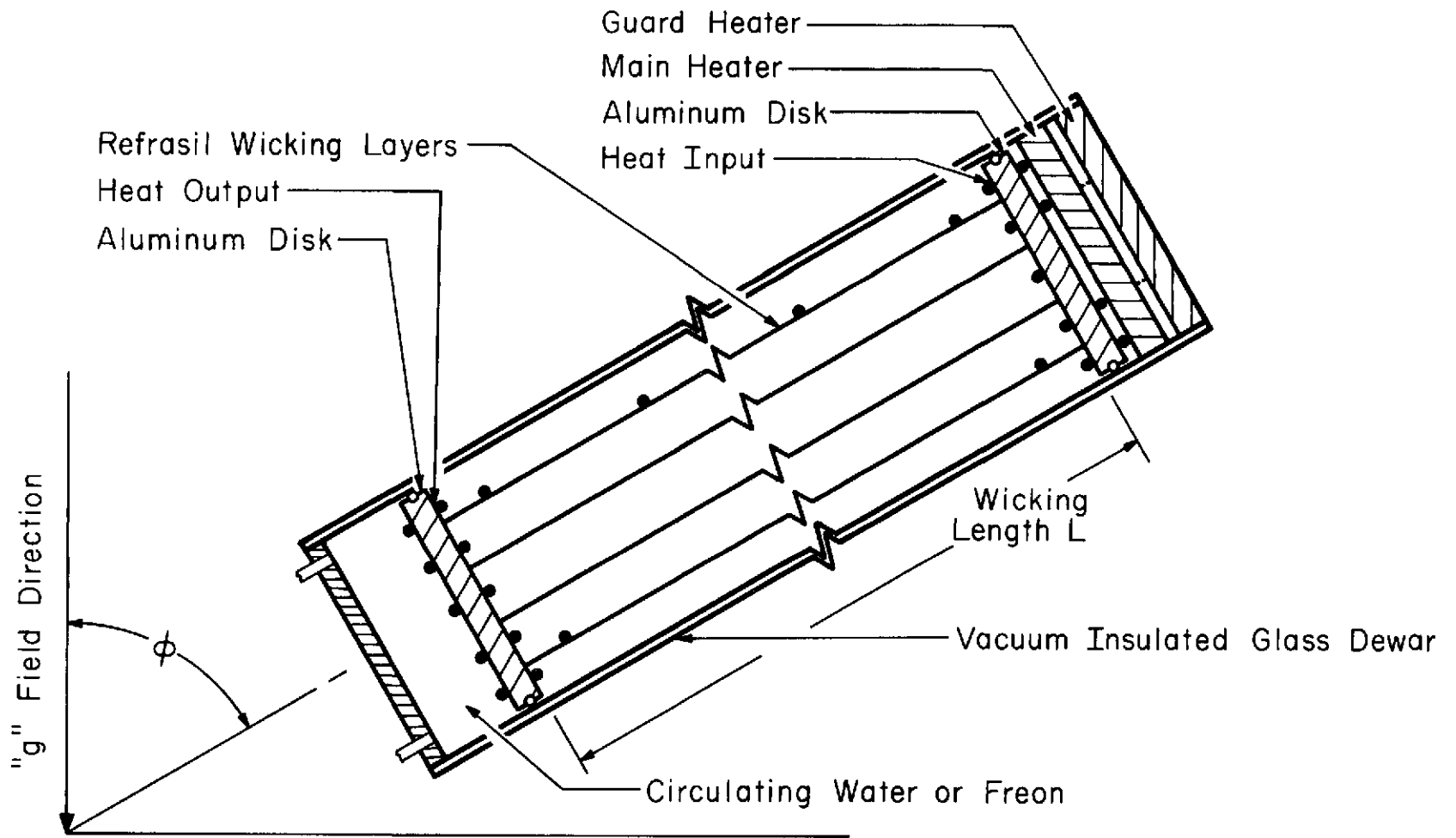


Figure 1. General Heat Pipe Design

In other words, the available pumping head must be sufficient to overcome the pressure losses caused by vapor transport, and by the viscous drag of the returning liquid. Gravity can aid or hinder, depending on the orientation of the evaporator with respect to the condenser. The following theory is patterned, in part, after Feldman's [3] analysis of heat pipe operation.

### 3.1 CAPILLARY PUMPING IN WICK

The capillary pumping term,  $\Delta P_c$ , may be written

$$\Delta P_c = 2\sigma \left( \frac{\cos \theta_e}{r_e} - \frac{\cos \theta_c}{r_c} \right), \quad (2)$$

where  $\sigma$  is the surface tension of the liquid,  $\theta_e$  is the liquid contact angle at the evaporator section,  $\theta_c$  is the liquid contact angle at the condenser section,  $r_e$  is the effective radius of the wick pore at the evaporator section, and  $r_c$  is the effective radius of the wick pore at the condenser section.

The maximum value of Eq. (2) is obtained when  $\theta_e = 0^\circ$ ,  $\theta_c = 90^\circ$ , and  $r_e$  is the actual pore radius of the wicking material. Equation (2) becomes

$$\Delta P_{c \max} = 2\sigma \left( \frac{1}{r} \right) = \frac{2\sigma}{r}, \quad (3)$$

where  $r = r_e$ .

### 3.2 VISCOUS LOSSES IN VAPOR

Pressure losses caused by vapor flow in the heat pipe may be

determined by using existing theory for either laminar or turbulent flow in pipes [4]. When the vapor flow pressure drop was calculated, it was found to be negligible when compared to other pressure losses in this heat pipe.

### 3.3 VISCOUS LOSSES IN LIQUID

Flow rates and velocities encountered with capillary flow in wicks may be assumed to be laminar\* and relatively free from inertial effects. Darcy's Law [5] for flow through porous media then can be applied to yield

$$\Delta P_L = \frac{\mu L \dot{m}}{\rho K A} = \frac{\mu L \dot{v}}{K A} \quad (4)$$

where  $\mu$  is the liquid viscosity,  $L$  is the wicking material length,  $\dot{m}$  is the liquid mass flow rate,  $\rho$  is the liquid density,  $K$  is the wick permeability,  $A$  is the total cross sectional area of the wick, and  $\dot{v}$  is the volume flow rate.

### 3.4 GRAVITATIONAL FIELD EFFECTS

The gravitational field can aid, hinder, or have no effect on the liquid flow in the wick. This effect depends upon the orientation of the evaporator and condenser sections relative to the direction of the gravitational field. The general equation for the pressure loss in the wick caused by gravity is

---

\*For the heat pipe considered in this report, the Reynolds numbers were 56.3 and 14.5 for the water flow in the Refrasil and the vapor flow in the wicking chamber, respectively.

$$\Delta P_g = \rho g L \cos \phi , \quad (5)$$

where  $\rho$  is the liquid density,  $L$  is the wick length,  $g$  is the acceleration of gravity, and  $\phi$  is the angle between the heat pipe axis and the gravitational field as shown in Fig. 1. The algebraic sign in Eq. (5) is

- (+) when the evaporator is above the condenser in the gravitational field (hinders),
- (-) when the condenser is above the evaporator in the gravitational field (aids),

and when the evaporator and the condenser are in a horizontal plane gravity has no effect, the term is zero.

The gravitational effects on the vapor flow are neglected in this report, since the density of the vapor is approximately 4000 times less than that of the liquid at 26°C.

### 3.5 MAXIMUM FLOW RATE IN THE WICK

By substituting Eqs. (3), (4), and (5) into Eq. (1), the maximum flow rate is obtained as

$$\dot{m} = \frac{\rho K A}{\mu L} \left( \frac{2\sigma}{r} - \rho g L \cos \phi \right) . \quad (6)$$

If the heat pipe is horizontal, Eq. (6) reduces to

$$\dot{m} = \frac{2\sigma\rho K A}{\mu r L} = \dot{v}\rho \quad (7)$$

since  $\phi = 90^\circ$ .

For given operating conditions, wicking fluid, and wicking material  $\sigma$ ,  $\rho$ ,  $\mu$ ,  $K$ ,  $A$ , and  $r$  are constant and Eq. (7) becomes

$$\dot{m}L = \frac{2\sigma\rho KA}{\mu r} = \dot{v}\rho L = C = \text{constant.} \quad (8)$$

### 3.6 MAXIMUM HEAT TRANSFER RATE

Because the rate of heat transfer attributed to latent heat transport is large and the temperature gradient along the heat pipe is small, conduction, radiation, and sensible convection heat transfer will be negligibly small. Therefore, assuming all thermal energy is transferred as latent heat, the heat transfer rate is

$$Q = \dot{m}h_{fg} = \dot{v}\rho h_{fg} \quad (9)$$

where  $h_{fg}$  is the latent heat of vaporization at the operating pressure and temperature of the system.

Combining Eqs. (6) and (9), the maximum heat transfer rate becomes

$$Q = \frac{\rho KA}{\mu L} \left( \frac{2\sigma}{r} - \rho g L \cos \phi \right) h_{fg} \quad (10)$$

If the heat pipe is horizontal, Eq. (10) reduces to

$$Q = \left( \frac{2\sigma\rho KA}{\mu r L} \right) h_{fg} \quad (11)$$

since  $\phi = 90^\circ$ .

The following assumptions were made in obtaining Eqs. (10) and (11):

1. Gravity effects on vapor flow are negligible.
2. Liquid flow in wick capillaries is laminar.
3. Viscous vapor flow losses are negligible.
4. Conduction, radiation, and sensible convection heat transfer along the heat pipe are negligible.
5. Liquid properties are constant along the heat pipe.
6. Flow and heat transfer are essentially one-dimensional.
7. Wick is uniform and evenly saturated.
8. Heat transfer is uniform over the evaporator and condenser surfaces.

## 4. EXPERIMENTAL WORK

### 4.1 HEAT PIPE DESIGN\*

#### Dewar

A 7.62 cm inside diameter, 8.90 cm outside diameter, and 101.5 cm long double open-ended, silvered glass dewar was used to contain the entire test setup. The inside and outside diameters were attained by using concentric glass cylinders with a high vacuum between them and sealed on the ends. This vacuum, between the silvered surfaces, provided the necessary insulation between the heat transfer area and the surrounding atmosphere†. The three main elements of the heat pipe previously mentioned were then fitted inside this dewar with a combination of o-rings and gaskets sealing axially down the dewar. A radial connection between the inside of the dewar and the exterior was provided. This connection was needed to allow charging the wicking chamber with the desired transfer medium or fluid and to provide access to the wicking chamber for thermocouple wires.

#### Heat Input Section (Evaporator)

The main requirement here was to have a heat input which could be measured accurately. The final system chosen was to use two electrical heaters. The main heater, closer to the heat transfer area, was used for the total heat input and the distant guard heater was used to

---

\*Initial design of the heat pipe was by Prof. John C. Chato of the University of Illinois, Urbana, Illinois.

†Unsilvered window strips allowed inspection of the interior after assembly.

minimize heat flux in the outward axial direction. By measuring the input wattage to the main heater, an accurate measurement of heat input to the system could be obtained. Both heaters were supplied electrical energy from variable transformers and the wattage inputs were measured by wattmeters (see Fig. 2).

#### Heat Transfer Section (Wicking Chamber)

The wicking material used was Refrasil #C100-28. This material had a water lift rate and horizontal transfer rate\* which were deemed the best from past experience.

Rather than arranging the wicking material in a cylindrical fashion, concentric with the dewar as is normally done, it was decided to assemble the wicking material in four horizontal layers. The two center strips were 5.0 cm wide while the top and bottom strips were approximately 3.8 cm wide. This arrangement eliminated any gravitational effects on a given cross section while the dewar was maintained in a horizontal attitude. Also a wicking cage was utilized for suspending the Refrasil (see Fig. 3). This cage consisted of four teflon disks, two stainless steel rods, and three intermediate supports. The three intermediate supports were required because the wicking cage was the primary device separating the two aluminum disks. Since a vacuum of approximately  $10^{-3}$  mm of Hg. was pulled in the chamber between the disks, the wicking cage was required to support a load of approximately 100 pounds in compression. Finally, circular sections of Refrasil were attached to the insides of the aluminum disks for the purpose of

---

\*See p. 27 for a plot of Transfer Distance vs. Time for the Refrasil #C100-28 and other Refrasils commonly used.

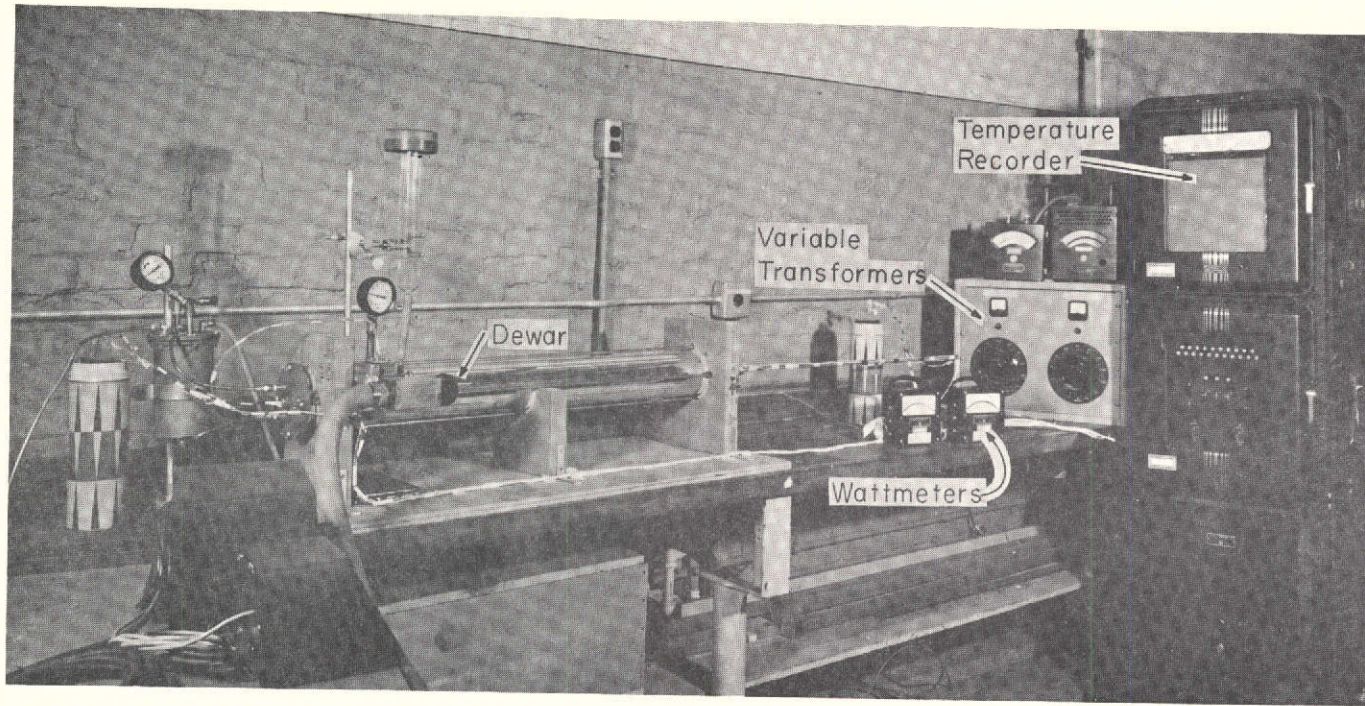


Figure 2. Heat Pipe System

Note : • Indicates Location of Thermocouple Points

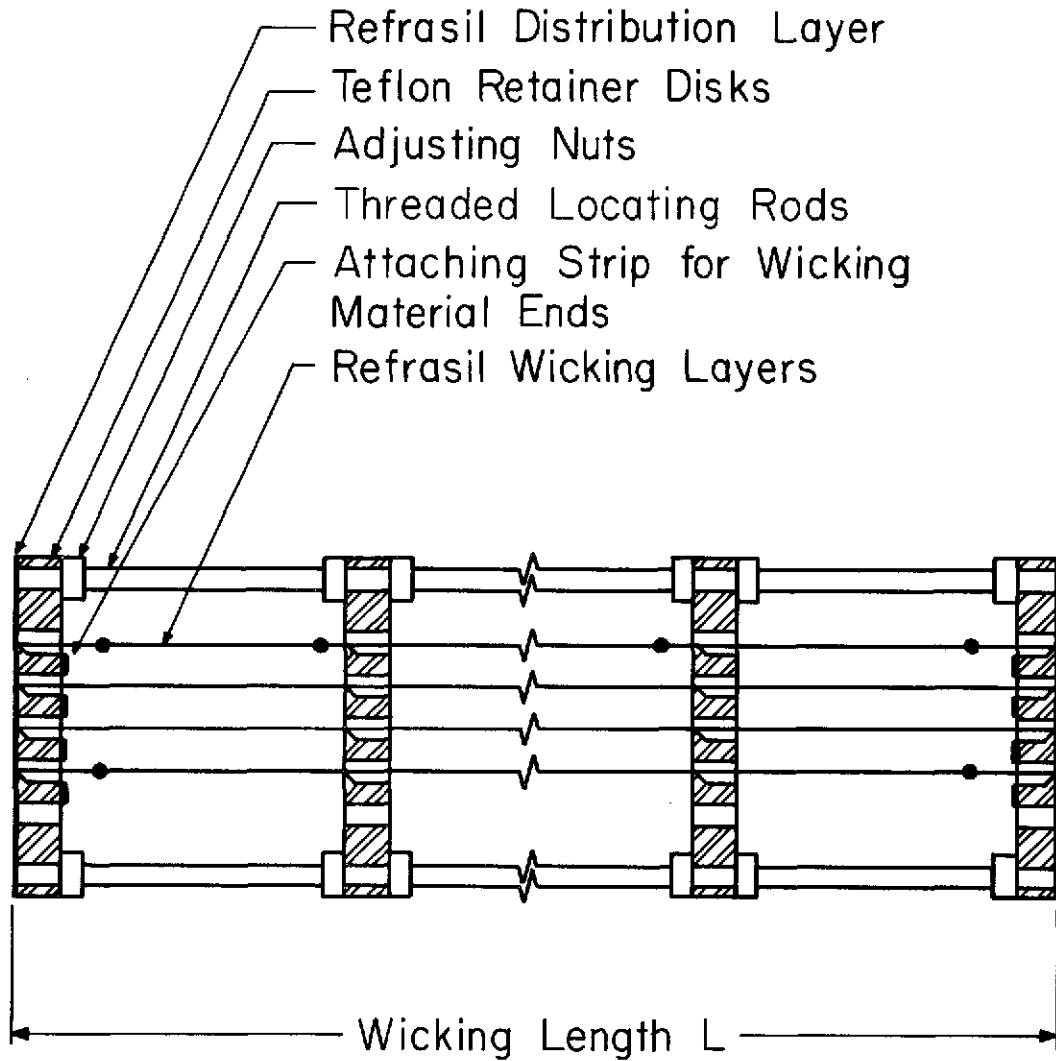


Figure 3. Wicking Cage Assembly

equalizing the distribution of fluid on each disk. These sections of Refrasil were lightly spot-epoxied to the aluminum disks.

#### Heat Removal Section (Condenser)

The heat transferred down the dewar by the wicking chamber was dissipated through the condenser aluminum disk. After the heat was conducted through the condenser aluminum disk, it was removed by circulating cool water through the condenser chamber and expending the water. An alternate method, which will be used in the future, uses a Freon in a liquid-vapor state circulating in a closed system. The closed system consists of the condenser end of the dewar and a storage tank (see Fig. 4). Copper cooling coils are located inside the storage tank and will be used to remove the heat from the Freon so that the pressure of the Freon in the tank remains within a reasonable range and that the temperature can be controlled to remove all the heat transferred. Water or any other cooling agent can be circulated through the cooling coils since the coils are isolated completely from the Freon inside the tank.

#### Temperature Measurement

Temperatures throughout the system were measured by copper-constantan thermocouple wires. Approximately forty-five different points in the system were monitored. Thermocouples were placed across mica disks between the two heaters for measuring the gradient existing there. Next, thermocouples were placed across the heater aluminum disk in order to determine the temperature gradient for heat input calculations. In the wicking chamber, six thermocouple points were distributed, two at each end and two distributed down the center of the wick for

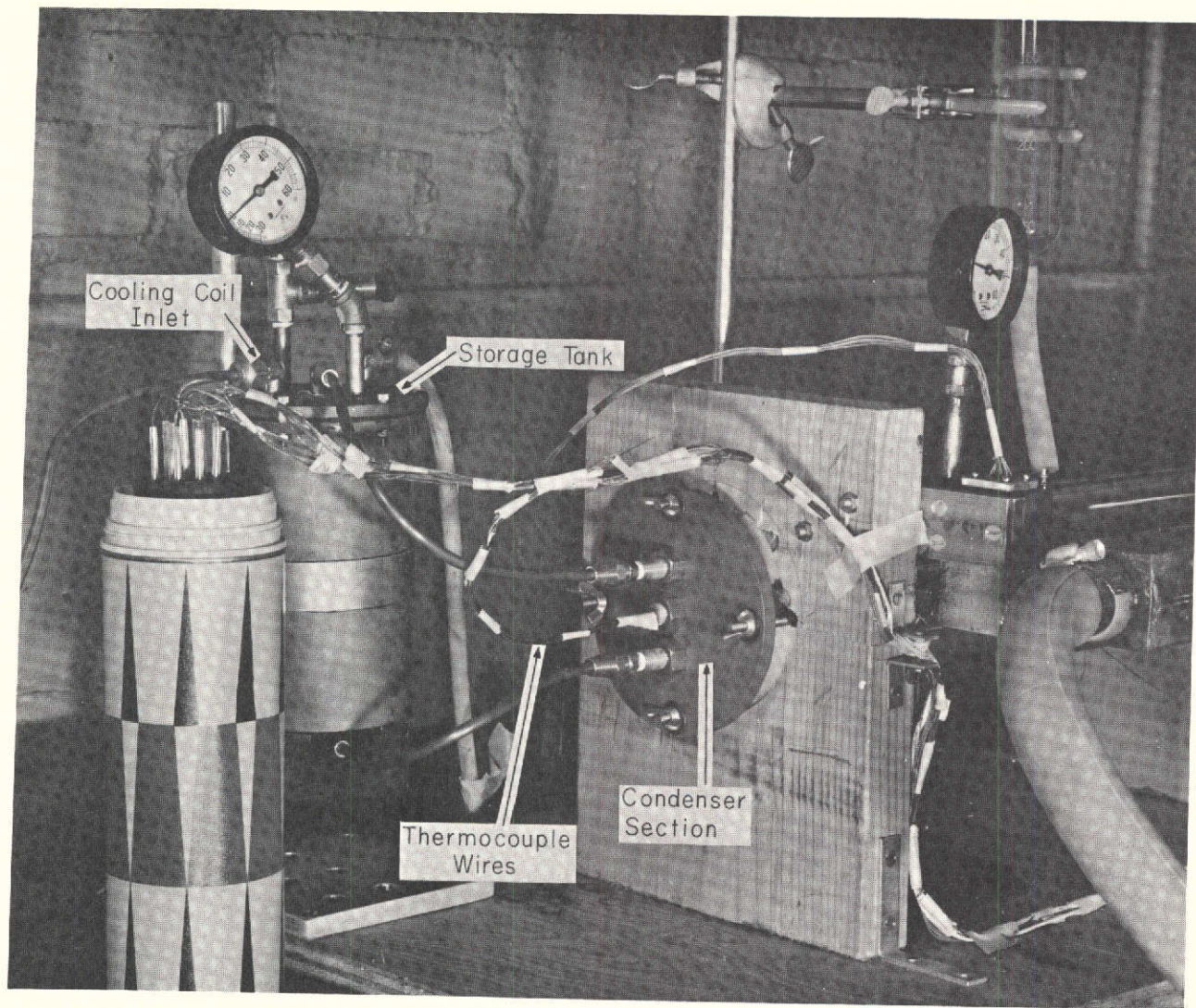


Figure 4. Heat Removal System

measuring temperatures and for determining when "burn out" (desiccation of the wick material) occurred. At the condenser end, thermocouples were used again to determine the temperature gradient for determining the heat flux out of the system. Accurate determination of the conductivity of the aluminum disks was made before the system was assembled. The product of conductivity and temperature difference indicated the heat flux.

#### Wicking Chamber Manifold

A manifold was constructed for use with the wicking chamber. First, the manifold had a large vacuum valve (see Fig. 5) which connected to a vacuum system (see Fig. 6) capable of vacuums to  $10^{-6}$  mm of Hg. for evacuating the wicking chamber. A transfer plug was adapted to the manifold for extracting the thermocouple wires from the wicking chamber. A small needle valve was attached to the manifold for charging the chamber with the working fluid. A union was also adapted to the manifold for connecting a combination pressure-vacuum gage for indicating the pressure in the chamber. Another union was adapted to the manifold for making the direct connection to the wicking chamber. The entire manifold, along with the valves and unions, was mounted to the dewar mounting stand near the wicking chamber outlet tube (see Fig. 7). Then, all of the necessary connections to the wicking chamber were made through the wicking chamber manifold.

#### Temperature Recording

A twenty-one point Leeds and Northrup millivolt recorder was used (see Fig. 2). Since all forty-five thermocouple points could not be recorded, the most representative points were chosen after monitoring

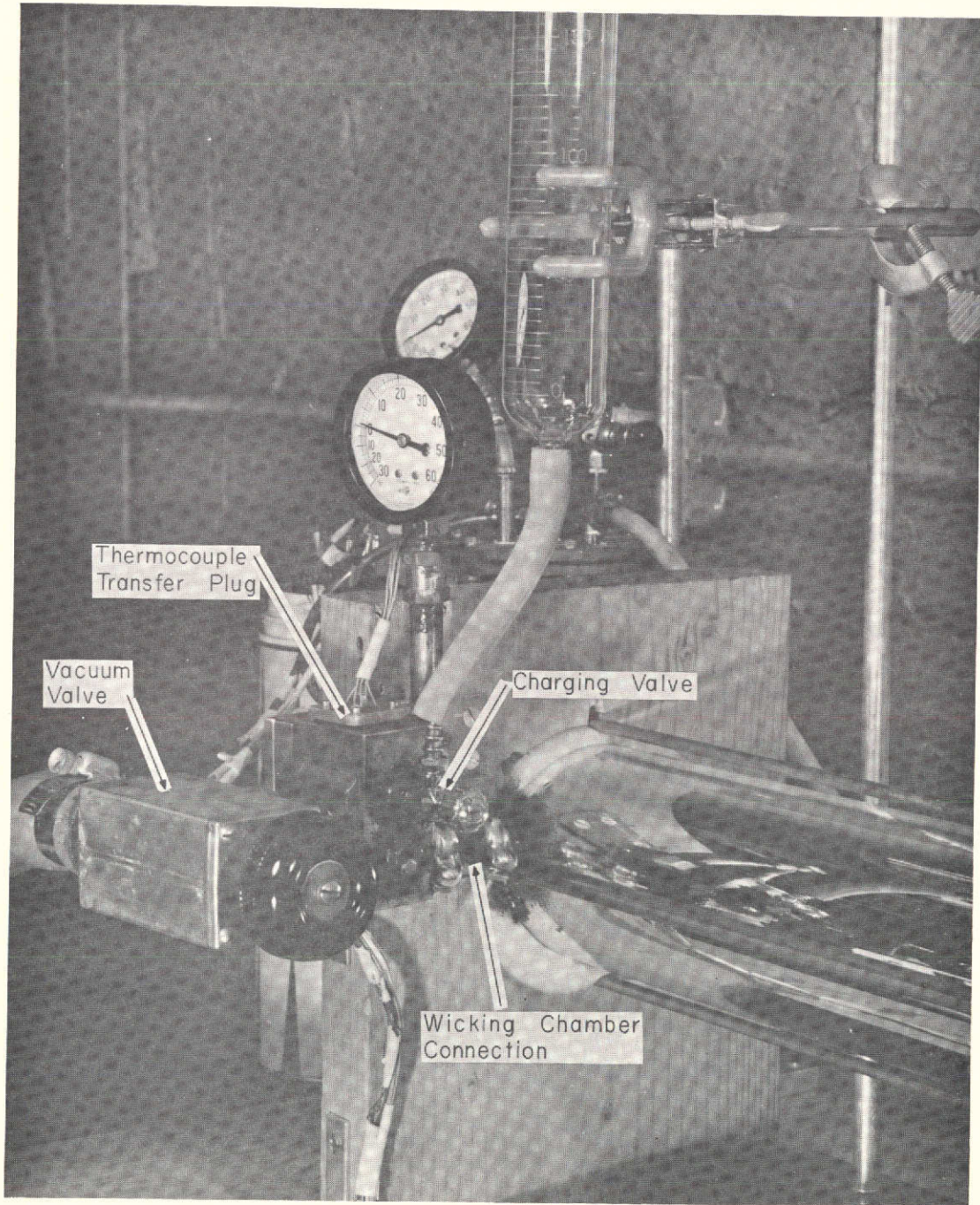


Figure 5. Wicking Chamber Manifold

47<

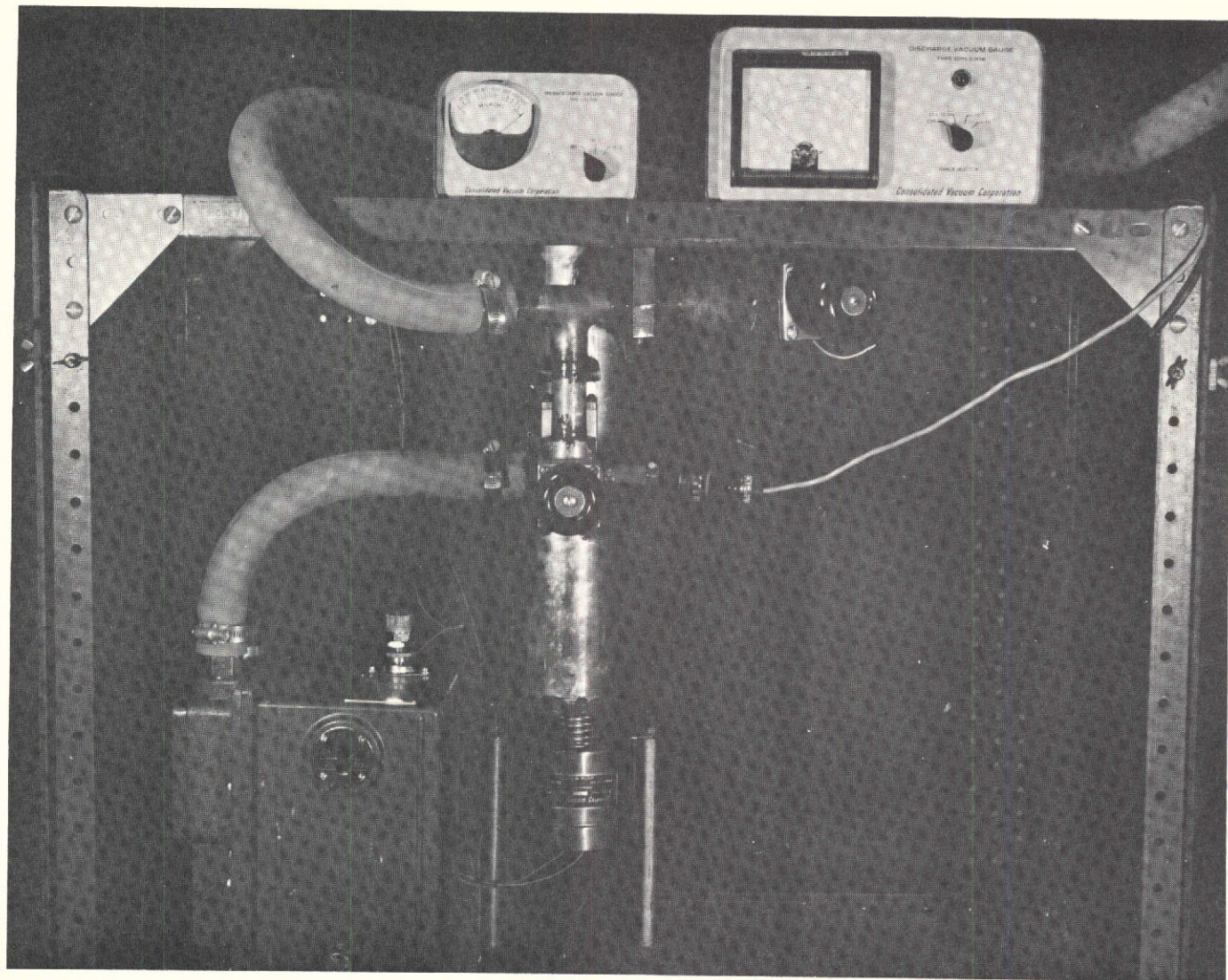


Figure 6. Vacuum System

48 >

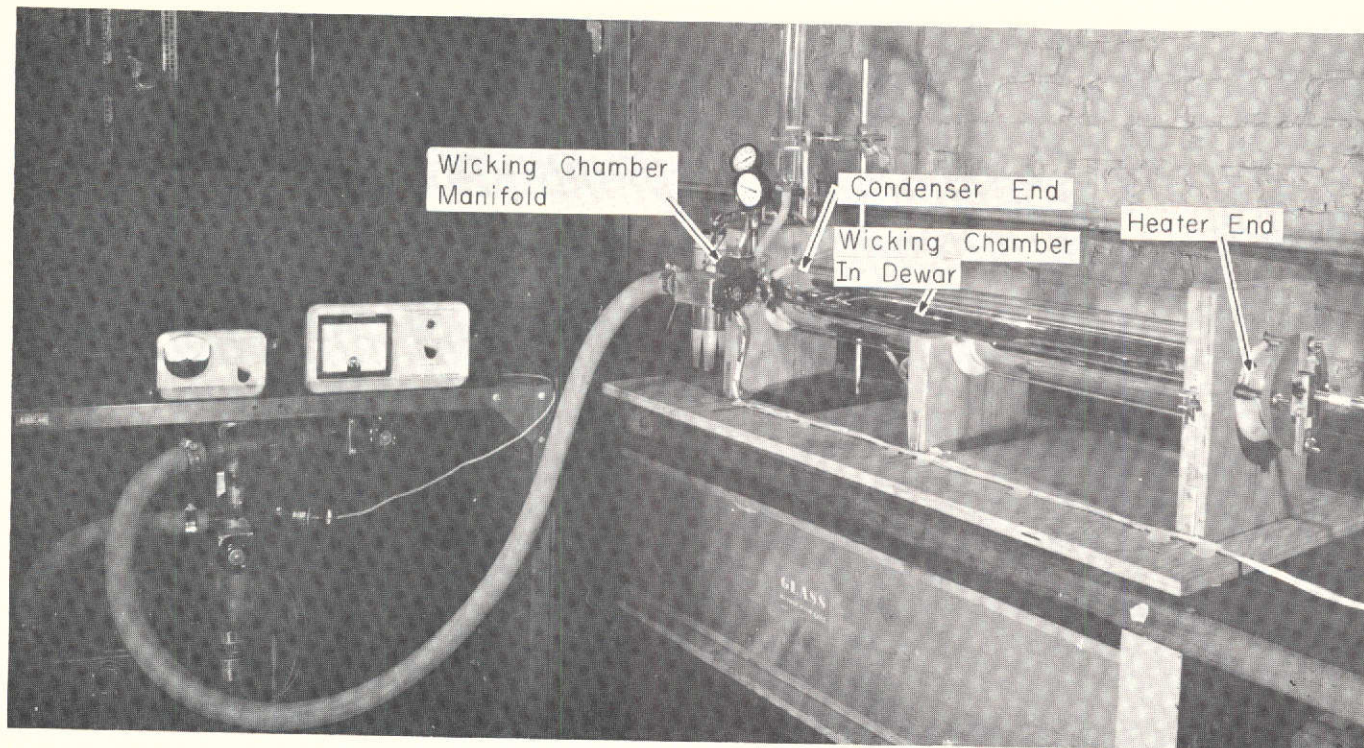


Figure 7. Heat Pipe and Vacuum System

all forty-five points for a period of time. A potentiometer was used to continuously monitor the temperature gradient between the main and guard heaters so that the guard heater variable transformer could be adjusted to minimize the heat loss from the main heater.

#### 4.2 INITIAL TESTING PROCEDURE

The wicking chamber was evacuated to an initial absolute pressure of  $8 \times 10^{-2}$  mm of Hg. However, under this first evacuation, the wicking cage collapsed by buckling the stainless steel rod columns. After sufficient strengthening of the cage, the chamber was evacuated to  $15 \times 10^{-2}$  mm of Hg. Six hundred milliliters of distilled water was then injected into the chamber. This large amount of water proved to be much more than was necessary.

During the first application of heat to the wicking chamber, no heat was transferred to the condenser end and a temperature distribution of 5 to  $10^{\circ}\text{C}$  was established. Much purging of the wicking chamber was required before the temperature in the chamber equalized and a temperature gradient across the condenser aluminum disk was established.\* After establishing the heat flux, further purging was required at about fifteen minute intervals. Without this purging, the temperature distribution in the wicking chamber widened and the wicking material appeared to begin "burn out" at less than 10 watts input power. With the intermittent purging, the maximum heat transport rate was approximately 10 watts.

---

\*Purging of the wicking chamber was performed by cracking (opening very slightly) the large vacuum valve while the mechanical vacuum pump was running. This procedure drew out of the chamber the non-condensable gases which had formed a barrier between the aluminum disk and the newly evaporated water vapor. The valve was opened for 1 to 5 second durations.

During testing, heat inputs were varied from an initial zero watts to a maximum of 60 watts at 5 watt intervals. Each input wattage was maintained until all temperature in the system stabilized. After stabilization, the heat input was stepped up or down, depending upon the test being performed. Even though runs of greater than 10 watts were obtained, 10 watts was the maximum repeatable heat flux before "burn out" occurred.

Since the time constant of the heater assembly and, in particular, the heater aluminum disk temperature were large (approximately seven minutes for 63.2% response of steady state for the aluminum disk), the "burn out" wattage was, at first, difficult to determine experimentally. When a given heat input was maintained for at least 10 to 15 minutes, 10 watts was the maximum maintainable input wattage. At wattage inputs above 10 watts, the heater aluminum disk temperature continued to increase without reaching a steady state value. This fact would indicate that the circular section of Refrasil attached to the aluminum disk began to dry out. Then the aluminum disk temperature could continue to increase and begin to diverge over the surface of the disk.

#### 4.3 NORMAL TEST RUN

After initial charging of the wicking chamber, the heat pipe continues to operate until either non-condensable gases collect at the condenser surface or both the heater and condenser ends are at the same temperature. If a temperature difference exists and the heat pipe is not operating, the wicking chamber must be purged lightly. The heat pipe should be allowed to operate without adding heat until both ends are } at the same temperature. Then the main heater should be set

at 2 or 5 watts, depending upon the size input change utilized. The temperature difference between the main and guard heaters should be monitored continuously. Then the guard heater is adjusted so that the temperature difference is approximately zero. The temperature difference should be monitored and the guard heater adjusted throughout the entire test run.

When the heater aluminum disk temperature stabilizes, the main heater input should be increased by the 2 or 5 watt change required. The guard heater wattage should also be increased accordingly to minimize the main to guard heater temperature difference. The variance of the wicking chamber temperatures should be observed continuously. When the variance exceeds  $\frac{1}{2}^{\circ}\text{C}$ , the chamber should be lightly purged. If the temperatures do not equalize within 20 seconds after the purge, the main heater should no longer be increased, for "burn out" is impending. At the same time, the temperature of the heater aluminum disk on the wicking chamber side should be observed. If these five temperatures on the disk continue to rise without reaching a steady state value or start diverging from each other, "burn out" could be impending. At "burn out" these temperatures will continue to diverge from each other regardless of the amount of purging. It is to be noted that the "burn out" can be a very gradual process.

Step down runs of the system were not performed successfully. The heat retention and time constants of the heater assembly and aluminum disk were too large.

After the wick "burn out", the heaters should be turned off. The wick must be allowed to resaturate before additional tests can be run.

#### 4.4 WICKING MATERIAL TESTS

The wicking material, Refrasil #C100-28, used in the heat pipe was performance tested outside the heat pipe. Figure 8 shows the test apparatus used in these tests. The two objectives of the tests were to obtain fluid front displacement and volume input as functions of time data. Then the volume transport rate of the wick for any length was calculated in two ways. First, the transport rate was found using the equation

$$\dot{v} = AV \quad (12)$$

where  $\dot{v}$  is the volume transport rate,  $A$  is the measured cross sectional area of the wick, and  $V$  is the velocity of the wetting front. The  $V$  term was determined by differentiating the displacement-time equation determined from Fig. 9. Second, the volume transport rate was determined by summing the total volume input to the wick over a given length. When this total volume was divided by the total elapsed time, the volume flow rate for a wick of one-half the total wick length used was determined. Equation (8) shows that the mass transport rate is inversely proportional to the total wick length. The volume rate for the length of wick desired can be scaled by multiplying by the appropriate ratio. This procedure for scaling the volume transport rates for different wick lengths was applicable only to the horizontal wick configurations, as can be seen from Eq. (6).

The wicking test apparatus, Fig. 8, consisted of three main elements. First, the distilled water was supplied by a 100 ml burette; all excess water dripping from the saturated end of the wick was

50

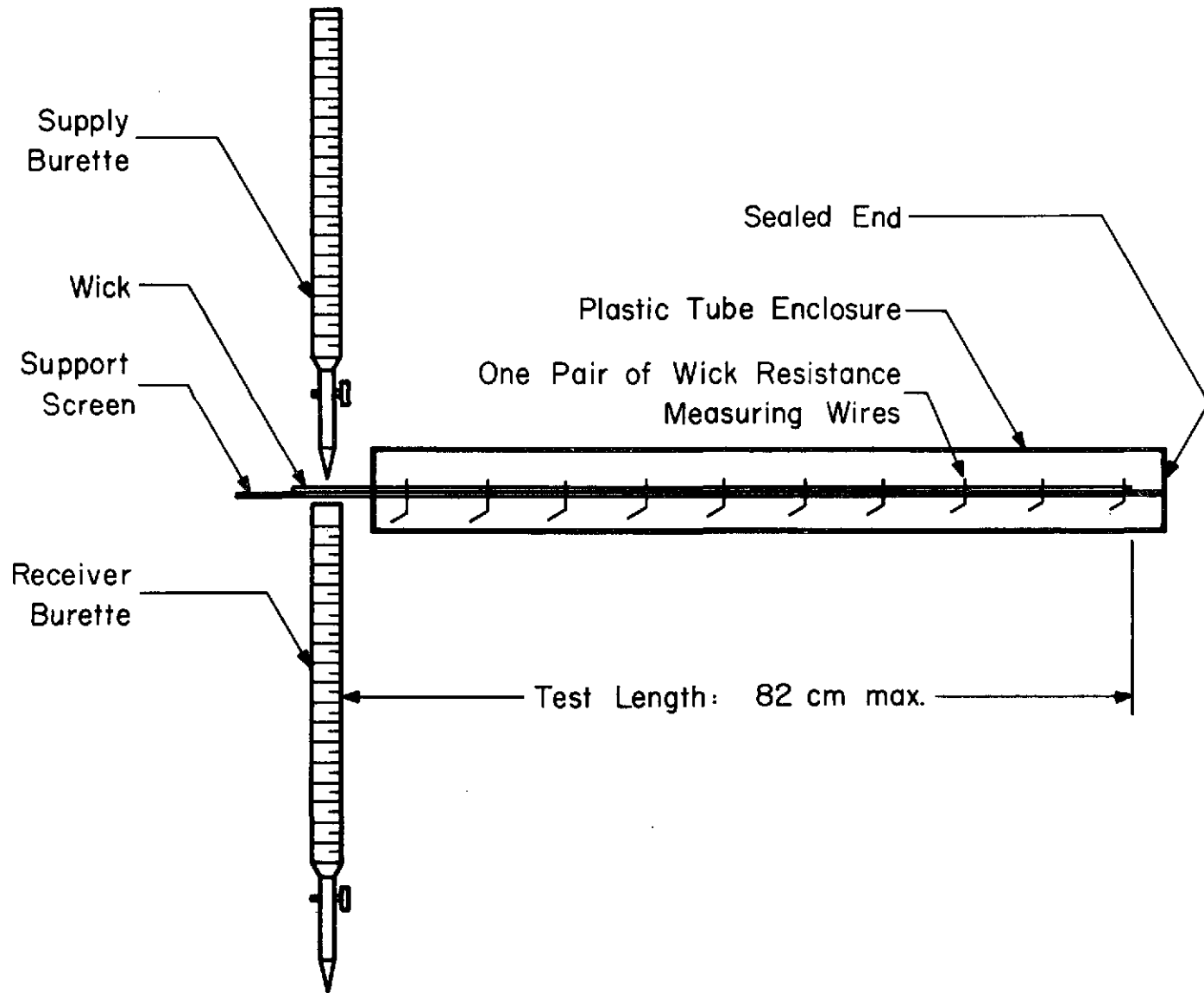


Figure 8. Schematic of Test Arrangement for Measurement of Capillary Flow in Horizontal Wicks

collected in a 50 ml receiver burette. The total volume transferred down the wick at any time was the difference between the readings of the supply and receiver burettes. Second, the wick was supported on a 1 cm-square mesh screen; a 3.2 cm inside diameter plexiglass tube was used to house the entire wick, except for the area where the water was introduced. This tube minimized losses from the wick by evaporation. Before each test, a saturated wick was placed inside the tube for several hours in order to saturate the atmosphere there. Third, pairs of copper wires were attached to the support screen at every 5 cm distance down the length of the wick. The insulation was removed from the ends of all the wires and the ends were then inserted into pores in the wick. The wires in each pair were separated by approximately 1 cm in a given cross section of the wick and each pair of wires was separated by a 5 cm distance down the wick. All the wires were connected to a 25-point thermocouple switch; the main connection of the switch was connected to an ohmmeter. When the wick was dry, the ohmmeter indicated an infinite resistance for any pair of wires. Immediately after the pores of the wick occupied by a pair of wires in any cross section were wetted, the resistance between wires changed (within approximately 2 sec) from an infinite to approximately  $1M\Omega$  resistance. When one cross section was wetted, the thermocouple switch was advanced to the next pair of wires to detect wetting of the wick at the next 5 cm interval. When the wetting front reached each pair of wires, all readings were taken. The readings included: supply and receiver burette volumes, total distance of wetting front down the wick, and total elapsed time of the test measured using a stop watch. From the distance and time data, a graph (Fig. 9) was constructed.

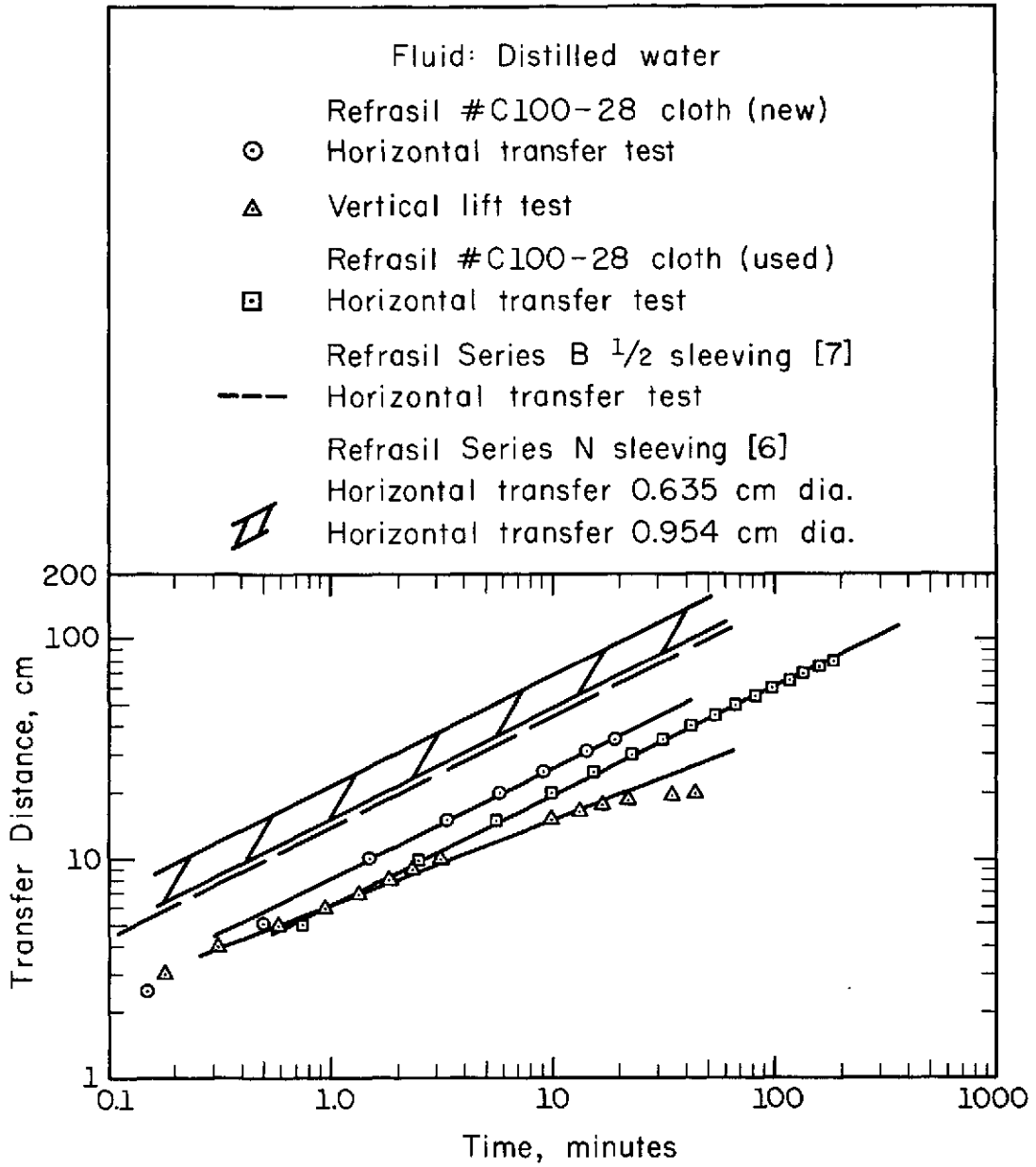


Figure 9. Wick Performance Graph

Maximum test wick width and length were 2.5 cm and 95 cm, respectively, for the test apparatus constructed.

## 5. DISCUSSION

For a "burn out" heat flux of 10 watts, which for the Refrasil #C100-28 used corresponds to 0.594 watts per cm width of wick, the volume transfer rate of water in the Refrasil wicking material required was

$$\dot{v} = \frac{Q}{h_{fg}\rho} = 0.247 \text{ cm}^3/\text{min} , \quad (9)$$

where  $Q$  equals the "burn out" wattage transferred and  $h_{fg}$  is the enthalpy of evaporation of water at 26.7°C (80°F). With a wick cross sectional area of 0.685 cm<sup>2</sup>, the volume transfer rate per unit area becomes 0.361 cm<sup>3</sup>/min-cm<sup>2</sup>. The wicking chamber temperatures for all tests were within 5°C of the 26.7°C temperature used for the calculations.

From the wick performance tests on the Refrasil #C100-28, the volume flow rates per area were 0.299 to 0.424 cm<sup>3</sup>/min-cm<sup>2</sup>. The lower value was determined from the volume input measurements, whereas the upper value came from velocity calculations on the test data (Fig. 8). This wicking material was unused.

Another wick performance test was conducted on the actual wick used in the heat pipe. The results indicated approximately 45% less than the volume transport rates per cm<sup>2</sup> area for the unused material; the values were 0.163 to 0.229 cm<sup>3</sup>/min-cm<sup>2</sup> for volume and velocity calculated, respectively. This decrease in wicking capability could be due primarily to wick contamination during the four months while it was used in the heat pipe. The used wick had acquired a yellow-brown appearance in contrast to the white color of the unused wick.

References [6] and [7] give water flow rates through horizontal wicks for different specimens of Refrasil. When scaled to the 81.9 cm length used in this heat pipe, the volume transfer rates per  $\text{cm}^2$  area from [6] were 1.39 and 2.82  $\text{cm}^3/\text{min}\text{-cm}^2$  for the 0.954 and 0.635 cm diameter sleeving, respectively. These values are from 365% to 567% greater than the wicking tests performed by the author. The results of [7] lie between the data of [6] and those obtained in this work. There are three main reasons for large variations in liquid transfer rates. First, the Refrasil used in this experiment probably had a different pore size than the samples used by the other authors. As shown in Eqs. (6) and (7), the pore radius is one of the independent variables for the mass or volume flow rates. Second, the sleeveings were flattened for the horizontal tests in the previous references. The interaction of the touching surfaces of the inside diameter may have caused errors in the transport rate. Third, in [6] the water was removed from the end of the wick by adding heat from a gas burner. This addition of heat created a large temperature rise and a resulting possible 20% change in the surface tension of the water. Since surface tension is the main pumping pressure, the temperature rise could cause error in the transfer rate. Figure 8 shows the comparison among the wicking materials.

The experimental "burn out" transfer rate per  $\text{cm}^2$  area (at 10 watts) of 0.361  $\text{cm}^3/\text{min}\text{-cm}^2$  lies well within the range predicted by the author's horizontal wick performance tests. Actually the experimental value coincides with the average of the predicted rates for the unused Refrasil #C100-28 and within 36% of the upper predicted value for the used Refrasil #C100-28.

The maximum vapor velocity in the wicking chamber at "burn out" was approximately 446 cm/min. This value was far below the speed of sound in water vapor,  $2.60 \times 10^6$  cm/min at 26.7°C. The corresponding Reynolds number at "burn out" was 14.5, indicating laminar flow.

If the entire cross sectional area of the wick were capable of transporting liquid, the water velocity in the wick while approaching "burn out" would be approximately 0.361 cm/min. Actually much of the area is not capable of transporting liquid due to the presence of the fibers of the Refrasil. The mean velocity of the liquid in the wick probably would be approximately 2 to 5 times that value stated above. A maximum value of 1.805 cm/min seems reasonable. The corresponding maximum Reynolds number was 56.3 in the wick with water at 26.7°C.

Usable data for the heat flux through the aluminum disks were not obtained. Thermocouple points had been attached to the aluminum disks with epoxy for the purpose of obtaining both absolute temperature readings on the disks and relative temperatures across the disks. This relative temperature, along with the accurately determined conductivity of the aluminum disks, was to be used for calculating the heat flux. However, a thin layer of epoxy had been applied to the bare thermocouple wires before attaching them to the disks in an effort to prevent electrical shorting of the thermocouple wires. The epoxy did indeed prevent electrical shorting, but also introduced a large thermal resistance. This resistance was large enough to cause errors in the differential temperature of 50 to 1500%. The maximum differential temperature times the disk conductivity yielded a heat flux of up to 15 times greater than the heat applied through the main heater. This measurement was obviously in error.

With the system used, no transient temperature lag from one end of the wicking chamber to the other end was observed during heat input changes. Apparently the time constants of the heat input changes were much larger than the temperature equalizing time constant of the wicking chamber. The time constant for the temperature on the wicking chamber side of the heater aluminum disk was approximately seven minutes for a 63.2% response of steady state.

## 6. CONCLUSIONS

The heat pipe construction was completed and initial experimental operating data were obtained. The maximum heat transport rate was 10 watts. For the Refrasil #C100-28 used, the 10 watt "burn out" point corresponds to 0.594 watts per cm width of the wick. This value was well within the power level of 8.27 to 11.8 watts predicted from horizontal wicking tests performed on the Refrasil #C100-28. Both vapor and liquid flows in the wicking chamber were found to be laminar.

Usable temperature drops across the aluminum disks were not obtained; temperature variances within the wicking chamber were found to be consistently less than  $\frac{1}{2}^{\circ}\text{C}$  over the entire 81.9 cm wick length. With the system used, no transient temperature lag from one end of the wicking chamber to the other end was observed during heat input changes. Apparently the time constants of the heat input changes were much larger than the temperature equalizing time constant of the wicking chamber.

During this initial testing, many problems were encountered. Most of them were solved during the test runs and the main operating parameters of the heat pipe system were determined. Perhaps the most important fact of the initial testing was the resulting closeness of the experimental "burn out" to that predicted from horizontal wicking tests performed by the author.

## 7. RECOMMENDATIONS

### 7.1 HEAT PIPE MODIFICATIONS

1. A new wicking cage should be made. Narrow supports for locating the wicking material should be provided at a 10 to 12 cm spacing. If the cage is made solid (nonadjustable), attachment of the wicking material may be facilitated greatly.

2. Since high temperature build up was encountered around the heater pack, several of the mica sheets and the copper disk should be removed from between the main heater and the heater aluminum disk. With less thermal insulation, a greater heat flux could be realized with less temperature differential.

3. Special thermocouple wires should be used. These wires should have measuring points coated with material having high electrical and low thermal resistances. The special wires could be placed on each side of the aluminum disks to accurately measure the differential temperature drops. With these temperature measurements, accurate values for the axial heat flux could be calculated.

4. A small needle valve should be inserted on the manifold between the vacuum system and the wicking chamber. This valve would provide fine control for purging non-condensibles from the wicking chamber.

5. During reassembly of the entire heat pipe, special care should be taken to double check all joints for possible leaks. After assembly of the heat pipe, all joints should be coated with several thin layers of "Glyptol" or its equivalent.

6. The wicking chamber of the heat pipe should be evacuated to about  $10^{-2}$  to  $10^{-3}$  mm of Hg. before charging the chamber with water.

When evacuated, the chamber should be charged with approximately 100 to 150 milliliters of distilled water. Over 150 milliliters of water may result in an excessively large pool of liquid on the bottom of the wicking chamber. If the heat pipe length is changed, the amount of charge should be changed proportionately.

## 7.2 WICKING MATERIAL TESTING

Wicking material testing experiments should be continued to determine the volume transport qualities of different wicking materials. The experiment should be carried out under constant temperature conditions. A burner should not be used at the evaporator end of the wick, since the elevated temperature may change the surface tension and viscosity of the working fluid. If obtained with heating, the data may not represent the true operating conditions inside the heat pipe.

## 7.3 FUTURE HEAT PIPE TESTS

1. Test runs should be performed on shorter lengths of the wicking chamber to determine what effect the wick length has on the "burn out" wattage. For the horizontal case Eq. (8) should be further verified.

2. Fluids other than water should be employed in the wicking chamber to determine their operating characteristics. These fluids should then be compared to water for possible future application.

3. Combinations of two different fluids should be employed in the wicking chamber. Compatibility and other operating characteristics should be determined for all *practical* combinations of the fluids.

4. A new heat input unit with a sufficiently small time constant, so that the transient phenomena inside the wicking chamber may be observed during heat input changes, should be designed and built.

## LIST OF REFERENCES

1. R. C. Turner and W. E. Harbaugh, "Design of a 50 000 Watt Heat Pipe Space Radiator," AVIATION AND SPACE, June 16-19, 1968, The American Society of Mechanical Engineers, New York, pp. 639-643.
2. Samuel Katzoff, "Heat Pipes and Vapor Chambers for Thermal Control of Spacecraft," AIAA THERMO-PHYSICS SPECIALIST CONFERENCE, New Orleans, Louisiana, April 17-20, 1967, p. 23.
3. K. T. Feldman, Jr., Heat Pipe Design and Analysis, The University of New Mexico, Albuquerque, New Mexico, April 20, 1968, p. 48.
4. V. L. Streeter, Fluid Mechanics, 4th edition, McGraw Hill Book Co., New York, 1966, p. 257.
5. A. E. Scheidegger, The Physics of Flow Through Porous Media, The Macmillan Co., 1960, pp. 68-90.
6. Arnold P. Shlosinger, Technology Study of Passive Control of Humidity in Space Suits, Northrop Corporation, Northrop Space Laboratories, Hawthorne, California, September, 1965, p. 73.
7. R. A. Farran and K. E. Starner, "Determining Wicking Properties of Compressible Materials for Heat Pipe Applications," AVIATION AND SPACE, June 16-19, 1968, The American Society of Mechanical Engineers, New York, pp. 659-670.

## LIST OF SYMBOLS

A	cross-sectional area of wick ( $\ell^2$ )*
$A_c$	minimum cross-sectional area of wicking chamber ( $\ell^2$ )
C	arbitrary constant (M- $\ell$ /t)
g	acceleration of gravity ( $\ell/t^2$ )
$h_{fg}$	latent heat of vaporization of liquid (q/M)
K	wick permeability ( $\ell^2$ )
L	actual length of wicking material ( $\ell$ )
$\dot{m}$	mass flow rate (M/t)
$\Delta P_c$	capillary pumping head ( $F/\ell^2$ )
$\Delta P_g$	gravitational head ( $F/\ell^2$ )
$\Delta P_L$	liquid viscous drag ( $F/\ell^2$ )
$\Delta P_v$	vapor pressure drop ( $F/\ell^2$ )
Q	heat transfer rate (q/t)
r	mean pore radius of wicking material ( $\ell$ )
$r_c$	effective pore radius of wick at condenser ( $\ell$ )
$r_e$	effective pore radius of wick at evaporator ( $\ell$ )
V	velocity ( $\ell/t$ )
$\dot{v}$	volume flow rate ( $\ell^3/t$ )
w	total wick width ( $\ell$ )
$\theta_c$	liquid contact angle in wick at condenser
$\theta_e$	liquid contact angle in wick at evaporator
$\mu$	absolute viscosity of liquid ( $F\cdot t/\ell^2$ ) or (M/t- $\ell$ )
$\nu$	kinematic viscosity of liquid or vapor ( $\ell^2/t$ )
$\rho$	liquid density (M/ $\ell^3$ )

\*Dimensions in parentheses are: F - force, M - mass,  $\ell$  - length, q - heat (F- $\ell$ ), t - time.

$\sigma$  liquid surface tension (F/l)  
 $\phi$  angle between heat pipe axis and gravitational field

## APPENDIX A: SAMPLE CALCULATIONS

"Burn out" power rating per cm width of wick (Refrasil #C100-28):

$$\frac{Q}{w} = \frac{10 \text{ watts}}{16.85 \text{ cm}} = 0.594 \text{ watts/cm}$$

Required transport rate of water in the Refrasil for a "burn out" wattage of 10 watts:

$$Q = \dot{v} h_{fg}$$

$$\dot{v} = \frac{Q}{h_{fg} \rho}$$

$$Q = 10 \text{ watts} = 143.5 \text{ cal/min}$$

$$h_{fg} = 582 \text{ cal/g @ } 26.7^\circ\text{C.}$$

$$\dot{v} = \text{volume transport rate}$$

$$\rho = 1 \text{ g/cm}^3 \text{ @ } 26.7^\circ\text{C. for water}$$

$$\dot{v} = \frac{143.5 \text{ cal/min}}{(582 \text{ cal/g})(1 \text{ g/cm}^3)}$$

$$\dot{v} = 0.247 \text{ cm}^3/\text{min}$$

Cross-sectional area of wick:

$$A = (\text{thickness})(\text{width})$$

$$\text{thickness} = 0.016 \text{ in.} = (4.06)(10^{-2}) \text{ cm}$$

$$\text{width} = 6.625 \text{ in.} = 16.85 \text{ cm}$$

$$A = (4.06)(10^{-2})(16.85) = 0.685 \text{ cm}^2$$

Required volume transport rate per  $\text{cm}^2$  cross-sectional area:

67a

$$\frac{\dot{v}}{A} = \frac{0.247 \text{ cm}^3/\text{min}}{0.685 \text{ cm}^2} = 0.361 \text{ cm}^3/\text{min-cm}^2$$

Available volume transport rates from horizontal wicking performance tests:

Wicking material: Refrasil #C100-28

Wicking fluid: distilled water

Fluid temperature: 26.7°C.

Unused material; 2.50 cm wide, 31.0 cm long

1. Calculated from volume input measurements:

$$\begin{aligned} \dot{v}(31.0/2 \text{ cm}) &= \frac{\text{total volume}}{\text{total time}} \\ &= \frac{2.30 \text{ cm}^3}{14.33 \text{ min}} \\ &= 0.1605 \text{ cm}^3/\text{min} \end{aligned}$$

$$\begin{aligned} \frac{\dot{v}}{A} (15.5 \text{ cm}) &= \frac{0.1605 \text{ cm}^3/\text{min}}{(2.50 \text{ cm}) (4.06)(10^{-2}) \text{ cm}} \\ &= 1.58 \text{ cm}^3/\text{min-cm}^2 \end{aligned}$$

$$\begin{aligned} \frac{\dot{v}}{A} (81.9 \text{ cm}) &= \frac{(15.5 \text{ cm})(1.58 \text{ cm}^3/\text{min-cm}^2)}{(81.9 \text{ cm})} \\ &= 0.299 \text{ cm}^3/\text{min-cm}^2 \end{aligned}$$

2. Calculated from velocity which was derived from displacement vs time plot:

$$\frac{\log x}{\log kt} = \frac{1}{2}, \quad kt = x^2$$

$$k = \frac{(25.0)^2}{9.00} = 69.4 \text{ cm}^2/\text{min} \text{ (using experimental point)}$$

$$69.4t = x^2$$

$$V = \frac{dx}{dt} = 34.7 \frac{1}{x} \text{ cm/min}$$

$$V = \frac{34.7}{81.9} = 0.424 \text{ cm/min}$$

$$\frac{\dot{V}}{A} = V = 0.424 \text{ cm/min} = 0.424 \text{ cm}^3/\text{min-cm}^2$$

$$= 0.424 \text{ cm}^3/\text{min-cm}^2 \text{ for } 81.9 \text{ cm wick length}$$

Used material; 2.5 cm wide, 80.0 cm long

1. Calculated from volume input measurements:

$$\begin{aligned} \frac{\dot{V}}{A} (40.0 \text{ cm}) &= \frac{\text{total volume}}{\text{total time}} \\ &= \frac{6.40 \text{ cm}^3}{188.5 \text{ min}} \\ &= 3.39 \times 10^{-2} \text{ cm}^3/\text{min} \end{aligned}$$

$$\begin{aligned} \frac{\dot{V}}{A} (40.0 \text{ cm}) &= \frac{3.39 \times 10^{-2} \text{ cm}^3/\text{min}}{(2.50 \text{ cm})(4.06 \times 10^{-2} \text{ cm})} \\ &= 0.334 \text{ cm}^3/\text{min-cm}^2 \end{aligned}$$

$$\begin{aligned} \frac{\dot{V}}{A} (81.9 \text{ cm}) &= \frac{(40.0 \text{ cm})(0.334 \text{ cm}^3/\text{min-cm}^2)}{(81.9 \text{ cm})} \\ &= 0.163 \text{ cm}^3/\text{min-cm}^2 \end{aligned}$$

2. Calculated from velocity which was derived from displacement vs time plot:

$$\frac{\log x}{\log kt} = \frac{1}{2}, kt = x^2$$

$$k = \frac{(60.0)^2}{96.0} = 37.6 \text{ cm}^2/\text{min}$$

$$37.6t = x^2$$

$$V = \frac{dx}{dt} = 18.8 \frac{1}{x} \text{ cm/min}$$

$$\frac{\dot{v}}{A} = V = \frac{18.8}{81.9} = 0.229 \text{ cm/min}$$

$$= 0.229 \text{ cm}^3/\text{min-cm}^2 \text{ for } 81.9 \text{ cm wick length}$$

Liquid velocity in wick as acquired from the required volume transport rate, also assuming that entire wick area was capable of transporting liquid:

$$V = \frac{\dot{v}}{A} = 0.361 \text{ cm}^3/\text{min-cm}^2$$

$$= 0.361 \text{ cm/min}$$

If actual wick area for transporting liquid was approximately 1/5 total area, A, due to the Refrasil fibers:

$$V_{(\text{max})} = 5V = 5(0.361 \text{ cm/min})$$

$$= 1.805 \text{ cm/min}$$

Maximum Reynolds number of liquid flow in wick based on  $L_{\max}$ :

$$Re_{\max} = \frac{V_{\max} L_{\max}}{\nu}$$

$$V_{\max} = 1.805 \text{ cm/min}$$

$$L_{\max} = \text{assumed to be total wick width}$$

$$= 16.85 \text{ cm}$$

$$\nu = 0.540 \text{ cm}^2/\text{min at } 26.7^\circ\text{C for liquid}$$

$$= \frac{(16.85 \text{ cm})(1.805 \text{ cm/min})}{(0.540 \text{ cm}^2/\text{min})}$$

$$= 56.3 \text{ for water in wick at } 26.7^\circ\text{C.}$$

Maximum vapor velocity in the wicking chamber as acquired from the required volume transport rate:

$$V_{\max} = \frac{\dot{v}_v}{A_c}$$

$$\dot{v}_v = \dot{v} \frac{\text{specific volume of vapor}}{\text{specific volume of fluid}}$$

$$V_{\max} = \frac{\dot{v} (\text{specific volume})_{\text{vapor}}}{A_c (\text{specific volume})_{\text{fluid}}}$$

$$\dot{v}_v = \text{vapor volume transport rate}$$

$$\dot{v} = \text{fluid volume transport rate}$$

$$= 0.247 \text{ cm}^3/\text{min}$$

$$A_c = 21.8 \text{ cm}^2$$

$$V_{\max} = \frac{(0.247 \text{ cm}^3/\text{min})(633.7)}{(21.8 \text{ cm}^2)(0.0161)} @ 26.7^\circ\text{C.}$$

$$= 446 \text{ cm/min}$$

Reynolds number of vapor flow in the wicking chamber, based on  $L_{\max}$ :

$$Re_{\max} = \frac{V_{\max} L_{\max}}{\nu}$$

$$V_{\max} = 446 \text{ cm/min}$$

$$L_{\max} = \text{dewar diameter}$$

$$= 7.62 \text{ cm}$$

$$\nu = 234 \text{ cm}^2/\text{min @ } 26.7^\circ\text{C for vapor}$$

$$\begin{aligned} \text{Re}_{\text{max}} &= \frac{(7.62 \text{ cm})(446 \text{ cm/min})}{(234 \text{ cm /min})} \\ &= 14.5 \text{ for water vapor @ } 26.7^\circ\text{C}. \end{aligned}$$

EXPERIMENTAL INVESTIGATION OF THE PERFORMANCE  
OF VARIOUS WICK CONFIGURATIONS IN SINGLE-  
AND TWO-FLUID HEAT PIPES OPERATING  
IN THE GRAVITATIONAL FIELD

D. L. Hunsberger

J. C. Chato

Technical Report No. ME-TR-187

October 1970

DEPARTMENT OF MECHANICAL AND INDUSTRIAL ENGINEERING  
PHYSICAL ENVIRONMENT UNIT  
ENGINEERING EXPERIMENT STATION  
UNIVERSITY OF ILLINOIS AT URBANA - CHAMPAIGN  
URBANA, ILLINOIS 61801



# EXPERIMENTAL INVESTIGATION OF THE PERFORMANCE OF VARIOUS WICK CONFIGURATIONS IN SINGLE- AND TWO-FLUID HEAT PIPES OPERATING IN THE GRAVITATIONAL FIELD

by

D. L. HUNSBERGER

J. C. CHATO

Technical Report No. ME-TR-187

October 1970

Supported by

National Aeronautics and Space Administration

under

Grant No. NGR-14-005-103

*I*

74<

EXPERIMENTAL INVESTIGATION OF THE  
PERFORMANCE OF VARIOUS WICK CONFIGURATIONS  
IN SINGLE- AND TWO-FLUID HEAT PIPES  
OPERATING IN THE GRAVITATIONAL FIELD

by

D. L. Hunsberger

J. C. Chato

Technical Report No. ME-TR-187

October 1970

Supported by  
National Aeronautics and Space Administration  
under  
Grant No. NGR 14-005-103

## ABSTRACT

In Part I, wicking material tests were made on Refrasil No. C100-28. The tests were run on 9-in. X 1-in. Refrasil strips. Displacement-time curves were extrapolated for predicting the performance of a 21-3/4 in. heat pipe.

In Part II, heat pipe tests were run with a well-defined wick length of 21-3/4 in. and a total width of 7 in. The same Refrasil was the wicking material. An open-ended dewar housed the heat pipe system which consisted of heat input, mass transfer, and heat removal sections. Two electric heaters supplied heat input, while circulating water was used for heat removal.

Both Parts I and II showed water to be a much better operating fluid than ethyl alcohol or 50 percent ethyl alcohol by weight. Ethyl alcohol appeared to be only slightly better than the 50 percent mixture. At zero degrees the maximum heat transfer capacities were 15, 4, and 2 watts, respectively, for the three fluids. The predicted wattages from Part I were generally higher due to greater ease in saturating the wicking material with fluid.

A gap effect created by sewing two layers of wicking material together greatly enhanced the heat pipe performance. At zero degrees, water transferred over 80 watts, as compared to 15 watts previously.

## TABLE OF CONTENTS

	Page
LIST OF FIGURES . . . . .	v
1. INTRODUCTION . . . . .	1
2. HEAT PIPE OPERATION . . . . .	3
3. GENERAL HEAT PIPE THEORY . . . . .	4
4. EXPERIMENTAL WORK, PART I . . . . .	6
5. EXPERIMENTAL WORK, PART II . . . . .	8
5.1 APPARATUS . . . . .	8
5.2 TEST PROCEDURE . . . . .	11
6. DISCUSSION AND RESULTS . . . . .	13
7. CONCLUSIONS AND RECOMMENDATIONS . . . . .	21
REFERENCES . . . . .	23
LIST OF SYMBOLS . . . . .	24
FIGURES . . . . .	25
APPENDIX . . . . .	40

## LIST OF FIGURES

	Page
Figure 1	Schematic of test arrangement for measurement of capillary flow in wicks in the gravitational field . . . . . 25
Figure 2	Wick distance vs time graph Wick No. 2. Single layer at 0° . . . . . 26
Figure 3	Wick distance vs time graph Wick No. 5. Double layer at 0° . . . . . 27
Figure 4	Wick distance vs time graph Wick No. 6. Double layer at 0° . . . . . 28
Figure 5	Wick distance vs time graph Wick No. 8. Single layer . . . . . 29
Figure 6	Wick distance vs time graph Wick No. 9. Double layer . . . . . 30
Figure 7	Heat pipe system . . . . . 31
Figure 8	Volumetric flow vs wick length graph Wick No. 2. Single layer at 0° . . . . . 32
Figure 9	Volumetric flow vs wick length graph Wick No. 5. Double layer at 0° . . . . . 33
Figure 10	Volumetric flow vs wick length graph Wick No. 6. Double layer at 0° . . . . . 34
Figure 11	Volumetric flow vs wick length graph Wick No. 8. Single layer with water . . . . . 35
Figure 12	Volumetric flow vs wick length graph Wick No. 8. Single layer with ethyl alcohol . . . 36
Figure 13	Volumetric flow vs wick length graph Wick No. 9. Double layer with water . . . . . 37
Figure 14	Volumetric flow vs wick length graph Wick No. 9. Double layer with ethyl alcohol . . . 38
Figure 15	Heat pipe temperature vs distance curves Single wicks at 0° . . . . . 39

## 1. INTRODUCTION

Future space exploration will entail more and more extravehicular activity. Consequently, it becomes necessary that the astronaut's space suit provide him with a suitable living environment. One necessity is provision of a satisfactory thermal environment.

Present systems utilize liquid-cooled undergarments which need an intricate system of valves, pumps, and auxiliary equipment. Heat pipes could be used to create a system of less complexity and greater efficiency. The complexity of the system could be reduced because a heat pipe is a closed system which needs no resupply or adjustment after assembly. No pumps, compressors, or auxiliary equipment are needed during operation. Efficiency is increased because a heat pipe commonly transfers heat on the order of 100-1000 times faster than the best conducting metals.

A space suit thermoregulatory system must be capable of transferring heat from the astronaut's body to an area on the suit where the heat can be rejected either to space by radiation or to a porous plate sublimator. In performing such tasks, there are no restrictions on the orientation of a heat pipe. Wicking materials are used to provide fluid travel from the heat rejection areas to the heat input areas, even against the force of gravity.

At temperatures below 32°F, a fluid such as alcohol or an alcohol-water mixture could be used. A mixture might compensate for the low latent heat of the alcohol since the two fluids will tend to separate

and occupy opposite ends of the heat pipes. Thus, the distance across which the alcohol must transfer heat would be reduced.

In space suit applications, the heat pipe configuration and heat transfer rates indicate that the ability of the wick to transfer the fluid will be more of a limiting factor than the pressure drop due to vapor flow. Consequently, this study was restricted to the performance of the wick.

During the last few years, there has been considerable activity in the study of heat pipes as indicated by the numerous technical sessions on the subject at the meetings of several professional societies, such as ASME [1]†, AIAA [2], and other combined meetings [3]. A detailed literature survey will not be presented here, however; only references which have direct bearing on this study will be given.

---

†Numbers in brackets refer to entries in REFERENCES.

## 2. HEAT PIPE OPERATION

A heat pipe consists of three distinct sections. First, a heat input section or evaporator section evaporates the operating fluid. Second, the small pressure gradient along the heat pipe forces the vapor through the mass (vapor state) transfer section to the third section, the heat rejection or condenser section. Here, the vapor condenses before returning to the heat input section via the mass (liquid state) transfer section. Capillary action or gravitational force is the means of returning the fluid.

Mass return to the heat input section by capillary action requires the use of a wicking material. Commonly used wicking materials are fine wire screens, porous solid materials, and natural or synthetic cloths.

### 3. GENERAL HEAT PIPE THEORY

For the purpose of this work, a relatively simple theory, such as given in [4,5], is quite adequate. This theory will only be briefly summarized here.

The temperature gradient along a wick limited heat pipe is very small due to the small pressure gradient. Consequently, conduction, radiation, and sensible convection heat transfer will all be negligible compared to heat transferred as latent heat of vaporization. Assuming all heat transferred is due to latent heat, the heat transfer rate ( $Q$ ) is the product of mass flow rate ( $\dot{m}$ ) of fluid in the wick and latent heat of vaporization ( $h_{fg}$ ) of the fluid at the operating temperature of the system. The maximum heat transfer capability of the heat pipe is then  $Q_{\max} = \dot{m}_{\max} h_{fg}$  where  $\dot{m}_{\max}$  may be interpreted as the flow rate occurring when the wicking material is dry at the evaporator end.

The following four basic parameters may be used to find an expression for the maximum mass flow rate. They are

- (i) the capillary pumping head of the wick ( $\Delta P_c$ ),
- (ii) the vapor pressure drop ( $\Delta P_v$ ),
- (iii) the liquid viscous drag ( $\Delta P_L$ ), and
- (iv) the gravity head ( $\Delta P_g$ ).

The acceleration effects in the wick can be ignored [5]. From a balance of pressure heads, the equation for the operation of a heat pipe becomes

$$\Delta P_c \geq \Delta P_v + \Delta P_L + \Delta P_g \quad (1)$$

Substituting appropriate terms for the pressure heads, Eq. (1) becomes

$$\frac{2\sigma}{r} \geq \frac{\mu L \dot{m}}{\rho KA} + \rho g L \cos \phi \quad (2)$$

where  $\Delta P_v$  has been assumed to be negligible.  $2\sigma/r$  is a maximum value for  $\Delta P_c$  which occurs where the wick becomes dry. Rearrangement of Eq. (2) gives

$$\dot{m} \leq \frac{\rho KA}{\mu L} \left( \frac{2\sigma}{r} - \rho g L \cos \phi \right) \quad (3)$$

Therefore,

$$\dot{m}_{\max} = \frac{\rho KA}{\mu L} \left( \frac{2\sigma}{r} - \rho g L \cos \phi \right) \quad (4)$$

and

$$Q_{\max} = \frac{\rho KA}{\mu L} \left( \frac{2\sigma}{r} - \rho g L \cos \phi \right) h_{fg} \quad (5)$$

## 4. EXPERIMENTAL WORK, PART I

## APPARATUS AND TEST PROCEDURE

The apparatus used for testing the wicking material Refrasil No. C100-28 is shown in Fig. 1. The objectives of the tests were to obtain fluid front displacement and volume transport data as functions of time.

Fluid was supplied to one end of the test wick by a 100 milliliter supply burette. Excess fluid dripping from the saturated end of the wick was collected in a 100 milliliter receiver burette. Therefore, the total volume transferred along the wick was the difference between readings of the supply and receiver burettes.

The test wick was supported on a 1 centimeter-square mesh screen. Fluid losses by evaporation were minimized by

- (i) placing the wick and screen in a 31 mm inside diameter plexiglas tube,
- (ii) using a hood to partially cover the area where the fluid was introduced, and
- (iii) saturating the atmosphere around the wick by leaving some of the test fluid in the tube before each test.

A copper wire was attached to the support screen at 2-in. intervals along the wick with an additional wire placed at the first location. After removing insulation from the ends of these wires, the ends were inserted into the wick pores. All wires were connected to a 25-point thermocouple switch whose main terminals were connected

to an ohmmeter. When the wick was dry, the ohmmeter indicated an infinite resistance between any wire and the additional wire at the first location. Immediately after the wick pores occupied by a wire were wetted, the resistance between that wire and the additional wire changed (over a period of about 1 second) from infinity to about 1 megohm. After one cross section was wetted, the thermocouple switch was advanced to the next wire to detect wetting there. As the wetting front reached each wire, as indicated by the first change in resistance, the total distance of wetting front down the wick and the total elapsed time of the test, measured by a stop watch, were recorded. At the 9-in. location, supply and receiver burette volumes were recorded as well. The curves in Figs. 2-6 were constructed using the displacement-time data. The results will be discussed after the description of Part II of the experimental work.

## 5. EXPERIMENTAL WORK, PART II

### 5.1 APPARATUS

Figure 7 shows the test set-up which is the same basic set-up used and described in detail previously [4,5].

Dewar: The three main elements of the heat pipe (heat input, mass transfer, and heat rejection sections) were housed in a 7.62 cm I.D., 8.90 cm O.D., 101.5 cm long double open-ended, silvered glass dewar. The dewar was made of two concentric glass cylinders with the surfaces in the annulus silvered. It provided insulation in the radial direction between the interior and the surroundings. Unsilvered window strips located axially along the top and bottom of the dewar allowed inspection of the interior after assembly. A combination of O-rings and gaskets was used to seal the dewar in the axial direction. Also, a radial tube between the inside of the dewar and the exterior was provided near the condenser end to allow changing of the wicking chamber with the desired fluid, and to provide connection of a vacuum system to the interior and passage of thermocouple wires entering the dewar.

Heat Input Section (Evaporator): Two electrical heating elements were used as the heat input source. The heater closer to the mass transfer section (main heater) was used for the total heat input, while the other (guard heater) was used to minimize axial heat flow away from the chamber. An accurate measurement of heat input to the mass transfer section could then be obtained by recording input wattage

to the main heater. Electrical energy was supplied to each heater from a variable transformer. Wattmeters were used to measure the power inputs. An O-ring sealed aluminum disc wall between the main heater and the mass transfer section provided a uniform source of heat to the chamber.

Heat Transfer Section (Wicking Chamber): Wicking material Refrasil No. Cl00-28 was used because past experience proved it to be superior in water lift rate and horizontal transfer rate.

Four horizontal strips of wicking material were used to eliminate gravitational effects over a given cross section of the heat pipe. The two center strips were 2-1/16 in. wide, while the top and bottom strips were 1-7/16 in. wide. A wicking cage was utilized to suspend the Refrasil, as well as to prevent axial movement of the heat input and heat rejection sections. Also, circular pieces of Refrasil were attached to the aluminum discs at each end forming the heat input and heat rejection sections to evenly distribute fluid and to supply fluid to the horizontal wicking strips.

Heat Rejection Section (Condenser): An O-ring sealed aluminum disc was used in the heat rejection section, as in the heat input section, to provide uniform heat transfer. After being conducted through the aluminum disc, the heat was removed by circulating cool water through the condenser section.

Temperature Measurement: Temperatures throughout the system were measured by monitoring twenty-two copper-constantan thermocouples. One thermocouple was placed across a mica disc between the main and guard

heaters. With the desired heat input set on the main heater, the guard heater was continually adjusted to keep the temperature gradient at zero. Thus, it was ensured that the desired heat input would flow into the mass transfer section. Another thermocouple was placed across the inlet and outlet cooling water lines as a check on the heat transferred along the heat pipe. The twenty remaining thermocouples were used to record temperatures at various locations on the heater and condenser aluminum discs and in the wicking chamber.

Wicking Chamber Manifold: A wicking chamber manifold was located near the condenser end to make the necessary connections to the wicking chamber. This manifold contained a large vacuum valve for evacuating the dewar through a glass access tube in the side, as well as a small needle vacuum valve to purge non-condensable gases from the chamber. Another small needle valve allowed the chamber to be charged with the working fluid. Passage of thermocouple wires into the chamber was made possible by a transfer plug. Connection of a pressure-vacuum gage to the chamber was accomplished by a union on the manifold. This union was later used in connecting a mercury manometer to the chamber. Finally, another union was made available for direct connection to the chamber itself.

Temperature Recording: A 21-point Leeds and Northrup millivolt recorder was used to record the twenty temperature measuring points. The temperature gradients between the two heaters and over the cooling water lines were monitored on a potentiometer.

## 5.2 TEST PROCEDURE

The wicking chamber was first evacuated to  $15 \times 10^{-2}$  mm of mercury. Then, for testing of single layers of Refrasil, 45 ml of working fluid was injected into the chamber. However, for testing double layers of material, difficulty was experienced in initially filling the gaps with fluid. This made it necessary to fill the entire chamber with liquid. Then, the greater part of the fluid was removed using a makeshift sump pump consisting of a gallon jug and the vacuum pump.

As heat was added through the heaters, non-condensable gases immediately began to build up in front of the condenser aluminum disc. This caused a temperature gradient to build over the length of the heat pipe. When the gradient reached  $5-10^{\circ}\text{C}$ , the needle vacuum valve was opened slightly to purge these gases from the system. At heat inputs below the burn-out wattage, the temperature gradient along the heat pipe reduced to about  $1^{\circ}\text{C}$  or a little larger for large heat inputs.

After purging several times (over a period averaging thirty minutes to an hour), the heat input was increased if burn-out had not occurred. Naturally, test runs were shorter for testing of double layers of Refrasil since the fluid flowed more rapidly. At or above the burn-out wattage, purging did not reduce the temperature of the heater aluminum disc to previous levels. Instead, the temperatures indicated by the thermocouples on the disc continued to increase.

When this happened, the heaters were shut off so the wicking material could resaturate with fluid.

Condensable gases purged from the system were condensed by a cold trap immersed in dry ice and methanol before they could reach the vacuum pump. The cold trap was changed every 2-3 hours as very little fluid accumulated there. The temperature gradient between heaters was monitored constantly during testing and the guard heater was adjusted accordingly to keep it at zero. Also, before increasing heat input, the temperature difference between the cooling water inlet and outlet lines was recorded, as was the cooling water flow rate. Unsuccessful attempts were made during purging of non-condensable gases to measure the volume and alcoholic content of fluid accumulated in the cold trap. The volume accumulated during a normal run was much too small for accurate measurement and analysis.

## 6. DISCUSSION AND RESULTS

In Part I, the fluid transport rate along the wick was found using the equation,

$$\dot{v} = A \frac{dx}{dt} \quad (6)$$

where  $\dot{v}$  is the volumetric flow rate, A is the cross-sectional area of flow and dx/dt is the velocity of the wetting front.

The velocity of the wetting front was found by differentiating the displacement-time equations plotted in Figs. 2-6. The equations of the curves were found using first-order, least squares approximation to the log-log plots.

Since the cross-sectional area of flow was not known, it was necessary to make an approximation using volumetric flow data. The total volume input over the test length divided by the total elapsed time gave the volumetric flow rate for a wick length about one-half that of the test length (see development in sample calculations). Since tests with water at zero degrees inclination produced the most consistent volumetric flow data, those data were used in finding the cross-sectional area of flow. This area was used as an approximate area for other tests. All testing in Part I was done on 9-in. X 1-in. test strips.

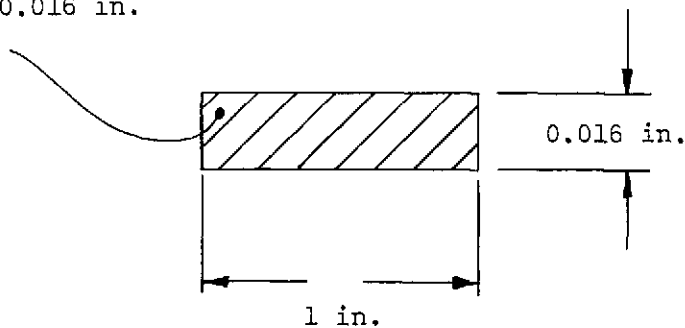
The results (see Tables I and II and Figs. 8-14) indicate water has the highest flow rate, while pure ethyl alcohol and 50 percent ethyl

TABLE I  
 SINGLE LAYER OF REFRASIL NO. C100-28  
 VOLUMETRIC FLOW RATE AT 21-3/4 IN. (ML/MIN)  
 PER INCH WIDTH

	H <sub>2</sub> O	E. Alc.	50% E. Alc.	
0°	0.073	0.017	0.006	} Wick #2 Figs. 2 and 8
0°	0.030†	0.011		
5°	0.032	0.004		} Wick #8 Figs. 5, 11, and 12
10°	0.027	0.001†		
15°	0.023	0.000††		
90°	0.009	0.002††		

Refrasil

$$A_{\text{solid}} = 0.016 \text{ in.}^2$$



$$\text{Area of flow} = 0.011 \text{ in.}^2$$

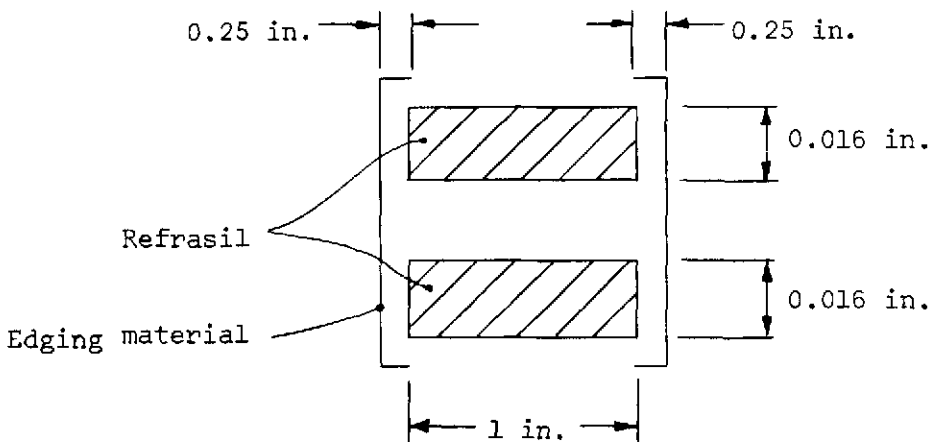
$$= 68 \text{ percent of } A_{\text{solid}}$$

†Figure 5 indicates a bad point; therefore, 0.074 ml/min may be more accurate.

††These numbers are only approximate due to the extremely small flow rates and relatively high evaporation rates of the fluid.

TABLE II  
 DOUBLE LAYER OF REFRASIL NO. C100-28  
 VOLUMETRIC FLOW RATE AT 21-3/4 IN. (ML/MIN)  
 PER INCH WIDTH

	H <sub>2</sub> O	E. Alc.	50% E. Alc.	
0°	0.865	0.346	0.617†	} Wick #5 Figs. 3 and 9
0°	0.809	0.213	0.191	
0°	0.735	0.400		} Wick #6 Figs. 4 and 10
5°	0.471	0.182		
10°	0.248	0.691		
15°	0.122	0.034		
90°	0.016	0.006		
				} Wick #9 Figs. 6, 13, and 14



Area of flow = 0.040 in.<sup>2</sup>  
 = 125 percent of 2A<sub>solid</sub>

†Appears to be inaccurate, comparing Figs. 9 and 10.

alcohol by weight were much lower. The pure alcohol appeared to be only slightly better than the 50 percent mixture. These results are in good qualitative agreement with the analytical studies of [6]. Comparison of Figs. 9 and 10 indicates the 50 percent alcohol run at zero degrees in Fig. 9 is inaccurate. This run is also shown in Fig. 3.

With a single layer of wicking material, the calculated water flow rate for a 21-3/4-in. X 1-in. wick was from 0.073 ml/min at zero degrees to 0.009 ml/min at ninety degrees. The flow rate for pure alcohol was from 0.011 ml/min at zero degrees to 0.002 ml/min at ninety degrees.† The 50 percent mixture flowed at 0.006 ml/min at zero degrees.

Two layers of wicking material sewn together increased the flow rate of water by a factor of about ten at zero degrees. This factor diminished to about two at ninety degrees, indicating that water did not flow in the vertically oriented gap. The improvement factor for alcohol was extremely erratic, although much larger than for water. The inconsistency suggests either inaccuracies in the extrapolation of distance-time curves or inconsistent filling of the gap. At zero degrees, the factor was about 25 and, at ninety degrees, the factor was 3. The 50 percent mixture increased by a factor of about 30 at zero degrees. The increase in flow rates due to a gap next to the wick has been suggested by previous workers [7,8].

---

†See second footnote in Table I.

Results of Part I were used to predict the heat transfer capacity of a 21-3/4-in. heat pipe operating with similar wicking, fluid, and inclination. Test results for a single wick gave predicted wattages of 21.0 at zero degrees and 2.6 at ninety degrees for water and 0.90 at zero degrees and 0.17 at ninety degrees for pure ethyl alcohol. A predicted range of 0.5-1.7 watts for the 50 percent mixture at zero degrees was found using latent heats of alcohol and water, respectively.

Results tabulated in Table III show that the burn-out wattages obtained with water in Part II were lower than those predicted from tests outside the heat pipe. Apparently, there is difficulty in saturating the wicking material in the heat pipe and in keeping the gaps between the wick completely filled. A bottleneck in the mass return process occurs at the condenser end where the fluid must travel vertically in the circular Refrasil patches. The differences are especially large for double layers of wicking material since rapidly moving fluid must be supplied to the gaps. The situation was alleviated somewhat by placing several circular Refrasil patches on the condenser aluminum plate. Ends of the horizontal strips were directed vertically downward between these patches to create a better gap effect. Also, thin spacers were placed between the aluminum disc and the wicking cage. Finally, the wicking cavity was temporarily filled with fluid prior to testing. After removing most of the fluid, the gaps could then resupply themselves by capillary action.

The equation for maximum heat transport in a heat pipe was given by Eq. (5).

TABLE III  
 PREDICTED (PART I) AND ACTUAL (PART II) BURN-OUT WATTAGES  
 FOR A WICK LENGTH OF 21-3/4 IN. AND  
 FOR A TOTAL WIDTH OF 7 INCHES

Fluid	Inclination to Horizontal†	Predicted Wattage (Part I)		Actual Wattage (Part II)	
		Single Wick	Double Wick	Single Wick	Double Wick
Water	0°	21.0	211, 232, 248	15 <sup>+1</sup> -2	≥ 80††
Water	1°			12 <sup>+1</sup> -2	
Water	2°			11 ±1	
Water	3°			9 ±1	
Water	4°			8 ±1	
Water	5°	9.1	135	7 ±1	45 ±5
Water	8°			5 ±1	
Water	10°	7.7	71	5 ±1	45 ±5
Water	15°	6.5	35	5 ±1	25 ±5
Water	90°	2.6	4.5		
Ethyl Alc.	0°	0.90, 1.4	17.9, 28.8, 33.5	4 ±1	
Ethyl Alc.	5°	0.33	15.2		
Ethyl Alc.	10°	0.08	5.8		
Ethyl Alc.	15°	0.00†††	2.8		
Ethyl Alc.	90°	0.17	0.5		
50% E. Alc.	0°	0.5-1.7	16-54.7	2 ±1	
25% E. Alc.	0°			1 ±1	
75% E. Alc.	0°			2 ±1	

†Flow against gravity if not 0°.

††This was the maximum power input of the heater.

†††See second footnote in Table I.

CJ

For the horizontal position, the maximum heat transfer capacity  $Q_{max}$  becomes inversely proportional to the wick length  $L$ . Tests by the author and by others [4,5] support this relationship with burn-out wattages of 15 (the author) and 10 for wick lengths of 21-3/4 in. and 32-1/4 in., respectively, for the same total width of 7 in.

Tests with water at various angles of inclination produced burn-outs from 15 watts at zero degrees to 5 watts at eight, ten, and fifteen degrees. The reduction in capacity change rate with an increasing operating angle agrees with the behavior of the cosine function [see Eq. (5)].

At zero degrees inclination, the burn-out wattage for pure ethyl alcohol was 4 watts. This represents a decrease by a factor of 3.75 from water. Equation (5), however, predicts a factor of about 13.5. However, the burn-out wattage of 4 is higher than predicted by tests outside the heat pipe. This is probably due to inaccuracy of heat input measurement for such low inputs. Second, the burn-out wattage of 15 for water is low because the wicking material in the heat pipe could not be thoroughly saturated with fluid. Part I tests indicated factors of 15.0-23.1 for a single wick and 6.30-13.9 for a double wick. Both ranges have the right order of magnitude when compared to the predicted value of 13.5.†

---

†It is notable that wick performance at times varied considerably for different test sections of Refrasil (see Tables I and II). This is probably due to variation in pore size.

Fifty percent alcohol had a burn-out wattage of only 2 watts at zero degrees. This was expected. A burn-out of 1 watt with 25 percent alcohol agrees with Woo [6], but disagrees with Feldman and Whitlow [9]. However, in a wick limited heat pipe, the effect of vapor flow is negligible, whereas in Ref. [9], the improvement may have been due to compression of the vapor. Seventy-five percent alcohol resulted in 2 watts burn-out.

Figure 15 shows temperature variation along the heat pipe for 25, 50, and 75 percent alcohol by weight mixtures. Due to the very low wattages, the 25 and 50 percent curves do not represent steady state conditions, so these curves may not be very useful for comparison of temperature differences. The curves, however, do seem to indicate correctly the location of a transition from alcohol at the condenser end to water at the heater end in agreement with Feldman and Whitlow [9].

Usable data for cooling water temperature change in Part II tests were not obtained. Such data could have been used with the cooling water flow rate as a check on heat input measurement. Heat conduction through the water piping and other heat losses prevented accurate thermocouple recordings. Also, purging of non-condensable gases from the system caused a refrigeration effect at the condenser end due to the small amounts of working fluid extracted. The magnitude of this effect was estimated to be about 1.5 watts from the material collected in the cold trap. Cooling water was actually cooled at times, instead of heated. Occasionally, formation of ice near the manifold in the vacuum hose as well as cooling of the manifold were noted.

## 7. CONCLUSIONS AND RECOMMENDATIONS

The simple experimental set-up shown in Fig. 1 can be used to obtain quantitative design data on wick materials with relatively volatile fluids, too. Appropriate precautions, however, must be made to minimize evaporative losses.

A liquid-filled gap adjacent to and running parallel to a wick increases the liquid transfer rate severalfold. Consequently, it can be recommended that a wick should always be designed with an adjacent gap provided by either another layer of wicking or a suitable wall. The gap should be as narrow as possible since refilling a wide gap inside a sealed heat pipe could be practically impossible. For the same reason, during the initial filling of the heat pipe, steps should be taken to ensure complete filling of all such gaps with the working fluid. The results of [7] indicate that gaps of any appreciable size, i.e., if the wick is not touching the wall or the next layer forming the gap, tend to lose their liquid fill, particularly in an adverse gravity gradient.

In a wick limited heat pipe, the addition of water to alcohol does not improve the performance, but tends to affect it adversely. A temperature difference, however, can be established across the heat pipe by the use of such mixtures. The property parameter suggested by [6],  $\rho_{fg} \sigma / \mu$ , seems to give good qualitative predictions for the performance of mixtures in a wick limited heat pipe. If the heat pipe is vapor-limited, however, the effect of higher vapor densities occurring with the mixtures could improve the heat transfer rates as suggested by [9].

The following recommendations can be made for future work on the heat pipes :

- (1) Circular Refrasil patches should be placed between the aluminum disc and the wicking cage at each end of the heat pipe. Longer wicking strips should then be employed so that the ends can be run vertically between the patches. This will increase fluid flow at the ends of the wicks, particularly at the condenser end.
- (2) Larger heater wires will allow finding the maximum heat transfer capability of double wick layers.
- (3) Tests should be run with the condenser end of the heat pipe kept at a temperature below 32°F. To do so, it would be necessary to use a fluid, such as Freon, circulating in a closed system through the cooling chamber at the condenser end. A refrigeration unit would be needed to cool the circulating Freon.
- (4) Investigate chemical methods of determining alcoholic content of purged gases. This will aid in determining how the two fluids in a mixture separate in the heat pipe.

## REFERENCES

1. ASME, Aviation and Space Conference, Los Angeles, California, June 1970.
2. AIAA, Thermophysics Conference, Berkeley, California, June 1969.
3. Fourth Intersociety Energy Conv. Eng. Conf., Washington, D.C., September 1969.
4. Streckert, J. H., and Chato, J. C., "Development of a Versatile System for Detailed Studies on the Performance of Heat Pipes," Technical Report No. ME-TR-64, Department of Mechanical and Industrial Engineering, University of Illinois, Urbana, Illinois, December 1968.
5. Chato, J. C., and Streckert, J. H., "Performance of a Wick-Limited Heat Pipe," ASME Paper No. 69-HT-20, 1969.
6. Woo, W., "Study of Passive Temperature and Humidity Control Systems for Advanced Space Suits," TRW System Group, Ames Research Center, Report No. 06462-6007-RO-00, November 1968, pp. 6-17.
7. Shaffer, J., "The Effects of the Proximity of a Wall on the Performance of a Wick," unpublished report, Department of Mechanical and Industrial Engineering, University of Illinois at Urbana-Champaign, 1969.
8. Kemme, J. E., Verbal Report, ASME, Aviation and Space Conference, Beverly Hills, California, June 1968.
9. Feldman, K. T., Jr., and Whitlow, G. L., "Experiments with a Two-Fluid Heat Pipe," Proc. 4th Intersociety Energy Conv. Eng. Conf., Washington, D.C., 1969, pp. 1025-1032.

## LIST OF SYMBOLS

A	cross-sectional area of wick ( $\ell^2$ )†
g	acceleration of gravity ( $\ell/t^2$ )
$h_{fg}$	latent heat of vaporization of liquid (q/M)
K	wick permeability ( $\ell^2$ )
L	actual length of wicking material ( $\ell$ )
$\dot{m}$	mass flow rate (M/t)
$\Delta P_c$	capillary pumping head ( $F/\ell^2$ )
$\Delta P_g$	gravitational head ( $F/\ell^2$ )
$\Delta P_L$	liquid viscous drag ( $F/\ell^2$ )
$\Delta P_v$	vapor pressure drop ( $F/\ell^2$ )
Q	heat transfer rate (q/t)
r	mean pore radius of wicking material ( $\ell$ )
V	velocity ( $\ell/t$ )
$\dot{v}$	volume flow rate ( $\ell^3/t$ )
$\mu$	absolute viscosity of liquid ( $F-t/\ell^2$ ) or (M/t- $\ell$ )
$\rho$	liquid density (M/ $\ell^3$ )
$\sigma$	liquid surface tension (F/ $\ell$ )
$\phi$	angle between heat pipe axis and gravitational field

---

†Dimensions in parentheses are: F--force, M--mass,  $\ell$ --length, q--heat (F- $\ell$ ), t--time.

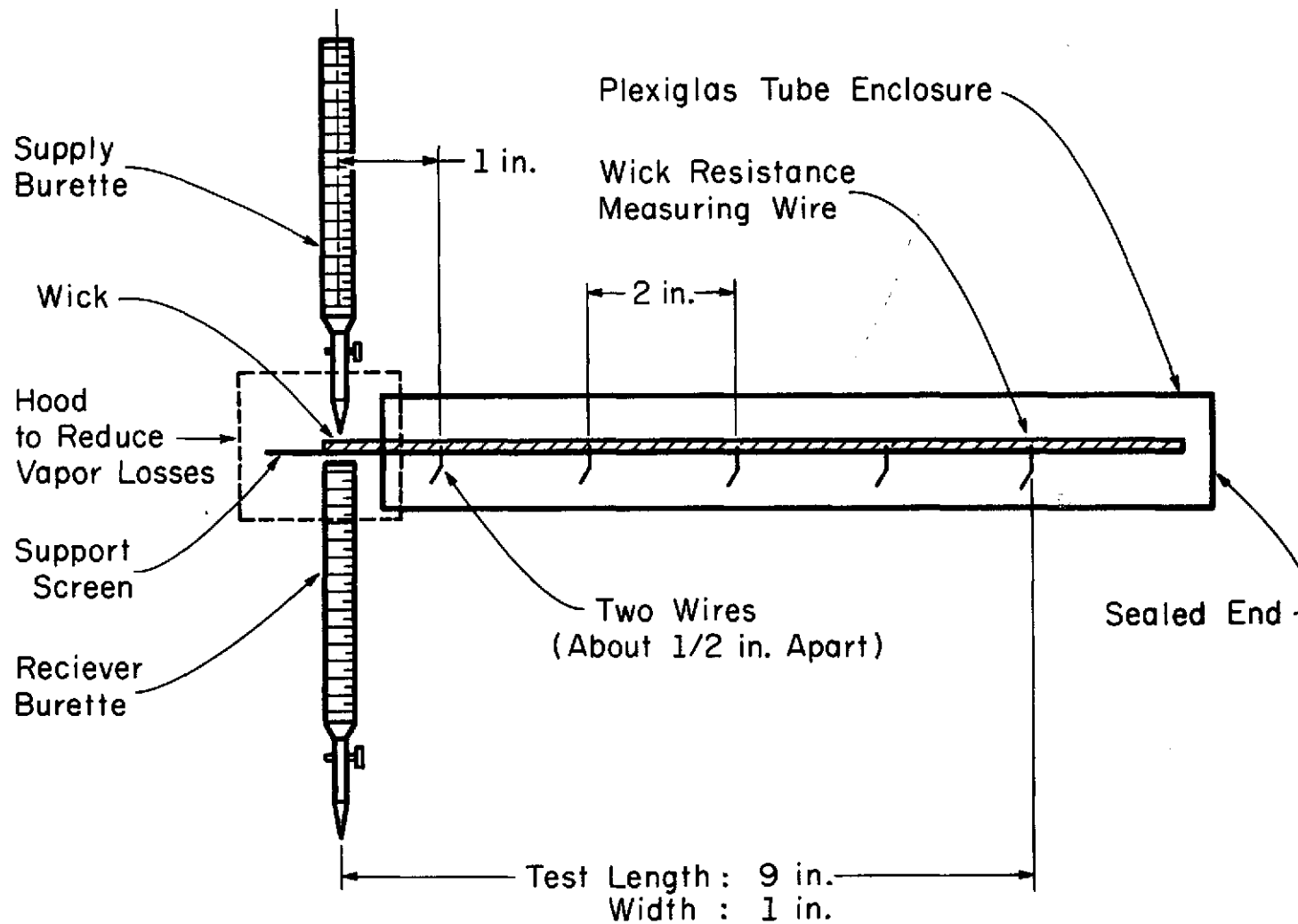


Figure 1. Schematic of test arrangement for measurement of capillary flow in wicks in the gravitational field

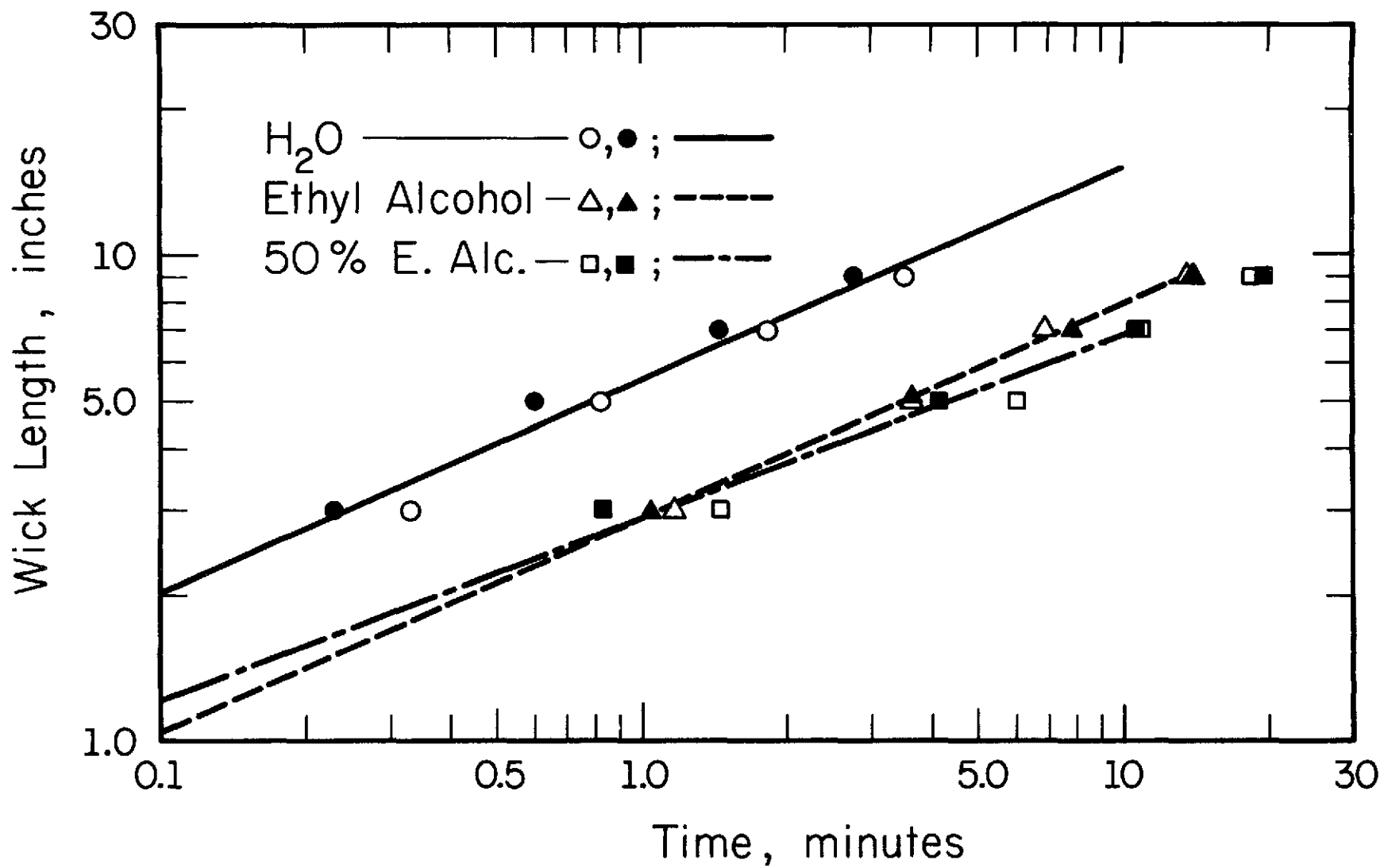


Figure 2. Wick distance vs time graph  
 Wick No. 2. Single layer at  $0^\circ$

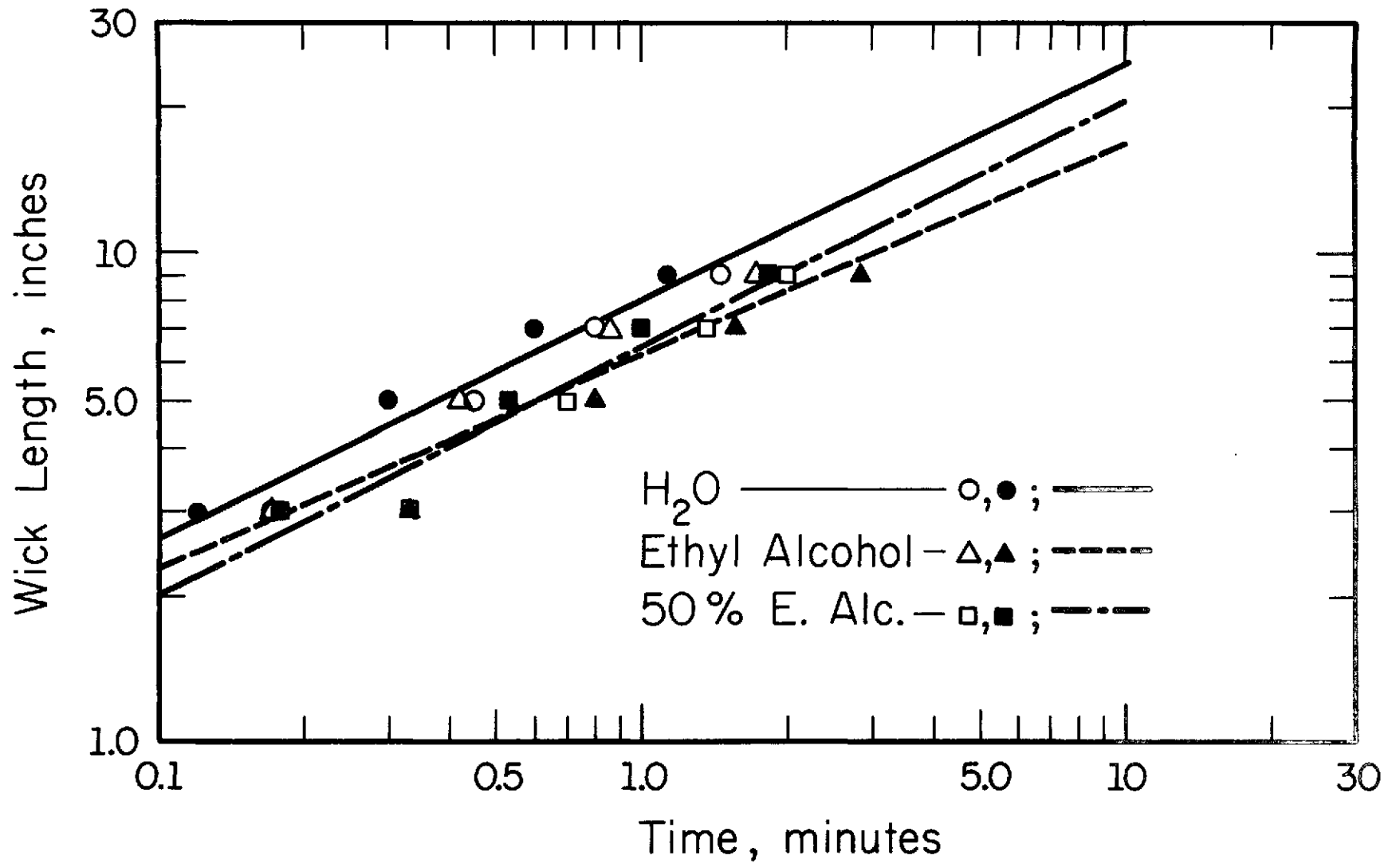


Figure 3. Wick distance vs time graph  
Wick No. 5. Double layer at 0°

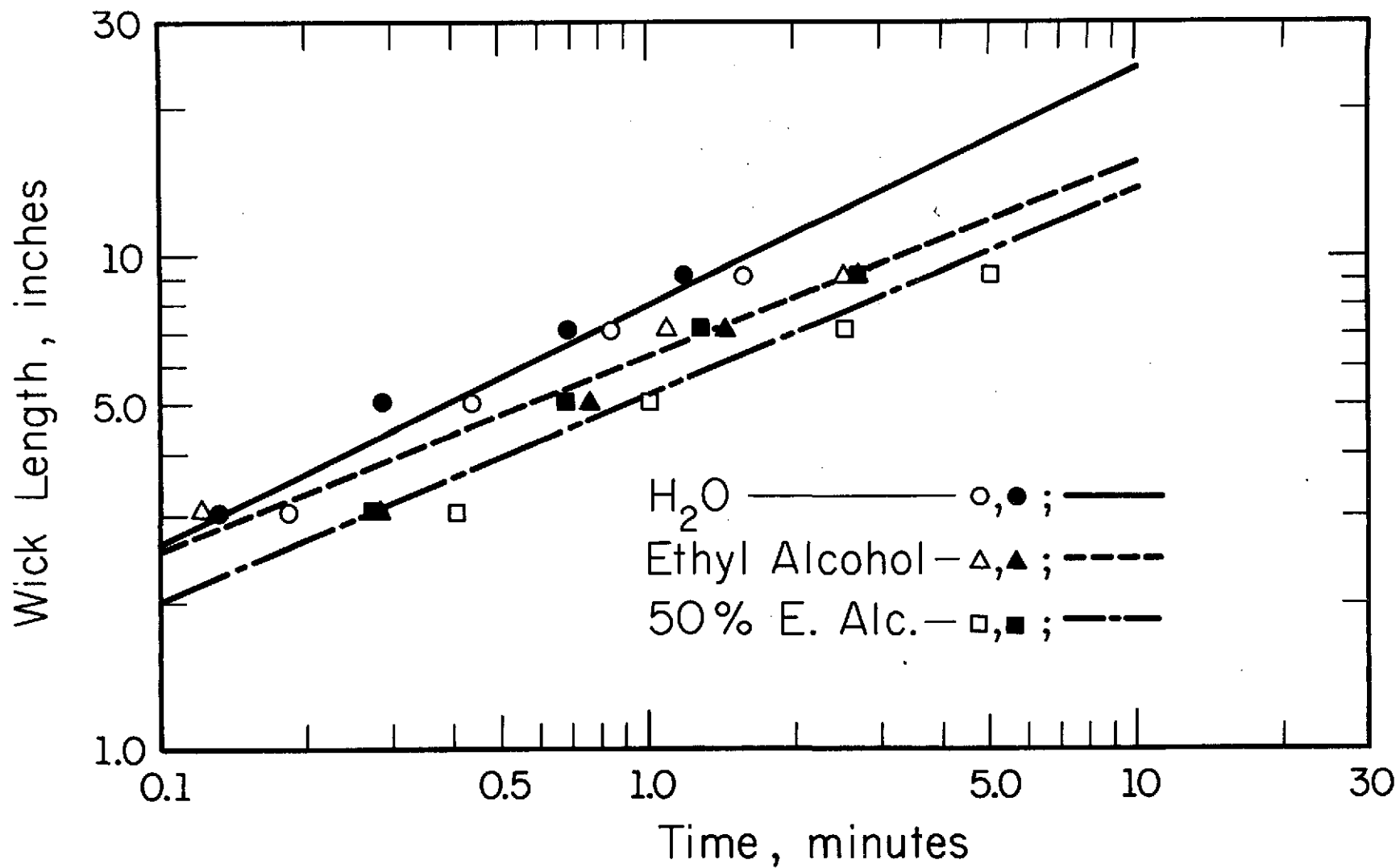


Figure 4. Wick distance vs time graph  
 Wick No. 6. Double layer at  $0^\circ$

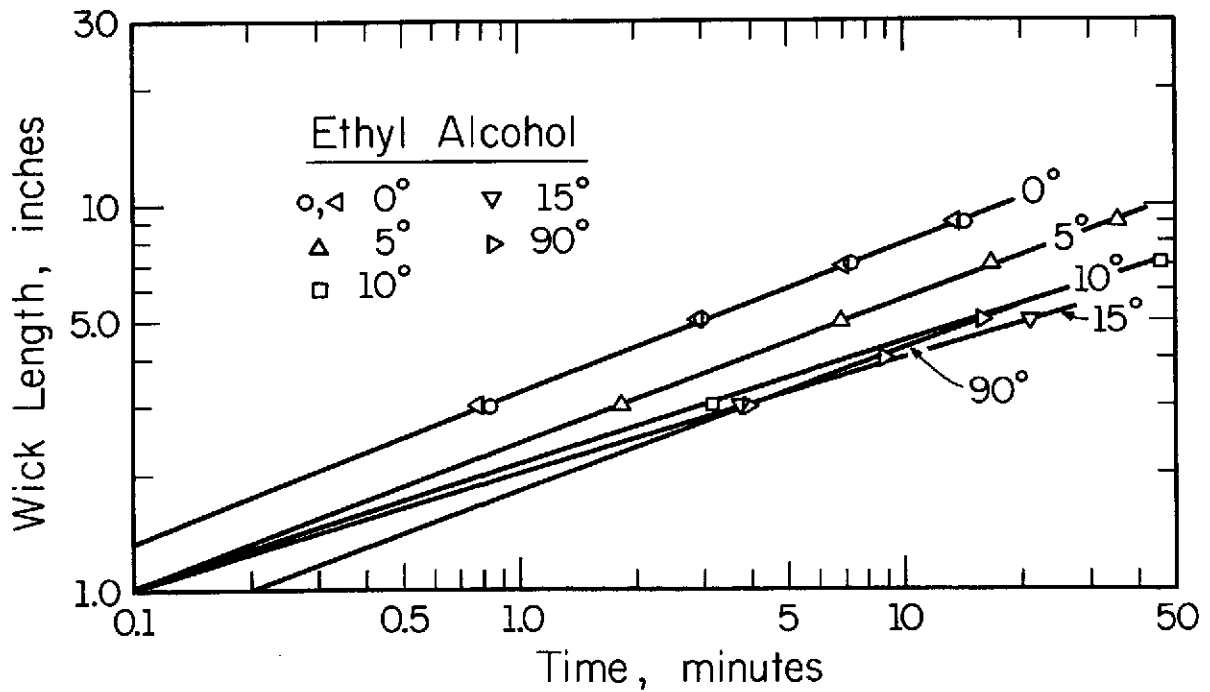
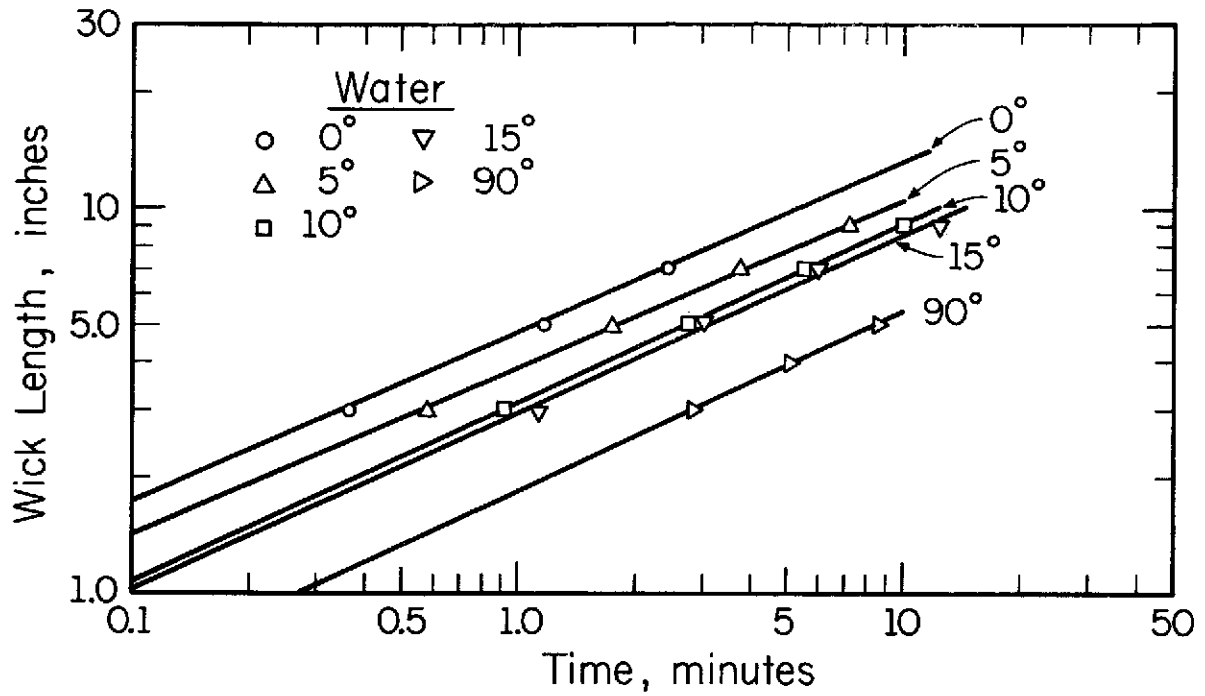


Figure 5. Wick distance vs time graph  
Wick No. 8. Single layer

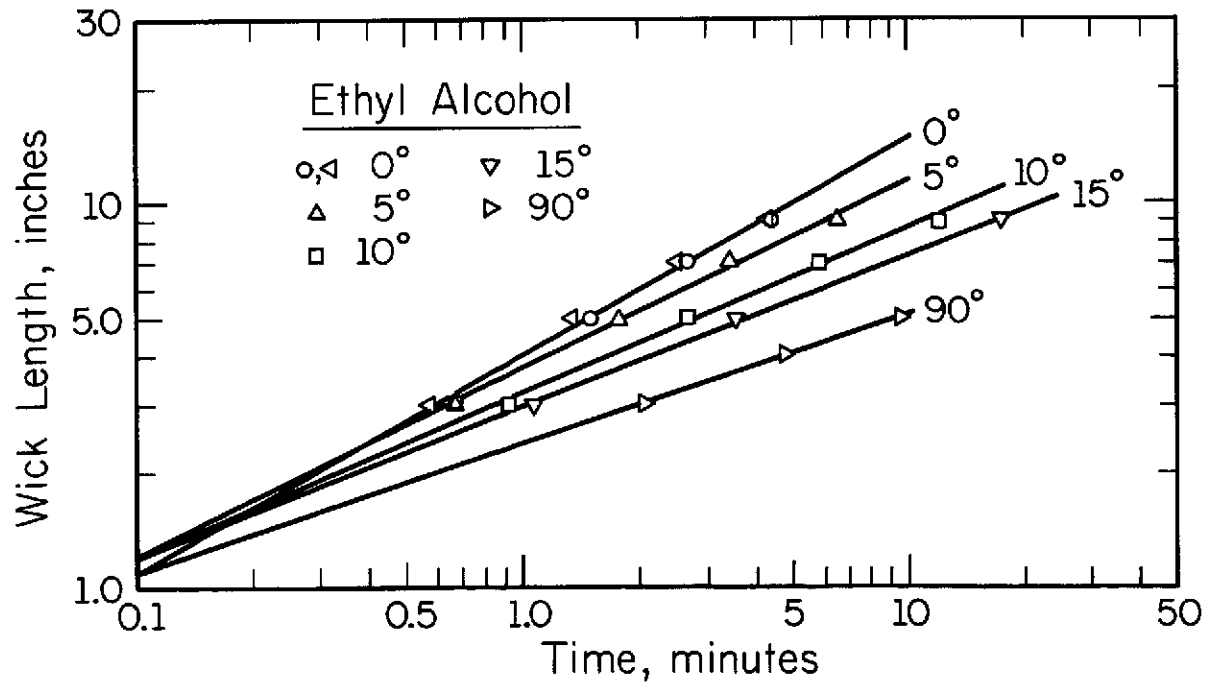
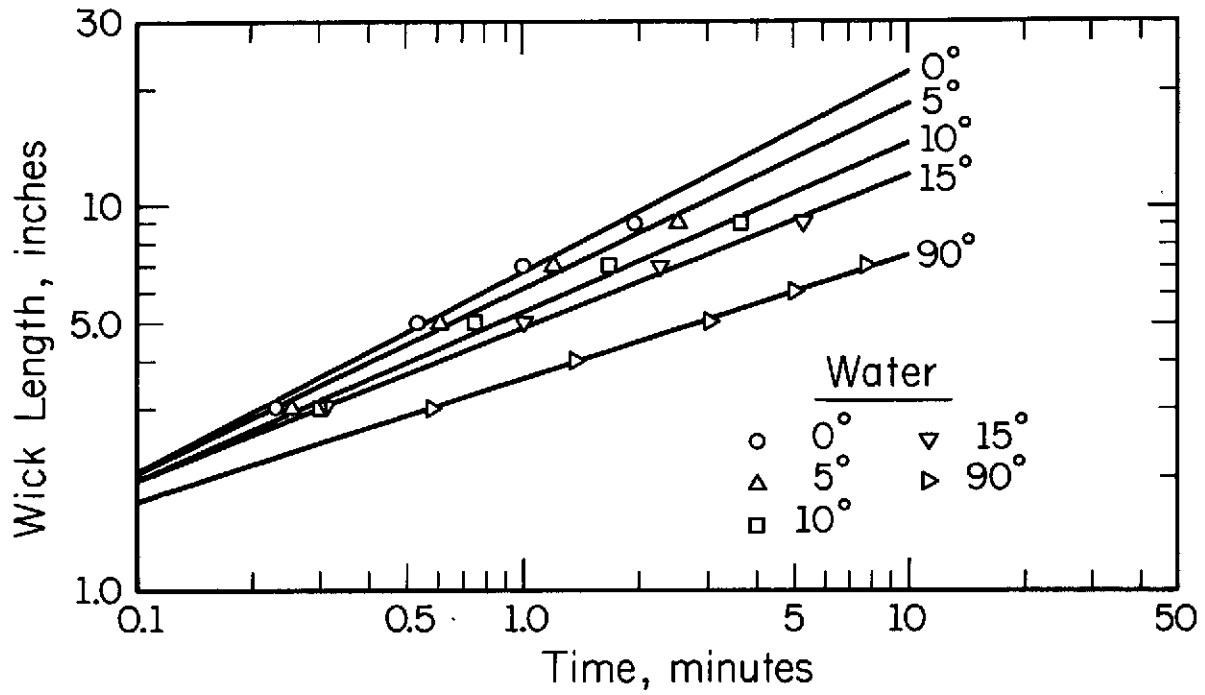


Figure 6. Wick distance vs time graph  
Wick No. 9. Double layer

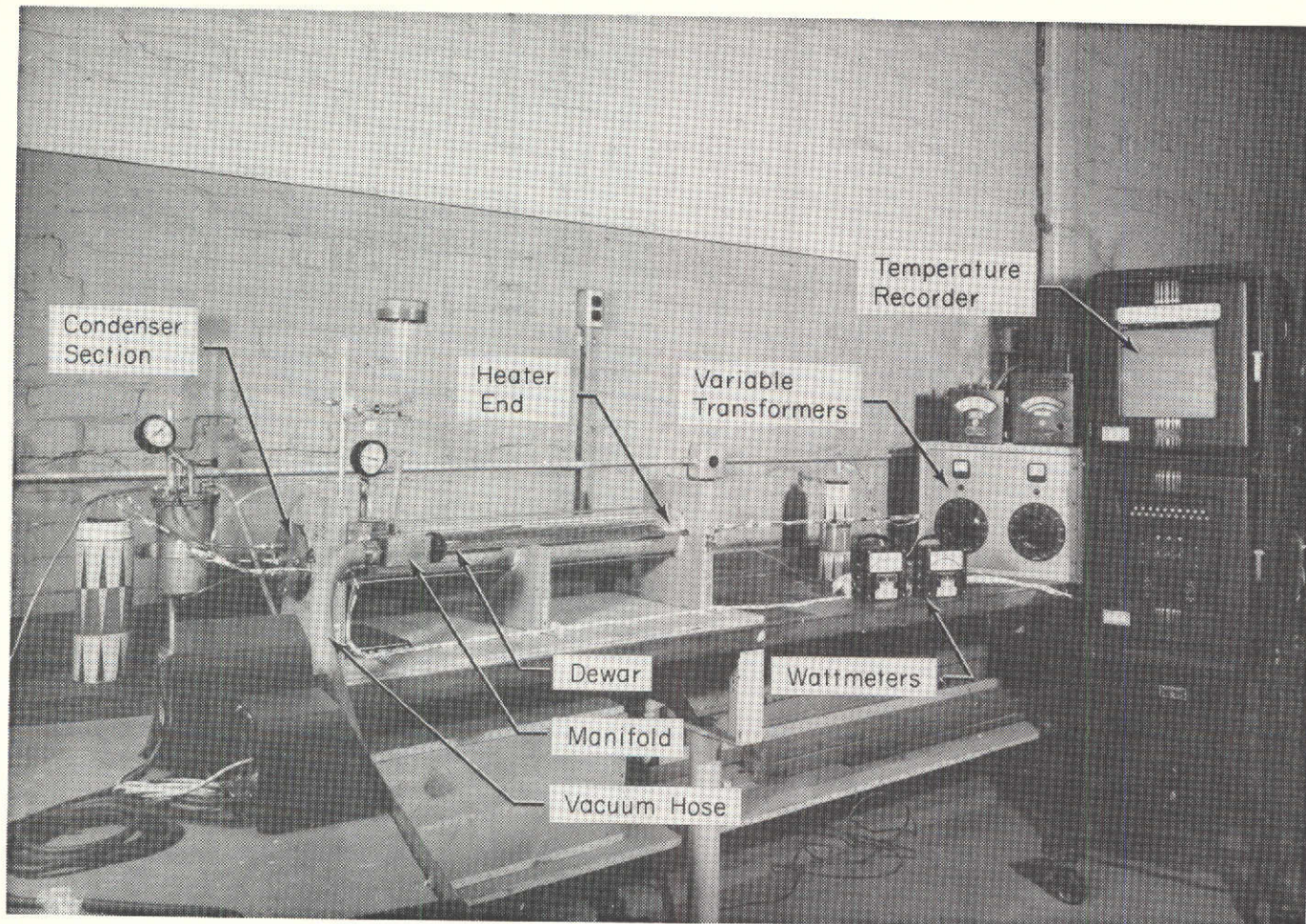


Figure 7. Heat pipe system

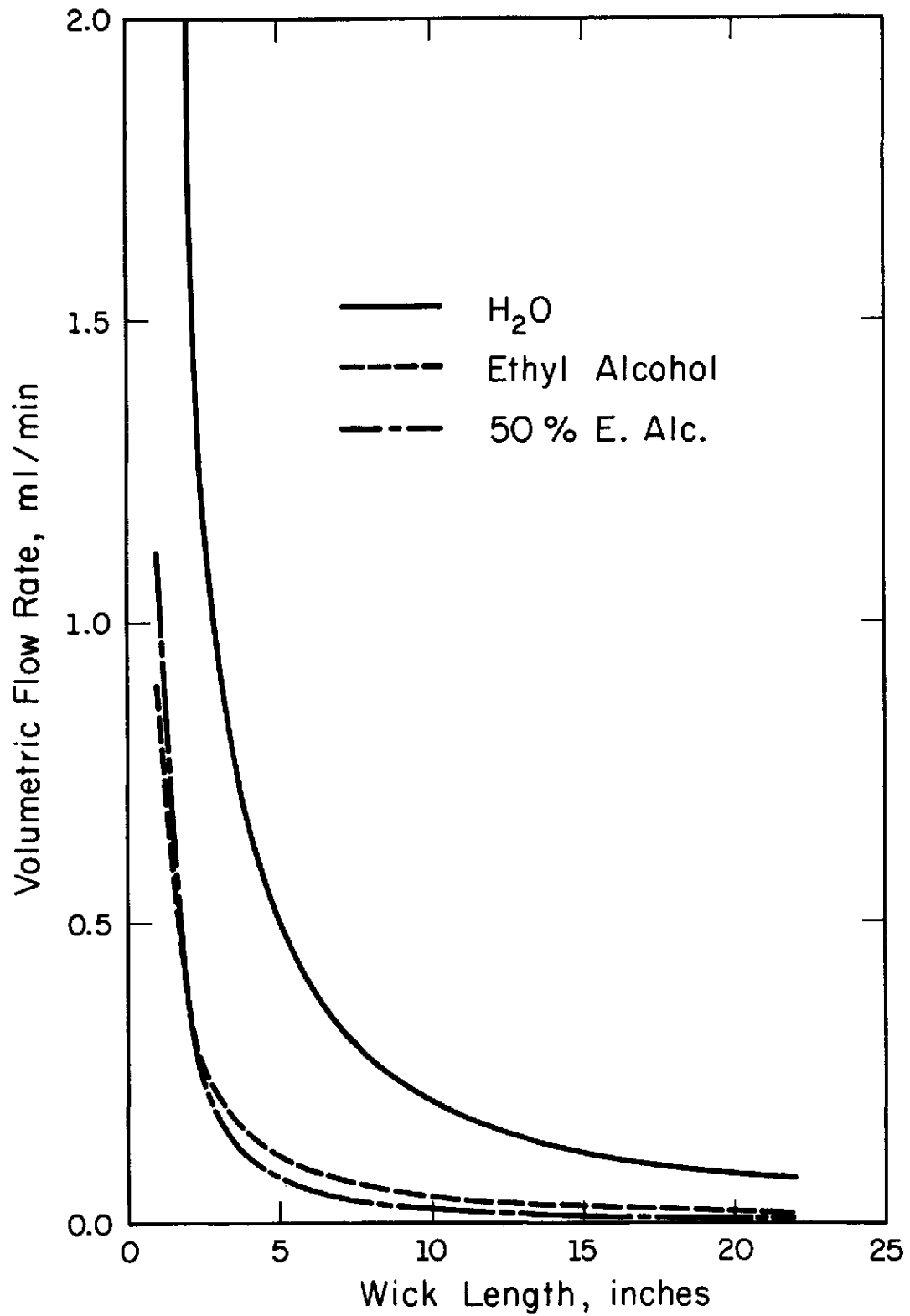


Figure 8. Volumetric flow vs wick length graph  
Wick No. 2. Single layer at 0°

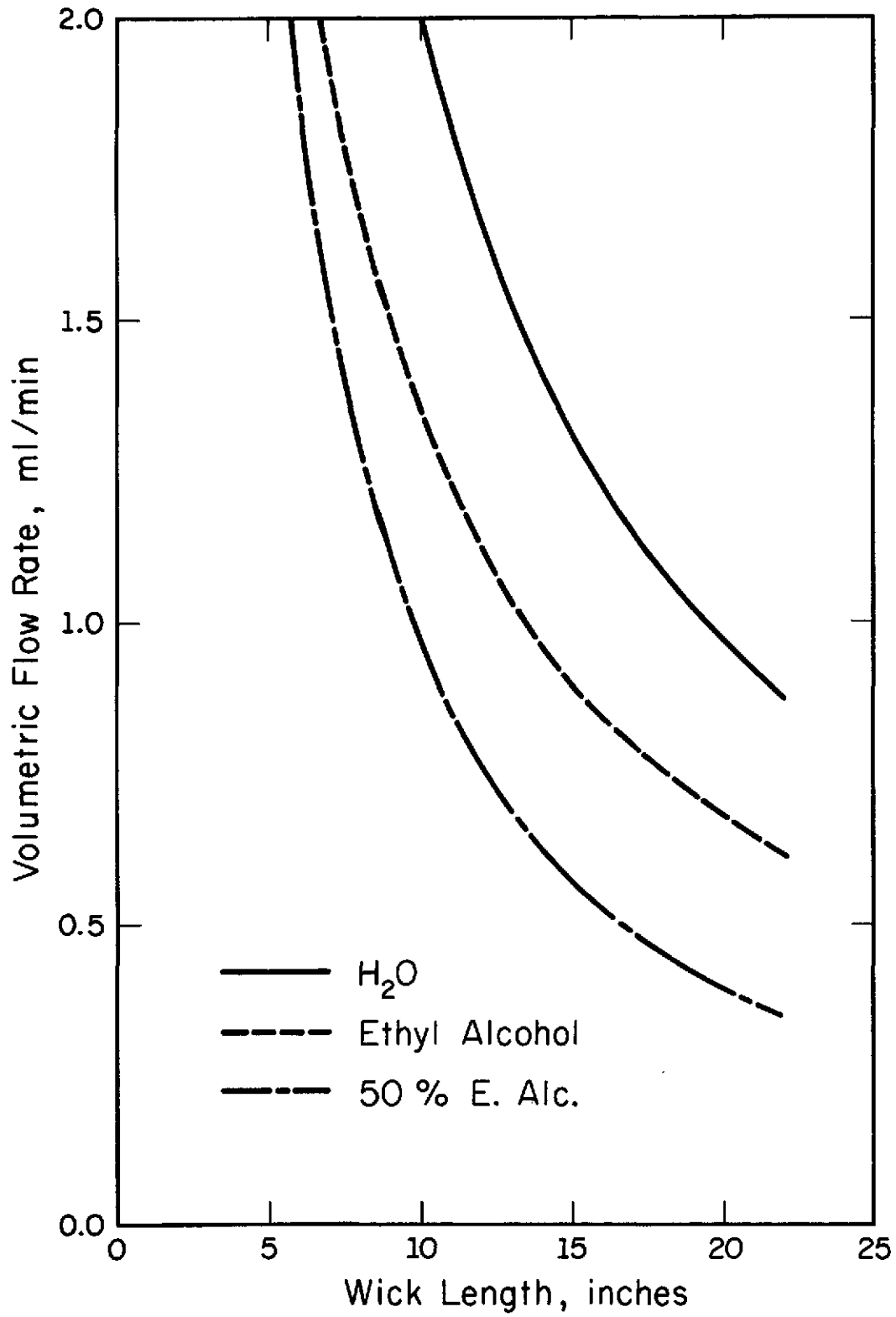


Figure 9. Volumetric flow vs wick length graph  
Wick No. 5. Double layer at 0°

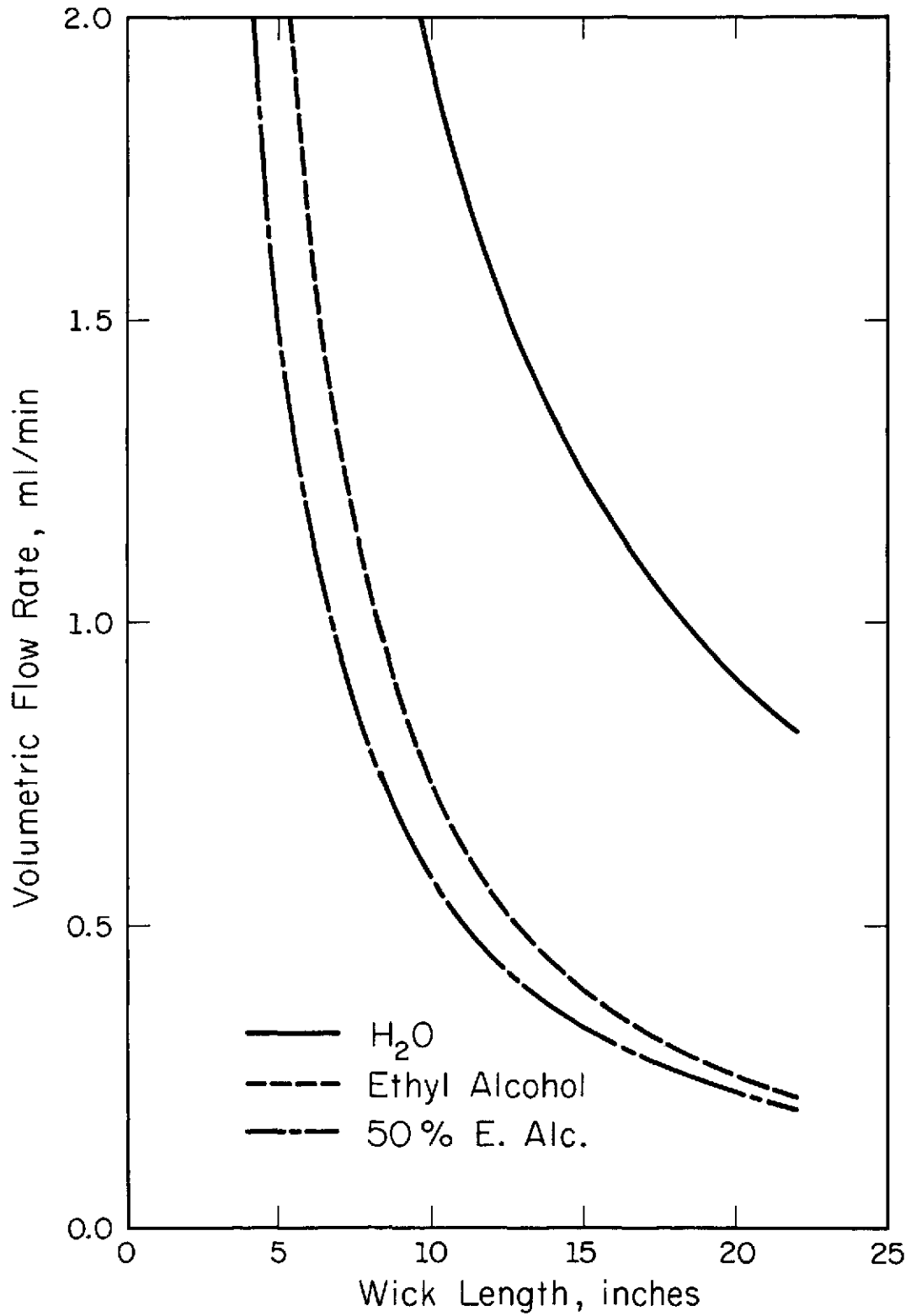


Figure 10. Volumetric flow vs wick length graph  
Wick No. 6. Double layer at 0°

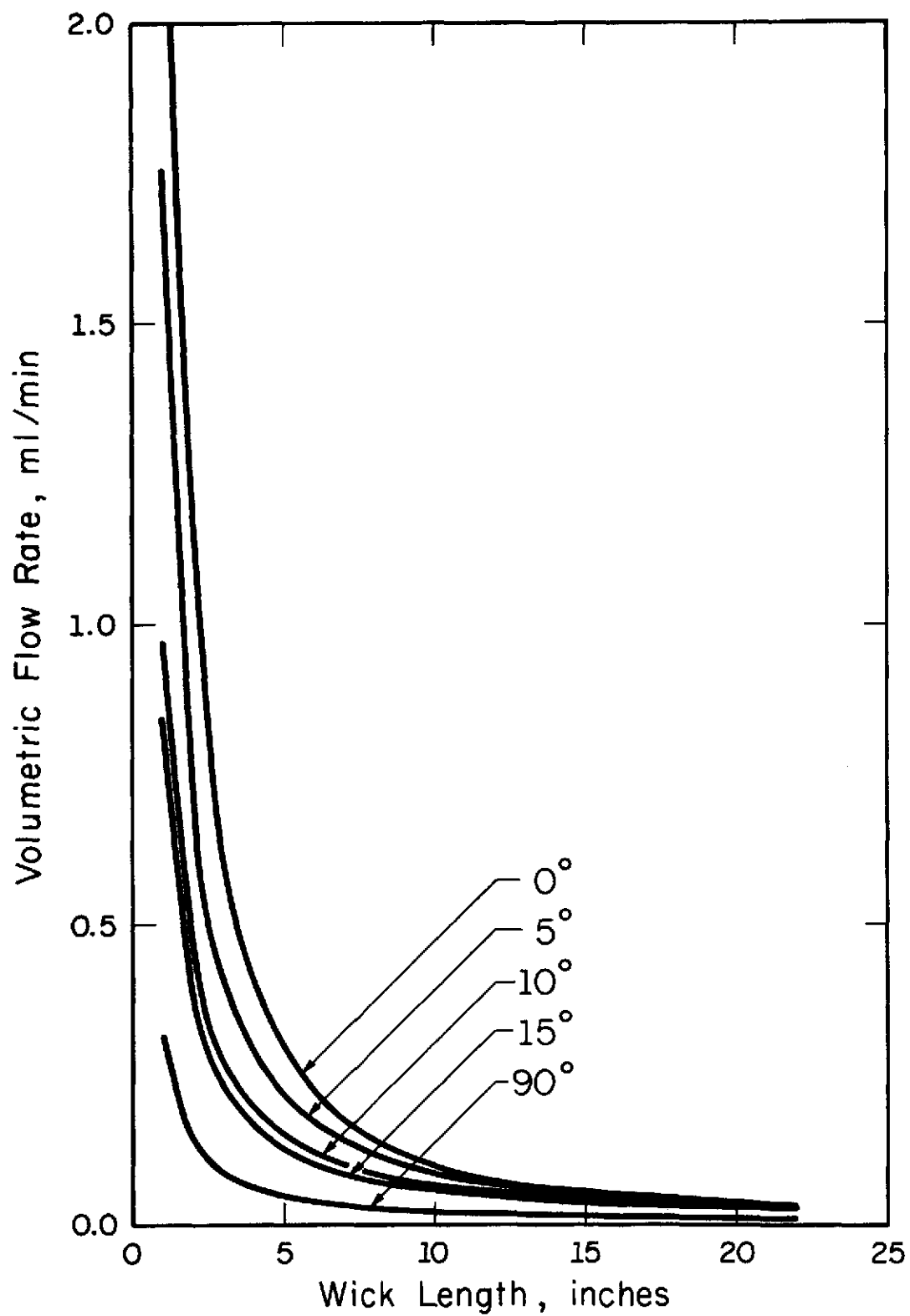


Figure 11. Volumetric flow vs wick length graph  
Wick No. 8. Single layer with water

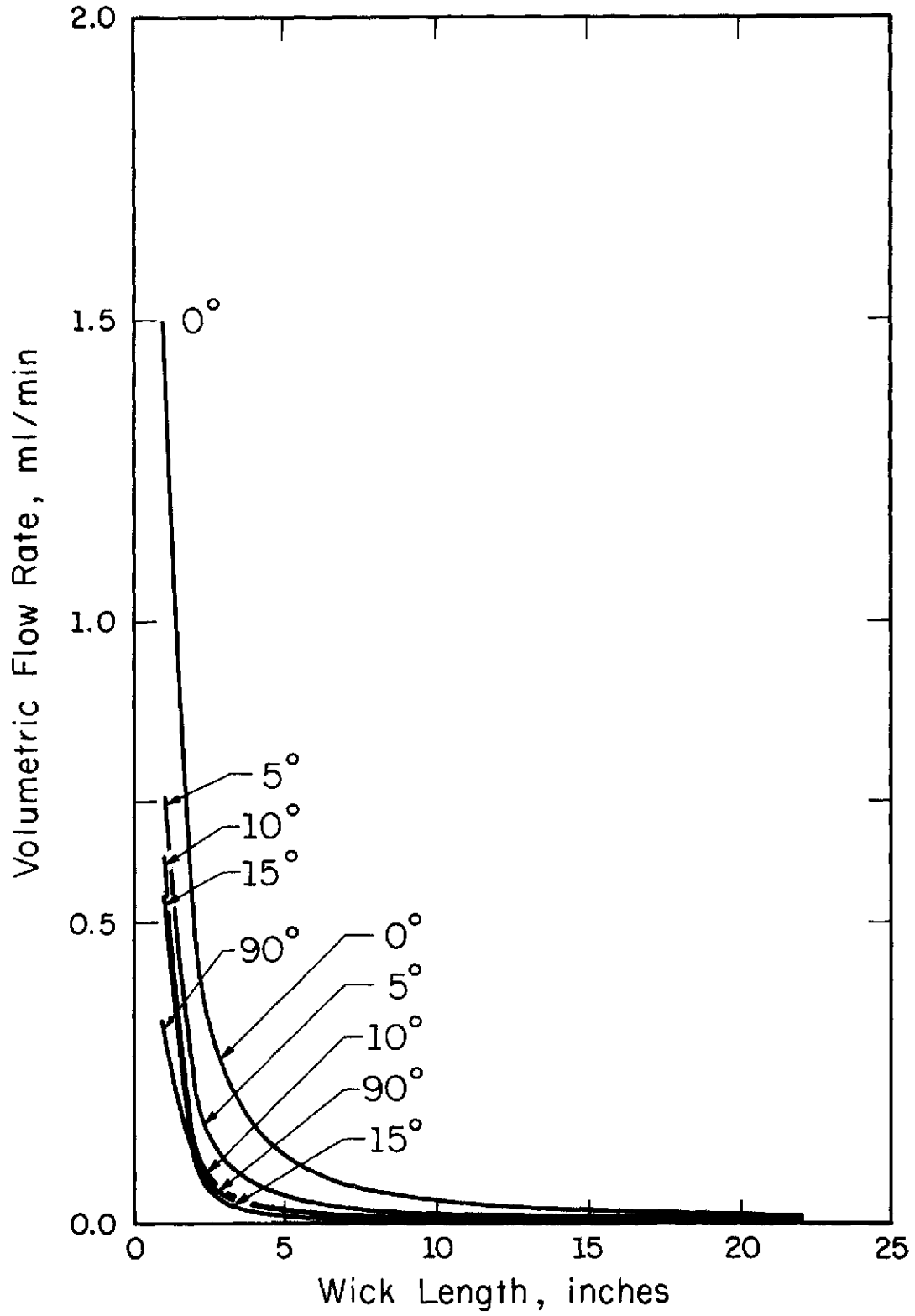


Figure 12. Volumetric flow vs wick length graph  
Wick No. 8. Single layer with ethyl alcohol

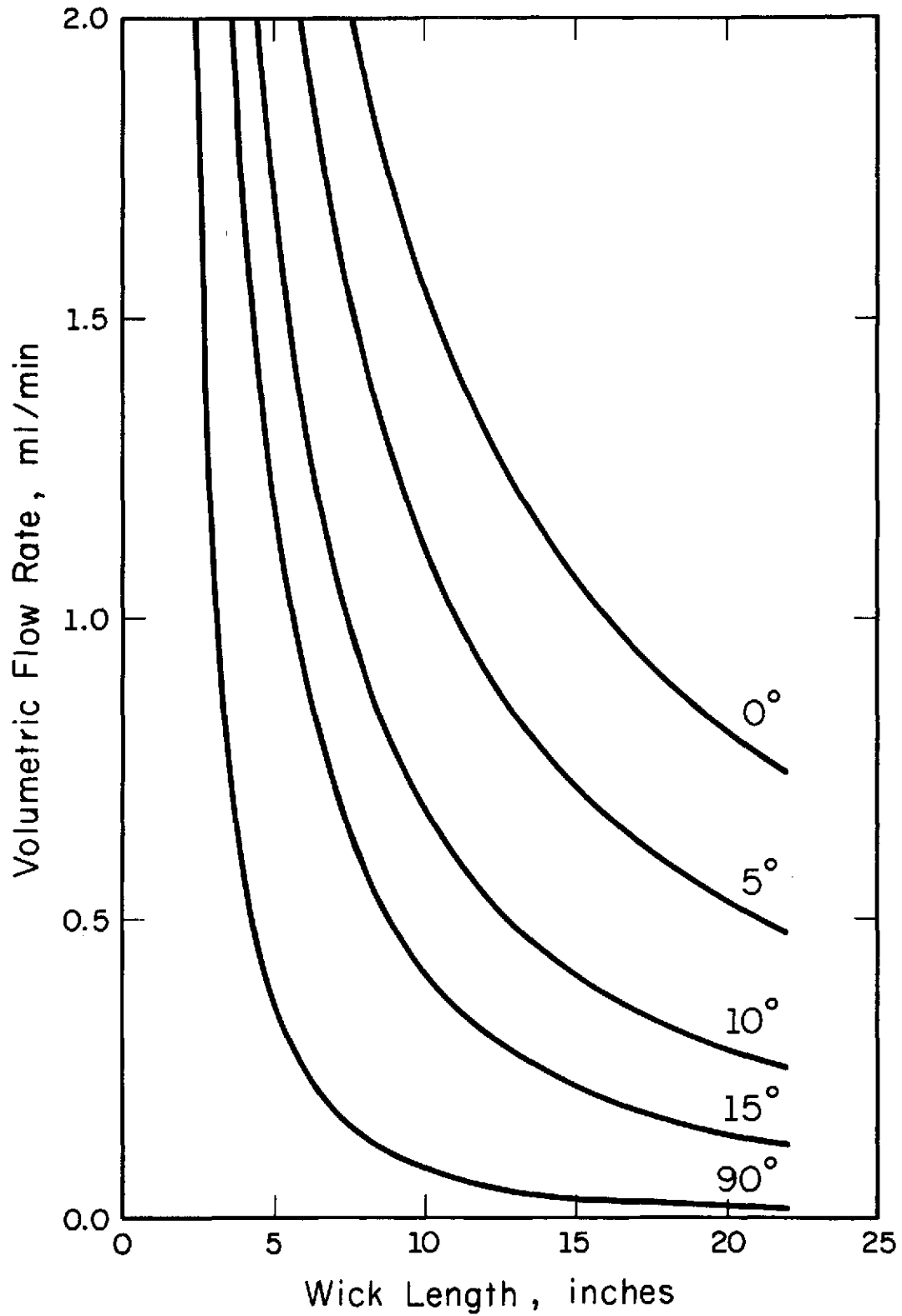


Figure 13. Volumetric flow vs wick length graph  
Wick No. 9. Double layer with water

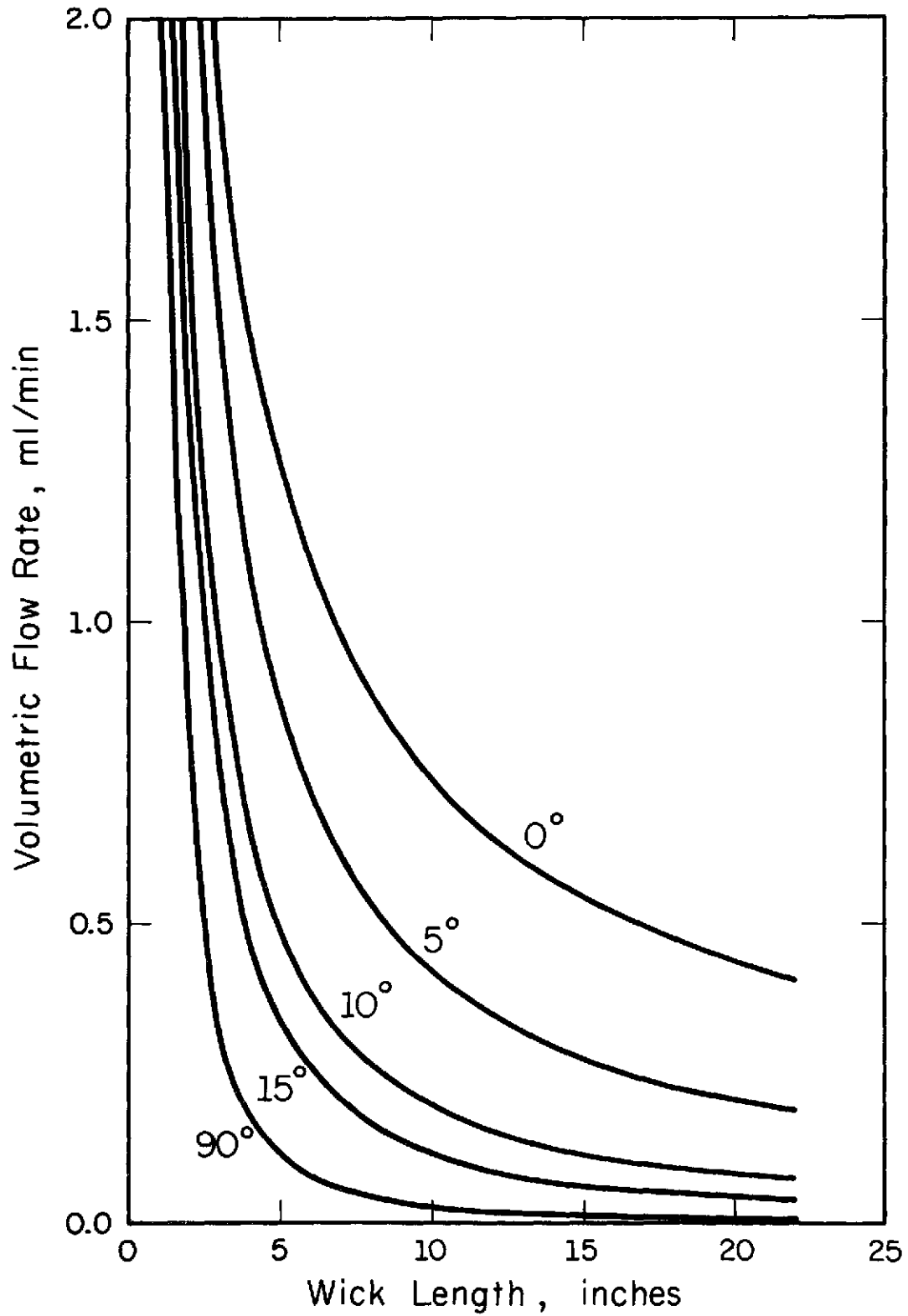


Figure 14. Volumetric flow vs wick length graph  
Wick No. 9. Double layer with ethyl alcohol

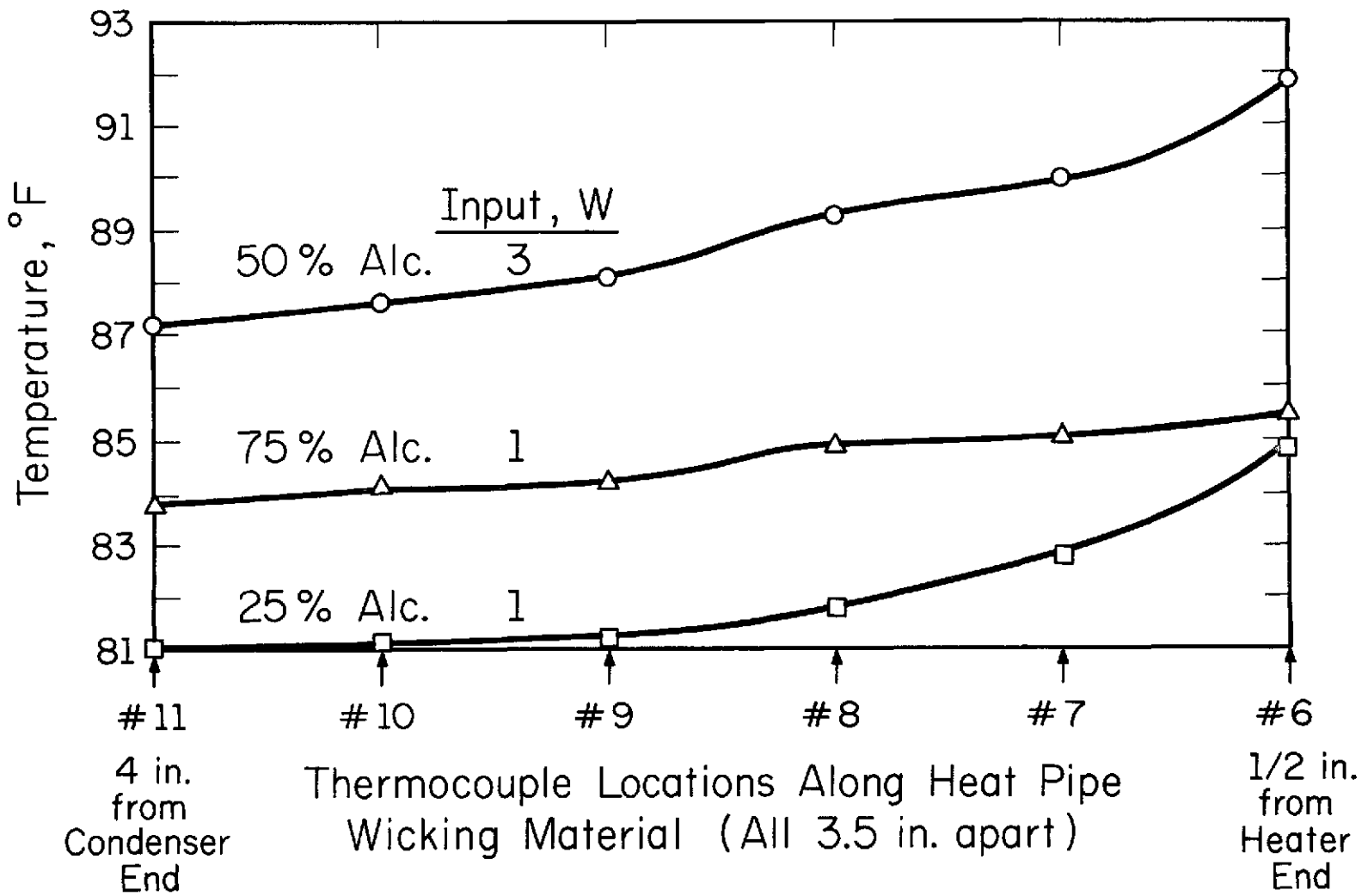


Figure 15. Heat pipe temperature vs distance curves  
Single wicks at 0°

## APPENDIX

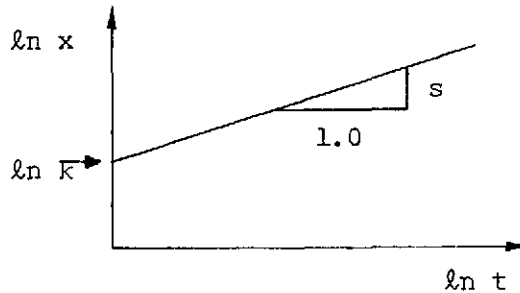
## SAMPLE CALCULATIONS

## I. Finding Area of Flow

$$\ln x = s \ln t + \ln k$$

$$x = kt^s$$

$$\frac{dx}{dt} = kst^{s-1}$$



Schematic layout of Figs. 2-6

$$v_o = AL$$

$v_o \equiv$  total volume in a wick of length  $L$  ( $\text{cm}^3 = \text{ml}$ )

$$A = \frac{v_o}{t_o} \frac{1}{L^{(s-1)/s} k^{1/s}}$$

$t_o \equiv$  time at which flow reaches  $L$  (min)

$$\dot{v} = A \frac{dx}{dt}$$

$\dot{v} \equiv$  volumetric flow rate at "x" (cm/min) (ml/min)

$$= \frac{v_o}{t_o} \frac{sx^{(s-1)/s}}{L^{(s-1)/s}}$$

$$\begin{aligned} \frac{dx}{dt} &= \text{flow velocity at "x" (cm/min)} \\ &= sk^{1/s} x^{(s-1)/s} \end{aligned}$$

$\dot{v}$  will be exactly  $v_o/t_o$  if  $sx^{(s-1)/s} = L^{(s-1)/s}$ .

Denoting this "x" by " $x_o$ ," we have

$$\left( \frac{x_o}{L} \right)^{(s-1)/s} = \frac{1}{s}$$

$$x_o = L/s^{s/(s-1)} \text{ (cm)}$$

$$A = \dot{v}/(dx/dt)$$

$$A = (v_o/t_o)/(k^{1/s} L^{(s-1)/s}) \text{ (cm}^2\text{)}$$

## A. Single Layer (Water at Zero Degrees)

$$\begin{aligned}
 s^{s/(s-1)} &= (0.437)^{0.437/-0.563} \\
 &= 1.90 \\
 x_o &= L/1.90 \\
 A &= (v_o/t_o)/k^{1/s} L^{(s-1)/s} \\
 &= \frac{0.614}{(15.0)^{1/0.437} (22.85)^{-0.563/0.437}} \\
 &= 0.070 \text{ cm}^2 \\
 &= 0.011 \text{ in.}^2
 \end{aligned}$$

## B. Double Layer (Water at Zero Degrees)

$$\begin{aligned}
 s^{s/(s-1)} &= (0.514)^{0.514/-0.486} \\
 &= 2.02 \\
 x_o &= L/2.02 \\
 A &= (v_o/t_o)/k^{1/s} L^{(s-1)/s} \\
 &= \frac{4.06}{(18.94)^{1/0.514} (22.85)^{-0.486/0.514}} \\
 &= 0.257 \text{ cm}^2 \\
 &= 0.040 \text{ in.}^2
 \end{aligned}$$

## II. Finding Predicted Wattages for Single Wick with Fluid at 80°F

### A. Water at Zero Degrees

$$\begin{aligned}
 Q_{\max} &= \dot{m}_{\max} h_{fg} \\
 &= \rho v h_{fg} \\
 &= (1)(0.074)(581)(1/14.35) \\
 &= \left[ \left( \frac{\text{gm}}{\text{cm}^3} \right) \left( \frac{\text{cm}^3}{\text{min-in. width}} \right) \left( \frac{\text{cal}}{\text{gm}} \right) \left( \frac{\text{watts}}{\text{cal/min}} \right) \right] \\
 &= 3.0 \text{ watts/in. of width} \\
 Q_{\text{heat pipe}} &= (3.0)(2) \left[ \left[ 2 \frac{1}{16} \right] + \left[ 1 \frac{7}{16} \right] \right] \\
 &= [(\text{watts/in. width}) (\text{in. width})] \\
 &= 21.0 \text{ watts}
 \end{aligned}$$

### B. Alcohol at Zero Degrees

$$\begin{aligned}
 Q_{\text{heat pipe}} &= (0.79)(0.011)(214)(1/14.35)(2) \left[ \left[ 2 \frac{1}{16} \right] + \left[ 1 \frac{7}{16} \right] \right] \\
 &= \left( \frac{\text{gm}}{\text{cm}^3} \right) \left( \frac{\text{cm}^3}{\text{min-in. width}} \right) \left( \frac{\text{cal}}{\text{gm}} \right) \left( \frac{\text{watts}}{\text{cal/min}} \right) (\text{in. width}) \\
 &= 0.91 \text{ watts}
 \end{aligned}$$

### C. Fifty Percent Ethyl Alcohol at Zero Degrees

$$\begin{aligned}
 Q_{\text{heat pipe}} \Big|_{\text{upper limit}} &= Q_{\text{heat pipe}} \Big|_{h_{fg} \text{ of H}_2\text{O}} = 1.7 \text{ watts} \\
 Q_{\text{heat pipe}} \Big|_{\text{lower limit}} &= Q_{\text{heat pipe}} \Big|_{h_{fg} \text{ of E. Alc.}} = 0.5 \text{ watts}
 \end{aligned}$$

A STUDY OF THE THERMAL BEHAVIOR OF  
LIVING BIOLOGICAL TISSUE WITH APPLICATION TO  
THERMAL CONTROL OF PROTECTIVE SUITS

A. Shitzer

J. C. Chato

B. A. Hertig

Technical Report No. ME-TR-207

January 1971

DEPARTMENT OF MECHANICAL AND INDUSTRIAL ENGINEERING  
LABORATORY FOR ERGONOMICS RESEARCH  
ENGINEERING EXPERIMENT STATION  
UNIVERSITY OF ILLINOIS AT URBANA - CHAMPAIGN  
URBANA, ILLINOIS 61801



# **A STUDY OF THE THERMAL BEHAVIOR OF LIVING BIOLOGICAL TISSUE WITH APPLICATION TO THERMAL CONTROL OF PROTECTIVE SUITS**

by

A. SHITZER  
J. C. CHATO  
B. A. HERTIG

Technical Report No. ME-TR-207  
January 1971

Supported by  
National Aeronautics and Space Administration  
under  
Grant No. NGR-14-005-103

I

122<

i

Errata for ME-TR-207

Page 28 Eq. (3.19), "f(x)" should be "f(ξ)."

29 TABLE 3.1, numbers in last row of third and fourth columns should be interchanged to read:

Heart Muscle	Rest of Body
0.0089	0.1375

42 At top of Fig. 3.10, " $-\frac{f(z)}{\partial k_1}$ " should be " $-\frac{f(z)}{k_1}$ ."

47 Eq. (3.44), last line, second term in denominator, " $wR_2 \psi_{\eta(\eta+1)}^1(wR_2)$ " should be " $wR_2 \psi_{(\eta+1)\eta}^1(wR_1)$ ."

52 Eq. (3.49), second line, " $\frac{2}{aK}$ " should be " $\frac{2}{bK}$ ."

55 Eq. (3.53), fourth line, " $\cos(\delta_1 x)$ " should be " $\cos(\delta_1 y)$ ."

63-65 Figs. 3.15-3.17, the vertical coordinate " $\frac{r}{b}$ " should be " $\frac{r - R_1}{b}$ ."

70 Fig. 3.20, in the figure the parameter " $Q_0$ " should be " $Q'$ ."

72 TABLE 3.3, in the next-to-last column, the decimal points should be moved in front of the numbers; i.e., "2.484" should be "0.2484" and "9.049" should be "0.9049."

73 Eq. (3.70), " $\left(\frac{n\pi}{a}\right)^2$ " should be " $\left[\frac{(2n-1)\pi}{2b}\right]^2$ ."

73 Item (2), seventh line from bottom, " $(kT_1/a^2)$ " should be " $(kT_1/b^2)$ ."

74 TABLE 3.4, last two lines should be

$\left[\frac{(2n-1)\pi}{2b}\right]^2$	1/m <sup>2</sup>	4,950	44,720
	1/ft <sup>2</sup>	460	4,160

162 and Figs. D.1 and D.3, in the figures delete the parameters "K"  
164 and "L" and add the identification,  $wR_1$ , for the numbers in columns on the right-hand sides.

A STUDY OF THE THERMAL BEHAVIOR OF LIVING  
BIOLOGICAL TISSUE WITH APPLICATION TO THERMAL  
CONTROL OF PROTECTIVE SUITS

by

A. Shitzer

J.C. Chato

B. A. Hertig

Research Supported by  
National Aeronautics and Space Administration  
under  
Grant No. NGR-14-005-103

Technical Report No. ME-TR-207

January 1971

Department of Mechanical and Industrial Engineering  
Laboratory for Ergonomics Research  
Engineering Experiment Station  
University of Illinois at Urbana-Champaign  
Urbana, Illinois 61801

## ABSTRACT

A biothermal model of living tissue has been studied which allows for the inclusion of the effects of blood flow, local heat generation, conduction, and storage of heat on the heat transfer processes occurring in the living tissue. A second order, partial differential equation, the "bio-heat" equation, was obtained for the model. Due to the lack of reliable and detailed data on the thermophysical properties involved, the tissue was assumed to be isotropic and homogeneous and all properties were assumed to be constant. Transient, as well as steady-state, closed form, analytical solutions were obtained for cylindrical and rectangular geometries, and for various parameters.

Based on the analysis, a few observations were made:

- (1) Blood flow plays a significant role in the transfer of heat inside the living tissue.
- (2) Transient times for reaching a so-called "fully developed" temperature profile in the tissue were estimated to be of the order of 5-20 minutes. These transient times were found to be strongly dominated by a geometrical parameter.
- (3) At elevated metabolic rates, maximum temperature may occur in the tissue rather than in the inner core.
- (4) Knowledge of the exact shape of the heat flux on the skin was found to be unimportant for the determination of the temperature distribution away from the skin surface.
- (5) Results obtained for the cylindrical and rectangular models were remarkably close for the practical range of variables. The rectangular geometry, however, was easier for computation.

The analysis was partially validated by measuring the temperature profiles on the skin of the thigh cooled by parallel tubes in contact with the skin.

Particular applications of the biothermal model were directed to the problem of extending the thermophysical capabilities of man. Providing a "micro-climate" to man by means of cooling tubes that are in direct contact with the skin, e.g., extravehicular space suits, was a major concern in this study. To this end, a cooling garment, including a cooling hood, was constructed. The garment consisted of sixteen individual pads made of Tygon tubes. These pads were grouped to provide independent supply of cooling water to six separate regions of the body: head, upper torso, lower torso, arms, thighs, and lower legs. Experiments with the cooling garment were directed at exploring the characteristics of independent control of temperature and removal of excess heat from separate regions of the body. Five activity schedules consisting of alternate sessions of standing and treadmill walking were used with five test subjects. Quasi-steady state and, to some extent, transient characteristics of the proposed scheme of independent regional cooling were studied. The results show that there are regions that require more cooling for this type of activity than others (thighs, lower legs, head). It was also demonstrated that heat strain was reduced as a result of wearing the cooling garment.



## NOMENCLATURE†

$a$	half distance between cooling tubes, [L]
$a_k$	coefficient in Eqs. (3.61) and (3.62)
$A$	total skin surface area, [L <sup>2</sup> ]
$A_1$	defined by Eq. (3.69)
$b$	depth of tissue layer, [L]
$b_k$	coefficient in Eqs. (3.61) and (3.62)
$c_1$	defined by Eq. (E.19)
$c_3$	defined by Eq. (E.20)
$c_b$	specific heat of blood [L <sup>2</sup> θ <sup>-2</sup> T <sup>-1</sup> ]
$c_k$	coefficient in Eqs. (3.61) and (3.62)
$c_p$	specific heat of tissue, [L <sup>2</sup> θ <sup>-2</sup> T <sup>-1</sup> ]
$C\{ \}$	Fourier cosine transform operator, defined by Eq. (3.28)
$E(y)$	defined by Eq. (3.13), [T]
$f$	heat flux, [Mθ <sup>-3</sup> ]
$f_a$	average heat flux, defined by Eq. (3.16), [Mθ <sup>-3</sup> ]
$F, F_0$	uniform heat flux, [Mθ <sup>-3</sup> ]
$G$	defined by Eq. (3.14), [L <sup>-1</sup> T]
$G(y, \tau)$	defined by Eq. (3.21)
$h$	height, [L]
$H(\zeta)$	defined by Eq. (3.15), [Mθ <sup>-3</sup> T <sup>-1</sup> ]
$I_i$	modified Bessel function of the first kind of order $i$
$J_i$	Bessel function of the first kind of order $i$
$k$	thermal conductivity, [MLθ <sup>-3</sup> T <sup>-1</sup> ]

---

†Units in brackets are: M, mass; L, length; θ, time; T, temperature.

$k^*$	ratio of thermal conductivities, defined by Eq. (B.8)
$K_i$	modified Bessel function of the second kind of order $i$
$M$	defined by Eqs. (3.40) or (3.42), $[L^{-1}T]$
$q_b$	rate of heat transported by blood, defined by Eq. (3.1), $[ML^{-1}\theta^{-3}]$
$q_m, Q'$	internal heat generation rate per unit volume, $[ML^{-1}\theta^{-3}]$
$Q$	defined by Eq. (3.10), $[L^{-2}T]$
$Q_m$	total metabolic rate, $[ML^2\theta^{-3}]$
$r$	radial coordinate, $[L]$
$\bar{R}$	defined under Eq. (D.6), $[L]$
$R_1$	radius of inner core in cylindrical model, $[L]$
$R_{12}$	radius of interface between skeletal muscle and skin layer in cylindrical model, $[L]$
$R_2$	radius of the skin surface in cylindrical model, $[L]$
$s$	defined under Eq. (D.6)
$t$	time, $[\theta]$
$t^*$	characteristic time, $[\theta]$
$T$	tissue temperature, $[T]$
$T_a$	arterial blood temperature, $[T]$
$T_1, T_2^*$	constant temperature at inner core, $[T]$
$T_{ref}$	reference temperature, $[T]$
$U(\zeta R)$	defined under Eq. (D.6)
$V$	volume, $[L^3]$
$w$	defined by Eq. (3.9), $[L^{-1}]$
$w_b$	blood perfusion rate per unit volume, $[ML^{-3}\theta^{-1}]$
$W$	weight $[ML\theta^{-2}]$

$W[\phi_1, \phi_2]$	Wronskian, defined by Eq. (3.24)
$x$	coordinate, normal to cooling tubes along the skin surface, [L]
$y$	coordinate, normal to skin surface, [L]
$Y_i$	Bessel function of the second kind of order $i$
$Y(y)$	defined by Eq. (3.26), [T]
$z$	coordinate, parallel to the axis of cooling tubes, [L]
$\alpha$	thermal diffusivity, [ $L^2 \theta^{-1}$ ]
$\alpha_n$	defined by Eq. (3.19), [ $L^{-1} T$ ]
$\beta$	ratio of width of cooling tube to cooling tube spacing
$\gamma$	Euler's constant
$\gamma_i$	defined by Eq. (3.51), [ $L^{-1}$ ]
$\delta_n$	defined by Eq. (3.50), [ $L^{-1}$ ]
$\epsilon_i$	defined by Eq. (3.60), [ $L^{-1}$ ]
$\zeta_i$	defined by Eq. (3.17), [ $L^{-1}$ ]
$\eta$	defined by Eq. (3.46)
$\theta$	defined by Eq. (3.8), [T]
$\theta^*(y)$	variable blood supply temperature, [T]
$\lambda_n$	defined by Eq. (3.18), [ $L^{-1}$ ]
$\Lambda(wr)$	defined by Eq. (3.38), [T]
$\mu_n$	defined by Eq. (3.59), [ $L^{-1}$ ]
$\nu_n$	defined by Eq. (3.31), [ $L^{-1}$ ]
$\xi$	dummy variable of integration, [L]
$\rho$	specific gravity of tissue, [ $ML^{-3}$ ]
$\rho^*$	ratio of radii, defined by Eq. (E.8)
$\sigma$	defined by Eq. (3.55), [ $L^{-1}$ ]

$\tau$	dummy variable of integration, [L]
$\phi$	angular coordinate in cylindrical model
$\Phi_1$	plane angle between two adjacent tubes in cylindrical model
$\Phi_1, \Phi_2$	defined by Eq. (3.22a)
$\chi(\mu_n r)$	defined by Eq. (3.58)
$\psi(n)$	Psi or Digamma function
$\psi_{k\ell}^j(\zeta_1 r)$	combination of modified Bessel functions, defined by Eq. (3.37)
$\Omega(\zeta_m)$	defined by Eq. (3.39), [ $M\theta^{-3} T^{-1}$ ]

### Subscripts

1	pertaining to skin layer or initial state
2	pertaining to skeletal muscle or final state
b	blood
i	integer
j	integer
k	integer
$\ell$	integer
m	integer
n	integer

## LIST OF FIGURES

	Page
Figure 3.1 Cross section of the normal skin. Copyright, 1967, CIBA Corporation, reproduced with permission from the Clinical Symposia by Frank H. Netter, M.D. . . . . .	18
Figure 3.2 Representative section of the cylindrical model with the cooling tubes on the skin running perpendicular to the axis of the cylinder. . . . .	20
Figure 3.3 Representative section of the cylindrical model with the cooling tubes on the skin running parallel to the axis of the cylinder. . . . .	21
Figure 3.4 Representative section of the rectangular model. . . . .	22
Figure 3.5 Geometry and boundary conditions for the rectangular model. Skin layer and skeletal muscle are considered as separate regions. . . . .	27
Figure 3.6 Temperature distribution in the separated tissue for the rectangular model. Dashed curves indicate temperature distribution obtained by Buchberg and Harrah [39] without blood flow. $Q_m = 2600$ Btu/hr, (760 w), $\beta = 0.1$ and constant temperature at inner core. . . . .	32
Figure 3.7 Effect of changing the specified flux function on the temperature of the skin for the rectangular model. $Q_m = 2600$ Btu/hr, (760 w), $\beta = 0.1$ and constant temperature at inner core. . . . .	34
Figure 3.8 Effect of increasing the contact area between the cooling tubes and the skin on the temperature distribution on the skin surface. $Q_m = 290$ Btu/hr (85 w), $f_2/f_1 = 1.5$ and constant temperature at inner core. . . . .	35
Figure 3.9 Steady state, one dimensional temperature distribution in the combined tissue with variable linear blood supply temperature for the rectangular model. Dashed line indicates locus of maxima. $Q_m = 2600$ Btu/hr (760 w), and constant temperature at inner core. . . . .	40
Figure 3.10 Geometry and boundary conditions for the cylindrical model with the cooling tubes on the skin running perpendicular to the axis of the cylinder. Skin layer and skeletal muscle are considered as separate regions. . . . .	42

Figure 3.11 Geometry and boundary conditions for the cylindrical model with the cooling tubes on the skin running parallel to the axis of the cylinder. Skin layer and skeletal muscle are considered as a combined tissue. . . . . 48

Figure 3.12 Transient temperature distribution in the combined tissue for the one-dimensional rectangular model. Step changes:  
 (a) from 290 Btu/hr (85 w) to 2600 Btu/hr (760 w)  
 (b) from 2600 Btu/hr (760 w) to 290 Btu/hr (85 w)  
 Constant temperature at inner core. . . . . 53

Figure 3.13 Transient temperature distribution on the skin of the combined tissue for the two-dimensional rectangular model. Step change assumed from 290 Btu/hr (85 w) to 2600 Btu/hr (760 w),  $\beta = 0.1$  and constant temperature at inner core. . . . . 56

Figure 3.14 Comparison between the steady state, two-dimensional solutions for rectangular and cylindrical models (tubes running perpendicular to the axis of the cylinder,  $R_1 = 0.15$  ft,  $V$  and  $b$  are constant).  $Q_m = 290$  Btu/hr (85 w),  $\beta = 0.1$  and constant temperature at inner core. . . . . 62

Figure 3.15 Comparison between steady state, one-dimensional solutions obtained for the rectangular and cylindrical models ( $V$  and  $b$  are constant). Constant temperature at inner core. . . . . 63

Figure 3.16 Comparison between steady state, one-dimensional solutions obtained for the rectangular and cylindrical models ( $B$  and  $A$  are constant). Constant temperature at inner core. . . . . 64

Figure 3.17 Comparison between steady state, one-dimensional solutions obtained for the rectangular and cylindrical models ( $A$  and  $b$  are constant). Constant temperature at inner core. . . . . 65

Figure 3.18 Steady state temperature distributions in the combined tissue for the one-dimensional rectangular model. Constant temperature at inner core. . . . . 67

Figure 3.19 Steady state temperature distributions in the combined tissue for the one-dimensional rectangular model. Constant flux at inner core. . . . . 68

Figure 3.20 Location of the maximum temperature in the combined tissue for the one-dimensional rectangular model. . . . . 70

	Page
Figure 4.1	General view of the cooling garment. . . . . 77
Figure 4.2	Schematic diagram of the cooling garment and the control, supply and measuring systems. . . . . 81
Figure 4.3	View of the water supply system, rotameter and potentiometer recorder used for the experiments with the cooling suit. . . . . 82
Figure 4.4	View of the treadmill, Tele-Thermometer and system for collecting samples for determining metabolic rates. . . . . 84
Figure 4.5	General view of the set-up used for the experiments with the cooling suit. A test subject is shown dressed up in the cooling suit walking on the treadmill. No tennis shoes are shown in this picture and the ear canal thermistor is not connected. . . . . 86
Figure 4.6	View of one of the individual pads. . . . . 88
Figure 4.7	Activity schedules used for the experiments with the cooling suit. . . . . 91
Figure 4.8	Front view of the cooling garment. . . . . 96
Figure 4.9	Side view of the cooling garment. . . . . 97
Figure 4.10	Back view of the cooling garment. . . . . 98
Figure 4.11	Front view of a test subject dressed up in the cooling and insulating garments. . . . . 99
Figure 4.12	A test subject shown walking on the treadmill and breathing through the system for measuring metabolic rates. No tennis shoes are shown in the picture. . . . . 100
Figure 4.13	General view of the set-up used for the experiments with the individual cooling pads. A test subject is shown pedalling the bicycle ergometer. . . . . 101
Figure 5.1	Mean values of metabolic rates and of the amounts of heat removed by the cooling suit and by respiration for Schedule I. . . . . 106
Figure 5.2	Mean values of metabolic rates and of the amounts of heat removed by the cooling suit and by respiration for Schedule II. . . . . 107
Figure 5.3	Mean values of metabolic rates and of the amounts of heat removed by the cooling suit and by respiration for Schedule III. . . . . 108

	Page
Figure 5.4 Mean values of metabolic rates and of the amounts of heat removed by the cooling suit and by respiration for Schedule IV. . . . .	109
Figure 5.5 Mean values of metabolic rates and of the amounts of heat removed by the cooling suit and by respiration for Schedule V. . . . .	110
Figure 5.6 Average ear canal temperatures for the various schedules. . . . .	111
Figure 5.7 Individual variations in the ear canal temperatures and heart rates for Schedule V. . . . .	119
Figure 5.8 Mean values of the amounts of heat removed by the cooling pads for Schedule I. . . . .	122
Figure 5.9 Mean values of the amounts of heat removed by the cooling pads for Schedule II. . . . .	123
Figure 5.10 Mean values of the amounts of heat removed by the cooling pads for Schedule III. . . . .	124
Figure 5.11 Mean values of the amounts of heat removed by the cooling pads for Schedule IV. . . . .	125
Figure 5.12 Mean values of the amounts of heat removed by the cooling pads for Schedule V. . . . .	126
Figure 5.13 Mean water inlet temperatures at the various regions of the body for Schedule II. . . . .	132
Figure 5.14 Comparison of measured and calculated temperature distribution on the surface of the skin for the rectangular model. Pad No. 1, $w_b = 83.4$ lb/hr-ft <sup>3</sup> , $Q' = 711$ Btu/hr-ft <sup>3</sup> and constant temperature at inner core. . . . .	138
Figure 5.15 Comparison of measured and calculated temperature distribution on the surface of the skin for the rectangular model. Pad No. 2, $w_b = 83.4$ lb/hr-ft <sup>3</sup> , $Q' = 805$ Btu/hr-ft <sup>3</sup> and constant temperature at inner core. . . . .	139
Figure 5.16 Comparison of measured and calculated temperature distribution on the surface of the skin for the rectangular model. Pad No. 3, $w_b = 83.4$ lb/hr-ft <sup>3</sup> , $Q' = 848$ Btu/hr-ft <sup>3</sup> and constant temperature at inner core. . . . .	140

	Page
Figure B.1 Comparison of steady state temperature distributions in the tissue for the two-dimensional, rectangular model without blood flow. $Q_m = 2600$ Btu/hr (760 w), $\beta = 0.1$ , constant temperature at inner core. . . . .	153
Figure B.2 Comparison of steady state temperature distributions in the combined tissue for the two-dimensional rectangular model with and without blood flow. $Q_m = 290$ Btu/hr (85 w), $\beta = 0.1$ , constant temperature at inner core. . . . .	154
Figure B.3 Effect of increasing the contact area between the cooling tubes and the skin on the temperature distribution on the skin surface. Blood flow effects are not included. $Q_m = 290$ Btu/hr (85 w), $f_2/f_1 = 1.5$ and constant temperature at inner core. . . . .	155
Figure C.1 Steady state temperature distribution in the combined tissue for the rectangular model. $Q_m = 2600$ Btu/hr, (760 w), $\beta = 0.1$ and constant temperature at inner core. . . . .	157
Figure C.2 Steady state temperature distribution in the combined tissue for the rectangular model. $Q_m = 290$ Btu/hr (85 w), $\beta = 0.1$ , constant flux at inner core. . . . .	159
Figure D.1 The function $\psi_{01}^1(wR)$ drawn on semi-log paper. . . . .	162
Figure D.2 The function $\psi_{00}^1(wR)$ . . . . .	163
Figure D.3 The function $\psi_{12}^1(wR)$ drawn on semi-log paper. . . . .	164
Figure E.1 Steady state temperature distribution in the combined tissue for the cylindrical model (cooling tubes on the skin running perpendicular to the axis of the cylinder). $Q_m = 2600$ Btu/hr (760 w), $\beta = 0.1$ , constant temperature at inner core. . . . .	166
Figure E.2 Steady state temperature and surface area of the skin as functions of $R_1$ for the one-dimensional cylindrical model. $V$ and $b$ are constant and constant temperature at inner core. . . . .	169
Figure E.3 Steady state temperature of the skin and depth of tissue as functions of $R_1$ for the one-dimensional cylindrical model. $V$ and $A$ are constant and constant temperature at inner core. . . . .	170

Figure E.4 Steady state temperature of the skin and volume of the tissue as functions of  $R_1$  for the one-dimensional cylindrical model. A and b are constant and constant temperature at inner core. . . . . 171

Figure E.5 Steady state temperature of the skin as function of  $R_1$  for the one-dimensional cylindrical model. Constant temperature at inner core. . . . . 172

Figure F.1 Metabolic rates and ear canal temperatures of subject SKB for experiments with and without the cooling suit during Schedule I. . . . . 176

Figure F.2 Metabolic rates and ear canal temperatures of subject SKB for experiments with and without the cooling suit during Schedule II. . . . . 177

Figure F.3 Metabolic rates and ear canal temperatures of subject SKB for experiments with and without the cooling suit during Schedule III. . . . . 178

Figure F.4 Metabolic rates and ear canal temperatures of subject SKB for experiments with and without the cooling suit during Schedule IV. . . . . 179

Figure F.5 Metabolic rates and ear canal temperatures of subject SKB for experiments with and without the cooling suit during Schedule V. . . . . 180

Figure F.6 Heart rates of subject SKB for experiments with and without the cooling suit during Schedule V. . . 181

LIST OF TABLES

	Page	
TABLE 3.1	PHYSICAL AND PHYSIOLOGICAL PROPERTIES OF THE RECTANGULAR BIOTHERMAL MODEL CORRESPONDING TO A 139 LB (63 KG) ADULT MALE WITH 90 MM HG MEAN ARTERIAL BLOOD PRESSURE AND TOTAL METABOLIC RATE OF 290 BTU/HR (85 W). REPRODUCED IN PARTS FROM BUCHBERG AND HARRAH [39] AND BRAD [59]. . . . .	29
TABLE 3.2	FIRST SIX ROOTS OF EQ. (3.59) AS A FUNCTION OF THE RATIO OF THE OUTER TO INNER RADII OF THE CYLINDRICAL MODEL, $R_2/R_1$ . THE RIGHTMOST COLUMN GIVES THE ASYMPTOTIC VALUES ( $[(2n - 1)\pi]/2b$ , RECTANGULAR MODEL) AS $R_1 \rightarrow \infty$ AND $R_2/R_1 \rightarrow 1$ . . . . .	60
TABLE 3.3	PHYSIOLOGICAL QUANTITIES AND THE CORRESPONDING DIMENSIONLESS PARAMETERS. $c_b = 1$ Btu/lb-°F (4187 J/kg-°C), $k = 0.311$ Btu/ft-hr-°F (0.540 w/m-°C), $b = 0.0731$ ft (0.0223 m), AND $A = 15.4$ ft <sup>2</sup> (1.43 m <sup>2</sup> ) . . . . .	72
TABLE 3.4	COMPARISON OF MAGNITUDES OF THE TERMS IN EQ. (3.70). $c_b = 1$ Btu/lb-°F (4187 J/kg-°C), $k = 0.311$ Btu/hr-ft-°F (0.540 w/m-°C), AND $a = 0.032$ ft (0.00975 m) . . . . .	74
TABLE 4.1a	DATA ON THE COOLING GARMENT . . . . .	78
TABLE 4.1b	DATA ON THE COOLING GARMENT . . . . .	79
TABLE 4.2	DATA ON THE INDIVIDUAL COOLING PADS . . . . .	87
TABLE 4.3	CHARACTERISTICS OF THE TEST SUBJECTS . . . . .	94
TABLE 4.4	CHARACTERISTICS OF SUBJECT TEK . . . . .	103
TABLE 5.1	ORDER OF PREFERRED CHANGES IN WATER INLET TEMPERATURES AND THE COMFORT VOTE FOR THE VARIOUS ACTIVITIES . . . . .	113
TABLE 5.2	WEIGHT LOSSES DURING TREADMILL EXPERIMENTS . . . . .	128
TABLE F.1	MEAN VALUES AND RANGES OF TOTAL METABOLIC RATES, HEAT REMOVED BY SUIT AND BY RESPIRATION AT THE VARIOUS SCHEDULES OF ACTIVITY . . . . .	182
TABLE F.2	MEAN VALUES AND RANGES OF WATER INLET TEMPERATURES FOR THE VARIOUS REGIONS AT DIFFERENT SCHEDULES OF ACTIVITY . . . . .	188



PRECEDING PAGE BLANK NOT FILMED

## TABLE OF CONTENTS

	Page
1. INTRODUCTION . . . . .	1
2. REVIEW OF RELATED WORKS . . . . .	4
2.1 ANALYTICAL THERMAL MODELING . . . . .	4
2.2 WATER COOLED GARMENTS . . . . .	12
2.3 MEASUREMENT OF THERMOPHYSICAL PROPERTIES . . . . .	12
3. THEORETICAL ANALYSIS . . . . .	14
3.1 DEVELOPMENT OF THE GOVERNING PARTIAL DIFFERENTIAL EQUATION . . . . .	14
3.2 GEOMETRIES, BOUNDARY AND INITIAL CONDITIONS . . . . .	17
3.3 ANALYTICAL SOLUTIONS . . . . .	23
3.4 STEADY STATE, RECTANGULAR COORDINATES . . . . .	24
3.5 STEADY STATE, CYLINDRICAL COORDINATES . . . . .	41
3.6 TRANSIENT STATE, RECTANGULAR COORDINATES . . . . .	50
3.7 TRANSIENT STATE, CYLINDRICAL COORDINATES . . . . .	57
3.8 COMPARISON OF STEADY STATE SOLUTIONS FOR RECTANGULAR AND CYLINDRICAL COORDINATES . . . . .	59
3.9 DIMENSIONLESS PARAMETERS ASSOCIATED WITH THE THERMAL BEHAVIOR OF LIVING BIOLOGICAL TISSUE . . . . .	66
4. EXPERIMENTS . . . . .	75
4.1 OBJECTIVES . . . . .	75
4.2 DESCRIPTION OF THE EXPERIMENTAL SETUPS . . . . .	75
4.2.1 Cooling Suit . . . . .	75
4.2.2 Individual Cooling Pads . . . . .	85
4.3 EXPERIMENTS WITH THE COOLING SUIT . . . . .	89
4.3.1 Activity Schedules . . . . .	89
4.3.2 Test Subjects . . . . .	92
4.3.3 Experimental Procedure . . . . .	93
4.3.4 Measured, Recorded and Calculated Quantities . . . . .	101
4.4 EXPERIMENTS WITH THE INDIVIDUAL PADS . . . . .	102
5. DISCUSSION . . . . .	105
5.1 EXPERIMENTS WITH THE COOLING SUIT . . . . .	105
5.2 EXPERIMENTS WITH THE INDIVIDUAL COOLING PADS . . . . .	135
6. SUMMARY AND CONCLUSIONS . . . . .	141

	Page
APPENDIX	
A. THE THERMOREGULATORY SYSTEM OF THE HOMEOTHERM . . . .	146
B. STEADY STATE, RECTANGULAR COORDINATES WITHOUT BLOOD FLOW . . . . .	149
C. STEADY STATE, RECTANGULAR COORDINATES WITH THE SKIN AND MUSCLE CONSIDERED AS A SINGLE REGION . . . .	156
D. THE FUNCTION $\psi_{k\ell}^j(\zeta_i r)$ . . . . .	160
E. STEADY STATE, CYLINDRICAL COORDINATES WITH THE SKIN AND MUSCLE CONSIDERED AS A SINGLE REGION . . . .	165
F. ADDITIONAL EXPERIMENTAL DATA . . . . .	175
LIST OF REFERENCES . . . . .	194

## 1. INTRODUCTION

The thermal system of homeotherms, and that of the human body in particular, has long been of interest to many researchers. The ability to maintain a fairly constant "deep body" temperature and to dissipate or preserve heat under widely varying environmental conditions have been among the most fascinating aspects of this system.

With the progress of scientific knowledge and methods, emphasis has shifted from mere observations of this system and its functions to more systematic studies. The efforts were directed to provide more understanding and insight into the nature and behavior of the mechanisms that govern such thermal phenomena. For completeness, a brief outline of the thermoregulatory system of homeotherms, as currently understood, is given in APPENDIX A.

In common with many branches of physiology, the study of the thermoregulatory system is approaching a stage in which work of descriptive nature will yield progressively less in the way of improved insight. Consequently, analytical approaches become more and more necessary. Analytical modeling of various aspects of the thermoregulatory system is expected to provide improved understanding of the mechanisms of thermoregulation and heat transfer. From these models new experimental directions are expected to emerge.

In our era of advanced technology, man has also been venturing into and exploring environments that are, among other things, thermally hostile to life. As a result, man's natural physiological abilities had to be augmented to render these hostile environments habitable.

The required artificial systems had to provide "micro-climates" to man that were capable of countering any adverse thermal changes in the environment.

As an example, the first such system used for pilots in the Royal Air Force was a gas-ventilated suit [1]†. Such suits proved to be of limited capacity for the removal of metabolic heat and hybrid systems emerged. These "second generation" suits were composed of two sub-systems; a water cooled garment, first suggested by Billingham in 1959 [2], fabricated from flexible tubes in contact with the skin and an overlying gas-ventilated system. In the current Apollo suits that are of this hybrid type [1], a change in body temperature and activity level is compensated by a uniform change in the cooling water inlet temperature. It would seem reasonable, however, to cool active muscles first; i.e., where heat is generated. Moreover, there are regions in the body that are more temperature sensitive, e.g., the back, that may render a uniform change in temperature less tolerable from a comfort standpoint.

Consideration of the above-mentioned points led to formulation of the specific objectives for this study:

- (1) Analytical modeling of the thermal behavior of the living biological tissue. Blood flow effects were included in the model explicitly because heat transfer is an important concomitant of the circulatory system.
- (2) Experiments with cooling pads directed at partially

---

†Numbers in brackets refer to entries in REFERENCES.

validating the temperature distributions obtained from the analysis.

- (3) Exploration of the characteristics of regional cooling, i.e., independently cooling various regions of the body.

## 2. REVIEW OF RELATED WORKS

During the last few decades, three major avenues have been pursued to study and modify the thermal behavior of biological media, namely:

- (1) Analytical modeling of the thermal system and partitional calorimetry relating to homeotherms.
- (2) Experimental studies of man-environment interactions involving whole-body or partial cooling devices, e.g., cooling garments, hoods.
- (3) Measurements of pertinent thermophysical and physiological properties, both "in vivo" and "in vitro."

The following is a brief review of works done in these three areas.

### 2.1 ANALYTICAL THERMAL MODELING

The fact that the body exchanges water vapor with the environment was first established by Santorio, an Italian physician living in the sixteenth and seventeenth centuries [3]. He spent a portion of the latter part of his life in a large balance; his food intake and excreta were accurately weighed. Santorio attributed the differences he found in the two weights to losses of water evaporated from the skin and carried by respiration. He termed these losses "insensible perspiration." Although not concerned with the heat transfer aspects of the processes he had observed, Santorio can still be considered as one of the founders of the "bio-heat transfer" school.

However, it was not until the second half of the eighteenth century, that Lavoisier [4] conceived the idea of the human body being a heat generator. With this concept, more rigorous studies of the

man-environment heat exchanges and the heat transfer processes occurring inside the body, have become feasible.

It appears that Burton [5] in 1934 was the first to apply heat transfer equations to the human body. He assumed a uni-dimensional, steady state model with constant properties and uniform heat generation in the tissue. Solving the equation analytically, he obtained a parabolic temperature distribution.

Eichna, et al. [6] in 1945, and Machle and Hatch [7] in 1947 adopted the concept of "core and shell" and applied it to the human body. In this method, two temperatures are assigned to the body, i.e., deep body (rectal) and skin temperatures. Skin temperature was taken as a weighted average of temperatures of various regions of the skin. Heat exchange between man and his environment was then calculated as a function of conductance and core and shell temperature differences. This approach to the problem has since then been popular particularly with physiologists. However, it is not concerned with the details of temperature distribution and effects of blood flow.

In 1948 Pennes [8] introduced two new concepts into the problem of modeling the thermal behavior of the human body. First, he depicted the human body as consisting approximately of cylinders with circular cross section. Second, he realized the important role that blood flow plays in the process of heat transfer in the tissue and introduced an additional term into the heat equation, making the heating effect due to blood flow proportional to its heat capacity rate and to its temperature change within the tissue. Further, assuming the body to be homogeneous and isotropic with constant physical properties and uniform rate of heat production, he obtained a steady

state solution in terms of Bessel functions for the temperature distribution in the forearm. The boundary condition satisfied at the skin was in accordance with Newton's cooling law (convective boundary condition). Pennes also commented that axial temperature gradients of the extremities can be neglected when compared to radial gradients and that the heat production in the skin and subcutaneous fat is of low order of magnitude.

As is suggested by the title of their article, Wyndham and co-workers in 1952 [9] examined the use of heat exchange equations to determine changes in body temperature.

Pursuing the concepts advanced by Pennes, Hertzman in 1953 [10] obtained correlations between skin temperature and cutaneous blood flow.

The "computer era" in thermal modeling began in 1955 when Taylor [11] advanced the idea of using an electrical analog to simulate heat transfer modes occurring inside the human body and between man and his thermal environment. He divided the body into five layers: skin, functional peripheral shell (subcutaneous tissue and part of the muscles), functional central section (skeletal muscle, heart and blood), core organs (liver, kidneys, central nervous system) and the inert tissue (skeleton and alimentary tract). He also assigned values of thermal capacity, conductance, and heat generation to these layers. Taylor proposed an electrical analog circuit composed of resistances, capacitances and potential sources to simulate the human-environment thermal system.

Herrington, in two articles in 1958 [12] and 1959 [13], discussed a full scale human body model for thermal exchanges. Using algebraic

and least-square concepts, he derived a five element linear differential equation to describe extensive calorimetric data collected from seated, clothed human subjects. Rate of change of the skin temperature with respect to metabolic heat input, evaporative cooling, ambient air and ambient radiation temperature, were the result of the former work. In the latter, the data were compared with those obtained for an electrically heated body model ("copper man").

In 1958 Westland [14] followed up the ideas developed by Taylor of a biothermal analog to simulate and study interior and exterior heat transfer mechanisms related to the human body. Assuming one-dimensional heat flow and equivalent conductance to account for blood flow and the thermal conductivity, he studied the transient response of the human body to thermal exposures. Osman in 1962 [15] refined and improved on Westland's work.

A similar approach to the problem of heat transfer associated with the human body was used by Wyndham and Atkins in 1960 [16]. They approximated the body by a series of concentric cylinders corresponding to the core, muscle, and skin; and considered radial heat flow only. Using a numerical technique and utilizing an analog computer they obtained transient solutions for their model. At about the same time, Crosbie, et al., [17] employed a similar technique and applied it to a one-dimensional slab model. They assumed the slab to be divided into the same three layers and assigned constant, uniform, but different temperatures to each of the layers and compared their results with physiological data. Neither of the latter two approaches included a blood flow term explicitly.

In 1961 Wissler [18,19] initiated a study of mathematical

modeling of the human thermal system. He divided the body into six cylinders corresponding to the extremities, trunk, and head. Including the blood flow term, he obtained analytical solutions for radial heat transfer for both the steady and transient states. He also introduced the concept of a central "pool," where blood from all regions is gathered, mixed, and redistributed, and the idea of lumped heat exchange between arteries and veins. Later, in 1964, he improved his model by dividing the body into fifteen circular cylinders interconnected by blood vessels [20]. These cylinders were subdivided into fifteen layers and numerical solutions were obtained on a digital computer. Just recently, Wissler increased the number of compartments into which the body is divided to include some 250 elements [21].

Perl, in 1962 [22], conceived of a method of indirect measurement of blood flow rates by employing Fick's second principle. He solved analytically the steady state and the transient problems and compared his results with experiments. Extensions of the initial work were published by him and co-workers in 1963 [23], 1965 [24], and 1966 [25].

The idea of using an analog computer for simulating temperature regulation in man was further utilized by Brown in 1963 [26]. He divided the body into four regions (central, muscle, subcutaneous region and skin) and studied interactions with the environment as well as heat distribution within the body. Further development of the biothermal analog computer was given by him in 1966 [27].

Numerical solutions for a uni-dimensional, four layer transient model were also obtained by Layné and Barker [28] in 1965 and by Stolwijk and Cunningham [29]. In 1966 Birkebak, et al., considered the application of heat transfer equations to the animal system [30].

In 1966 Soltwijk and Hardy [31] represented the human body by three cylinders corresponding to the head, trunk, and extremities and assumed the ends to be perfectly insulated. Each of the cylinders was subdivided into layers to represent the skin, muscle, viscera, brain, etc., and each sublayer was assumed to be at a constant temperature. Only radial heat flow was assumed and the effect of blood flow, as well as metabolic heat production, was included. Eight simultaneous differential equations were written for the various sublayers and three "controller" equations. These equations corresponded to evaporative heat losses, muscle blood flow changes with temperature and exercise rate, and also took into consideration the effects of shivering on heat transfer. The set of equations was solved on an analog computer yielding transient temperature distributions for various environmental and metabolic conditions. These two researchers were the first to introduce the concept of the passive system and active controller as applied to the human thermoregulatory system. According to this concept, the passive system represents a complex transfer function between the controller and the disturbance. The controller is responsible for maintaining the human body within the narrow limits of acceptable thermal conditions by activating the various thermoregulatory mechanisms, i.e., vasoconstriction or dilatation, sweating, and shivering.

A group from the University of Washington became interested, in 1967 [32], in the effects of electromagnetic heating patterns in human tissue. One year later [33], they also studied the propagation of acoustic waves and the resulting thermal effect in biological materials. In 1969, two solutions to the problem, one using an analytical method

[34] and the other a finite difference method [35], were presented by this group.

Richardson and Whitelaw in 1968 [36] studied transient heat transfer in the human skin. They constructed two probes: a cylindrical and a rectangular slab. The probes were made of nylon and methyl methacrylate (Perspex), respectively, and had thermocouples embedded in them at known locations. After being immersed in a constant temperature bath, the probes were brought into contact with the skin (enclosed areas of arm-pit and clenched hand) and the temperature of the thermocouples was recorded. Using available analytical solutions to the heat conduction equation in solids, the conductance of the human skin was evaluated. It was found that the change in conductance was independent of the surface temperature and heat flux to which the skin was exposed.

Infrared thermometry was utilized by Gros and Gautherie in 1968 [37] to study transient changes in human skin temperature as a function of ambient temperature. By means of a simplified model of heat exchange between the organism and the environment (only one-dimensional, transient conduction was considered), a mathematical law was derived. This law, obtained by using Laplace transform, was expressed by error functions and gave satisfactory representation of the experimental data.

At about the same time Mitchell and Myers [38] developed an analytical model for countercurrent heat exchange between arteries and veins. They proposed two different configurations for the countercurrent heat exchange that can be found in animals. These were: equal number of arteries and veins (arm of man, leg of bird, rete of a sloth's leg) and veins encircling a single artery (fins of whales and

porpoises). Applying the principle of conservation of energy they obtained analytical solutions to the various configurations and compared their results with available experimental data.

Buchberg and Harrah [39] in 1968 tried a numerical solution of a two-dimensional, steady state model cooled by a network of tubes at the skin. They divided the slab into four layers corresponding to the core, musculature, a so-called functional periphery, and the skin. They assumed the thermal conductivity of the tissue to be a function of temperature and no heat to be generated in the skin. They did not include a blood flow term explicitly.

Chato in 1968 [40] reported on a method for measuring both local thermal diffusivity and blood perfusion rate. He modeled the tissue as an infinitely large medium with a spherical heat source (thermistor bead) embedded in it. He obtained analytical solutions and satisfactory results were obtained experimentally.

In 1968 Trezek and Jewett [41] initiated a study of the thermal field emanating from a cylindrical probe embedded in a tissue, in general, and in a brain, in particular. They were initially interested in applications to cryo-surgical probes. Other works on the subject were published later by Trezek and Cooper in 1968 [42], Trezek in 1969 [43], and Cooper in 1970 [44].

A study of the stationary heat transport from a heated spherical probe located in a tissue was made in 1969 by Priebe and Betz [45]. The tissue was assumed to be of spherical shape, too, and was considered to be isotropic and homogeneously perfused by blood. Assuming the discrete capillary heat sinks as well as the venous heat sources to

be "smeared" over the whole volume of the tissue, they obtained analytical solutions to the problem. This treatment provided a method for estimating local blood flows. Also, thermal conductivity as a function of blood flow was obtained.

Just recently, Keller and Seiler [46] reported on an analysis of peripheral heat transfer in humans. In a steady state, one-dimensional continuum model, they accounted for effects of heat conduction, convection by blood flow and vascular heat exchange. They did not assume heat to be generated inside the tissue. Solving the resulting three simultaneous differential equations, they obtained general expressions for the effective conductivity of the tissue. They also discussed a method for estimating the degree of arterial precooling by the vessel spacing.

## 2.2 WATER COOLED GARMENTS

A most complete review on water cooled garments (WCG) was recently given by S. A. Nunneley [47]. She discussed the history of water cooled garments in the United States and in the United Kingdom. The discussion also includes variables affecting WCG design and operation, the development of automatic control and possible uses for regional cooling. Some 118 references are cited in this work and form a complete list of works pertinent to the subject.

## 2.3 MEASUREMENT OF THERMOPHYSICAL PROPERTIES

A large number of works describing methods and techniques for measuring the thermophysical properties of biological tissues has

been published. These include both "in vitro" and, to a lesser extent, "in vivo" measurements.

Webb in 1964 [48] published a monograph entitled "Bioastronautics Data Book" in which he listed extensive data on the human body. He also included a chapter on thermophysical properties.

In 1966 Chato [49] made a rather extensive survey of thermal diffusivity and conductivity data on biological materials. This work was extended in 1968 [50]. He reported the data available at that time to include properties of internal organs, skin, biological fluids, frozen and then thawed materials and animal integuments.

Pond in 1968 [51] measured the thermal conductivity of rat brain. For the measurements he utilized a thermistor bead and used the same concepts as those suggested earlier by Chato [40].

Recently, Cooper [44] completed the development of a needle-probe for measuring thermal properties of human organs. The needle probe is essentially a copper-constantan thermocouple in the shape of a long, thin cylinder. This probe, while being at a temperature different than that of the organ, is suddenly plunged into the tissue. The changes in temperature of the probe are then recorded until it reaches the temperature of the medium. Thermal diffusivity values are calculated from the initial portion of the response curve. This method was developed to allow for blood flow effects to be taken into account and thus may be used for both "in vivo" and "in vitro" measurements. Cooper and Trezek report data obtained via the needle probe technique elsewhere [52].

Chato and co-workers further applied the thermistor bead to measure effective conductivity values of cat brain and hind leg muscle "in vivo" and "in vitro" [53].

### 3. THEORETICAL ANALYSIS

#### 3.1 DEVELOPMENT OF THE GOVERNING PARTIAL DIFFERENTIAL EQUATION

Among the factors to be considered when attempting the modeling of the human thermal system are the following:

- (1) Geometry of the body.
- (2) Heat capacity of the body (thermal inertia).
- (3) Conduction of heat due to thermal gradients.
- (4) Metabolic heat production.
- (5) The role of blood flow in heat transfer; i.e., transport of heat by circulating blood and countercurrent heat exchange between large blood vessels.
- (6) Thermoregulatory mechanisms in the body and their functions; i.e., vasomotor activity, sweating, shivering, increased metabolism due to glandular activity, and pilo-motor activity (goose flesh). (In warm-blooded species other than humans, an additional mechanism of panting is also of importance.)
- (7) Thermophysical and physiological properties of various organs and tissues; e.g., thermal conductivity, specific heat, density, blood perfusion rates, etc., and their dependence upon temperature and location.
- (8) The interaction with the environment and its condition; i.e., dry and wet bulb temperatures, pressure, and air motion relative to the body.

In what follows, these factors will be considered while a heat balance on a differential element of tissue will be established.

Storage, conduction, and production of heat within the tissue will be assumed to be represented by the well-known heat equation. The additional term representing the heat transported by the blood stream will be derived using Fick's principle. This principle, when applied to biological systems, can be stated as, "the amount of a substance taken up by an organ (or by the whole body) per unit time is equal to the arterial level of the substance minus the venous level times the blood flow" [54]. When applied to the amount of heat gained (lost) by the blood perfusing an element of tissue, it yields

$$q_b = w_b c_b (T_{i n} - T_{o u t}) \quad (3.1)$$

Equation (3.1), when combined with the heat equation, obtains

$$\rho c_p \frac{\partial T}{\partial t} = \nabla(k \nabla T) + w_b c_b (T_{i n} - T_{o u t}) + q_m \quad (3.2)$$

Equation (3.2) is the mathematical statement of the first law of thermodynamics describing the "in vivo" relationship between the various modes of heat transfer, storage, and production within a biological tissue. It may be referred to as the "bio-heat" equation. Similar forms were obtained by Pennes [8], Hertzman [10], Wissler [18], Perl [22], Chato [40], Trezek [42], and Keller and Seiler [46].

In view of the complexity of the thermal behavior and structure of a living tissue and also because of the lack of accurate, detailed

data of the thermophysical properties and the distribution of blood perfusion and metabolic heat production rates in the body, a number of assumptions should be made to facilitate analytical modeling.

- (1) The thermophysical properties of the tissue will be assumed constant and the tissue will be assumed to be homogeneous and isotropic.
- (2) The temperature of blood leaving the tissue will be assumed equal to the temperature of the tissue. This assumption can be justified by the structure of the capillary bed and the slow rate of flow of blood through the capillaries which makes them almost perfect heat exchangers.
- (3) The temperature of blood entering the tissue will be assumed constant and equal to the temperature of the artery. Later, however, this assumption will be changed and an arbitrary function will be assumed to represent the inlet temperature of blood perfusing the tissue.
- (4) Blood perfusion and metabolic heat production rates will be assumed uniform and constant throughout the entire layer of tissue and will be assumed to represent average values.

Accordingly, Eq. (3.2) becomes

$$\rho c_p \frac{\partial T}{\partial t} = k \nabla^2 T + w_b c_b (T_a - T) + q_m \quad (3.3)$$

Equation (3.3) will be applied to the various layers of tissue and analytical solutions will be given for different geometries and boundary conditions.

The various thermoregulatory mechanisms outlined above are included in the present model indirectly. The major role that these mechanisms play in the thermoregulation of the homeotherm [55] is expressed, among other effects, by the modification of local heat transfer characteristics, such as blood perfusion (vasomotor activity) and metabolic heat production rates (shivering and glandular activity), and the boundary conditions (sweating and pilo-motor activity). Accordingly, the effect of the thermoregulatory mechanisms on the transport of heat in the tissue can be incorporated by properly changing the values of the rate of blood flow and heat generation. The interaction with the environment will be accounted for in the following section via the boundary conditions.

### 3.2 GEOMETRIES, BOUNDARY AND INITIAL CONDITIONS

This study will be primarily concerned with the removal of metabolic heat produced in the body by means of a network of cooling tubes that are in direct contact with the skin. Consequently, it is possible to approximate the very involved geometry of the body by circular cylinders or even by strips of rectangular cross section.

To this end, the tissue is assumed to be divided into three layers:

- (1) A skin layer composed of epidermis, dermis, and subcutaneous fat as shown in Fig. 3.1. The actual thickness of the layer varies from 1-6 mm [56]. All excess metabolic heat will be assumed to be removed at the contact areas between the epidermis and the cooling tubes.

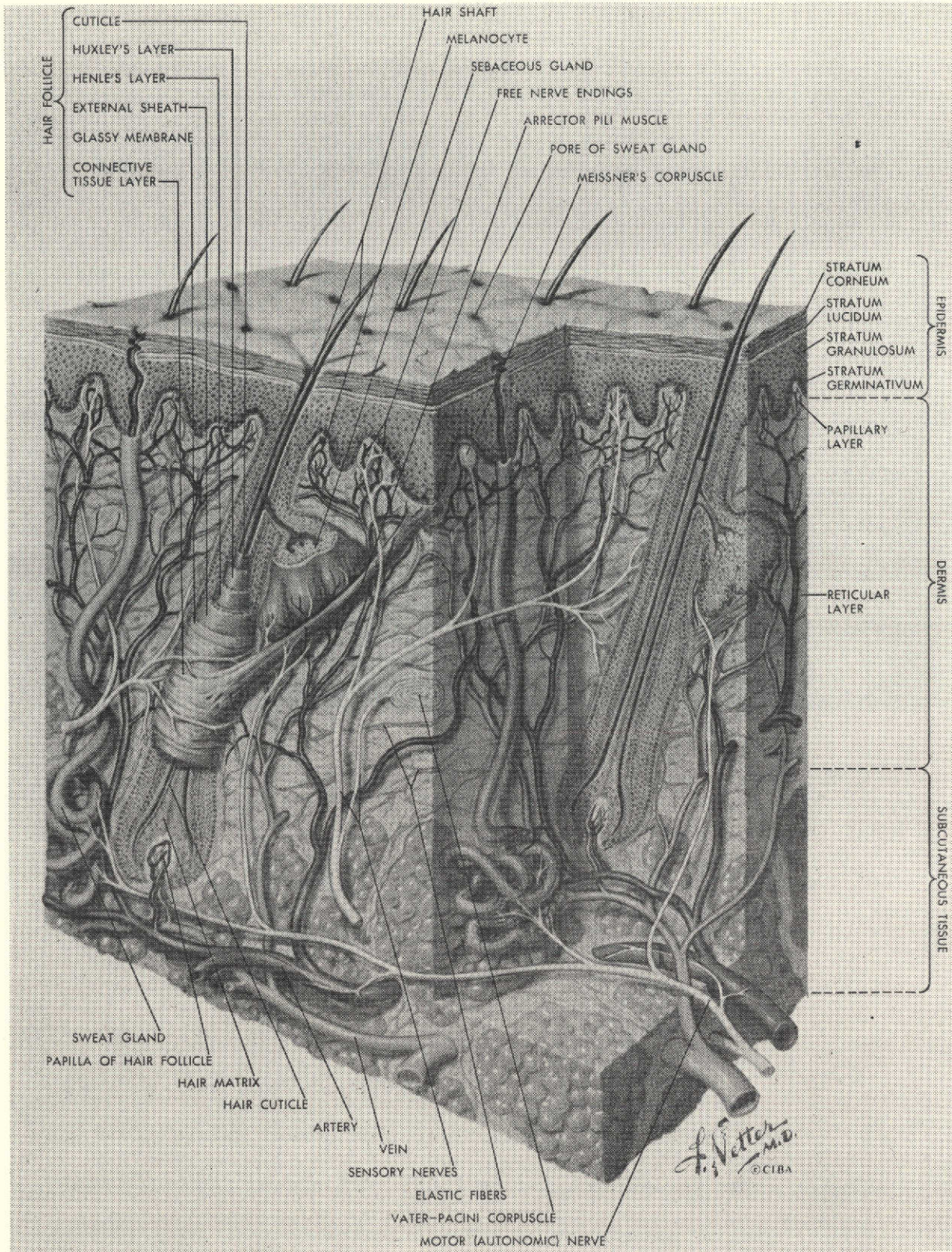


Figure 3.1 Cross section of the normal skin. Copyright, 1967, CIBA Corporation, reproduced with permission from the Clinical Symposia by Frank H. Netter, M.D.

- (2) A layer called skeletal muscle composed of all the muscles.
- (3) An inner core layer consisting of the skeleton and all the internal organs. At steady state, this layer will be assumed to be at a constant temperature which will vary with metabolic rates [57].

Assuming the body to be represented by cylinders of circular cross section, two configurations of cooling tubes seem conceivable:

- (1) The tubes running perpendicular to the axis of the cylinder, Fig. 3.2.
- (2) The tubes running parallel to the axis of the cylinder, Fig. 3.3.

Other intermediate configurations of the cooling tubes can be represented as a combination of these two. However, as the inside diameter of the cylinders becomes larger (which is the case with the trunk, thighs, and lower legs and approximately with the arms, too), the cylindrical configuration can be replaced by strips of rectangular cross section, Fig. 3.4. The calculations of the temperature distribution inside the tissue thus become simpler and easier without any significant loss of accuracy, as is demonstrated later.

As mentioned above, the temperature of the interface between the skeletal muscle and the inner core is assumed constant and uniform and equal to that of the inner core. An assumption of a constant, uniform flux at this interface is also possible and the two will be considered separately. At the skin surface, a heat flux corresponding to the amount of heat to be removed by the tubes will be assumed.

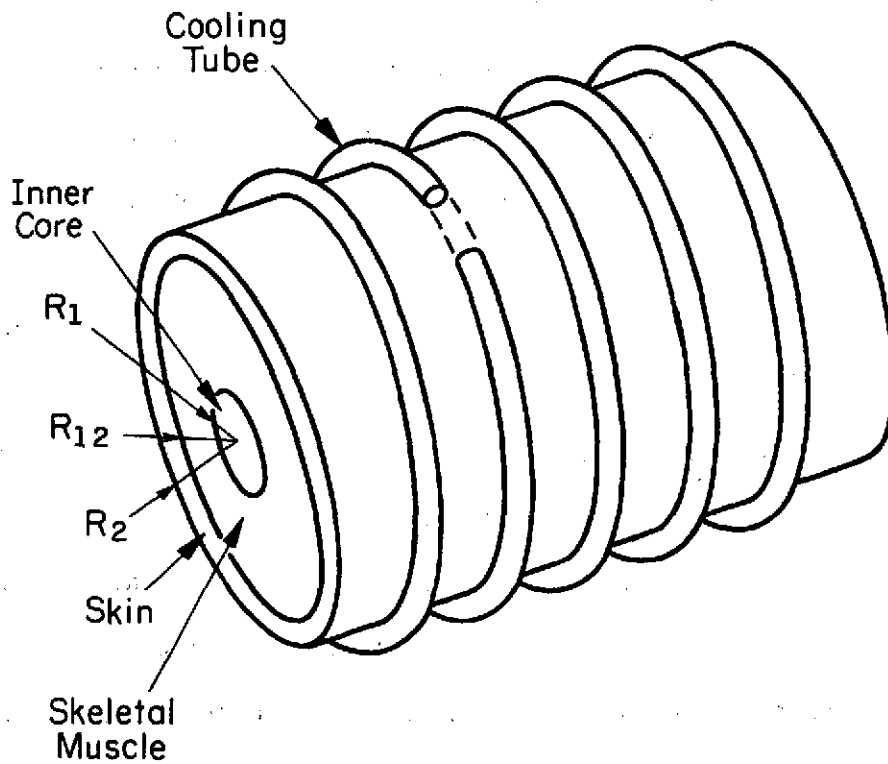


Figure 3.2 Representative section of the cylindrical model with the cooling tubes on the skin running perpendicular to the axis of the cylinder.

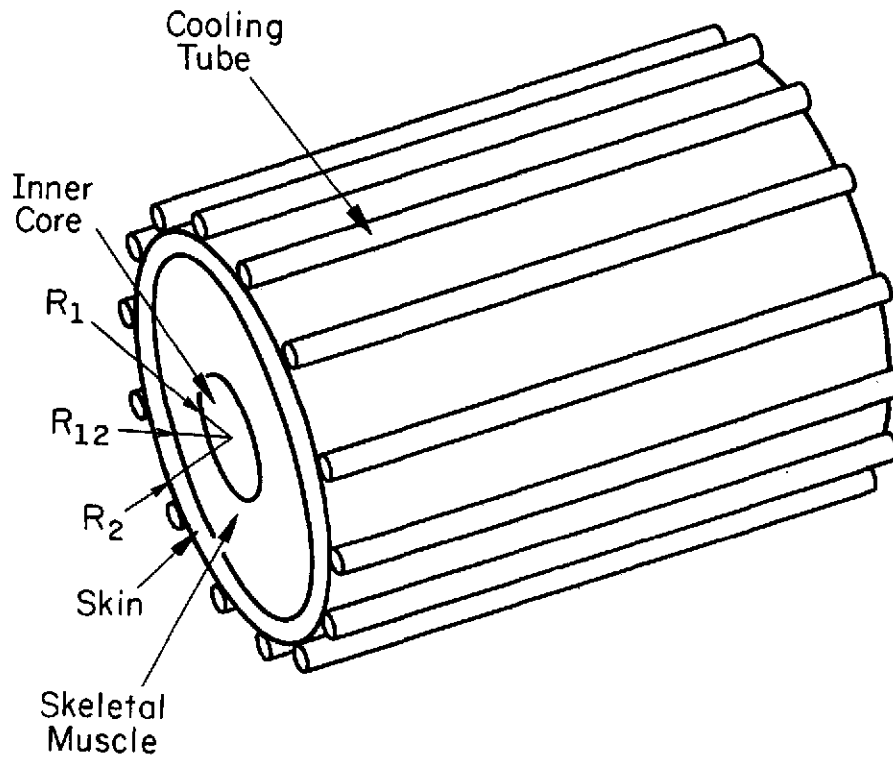


Figure 3.3 Representative section of the cylindrical model with the cooling tubes on the skin running parallel to the axis of the cylinder.

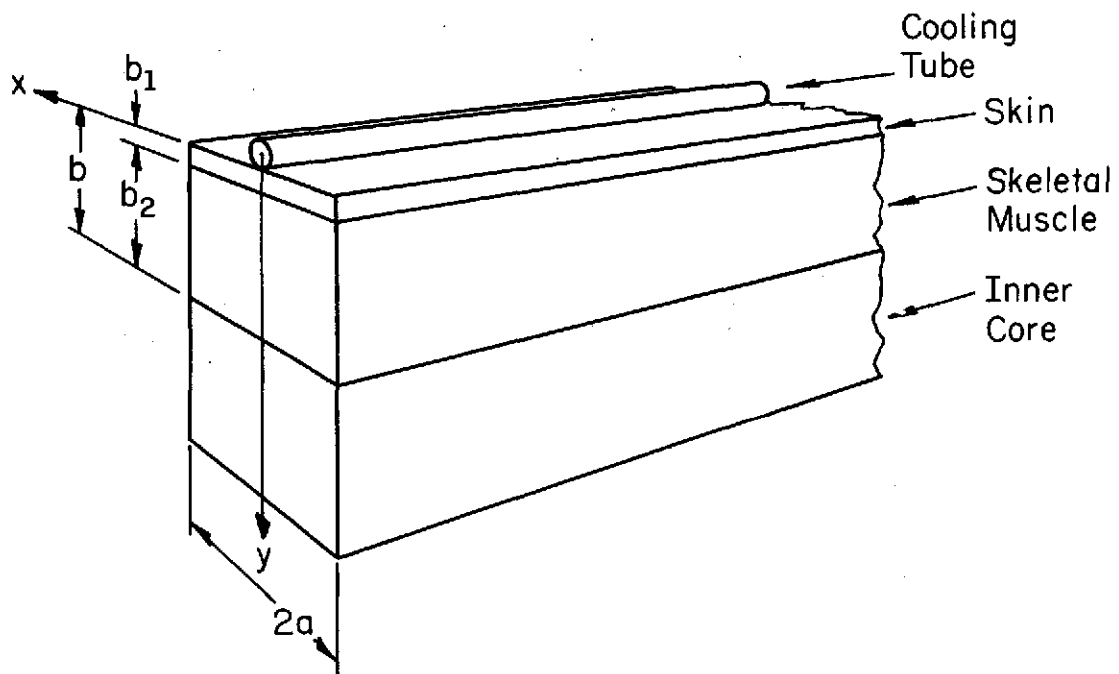


Figure 3.4 Representative section of the rectangular model.

First, an arbitrary distribution of the flux will be assumed,<sup>†</sup> but, later, it will be shown that knowledge of the actual shape of the flux function is not necessary as long as the heat is removed only by the tubes [58]. Because of the symmetry of the problem, the lines of symmetry running through the tubes and half-way between two adjacent tubes can be assumed adiabatic. At the interface between the skin layer and the skeletal muscle, two matching conditions will be satisfied: equal temperatures and equal heat fluxes.

The steady state temperature distribution in the tissue at a given metabolic rate will be assumed to be the initial condition for the transient state.

### 3.3 ANALYTICAL SOLUTIONS

It will be assumed that the changes along the axes of the cooling tubes are small compared to those occurring in the directions perpendicular to the tubes. In mathematical notation, this statement becomes

$$\frac{\partial}{\partial z} = 0 \quad (3.4)$$

and, consequently, the problem becomes two dimensional. Steady state solutions in the two most relevant coordinate systems, i.e., rectangular and cylindrical, will be given first. These solutions will

---

<sup>†</sup>By properly modifying the distribution of the specified flux function over the skin, heat removed by sweat evaporation and convection can be incorporated, too.

be used as initial conditions for the more general transient cases.

### 3.4 STEADY STATE, RECTANGULAR COORDINATES

The first case to be studied is the one with the skin and skeletal muscle considered as separate regions using rectangular coordinates. All metabolic heat is assumed to be removed at the skin along the portion contacted by the cooling tubes. No heat is assumed to be removed at the rest of the skin surface. At the interface between the skeletal muscle and the inner core, a constant temperature, equal to that of the inner core, is assumed. Because of the symmetry of the problem, the boundaries at  $x = 0$  and  $x = a$  are assumed to be adiabatic. Two matching conditions of equal temperature and equal heat flux are satisfied at the interface between the skin and the skeletal muscle. Although the problem as formulated above neglects end effects, it can still be considered general; for, the solution presented below pertains to the areas covered by the cooling pads, modeled as rectangular, symmetrical, two-dimensional strips. Temperature distributions in the tissue underneath the areas not covered by the cooling pads can be obtained by properly modifying the heat flux at the skin while using the same approach as presented below. The problem, in mathematical notation, becomes:

SKIN

$$\frac{\partial^2 \theta_1}{\partial x^2} + \frac{\partial^2 \theta_1}{\partial y_1^2} - w_1^2 \theta_1 = -Q_1 \quad (3.5a)$$

$$0 \leq x \leq a, \quad 0 \leq y_1 \leq b_1$$

$$\text{at } y_1 = b_1, \quad \left\{ \begin{array}{l} \frac{\partial \theta_1}{\partial y_1} = -\frac{f(x)}{k_1}, \quad 0 \leq x < \beta a \\ \frac{\partial \theta_1}{\partial y_1} = 0, \quad \beta a < x \leq a \end{array} \right\} \quad (3.5b)$$

$$\text{at } x = 0, \quad \frac{\partial \theta_1}{\partial x} = 0 \quad (3.5c)$$

$$\text{at } x = a, \quad \frac{\partial \theta_1}{\partial x} = 0 \quad (3.5d)$$

SKELETAL MUSCLE

$$\frac{\partial^2 \theta_2}{\partial x^2} + \frac{\partial^2 \theta_2}{\partial y_2^2} - w_2^2 \theta_2 = -Q_2 \quad (3.6a)$$

$$0 \leq x \leq a, \quad 0 \leq y_2 \leq b_2$$

$$\text{at } y_2 = b_2, \quad \theta_2 = 0 \quad (3.6b)$$

$$\text{at } x = 0, \quad \frac{\partial \theta_2}{\partial x} = 0 \quad (3.6c)$$

$$\text{at } x = a, \quad \frac{\partial \theta_2}{\partial x} = 0 \quad (3.6d)$$

matching conditions at  $y_1 = y_2 = 0$ ,

$$\theta_1 = \theta_2 \quad (3.7a)$$

$$k_1 \frac{\partial \theta_1}{\partial y_1} = -k_2 \frac{\partial \theta_2}{\partial y_2} \quad (3.7b)$$

where

$$\theta_i \equiv T_i(x, y_i) - T_2^* \quad (3.8)$$

$$w_i^2 \equiv \frac{w_i c_b}{k_i} \quad (3.9)$$

$$Q_i \equiv \frac{Q_i'}{k_i} \quad (3.10)$$

$f(x)$  is an arbitrary function representing the flux of heat removed by the cooling tubes at the skin. Figure 3.5 shows the two regions, the coordinate system, and the boundary conditions for this case.

The solutions to the above two simultaneous sets were obtained by using appropriate transformations and Fourier series expansions. In terms of regional temperatures, these solutions are:

For the skin layer,

$$\begin{aligned} T_1(x, y_1) = & T_2^* + \frac{Q_1}{w_1} + E(0) \cosh(w_1 y_1) - \left[ \frac{\beta f_a}{k_1} + \frac{G}{\cosh(w_1 b_1)} \right] \\ & \cdot \frac{\sinh(w_1 y_1)}{w_1} - \left[ \frac{Q_1 k_2 w_2}{w_1^2} + \frac{k_1 G \tanh(w_2 b_2)}{\cosh(w_1 b_1)} \right] \\ & \cdot \frac{\cosh[w_1(b_1 - y_1)]}{H(w)} + k_1 \sum_{n=1}^{\infty} \frac{\alpha_n}{\cosh(\zeta_1 b_1)} \\ & \left\{ \frac{\tanh(\zeta_2 b_2) \cosh[\zeta_1(b_1 - y_1)]}{H(\zeta)} \right. \\ & \left. + \frac{\sinh(\zeta_1 y_1)}{k_1 \zeta_1} \right\} \cos(\lambda_n x) \quad (3.11) \end{aligned}$$

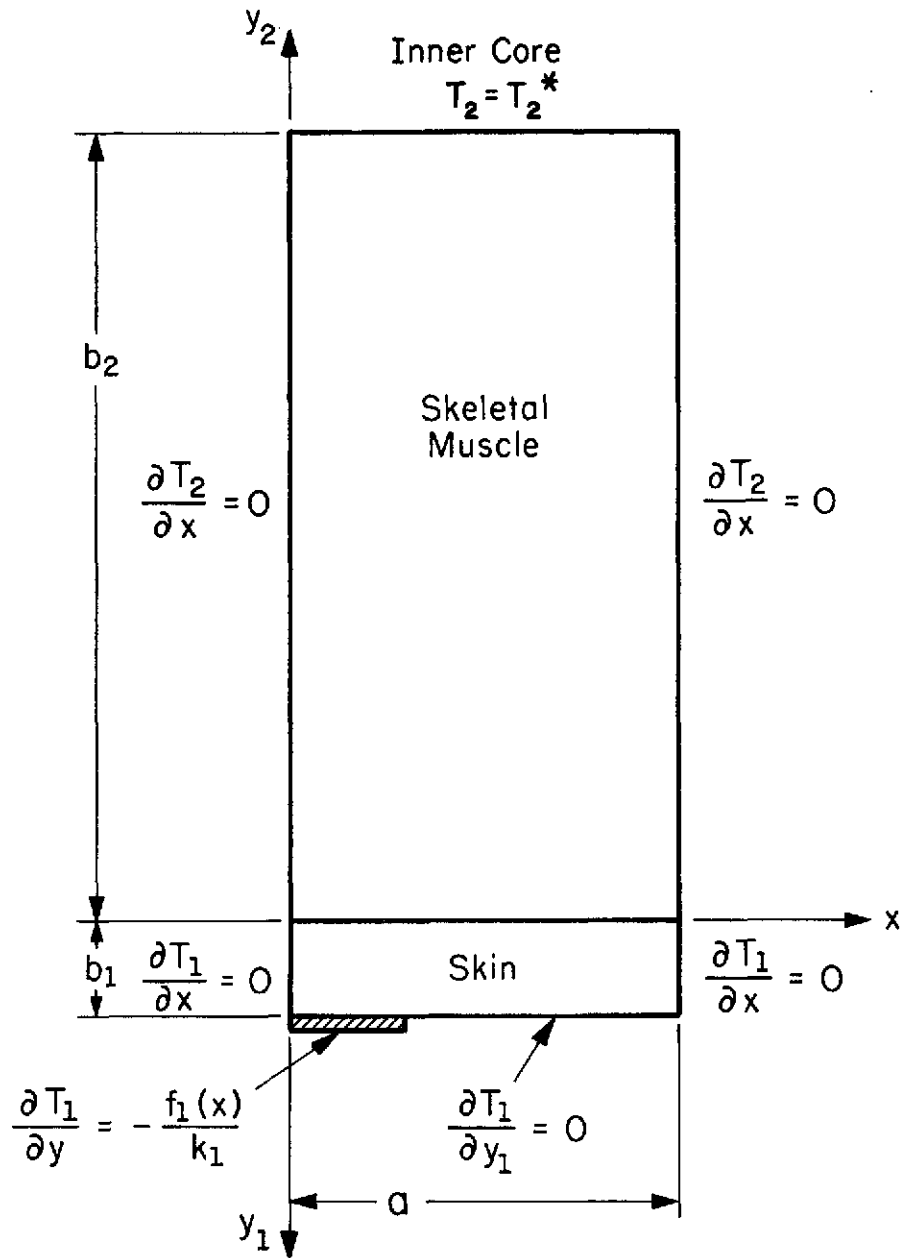


Figure 3.5 Geometry and boundary conditions for the rectangular model. Skin layer and skeletal muscle are considered as separate regions.

For the skeletal muscle layer,

$$\begin{aligned}
 T_2(x, y_2) = & T_2^* + E(y_2) + \left[ \frac{Q_1 \sinh(w_1 b_1)}{w_1} - G \right] \\
 & \cdot \frac{k_1 \sinh[w_2(b_2 - y_2)]}{H(w) \cosh(w_2 b_2)} + k_1 \sum_{n=1}^{\infty} \\
 & \cdot \frac{\alpha_n \sinh[\zeta_2(b_2 - y_2)]}{H(\zeta) \cosh(\zeta_2 b_2)} \cos(\lambda_n x)
 \end{aligned} \tag{3.12}$$

where

$$E(y) \equiv \frac{Q_2}{w_2} \left[ 1 - \frac{\cosh(w_2 y)}{\cosh(w_2 b_2)} \right] - \frac{\beta f_a}{k_2 w_2} \frac{\sinh[w_2(b_2 - y)]}{\cosh(w_2 b_2)} \tag{3.13}$$

$$G \equiv w_1 E(0) \sinh(w_1 b_1) - \frac{\beta f_a}{k_1} [\cosh(w_1 b_1) - 1] \tag{3.14}$$

$$H(\zeta) \equiv k_2 \zeta_2 \cosh(\zeta_1 b_1) + k_1 \zeta_1 \sinh(\zeta_1 b_1) \tanh(\zeta_2 b_2) \tag{3.15}$$

$$f_a = \frac{1}{\beta a} \int_0^{\beta a} f(\xi) d\xi \tag{3.16}$$

$$\zeta_1^2 \equiv w_1^2 + \lambda_n^2 \tag{3.17}$$

$$\lambda_n \equiv \frac{n\pi}{a} \tag{3.18}$$

$$\alpha_n \equiv \frac{2}{a} \int_0^{\beta a} \frac{f(x)}{k_1} \cos(\lambda_n \xi) d\xi \tag{3.19}$$

Equations (3.11) through (3.19) were programmed on the digital computer and temperature distributions for various values of parameters and metabolic rates were obtained. TABLE 3.1 gives dimensions and thermophysical properties of the model used for the numerical

TABLE 3.1

PHYSICAL AND PHYSIOLOGICAL PROPERTIES OF THE RECTANGULAR BIOTHERMAL MODEL CORRESPONDING TO A 139 LB (63 KG) ADULT MALE WITH 90 MM HG MEAN ARTERIAL BLOOD PRESSURE AND TOTAL METABOLIC RATE OF 290 BTU/HR (85 W). REPRODUCED IN PARTS FROM BUCHBERG AND HARRAH [39] AND BRAD [59].†

Property		Region				
		Skin	Skeletal Muscle	Inner Core		Whole Body
				Heart Muscle	Rest of Body	
Mass	kg	3.6	31.0	0.3	28.1	63.0
	lb	7.94	68.40	0.66	62.00	139.00
Volume	m <sup>3</sup>	0.00350	0.02800	0.00028	0.02700	0.05878
	ft <sup>3</sup>	0.125	1.000	0.010	0.965	2.100
Depth	m	0.02475	0.019800	--	0.019350	0.041625
	ft	0.00812	0.06500	--	0.06350	0.13662
Width of Strip	m	0.01945	0.01945	--	0.01945	--
	ft	0.064	0.064	--	0.064	--
Blood Flow Rate	ml/min	462	840	250	3848	5400
	ft <sup>3</sup> /min	0.0165	0.0300	0.1375	0.0089	0.1929

†These numerical values were used in the computations, but they do not imply accuracies corresponding to the number of digits given.

(continued)

TABLE 3.1 continued

Property		Region				
		Skin	Skeletal Muscle	Inner Core		Whole Body
				Heart Muscle	Rest of Body	
Oxygen Consumption	ml/min	12	50	29	159	250
	ft <sup>3</sup> /min	0.000429	0.001785	0.001035	0.005675	0.008924
Percent of Total	Blood Flow Rate	8.6	15.6	4.7	71.1	100.0
	Oxygen Consumption	4.8	20.0	11.6	63.6	100.0
Thermal Conductivity	w/m-°C	0.419	0.540	--	--	--
	Btu/hr-ft-°F	0.242	0.311	--	--	--

computations. The first twenty terms of the series were used in the numerical solution. It was found that by doing so the truncation error introduced was less than 0.01; i.e.,  $|\alpha_{20}| - |\alpha_{21}| < 0.01$  °F/ft. A typical temperature distribution in the tissue for one set of parameters is shown in Fig. 3.6.

Three observations were made based on the preceding analysis:

- (1) If  $y/x > 2$  (the ratio of  $b/a$  in the present rectangular model was about 2.3), the isotherms become essentially independent of  $x$ ; i.e., the isotherms become parallel and a function of depth only as illustrated in Fig. 3.6. This observation leads to the conclusion that, at the interface between the inner core and the skeletal muscle, the boundary conditions of constant, uniform flux or temperature become identical for any practical purposes. From a physiological standpoint, this conclusion is not surprising. It is known that, in a steady state, inner body temperature is maintained at a fairly constant level while, at the same time, most of the heat generated inside the body is removed at the skin. The heat to be removed at the skin is transported there by the blood stream and by conduction through the tissue, mechanisms that are included in the present mathematical model.
- (2) One of the most difficult parameters to assess is the shape of the flux at the portion of the skin contacted by the cooling tubes. Fortunately, it was demonstrated [58] that the actual shape of this function is not of great importance

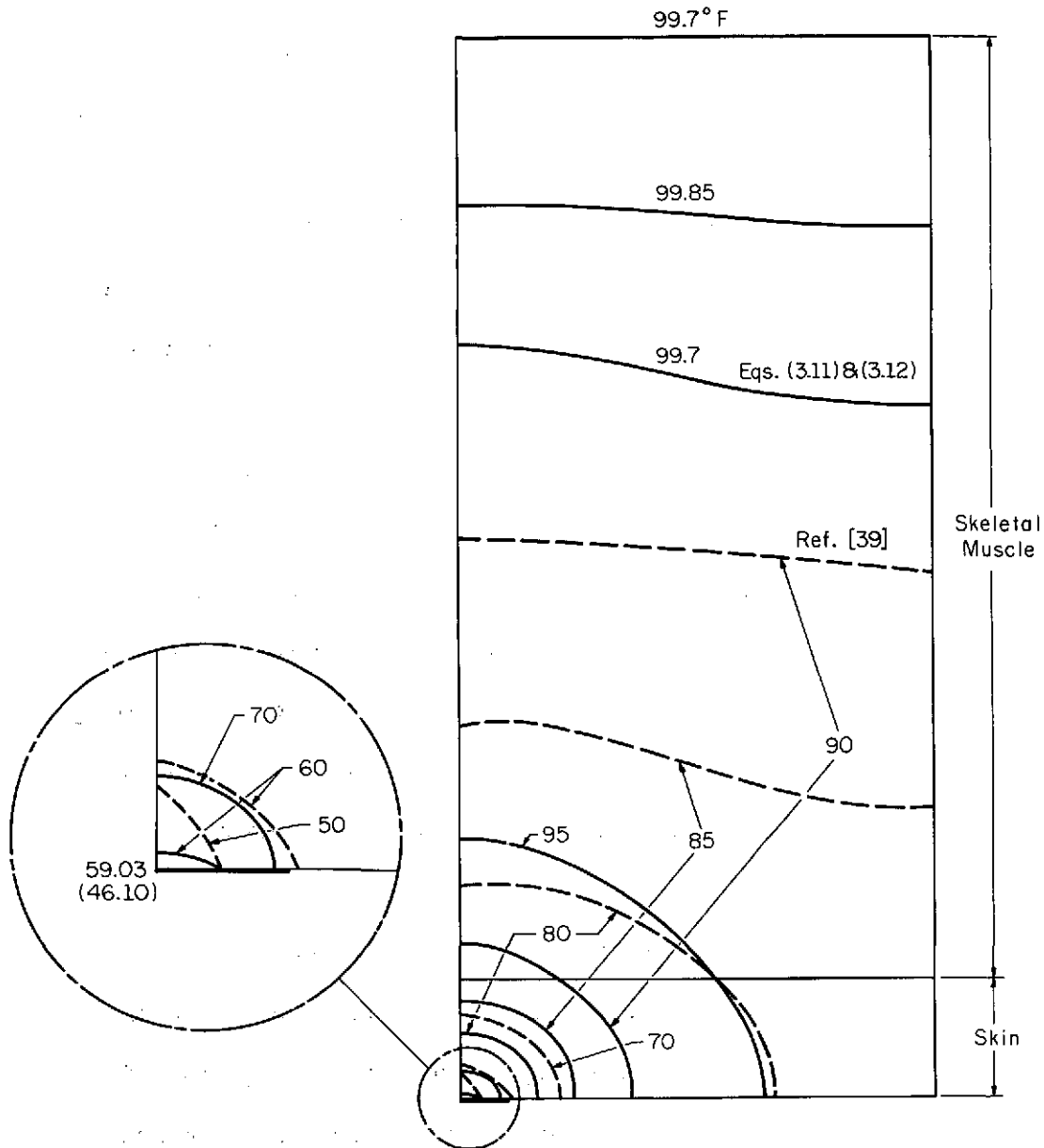


Figure 3.6 Temperature distribution in the separated tissue for the rectangular model. Dashed curves indicate temperature distribution obtained by Buchberg and Harrah [39] without blood flow.  $Q_m = 2600$  Btu/hr, (760 w),  $\beta = 0.1$  and constant temperature at inner core.

so long as it provides for the removal of all the excessive heat at the skin. This was done by assuming an arbitrary, linear heat flux function at the skin. This function varied from its maximum value at  $x = 0$  (centerline of the cooling tube) to  $2/3$  of the maximum at  $x = \beta a$  (edge of the cooling tube) or  $f_2/f_1 = 1.5$ . The mean value of the flux over the area covered by the cooling tube was taken to correspond to the appropriate amount of heat to be removed. As a second choice, this function was reversed; i.e.,  $f_2/f_1 = 1/1.5$ . With these two extreme assumptions, the temperature distribution in the tissue was evaluated. The effect of selecting different flux functions at the skin was noticeable only in the vicinity of the cooling tubes and became indistinguishable at a very short distance away. Thus, knowledge of the exact shape of the flux function is not essential and the error introduced by various functions is insignificant so long as the above obvious condition is satisfied. Figure 3.7 demonstrates this finding. Figure 3.8 shows the effect of increasing the contact area between the cooling tubes and the skin (increasing  $\beta$ ) while  $f_2/f_1$  is maintained at 1.5.

- (3) It was found that, if  $b \cdot (w_b c_b / k)^{1/2} > 2.3$ , the maximum temperature of the body occurs in the skeletal muscle rather than in the inner core. This observation demonstrates, among other things, the important role that the blood stream plays in the transport of heat in the body; for, without

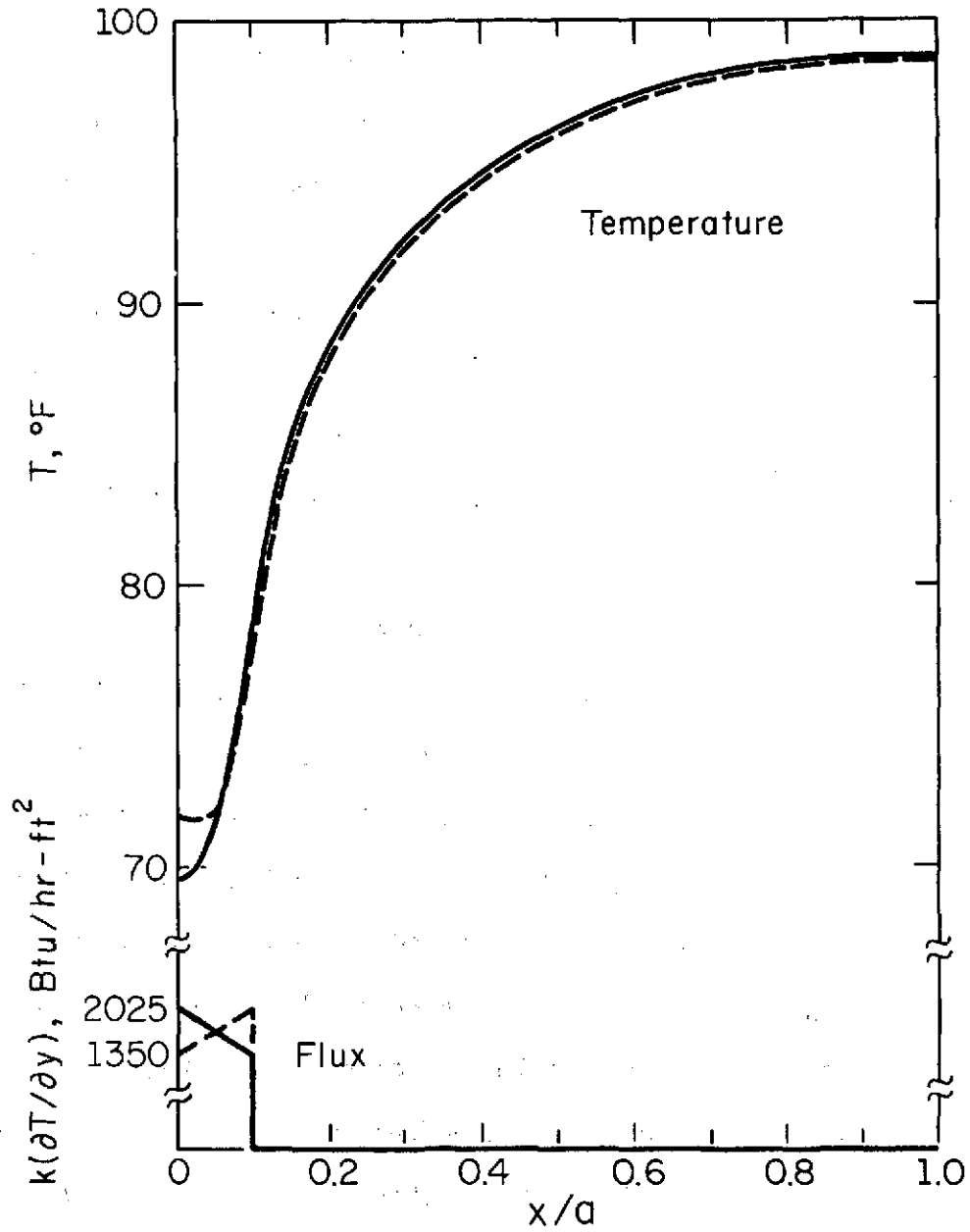


Figure 3.7 Effect of changing the specified flux function on the temperature of the skin for the rectangular model.  $Q_m = 2600$  Btu/hr, (760 w),  $\beta = 0.1$  and constant temperature at inner core.

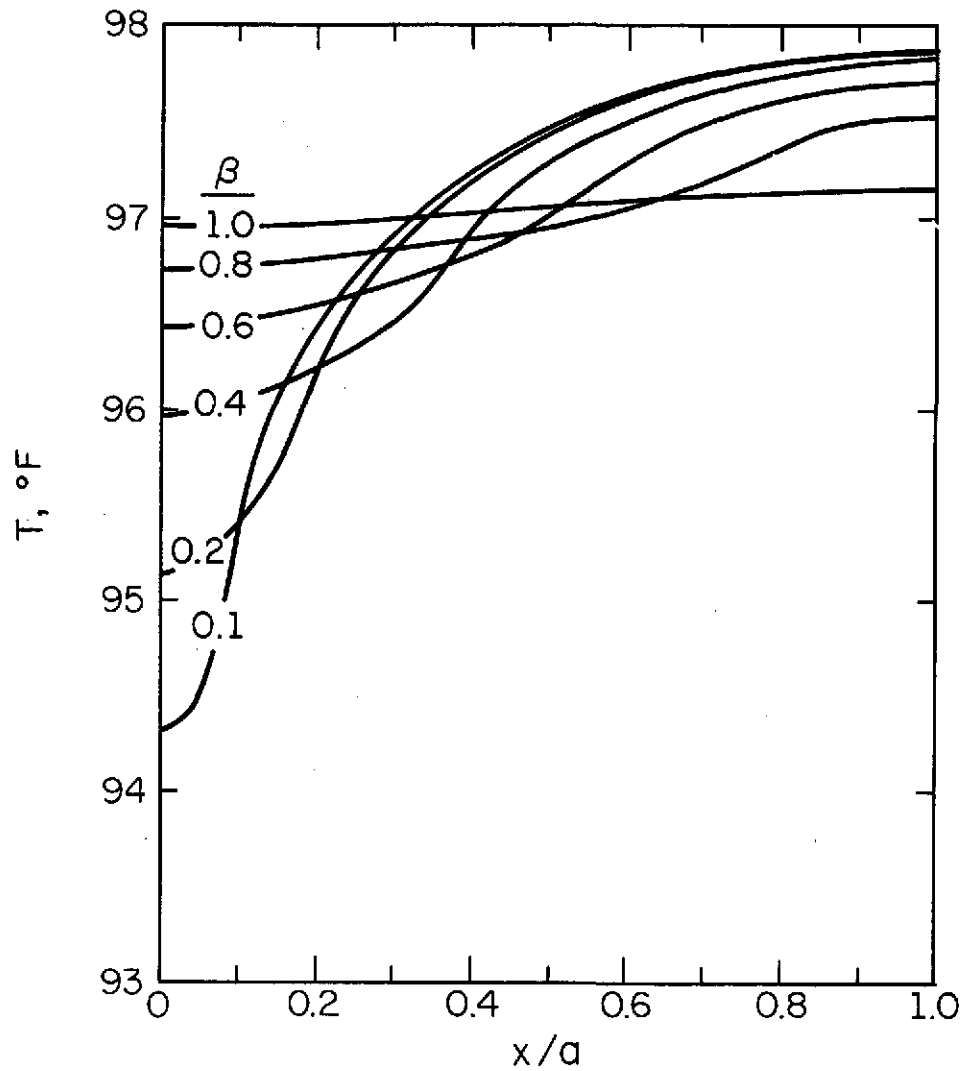


Figure 3.8 Effect of increasing the contact area between the cooling tubes and the skin on the temperature distribution on the skin surface.  $Q_m = 290$  Btu/hr (85 w),  $f_2/f_1 = 1.5$  and constant temperature at inner core.

this mode of heat transfer, the occurrence of a maximum temperature inside the tissue will mean inability to adequately dissipate heat with all the acute physiological consequences. Only heat transported by the blood stream can by-pass this "barrier" and reach the skin where it will eventually be removed. From a mathematical standpoint, when the term representing blood flow is not included in Eq. (3.3), as was done by Buchberg and Harrah [39], the above-mentioned phenomenon does not occur (Fig. 3.6, dashed lines). However, there are cases when blood flow reduces significantly or even vanishes; e.g., vasoconstriction. Therefore, a solution for this limiting case,  $w_b \rightarrow 0$ , is presented and compared in APPENDIX B with the more general result that includes blood flow and the results of Ref. [39].

As was mentioned before, very little accurate and reliable data are available pertaining to the thermophysical properties of the tissue, local blood perfusion and metabolic heat production rates. The most comprehensive source of thermophysical properties was given by Chato [50]. Scant physiological data can be found in medical or physiological textbooks, such as the one by Brad [59]. Consequently, any attempt to improve on the preceding analysis will have to be delayed until such data become available.

Nevertheless, two additional sets of solutions will be given. The first additional solution is less detailed than the previous one. It is obtained when the skin and skeletal muscle zones are combined

to form a single zone.† The result is of gross nature, but, in view of the inadequacy of the available data, it is almost as good as the more complete one with the two zones separated and is easier for computation. This case is presented and discussed in APPENDIX C.

The second additional solution assumes a variable, arbitrary blood supply temperature rather than a constant one. Since this solution is more detailed and requires more information on the actual changes that the temperature of the blood perfusing the tissue undergoes, it seemed sufficient to assume a one-dimensional model with uniform flux at the skin. It is believed that the extension of this solution to two dimensions should not present any major difficulties.

In mathematical notation,

$$\frac{d^2 T}{dy^2} + w^2 [\theta^*(y) - T] = -Q \quad (3.20a)$$

and the boundary conditions are

$$\text{at } y = 0, \quad \frac{dT}{dy} = \frac{F}{k} \quad (3.20b)$$

$$\text{at } y = b, \quad T = T_1 \quad (3.20c)$$

where  $F$  is the uniform flux at the skin.

This set was integrated using a Green function [60],

---

†This procedure amounts to carrying the above solution to the limit  $b_1 \rightarrow 0$  and  $b_2 \rightarrow b$ , or  $b_2 \rightarrow 0$  and  $b_1 \rightarrow b$ , while assuming  $k_1 = k_2$ ,  $w_1 = w_2$ , and  $Q_1 = Q_2$  and reversing the sign of the flux at the skin.

$$G(y, \tau) = \begin{cases} \frac{\Phi_1(\tau)\Phi_2(y)}{W[\Phi_1, \Phi_2]}, & y < \tau \\ \frac{\Phi_1(y)\Phi_2(\tau)}{W[\Phi_1, \Phi_2]}, & y > \tau \end{cases} \quad (3.21)$$

where  $\Phi_1(y)$  and  $\Phi_2(y)$  are two independent solutions of the homogeneous differential equation,

$$\Phi''(y) - w^2\Phi(y) = 0 \quad (3.22a)$$

satisfying,

$$\Phi_1'(0) = 0 \quad (3.22b)$$

$$\Phi_2(b) = 0 \quad (3.22c)$$

namely,

$$\Phi_1(y) = \cosh(wy) \quad (3.23a)$$

$$\Phi_2(y) = \sinh[w(b-y)] \quad (3.23b)$$

and  $W[\Phi_1, \Phi_2]$  is the Wronskian defined

$$W[\Phi_1, \Phi_2] = \begin{vmatrix} \Phi_1 & \Phi_2 \\ \Phi_1' & \Phi_2' \end{vmatrix} \quad (3.24)$$

The solution obtained is

$$\begin{aligned}
T(y) = T_1 + \frac{Q}{w} \left[ 1 - \frac{\cosh (wy)}{\cosh (wb)} \right] - \frac{F}{kw} \frac{\sinh [w(b-y)]}{\cosh (wb)} \\
- \frac{w}{\cosh (wb)} \left\{ \sinh [w(b-y)] \int_0^y Y(\tau) \cosh (w\tau) d\tau \right. \\
\left. + \cosh (wy) \int_y^b Y(\tau) \sinh [w(b-\tau)] d\tau \right\} \quad (3.25)
\end{aligned}$$

where, with the dummy variable  $\tau$  replaced by  $y$ ,

$$Y(y) = T_1 - \theta^*(y) \quad (3.26)$$

and  $\theta^*(y)$  is an arbitrary function describing the variations of the blood supply temperature. Figure 3.9 shows typical results obtained for assumed linear temperature variations of the blood supply. It can be seen that, as the slope of blood supply temperature increases, skin temperature decreases and the maximum temperature of the tissue is shifted toward the inner core.

If the boundary condition at the inner core, Eq. (3.20c) is changed

$$\text{at } y = b, \quad \frac{dT}{dy} = \frac{F_o}{k} \quad (3.27)$$

(uniform flux instead of uniform temperature), a solution for the temperature inside the tissue can be obtained by employing the finite cosine Fourier transform

$$C\{\Phi(y)\} = \int_0^b \Phi(\tau) \cos (v_n \tau) d\tau \quad (3.28)$$

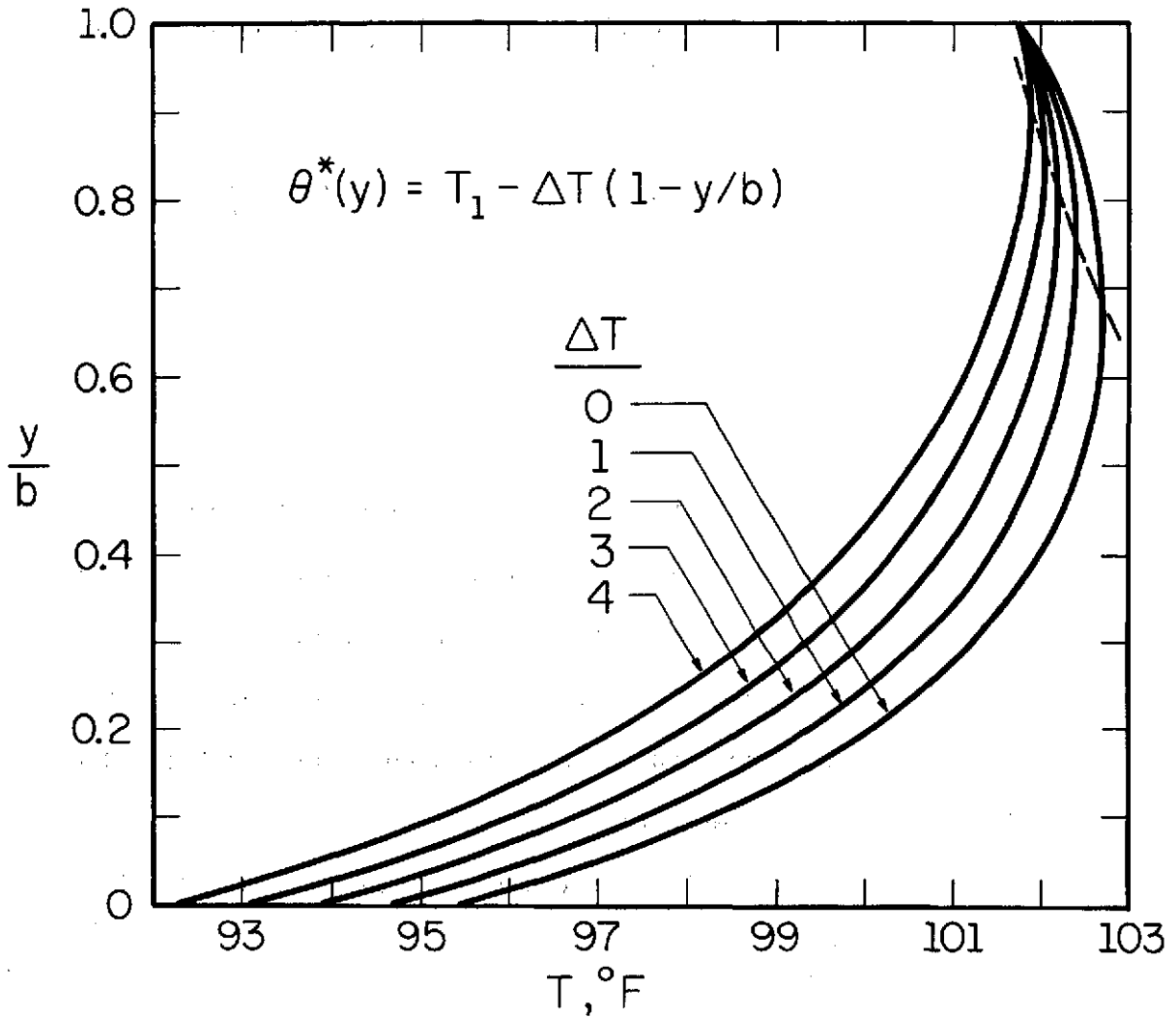


Figure 3.9 Steady state, one dimensional temperature distribution in the combined tissue with variable, linear blood supply temperature for the rectangular model. Dashed line indicates locus of maxima.  $Q_m = 2600$  Btu/hr (760 w), and constant temperature at inner core.

$$C\{\Phi''(y)\} = -v_n^2 C\{\Phi(y)\} + (-1)^n \Phi'(b) - \Phi'(0) \quad (3.29)$$

to obtain

$$T(y) = T_{ref} + \frac{Q}{w} + \frac{1}{kw} \frac{F_o \cosh(wy) - F \cosh[w(b-y)]}{\sinh(wb)} + \frac{1}{b} \left\{ \int_0^b \theta^*(\tau) d\tau + 2w^2 \sum_{n=1}^{\infty} \frac{\int_0^b \theta^*(\tau) \cos(v_n \tau) d\tau}{w^2 + v_n^2} \right\} \quad (3.30)$$

where

$$v_n = \frac{n\pi}{b} \quad (3.31)$$

and  $\theta^*(y)$  is the arbitrary function defined above.

### 3.5 STEADY STATE, CYLINDRICAL COORDINATES

In many cases, a closer approximation of the geometry of the human body is achieved by representing it as a set of cylinders. This is particularly true for the extremities and was used by many investigators [8,16,18,31,33].

Two general cases were studied: the cooling tubes running on the skin perpendicular to the cylinder (limb) axis, Fig. 3.2, and the tubes running parallel to the axis, Fig. 3.3. The first case was studied with the two zones separated, whereas only a solution for the combined tissue was obtained for the second.

The geometry of the first case (assuming the gradients along the axis of the cylinder to be negligible compared to those in the plane perpendicular to it) is essentially rectangular and similar to the one shown in Fig. 3.5. For completeness, the exact geometry and boundary conditions are shown in Fig. 3.10.

The mathematical formulation for this case is

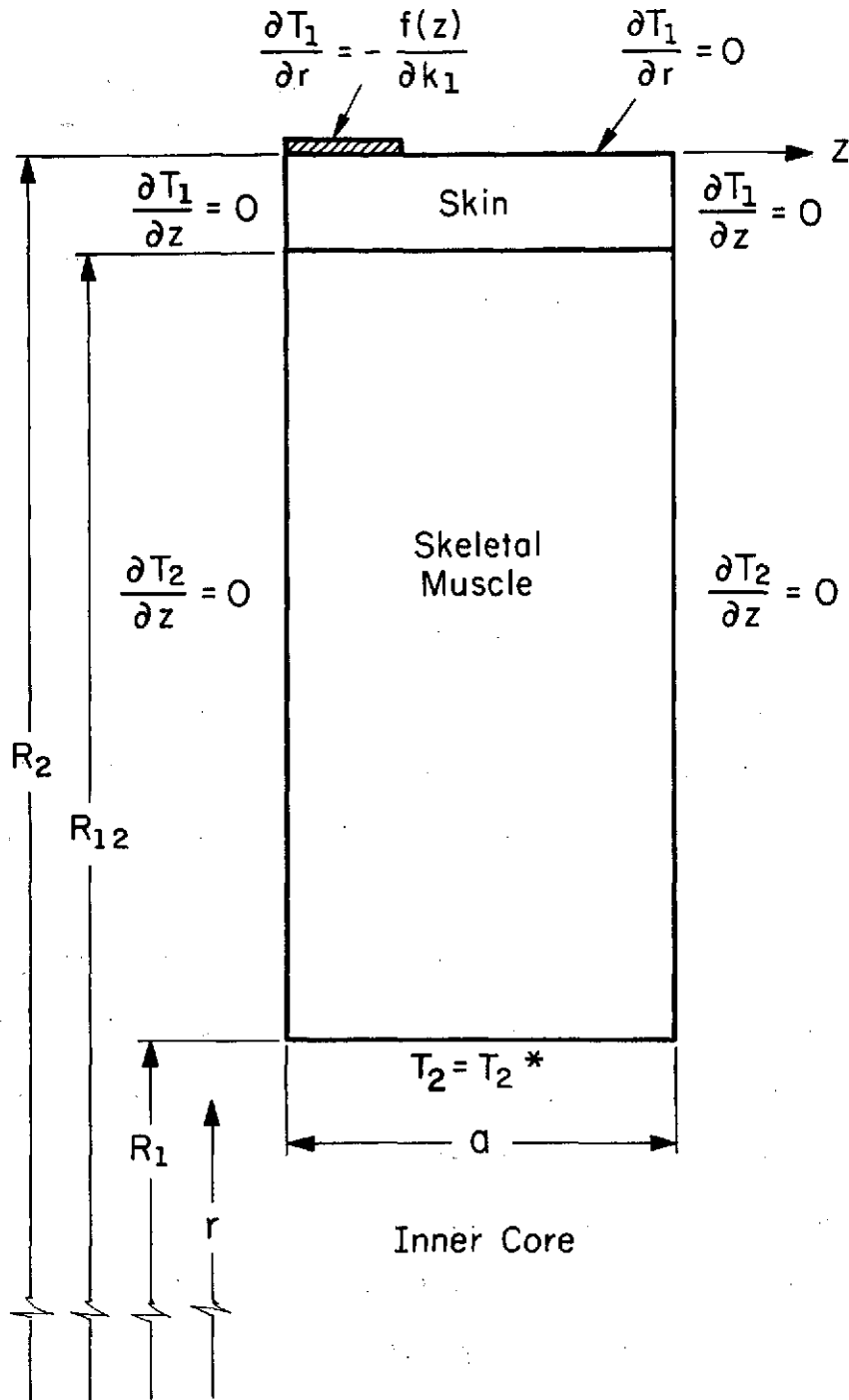


Figure 3.10 Geometry and boundary conditions for the cylindrical model with the cooling tubes on the skin running perpendicular to the axis of the cylinder. Skin layer and skeletal muscle are considered as separate regions.

SKIN

$$\frac{1}{r} \frac{\partial}{\partial r} \left( r \frac{\partial \theta_1}{\partial r} \right) + \frac{\partial^2 \theta_1}{\partial z^2} - w_1^2 \theta_1 = -Q_1 \quad (3.32a)$$

$$R_{12} < r \leq R_2; \quad 0 \leq z \leq a$$

$$\text{at } r = R_2, \quad \left\{ \begin{array}{l} \frac{\partial \theta_1}{\partial r} = -\frac{f(z)}{k_1}, \quad 0 \leq z < \beta a \\ \frac{\partial \theta_1}{\partial r} = 0, \quad \beta a < z \leq a \end{array} \right\} \quad (3.32b)$$

$$\text{at } z = 0, \quad \frac{\partial \theta_1}{\partial z} = 0 \quad (3.32c)$$

$$\text{at } z = a, \quad \frac{\partial \theta_1}{\partial z} = 0 \quad (3.32d)$$

SKELETAL MUSCLE

$$\frac{1}{r} \frac{\partial}{\partial r} \left( r \frac{\partial \theta_2}{\partial r} \right) + \frac{\partial^2 \theta_2}{\partial z^2} - w_2^2 \theta_2 = -Q_2 \quad (3.33a)$$

$$R_1 \leq r < R_{12}; \quad 0 \leq z \leq a$$

$$\text{at } r = R_1, \quad \theta_2 = 0 \quad (3.33b)$$

$$\text{at } z = 0, \quad \frac{\partial \theta_2}{\partial z} = 0 \quad (3.33c)$$

$$\text{at } z = a, \quad \frac{\partial \theta_2}{\partial z} = 0 \quad (3.33d)$$

matching conditions at  $r = R_{12}$ ,

$$\theta_1 = \theta_2 \quad (3.34a)$$

$$k_1 \frac{\partial \theta_1}{\partial r} = k_2 \frac{\partial \theta_2}{\partial r} \quad (3.34b)$$

where all the parameters are defined by Eqs. (3.8), (3.9), and (3.10).

The solution obtained is:

For the skin layer ( $R_{12} < r \leq R_2$ ),

$$\begin{aligned}
 T_1(r, z) = & T_2^* + \Lambda(w_2 R_{12}) \frac{\psi_{01}^{12}(w_1 r)}{\psi_{01}^{12}(w_1 R_{12})} + \frac{\beta f_a}{k_1 w_1} \frac{\psi_{00}^{12}(w_1 r)}{\psi_{10}^{12}(w_1 R_{12})} \\
 & - \frac{M}{w_1 K_1(w_1 R_2)} \\
 & \cdot \left[ \frac{k_2 w_2 K_0(w_1 R_{12}) \psi_{10}^1(w_2 R_{12}) - k_1 w_1 K_1(w_1 R_{12}) \psi_{00}^1(w_2 R_{12})}{\Omega(w R_{12})} \right. \\
 & \cdot \left. \psi_{01}^2(w_1 r) - K_0(w_1 r) \right] \\
 & + \frac{Q_1}{w_1} \left[ 1 + \frac{w_2 k_2 \psi_{10}^1(w_2 R_{12}) \psi_{01}^2(w_1 r)}{\Omega(w R_{12})} \right] - \sum_{n=1}^{\infty} \frac{\alpha_n}{\zeta_1 K_1(\zeta_1 R_2)} \\
 & \cdot \left\{ \frac{k_2 \zeta_2 K_0(\zeta_1 R_{12}) \psi_{10}^1(\zeta_2 R_{12}) + k_1 \zeta_1 K_1(\zeta_1 R_{12}) \psi_{00}^1(\zeta_2 R_{12})}{\Omega(\zeta R_{12})} \right. \\
 & \cdot \left. \psi_{01}^2(\zeta_1 r) - K_0(\zeta_1 r) \right\} \cos(\lambda_n z) \quad (3.35)
 \end{aligned}$$

For the skeletal muscle ( $R_1 \leq r < R_{12}$ ),

$$\begin{aligned}
T_2(r, z) = & T_2^* + \Lambda(w_2 r) + \frac{Q_1}{w_1} \frac{w_1 k_1 \psi_{11}^2(w_1 R_{12}) \psi_{00}^1(w_2 r)}{\Omega(w R_{12})} \\
& + \frac{k_1 M}{K_1(w_1 R_2)} \\
& \cdot \frac{K_1(w_1 R_{12}) \psi_{01}^2(w_1 R_{12}) + K_0(w_1 R_{12}) \psi_{11}^2(w_1 R_{12})}{\Omega(w R_{12})} \psi_{00}^1(w_2 r) \\
& - k_1 \sum_{n=1}^{\infty} \frac{\alpha_n}{K_1(\zeta_1 R_2)} \\
& \cdot \frac{K_1(\zeta_1 R_{12}) \psi_{01}^2(\zeta_1 R_{12}) + K_0(\zeta_1 R_{12}) \psi_{11}^2(\zeta_1 R_{12})}{\Omega(\zeta R_{12})} \\
& \cdot \psi_{00}^1(\zeta_2 r) \cos(\lambda_n z) \tag{3.36}
\end{aligned}$$

where

$$\psi_{k\ell}^j(\zeta_i r) \equiv I_k(\zeta_i r) K_\ell(\zeta_i R_j) + (-1)^{k+\ell+1} I_\ell(\zeta_i R_j) K_k(\zeta_i r) \tag{3.37}$$

$$\Lambda(wr) \equiv \frac{Q_2}{w} \left[ 1 - \frac{\psi_{01}^{12}(wr)}{\psi_{01}^{12}(w R_{12})} \right] - \frac{\beta F_a}{k_2 w} \frac{\psi_{00}^1(wr)}{\psi_{10}^1(w R_{12})} \tag{3.38}$$

$$\begin{aligned}
\Omega(\zeta R_{12}) \equiv & k_1 \zeta_1 \psi_{11}^2(\zeta_1 R_{12}) \psi_{00}^1(\zeta_2 R_{12}) \\
& - k_2 \zeta_2 \psi_{01}^2(\zeta_1 R_{12}) \psi_{10}^1(\zeta_2 R_{12}) \tag{3.39}
\end{aligned}$$

$$\begin{aligned}
M \equiv & - \frac{\beta F_a}{k_1} \left\{ 1 - \frac{\psi_{10}^{12}(w_1 R_2)}{\psi_{10}^{12}(w_1 R_{12})} \right. \\
& \left. + \frac{k_1 w_1 \psi_{00}^1(w_2 R_{12}) \psi_{11}^{12}(w_1 R_2)}{k_2 w_2 \psi_{10}^1(w_2 R_{12}) \psi_{10}^{12}(w_1 R_{12})} \right\} \tag{3.40}
\end{aligned}$$

Observing that [61]

$$\psi_{k, k+1}^j(w R_j) = \frac{1}{w R_j} \tag{3.41}$$

Equation (3.40) can be rewritten

$$M \equiv - \frac{\beta f_a}{k_1} \left\{ 1 - (w_1 R_{12}) \psi_{10}^{12}(w_1 R_2) + \frac{k_1 w_1^2 R_{12}}{k_2 w_2} \cdot \frac{\psi_{00}^1(w_2 R_{12}) \psi_{11}^{12}(w_1 R_2)}{\psi_{10}^1(w_2 R_{12})} \right\} \quad (3.42)$$

$I_i$  and  $K_i$  are the modified Bessel functions of the first and second kind of order  $i$  and  $w_i$ ,  $f_a$ ,  $\xi_i$ ,  $\lambda_n$ , and  $\alpha_n$  are defined by Eqs. (3.9), (3.16), (3.17), (3.18), and (3.19), respectively.

The solution to the cylindrical case exhibits the same characteristics as the one for the rectangular case. However, it is more difficult to obtain numerical results because of the presence of the Bessel functions in the series part of the solution. Still, temperature distribution of limited accuracy for this case for the skin layer and skeletal muscle considered as one combined tissue is shown in Fig. E.1. Fortunately, it was found that, without any significant loss in accuracy, the rectangular case yields results that are remarkably close to the cylindrical ones, as will be demonstrated in a separate chapter.

A special function,  $\psi_{k\ell}^j(\zeta_1, r)$ , was defined to simplify the mathematical derivation, Eq. (3.37). It is a combination of modified Bessel functions of the first and second kind which was found to recur in the solution many times. This function is further discussed in some detail in APPENDIX D.

As was done for the rectangular model, additional solutions for the combined tissue, including the limiting ones for no blood flow, are presented in APPENDIX E.

The second steady state case in cylindrical coordinates is the one with the cooling tubes running parallel to the cylinder axis. Figure 3.11 shows the geometry and boundary conditions for this case.

The mathematical formulation for this case is

$$\frac{1}{r} \frac{\partial}{\partial r} \left( r \frac{\partial \theta}{\partial r} \right) + \frac{1}{r^2} \frac{\partial^2 \theta}{\partial \phi^2} - w^2 \theta = -Q \quad (3.43a)$$

$$R_1 \leq r \leq R_2, \quad 0 \leq \phi \leq \Phi_1$$

with the boundary conditions,

$$\text{at } r = R_1, \quad \theta = 0 \quad (3.43b)$$

$$\text{at } r = R_2, \quad \left\{ \begin{array}{l} \frac{\partial \theta}{\partial r} = -\frac{f(\phi)}{k}, \quad 0 \leq \phi < \beta \Phi_1 \\ \frac{\partial \theta}{\partial r} = 0, \quad \beta \Phi_1 < \phi \leq \Phi_1 \end{array} \right\} \quad (3.43c)$$

$$\text{at } \phi = 0, \quad \frac{\partial \theta}{\partial \phi} = 0 \quad (3.43d)$$

$$\text{at } \phi = \Phi_1, \quad \frac{\partial \theta}{\partial \phi} = 0 \quad (3.43e)$$

Solution for this set was obtained by using the same technique as before to yield

$$\begin{aligned} T(r, \phi) = T_1 + \frac{Q}{w^2} \left[ 1 - \frac{\psi_{01}^2(wr)}{\psi_{01}^2(wR_2)} \right] - \frac{\beta f_a}{kw} \frac{\psi_{00}^1(wr)}{\psi_{01}^2(wR_1)} \\ - R_2 \sum_{n=1}^{\infty} \frac{\alpha_n \psi_{n\eta}^1(wr)}{\eta \psi_{n\eta}^1(wR_2) + wR_2 \psi_{n(\eta+1)}^1(wR_2)} \cos(\eta\phi) \quad (3.44) \end{aligned}$$

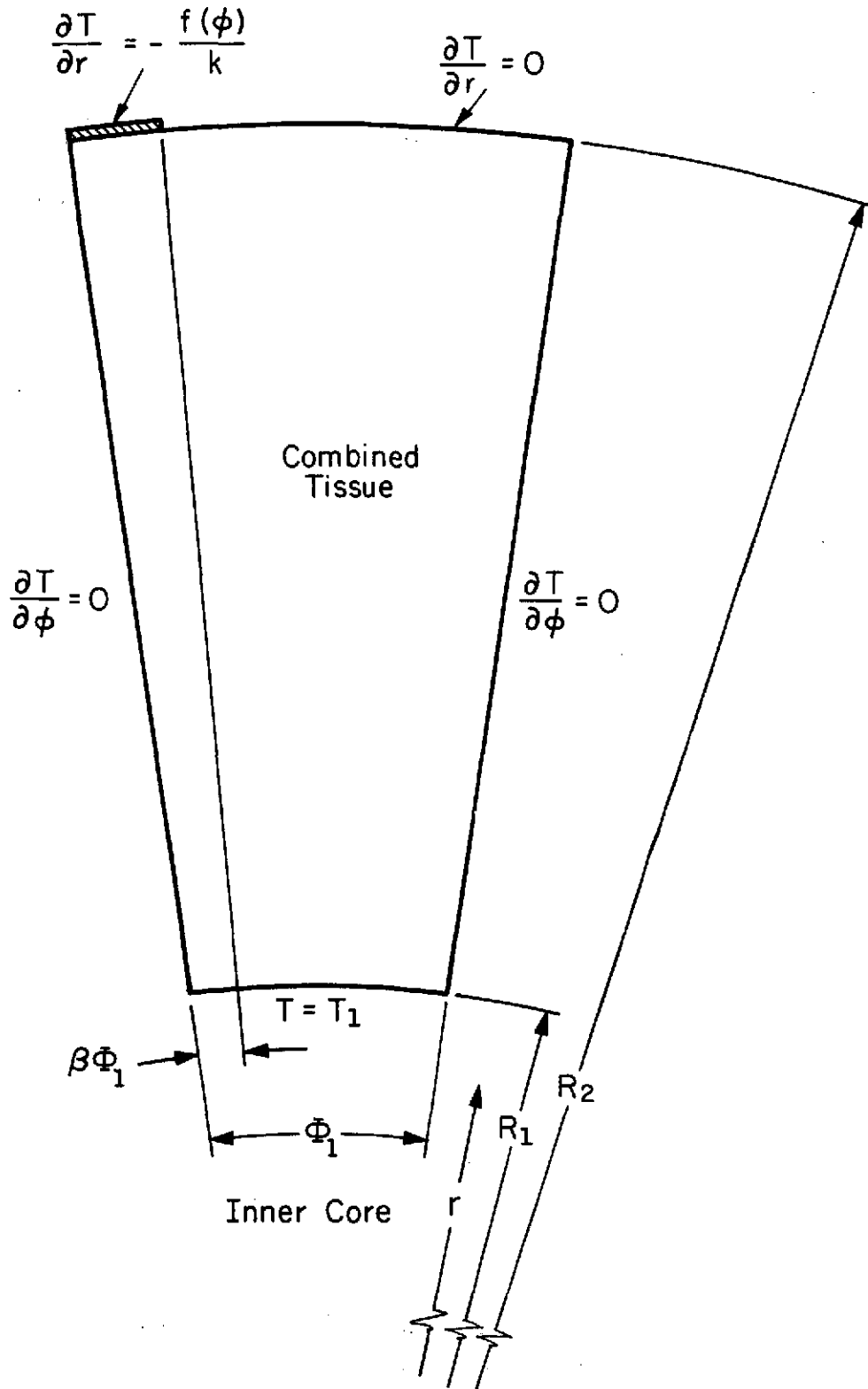


Figure 3.11 Geometry and boundary conditions for the cylindrical model with the cooling tubes on the skin running parallel to the axis of the cylinder. Skin layer and skeletal muscle are considered as a combined tissue.

where

$$\alpha_n = \frac{2}{\Phi_1} \int_0^{\beta\Phi_1} \frac{f(\xi)}{k} \cos(\eta\xi) d\xi \quad (3.45)$$

$$\eta = nm \quad (3.46)$$

$m$  is the number of equally spaced tubes on the circumference.

The presence of the function  $\psi_{\eta\eta}^i(wr)$  in the series of Eq. (3.44) hindered accurate computation of the temperature distributions in the tissue. This was true particularly in the vicinity of the cooling tubes. For example, if one assumes  $m = 20$ , the capacity of the computer is exceeded after the first two terms of the series for a low metabolic rate. Also, when  $R_1$  increases (while still being meaningful physiologically), the accuracy of the computation is further limited. Consequently, the temperature distribution obtained for this case was considered of limited value and is not presented here. This computational limitation was also one of the reasons why this case was not studied with the zones separated.

Solutions for cases where the tubes run diagonally on the skin, i.e., not parallel or perpendicular to the cylinder axis, can be obtained as linear combinations of the above two extreme cases. This can be done by resolving the flux function at the skin into two components corresponding to the above two cases. Because of the linearity of the equation, a linear combination of solutions constitutes a solution to this more general case.

### 3.6 TRANSIENT STATE, RECTANGULAR COORDINATES

Available experimental evidence shows that the thermal transients in the human body are of the order of a half hour [62]. Consequently, the steady state solutions become of limited importance and transient solutions should be sought.

The lack of accurate and detailed thermophysical and physiological data hinders any detailed analysis. This is even more noticeable in the transient cases. Therefore, the analysis presented below, although successful in obtaining solutions to the problem, should be considered approximate only. In view of these limitations, the following assumptions will be made:

- (1) The two outer zones, i.e., skin and skeletal muscle, will be considered to constitute one combined tissue.
- (2) All properties will be assumed to be constant and independent of time, temperature, and location.
- (3) The temperature at the interface between the inner core and the combined tissue will be assumed uniform and constant and will correspond to the final condition.
- (4) Step-like functions will be assumed to represent changes in blood perfusion and metabolic heat generation rates; that is, at  $t \geq 0$ , values of blood perfusion and heat generation rates correspond to the final ones. This assumption can be justified on the grounds that the transient time for changes in these quantities is much shorter than the thermal transients.

- (5) The initial temperature in the tissue will be taken as the steady state distribution. The final temperature distribution, as  $t \rightarrow \infty$ , was expected to correspond to the steady state at the new metabolic activity level.

Two cases will be studied: one with a uniform heat flux at the skin, i.e., one-dimensional, and the other with variable flux over the skin, similar to the steady state case presented in APPENDIX C.

CASE 1:

$$\frac{1}{\alpha} \frac{\partial \theta}{\partial t} = \frac{\partial^2 \theta}{\partial y^2} - w_2^2 \theta + Q_2 \quad (3.47a)$$

$$0 \leq y \leq b ; \quad 0 \leq t$$

with the boundary and initial conditions,

$$\text{at } y = 0 , \quad \frac{\partial \theta}{\partial y} = \frac{F_2}{k} \quad (3.47b)$$

$$\text{at } y = b , \quad \theta = 0 \quad (3.47c)$$

$$\text{at } t \leq 0 , \quad \theta = \frac{Q_1}{w_1} \left[ 1 - \frac{\cosh (w_1 y)}{\cosh (w_1 b)} \right] - \frac{F_1}{kw_1} \\ \cdot \frac{\sinh [w_1 (b - y)]}{\cosh (w_1 b)} \quad (3.47d)$$

where

$$\theta \equiv T(y,t) - T_1 \quad (3.48)$$

and all the other parameters were defined before. Index 1 indicates values prior to the step,  $t \leq 0$ , and index 2 values after the step,  $t > 0$ .

The solution to this case is

$$\begin{aligned}
 T(y,t) = & T_1 + \frac{Q_2}{w_2} \left[ 1 - \frac{\cosh(w_2 y)}{\cosh(w_2 b)} \right] - \frac{F_2}{kw_2} \frac{\sinh[w_2(b-y)]}{\cosh(w_2 b)} \\
 & + \frac{2}{ak} \sum_{n=1}^{\infty} \left\{ \frac{F_2}{\gamma_2} - \frac{F_1}{\gamma_1} + \frac{(-1)^n}{\delta_n} \left[ \frac{Q_2'}{\gamma_2} - \frac{Q_1'}{\gamma_1} \right] \right\} \cos(\delta_n y) \\
 & \cdot \exp(-\alpha \gamma_2^2 t) \tag{3.49}
 \end{aligned}$$

where

$$\delta_n \equiv \frac{(2n-1)\pi}{2b} \tag{3.50}$$

$$\gamma_i^2 \equiv w_i^2 + \delta_n^2 \tag{3.51}$$

Figure 3.12 shows results obtained for step changes in metabolic rates. It is clearly seen that most of the changes in temperature occur during the first five minutes when the step is from the low to the high rate, and during the first twenty minutes when the step is from the high to the low rate. After these periods, the temperature of the tissue is essentially equal to the steady state temperature. It should be noted that the temperature at the interface between the inner core and the combined tissue was assumed constant. This assumption, however, does not conform to the actual situation. Deep body temperature is known to change almost linearly with changes in metabolic rates [57]. However, the transient times of these changes are much longer than those obtained for the temperature profile inside the tissue. Consequently, the final configuration of the temperature distribution inside the tissue will be reached after about 5-20 minutes from the onset of a change in metabolic rate. From then on, only a shift of the "fully developed" temperature profile will occur.

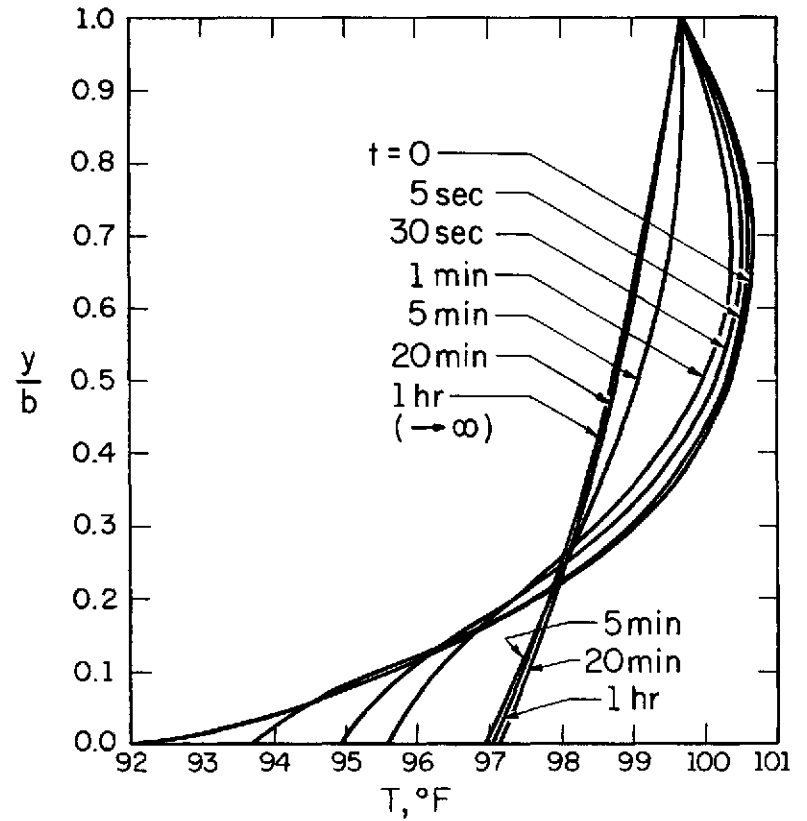
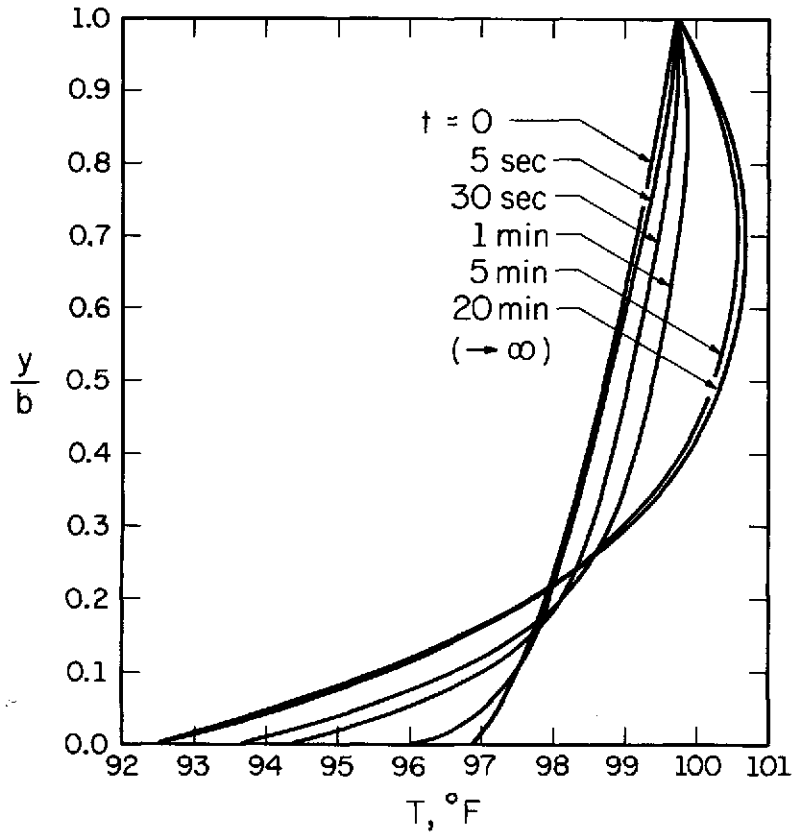


Figure 3.12 Transient temperature distribution in the combined tissue for the one-dimensional rectangular model. Step changes:  
 (a) from 290 Btu/hr (85 w) to 2600 Btu/hr (760 w)  
 (b) from 2600 Btu/hr (760 w) to 290 Btu/hr (85 w)  
 Constant temperature at inner core.

When a variable flux is assumed at the skin, the problem becomes

CASE 2:

$$\frac{1}{\alpha} \frac{\partial \theta}{\partial t} = \nabla^2 \theta - w_2 \theta + Q_2 \quad (3.52a)$$

$$0 \leq x \leq a, \quad 0 \leq y \leq b, \quad 0 \leq t$$

with the boundary and initial conditions,

$$\text{at } y = 0, \quad \left\{ \begin{array}{l} \frac{\partial \theta}{\partial y} = \frac{f_2(x)}{k}, \quad 0 \leq x < \beta a \\ \frac{\partial \theta}{\partial y} = 0, \quad \beta a < x \leq a \end{array} \right\} \quad (3.52b)$$

$$\text{at } y = b, \quad \theta = 0 \quad (3.52c)$$

$$\text{at } x = 0, \quad \frac{\partial \theta}{\partial x} = 0 \quad (3.52d)$$

$$\text{at } x = a, \quad \frac{\partial \theta}{\partial x} = 0 \quad (3.52e)$$

$$\begin{aligned} \text{at } t \leq 0, \quad \theta = & \frac{Q_1}{w_1} \left[ 1 - \frac{\cosh(w_1 y)}{\cosh(w_1 b)} \right] - \frac{\beta f_{a1}}{k w_1} \\ & \cdot \frac{\sinh[w_1(b-y)]}{\cosh(w_1 b)} + \sum_{n=1}^{\infty} \\ & \cdot \frac{\alpha_{n,1} \sinh[\zeta_1(b-y)]}{\zeta_1 \cosh(\zeta_1 b)} \cos(\lambda_{n,1} x) \end{aligned} \quad (3.52f)$$

The solution to this set was obtained by using transformations and a double Fourier series expansion to yield

$$\begin{aligned}
T(x,y,t) = & T_1 + \frac{Q_2}{w_2} \left[ 1 - \frac{\cosh(w_2 y)}{\cosh(w_2 b)} \right] - \frac{\beta f_{a2}}{kw_2} \frac{\sinh[w_2(b-y)]}{\cosh(w_2 b)} \\
& - \frac{2}{ak} \sum_{j=1}^{\infty} \frac{\alpha_{j,2} \sinh[\zeta_{j,2}(b-y)]}{\zeta_{j,2} \cosh(\zeta_{j,2} b)} \cos(\lambda_j x) \\
& + \frac{2}{bk} \sum_{i=1}^{\infty} \left\{ \frac{\beta f_{a2}}{\gamma_2^2} - \frac{\beta f_{a1}}{\gamma_1^2} + \frac{(-1)^i}{\delta_i} \right. \\
& \cdot \left. \left[ \frac{Q_2'}{\gamma_2^2} - \frac{Q_1'}{\gamma_1^2} \right] \right\} \cos(\delta_i x) \exp(-\alpha \gamma_2^2 t) + \frac{4}{abk} \\
& \cdot \sum_{n=1}^{\infty} \sum_{m=1}^{\infty} \left\{ \frac{\alpha_{n,1}}{\zeta_{n,1}^2 + \delta_m^2} - \frac{\alpha_{n,2}}{\zeta_{n,2}^2 + \delta_m^2} \right\} \\
& \cdot \cos(\lambda_n x) \cos(\delta_m y) \exp(-\alpha \sigma_2^2 t) \tag{3.53}
\end{aligned}$$

where

$$\alpha_{i,j} \equiv \int_0^{\beta a} f_j(\xi) \cos(\lambda_i \xi) d\xi \tag{3.54}$$

$$\sigma_2^2 \equiv w_2^2 + \lambda_n^2 + \delta_m^2 = w_2^2 + \pi^2 \left[ \left( \frac{n}{a} \right)^2 + \frac{(2m-1)^2}{4b^2} \right] \tag{3.55}$$

and  $w_1$ ,  $f_a$ ,  $\zeta_i$ ,  $\lambda_i$ ,  $\delta_i$ , and  $\gamma_i$  are defined by Eqs. (3.9), (3.16), (3.17), (3.18), (3.50), and (3.51), respectively.

Temperature variations on the skin are shown for this case in Fig. 3.13. These results exhibit the same basic characteristics as do those for the one-dimensional case; i.e., most of the changes in temperature occur during the first 5-20 minutes from the onset of a change in level of activity.

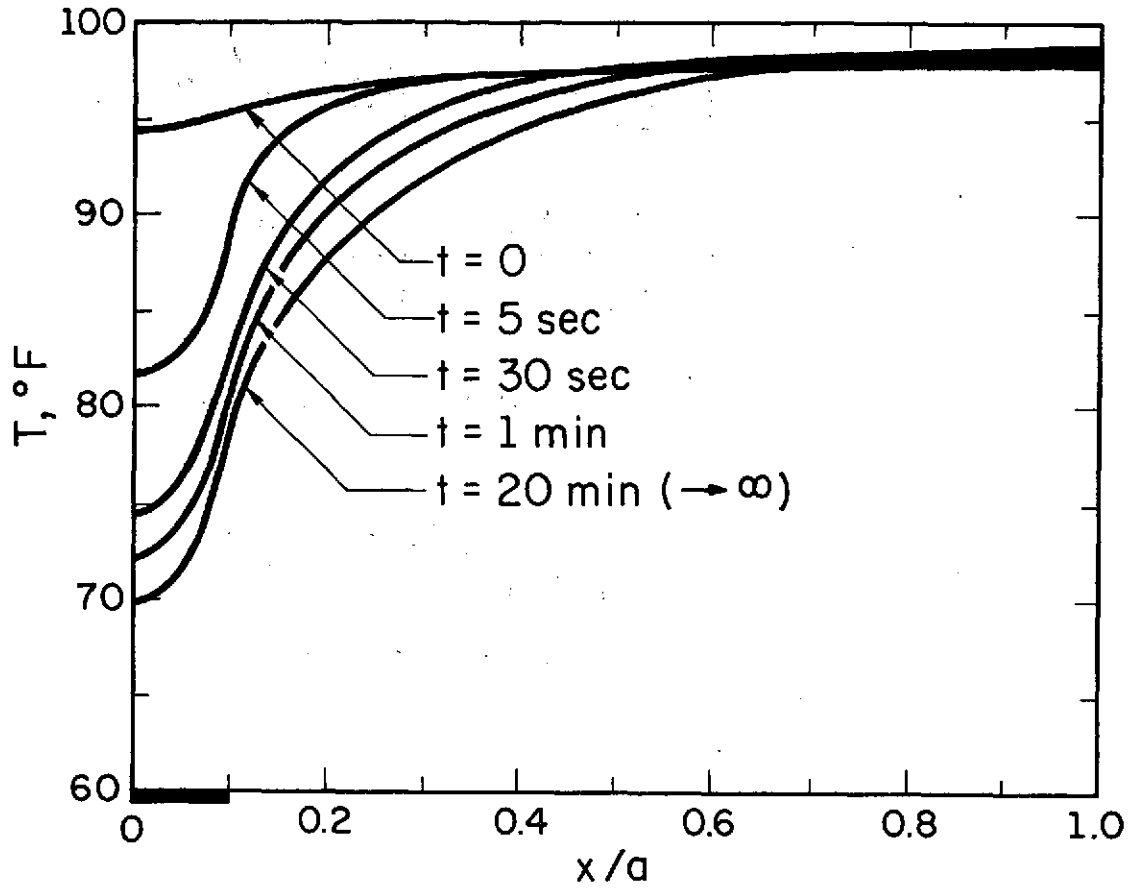


Figure 3.13 Transient temperature distribution on the skin of the combined tissue for the two-dimensional rectangular model. Step change assumed from 290 Btu/hr (85 w) to 2600 Btu/hr (760 w),  $\beta = 0.1$  and constant temperature at inner core.

Examination of the time dependent exponent in Eq. (3.49) leads to the following two conclusions:

- (1) The exponent is strongly dominated by the separation coefficient  $\lambda_n$  rather than by the blood flow term. This becomes even more noticeable for low blood flow rates. The effect of the blood can, in any case, be neglected for  $n > 2$ .
- (2) Time constants (transients) appear to be in the range of 5-20 minutes. This observation is supported by experimental evidence and partially validates the analysis.

Extension of the transient solutions outlined in this section to account for the actual changes occurring in the tissue will have to be delayed until more reliable experimental data become available. This extension, however, appears to be possible by using Duhamel's method [63].

### 3.7 TRANSIENT STATE, CYLINDRICAL COORDINATES

As a result of the preceding analysis, it was felt that an extensive solution of the transient problem in cylindrical coordinates, i.e., variable flux at the skin, could be neglected at present; for, the small amount of additional information obtained from such a solution would not justify the effort required. Consequently, only the case with uniform flux at the skin was studied as presented below.

$$\frac{1}{\alpha} \frac{\partial \theta}{\partial t} = \frac{1}{r} \frac{\partial}{\partial r} \left( r \frac{\partial \theta}{\partial r} \right) - w_2^2 \theta + Q_2 \quad (3.56a)$$

$$R_1 \leq r \leq R_2, \quad 0 \leq t$$

with the boundary and initial conditions,

$$\text{at } r = R_1, \theta = 0 \quad (3.56b)$$

$$\text{at } r = R_2, \frac{\partial \theta}{\partial r} = -\frac{F_2}{k} \quad (3.56c)$$

$$\text{at } t \leq 0, \theta = \frac{Q_1}{w_1} \left[ 1 - \frac{\psi_{01}^2(w_1 r)}{\psi_{01}^2(w_1 R_1)} \right] - \frac{F_1}{kw_1} \frac{\psi_{00}^1(w_1 r)}{\psi_{01}^2(w_1 R_1)} \quad (3.56d)$$

Using the same technique as for the rectangular case, the following solution was obtained

$$\begin{aligned} T(r,t) = & \frac{Q_2}{w_2} \left[ 1 - \frac{\psi_{01}^2(w_2 r)}{\psi_{01}^2(w_2 R_1)} \right] - \frac{F_2}{kw_2} \frac{\psi_{00}^1(w_2 r)}{\psi_{01}^2(w_2 R_1)} \\ & + \frac{\pi}{k} \sum_{n=1}^{\infty} \frac{\left[ \frac{Q_2'}{\epsilon_2} - \frac{Q_1'}{\epsilon_1} \right] Y_1(\mu_n R_2) - \mu_n \left[ \frac{F_2}{\epsilon_2} - \frac{F_1}{\epsilon_1} \right] Y_0(\mu_n R_1)}{Y_0^2(\mu_n R_1) - Y_1^2(\mu_n R_2)} \\ & \cdot Y_1(\mu_n R_2) \chi_n(\mu_n r) \exp(-\alpha \epsilon_2^2 t) \end{aligned} \quad (3.57)$$

where

$$\chi_n(\mu_n r) = J_0(\mu_n r) Y_0(\mu_n R_1) - J_0(\mu_n R_1) Y_0(\mu_n r) \quad (3.58)$$

and  $\mu_n$  are the roots of

$$J_0(\mu_n R_1) Y_1(\mu_n R_2) - J_1(\mu_n R_2) Y_0(\mu_n R_1) = 0 \quad (3.59)$$

$$\epsilon_i^2 = \mu_n^2 + w_i^2 \quad (3.60)$$

$J_i$  and  $Y_i$  are Bessel functions of the first and second kind, respectively, of order  $i$ .

No numerical solutions were obtained for this case because of the appearance of the combination of Bessel functions in the time dependent series in Eq. (3.57). These functions reach high numerical values at relatively small arguments and, therefore, exceed the calculating capacity of the computer. However, the first six roots of Eq. (3.59) were computed using Newton-Raphson's method as a function of the ratio  $R_2/R_1$  and are presented in TABLE 3.2. As this ratio approaches unity (rectangular model), the roots approach the limiting value for the rectangular case; i.e.,  $\mu_n \rightarrow \delta_n$ , as was to be expected.

### 3.8 COMPARISON OF STEADY STATE SOLUTIONS FOR RECTANGULAR AND CYLINDRICAL COORDINATES

As was noted above, the human body can be more closely approximated by cylinders rather than by rectangular slabs. According to Wissler [18], the outside radii of these cylinders vary from 0.15 ft for the arm to about 0.43 ft for the trunk. Unfortunately, the expressions obtained for the cylindrical coordinates are more difficult for numerical evaluation because of the presence of the combination of modified Bessel function in the solution for the cylindrical case, Eqs. (3.35) and (3.36). This combination, when programmed on a digital computer, caused an overflow after the first few terms of the series and rendered the numerical results inaccurate.

A comparison of the simpler, rectangular and the cylindrical cases revealed that the temperature distributions obtained for the two cases do not differ significantly. This fact became even more apparent as  $R_1$  increased. For  $R_1 \geq 0.20$  ft, the results obtained

TABLE 3.2

FIRST SIX ROOTS OF EQ. (3.59) AS A FUNCTION OF THE RATIO OF THE OUTER TO INNER RADII OF THE CYLINDRICAL MODEL,  $R_2/R_1$ . THE RIGHTMOST COLUMN GIVES THE ASYMPTOTIC VALUES ( $[(2n - 1)\pi]/2b$ , RECTANGULAR MODEL) AS  $R_1 \rightarrow \infty$  AND  $R_2/R_1 \rightarrow 1$ .

$n \backslash R_2/R_1$	2.46	1.73	1.37	1.24	1.18	1.15	1
$n \backslash R_1$ (ft)	0.05	0.10	0.20	0.30	0.40	0.50	$\infty$
1	17.83	19.18	20.16	20.55	20.76	20.90	21.49
2	63.29	63.74	64.04	64.16	64.23	64.27	64.46
3	106.74	107.01	107.19	107.26	107.30	107.33	107.44
4	149.91	150.11	150.24	150.29	150.32	150.34	150.42
5	193.00	193.15	193.24	193.30	193.32	193.33	193.39
6	236.05	236.17	236.25	236.29	236.30	236.32	236.37

for the rectangular model were adequate for any practical purpose. Figures 3.14, 3.15, 3.16, and 3.17 demonstrate this finding for uniform and variable heat fluxes at the skin (see APPENDIX E).

A partial explanation to this similarity of the solutions can be given as follows. If the argument of the modified Bessel function is greater than 10, which is mostly the case here ( $wR_1 > 10$ ), the following expressions can be used to approximate the modified Bessel functions of the first and second kind [64],

$$I_k(z) \approx \frac{0.3989 \exp(z)}{z^{1/2}} \left\{ 1 + (-1)^k \left[ \frac{a_k}{8z} + \frac{b_k}{128z^2} + \frac{c_k}{1024z^3} \right] \right\} \quad (3.61)$$

$$K_k(z) \approx \frac{1.2533 \exp(z)}{z^{1/2}} \left\{ 1 + (-1)^{k+1} \left[ \frac{a_k}{8z} + \frac{b_k}{128z^2} + \frac{c_k}{1024z^3} \right] \right\} \quad (3.62)$$

where  $a_k$ ,  $b_k$ , and  $c_k$  are constants and  $k = 0$  or  $1$ . When these expressions are substituted into Eq. (3.37), an essentially exponential expression results. This expression corresponds to the hyperbolic functions that appear in the solution for the rectangular case.

It should be noted that the above comparison is valid for the cylindrical case with the cooling tubes running perpendicular to the axis of the cylinder, Fig. 3.2. The reason is the similarity of the resulting rectangular geometry.

99.7 °F

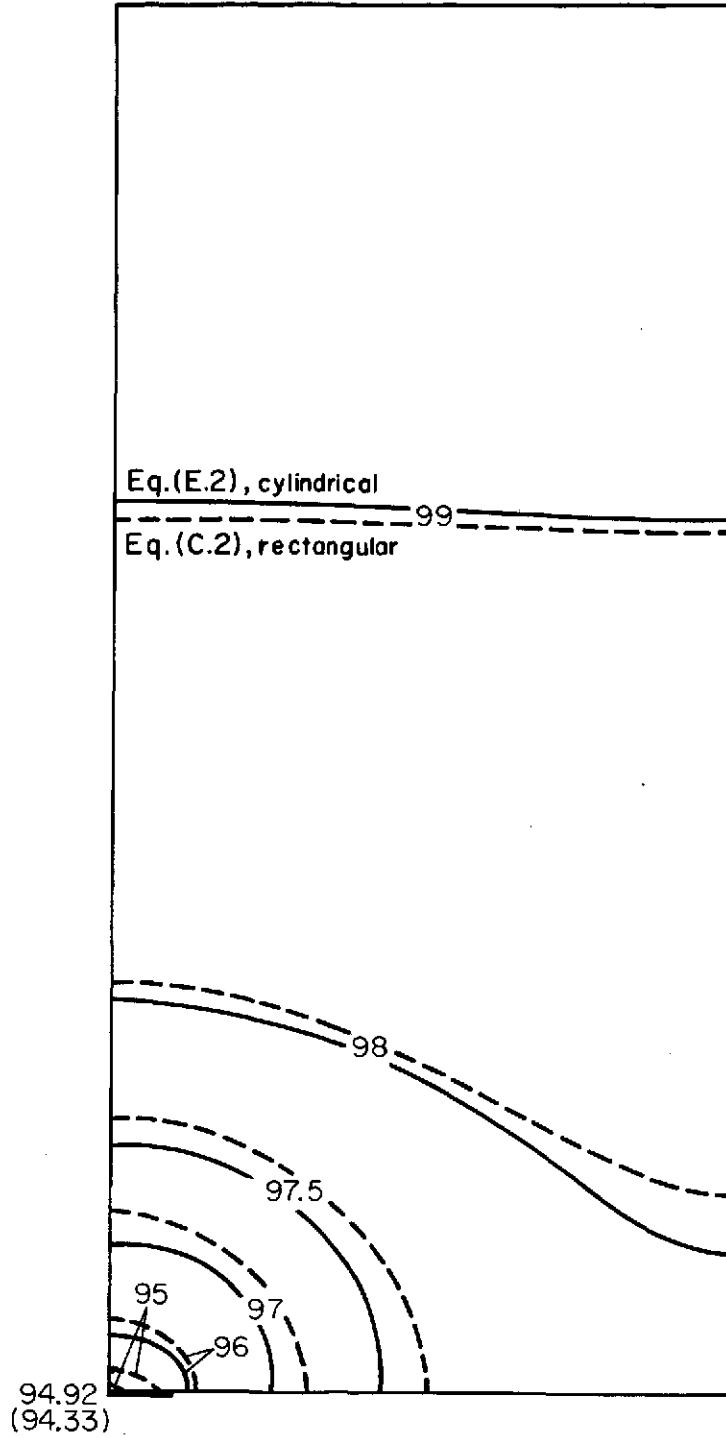


Figure 3.14 Comparison between the steady state, two-dimensional solutions for rectangular and cylindrical models (tubes running perpendicular to the axis of the cylinder,  $R_1 = 0.15$  ft,  $V$  and  $b$  are constant).  $Q_m = 290$  Btu/hr (85),  $\beta = 0.1$  and constant temperature at inner core.

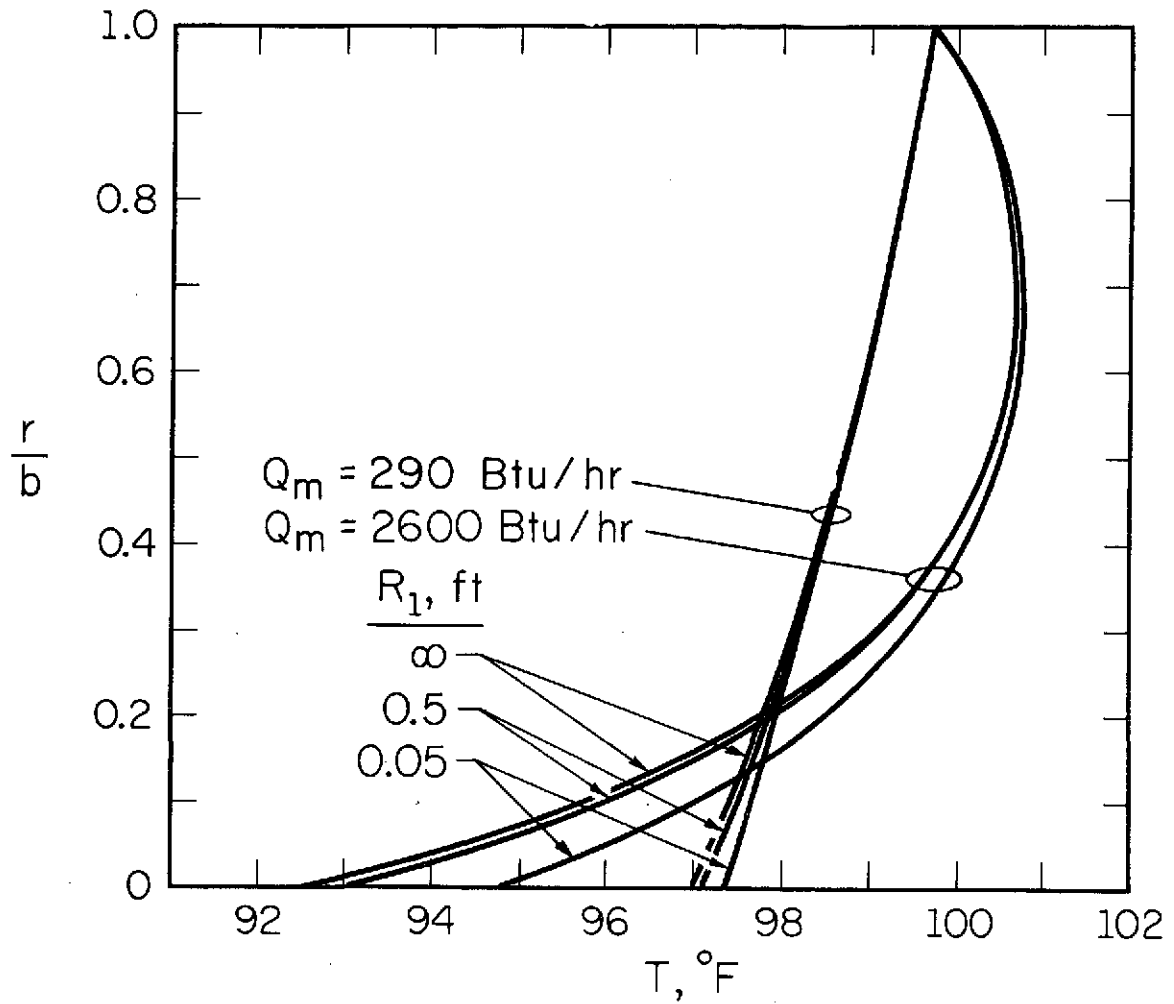


Figure 3.15 Comparison between steady state, one-dimensional solutions obtained for the rectangular and cylindrical models ( $V$  and  $b$  are constant). Constant temperature at inner core.

— R. G. B.

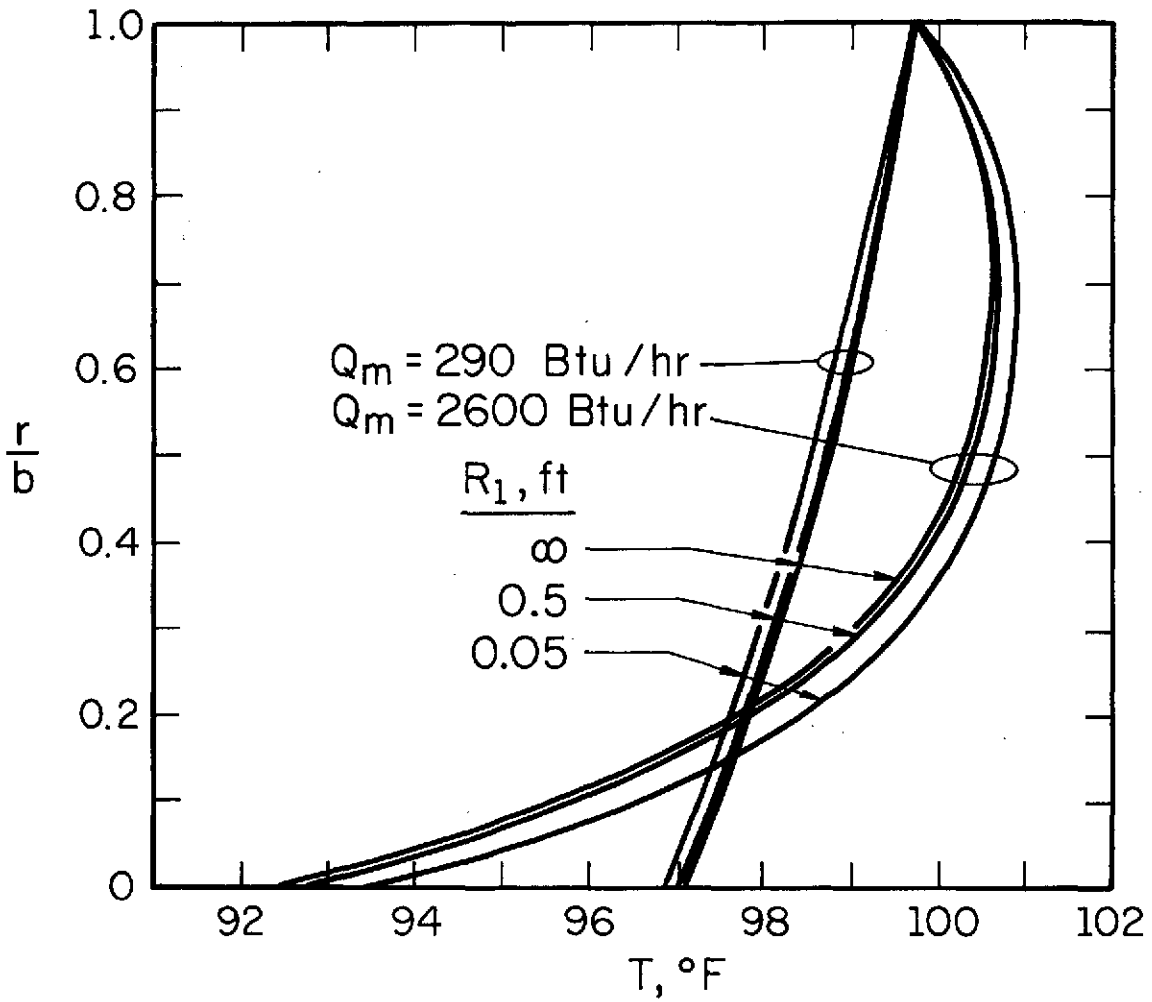


Figure 3.16 Comparison between steady state, one-dimensional solutions obtained for the rectangular and cylindrical models ( $V$  and  $A$  are constant). Constant temperature at inner core.

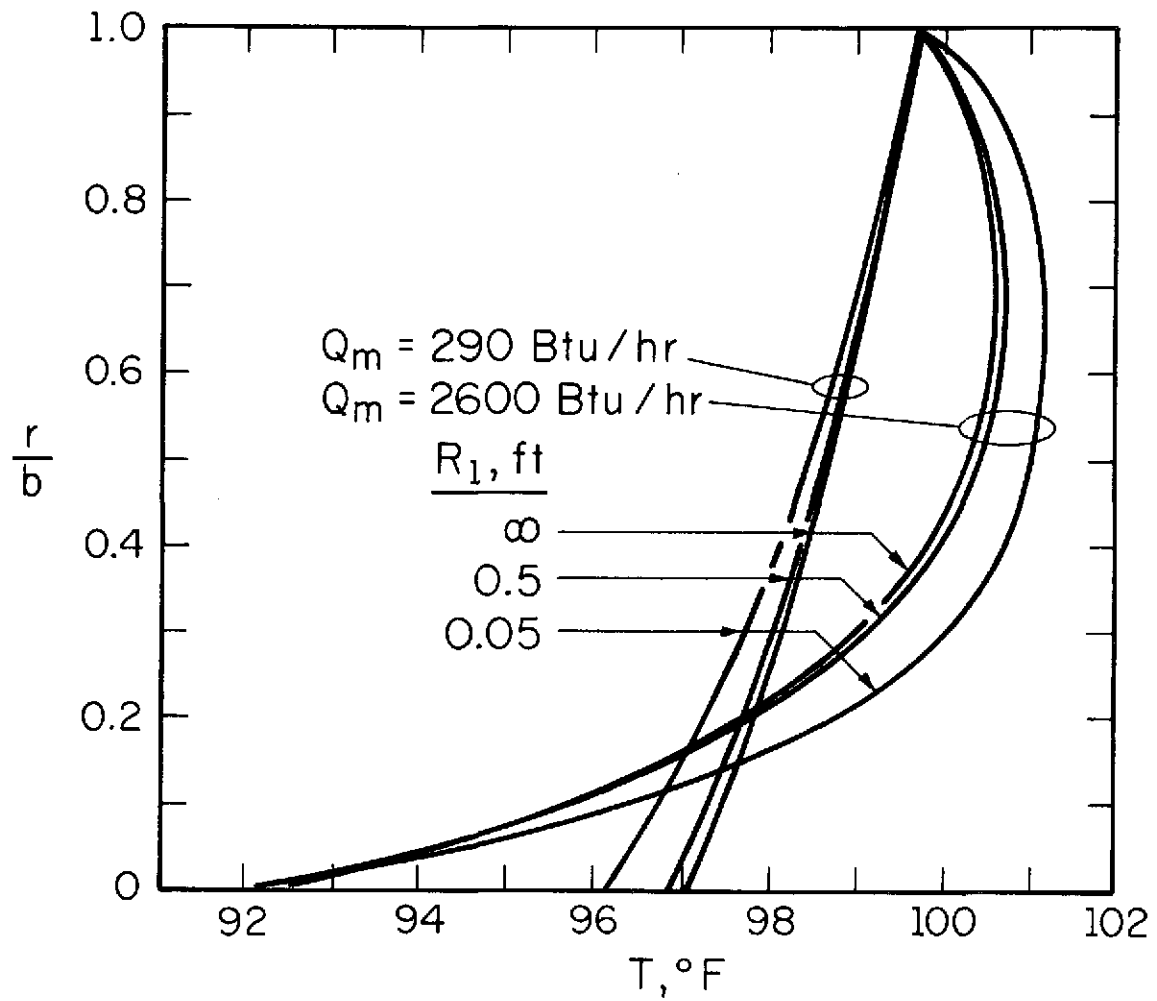


Figure 3.17 Comparison between steady state, one-dimensional solutions obtained for the rectangular and cylindrical models ( $A$  and  $b$  are constant). Constant temperature at inner core.

### 3.9 DIMENSIONLESS PARAMETERS ASSOCIATED WITH THE THERMAL BEHAVIOR OF LIVING BIOLOGICAL TISSUE

It is always desirable, from an engineering viewpoint, to have appropriate dimensionless parameters for the description of any physical phenomena. The best method for obtaining these parameters is via an analytical model.

Consider a one-dimensional, steady state case in rectangular coordinates. The analytical expressions for the temperature distributions in the tissue can be obtained from Eqs. (C.2) and (C.4) to yield, for constant temperature at the inner core,

$$T(y) = T_1 + \frac{Q}{w} \left[ 1 - \frac{\cosh(wy)}{\cosh(wb)} \right] - \frac{F}{kw} \frac{\sinh[w(b-y)]}{\cosh(wb)} \quad (3.63)$$

and, for a constant heat flux at the inner core,

$$T(y) = T_1 + \frac{Q}{w} + \frac{1}{kw \sinh(wb)} \left\{ F \cosh(wy) - F_0 \cosh[w(b-y)] \right\} \quad (3.64)$$

Figures 3.18 and 3.19 show results obtained for Eqs. (3.63) and (3.64), respectively, for both low (290 Btu/hr, 85 W) and high (2600 Btu/hr, 760 W) metabolic rates.

As was noted above, a maximum temperature was found to occur in the combined tissue rather than in the inner core (Fig. 3.18). In order to obtain the location of these maxima, Eqs. (3.63) and (3.64) were differentiated and equated with zero to obtain [65],

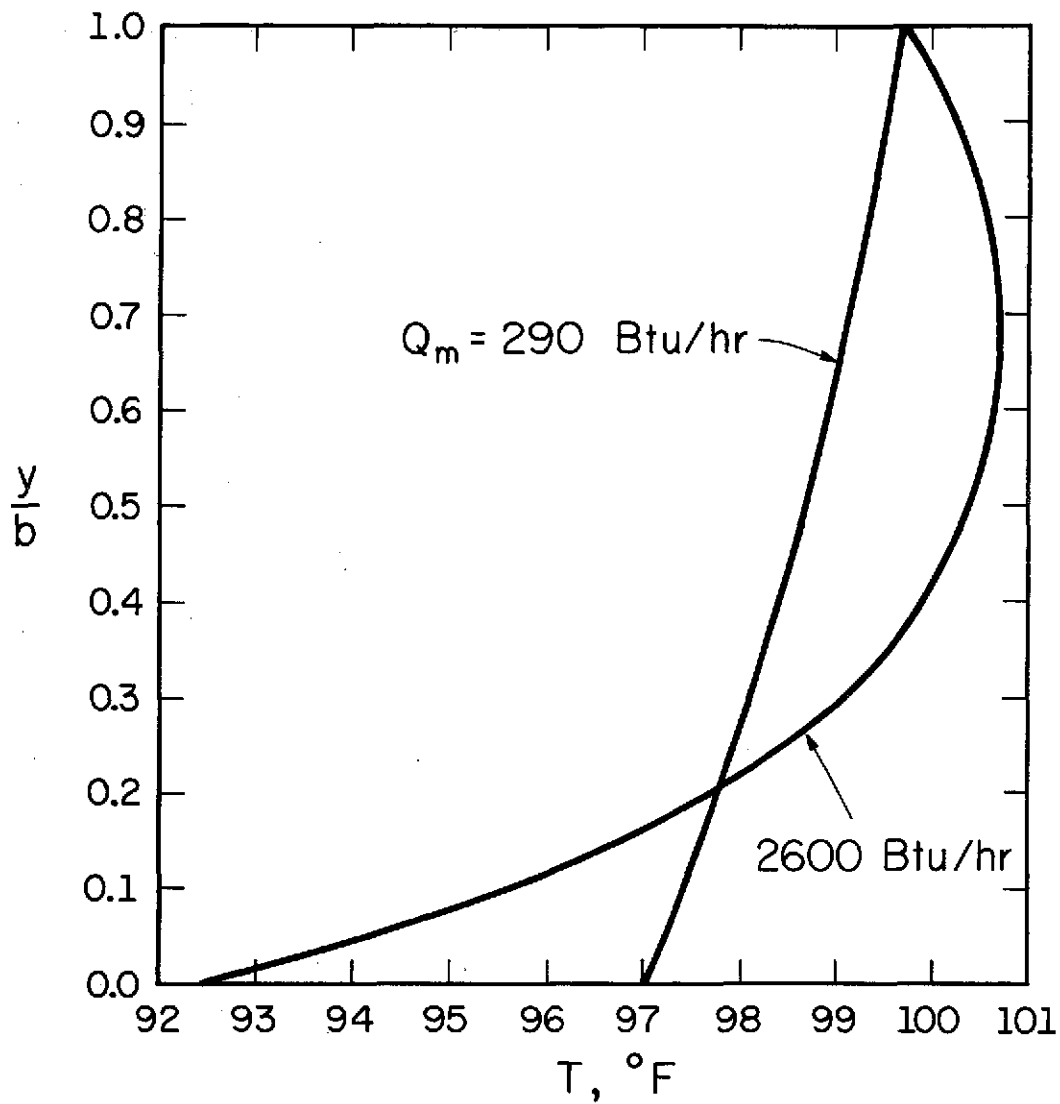


Figure 3.18 Steady state temperature distributions in the combined tissue for the one-dimensional rectangular model. Constant temperature at inner core.

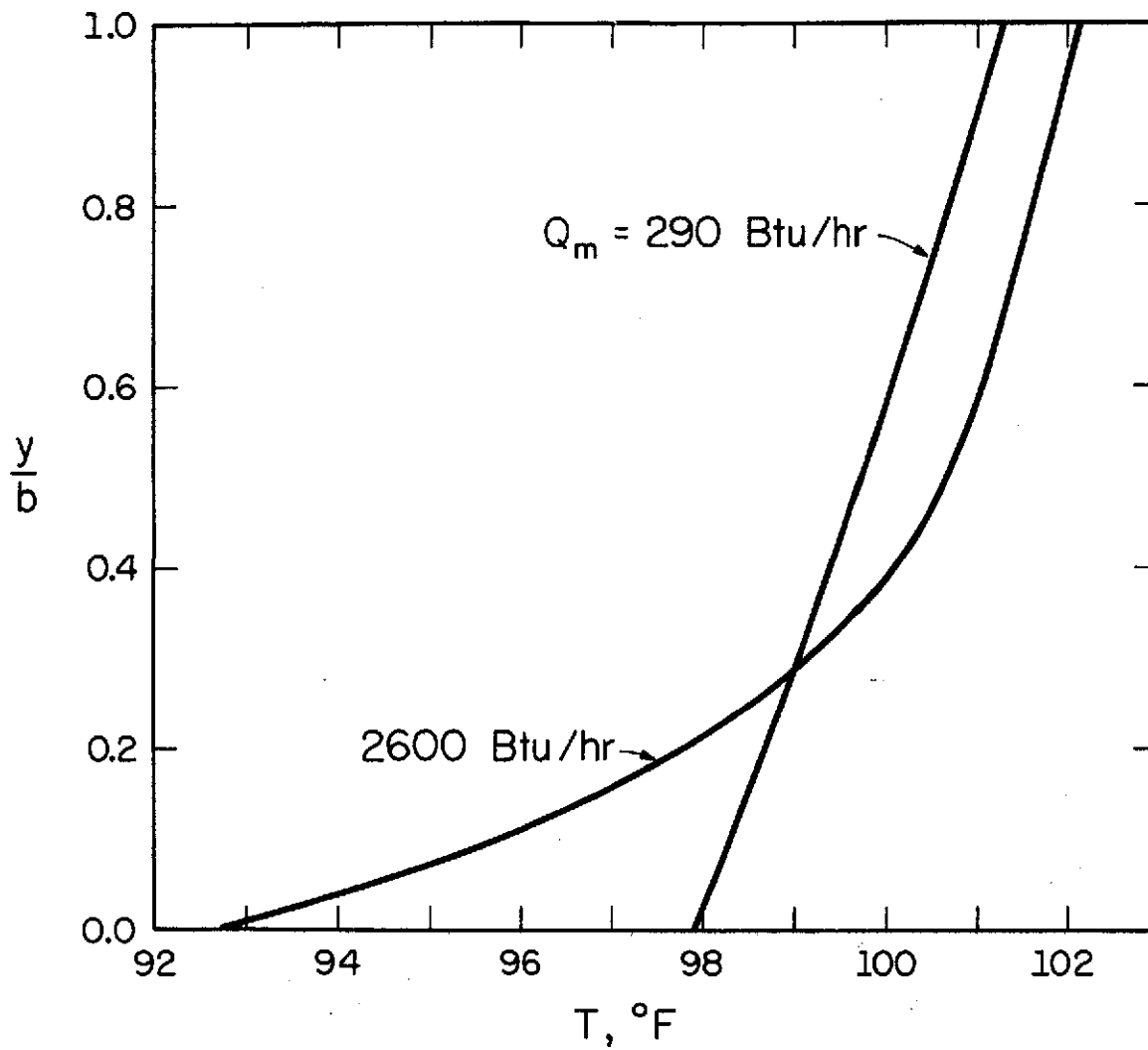


Figure 3.19 Steady state temperature distributions in the combined tissue for the one-dimensional rectangular model. Constant flux at inner core.

$$\tanh \left[ (wb) \frac{y}{b} \right] = \frac{\cosh (wb)}{\frac{Q'Ab}{Q_m} \frac{1}{wb} + \sinh (wb)} \quad (3.65)$$

$$\tanh \left[ (wb) \frac{y}{b} \right] = \frac{\sinh (wb)}{\frac{Q'Ab}{Q_m} - 1 + \cosh (wb)} \quad (3.66)$$

No maximum temperature was found to occur inside the tissue for the case with a specified flux at the inner core, Eqs. (3.64) and (3.66). This result is to be expected since, by imposing a heat flux from the inner core into the combined tissue, the temperature gradients must sustain heat flow toward the skin only. Equation (3.65), however, was solved for the  $y/b$  values for which the maximum temperature occurs as a function of the parameters present in it. The location of the maximum was found to be independent of inner body temperature. Results are shown in Fig. 3.20.

Based on the preceding analysis, three dimensionless parameters, which have significant effects on the steady state heat transfer in the living tissue, emerged. These are:

- (1)  $wb = (w_b c_b / k)^{1/2} b$  -- ratio of heat transported by the blood stream to the heat transferred by conduction through the tissue.
- (2)  $Q'Ab/Q_m$  -- ratio of rate of heat generated in the tissue to the total metabolic heat generation rate.
- (3)  $(Q'Ab/Q_m) [(w_b c_b / k)^{-1/2} b^{-1}]$  -- the quotient of the first and second groups which contains most of the physical and physiological properties describing the thermal condition of the human body. From the scant physiological data available [59], this third group appeared to be almost constant at 0.2 for a wide range of metabolic rates. If this value

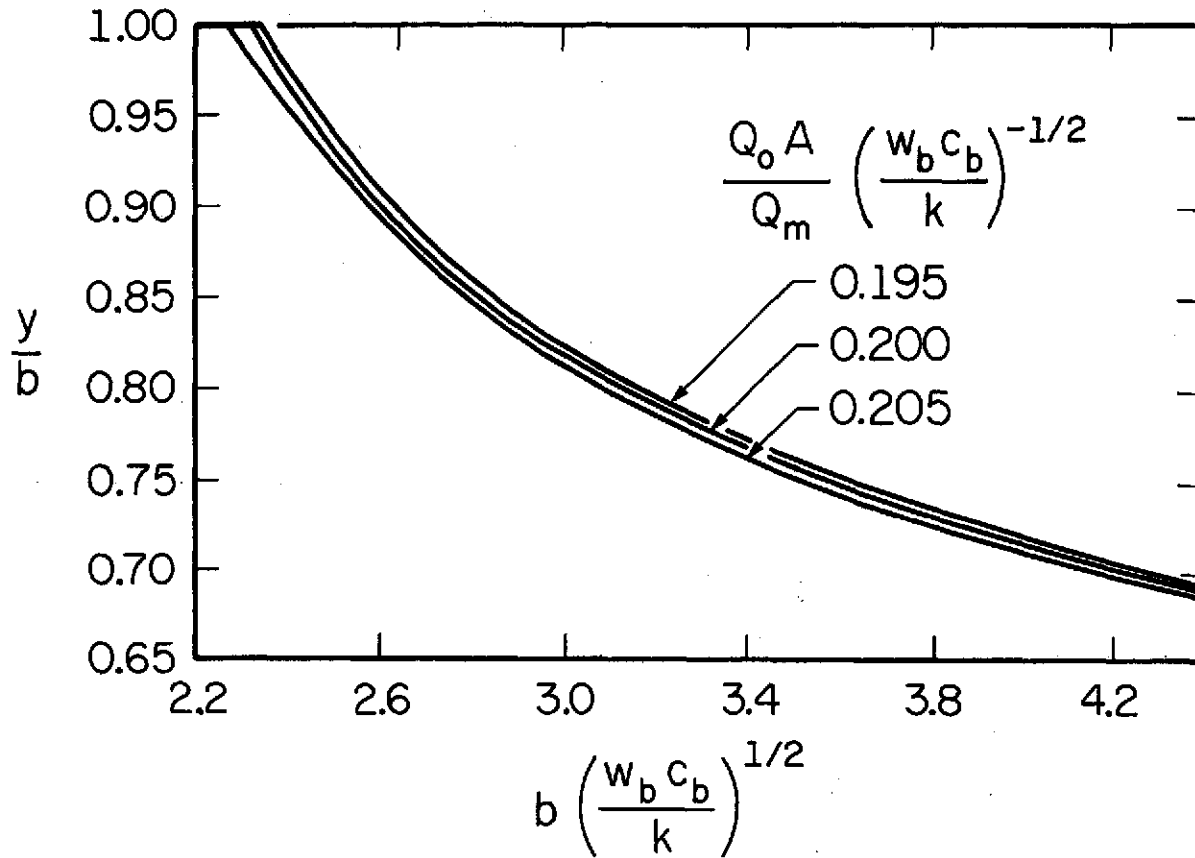


Figure 3.20 Location of the maximum temperature in the combined tissue for the one-dimensional rectangular model.

could be verified experimentally, which is beyond the scope of this work, a very strong physiological tool would become available, which would facilitate the calculation of quantities such as blood perfusion or heat generation rates that are very difficult to measure.

TABLE 3.3 summarizes the physiological quantities and the corresponding values of the above parameters.

No additional information was obtained from studying the corresponding cylindrical case. It is, however, presented below for completeness.

The temperature distribution in the cylindrical shell, which is uniformly cooled at the skin and has a constant temperature at the inner core, is

$$T(r) = T_1 + \frac{Q}{w^2} \left[ 1 - \frac{\psi_{01}^2(wr)}{\psi_{01}^2(wR_1)} \right] - \frac{F}{kw} \frac{\psi_{00}^1(wr)}{\psi_{01}^2(wR_1)} \quad (3.67)$$

with the resulting expression for the location of the maximum temperatures

$$\frac{I_1 \left[ (wR_1) \frac{r}{R_1} \right]}{K_1 \left[ (wR_1) \frac{r}{R_1} \right]} = \frac{A_1 I_1(wR_2) - I_0(wR_1)}{A_1 K_1(wR_2) + K_0(wR_1)} \quad (3.68)$$

where

$$A_1 = \frac{Q'AR_1}{Q_m} \frac{1}{wR_1} \quad (3.69)$$

TABLE 3.3

PHYSIOLOGICAL QUANTITIES AND THE CORRESPONDING DIMENSIONLESS PARAMETERS.

$c_b = 1$ , Btu/lb-°F (4187 J/kg-°C),  $k = 0.311$  Btu/ft-hr-°F (0.540 w/m-°C),  $b = 0.0731$  ft (0.0223 m),  
 AND  $A = 15.4$  ft<sup>2</sup> (1.43 m<sup>2</sup>)

$Q_m$		$Q'$		$w_b$		$(w_b c_b / k)^{1/2} b$	$Q' Ab / Q_m$	$(Q' Ab / Q_m)(1/wb)$
Btu/hr	w	Btu/hr-ft <sup>3</sup>	w/m <sup>3</sup>	lb/hr-ft <sup>3</sup>	kg/hr-m <sup>3</sup>			
290	85	64	660	94	1,510	1.273	2.484	0.195
2,600	760	2,090	21,600	1,120	18,000	4.394	9.049	0.206

210

In the cylindrical model, two groups appear,  $wR_1$  and  $wR_2$ , representing ratios of heat transported by blood to that conducted through the tissue.

For the transient case, an additional dimensionless parameter appears [from Eq. (3.49)],

$$\alpha[w^2 + \lambda_n^2]t \equiv \frac{k}{\rho c_p} \left[ \frac{w_b c_b}{k} + \left( \frac{n\pi}{a} \right)^2 \right] t \quad (3.70)$$

Equation (3.70) may be resolved into two expressions after multiplying and dividing it by the temperature of the inner core,  $T_1$ . The results are the following two dimensionless groups:

- (1)  $(w_b c_b T_1)/(\rho c_p T_1/t^*)$ --ratio of rate of heat transported by the blood stream to rate of energy stored in the tissue.
- (2)  $(kT_1/a^2)/(\rho c_p T_1/t^*)$ --ratio of rate of heat conducted through the tissue to rate of energy stored in it.

In the above two expressions,  $t^*$  is some characteristic time.

TABLE 3.4 gives values of the two expressions in the brackets of Eq. (3.70). It clearly demonstrates the dominance of the geometrical separation coefficient relative to the term containing blood flow for  $n \geq 2$ .

TABLE 3.4

COMPARISON OF MAGNITUDES OF THE TERMS IN EQ. (3.70).

$c_p = 1 \text{ Btu/lb-}^\circ\text{F}$  (4187 J/kg- $^\circ\text{C}$ ),  $k = 0.311 \text{ Btu/hr-ft-}^\circ\text{F}$   
 (0.540 w/m- $^\circ\text{C}$ ), AND  $a = 0.032 \text{ ft}$  (0.00975 m)

$Q_m$	w	85	760
	Btu/hr	290	2,600
$w_p c_p / k$	1/m	3,230	38,750
	1/ft	300	3,600
n		1	2
$(n\pi/a)^2$	1/m	103,200	427,000
	1/ft	9,600	39,700

## 4. EXPERIMENTS

### 4.1 OBJECTIVES

The experimental phase of this work was undertaken with the following objectives:

- (1) Exploration of the feasibility and operating characteristics of independently cooling separate regions of the body (regional cooling). This part was to determine preferable water inlet temperatures, amount of heat removed at each region and the order of cooling or warming preferences at different metabolic rates. The subjects' own sense of comfort was the criterion for determining these data.
- (2) Partial validation of the analytical predictions. This was planned to be achieved by measuring skin temperatures between two adjacent cooling tubes. No penetration of the skin was contemplated.

### 4.2 DESCRIPTION OF THE EXPERIMENTAL SETUPS

#### 4.2.1 Cooling Suit

A water cooled suit was constructed for the purpose of testing the characteristics of the proposed differential scheme of cooling the body. The suit consisted of sixteen individual pads made of 3/32 in. I.D. by 5/32 in. O.D. Tygon tubes running parallel 5/8 in. apart. The spacings between the tubes were maintained by the use of Mylar strips and heavy cotton thread. This assembly was stitched onto cotton fabric pieces, cut to fit the dimensions of the

various parts of the body. "Velcro" strips were glued to the fabric to facilitate quick fastening and to accommodate subjects of different sizes (Fig. 4.1).

The cooling pads covered the head (2)†, front and back, upper and lower torso (4), upper and lower, right and left arms (4), right and left thighs (4), and right and left lower legs (2). The face, neck, hands and feet were not covered with cooling tubes. TABLE 4.1 gives pertinent dimensions of the cooling pads and the whole suit.

All the pads, excluding the one for the head, were stitched onto the inside of a No. 44 long sleeve, Towncraft, Raschel knit, men's thermal union underwear garment. The cooling hood was made of a snow suit hood with the cooling tubes stitched onto the inside. The 3/8 in. O.D. main supply Tygon tubes were stitched on the outside of the garment.

The body was divided into six separate regions:

- (1) Head,
- (2) Upper torso,
- (3) Lower torso,
- (4) Arms,
- (5) Thighs, and
- (6) Lower legs.

These regions were supplied with water from cold and hot headers. Inlet pressure of the water was maintained at 20 psig by pressure regulators. Before entering the cooling pads, the two streams were mixed, thus allowing for continuous regulation of water inlet temperature. Water inlet temperatures were measured by means of No. 30 gage copper-

---

†Numbers in parentheses here represent number of pads in region.

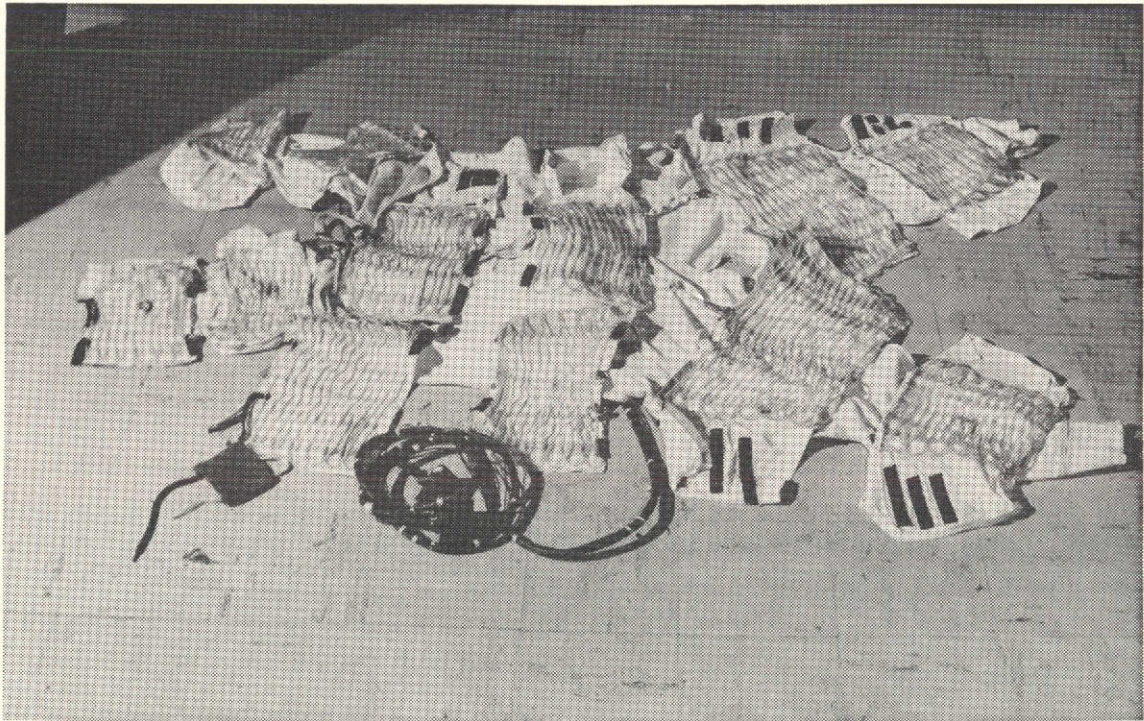


Figure 4.1 General view of the cooling garment.

TABLE 4.1a

## DATA ON THE COOLING GARMENT

Pad	Number of Pads	Number of Tube Rows in Pad	Area Covered by Pad		Total Area Covered by Pads		Percent Area Covered
			in. <sup>2</sup>	cm <sup>2</sup>	in. <sup>2</sup>	cm <sup>2</sup>	
Head	2	12	65	419	130	838	9.6
Front and Back, Upper and Lower Torso	4	14	111	716	444	2864	33.0
Upper Arms	2	11	62	400	124	800	9.2
Lower Arms	2	12	60	387	120	774	8.9
Upper Thighs	2	7	83	535	166	1070	12.3
Lower Thighs	2	10	96	619	192	1238	14.2
Lower Legs	2	16	86	555	172	1110	12.8
Total	16	--	--	--	1348	8694	100

TABLE 4.1b

## DATA ON THE COOLING GARMENT

	Cooling Garment		Insulating Suit		Cooling Hood		Insulating Hood		Total	
	kg	lb	kg	lb	kg	lb	kg	lb	kg	lb
Weight, dry	4.41	9.72	0.80	1.61	0.25	0.55	0.31	0.68	5.77	12.56
Weight, wet	4.88	10.77	--	--	0.30	0.66	--	--	6.29	19.33

constantan thermocouples using a Leeds and Northrup millivolt potentiometer. At a later stage, the thermocouples were replaced by interchangeable, multipurpose No. 401 thermistors using a Yellow Springs Instrument Co. Tele-Thermometer.

The difference between outlet and inlet temperature of each individual pad was measured by thermopiles consisting of five No. 30 gage copper-constantan thermocouples. These were connected in series to increase the sensitivity of the measurement. The thermopiles were glued to special Plexiglas connectors using 910 Eastman adhesive. The temperatures were continuously recorded on a Leeds and Northrup Speedomax Type G recording potentiometer. Water flow rates of each of the regions were measured by a Fisher and Porter rotameter. All the thermocouple assemblies and thermistors were precalibrated in a constant temperature bath against a precision platinum resistance thermometer. Figure 4.2 shows a schematic of the cooling pads and the control, supply, and measuring systems. Figure 4.3 shows the water supply system, the rotameter, and the potentiometer recorder.

On top of the underwear garment, the subjects donned an insulating suit which thermally isolated them from the environment. A heavily furred hood was used for the same purpose on the head. On the feet, all test subjects wore tennis shoes.

An A. R. Young treadmill was used for the walking sessions. The speed of the treadmill belt was controlled to correspond to the desired level of activity and was timed by a stop watch.

For metabolic measurements, expired air samples were taken with metalized Douglass bags [66]. The bags were placed inside a tightly

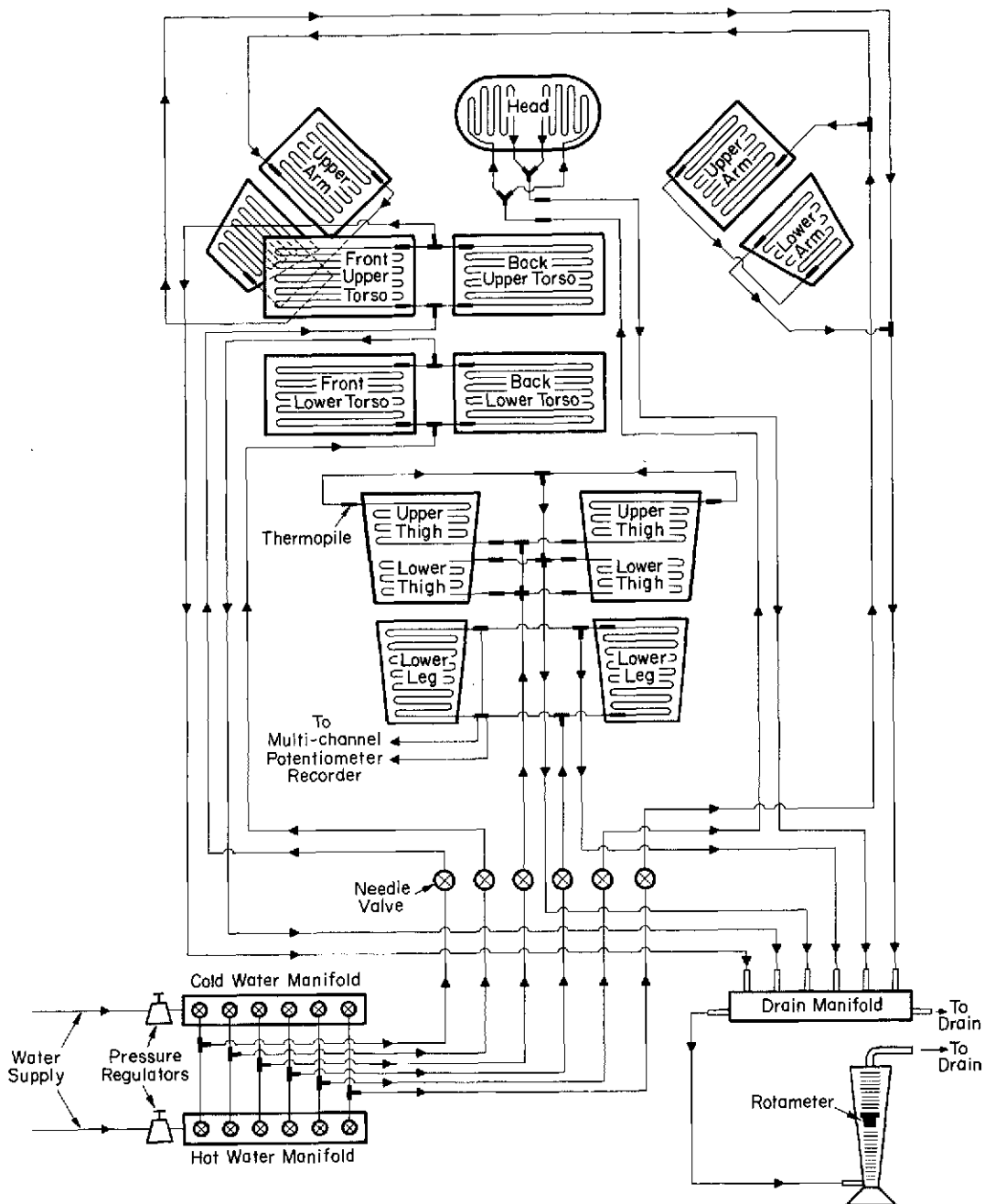


Figure 4.2 Schematic diagram of the cooling garment and the control, supply and measuring systems.

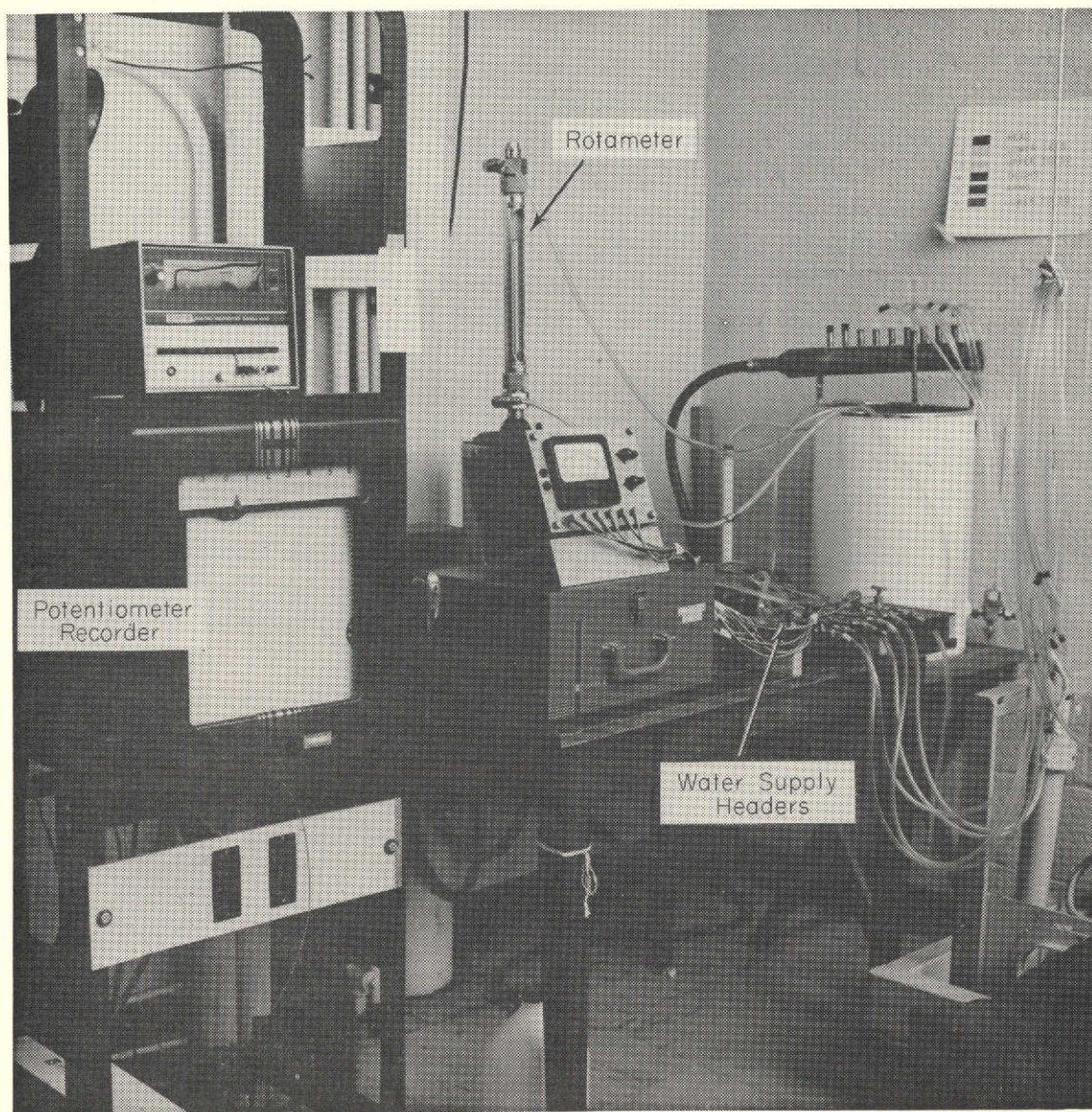


Figure 4.3 View of the water supply system, rotameter and potentiometer recorder used for the experiments with the cooling suit.

sealed Plexiglas chamber that was under vacuum of about 5 mm Hg [67]. Air was inhaled and exhaled through a mouth piece while the nostrils were blocked with a noseclip. Two sets of one-way rubber valves insured the separation of the two streams. The expired air was then directed through a 1 in. I.D. rubber hose into a mixing chamber. One minute sampling was achieved by opening a one-way stopcock valve thus exposing a previously evacuated metalized bag to the exhaled air.

Air volumetric flow rates were measured by means of a Parkinson-Cowan dry gas meter. Inlet and outlet air temperatures were measured by two interchangeable, multipurpose, No. 401 Yellow Springs thermistors using the company's Tele-Thermometer. Figure 4.4 shows part of the treadmill and the system used for collecting air samples. Air samples were analyzed for  $\text{CO}_2$  and  $\text{O}_2$  content. A Godart-Mijnhardt  $\text{CO}_2$  thermal conductivity meter, Pulmo Analyser Type 44-A-2 and a Beckmann Paramagnetic  $\text{O}_2$  analyzer, Model C2, were used. The results of this analysis together with the corresponding air flow rates were then used to evaluate the energy expenditure [68].

The temperature of the ear canal was taken as a measure of deep body temperature. This was done by an ear thermistor No. 510 and a Yellow Springs Instrument Co. Tele-Thermometer. The thermistor was inserted approximately one-half inch into the ear canal and was held in place by a specially prepared ear plug made of medical grade silicone rubber. The outside ear was covered by a piece of polyurethane foam to exclude possible effects of the cooling tubes. The reasons for measuring the temperature of the ear canal rather than the more commonly used rectal temperature were twofold: first, it was more convenient for walking; and second, it gave a closer indication to the

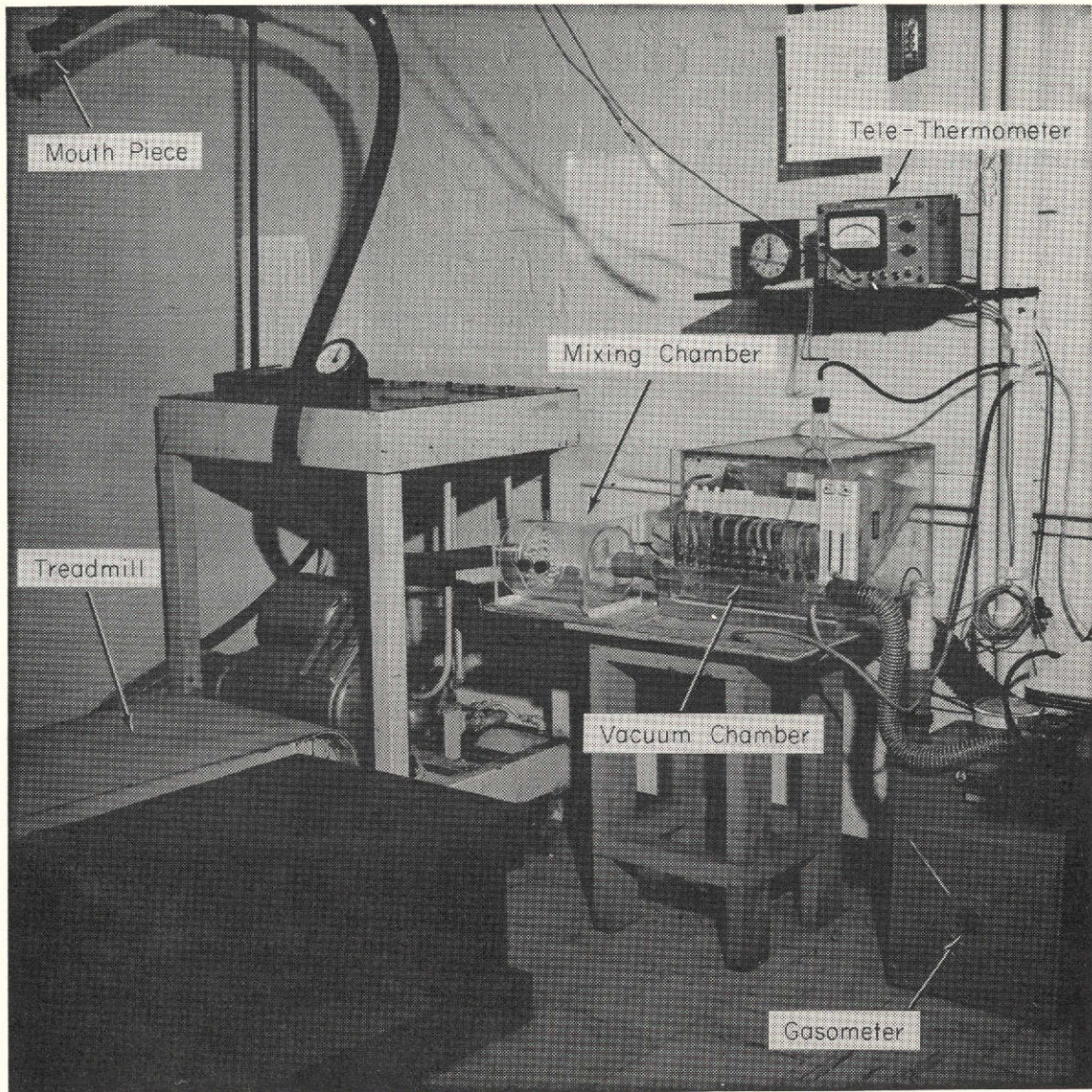


Figure 4.4 View of the treadmill, Tele-Thermometer and system for collecting samples for determining metabolic rates.

temperature regulated by the body, i.e., the temperature of the hypothalamus. Figure 4.5 shows a general view of the experimental set-up with a test subject dressed up with the cooling and insulating suits walking on the treadmill. Ear canal thermistor is not shown connected in this picture.

A Buffalo special physiological beam scale was used to weigh the subjects before and after the experiments. The capacity of this scale is 125 kg and the sensitivity is  $\pm 0.25$  gr.

#### 4.2.2 Individual Cooling Pads†

Three different individual cooling pads were constructed for the purpose of partially validating the analytical predictions. These pads were designed to fit over the thigh of a test subject. They were all made of gum rubber with parallel Tygon tubing glued onto one side using RTV glue. TABLE 4.2 gives pertinent data on the individual pads.

Number 30 gage copper-constantan thermocouples were used to measure cooling water temperatures and skin temperatures between two adjacent tubes. The thermocouples were equally spaced along a diagonal between the tubes and were pressed against the skin to insure good thermal contact. Figure 4.6 illustrates one of the cooling pads and the thermocouples.

The cooling pads were supplied with water by the same system as described in the preceding section. Water supply temperature and the difference between water outlet and inlet temperatures were

---

†This set-up was built and these experiments were performed by Mr. R. J. Leo under the supervision of the author.



Figure 4.5 General view of the set-up used for the experiments with the cooling suit. A test subject is shown dressed up in the cooling suit walking on the treadmill. No tennis shoes are shown in this picture and the ear canal thermistor is not connected.

TABLE 4.2

## DATA ON THE INDIVIDUAL COOLING PADS

	Outside Diameter of Tubes		Spacing of Tubes		Number of Rows of Tubes	Total Length of Tubes		Area Covered by Pad		Approximate Contact Area with the Skin		Percent of Area in Contact with Tubes
	in.	cm	in.	cm		in.	cm	in. <sup>2</sup>	cm <sup>2</sup>	in. <sup>2</sup>	cm <sup>2</sup>	
Pad No. 1	5/32	0.397	1	2.54	10	163	414	140	910	22.9	148	16.4
Pad No. 2	5/32	0.397	5/8	1.59	14	228	580	132	852	32.1	207	24.3
Pad No. 3	7/32	0.556	1	2.54	10	163	414	145	937	28.5	184	19.7

2025  
A

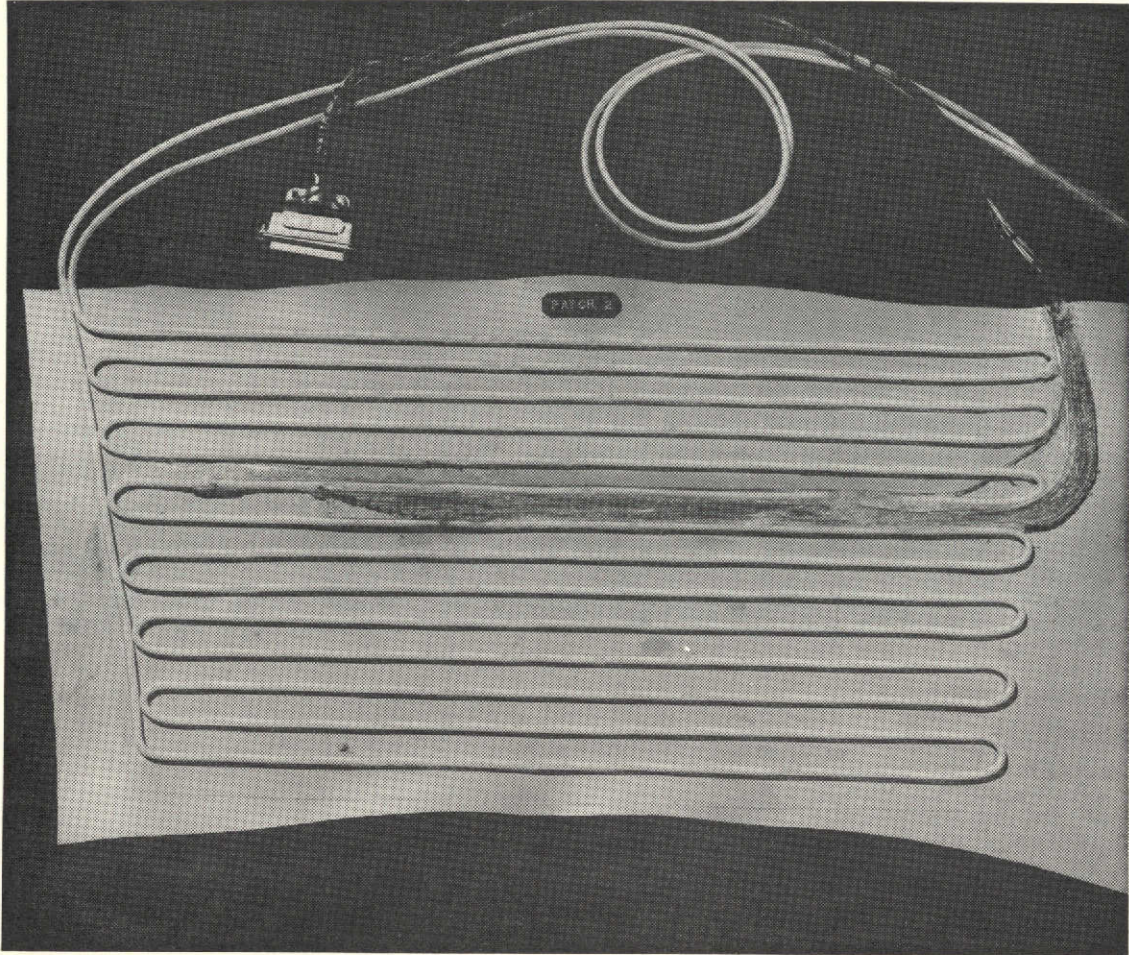


Figure 4.6 View of one of the individual pads.

continuously recorded by a Brush Mark 280 Recorder. Thermopiles consisting of five copper-constantan thermocouples connected in series and a Brush pre-amplifier were used to increase the sensitivity of the reading of the difference between outlet and inlet water temperatures.

For metabolic measurements, the same system as described in the preceding section was used. Ear canal temperatures were taken using the same technique as was used for the experiments with the cooling suit.

A Leeds and Northrup Speedomax W, 12-point potentiometer-recorder was used for continuously monitoring and recording the temperature of the cooling water and the skin temperatures between the adjacent tubes.

During the experiments the subject pedalled a Monark bicycle ergometer at a constant preset speed and load.

#### 4.3 EXPERIMENTS WITH THE COOLING SUIT

##### 4.3.1 Activity Schedules

Five different schedules of activity were used for all the test subjects. The schedules consisted of alternate periods of standing and level walking on the treadmill with or without the cooling suit. The various levels of activity were chosen to cover a variety of different activity loads. The steady state and, to some extent, transient state characteristics of the cooling suit were studied under those conditions. Each of the schedules started with the subject standing still for at least 45 minutes. During this period water inlet temperatures were adjusted to correspond to the subject's own sense of comfort. The duration of each of the standing and walking sessions (except the second part of Schedule V) was 45 minutes. It was assumed that after 45 minutes

from the onset of a change in activity level the subjects reached a thermal quasi-steady state. Figure 4.7 illustrates schematically the details of the five activity schedules.

Schedule I, with the lowest activity levels, consisted of four step changes: standing; walking at 2 mph; standing; walking at 2.5 mph; and standing. Two mph was the slowest speed that could be obtained from the treadmill with the subject on it. Once the subject's comfort was achieved while standing, no deliberate changes in water inlet temperatures were made. The small changes in water inlet temperatures were due to the instability of the water supply system. The purpose for maintaining constant temperature was to test the cooling capacity of the suit at higher metabolic rates while operating at the same temperature levels which were considered comfortable at the lower metabolic rate.

Schedule II was designed to compare the effect of changing the water inlet temperature at the same activity level. It consisted of two identical, periodic step changes: standing; walking at 3 mph; standing; and again walking at 3 mph and standing. During the first walking session, no adjustments in water inlet temperatures were permitted. During the second cycle, however, the water temperatures were adjusted to correspond to the subject's comfort.

Schedule III consisted of four step changes: standing; walking at 2 mph; walking at 4 mph; walking at 2 mph; and standing. The purpose of this schedule of activities was to study the characteristics of the suit at a moderately high activity level. (Approximately 1650 Btu/hr, 482 w ) The intermediate 2 mph walking sessions were used for two

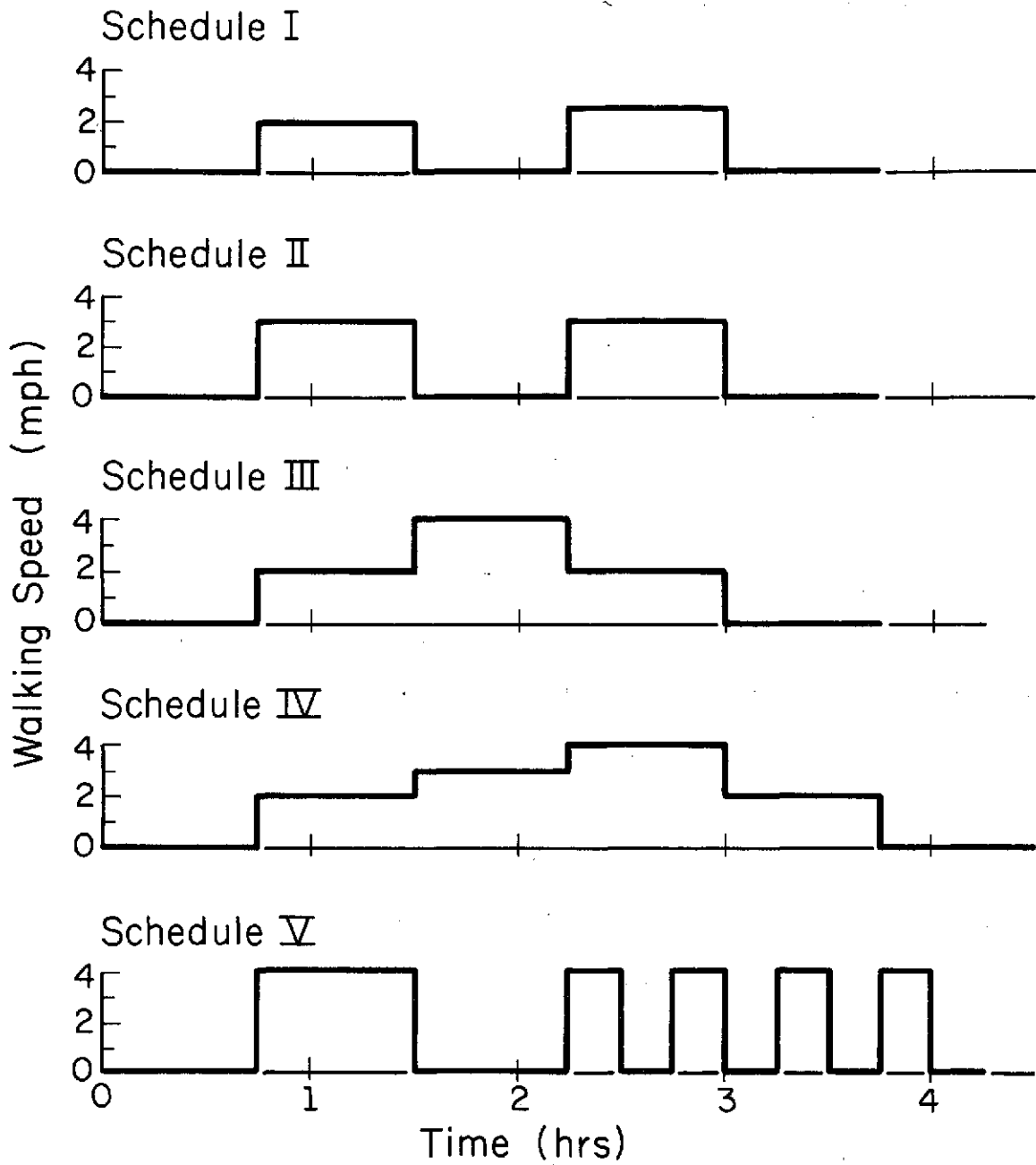


Figure 4.7 Activity schedules used for the experiments with the cooling suit.

reasons: first, to allow a gradual change to the high activity level and, second, to some extent, to acquaint the subjects with the relatively high speed that was also included in the last two schedules. Adjustments of water inlet temperatures were permitted throughout the entire duration of the experiment.

Schedule IV was almost identical to Schedule III, but it included an additional walking session at 3 mph immediately preceding the 4 mph walking period. This was done to study the effect of a more gradual change in activity level.

Schedule V was used to study two features: first, to examine the performance of the suit at a step from standing to the moderately high activity level without any intermediate changes and, second, to determine the characteristics of the suit with thermal transient changes at the same activity levels. This schedule consisted of the following step changes: standing; walking at 4 mph and standing followed by four short identical periodic sessions of walking at 4 mph and standing. The duration of each of the short walking and standing sessions was 15 minutes. Readjustments in water inlet temperatures were permitted throughout this entire schedule.

#### 4.3.2 Test Subjects

Five male students, ranging in age from 18 to 29 years, volunteered to serve as test subjects. They were all required to pass a thorough physical examination. They represented a variety of physical fitnesses ranging from poor to athletic. There were limits on the height and weight of the subjects dictated by the size of the cooling

suit. The physical characteristics of the test subjects are summarized in TABLE 4.3. Surface areas were determined from the Dubois height/weight formula [69]†. All but one subject completed all five experiments. Subject PF did not complete Schedule V due to a stiff thigh muscle.

#### 4.3.3 Experimental Procedure

All the experiments were performed at the Laboratory for Ergonomics Research, University of Illinois at Urbana-Champaign. This laboratory is permanently air conditioned at about 23°C and 60 percent relative humidity. The experiments were all run during July and August 1970 and were scheduled at the subject's convenience. The subjects performed at least once a week and usually more often.

A total of 29 experiments were run. Of these, 24 were performed with the cooling suit. Five pilot runs were performed by subject SKB repeating the regular activity schedules without the suit. During the pilot runs subject SKB wore tennis shoes, shorts and a light T shirt. All subjects started with Schedule I and, in order, completed the other schedules sequentially. The subjects were permitted to listen to the radio, and read while standing, but no eating, drinking or smoking was allowed during the experiments.

At the beginning and end of each experiment the subjects were weighed, and their oral temperature and blood pressure were taken. The last two measurements were taken only as precautionary measures against any acute effects of the experiment on the subject. Also the barometric

---

†Surface area [cm<sup>2</sup>] = 71.84 W[kg]<sup>0.425</sup> · h[cm]<sup>0.725</sup>.

TABLE 4.3  
CHARACTERISTICS OF THE TEST SUBJECTS

Subject	Age	Height		Weight		Surface Area		Percent Area Covered by Cooling Pads
		cm	in.	kg	lb	m <sup>2</sup>	ft <sup>2</sup>	
A. SGP	20	173	68	65.7	144.8	1.78	19.2	48.8
B. SKB	22	170	67	61.1	134.7	1.71	18.4	50.8
C. HNT	27	170	67	64.2	141.5	1.74	18.7	50.0
D. RET	18	169	66.5	64.2	141.5	1.74	18.7	50.0
E. PF	29	161	63.5	55.8	123.0	1.58	17.0	55.0
Means	23.2	169	66.4	62.2	137.1	1.71	18.4	50.9

pressure was measured. During the experiments the following data were collected: ear canal temperatures, water inlet temperatures, differences between water inlet and outlet temperatures at each of the six regions of the body, water flow rates, respiratory volumetric rates and temperatures of expired air. During the runs of Schedule V and during the pilot runs without the suit, pulse rates were also taken. All measurements were taken at the end of each activity in the schedule and were assumed to represent the quasi-steady state values.

After the preliminary measurements, the subjects donned the cooling garment. Each of the cooling pads was fastened in place to insure good thermal contact. The thermally insulated suit was then put over the cooling garment. Next, the ear thermistor was inserted into the ear and the ear was covered to exclude possible thermal effects of the cooling hood. Finally, the water inlet and outlet tubes were connected, flow was started and the leads of the thermopiles were connected to the potentiometer recorder. Figures 4.8 through 4.11 show one of the subjects at various stages of dressing.

The subjects stood on a bench and water inlet temperatures were adjusted to conform to their sense of comfort. When a thermal quasi-steady state† was reached, as indicated by the potentiometer recorder, the treadmill was started. With the support of the supervisor of the experiment, the subjects stepped on the moving belt and started to walk. The speed of the treadmill was then quickly adjusted to the desired level. Step changes from walking to standing were done in the same manner. Figure 4.12 shows one of the subjects while walking and breathing through the system

---

†Quasi-steady state was defined as that state wherein no significant changes in the difference in outlet and inlet water temperatures was noticeable.

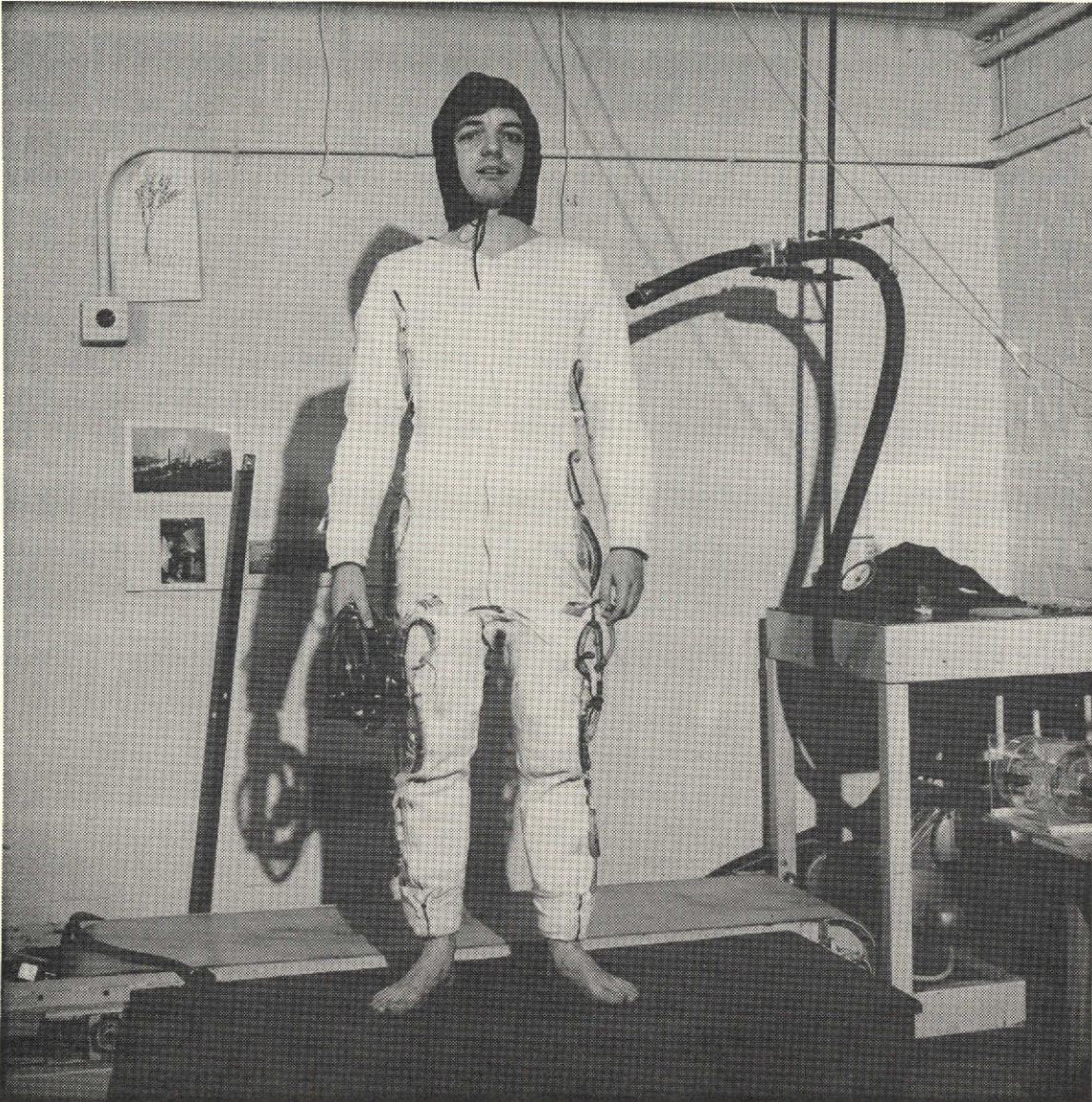


Figure 4.8 Front view of the cooling garment.

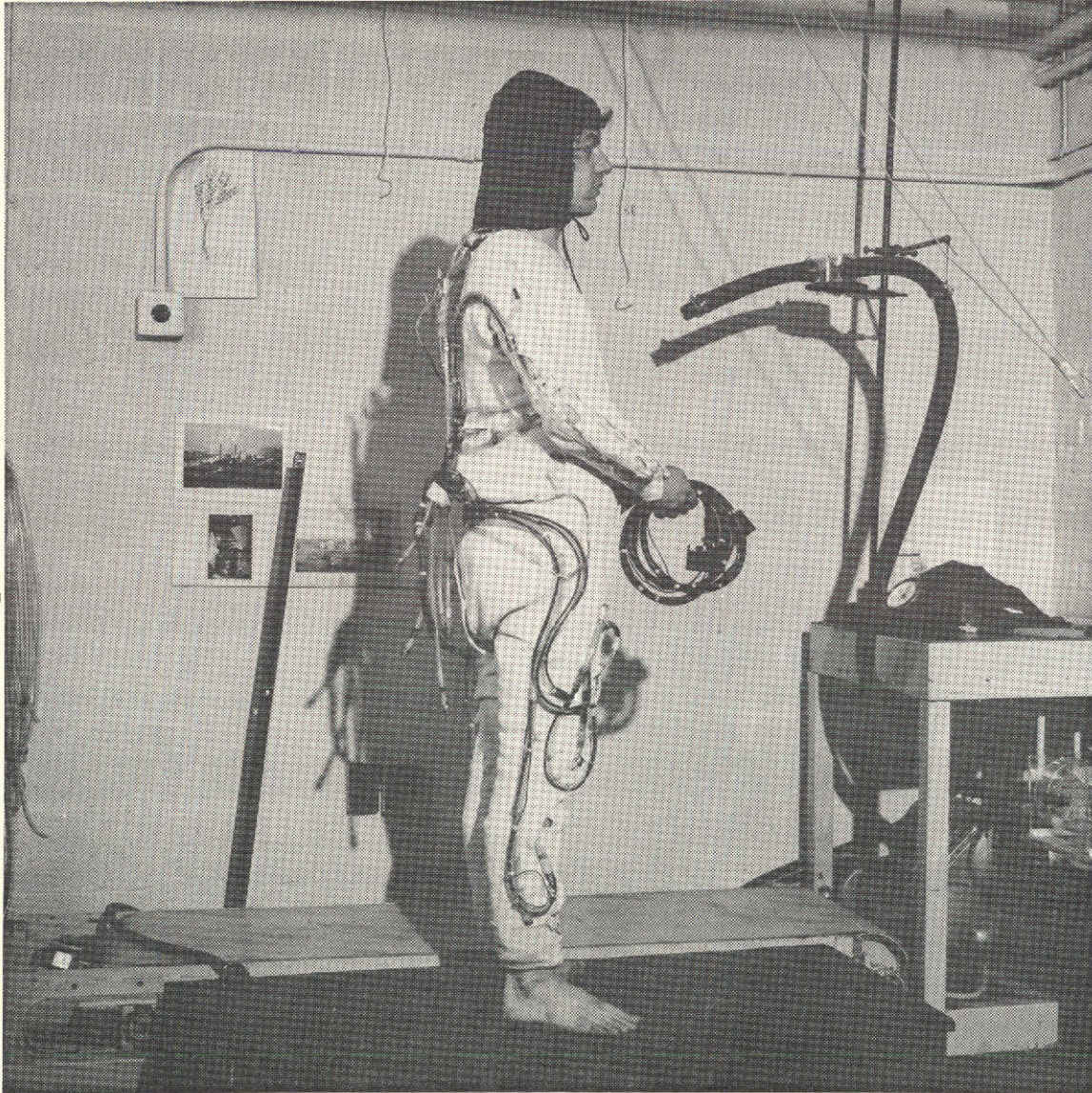


Figure 4.9 Side view of the cooling garment.

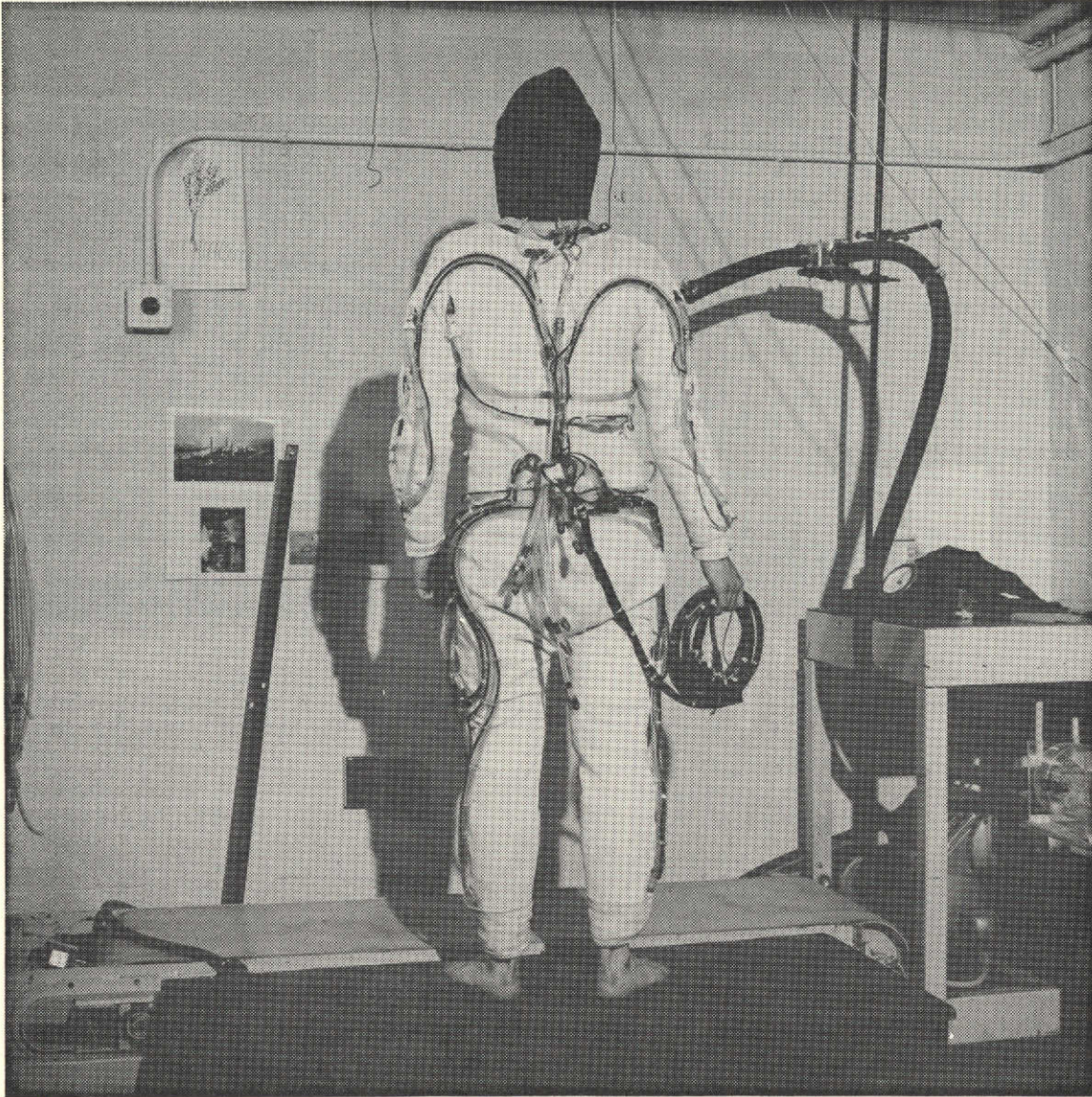


Figure 4.10 Back view of the cooling garment.



Figure 4.11 Front view of a test subject dressed up in the cooling and insulating garments.

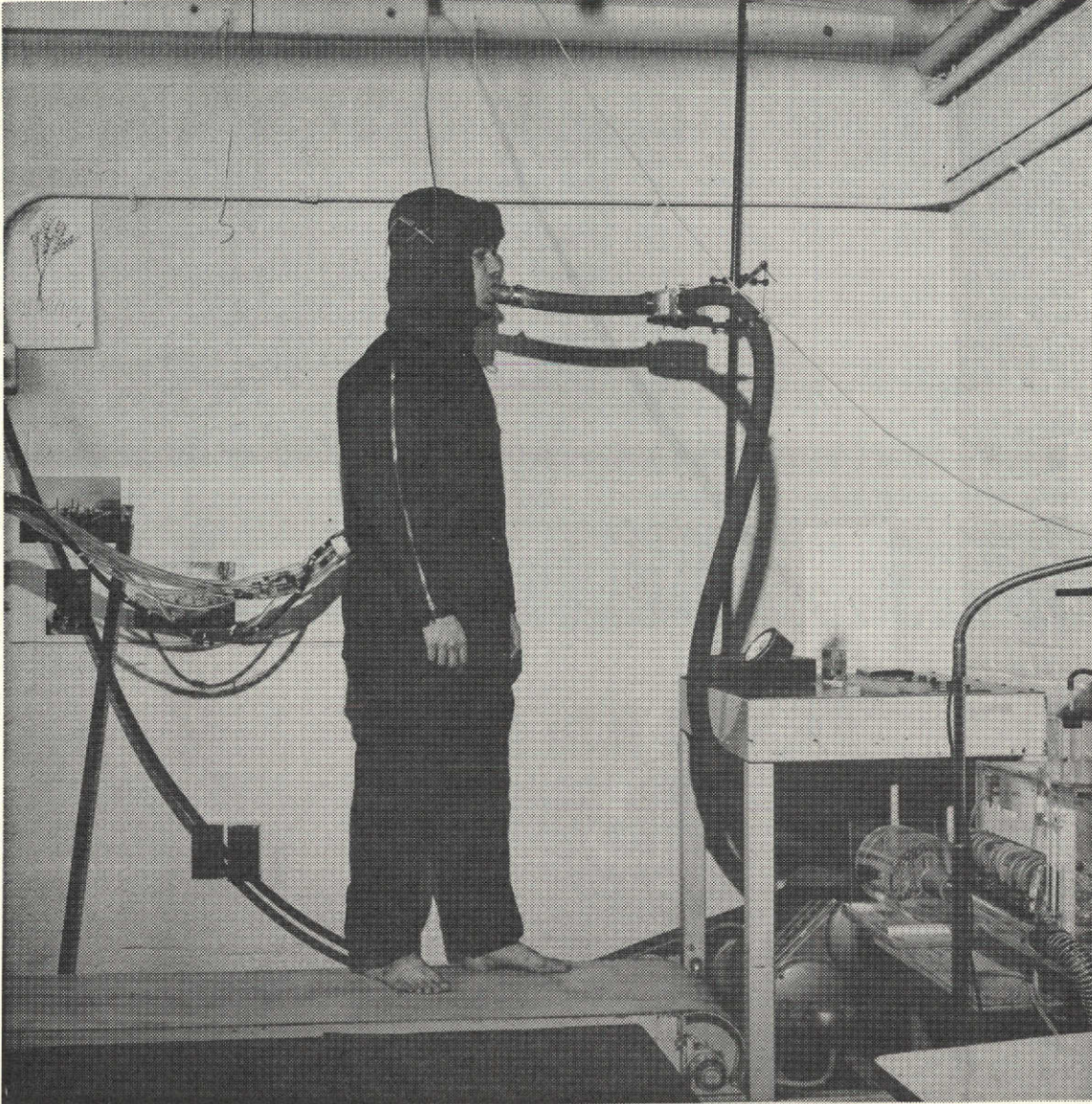


Figure 4.12 A test subject shown walking on the treadmill and breathing through the system for measuring metabolic rates. No tennis shoes are shown in the picture.

for measuring the metabolic rate.

#### 4.3.4 Measured, Recorded and Calculated Quantities

The following quantities were measured, recorded, or calculated from other measured data:

- (1) Total metabolic rate. This was calculated from volumetric flow rate of the expired air and the oxygen content obtained from the gas analysis. The caloric value of oxygen was assumed at 5.0 kcal/lit [70]. This value, although slightly high, conformed well with the respiratory quotients found in most of the runs. Maximum deviation from the actual caloric value was assumed to be about 4 percent.
- (2) Rate of heat removed by the suit at each region. This was taken as the product of the difference between water inlet and outlet temperatures and water flow rate. Specific heat of water was assumed to be unity.
- (3) Rate of heat lost by respiration. Flow rate, temperature and enthalpy of the expired air, assuming it to be saturated, were used for calculating this quantity.
- (4) Weight loss during the experiment. Taken as the difference between the initial and final weights of the subject.
- (5) Ear canal temperature. Measured by an ear thermistor and was assumed to simulate closely the temperature of the body that is regulated by the central temperature control mechanism.
- (6) Water inlet temperatures to each of the regions at the various activity levels. These were measured by thermistors that were

inserted into the water streams.

- (7) Order of preferred changes in water inlet temperatures to the different regions. This was recorded for the purpose of identifying those regions of the body that require changes in water temperature and the preferred order of the changes as a function of activity level.
- (8) Comfort vote. Based on the subject's own evaluation of his state of comfort. Only three choices were suggested: slightly cold, thermally comfortable, too warm.
- (9) Pulse rate. This was measured only during the experiments of Schedule V and the pilot runs without the suit. The pulse rate was assumed to be an index of the metabolic and cardiac costs of the physical work. Pulse rate was not taken during the experiments of the other schedules because these schedules were considered to represent quasi-steady states.

#### 4.4 EXPERIMENTS WITH THE INDIVIDUAL PADS

Three identical tests were conducted with the individual cooling pads. These tests were designed to compare the steady state temperature distribution on the skin for different cooling pads at the same level of activity. All experiments consisted of riding the bicycle ergometer at a constant speed and load for about two hours, corresponding to a total metabolic rate of about 1200 Btu/hr (352 w).

One male student volunteered to serve as a test subject for the experiments with the individual cooling pads. The physical characteristics of this subject are summarized in TABLE 4.4. At the beginning and end of

TABLE 4.4 CHARACTERISTICS OF SUBJECT TEK

Subject	Age	Height		Weight		Surface Area	
		cm	in.	kg.	lb.	m <sup>2</sup>	ft <sup>2</sup>
TEK	19	189	74.5	79.7	175.5	2.02	21.7

each of the experiments, the same procedure as was used for the experiments with the cooling suit was repeated (weighing, measuring blood pressure, etc.). Then the cooling pad was put in place on the thigh of the right leg. The water supply tubes were then connected, flow was started and the leads of the various measuring devices were connected to the appropriate recording instruments.

The subject started to bicycle at the preset speed and load and continued to do so until a steady state was reached. The steady state was obtained when no changes could be noticed in any of the measured parameters.

Figure 4.13 gives a general view of the set-up used for the experiments with the individual cooling pads with a test subject shown pedalling the bicycle ergometer.



Figure 4.13 General view of the set-up used for the experiments with the individual cooling pads. A test subject is shown pedalling the bicycle ergometer.

## 5. DISCUSSION

## 5.1 EXPERIMENTS WITH THE COOLING SUIT

In order to present the large amount of data that was gathered during the experiments, most of the results of each schedule were averaged and are presented in this form. Wherever it was feasible, entire ranges of individual variations were also shown. All the data, excluding the weight losses, were measured or calculated at the end of each of the step changes in activity level.

Figures 5.1 through 5.5 show mean values of metabolic rates and of heat removed by the suit and by respiration during the various schedules of activity. Also shown are the ranges of metabolic rates included in the mean values. It is seen that during the standing sessions of Schedules I through IV and the first part of Schedule V, most of the heat produced in the body was removed by the cooling suit. In many cases the amount of heat removed by the suit even exceeded slightly the total metabolic rate. This phenomenon is believed to be due to possible thermal transients indicated by a decrease in "deep body" temperature following a change in activity from walking to standing (Fig. 5.6) and cumulative measurement errors.

During all of the walking sessions the relative amount of heat removed by the suit dropped significantly. At best, only about 70 percent of the total metabolic rate was removed by the suit during the walking sessions; this value was usually closer to 50 percent. Possible explanations to account for the portion of the total metabolic rate that was not removed by the cooling suit are the following:

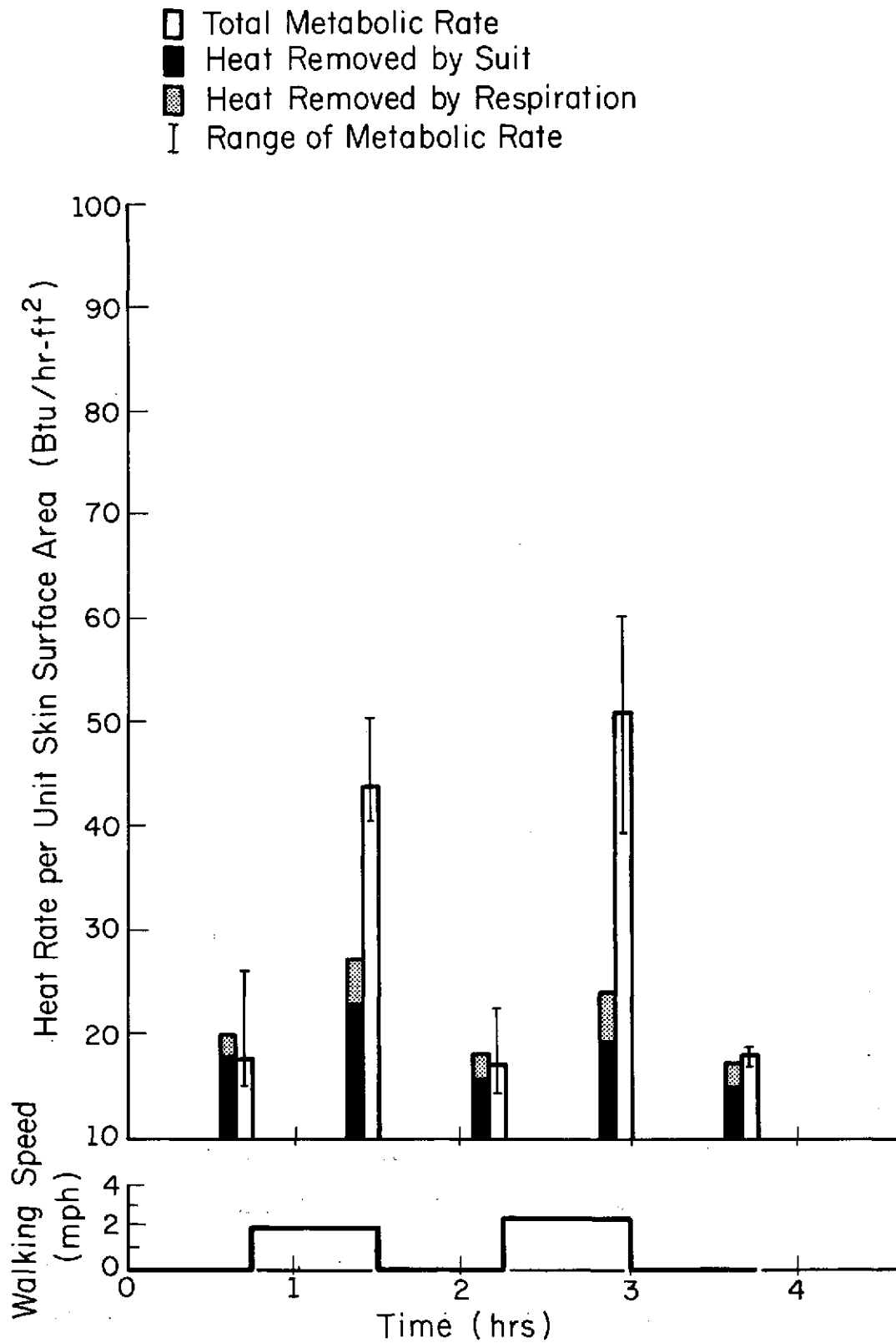


Figure 5.1 Mean values of metabolic rates and of the amounts of heat removed by the cooling suit and by respiration for Schedule I.

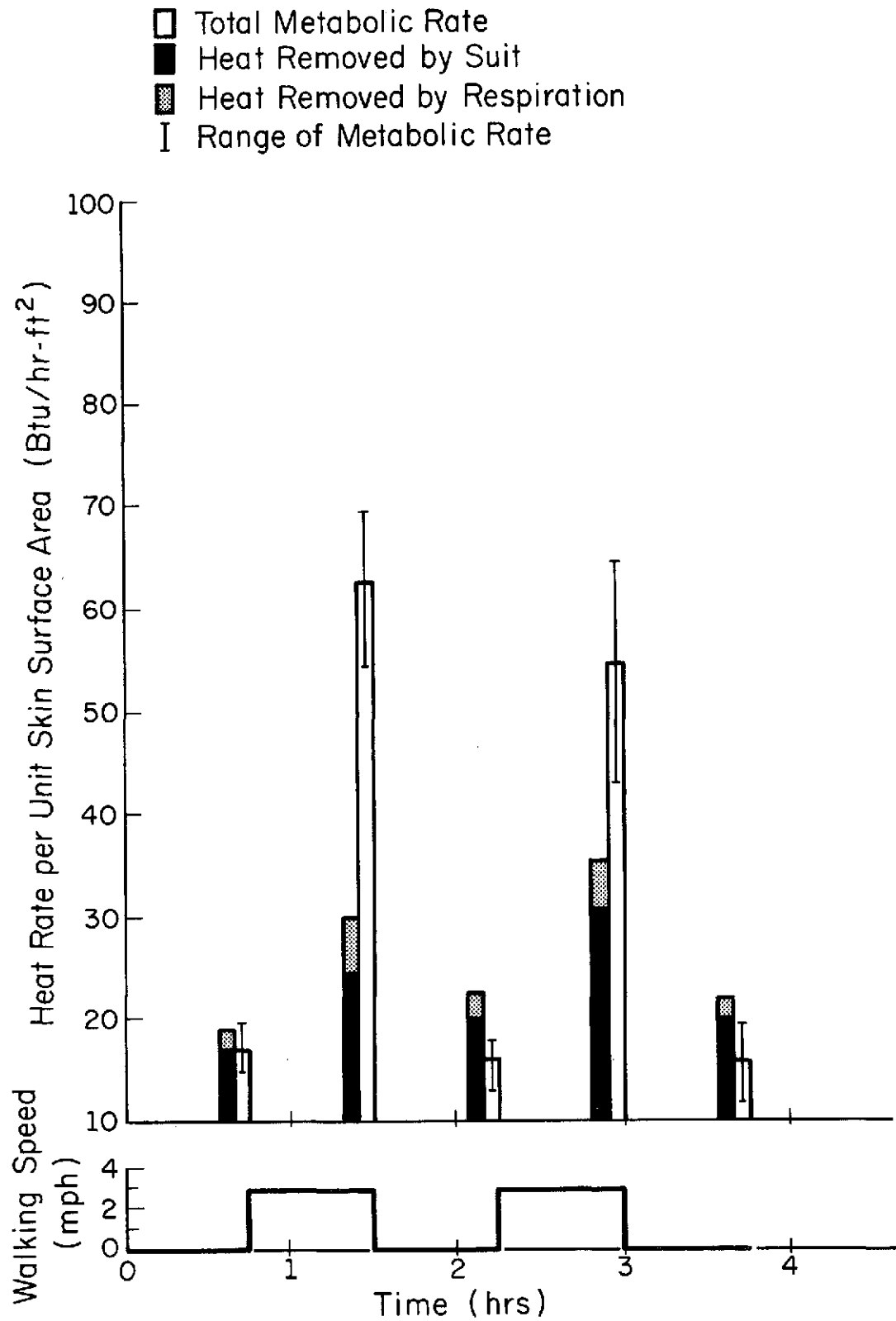


Figure 5.2 Mean values of metabolic rates and of the amounts of heat removed by the cooling suit and by respiration for Schedule II.

- Total Metabolic Rate
- Heat Removed by Suit
- ▨ Heat Removed by Respiration
- I Range of Metabolic Rate

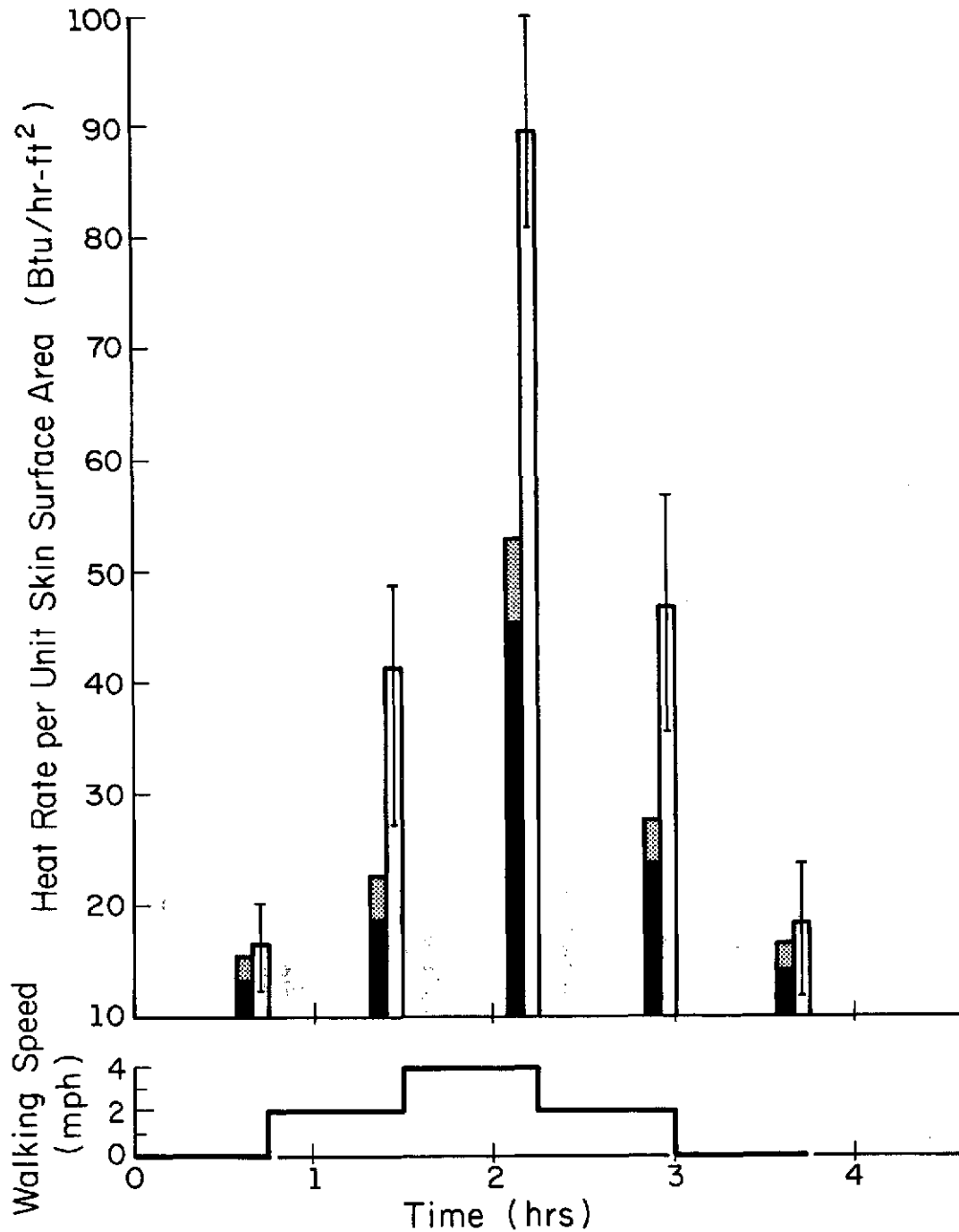


Figure 5.3 Mean values of metabolic rates and of the amounts of heat removed by the cooling suit and by respiration for Schedule III.

- Total Metabolic Rate
- Heat Removed by Suit
- ▨ Heat Removed by Respiration
- I Range of Metabolic Rate

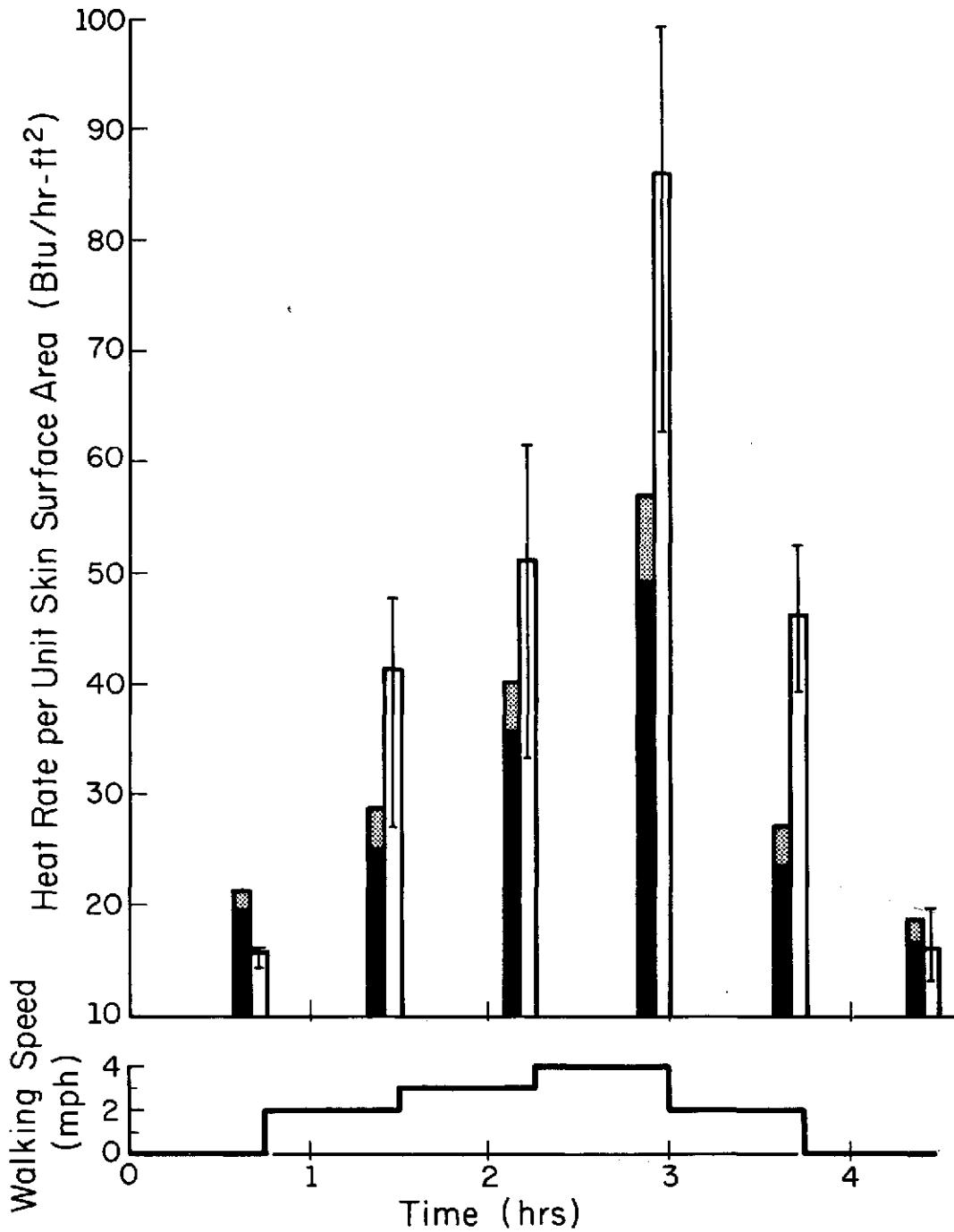


Figure 5.4 Mean values of metabolic rates and of the amounts of heat removed by the cooling suit and by respiration for Schedule IV.

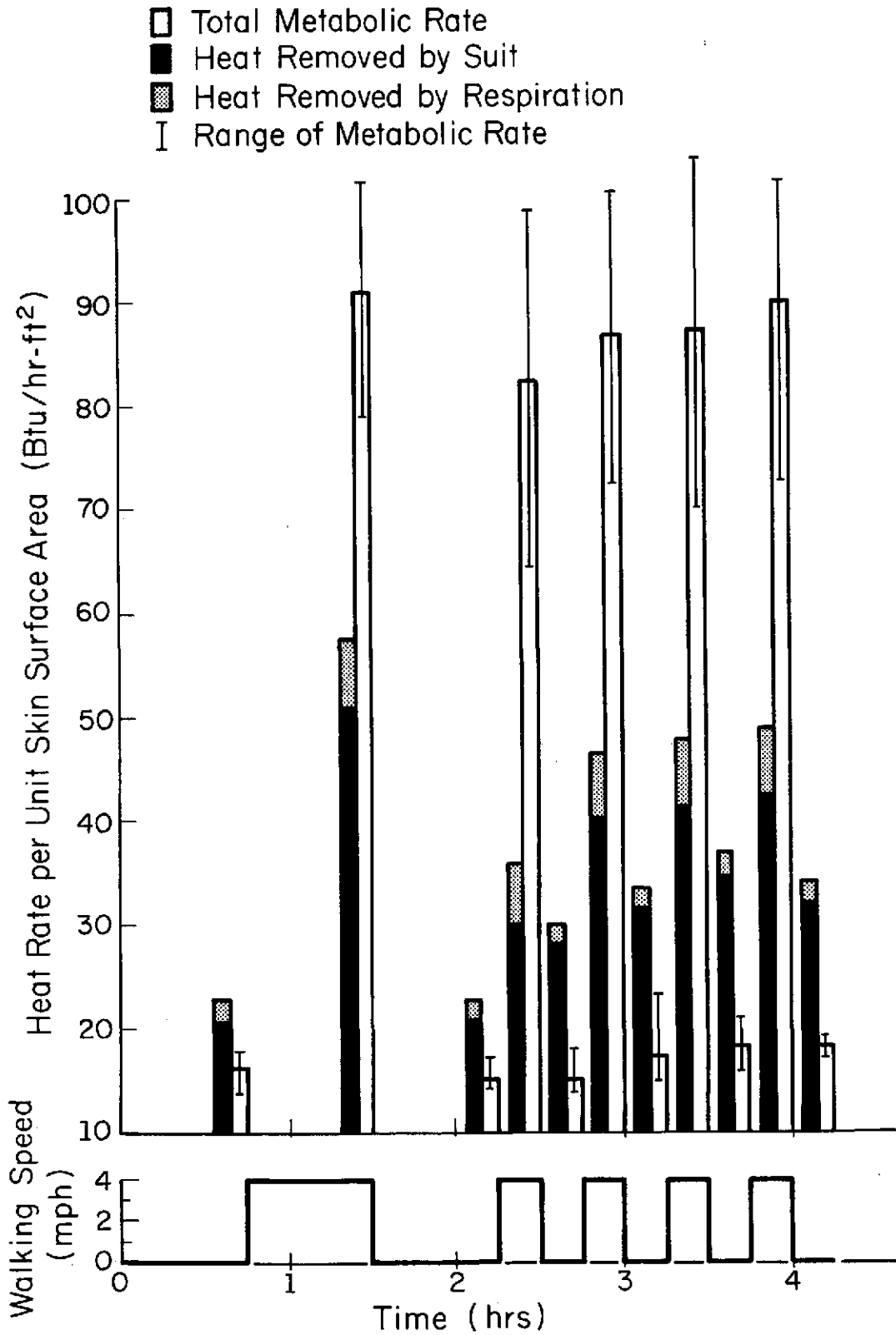


Figure 5.5 Mean values of metabolic rates and of the amounts of heat removed by the cooling suit and by respiration for Schedule V.

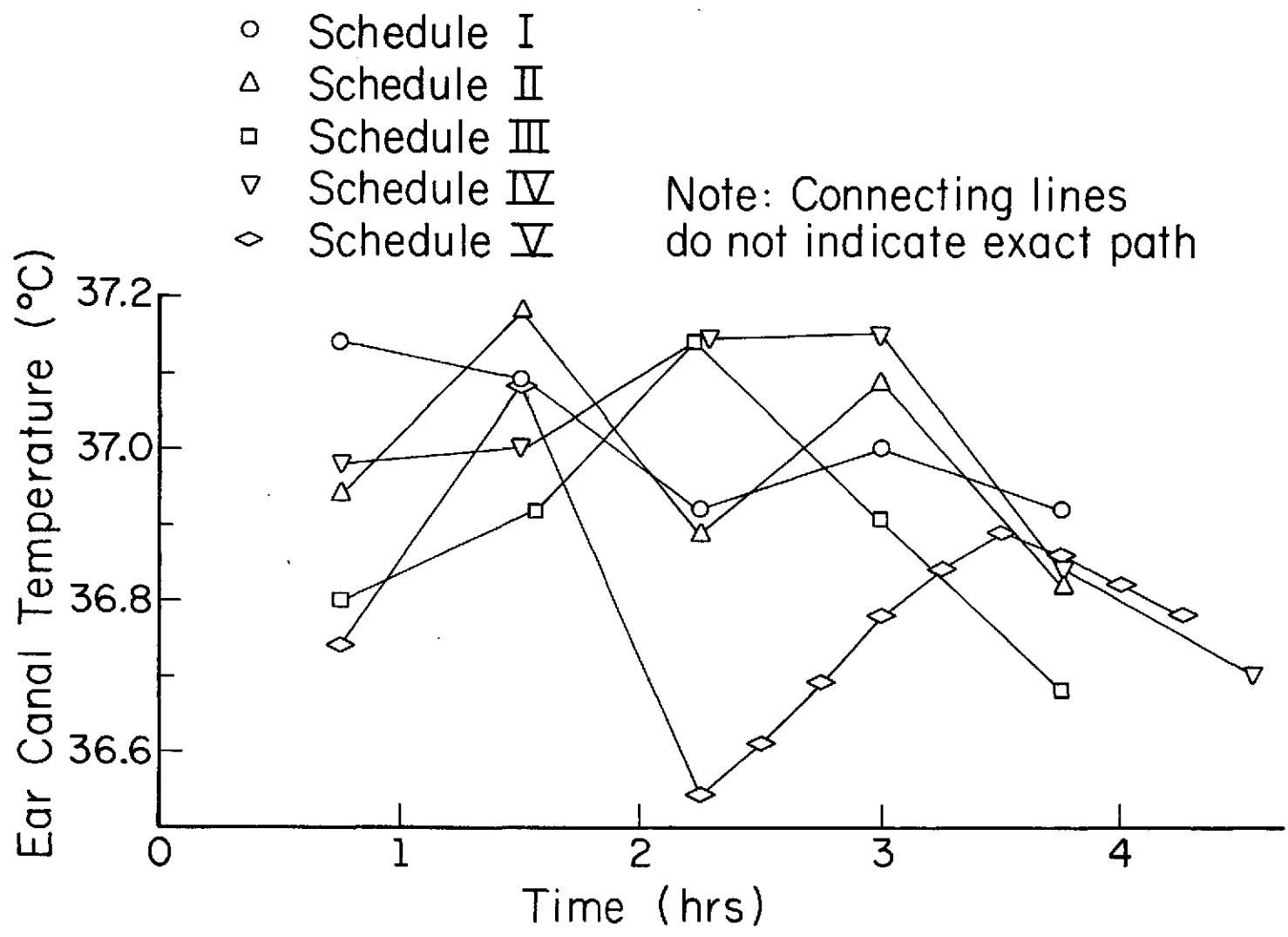


Figure 5.6 Average ear canal temperatures for the various schedules.

- (1) Thermal transient states with heat still being stored inside the body. (Increase in "deep body" temperatures, Fig. 5.6.)
- (2) Heat dissipated to the environment from the uncovered surfaces, e.g., face, forehead and hands.
- (3) Heat removed by the respiratory system.
- (4) Heat removed by perspiration aided by air that was pumped under the somewhat loose thermal insulating suit.
- (5) Work done by the muscles.
- (6) Measurement errors and inaccuracies.
- (7) Heat lost to the environment through the clothing assembly.

From these, only the contribution of item 3, i.e., respiration, was estimated. It was calculated that the amount of heat dissipated by the respiratory system ranged from 7.3 percent to 14.8 percent of the total metabolic rate. These values are consistent with values reported by Bazett [55]. With the increase in metabolic rate the amount of heat carried away by respiration also increased. However, the relative amount of heat removed by the exhaled air decreased. The remaining unaccounted-for portion of the metabolic rate is assumed to have been removed by the other channels that were mentioned above.

It was found that, from the comfort standpoint, the present cooling system was not sufficient to accommodate for metabolic rates in excess of about 1200 Btu/hr (352 w). This finding was manifested by the consistent comfort votes of "too warm" at the moderately high activity levels (TABLE 5.1). It is assumed that the insufficiency of the cooling system was due to two reasons: too small a contact area

TABLE 5.1

ORDER OF PREFERRED CHANGES IN WATER INLET  
TEMPERATURES AND THE COMFORT VOTE FOR THE VARIOUS ACTIVITIES

	Change in Water Inlet Temperature	Subjects				
		SGP	SKB	HNT	RET	PF
SCHEDULE II						
Standing to 3 mph	Decrease	All over the body	Not Recorded	Not Recorded	1. Upper Torso 2. Lower Legs 3. Thighs 4. Lower Torso	All over the body
Comfort Vote		Comfortable	Comfortable	Comfortable	Comfortable	Comfortable
3 mph to Standing	Increase	No Changes	Not Recorded	Not Recorded	All over the body <u>but</u> the lower legs	No Changes
Comfort Vote		Comfortable	Comfortable	Comfortable	Comfortable	Comfortable

(continued)

251

113

TABLE 5.1 continued

	Change in Water Inlet Temperature	Subjects				
		SGP	SKB	HNT	RET	PF
SCHEDULE III						
Standing to 2 mph	Decrease	Not Recorded	No Changes	1. Legs 2. Arms	All over the body	1. Head 2. Upper Torso
Comfort Vote		Comfortable	Comfortable	Comfortable	Comfortable	Comfortable
2 mph to 4 mph	Decrease	Not Recorded	1. Legs 2. Lower Torso 3. Head 4. Arms 5. Upper Torso	All over the body	1. Lower Torso 2. Lower Legs 3. Upper Torso	1. Head 2. Upper Torso
Comfort Vote		Too Warm	Too Warm	Too Warm	Too Warm	Too Warm
4 mph to 2 mph	Increase	Not Recorded	1. Upper Torso 2. Arms	No Changes	1. Head 2. Arms 3. Upper Torso	No Changes
Comfort Vote		Comfortable	Comfortable	Comfortable	Comfortable	Comfortable
2 mph to Standing	Increase	Not Recorded	No Changes	1. All over the body 2. Lower Torso	1. Arms 2. Upper Torso 3. Thighs	No Changes
Comfort Vote		Comfortable	Comfortable	Comfortable	Comfortable	Comfortable

(continued)

252 >

114

TABLE 5.1 continued

	Change in Water Inlet Temperature	Subjects				
		SGP	SKB	HNT	RET	PF
SCHEDULE IV						
Standing to 2 mph	Decrease	1. Thighs 2. Arms 3. Upper Torso	No Changes	1. Lower Torso 2. Lower Legs 3. Upper Torso 4. Arms	No Changes	No Changes
Comfort Vote		Comfortable	Comfortable	Comfortable	Comfortable	Comfortable
2 mph to 3 mph	Decrease	1. Thighs 2. Upper Torso 3. Arms 4. Lower Torso	1. Lower Legs 2. Upper Torso	1. Lower Torso 2. Lower Legs 3. Head	1. Lower Legs 2. Lower Torso 3. Thighs 4. Upper Thighs	No Changes
Comfort Vote		Comfortable	Comfortable	Comfortable	Comfortable	Comfortable
3 mph to 4 mph	Decrease	All over the body	All over the body	1. Lower Torso 2. Lower Legs 3. Head 4. All over the body	1. Lower Torso 2. Thighs 3. Lower Legs 4. Head 5. Lower Legs	Head
Comfort Vote		Too Warm	Too Warm	Too Warm	Too Warm	Too Warm

(continued)

253 >

115

TABLE 5.1 continued

	Change in Water Inlet Temperature	Subjects				
		SGP	SKB	HNT	RET	PF
SCHEDULE IV cont.						
4 mph to 2 mph	Increase	All over the body	1. Upper Torso 2. Lower Torso 3. Arms	No Changes	All over the body	No Changes
Comfort Vote		Comfortable	Comfortable	Comfortable	Comfortable	Comfortable
2 mph to Standing	Increase	No Changes	1. Upper Torso 2. Lower Torso 3. Arms 4. Head 5. Lower Legs	1. All over the body 2. Lower Torso 3. Lower Legs	All over the body	No Changes
Comfort Vote		Slightly Cool	Comfortable	Comfortable	Comfortable	Comfortable

(continued)

25A

TABLE 5.1 continued

	Change in Water Inlet Temperature	Subjects			
		SGP	SKB	HNT	RET
SCHEDULE V					
Standing to 4 mph (45 min run)	Decrease	1. Upper Torso 2. Lower Torso 3. Thighs 4. Upper Torso 5. Head	1. Lower Legs 2. All over the body 3. Head	All over the body	All over the body
Comfort Vote		Too Warm	Too Warm	Too Warm	Too Warm
4 mph to Standing (45 min run)	Increase	1. Upper Torso 2. Arms 3. Thighs	1. Thighs 2. Upper Torso 3. Arms 4. Upper Torso	1. Lower Torso 2. Lower Legs	All over the body
Comfort Vote		Comfortable	Comfortable	Comfortable	Comfortable
Standing to 4 mph (15 min run)	Decrease	No Changes	No Changes	All over the body	No Changes
Comfort Vote		Comfortable	Comfortable	Comfortable	Comfortable
Rest of Experiment (4 mph and standing alternately)		No Changes	No Changes	No Changes	Alternate Changes All over the Body
Comfort Vote		Comfortable	Comfortable	Comfortable	Comfortable

21  
01  
A

between the skin and the cooling tubes and too high water inlet temperatures. The actual contact area between the skin and the cooling tubes was estimated to be about 10 percent of the total skin surface area. The lowest water inlet temperature that was obtained in most of the experiments was about 16°C. Increasing the contact area between the skin and the cooling tubes and/or lowering water inlet temperatures should improve the cooling capacity of the suit. This conclusion was suggested by the results obtained by Webb and Annis [71], who also reported experiments with a cooling suit. They estimated that 22 percent of the total skin surface area was in contact with the cooling tubes in their experiments. All of their subjects were reported to have been comfortable with the lowest water inlet temperature of 16°C and high metabolic rates of 2400 Btu/hr (700 w) for two hours.

It is evident that during the second part of the experiments of Schedule V, a quasi-steady state was never reached. This finding was true for the metabolic rates and amounts of heat removed by the cooling suit (Fig. 5.5) and also for the heart rates and ear canal temperatures (Fig. 5.7). These quantities show a clear trend of increase with time at least during the two hours of the short (15 minutes each) alternate changes in levels of activity. The amount of heat removed by respiration, however, seems to have reached a quasi-steady state after 15 minutes or less from the onset of a change in the exercise level (Fig. 5.5 and TABLE F.1). This result indicates that the transient time of the respiratory system is much shorter than that of the thermal system of the human body within the investigated range.

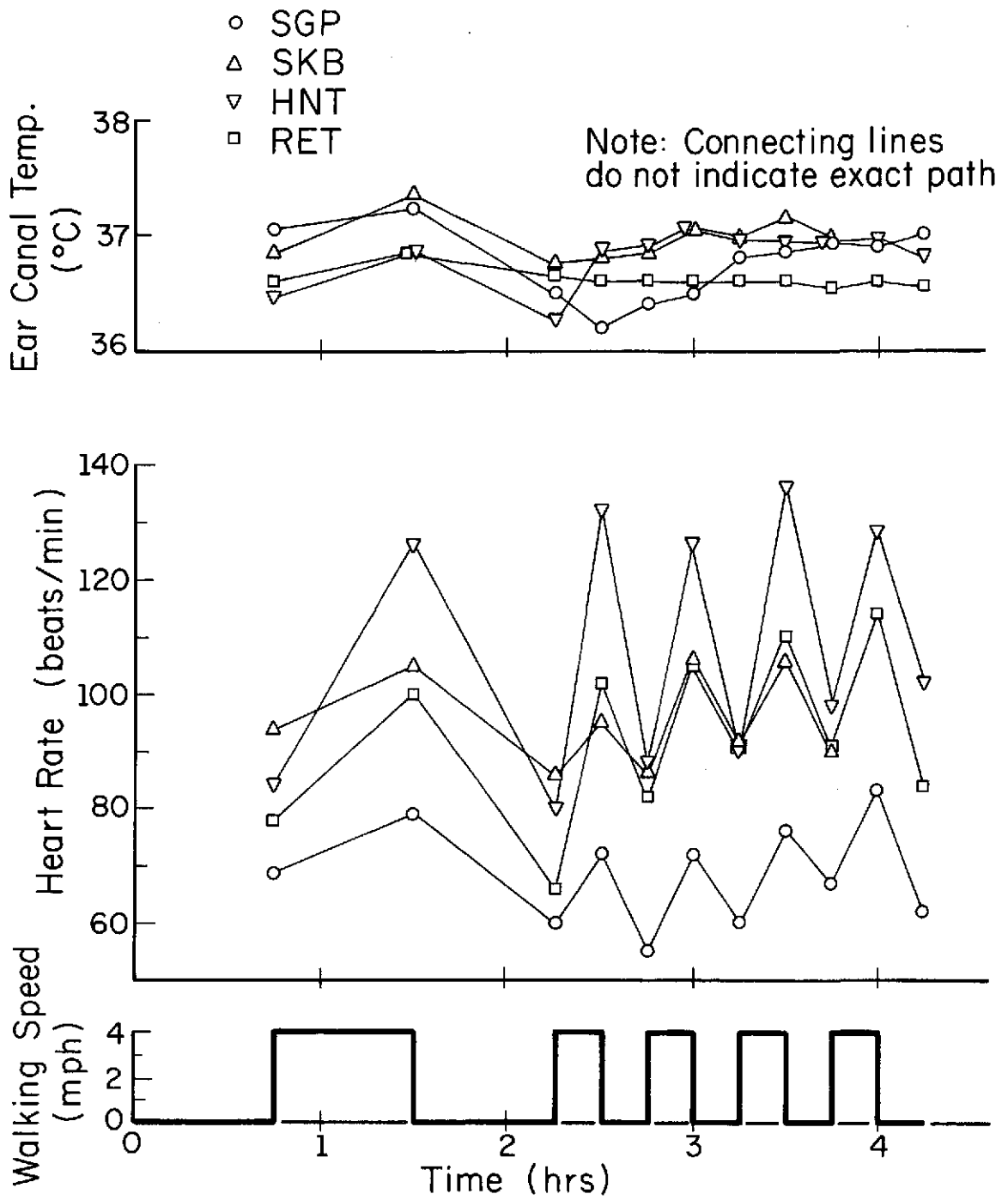


Figure 5.7 Individual variations in the ear canal temperatures and heart rates for Schedule V.

During the second part of the experiments of Schedule V, heart rates not only showed a trend to increase with time but also exceeded the values found in the first part. This observation is a possible indication of a fatigue effect that was supported by the feeling of all the subjects. It is also indicative of a lack of steady state.

During the experiments of Schedules III, IV, and V, the effects of gradual and abrupt step changes from standing to walking at 4 mph, were considered. No significant differences were found in total metabolic rates and amounts of heat removed by the cooling suit (Figs. 5.3, 5.4, and 5.5). Of those two quantities, only the cooling effectiveness† of the cooling suit seemed to have changed during the experiments of that schedule which included two intermediate steps (Schedule IV). This result may mean that during the experiments of Schedule IV the thermal steady state of the moderately high activity level was more nearly attained because of the two intermediate step changes preceding it. However, there were differences in the temperature of the ear canal. It was found to be lower by about 0.5°C when a step change from standing to walking at 4 mph was introduced without any intermediate changes (Fig. 5.6). There were no major differences between the temperatures of the ear canal measured during both experiments that involved gradual changes (Schedules III and IV). This observation probably indicates that the transient time for a thermal steady state in the human body is longer than 45 minutes and is more likely of the order of two hours.

TABLE F.1 in APPENDIX F summarizes the mean values and the ranges of the total metabolic rates and of the amounts of heat removed by the

---

†Cooling effectiveness of the cooling suit was defined as the ratio of the rate of heat removed by the suit to the total metabolic rate.

suit and by respiration at the various schedules of activity.

Figures 5.8 through 5.12 show the relative amounts of heat removed by the suit at the various regions of the body as functions of the different schedules of activity. Based on these data, the following observations were made:

- (1) The relative amount of heat removed from the arms by the arm pads was the lowest in most cases. It ranged from 1.7 percent to 7.2 percent of the total removed by the suit and was usually around 3 to 4 percent. This was despite the fact that the arm pads covered about 18 percent of the total skin surface area covered by the suit. It is assumed that this finding should be attributed to the nature of the schedules of activity used in this study; these were composed primarily of work of the leg muscles and did not involve much arm work. This assumption is supported by the fact that the relative value of the heat removed at the arms increased during the walking sessions with the subjects swinging their arms.
- (2) The largest amount of heat removed by the suit from a single region came from the thighs. It ranged from a low of 25.8 percent (while standing) to a high of 41.7 percent (while walking at 3 mph) of the total removed by the suit. As the metabolic rate exceeded the upper limit that could be accommodated by the suit, the relative amount of heat removed from the thighs decreased. This is probably due to the too high water inlet temperatures and the too small contact areas between the skin overlying the thighs and the cooling tubes. As a result, heat

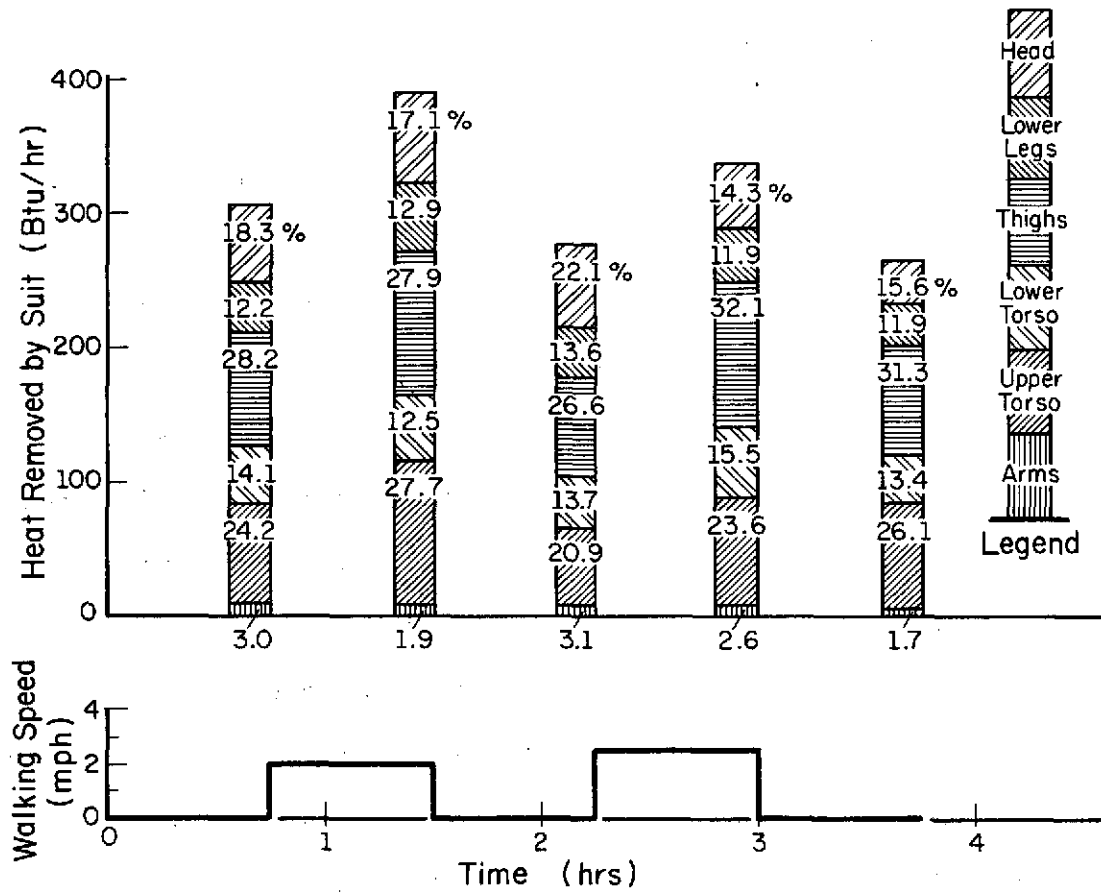


Figure 5.8 Mean values of the amounts of heat removed by the cooling pads for Schedule I.

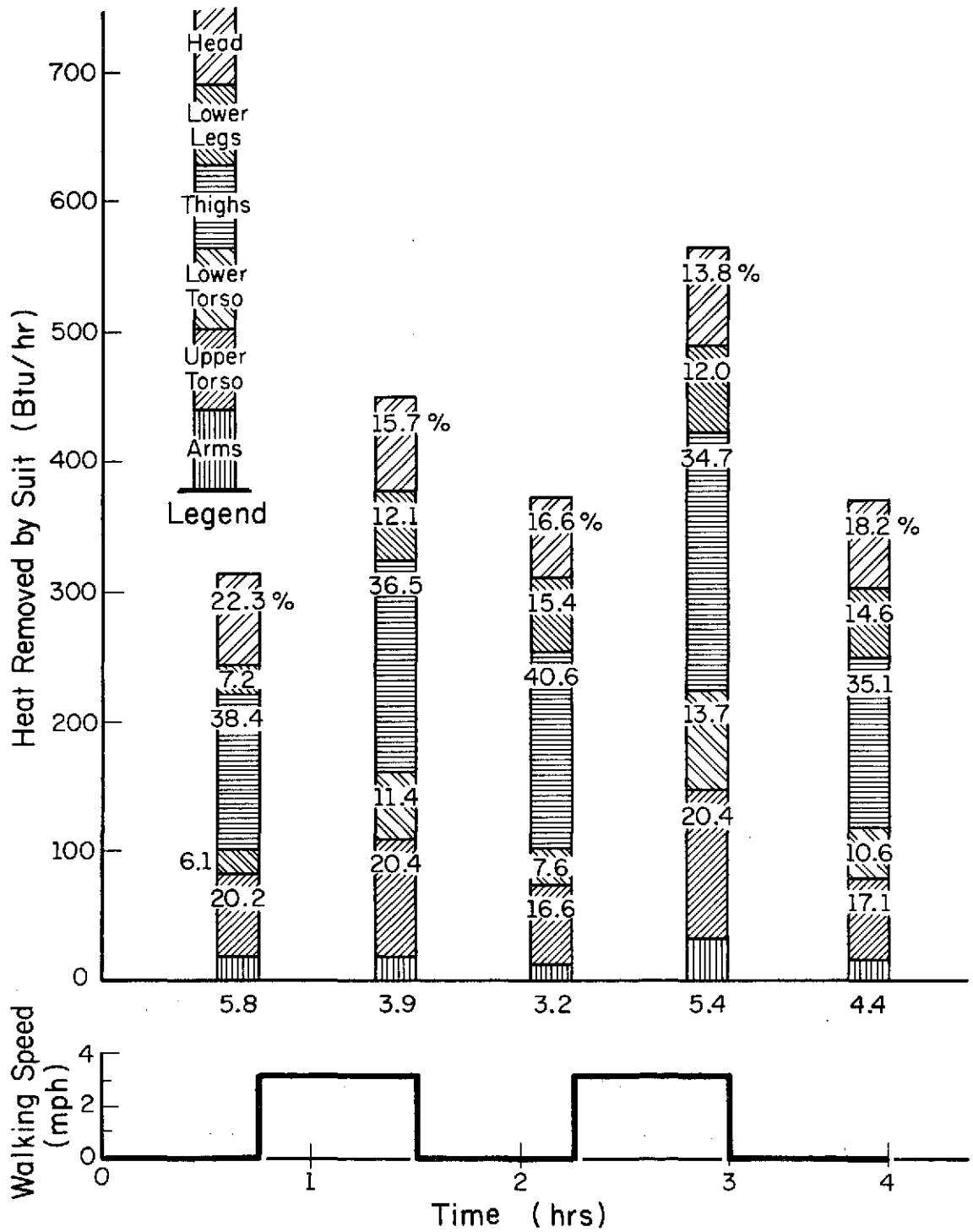


Figure 5.9 Mean values of the amounts of heat removed by the cooling pads for Schedule II.

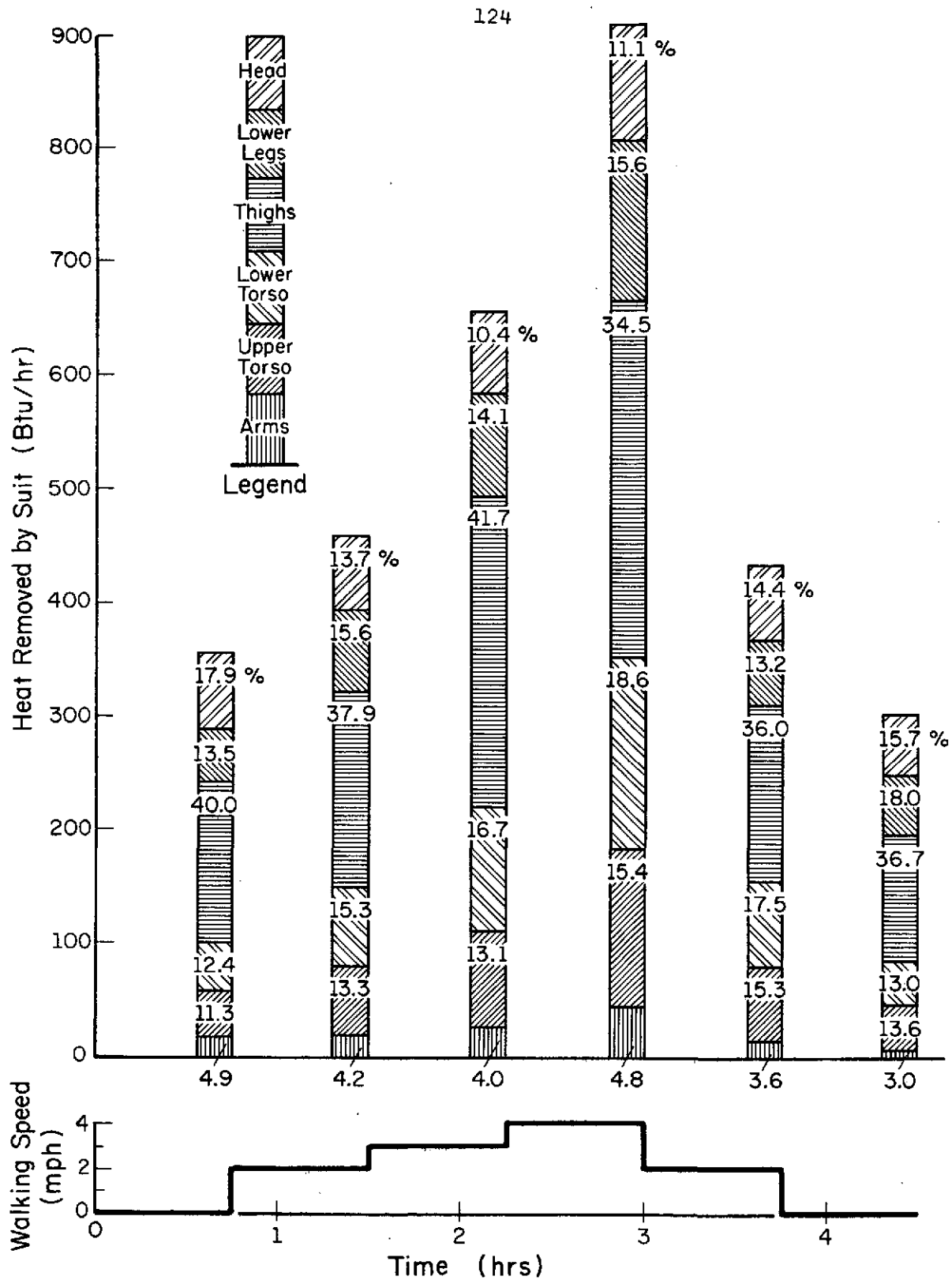


Figure 5.10 Mean values of the amounts of heat removed by the cooling pads for Schedule III.

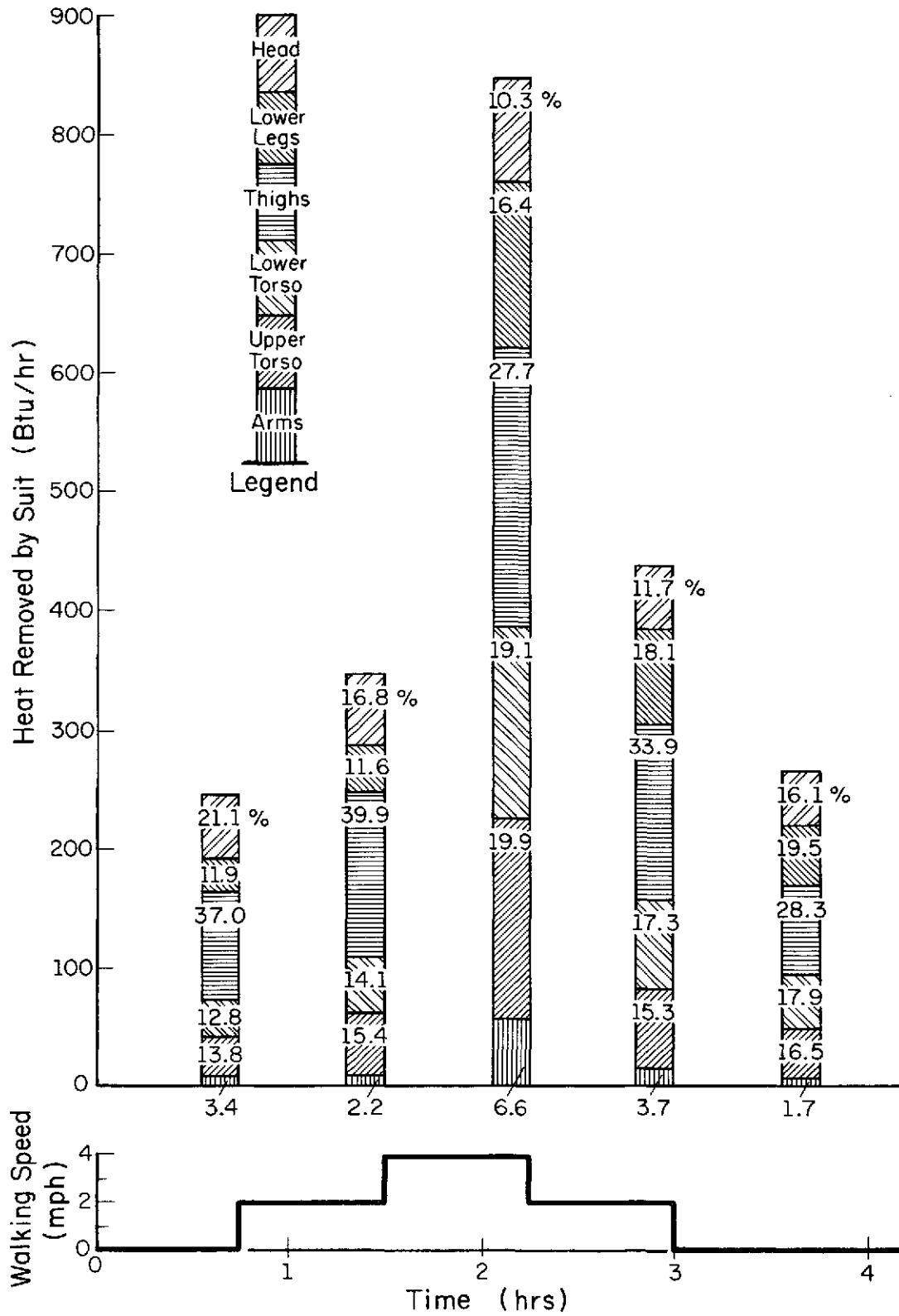


Figure 5.11 Mean values of the amounts of heat removed by the cooling pads for Schedule IV.

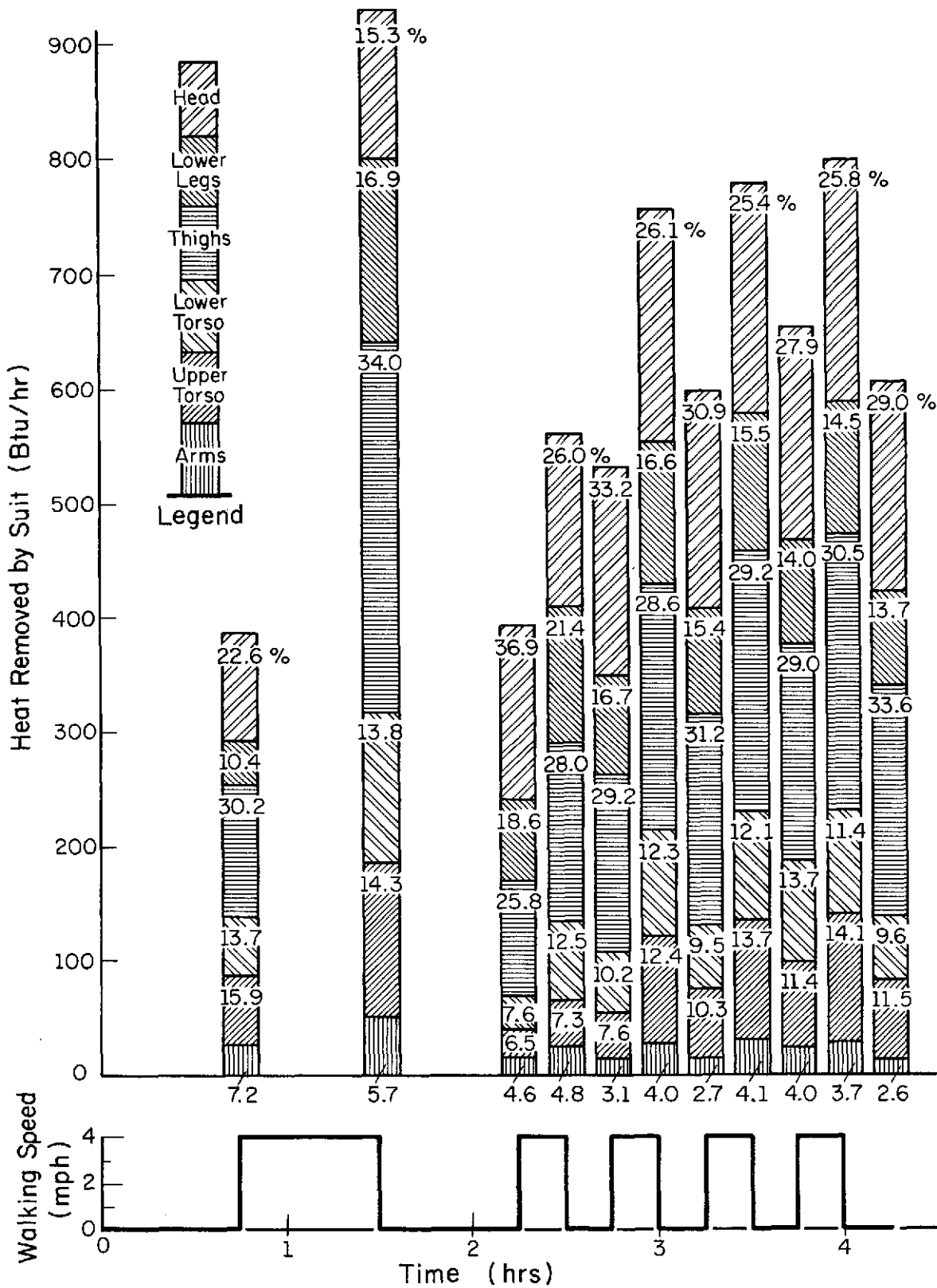


Figure 5.12 Mean values of the amounts of heat removed by the cooling pads for Schedule V.

was probably carried away from the thighs by the blood stream to be dissipated elsewhere where conditions were more favorable. Also, the "deep body" temperature increased and sweating was enhanced, as indicated by higher weight losses (TABLE 5.2).

- (3) A relatively high percentage of the total heat removed by the suit came from the head which constitutes about 7 percent of the total surface area. It ranged from 10.3 percent to 36.9 percent. The highest values were obtained during the second part of the experiments of Schedule V (Fig. 5.12). This result seems to indicate that during the thermal transient period from the onset of a change in activity level, relatively high amounts of heat are removed from the head. According to Nunneley [72], up to 40 percent of the total metabolic rate was removed from the head during resting and steady states by a cap consisting of cooling tubes. In her study, however, she did not use a cooling suit along with the hood. Another study with a cooling suit that included a cooling hood was reported by Shvartz [73]. He found that during steady states, the hood removed about 40 percent of the total removed by the cooling suit assembly. However, 12 percent of the total surface area was covered by the hood in his studies as compared to only about 5 percent that was covered by the hood in the present study.
- (4) During the experiments of Schedule I more heat was removed

TABLE 5.2

## WEIGHT LOSSES DURING TREADMILL EXPERIMENTS

Subject		Schedule				
		I	II	III	IV	V
SGP	Weight loss- $\Delta w$ (gr)	--†	450	875††	738	472
	$\Delta w/w$ (gr/kg)	--	6.89	13.02	11.16	7.25
	$\Delta w/t$ (gr/hr)	--	94.7	145.8	118.1	75.5
	$\Delta w/w/t$ (gr/kg,hr)	--	1.45	2.17	1.79	1.16
SKB	Weight loss- $\Delta w$ (gr)	390	346	516	478	412†††
	$\Delta w/w$	6.46	5.74	8.44	7.78	6.75
	$\Delta w/t$	78	65.9	114.7	95.8	91.6
	$\Delta w/w/t$	1.29	1.09	1.88	1.56	1.50
HNT	Weight loss- $\Delta w$ (gr)	262	370	758	718	930
	$\Delta w/w$	4.01	5.81	11.92	11.04	14.49
	$\Delta w/t$	61.6	70.5	126.3	131.7	169.1
	$\Delta w/w/t$	0.94	1.11	2.00	2.03	2.63
RET	Weight loss- $\Delta w$ (gr)	232	456	468	506	636
	$\Delta w/w$	3.61	7.05	7.31	7.96	9.87
	$\Delta w/t$	48.8	96.0	98.5	113.7	127.2
	$\Delta w/w/t$	0.76	1.48	1.54	1.79	1.97
PF	Weight loss- $\Delta w$ (gr)	382	424	590	662	--†
	$\Delta w/w$	6.88	7.64	10.47	11.82	--
	$\Delta w/t$	63.7	84.8	131.1	132.4	--
	$\Delta w/w/t$	1.15	1.53	2.33	2.36	--

†Did not complete the schedule.

††Irregular schedule.

†††Shorter activity schedule.

(continued)

TABLE 5.2 continued

Subject		Schedule				
		I	II	III	IV	V
MEAN	Weight loss- $\Delta w$ (gr)	317†	409	583†	620	679††
	$\Delta w/w$	5.62	6.63	9.53	9.95	9.59
	$\Delta w/t$	64.4	82.4	117.7	118.3	115.8
	$\Delta w/w/t$	1.05	1.33	1.94	1.91	1.82
SKB WITHOUT SUIT	Weight loss- $\Delta w$ (gr)	414	382	382	654	646
	$\Delta w/w$	6.72	6.19	6.15	10.60	10.52
	$\Delta w/t$	82.8	84.9	89.9	124.6	143.6
	$\Delta w/w/t$	1.34	1.38	1.45	2.02	2.34

---

†Average of 4 runs.

††Average of 3 runs.

by the cooling suit during the first walking session at two mph than that removed during the second at 2.5 mph (Fig. 5.8). The reason was the unexpected drop in "deep body" temperature as indicated by the temperature of the ear canal (Fig. 5.6). It should be noted that no readjustments in water inlet temperatures were permitted during these experiments. All changes were due to the instability of the cooling system. Therefore, this phenomenon of less heat removed by the suit at a higher metabolic rate is not considered to have any physiological meaning.

- (5) During the experiments of Schedule II readjustments of the water inlet temperatures at the same level of activity resulted in the following changes:
- (a) The total metabolic rate decreased, (Fig. 5.2),
  - (b) The amount of heat removed by the cooling suit increased, (Fig. 5.9), and
  - (c) The temperature of the ear canal dropped, (Fig. 5.6).
- Consequently, the cooling effectiveness of the suit increased from 0.39 to 0.56, (TABLE F.1). Also, it is clear that adjustments of water inlet temperature actually did diminish the subjects' heat strain.† This reduction of heat strain was in spite of the consistent comfort vote of

---

†Heat strain is often referred to as the physiological response in consequence of a heat load [74]. This should be distinguished from the heat stress which is used to denote the heat load imposed on man [74]. A commonly used index to assess physiological strain was developed by Craig [75] and modified by others [76]. It is a linear combination of heart rate, rise in rectal temperature and sweat production rate.

"comfortable" obtained throughout the experiments of Schedule II (TABLE 5.1). The findings of this section indicate that additional cooling provided by some artificial means, e.g., a cooling suit, may reduce heat strain beyond that which is considered "comfortable" by human subjects.

A similar conclusion was reached by Gold and Zornitzer [77].

Figure 5.13 shows the average values of water inlet temperatures at the various regions of the body for Schedule II. This schedule was selected for comparative presentation for two reasons:

- (1) The effect of additional cooling at the same level of activity was studied during the experiments of this schedule and
- (2) The metabolic rates encountered during the experiments of this schedule did not exceed the cooling capacity of the suit.

It can be seen that during the initial standing session, most of the subjects preferred an almost uniform temperature all over the body (Fig. 5.13a). This situation did not change during the first walking session where no additional cooling was permitted (Fig. 5.13b). Immediately following the first walking session, the restriction on the additional cooling was removed. A decrease in most water inlet temperatures was then requested by all of the subjects (Fig. 5.13c). The average changes requested for the arms and thighs were about 1.2 to 1.3°C, the head and upper and lower torso 0.2 to 0.6°C; and the highest decrease in water inlet temperature, 2.3°C, was requested for the lower

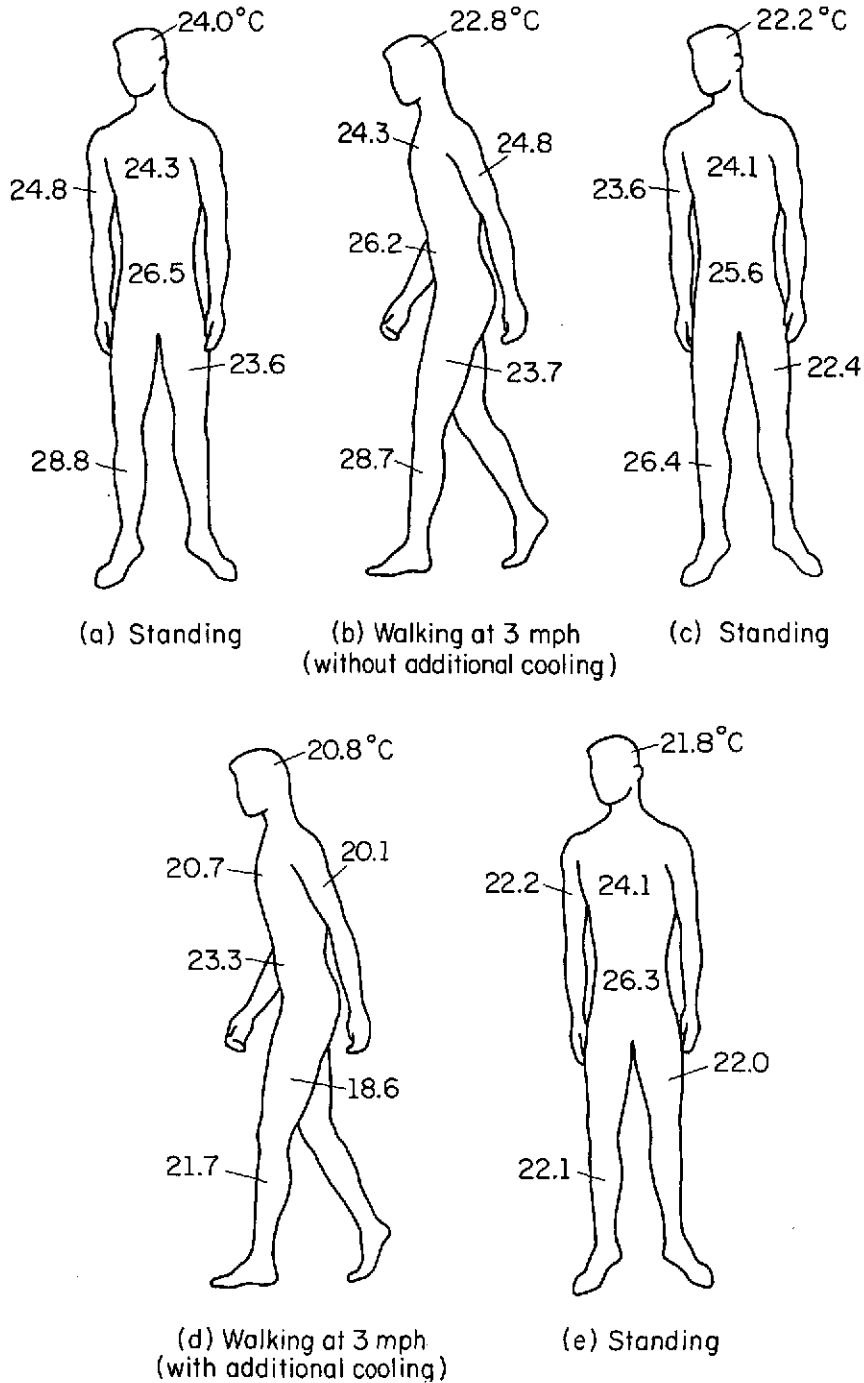


Figure 5.13 Mean water inlet temperatures at the various regions of the body for Schedule II.

legs. During the second walking session at 3 mph (Fig. 5.13d) the requests for decreases in water inlet temperatures were as follows: arms, upper torso, and thighs, 3.4 to 3.8°C; head, 1.4°C; lower torso, 2.5°C; and, again, the highest decrease in water inlet temperature, 4.7°C, was requested for the lower legs. During the last standing period, requested changes in water inlet temperatures to the various regions of the body were essentially such that they retraced the situation that prevailed during the second standing session. Only minor changes were noticeable, (Fig. 5.13e).

As a consequence of the results presented in the preceding section, the following observations were made:

- (1) The working muscles, i.e., thighs and lower legs, exhibited the highest variability in water inlet temperatures. This was expected and does not seem to require any further discussion.
- (2) The changes in water inlet temperatures to the head were the smallest. At the same time, the temperature of the water entering the cooling hood was, on the average, the lowest water inlet temperature of all. This indicates that cooling the head may have a profound effect on the sensation of comfort, as noted by Nunneley [72] and Shvartz [73].

A complete listing of the water inlet temperatures and their ranges at the various schedules of activity is given in TABLE F.2. It should, however, be kept in mind that the values shown there for the moderately high activity levels (walking at 4 mph) are of limited meaning. This is because the limited cooling capacity of the present

cooling system was definitely exceeded during these schedules of activity.

In TABLE 5.1, the orders of preferred changes in water inlet temperatures, from the onset of a change in the level of activity, are shown. There does not seem to be any consistency in the order of changes requested by different subjects. Many more experiments with more subjects are needed to identify those regions in the body which require faster cooling or warming as a result of a change in the level of activity.

Weight losses during treadmill experiments are shown in TABLE 5.2. The mean values of weight losses range from about 65 gr/hr (Schedule I) to about 118 gr/hr (Schedules III and IV). These values, although slightly higher, are consistent with values reported by Webb and Annis [71]. In four out of five cases, the sweat rates were higher during the runs without the suit as compared to the runs with the suit. No fundamental explanation was found for the one run (Schedule III) that exhibited a higher weight loss with the suit. The reason for that may have been due to a measurement error.

Total metabolic rates for subject SKB with and without the cooling suit are compared in Figs. F.1 through F.5. Also compared in these figures are the temperatures of the ear canal. In most cases, the total metabolic rate was higher during the experiments with the cooling suit. This finding is probably due to the fact that there is a certain energy cost for wearing the suit (higher heat stress). At the same time, the temperature of the ear canal seemed to have been slightly lower during the experiments without the cooling suit.

Also, as shown in Fig. F.6, the heart rate was usually lower during at least the comparative experiments of Schedule V with the cooling suit. Heart rate was not measured during the other experiments with the suit. These two, i.e., slightly higher "deep body" temperatures and lower heart rates, indicate that the heat strain probably was reduced during the experiments with the cooling suit.

## 5.2 EXPERIMENTS WITH THE INDIVIDUAL COOLING PADS

Temperature distributions on the skin between two adjacent tubes were measured for the three individual cooling pads. The measurements were taken after the test subject had been pedalling for two hours on the bicycle ergometer at a constant load and speed [corresponding to a total metabolic rate of about 1200 Btu/hr (352 w)]. The measured values were assumed to represent steady state data.

The theoretical steady state temperature distribution on the skin for the rectangular model with the skin layer and skeletal muscle considered as one combined tissue was obtained from Eq. (C.2) to yield

$$T(x,0) = T_o + \frac{Q'}{w_b c_b} \left[ 1 - \frac{1}{\cosh(wb)} \right] - \frac{\beta f_a}{\sqrt{w_b c_b k}} \tanh(wb) - \sum_{n=1}^{\infty} \frac{\alpha_n \tanh(\zeta b)}{\zeta} \cos(\lambda_n x) \quad (5.1)$$

As can be seen from Eq. (5.1), the parameters affecting the steady state temperature of the skin are:

- (1) Temperature of the inner core,  $T_o$ .

- (2) Specific heat of blood,  $c_b$ .
- (3) Thermal conductivity of the combined tissue,  $k$ .
- (4) Ratio of cooling tube width to cooling tube spacing,  $\beta$ .
- (5) Cooling tube spacing,  $a$ .
- (6) Average heat flux at the skin surface,  $f_a$ .
- (7) Number of terms in the series used for computation.
- (8) Shape of the specified flux function,  $f(x)$ .
- (9) Average heat generation rate per unit volume of tissue,  $Q'$ .
- (10) Average blood perfusion rate per unit volume of tissue,  $w_b$ .
- (11) Depth of tissue,  $b$ .

From these parameters, the first seven could either be measured or estimated. The remaining four, i.e.,  $f(x)$ ,  $Q'$ ,  $w_b$ , and  $b$ , were left to be estimated by the method of fitting a theoretical curve to the experimental data. Curve fitting was done with the aid of a digital computer. A program was written for evaluating Eq. (5.1) for various combinations of the unknown parameters. The computer output was then analyzed to determine that combination of parameters which yielded a curve fitting closely with the experimental data while the parameters met a set of predetermined criteria. These criteria were:

- (1) The lowest temperature of the skin should not be below 60°F.

This assumption was based on the cooling water temperature which was measured at 55°F.

- (2) The depth of tissue should not exceed 0.2 ft or be less than 0.05 ft.
- (3) Only measurements taken away from the cooling tubes were considered accurate. Measurements underneath the cooling tube were assumed questionable because of the interference of the thermocouple with the contact between the cooling tube and the skin.
- (4) The blood perfusion and heat generation rates per unit volume of tissue should not exceed values found in the literature.

The results obtained for the three individual pads are shown in Figs. 5.14, 5.15, and 5.16. In view of the complexity of the problem, the agreement between the measured and calculated values is remarkably good. It should, however, be noted that the set of parameters that yielded a good fit to the measured data is not unique. Improved techniques for measuring the unknown parameters are required to render the analysis presented in this chapter physiologically more meaningful.

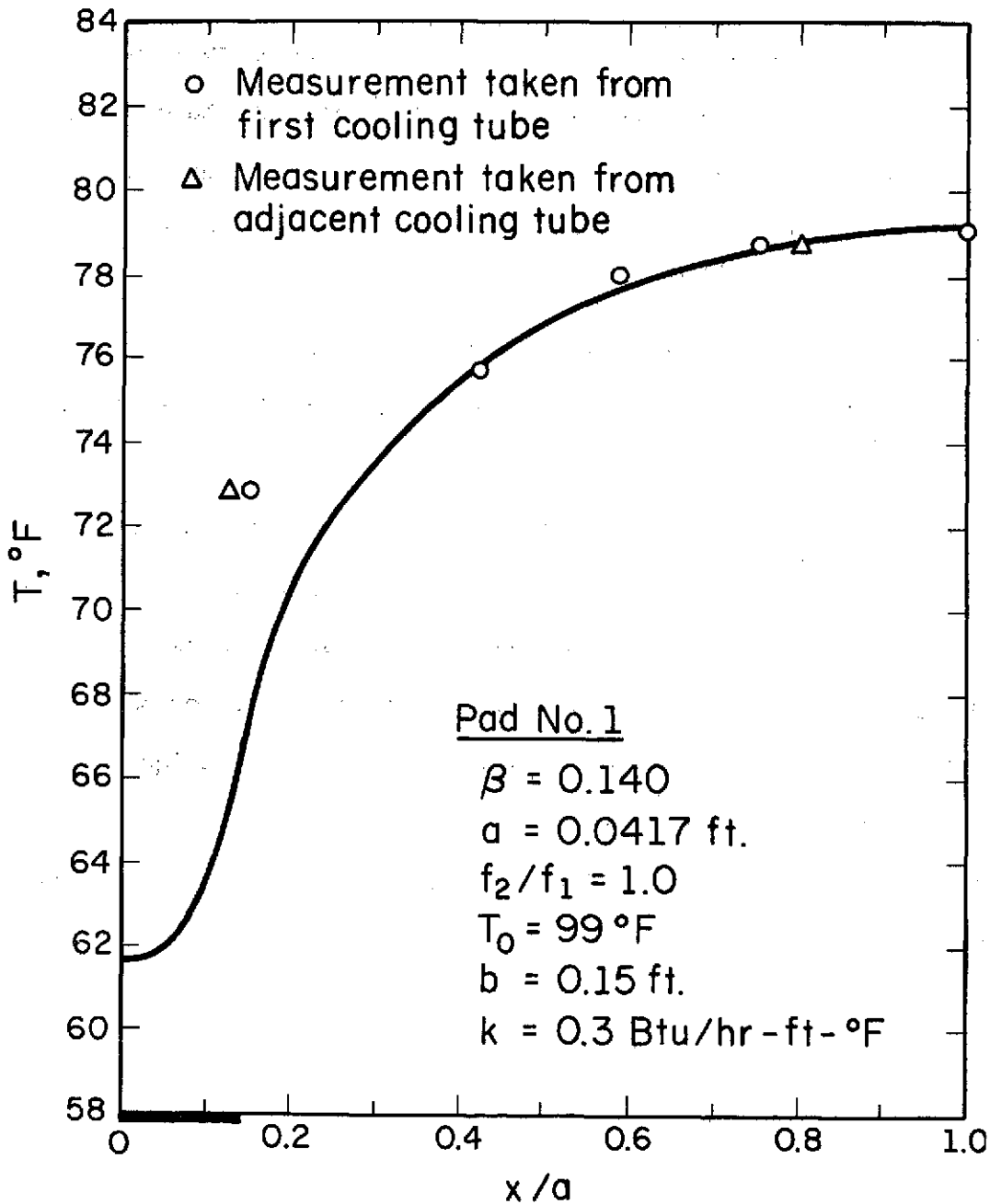


Figure 5.14 Comparison of measured and calculated temperature distribution on the surface of the skin for the rectangular model. Pad No. 1,  $w_b = 83.4 \text{ lb/hr-ft}^3$ ,  $Q' = 711 \text{ Btu/hr-ft}^3$  and constant temperature at inner core.

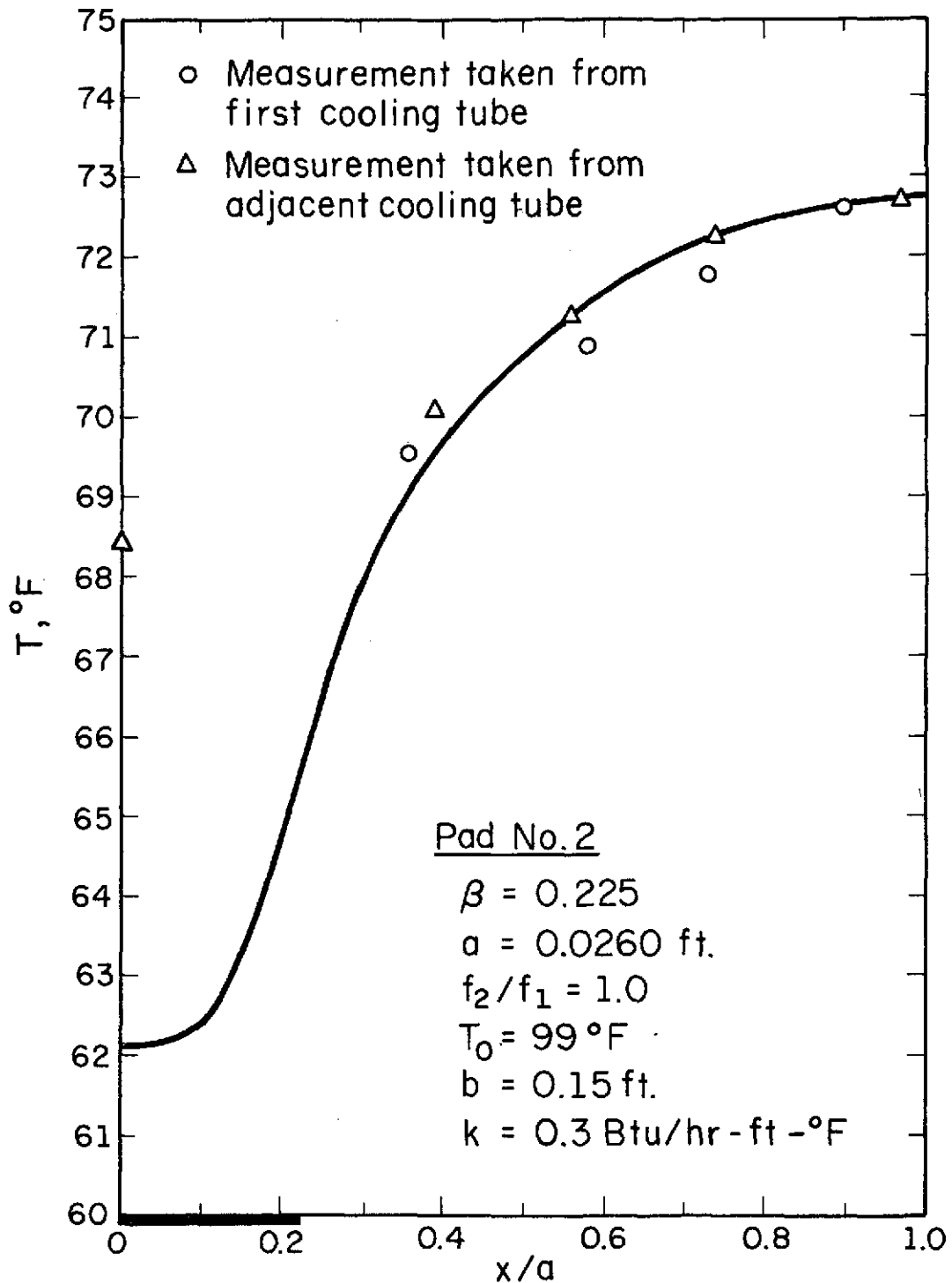


Figure 5.15 Comparison of measured and calculated temperature distribution on the surface of the skin for the rectangular model. Pad No. 2,  $\dot{w}_b = 83.4 \text{ lb/hr-ft}^3$ ,  $Q' = 805 \text{ Btu/hr-ft}^3$  and constant temperature at inner core.

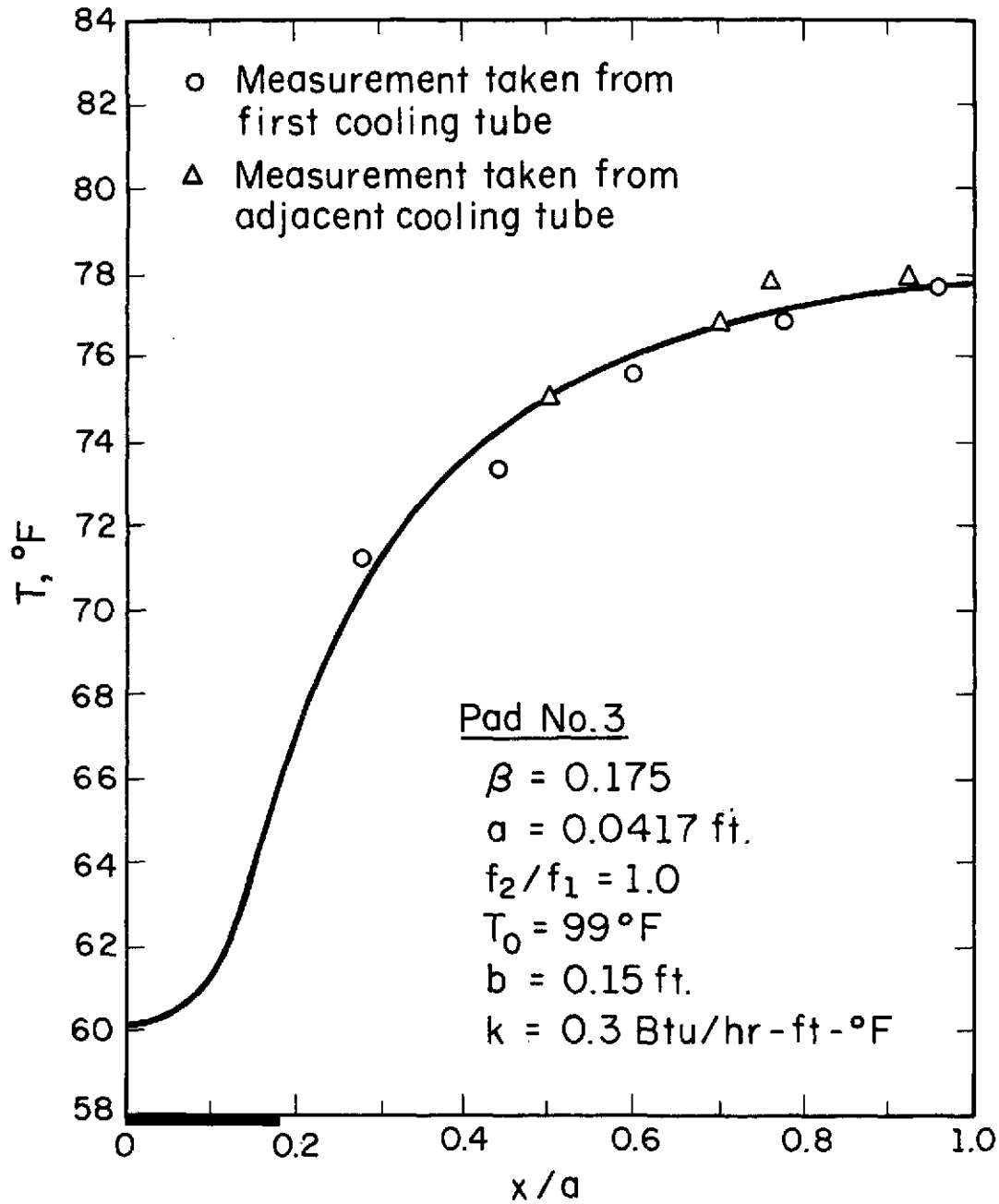


Figure 5.16 Comparison of measured and calculated temperature distribution on the surface of the skin for the rectangular model. Pad No. 3,  $w_b = 83.4 \text{ lb/hr-ft}^3$ ,  $Q' = 848 \text{ Btu/hr-ft}^3$  and constant temperature at inner core.

## 6. SUMMARY AND CONCLUSIONS

This study was directed to the exploration of two aspects related to thermal comfort of man:

- (1) The analytical modeling of the thermal behavior of living biological tissue and partial experimental validation of the analytical predictions.
- (2) The exploration of the characteristics of independent regional cooling of the body by means of a water-cooled garment (thermal protective suit).

A biothermal model of living biological tissue has been proposed and studied. This model includes the effects of blood flow, local heat generation rates, conduction and storage of heat on the heat transfer processes occurring in the living tissue. A second order, partial differential equation (referred to as the "bio-heat" equation) was obtained and analyzed. Closed form, steady and transient state analytical solutions were obtained for two relevant geometries (cylindrical and rectangular). Good agreement was obtained between the measured and predicted temperature profiles on the skin surface.

Based on the analysis, the following conclusions were reached:

- (1) Blood flow plays a significant role in the transfer of heat in the living tissue and, therefore, should be explicitly included in any analytical model of the thermal behavior of the tissue.
- (2) Much more detailed and accurate data of the thermophysical and physiological properties of the body, e.g., thermal conductivities and local blood flow rates, are required

before any extension of the present model should be attempted.

- (3) Transient times for reaching a so-called "fully developed" temperature profile in the tissue are of the order of 5 to 20 minutes.
- (4) Transient changes in tissue temperature are strongly dominated by a geometrical parameter (separation coefficient).
- (5) Under certain conditions, maximum temperature may occur in the tissue rather than in the inner core ( $w/b > 2.3$ ). The location of the maximum temperature was found to be independent of "deep body" temperature.
- (6) For  $y/b > 2$ , isotherms in the tissue become parallel. This observation renders assumptions of constant temperature or constant flux at the interface between the skeletal muscle and the inner core equivalent.
- (7) The exact shape of the heat flux on the skin has an insignificant effect on the temperature distribution inside the tissue at a short distance away from the skin surface. It does have, however, a noticeable effect on the temperature on the skin surface.
- (8) For  $R_1 > 0.15$  ft (radius of inner core in the cylindrical model) the results obtained from the cylindrical and rectangular models are so close that the simpler, rectangular model can be used without loss of accuracy.

A water cooled garment was constructed and used to study the characteristics of independent regional cooling of the body in contrast to the current practice of uniform cooling. The cooling garment consisted

of sixteen individual cooling pads made of 5/32 in. O.D. Tygon tubes. The pads were grouped to provide independent control of water inlet temperatures and flow rates to six regions: head, upper torso, lower torso, arms, thighs and lower legs. Experiments with and without the cooling suit assembly were conducted with the five test subjects standing and walking on a treadmill on selected schedules. Steady and, to a lesser extent, transient state characteristics of the cooling suit were obtained.

Based on the experiments with the cooling suit the following conclusions were reached:

- (1) There are regions in the body that require more cooling during walking than others, e.g., thighs, head and lower legs.
- (2) During standing, an almost uniform water inlet temperature was requested for all regions of the body by the test subjects. This situation changed significantly during exercise. Conclusions 1 and 2 indicate that independent regional cooling may be more efficient than the present scheme of uniform cooling.
- (3) Cooling of the head during exercise has a profound effect on comfort.
- (4) Transient times for reaching a thermal steady state from the onset of exercise are of the order of two hours. This transient time, however, includes a relatively slow active response of the human thermoregulatory system to changes in exercise rates, e.g., the shifting of the deep body temperature.

- (5) During exercise the thermal effectiveness of the cooling suit decreased as compared to the values obtained for standing.
- (6) Intermediate changes in the level of activity between an initial and a final level do not have a noticeable effect on the thermal state so long as sufficient time is allowed for reaching a steady state corresponding to the final level of activity.
- (7) The cooling suit did actually diminish the heat strain of the test subjects beyond what was considered comfortable by them.
- (8) The regional order of preferred changes in water inlet temperatures from the onset of a change in the level of activity could not be determined. More experiments are required to identify the regions of the body that require faster cooling (or warming) than others.

Based on the comparative experiments with and without the cooling suit, the following observations were made:

- (1) Metabolic rates were, in most cases, higher during the experiments with the cooling suit, indicating that a certain energy cost was associated with wearing the suit, i.e., the subject was under higher heat stress.
- (2) Ear canal temperatures were usually lower during the experiments without the cooling suit.
- (3) Heart rates seem to have been lower during the experiments with the cooling suit.

- (4) Weight losses were usually lower during the experiments with the cooling suit.

Thus, the cooling suit seems to have reduced the heat strain even though the heat stress was increased slightly.

Recommendations for future work are the following:

- (1) Application of optimization techniques to obtain design guidelines for the construction of more efficient cooling suits.
- (2) Extension of the model to include the local and temperature dependent variations of the physiological properties. This phase, however, should be delayed until more detailed physiological data become available.
- (3) Experimentation with various combinations of individual cooling pads, e.g., hood and thigh pad, to determine the local effects of cooling at various heat stresses and activities.
- (4) Experimentation with cooling suits while exercising other parts of the body, e.g., arms, in order to determine preferred temperature patterns for the coolant.

## APPENDIX A

## THE THERMOREGULATORY SYSTEM OF THE HOMEOTHERM

A homeotherm, or warm-blooded animal, exhibits a tendency to stability in the normal body states (fixed internal environment). The objective of the thermoregulatory system is counter any external or internal changes in heat stress while maintaining the temperature and metabolism (the transformation by which energy is made available for the uses of the organism) at the levels essential to life. This thermoregulatory system is composed of three interconnected elements: control, sensory, and regulatory mechanisms.

It is generally accepted that the center of thermal control is located in the hypothalamus, a structure in the brain which forms the floor and part of the lateral wall of the third ventricle [78, 79]. There appear to be two centers in the hypothalamus that are concerned with temperature control; the more posterior one, concerned with protection against cold, and the anterior one, concerned with protection against heat. These two centers are mutually inhibitory. The temperature which is being regulated, usually referred to as "deep body" temperature, is, however, not constant. It changes, within a narrow range above and below the "normal" temperature, with the metabolic rate. This concept of a "set point" rather than a fixed one was postulated by Hardy [80].

Thermal receptors in the skin are the major components of the sensory system [81]. In addition, there are indications that temperature-sensitive structures exist in the spinal cord [82], in the voluntary muscles [81], in the hypothalamus [55], and in the respiratory

tract [83], which play a subsidiary role in thermoregulation. Changes in skin temperature and probably also in heat flux at the skin [55] trigger a signal which is received by the thermal receptors and which is sent through the afferent pathways to the hypothalamus.

There exist regulatory mechanisms in the human body that make up the third element of the thermal system. These mechanisms are activated in response to need and, in turn, by the control through the nervous system. Adjustment to cold stress follows the sequence:

- (1) Superficial vasoconstriction that diminishes the amount of heat transported by the blood stream to the skin. This is balanced by splanchnic dilatation; i.e., dilatation of blood vessels in the internal cavities of the body.
- (2) Pilo-motor activity ("goose flesh") that reduces air movement at the skin and thereby diminishes heat convection.
- (3) Increased heat production that can take either (or both) of two forms: mechanical and glandular. The mechanical part is achieved by the muscles and is manifested as shivering; the glandular part involves secretion of adrenalin by the suprarenal gland. The function of the circulating adrenalin is to cause modifications in the circulation which favor blood supply to active muscles and liberation of glucose from liver glycogen and, consequently, a considerable increase in heat production (20-30 percent increase in resting metabolism [55]).
- (4) Long-term adaptation--decreased blood volume and accumulation of fat in the outer layers to increase thermal insulation.

Conversely, the sequence of adjustment to heat stress is as follows:

- (1) Superficial vasodilatation that increases blood flow and, consequently, the amount of heat transported to the skin.
- (2) Sweating which enhances the removal of heat by evaporation of water vapor from the surface of the skin. Sweating will follow an increase in deep body temperature caused by heat storage in the body.
- (3) Increased respiration that promotes more heat removal by expired air. In mammals other than humans, e.g., dogs, this mechanism, known as panting, is of great importance. This mechanism, as well as sweating, loses its effectiveness in saturated or very humid environments.
- (4) Long-term adaptation--increased blood volume and decreased basal metabolism (the minimal energy expended for maintenance of life) due to reduced activity of the thyroid.

An extensive and detailed description of the thermoregulatory system and its functions was given by Bazett [55].

## APPENDIX B

## STEADY STATE, RECTANGULAR COORDINATES WITHOUT BLOOD FLOW

If the term representing blood flow is eliminated from Eq. (3.3), the following heat equation is obtained

$$\rho c_p \frac{\partial T}{\partial t} = k \nabla^2 T + q_m \quad (\text{B.1})$$

or, assuming a steady state,

$$k \nabla^2 T = -q_m \quad (\text{B.2})$$

which is often referred to as the Poisson equation.

Solution to Eq. (B.2) for the geometry shown in Fig. (3.4) is desirable for two reasons:

- (1) There are cases when blood flow diminishes or even vanishes, e.g., vasoconstriction, and conduction remains as almost the sole mechanism for heat transfer in the tissue.
- (2) From a more general engineering viewpoint, Eq. (B.2) describes the energy balance in a material wherein heat is conducted and generated. Such cases occur frequently in engineering and a solution may be useful.

Examination of Eqs. (3.11) through (3.15) reveals that obtaining the solution for this limiting case, i.e.,  $w_1 \rightarrow 0$ , is not straightforward, but involves fairly complicated limit operations. Therefore, the complete problem will be formulated and presented below.

SKIN

$$\frac{\partial^2 \theta_1}{\partial x^2} + \frac{\partial^2 \theta_1}{\partial y_1^2} = -Q_1 \quad (\text{B.3a})$$

$$0 \leq x \leq a ; 0 \leq y_1 \leq b_1$$

$$\text{at } y_1 = b_1 , \left\{ \begin{array}{l} \frac{\partial \theta_1}{\partial y_1} = -\frac{f(x)}{k_1} , \quad 0 \leq x < \beta a \\ \frac{\partial \theta_1}{\partial y_1} = 0 \quad \quad \quad \beta a < x \leq a \end{array} \right\} \quad (\text{B.3b})$$

$$\text{at } x = 0 , \quad \frac{\partial \theta_1}{\partial x} = 0 \quad (\text{B.3c})$$

$$\text{at } x = a , \quad \frac{\partial \theta_1}{\partial x} = 0 \quad (\text{B.3d})$$

SKELETAL MUSCLE

$$\frac{\partial^2 \theta_2}{\partial x^2} + \frac{\partial^2 \theta_2}{\partial y_2^2} = -Q_2 \quad (\text{B.4a})$$

$$0 \leq x \leq a ; 0 \leq y_2 \leq b_2$$

$$\text{at } y_2 = b_2 , \theta_2 = 0 \quad (\text{B.4b})$$

$$\text{at } x = 0 , \quad \frac{\partial \theta_2}{\partial x} = 0 \quad (\text{B.4c})$$

$$\text{at } x = a , \quad \frac{\partial \theta_2}{\partial x} = 0 \quad (\text{B.4d})$$

matching conditions at  $y_1 = y_2 = 0$ ,

$$\theta_1 = \theta_2 \quad (\text{B.5a})$$

$$k_1 \frac{\partial \theta_1}{\partial y_1} = -k_2 \frac{\partial \theta_2}{\partial y_2} \quad (\text{B.5b})$$

where  $\theta_i$  and  $Q_i$  are defined by Eqs. (3.8) and (3.10), respectively.

The solutions for the two zones are: for the skin layer,

$$\begin{aligned}
 T_1(x, y_1) = & T_2^* + \frac{Q_2}{2} b_2^2 + \frac{Q_1}{2k^*} [2b_1 b_2 + k^* y_1 (2b_1 - y_1)] \\
 & - \frac{\beta f_a}{k_2} (k^* y_1 + b_2) + k_1 \sum_{n=1}^{\infty} \frac{\alpha_n}{\cosh(\lambda_n b_1)} \\
 & \cdot \left[ \frac{\tanh(\lambda_n b_2) \cosh[\lambda_n (b_1 - y_1)]}{H(\lambda)} \right. \\
 & \left. + \frac{\sinh(\lambda_n y_1)}{k_1 \lambda_n} \right] \cos(\lambda_n x) \quad (B.6)
 \end{aligned}$$

and, for the skeletal muscle layer,

$$\begin{aligned}
 T_2(x, y_2) = & T_2^* + \frac{Q_2}{2} (b_2^2 - y_2^2) + \frac{Q_1}{k^*} b_1 (b_2 - y_2) \\
 & - \frac{\beta f_a}{k_2} (b_2 - y_2) \\
 & + k_1 \sum_{n=1}^{\infty} \frac{\alpha_n \sinh[\lambda_n (b_2 - y_2)]}{H(\lambda) \cosh(\lambda_n b_2)} \cos(\lambda_n x) \quad (B.7)
 \end{aligned}$$

where

$$k^* \equiv \frac{k_2}{k_1} \quad (B.8)$$

and  $H(\lambda)$ ,  $f_a$ , and  $\alpha_n$  are defined by Eqs. (3.15), (3.16), and (3.19), respectively.

As was noted in the text (Chapter 3), no maximum temperature is found in the tissue. However, in order for all the excess heat

to be removed at the skin, the temperature gradients become steeper. As one result, the temperatures on the skin become lower since deep body temperature is maintained at about the same level as in the case with blood flow. In the vicinity of the cooling tube, the temperatures may become intolerably low or even dangerous, particularly if the cooling strip is relatively narrow (small  $\beta$ ) [84].

Buchberg and Harrah studied a similar case [39]. They assumed no heat to be generated in the skin layer ( $Q_1 = 0$ ), but assumed the thermal conductivity to be a function of temperature. By such means, they have tried to account for blood flow effects. Employing a numerical method, they obtained the temperature distribution in the separated layers for a total metabolic rate of 2600 Btu/hr (760 w). Their results are compared with those obtained here for  $Q_1 = 0$  in Fig. B.1 [85]. Considering the major differences in the calculation procedures, the results are remarkably close. The numerical results obtained for Eq. (B.6) and (B.7) without blood flow (combined tissue,  $b_1 \rightarrow b_2, k_1 \rightarrow k_2$ ) and Eq. (C.2) with blood flow are compared in Fig. B.2. The effect of the blood stream on the temperature distribution is clearly seen.

Figure B.3 shows the effect of increasing the contact area between the cooling tubes and the skin on the temperature distribution on the skin surface. When this figure is compared to Fig. 3.8, it is evident that one of the effects of blood flow is a higher temperature at the skin surface.

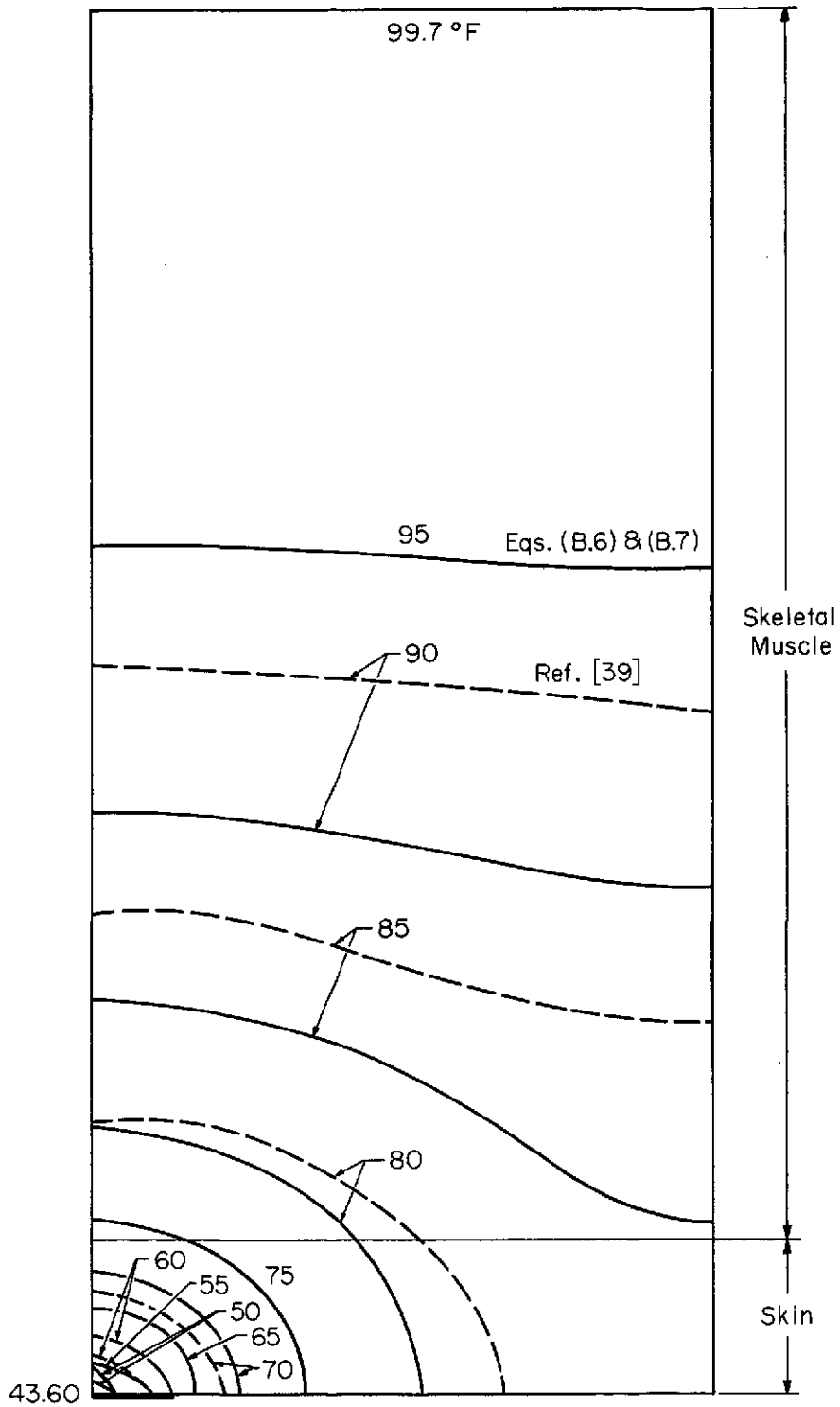


Figure B.1 Comparison of steady state temperature distributions in the tissue for the two-dimensional, rectangular model without blood flow.  $Q_m = 2600$  Btu/hr (760 w),  $\beta = 0.1$ , constant temperature at inner core.

99.7°F

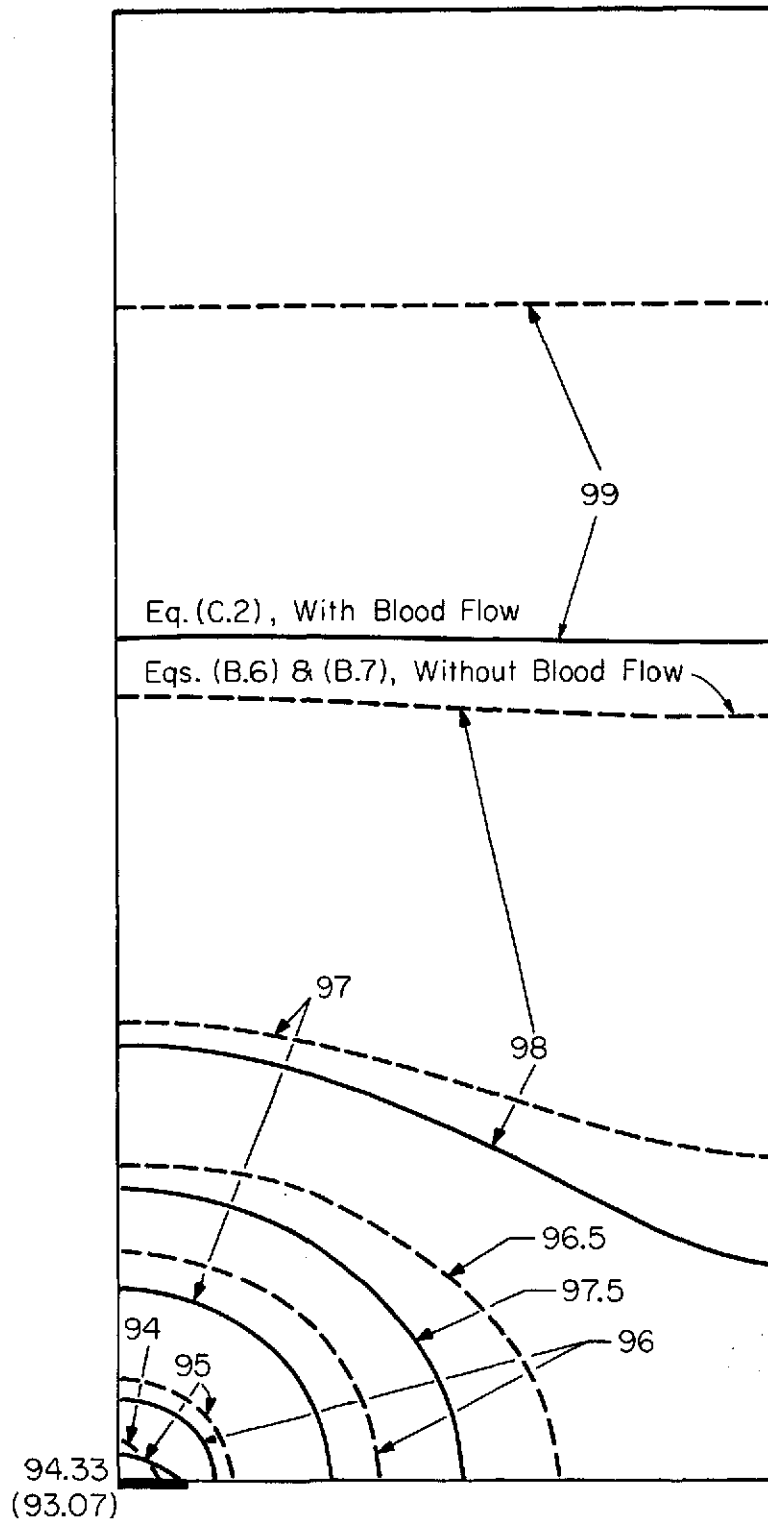


Figure B.2 Comparison of steady state temperature distributions in the combined tissue for the two-dimensional rectangular model with and without blood flow.  $Q_m = 290$  Btu/hr (85 w),  $\beta = 0.1$ , constant temperature at inner core.

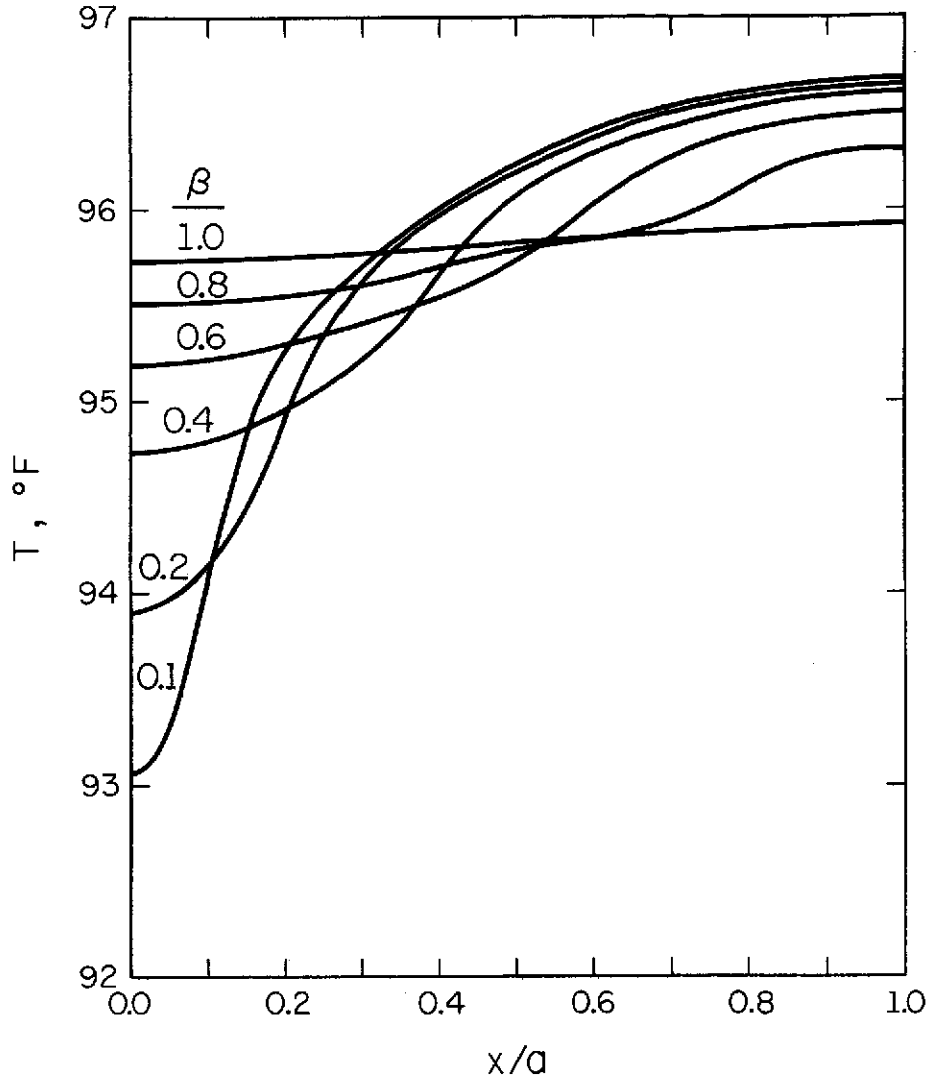


Figure B.3 Effect of increasing the contact area between the cooling tubes and the skin on the temperature distribution on the skin surface. Blood flow effects are not included.  $Q_m = 290$  Btu/hr (85 w),  $f_2/f_1 = 1.5$  and constant temperature at inner core.

## APPENDIX C

STEADY STATE, RECTANGULAR COORDINATES WITH THE SKIN  
AND MUSCLE CONSIDERED AS A SINGLE REGION

If the skin and skeletal muscle layers are combined to form one layer and if both the thermophysical and the physiological properties are averaged, the problem becomes

$$\nabla^2 \theta - w^2 \theta = -Q \quad (\text{C.1a})$$

$$0 \leq x \leq a ; 0 \leq y \leq b$$

with the boundary conditions,

$$\text{at } x = 0 , \quad \frac{\partial \theta}{\partial x} = 0 \quad (\text{C.1b})$$

$$\text{at } x = a , \quad \frac{\partial \theta}{\partial x} = 0 \quad (\text{C.1c})$$

$$\text{at } y = 0 , \quad \left\{ \begin{array}{l} \frac{\partial \theta}{\partial y} = \frac{f(x)}{k} , \quad 0 \leq x < \beta a \\ \frac{\partial \theta}{\partial y} = 0 , \quad \beta a < x \leq a \end{array} \right\} \quad (\text{C.1d})$$

$$\text{at } y = b , \quad \theta = 0 \quad (\text{C.1e})$$

The solution to this set is [58]

$$\begin{aligned} T(x,y) = T_1 + \frac{Q}{w} \left[ 1 - \frac{\cosh(wy)}{\cosh(wb)} \right] - \frac{\beta f_a}{kw} \frac{\sinh[w(b-y)]}{\cosh(wb)} \\ - \sum_{n=1}^{\infty} \frac{\alpha_n \sinh[\zeta(b-y)]}{\zeta \cosh(\zeta b)} \cos(\lambda_n x) \end{aligned} \quad (\text{C.2})$$

Figure C.1 shows results that were obtained for Eq. (C.2).

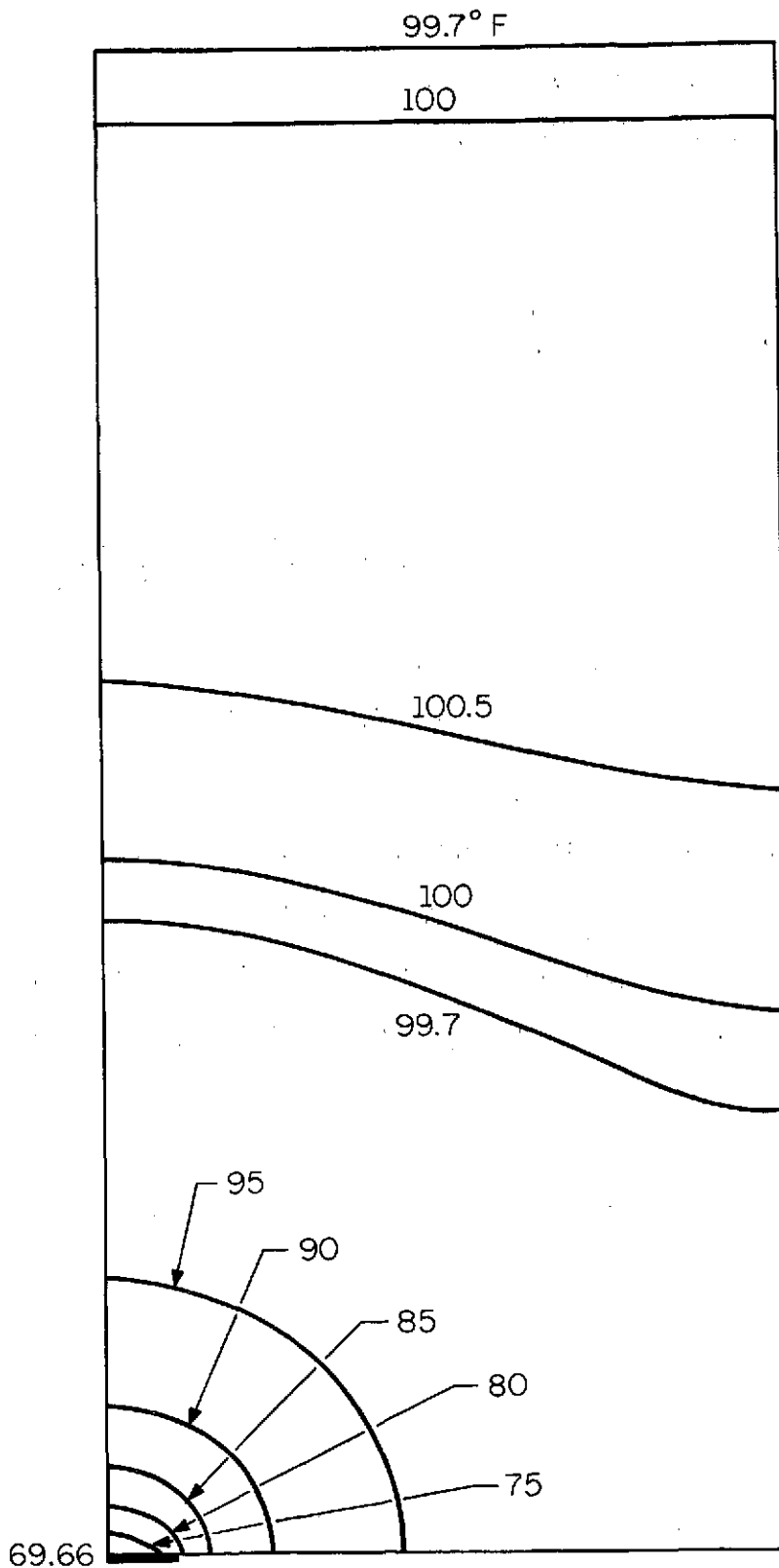


Figure C.1 Steady state temperature distribution in the combined tissue for the rectangular model.  $Q_m = 2600$  Btu/hr, (760 w),  $\beta = 0.1$  and constant temperature at inner core.

If the fourth boundary condition, Eq. (C.1e), is changed to uniform flux at the interface between the combined tissue and the inner core, that is,

$$\text{at } y = b, \quad \frac{\partial \theta}{\partial y} = \frac{F_o}{k} \quad (\text{C.3})$$

a solution is obtained [58],

$$T(x,y) = T_1 + \frac{Q}{w} - \frac{\beta f_a}{kw} \frac{\cosh [w(b-y)]}{\sinh (wb)} + \frac{F_o}{kw} \frac{\cosh (wy)}{\sinh (wb)} - \sum_{n=1}^{\infty} \frac{\alpha_n \cosh [\zeta(b-y)]}{\zeta \sinh (wb)} \cos (\lambda_n x) \quad (\text{C.4})$$

Figure C.2 shows results that were obtained for Eq. (C.4).

Solutions for the corresponding one-dimensional cases, i.e., uniform cooling at the skin, may be readily obtained from Eqs. (C.3) and (C.4) by eliminating the x-dependent series and replacing the term  $\beta f_a$  by  $F$ .

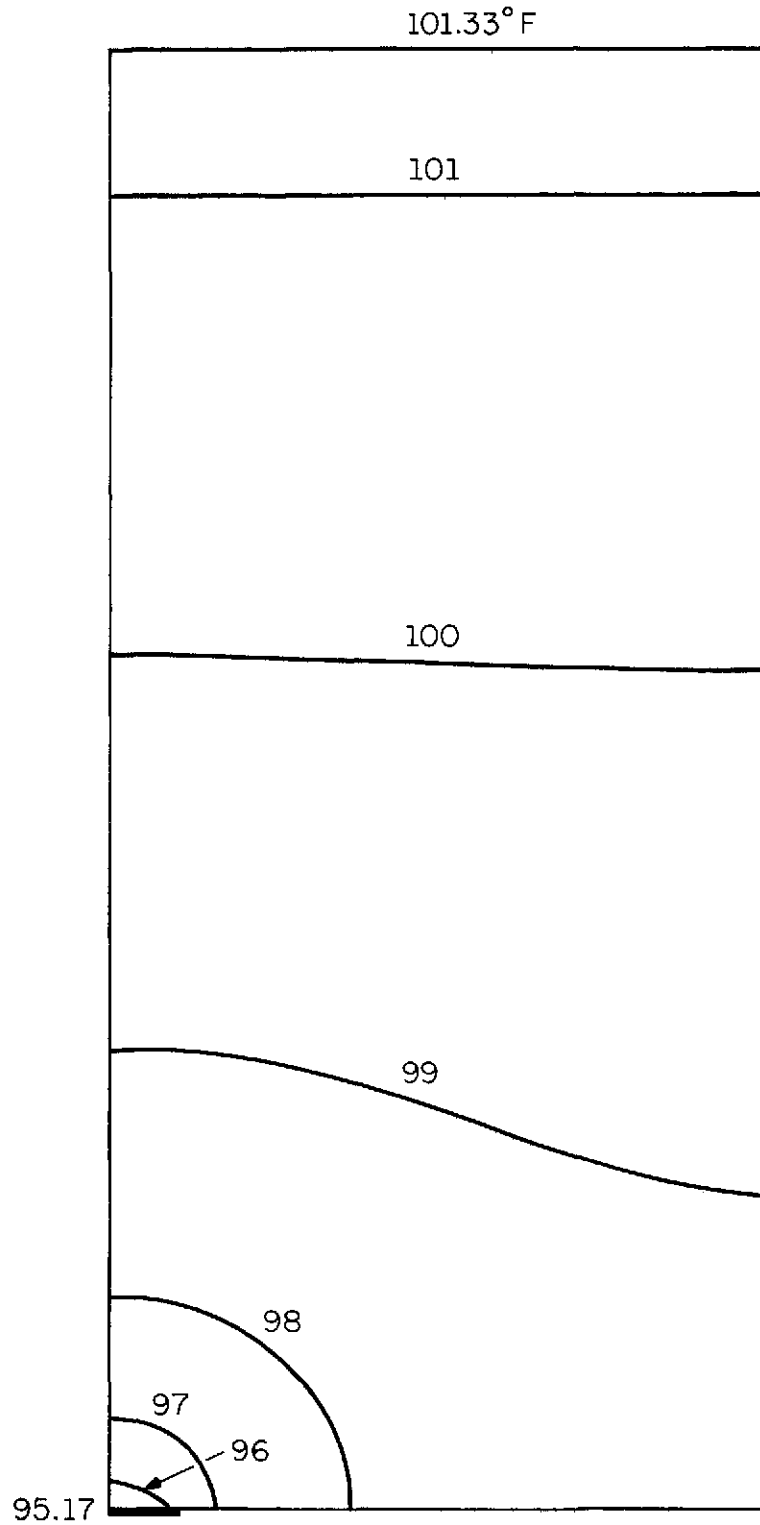


Figure C.2 Steady state temperature distribution in the combined tissue for the rectangular model.  $Q_m = 290$  Btu/hr (85 w),  $\beta = 0.1$ , constant flux at inner core.

## APPENDIX D

THE FUNCTION  $\psi_{k\ell}^j(\zeta_i r)$ 

During the mathematical derivation of the cylindrical model, a combination of modified Bessel function was found to recur; namely,

$$\psi_{k\ell}^j(\zeta_i r) \equiv I_k(\zeta_i r)K_\ell(\zeta_i R_j) + (-1)^{k+\ell+1}I_\ell(\zeta_i R_j)K_k(\zeta_i r) \quad (3.37)$$

This shorthand definition simplified the derivation considerably.

A few characteristics of this function are given below.

- (1) The function  $\psi_{k\ell}^j(\zeta_i r)$  satisfies the modified Bessel equation of order  $k$ ,

$$\frac{1}{r} \frac{d}{dr} \left[ r \frac{d\psi_{k\ell}^j(\zeta_i r)}{dr} \right] - \left( \zeta_i^2 + \frac{k^2}{r^2} \right) \psi_{k\ell}^j(\zeta_i r) = 0 \quad (D.1)$$

- (2) This function obeys the same differentiation rule as does the modified Bessel function of the first kind [64]

$$r \frac{d}{dr} \left[ \psi_{k\ell}^j(\zeta_i r) \right] = k\psi_{k\ell}^j(\zeta_i r) + \zeta_i r \psi_{(k+1)\ell}^j(\zeta_i r) \quad (D.2)$$

Therefore, it is not a so-called cylinder function [64].

- (3) For two consecutive indices, it satisfies [61]

$$\psi_{k(k+1)}^j(\zeta_i R_j) = \frac{1}{\zeta_i R_j} \quad (D.3)$$

- (4) If the indices of the function are reversed in order, the following expression is obtained

$$\psi_{k\ell}^i(\zeta_j r) = (-1)^{k+\ell+1} \psi_{\ell k}^j(\zeta_i r) \quad (D.4)$$

(5) For identical indices the following identity is obtained

$$\psi_{kk}^j(\zeta_i R_j) \equiv 0 \quad (\text{D.5})$$

When drawn on a semi-log paper, the function  $\psi_{k\ell}^j(wR)$  appears to behave as a straight line away from the minima (Fig. D.1,  $k = 0$ ,  $\ell = 1$ ,  $j = 1$ ). Also the slopes of these straight lines appear to be identical. This phenomenon suggests approximation of the function by using exponential expressions of the kind,

$$\psi_{k, k+1}^j(\zeta_i r) = U(\zeta_i R_j) \exp(s\zeta_i r) \quad (\text{D.6})$$

$$r \begin{matrix} < \\ > \end{matrix} \bar{R}$$

where  $U$  is the function describing the dependency on the parameter  $\zeta_i R_j$ ,  $s$  is the common slope, and  $\bar{R}$  is the value of the variable beyond which this approximation is valid.

Figures D.2 and D.3 show the functions  $\psi_{00}^1(wR)$  and  $\psi_{12}^1(wR)$ . As can be seen, these two functions exhibit the same characteristics as noted above, i.e., linearity on a semi-log paper, and, therefore, can also be approximated by expressions such as Eq. (D.6).

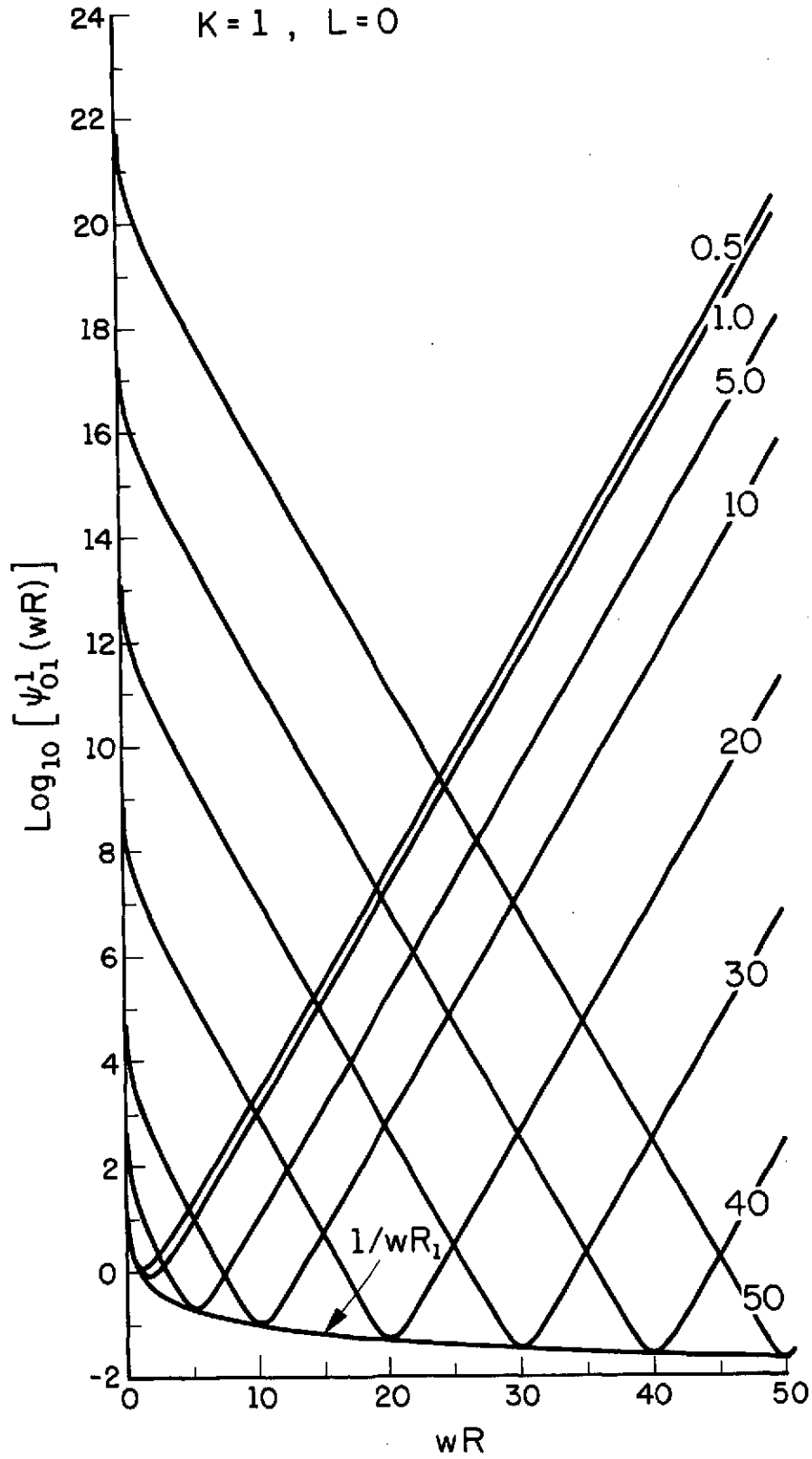


Figure D.1 The function  $\psi_{01}^1(wR)$  drawn on semi-log paper.

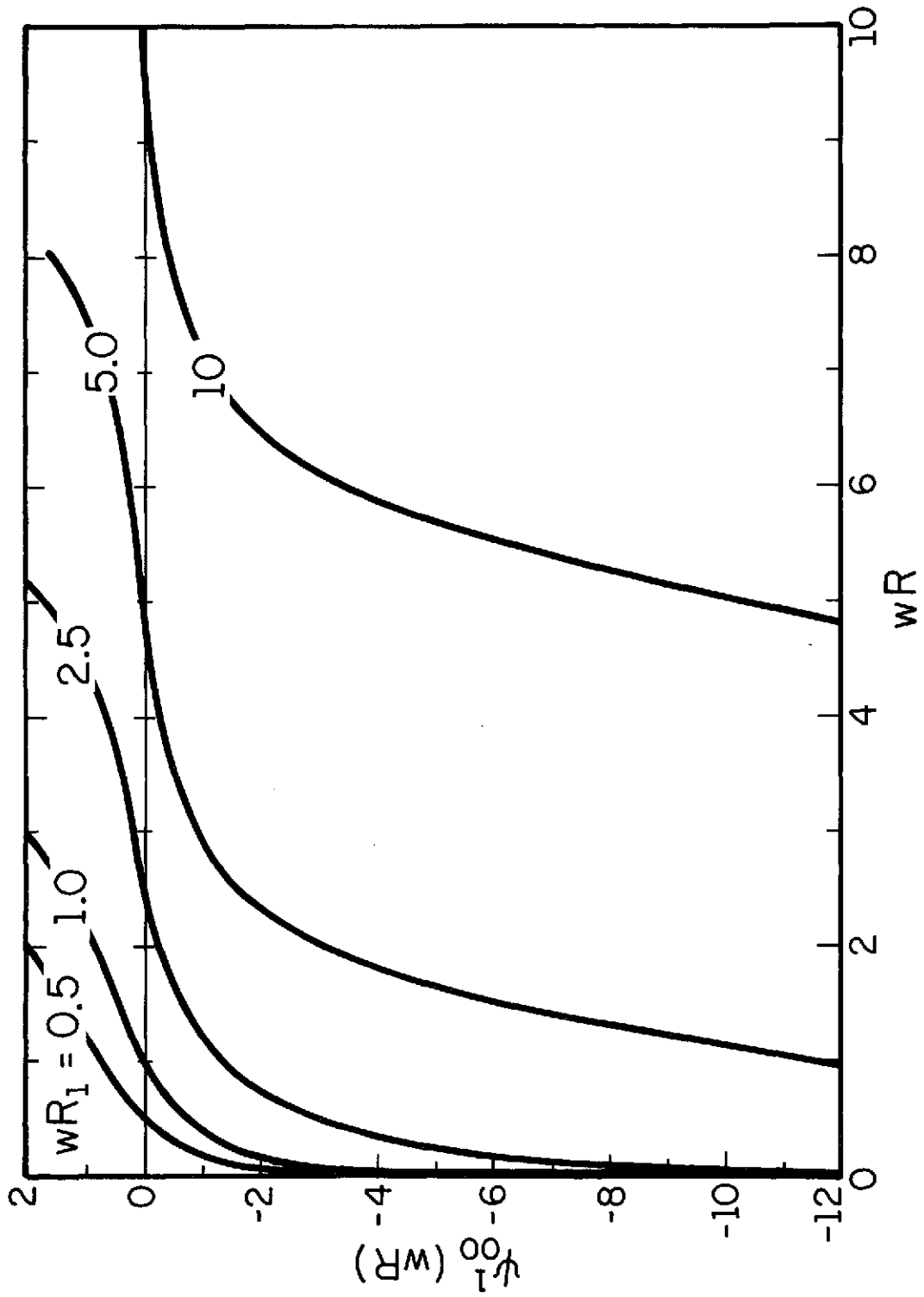


Figure D.2 The function  $\psi_{00}^1(wR)$ .

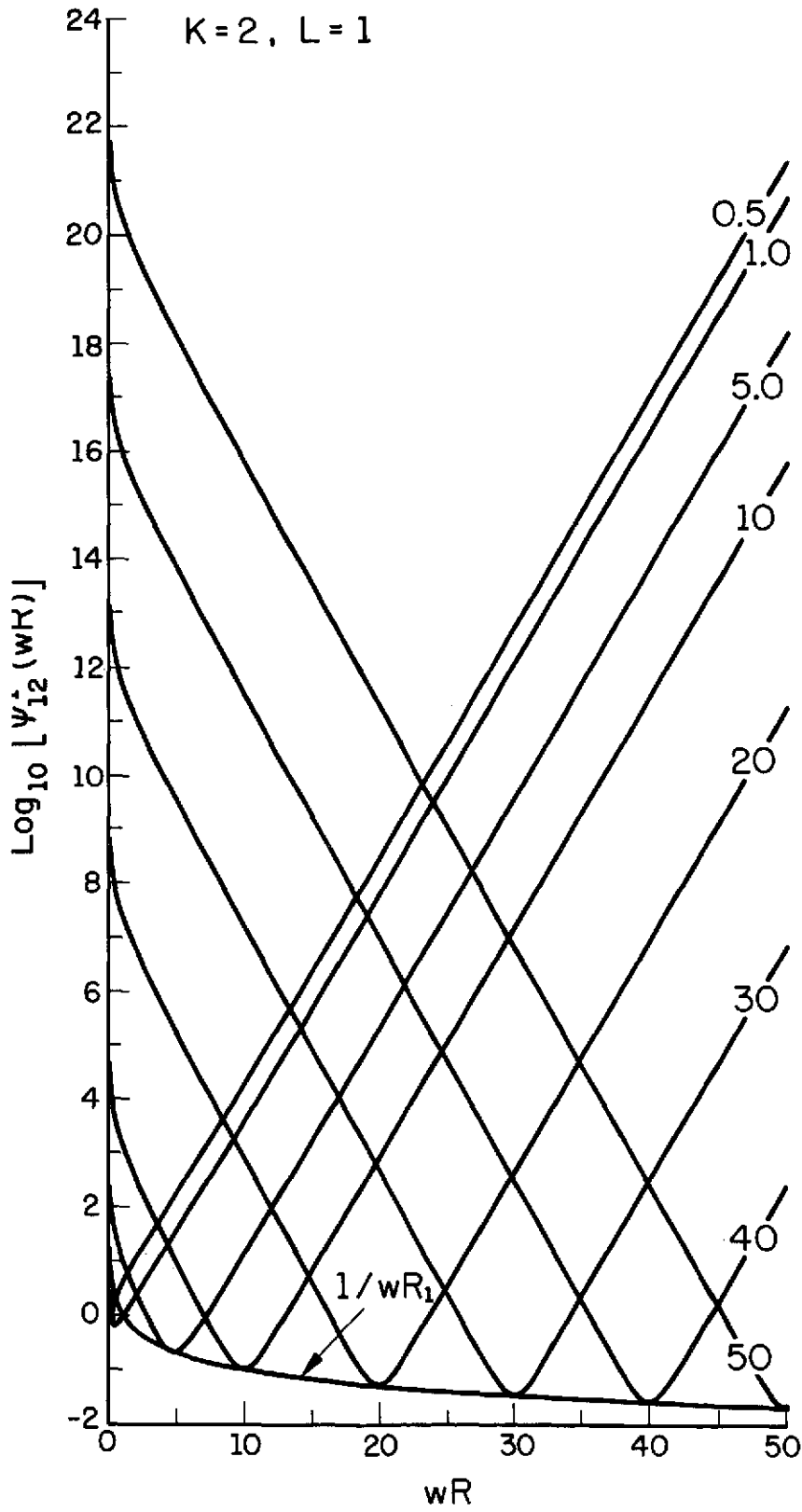


Figure D.3 The function  $\psi_{12}^1(wR)$  drawn on semi-log paper.

## APPENDIX E

STEADY STATE, CYLINDRICAL COORDINATES WITH THE SKIN AND MUSCLE  
CONSIDERED AS A SINGLE REGION

Combining the two layers into a single, averaged layer yields

$$\frac{1}{r} \frac{\partial}{\partial r} \left( r \frac{\partial \theta}{\partial r} \right) + \frac{\partial^2 \theta}{\partial z^2} - w^2 \theta = -Q \quad (\text{E.1a})$$

$$R_1 \leq r \leq R_2, \quad 0 \leq z \leq a$$

with the boundary conditions,

$$\text{at } r = R_1, \quad \theta = 0 \quad (\text{E.1b})$$

$$\text{at } r = R_2, \quad \left\{ \begin{array}{l} \frac{\partial \theta}{\partial r} = -\frac{f(z)}{k}, \quad 0 \leq z < \beta a \\ \frac{\partial \theta}{\partial r} = 0, \quad \beta a < z \leq a \end{array} \right\} \quad (\text{E.1c})$$

$$\text{at } z = 0, \quad \frac{\partial \theta}{\partial z} = 0 \quad (\text{E.1d})$$

$$\text{at } z = a, \quad \frac{\partial \theta}{\partial z} = 0 \quad (\text{E.1e})$$

The solution is

$$\begin{aligned} T(r,z) = T_1 + \frac{Q}{w} \left[ 1 - \frac{\psi_{01}^2(wr)}{\psi_{01}^2(wR_1)} \right] - \frac{\beta f_a}{kw} \frac{\psi_{00}^1(wr)}{\psi_{01}^2(wR_1)} \\ - \sum_{n=1}^{\infty} \frac{\alpha_n \psi_{00}^1(\zeta r)}{\zeta \psi_{01}^2(\zeta R_1)} \cos(\lambda_n z) \end{aligned} \quad (\text{E.2})$$

Figure E.1 shows results that were obtained for this case.

99.7°F

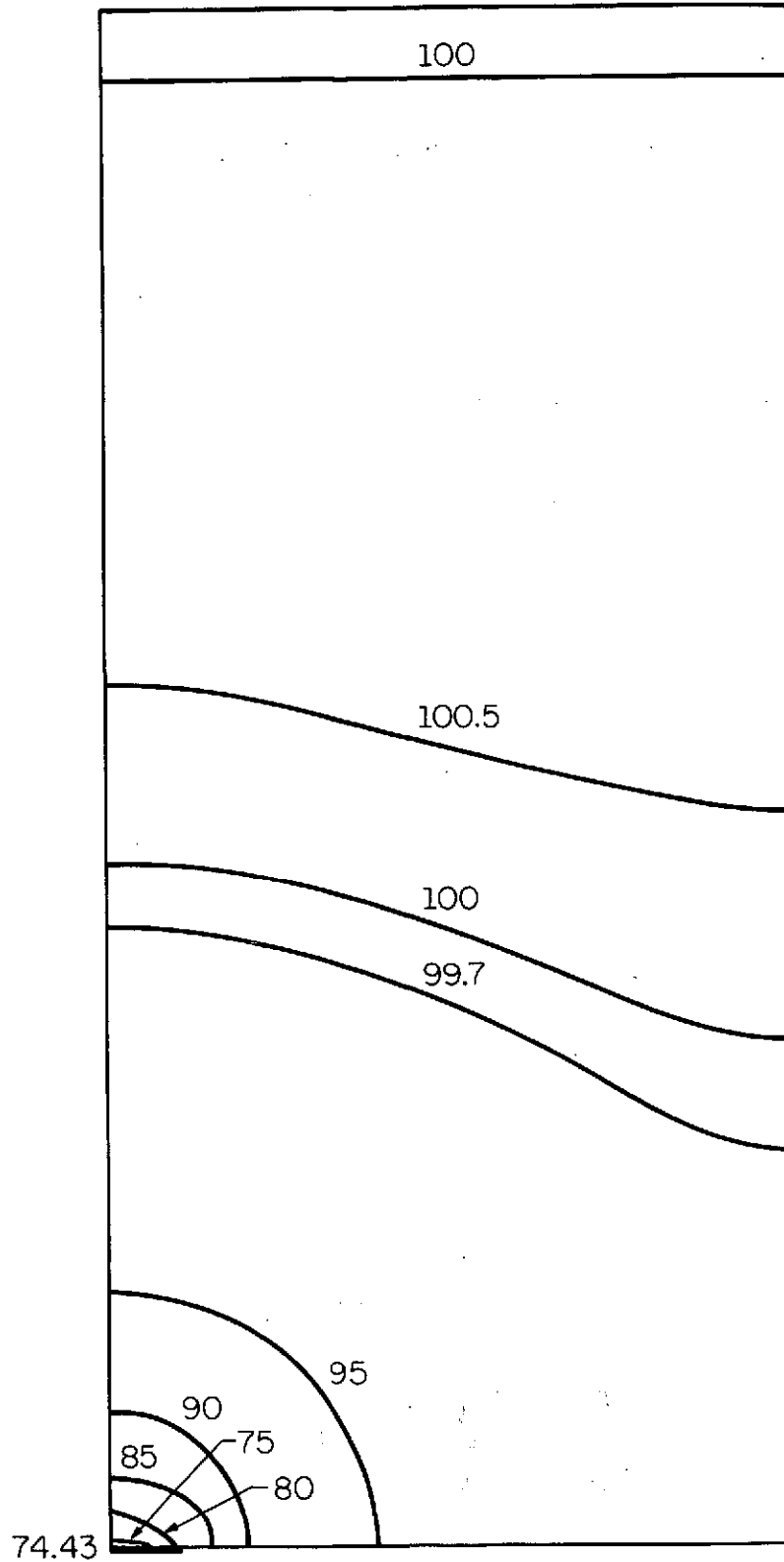


Figure E.1 Steady state temperature distribution in the combined tissue for the cylindrical model (cooling tubes on the skin running perpendicular to the axis of the cylinder).  $Q_m = 2600$  Btu/hr (760 w),  $\beta = 0.1$ , constant temperature at inner core.

Modifying the first boundary condition, Eq. (E.1b), to the constant flux case, that is,

$$\text{at } r = R_1, \quad \frac{\partial \theta}{\partial r} = - \frac{F_o}{k} \quad (\text{E.3})$$

yields

$$\begin{aligned} T(r,z) = T_1 + \frac{Q}{w^2} - \frac{\beta f_a}{kw} \frac{\psi_{01}^1(wr)}{\psi_{11}^2(wR_1)} - \frac{F_o}{kw} \frac{\psi_{01}^2(wr)}{\psi_{11}^2(wR_1)} \\ - \sum_{n=1}^{\infty} \frac{\alpha_n \psi_{01}^1(\zeta r)}{\zeta \psi_{11}^2(\zeta R_1)} \cos(\lambda_n z) \end{aligned} \quad (\text{E.4})$$

Because of the cylindrical geometry, an additional parameter appeared; namely,  $wR_2$ . If the body is assumed to be represented by one cylinder, an assumption which is equivalent to the rectangular case, three independent combinations arise as  $R_1$  is changed:

- (1) The volume and thickness of the cylindrical shell are constant while the skin surface area changes,

$$A = \frac{2V}{b(1 + \rho^*)} \quad (\text{E.5})$$

- (2) The volume and surface area of the cylindrical shell are constant while the thickness changes,

$$b = \frac{V}{A} - R_1 + \sqrt{R_1^2 + \left(\frac{V}{A}\right)^2} \quad (\text{E.6})$$

- (3) The surface area and the thickness of the cylindrical shell are constant while the volume changes,

$$v = \frac{Ab}{2} [1 + \rho^*] \quad (E.7)$$

where

$$\rho^* \equiv \frac{R_1}{R_2} \quad (E.8)$$

Assuming a uniform flux at the skin, the above three cases were evaluated, as functions of  $R_1$ , and are compared to the limiting case as  $R_1 \rightarrow \infty$  (rectangular case). The results are presented in Figs.

E.2, E.3, E.4, and E.5.

For completeness, the limiting cases for no blood flow,  $w_b \rightarrow 0$ , are presented below.

Using limit calculation techniques, it can be shown

$$\lim_{w \rightarrow 0} \frac{\psi_{01}^2(wr)}{\psi_{01}^2(wR_1)} = 1 \quad (E.9)$$

$$\lim_{w \rightarrow 0} \frac{1}{w} \left[ 1 - \frac{\psi_{01}^2(wr)}{\psi_{01}^2(wR_1)} \right] = \frac{1}{4} (R_1^2 - r^2) + \frac{1}{2} R_2^2 \ln \frac{r}{R_1} \quad (E.10)$$

$$\lim_{w \rightarrow 0} \frac{1}{w} \frac{\psi_{00}^1(wr)}{\psi_{10}^1(wR_2)} = R_2 \ln \frac{r}{R_2} \quad (E.11)$$

and

$$\lim_{w \rightarrow 0} \frac{1}{\zeta} \frac{\psi_{00}^1(\zeta r)}{\psi_{10}^1(\zeta R_2)} = \frac{1}{\lambda_n} \frac{\psi_{00}^1(\lambda_n r)}{\psi_{10}^1(\lambda_n R_2)} \quad (E.12)$$

Then, the solution for the cylindrical case with constant temperature at the interface between the combined tissue and the inner core, Eqs. (E.1a) through (E.1e), but  $w = 0$ , can be obtained from Eq. (E.2),

307

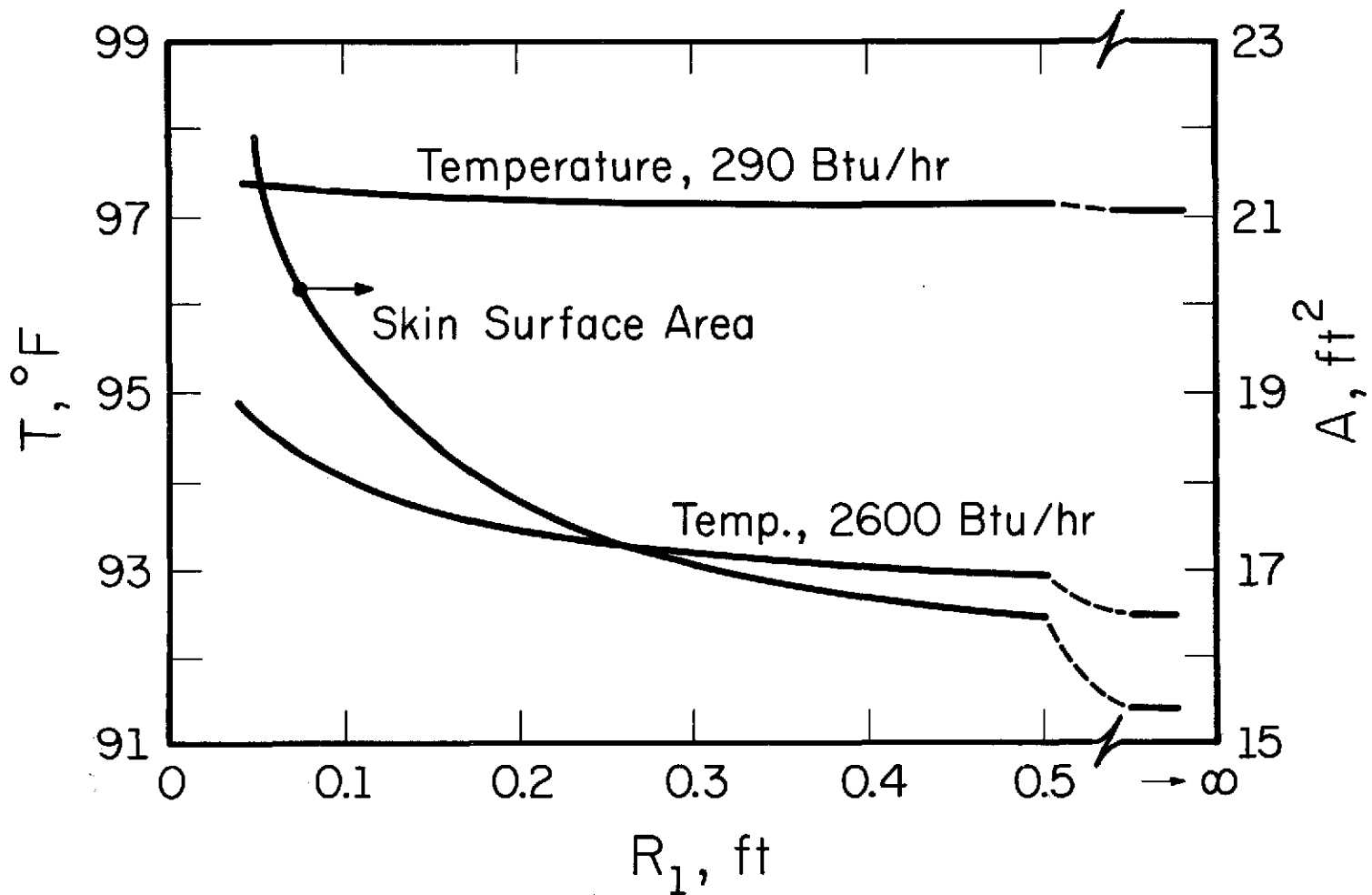


Figure E.2 Steady state temperature and surface area of the skin as functions of  $R_1$  for the one-dimensional cylindrical model.  $V$  and  $b$  are constant and constant temperature at inner core.

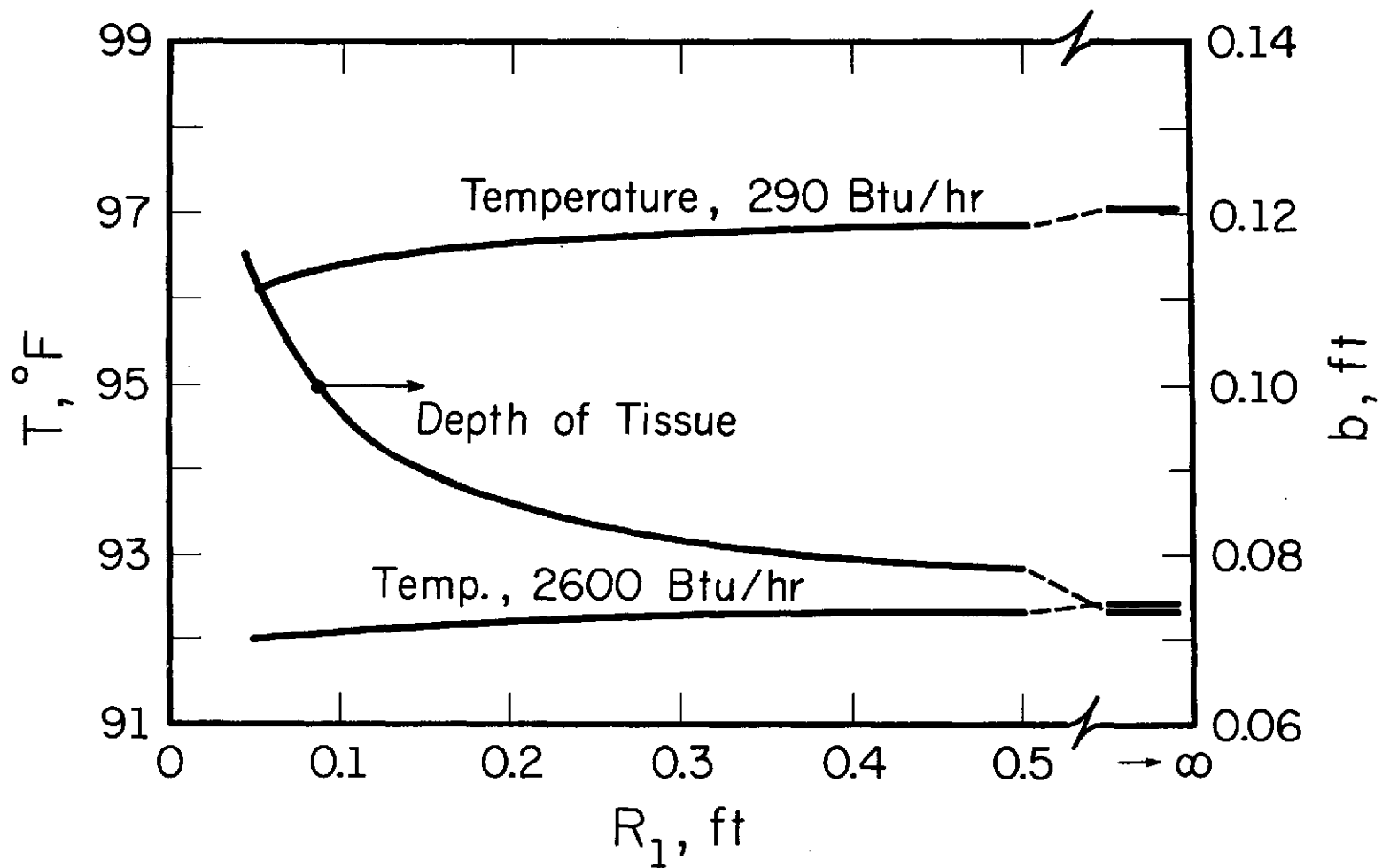


Figure E.3 Steady state temperature of the skin and depth of tissue as functions of  $R_1$  for the one-dimensional cylindrical model.  $V$  and  $A$  are constant and constant temperature at inner core.

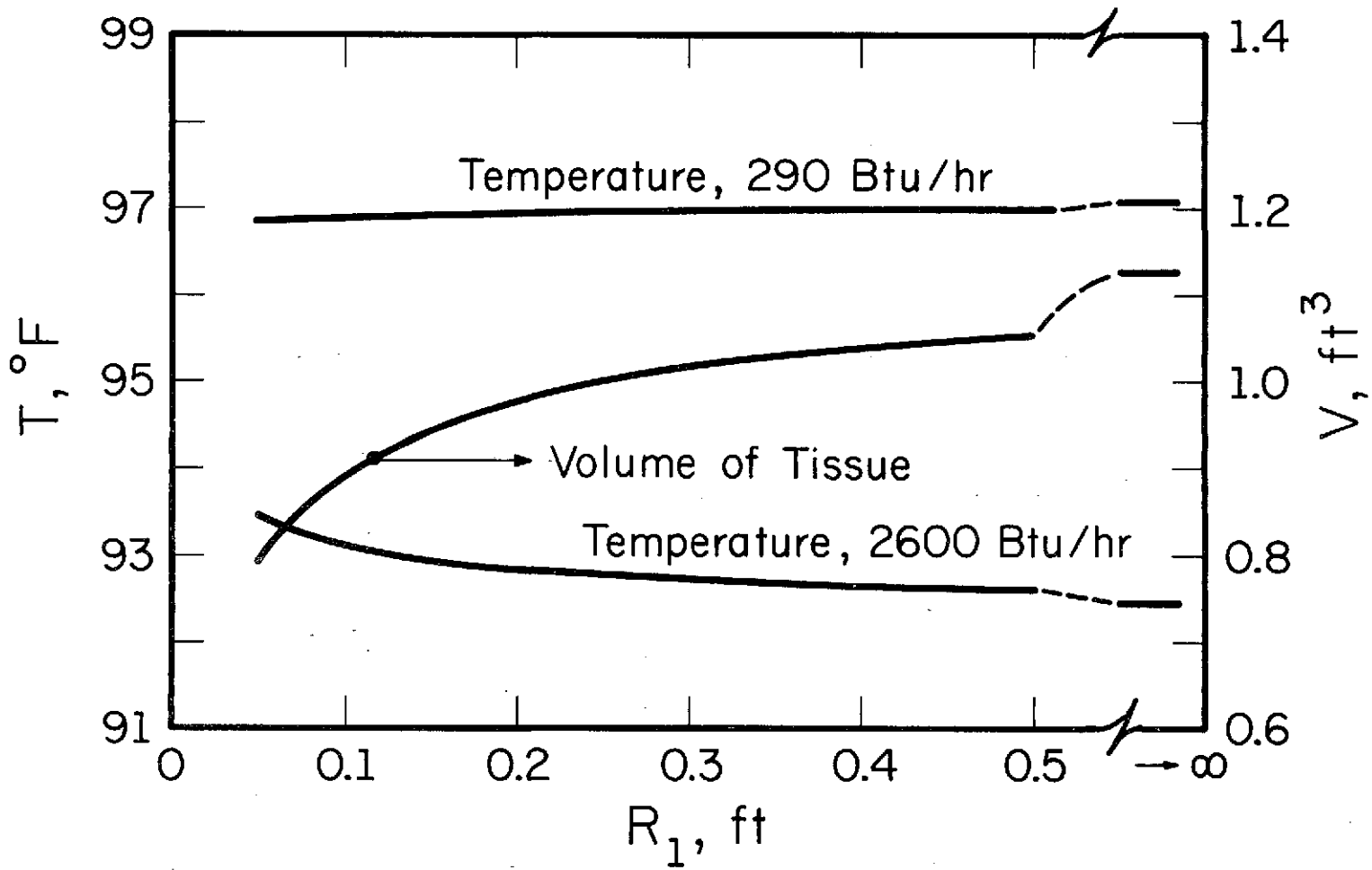


Figure E.4 Steady state temperature of the skin and volume of the tissue as functions of  $R_1$  for the one-dimensional cylindrical model.  $A$  and  $b$  are constant and constant temperature at inner core.

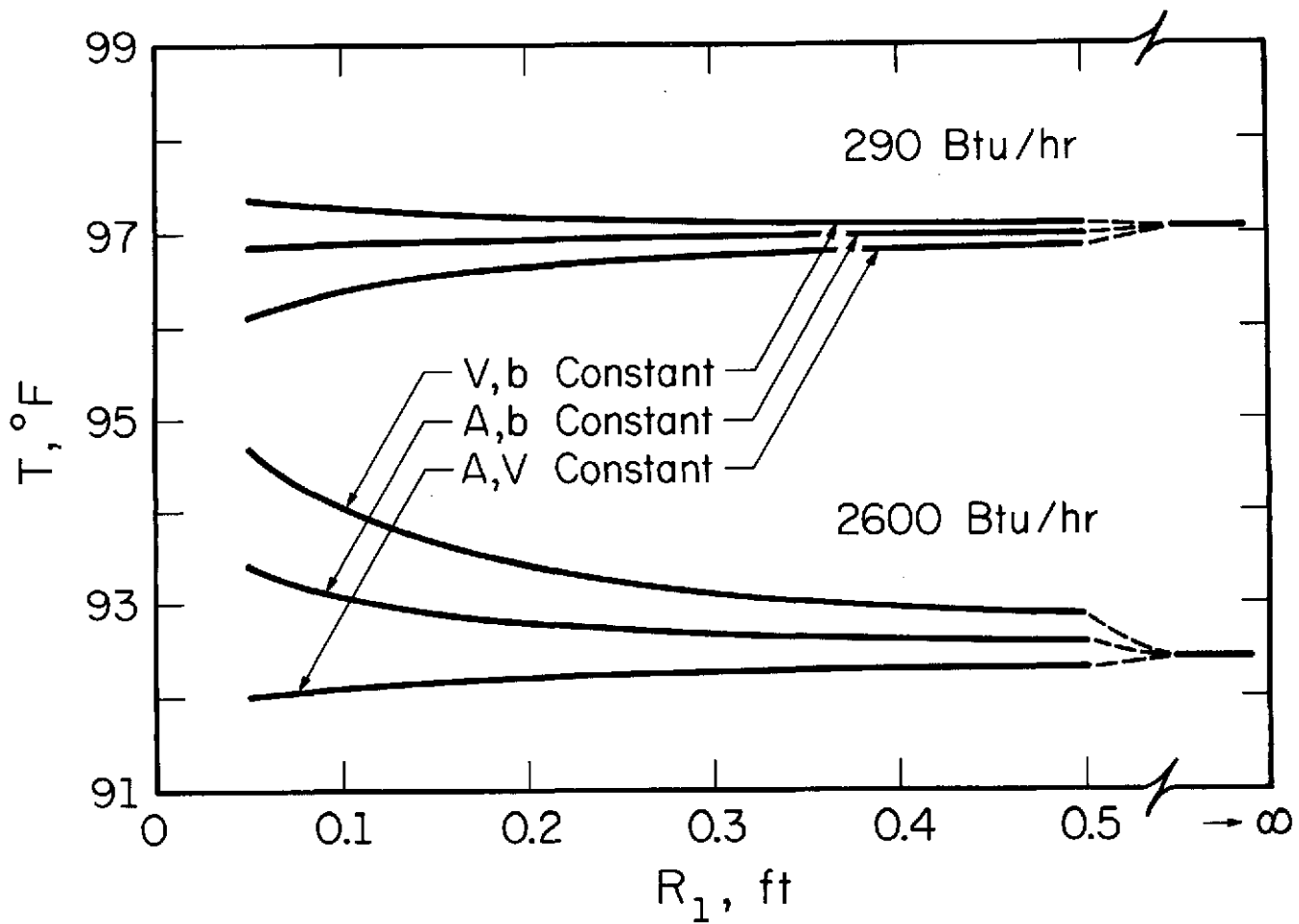


Figure E.5 Steady state temperature of the skin as function of  $R_1$  for the one-dimensional cylindrical model. Constant temperature at inner core.

$$T(r,z) = T_1 + \frac{Q}{4} (R_1^2 - r^2) + \left[ \frac{\beta F_a}{k} + \frac{QR_2}{2} \right] R_2 \ln \frac{r}{R_1} - \sum_{n=1}^{\infty} \frac{\alpha_n \psi_{00}^1(\lambda_n r)}{\lambda_n \psi_{10}^1(\lambda_n R_2)} \cos(\lambda_n z) \quad (E.13)$$

Similarly, using the energy balance equation

$$R_2 \beta f_a = R_1 F_o + \frac{Q'}{2} (R_2^2 - R_1^2) \quad (E.14)$$

Eq. (E.4) can be rewritten

$$T(r,z) = T_1 + \frac{Q'}{2R_2 k} \frac{2R_2 \psi_{11}^1(wR_2) - w(R_2^2 - R_1^2) \psi_{01}^1(wr)}{w^2 \psi_{11}^1(wR_2)} - \frac{F_o R_1 \psi_{01}^1(wr) - R_2 \psi_{01}^2(wr)}{R_2 w \psi_{11}^1(wR_2)} + \sum_{n=1}^{\infty} \frac{\alpha_n \psi_{01}^1(\zeta r)}{\zeta \psi_{11}^1(\zeta R_2)} \cos(\lambda_n z) \quad (E.15)$$

and, by using limit calculation techniques, it can be shown

$$\lim_{w \rightarrow 0} \frac{2R_2 \psi_{11}^1(wR_2) - w(R_2^2 - R_1^2) \psi_{01}^1(wr)}{w^2 \psi_{11}^1(wR_2)} = R_1 R_2 \left[ R_1 \ln r - \frac{r^2}{2R_1} \right] + R_1 R_2 \left\{ \frac{R_1}{R_2^2 - R_1^2} [R_1^2 \ln R_1 - R_2^2 \ln R_2] + \frac{R_2^2 + R_1^2}{4R_1} \right\} + R_1 (2c_1 - c_3) \quad (E.16)$$

$$\lim_{w \rightarrow 0} \frac{R_1 \psi_{01}^1(wr) - R_2 \psi_{01}^2(wr)}{w \psi_{11}^1(wR_2)} = R_1 R_2 \ln r + R_1 R_2 \left\{ \frac{R_1^2 \ln R_1 - R_2^2 \ln R_2}{R_2^2 - R_1^2} + 2c_1 - c_3 \right\} \quad (\text{E.17})$$

and

$$\lim_{w \rightarrow 0} \frac{\frac{1}{\zeta} \frac{\psi_{01}^1(\zeta r)}{\psi_{11}^1(\zeta R_2)}}{\frac{1}{\lambda_n} \frac{\psi_{01}^1(wr)}{\psi_{11}^1(wR_2)}} = \frac{1}{\lambda_n} \frac{\psi_{01}^1(wr)}{\psi_{11}^1(wR_2)} \quad (\text{E.18})$$

where

$$c_1 = \frac{\psi(1) + \psi(2) + 2 \ln 2}{4} \quad (\text{E.19})$$

$$c_3 = \ln 2 - \gamma \quad (\text{E.20})$$

$\psi(n)$  is the Psi or Digamma function and  $\gamma$  is Euler's constant.

Using the above results, the solution for the cylindrical case with constant flux at the interface between the combined tissue and the inner core, Eqs. (E.1a), (E.1c), (E.1d), (E.1e), and (E.3), but  $w = 0$ , can be obtained from Eq. (E.15),

$$\begin{aligned} T(r,z) = & T_1 + \frac{Q'}{2k} \left[ R_1^2 \ln r - \frac{r^2}{2} \right] - \frac{F_0 R_1}{k} \ln r \\ & + \frac{R_1}{k} \left[ \frac{Q' R_1}{2} - F_0 \right] \cdot \left\{ \frac{1}{R_2^2 - R_1^2} [R_1^2 \ln R_1 - R_2^2 \ln R_2] \right. \\ & \left. + \frac{1}{2} \right\} + \frac{Q'}{8k} (R_2^2 + R_1^2) + \sum_{n=1}^{\infty} \frac{\alpha_n \psi_{01}^1(wr)}{\lambda_n \psi_{11}^1(wR_2)} \\ & \cdot \cos(\lambda_n z) \end{aligned} \quad (\text{E.21})$$

APPENDIX F  
ADDITIONAL EXPERIMENTAL DATA

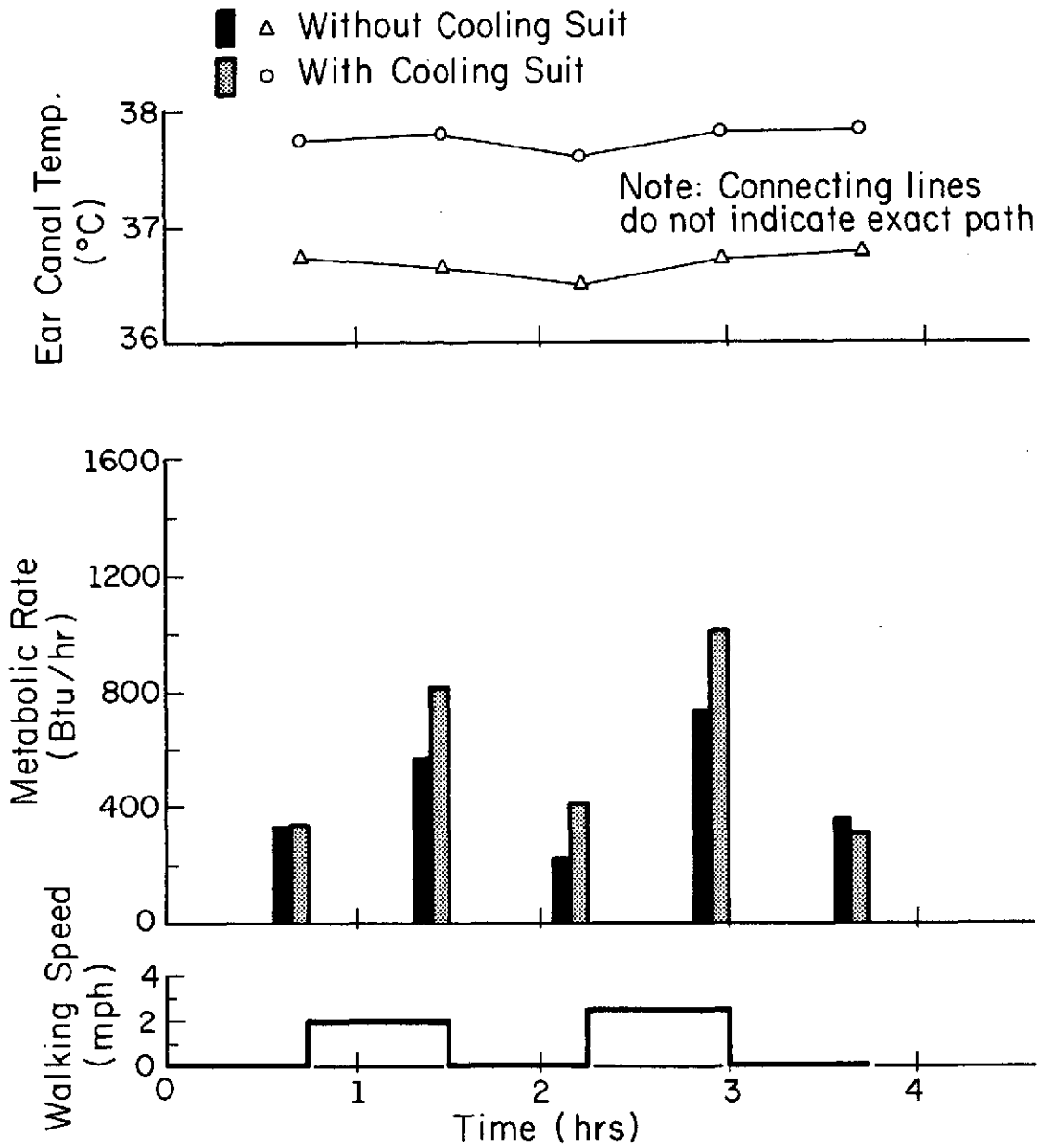


Figure F.1 Metabolic rates and ear canal temperatures of subject SKB for experiments with and without the cooling suit during Schedule I.

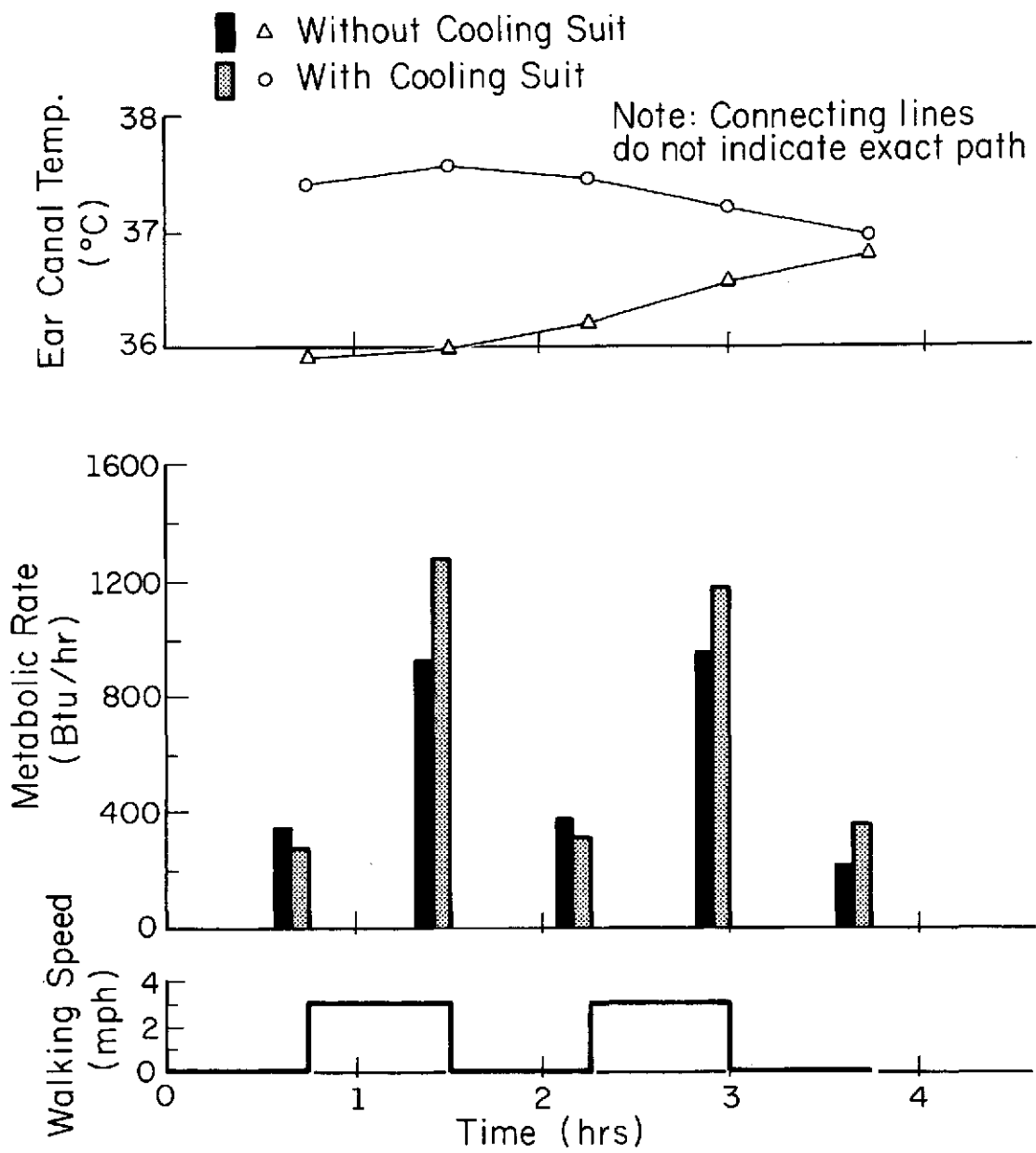


Figure F.2 Metabolic rates and ear canal temperatures of subject SKB for experiments with and without the cooling suit during Schedule II.

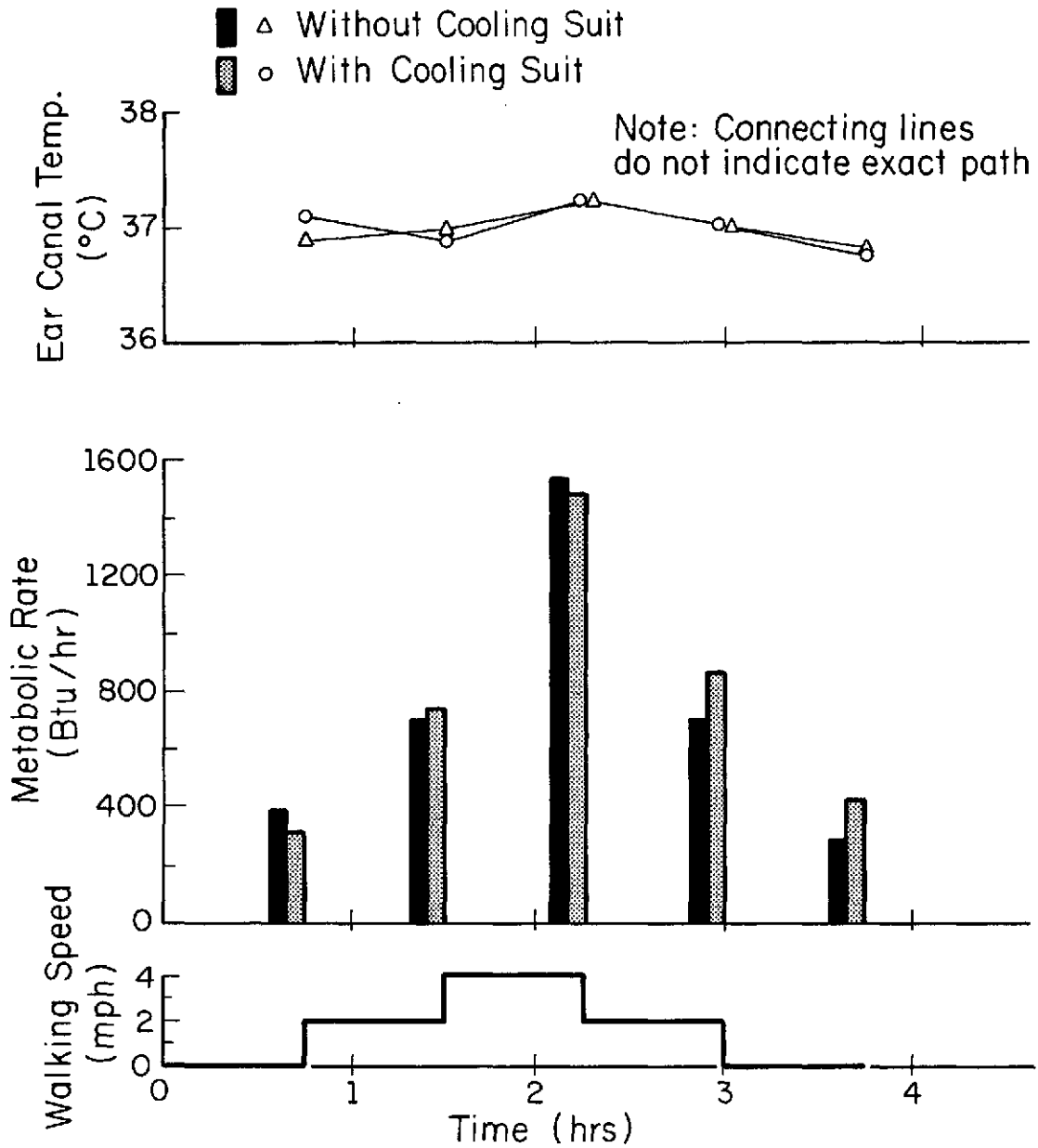


Figure F.3 Metabolic rates and ear canal temperatures of subject SKB for experiments with and without the cooling suit during Schedule III.

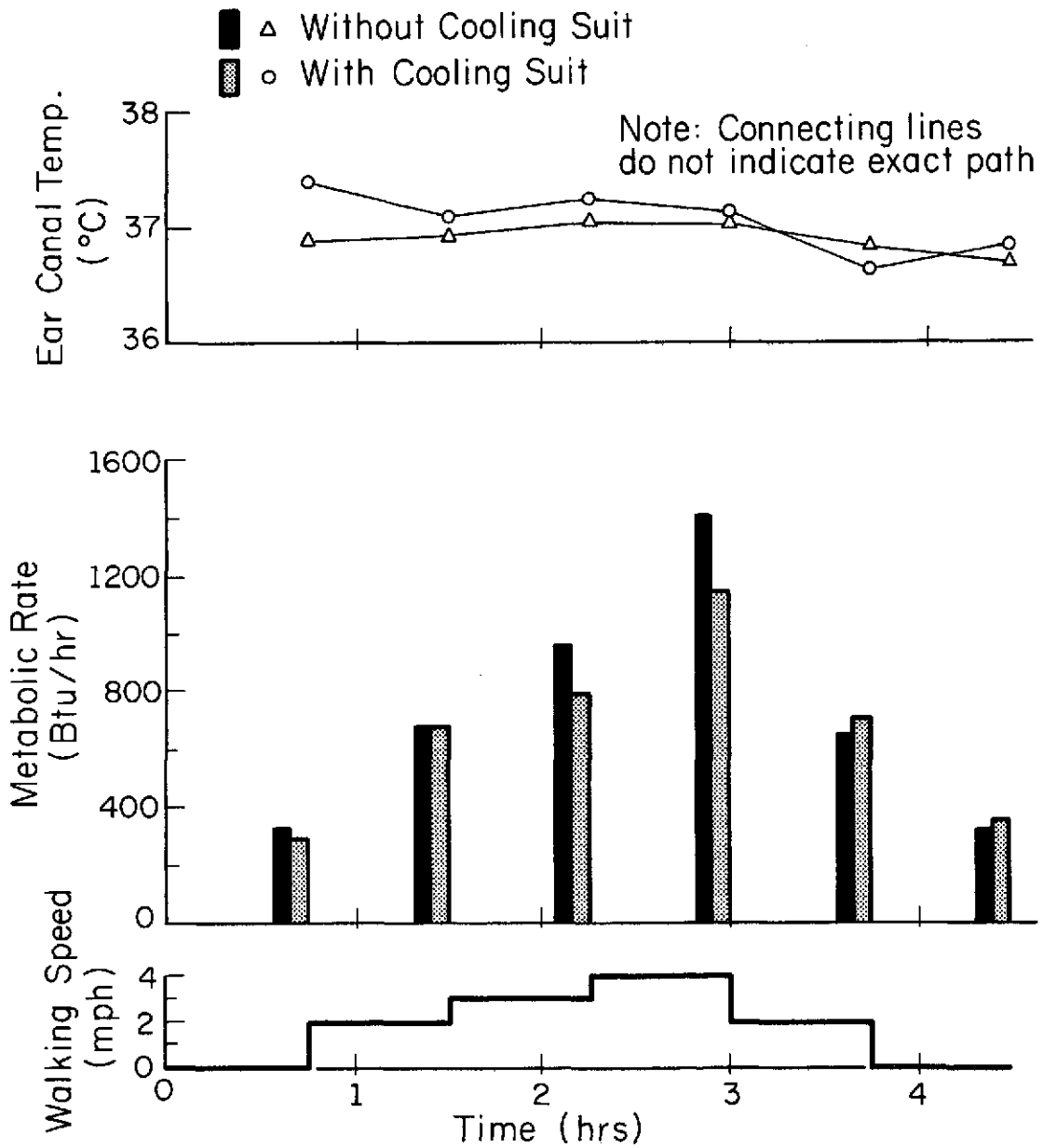


Figure F.4 Metabolic rates and ear canal temperatures of subject SKB for experiments with and without the cooling suit during Schedule IV.

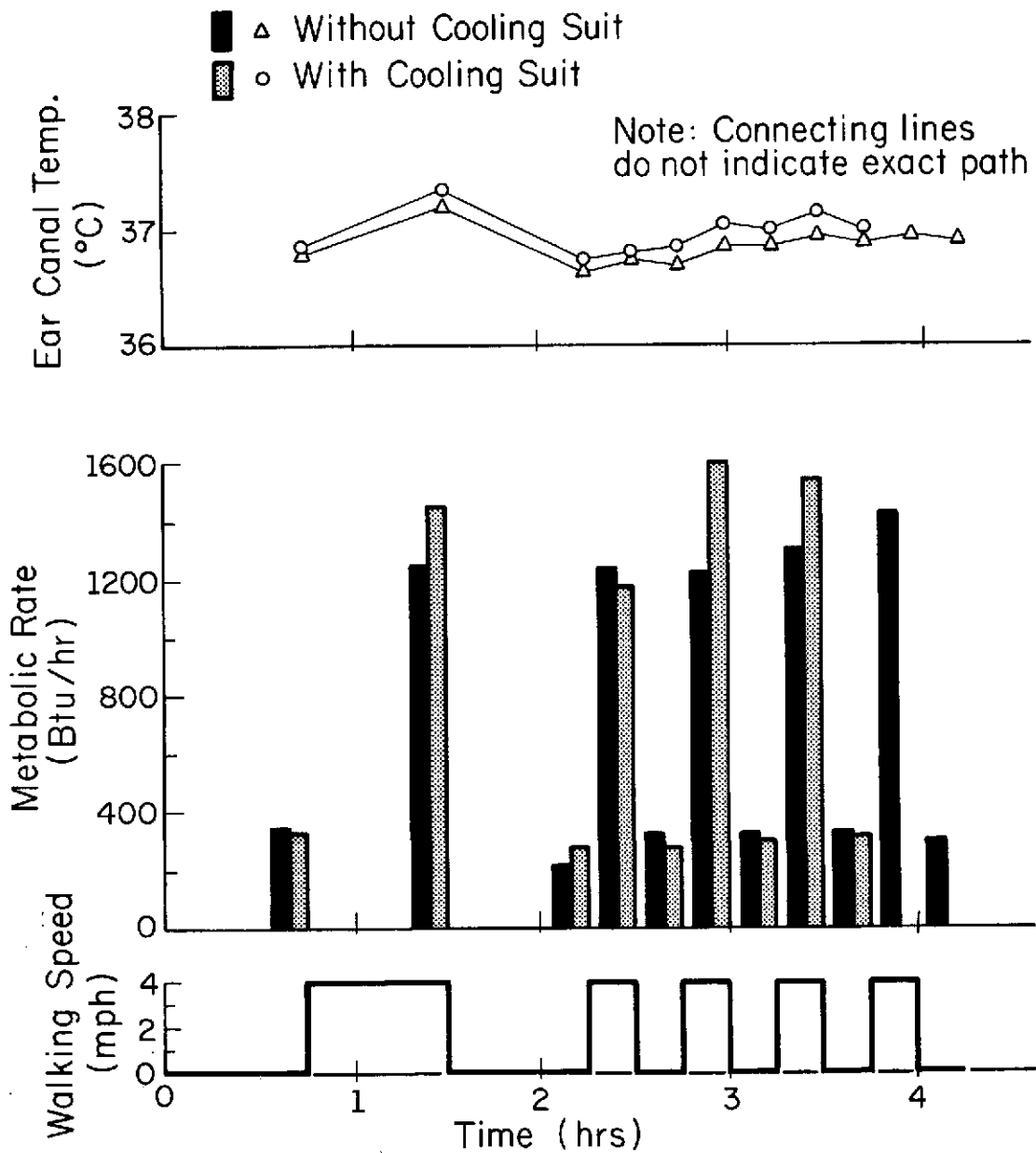


Figure F.5 Metabolic rates and ear canal temperatures of subject SKB for experiments with and without the cooling suit during Schedule V.

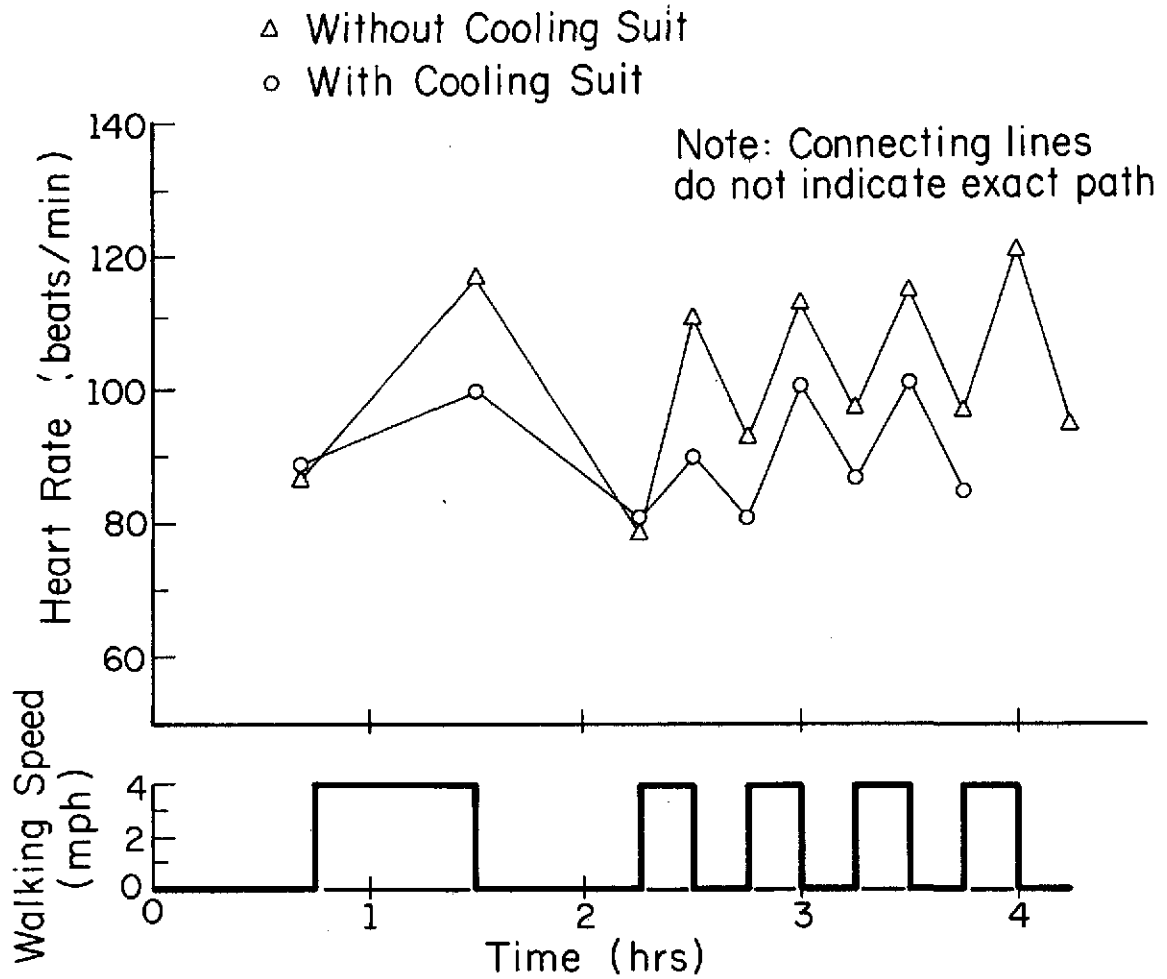


Figure F.6 Heart rates of subject SKB for experiments with and without the cooling suit during Schedule V.

TABLE F.1

MEAN VALUES AND RANGES OF TOTAL METABOLIC RATES, HEAT REMOVED  
BY SUIT AND BY RESPIRATION AT THE VARIOUS SCHEDULES OF ACTIVITY

Activity		Metabolic Rate Btu/hr-ft <sup>2</sup>	Heat Removed by Suit Btu/hr-ft <sup>2</sup>	Heat Removed by Respiration Btu/hr-ft <sup>2</sup>	Mean Percent Heat Removed	
					Suit	Respiration
SCHEDULE I						
Standing	Mean	17.7	17.9	2.2	--	12.5
	Range	15.0-26.1	12.9-22.4	2.0-3.1		
2 mph	Mean	43.9	22.9	4.2	52.2	9.7
	Range	40.5-50.5	18.3-28.2	3.9-4.9		
Standing	Mean	17.1	15.8	2.3	92.1	13.6
	Range	14.4-22.6	11.6-23.5	1.7-3.3		
2.5 mph	Mean	50.7	19.4	4.7	38.4	9.3
	Range	39.5-60.1	15.8-25.5	4.1-7.3		
Standing	Mean	18.0	15.1	2.3	83.8	12.6
	Range	17.0-18.8	12.8-18.3	2.0-3.3		

(continued)

TABLE F.1 continued

Activity		Metabolic Rate Btu/hr-ft <sup>2</sup>	Heat Removed by Suit Btu/hr-ft <sup>2</sup>	Heat Removed by Respiration Btu/hr-ft <sup>2</sup>	Mean Percent Heat Removed	
					Suit	Respiration
SCHEDULE II						
Standing	Mean	17.0	17.0	1.9	100.0	11.3
	Range	14.8-19.6	14.5-23.4	1.3-2.5		
3 mph (w/o additional cooling)	Mean	62.6	24.5	5.4	39.1	8.7
	Range	54.3-69.5	21.1-26.4	3.0-8.7		
Standing	Mean	16.1	20.2	2.4	--	14.8
	Range	12.9-17.9	15.0-23.3	1.3-4.2		
3 mph (with additional cooling)	Mean	54.8	30.7	4.9	56.0	9.0
	Range	42.9-64.6	24.9-37.9	2.3-7.1		
Standing	Mean	16.0	20.1	2.1	--	12.9
	Range	11.8-19.6	15.6-28.2	1.2-3.5		

(continued)

321

183

TABLE F.1 continued

Activity		Metabolic Rate Btu/hr-ft <sup>2</sup>	Heat Removed by Suit Btu/hr-ft <sup>2</sup>	Heat Removed by Respiration Btu/hr-ft <sup>2</sup>	Mean Percent Heat Removed	
					Suit	Respiration
SCHEDULE III						
Standing	Mean	16.6	13.3	2.3	80.0	13.9
	Range	12.3-20.3	11.2-15.3	1.2-3.1		
2 mph	Mean	41.2	18.8	3.9	45.6	9.4
	Range	27.2-48.8	14.7-28.7	2.8-4.8		
4 mph	Mean	89.4	45.5	7.4	50.9	8.3
	Range	80.7-100.3	30.0-60.5	5.2-9.6		
2 mph	Mean	46.8	23.6	4.0	50.5	8.5
	Range	35.5-56.7	21.3-26.0	2.6-6.4		
Standing	Mean	18.4	14.2	2.4	77.2	13.2
	Range	11.8-23.8	6.6-21.9	1.3-4.6		

(continued)

TABLE F.1 continued

Activity		Metabolic Rate Btu/hr-ft <sup>2</sup>	Heat Removed by Suit Btu/hr-ft <sup>2</sup>	Heat Removed by Respiration Btu/hr-ft <sup>2</sup>	Mean Percent Heat Removed	
					Suit	Respiration
SCHEDULE IV						
Standing	Mean	15.7	19.5	1.8	--	11.6
	Range	14.2-15.9	11.5-23.3	1.3-2.3		
2 mph	Mean	41.1	24.9	3.6	60.6	8.9
	Range	27.0-47.7	16.7-31.7	2.4-5.0		
3 mph	Mean	51.0	35.5	4.4	69.5	8.6
	Range	33.0-61.2	31.1-41.4	3.0-5.9		
4 mph	Mean	85.7	49.0	7.7	57.1	9.0
	Range	62.5-98.8	35.7-60.7	4.2-10.0		
2 mph	Mean	46.1	23.4	3.6	50.8	7.7
	Range	38.9-52.2	17.5-30.5	3.1-4.6		
Standing	Mean	16.0	16.4	2.1	--	13.4
	Range	12.9-19.6	9.1-23.5	1.2-3.9		

(continued)

323

TABLE F.1 continued

Activity		Metabolic Rate Btu/hr-ft <sup>2</sup>	Heat Removed by Suit Btu/hr-ft <sup>2</sup>	Heat Removed by Respiration Btu/hr-ft <sup>2</sup>	Mean Percent Heat Removed	
					Suit	Respiration
SCHEDULE V						
Standing	Mean	16.1	20.6	2.1	--	13.0
	Range	13.7-17.9	12.9-31.6	1.2-3.1		
4 mph	Mean	91.1	50.9	6.6	55.8	7.3
	Range	78.8-101.4	37.6-61.5	3.5-8.9		
Standing	Mean	15.1	20.9	1.9	--	12.6
	Range	14.1-17.2	10.0-29.0	1.4-2.4		
4 mph	Mean	82.4	29.8	6.1	36.1	7.4
	Range	64.3-98.7	26.1-36.8	3.4-8.9		
Standing	Mean	15.2	28.2	1.9	--	12.2
	Range	13.8-18.0	27.0-31.3	1.3-2.3		
4 mph	Mean	86.8	40.3	6.4	46.4	7.4
	Range	72.4-100.6	28.1-59.3	3.5-8.8		

(continued)

TABLE F.1 continued

Activity		Metabolic Rate Btu/hr-ft <sup>2</sup>	Heat Removed by Suit Btu/hr-ft <sup>2</sup>	Heat Removed by Respiration Btu/hr-ft <sup>2</sup>	Mean Percent Heat Removed	
					Suit	Respiration
SCHEDULE V cont.						
Standing	Mean	17.4	31.8	1.9	--	10.8
	Range	14.9-23.3	22.5-37.3	1.3-3.0		
4 mph	Mean	87.3	41.4	6.6	47.4	7.5
	Range	69.8-103.8	34.4-44.8	3.2-9.0		
Standing	Mean	18.3	34.8	2.3	--	12.3
	Range	15.9-21.2	22.8-42.8	1.6-2.9		
4 mph	Mean	90.1	42.5	6.6	47.1	7.3
	Range	72.7-101.6	34.6-50.9	4.0-9.2		
Standing	Mean	18.3	32.2	2.0	--	10.9
	Range	17.1-19.3	27.4-35.9	1.6-2.6		

63  
73  
67  
A

TABLE F.2

MEAN VALUES AND RANGES OF WATER INLET TEMPERATURES FOR THE VARIOUS REGIONS  
AT DIFFERENT SCHEDULES OF ACTIVITY

Activity		Water Inlet Temperature, deg C					
		Region					
		Head	Arms	Upper Torso	Lower Torso	Thighs	Lower Legs
SCHEDULE †							
Standing	Mean	19.6	24.9	22.7	23.1	24.5	23.8
	Range	12.6-22.9	22.1-29.4	12.7-28.9	12.8-28.5	22.6-28.2	20.2-27.6
2 mph	Mean	19.3	24.8	25.5	23.4	24.2	24.4
	Range	14.5-23.3	22.3-28.2	20.8-31.1	14.3-31.4	22.1-29.6	19.7-29.6
Standing	Mean	19.5	25.6	26.5	23.8	26.0	25.3
	Range	15.2-24.1	22.1-29.0	21.2-32.9	15.1-33.2	22.0-31.7	19.5-31.0
2.5 mph	Mean	19.6	25.5	26.3	24.2	25.7	25.2
	Range	15.7-24.6	21.5-28.7	21.0-32.6	15.5-33.6	20.9-31.7	19.0-30.9
Standing	Mean	20.3	25.0	25.8	24.3	25.3	24.7
	Range	15.9-24.6	21.3-27.6	20.5-32.1	15.8-34.1	21.2-31.0	19.0-30.3

†Averages of 5 runs.

(continued)

TABLE F.2 continued

Activity		Water Inlet Temperature, deg C					
		Region					
		Head	Arms	Upper Torso	Lower Torso	Thighs	Lower Legs
SCHEDULE II†							
Standing	Mean	24.0	24.8	24.3	26.5	23.6	28.8
	Range	15.5-33.1	21.7-27.6	20.2-28.6	21.4-30.1	21.5-25.7	26.3-31.1
3 mph (w/o additional cooling)	Mean	22.8	24.8	24.3	26.2	23.7	28.7
	Range	15.5-29.1	21.7-28.5	20.6-29.2	21.8-29.8	21.2-26.0	26.4-31.8
Standing	Mean	22.2	23.6	24.1	25.8	22.4	26.4
	Range	15.2-29.7	22.3-26.2	20.6-27.2	21.8-28.6	19.1-25.3	18.2-31.4
3 mph (with additional cooling)	Mean	20.8	20.1	20.7	23.3	18.6	21.7
	Range	14.9-26.1	14.8-23.0	14.8-22.6	17.5-29.1	17.0-19.3	16.9-29.5
Standing	Mean	21.8	22.2	24.1	26.3	22.0	22.1
	Range	15.0-34.4	19.8-25.8	22.0-28.8	24.4-28.5	19.0-26.6	17.4-28.6

†Averages of 5 runs.

(continued)

367

TABLE F.2 continued

Activity		Water Inlet Temperature, deg C					
		Region					
		Head	Arms	Upper Torso	Lower Torso	Thighs	Lower Legs
SCHEDULE III†							
Standing	Mean	22.5	25.7	27.8	26.5	26.9	28.3
	Range	18.4-26.0	19.1-29.1	22.3-32.2	24.6-29.0	23.2-29.8	25.9-31.3
2 mph	Mean	19.5	25.3	25.1	26.7	25.3	28.3
	Range	16.6-25.1	19.7-30.1	22.1-29.5	23.4-29.0	21.9-30.4	25.8-33.4
4 mph	Mean	17.0	18.7	17.9	18.2	18.8	18.6
	Range	16.1-18.4	16.0-27.1	16.0-22.9	16.0-25.6	16.0-28.6	16.0-27.7
2 mph	Mean	19.5	22.0	19.2	21.0	23.8	20.2
	Range	16.3-25.2	16.5-27.2	16.5-23.0	16.6-25.6	16.7-32.5	16.6-27.8
Standing	Mean	21.6	22.5	21.6	24.1	25.3	21.7
	Range	16.3-28.4	16.5-28.6	16.5-24.9	16.8-29.2	19.4-33.5	16.6-29.3

†Averages of 5 runs.

(continued)

518  
A

190

TABLE F.2 continued

Activity		Water Inlet Temperature, deg C					
		Region					
		Head	Arms	Upper Torso	Lower Torso	Thighs	Lower Legs
SCHEDULE IV†							
Standing	Mean	22.9	27.6	26.7	25.0	23.8	25.6
	Range	17.3-28.2	21.2-36.6	25.1-28.4	19.1-29.4	19.7-31.7	19.3-30.8
2 mph	Mean	23.3	25.1	26.0	24.8	22.4	24.2
	Range	17.1-32.1	19.0-31.3	22.6-28.3	20.1-27.7	20.7-25.0	20.4-30.5
3 mph	Mean	22.3	23.6	24.8	21.5	19.5	22.6
	Range	17.4-25.1	18.6-29.0	20.6-28.1	17.2-25.0	17.3-23.2	17.6-30.5
4 mph	Mean	16.9	19.7	19.6	18.5	18.1	18.2
	Range	16.2-17.3	16.6-30.3	17.0-29.0	16.5-25.8	16.6-23.4	16.6-23.9
2 mph	Mean	18.9	22.2	21.9	20.9	19.8	19.5
	Range	17.1-23.2	16.8-29.6	17.3-28.5	16.8-25.4	17.0-23.2	16.8-23.6
Standing	Mean	23.7	26.5	25.4	24.9	22.5	22.3
	Range	17.2-32.5	22.0-29.5	22.2-28.9	20.5-29.1	20.9-24.7	19.9-24.6

†Averages of 5 runs.

(continued)

TABLE F.2 continued

Activity		Water Inlet Temperature, deg C					
		Region					
		Head	Arms	Upper Torso	Lower Torso	Thighs	Lower Legs
SCHEDULE V†							
Standing	Mean	22.1	24.9	25.3	28.0	25.7	26.9
	Range	19.0-25.4	19.7-32.6	20.5-29.9	24.7-31.4	21.8-27.8	25.0-29.0
4 mph	Mean	17.0††	20.2	18.3	19.7	16.9	16.8
	Range	16.8-17.4	16.6-30.1	17.1-21.1	16.5-21.1	16.7-17.2	16.5-17.1
Standing	Mean	19.8	23.1	27.2	26.1	24.0	20.6
	Range	17.8-21.7	17.1-25.6	17.6-38.6	17.4-34.5	21.0-25.4	17.6-25.2
4 mph	Mean	19.6	23.0	27.0	23.2	21.9	18.6
	Range	17.2-21.5	16.8-25.5	17.3-38.0	16.8-34.4	16.9-25.4	16.8-22.5
Standing	Mean	19.7	22.9	25.9	23.3	21.9	18.5
	Range	17.0-21.8	16.7-25.4	17.2-33.6	16.7-35.0	16.8-25.4	16.6-22.0
4 mph	Mean	19.4	21.9	23.2	21.7	20.6	18.4
	Range	17.1-21.4	16.8-26.0	17.3-27.8	16.8-29.1	16.9-24.4	16.7-21.9

†Averages of 4 runs.

††Averages of 3 runs.

(continued)

TABLE F.2 continued

Activity		Water Inlet Temperature, deg C					
		Region					
		Head	Arms	Upper Torso	Lower Torso	Thighs	Lower Legs
SCHEDULE V cont.†							
Standing	Mean	19.2	21.7	22.8	21.4	20.3	17.9
	Range	16.8-21.3	16.6-25.6	17.1-26.9	16.5-28.5	16.7-24.2	16.5-21.4
4 mph	Mean	19.3	21.7	22.8	21.4	20.4	18.2
	Range	16.9-21.4	16.7-25.6	17.2-27.0	16.7-28.3	16.8-24.4	16.6-21.4
Standing	Mean	19.3	21.8	23.0	21.4	20.4	18.3
	Range	17.1-21.1	16.9-26.1	17.4-27.7	16.9-28.0	17.0-24.0	16.8-21.5
4 mph	Mean	18.1	21.8	20.3	19.8††	20.0	18.6
	Range	17.3-19.8	17.0-28.1	17.4-22.6	17.0-25.3	17.0-22.1	16.9-23.0
Standing	Mean	18.7	21.5	21.1	19.3††	20.3	18.4
	Range	17.2-20.1	16.9-26.3	17.5-22.8	17.0-24.1	17.0-22.7	16.9-22.3

†Averages of 4 runs.

††Averages of 3 runs.

CSA

## LIST OF REFERENCES

1. Chambers, A. B., "Controlling Thermal Comfort in the EVA Space Suit," ASHRAE Journal, Vol. 12, 1970, pp. 33-38.
2. Billingham, J., "Heat Exchange Between Man and His Environment on the Surface of the Moon," Journal of the British Interplanetary Society, Vol. 17, 1959, pp. 297-300.
3. Best, C. H. and Taylor, N. B., The Living Body, Holt, Reinhardt and Winston, Fourth Edition, 1958, pp. 11-12, 377.
4. Lavoisier, A. L., "Experiences sur la Respiration des Animaux," Memoire de l'Academie des Sciences, 1777.
5. Burton, A. C., "The Application of the Theory of Heat Flow to The Study of Energy Metabolism," Journal of Nutrition, Vol. 7, 1934, pp. 497-533.
6. Eichna, L. W., Ashe, W. F., Bean, W. B., and Shelley, W. B., "The Upper Limits of Environmental Heat and Humidity Tolerated by Acclimatized Men Working in Hot Environments," Journal of Industrial Hygiene and Toxicology, Vol. 27, 1945, pp. 59-84.
7. Machle, W., and Hatch, T. F., "Heat: Men's Exchanges and Physiological Response," Physiological Review, Vol. 27, 1947, pp. 200-227.
8. Pennes, H. H., "Analysis of Tissue and Arterial Blood Temperature in the Resting Human Forearm," Journal of Applied Physiology, Vol. 1, 1948, pp. 93-122.
9. Wyndham, W., Bouwer, N., Devine, M. G., Patterson, H. E., and Macdonald, D. K. C., "Examination of Use of Heat Exchange Equations for Determining Changes in Body Temperature," Journal of Applied Physiology, Vol. 5, 1952, pp. 299-307.
10. Hertzman, A. B., "Some Relations between Skin Temperature and Blood Flow," American Journal of Physical Medicine, Vol. 32, 1953, pp. 233-251.
11. Taylor, C. L., "Heat Transfer Applications in the Human Body," Mechanical Engineering, Vol. 77, 1955, pp. 511-513.
12. Herrington, L. P., "The Biotechnical Problem of the Human Body as a Heat Exchanger," Transactions ASME, Vol. 80, 1958, pp. 343-346.
13. Herrington, L. P., "Full Scale Human-Body-Model Thermal Exchange Compared with Equational Condensation of Human Calorimetric Data," Journal of Heat Transfer, Vol. 81, Ser. C, 1959, pp. 187-194.

14. Westland, R. A., "A Biothermal Analog," U.C.L.A. Master's Thesis, 1958.
15. Osman, D. B., "An Electrical Analog of the Biothermal System," U.C.L.A. Master's Thesis, 1962.
16. Wyndham, C. H., and Atkins, A. R., "An Approach to the Solution of the Human Biothermal Problem with the Aid of an Analog Computer," Proceedings of the Third International Conference on Medical Electronics, London, England, 1960, pp. 32-38.
17. Crosbie, R. J., Hardy, J. D., and Fessenden, E., "Electrical Analog Simulation of Temperature Regulation in Man," in Temperature, Its Measurement and Control in Science and Industry, J. D. Hardy, editor, Vol. 3, Part 3, Reinhold, New York, 1963, pp. 627-635.
18. Wissler, E. H., "Steady State Temperature Distribution in Man," Journal of Applied Physiology, Vol. 16, 1961, pp. 734-740.
19. Wissler, E. H., "An Analysis of Factors Affecting Temperature Levels in the Nude Human," in Temperature, Its Measurement and Control in Science and Industry, J. D. Hardy, editor, Vol. 3, Part 3, Reinhold, New York, 1963, pp. 603-612.
20. Wissler, E. H., "A Mathematical Model of the Human Thermal System," Bulletin of Mathematical Biophysics, Vol. 26, 1964, pp. 147-166.
21. Wissler, E. H., "Comparison of Computer Results from Two Mathematical Models--A Simple 14-Node Model and a Complex 250 Node Model," Symposium International de Thermoregulation Comportementale, Lyon, France, 7-11, September 1970.
22. Perl, W., "Heat and Matter Distribution in Body Tissues and the Determination of Tissue Blood Flow by Local Clearance Methods," Journal of Theoretical Biology, Vol. 2, 1962, pp. 201-235.
23. Perl, W., "An Extension of the Diffusion Equation to Include Clearance by Capillary Blood Flow," Annals of the New York Academy of Science, Vol. 108, 1963, pp. 92-105.
24. Perl, W., and Cucinell, S. A., "Local Blood Flow in Human Leg Muscle Measured by a Transient Response Thermoelectric Method," Biophysical Journal, Vol. 5, 1965, pp. 211-230.
25. Perl, W., and Hirsch, R. L., "Local Blood Flow in Kidney Tissue by Heat Clearance Measurement," Journal of Theoretical Biology, Vol. 10, 1966, pp. 251-280.
26. Brown, A. C., "Analog Computer Simulation of Temperature Regulation in Man," Technical Documentary Report AMRL-TDR-63-116, Aerospace Medical Research Laboratories, Wright-Patterson AFB, Ohio, 1963.

27. Brown, A. C., "Further Development of the Biothermal Analog Computer," Final Report AMRL-TR-66-197, Medical Research Laboratories, Wright-Patterson AFB, Ohio, 1966.
28. Layne, R. S., and Barker, R. S., "Digital Computer Simulation of the Biothermal Man," Paper No. 3369, Douglas Missile and Spacecraft Division, 1965.
29. Stolwijk, A. J. A., and Cunningham, D. J., "A Study of Heat Exchange between Man and His Environment in Project Apollo," Contract No. NAS-9-4522, Final Report, John B. Pierce Foundation.
30. Birkebak, R. C., Cremers, C. J., and Lafebre, E. A., "Heat Transfer Applied to Animal Systems," Transactions ASME, Ser. C., Vol. 88, 1966, pp. 125-130.
31. Stolwijk, A. J. A., and Hardy, J. D., "Temperature Regulation in Man--A Theoretical Study," Pflügers Archiv. f.d. gesamte Physiologie des Menschen und der Tiere, Vol. 291, 1965, pp. 129-162.
32. Guy, A. W., and Lehman, J. F., "Determination of Electromagnetic Heating Patterns in Human Tissue by Thermographic Studies on Phantom Models," Digest of the Seventh International Conference on Medical and Biological Engineering, Stockholm, Sweden, 1967.
33. Chan, A. K., Sigelmann, R. A., Guy, A. W., and Lehman, J. F., "Thermal Effect Due to Propagation of Acoustic Waves in Biological Materials," Proceedings of the Twenty-First Annual Conference on Engineering in Medicine and Biology, Houston, Texas, 1968, p. 19.3.
34. Ho, H. S., Guy, A. W., Sigelmann, R. A., and Lehman, J. F., "Electromagnetic Heating Patterns in Circular Cylindrical Models of Human Tissue," Proceedings of the Twenty-Second Annual Conference on Engineering in Medicine and Biology, 1969, Chicago, Illinois. P. 27.4.
35. Chan, A. K., Sigelmann, R. A., Guy, R. W., and Lehman, J. F., "Calculation of Temperature Distribution in Layered Tissue due to Distributed Thermal Sources by Finite Difference Method," Proceedings of the Twenty-Second Annual Conference on Engineering in Medicine and Biology, Chicago, Illinois, 1969, p. 27-3.
36. Richardson, P. D., and Whitelaw, J. H., "Transient Heat Transfer in Human Skin," Journal of The Franklin Institute, Vol. 286, 1968, pp. 169-181.
37. Gros, C., and Gautherie, "Etudi par Thermometrie Infrarouge de l'Evolution au Cours du Temps des Temperatures Cutnee's Humaines en Fonction de la Temperature Ambiante. Notion de'Adaptance Thermique Cutanee," Revue Francaise Etudes Cliniques et Biologiques, Vol.13, 1968, pp. 697-703.

38. Mitchell, J. W., and Myers, G. E., "Analytical Model of the Countercurrent Heat Exchange Phenomena," Biophysical Journal, Vol. 8, 1968, pp. 897-911.
39. Buchberg, H., and Harrah, C. B., "Conduction Cooling of the Human Body--A Biothermal Analysis," Thermal Problems in Biotechnology, ASME Symposium Series, New York, 1968, pp. 82-95.
40. Chato, J. C., "A Method for the Measurement of Thermal Properties of Biological Materials," Thermal Properties in Biotechnology, ASME Symposium Series, 1968, pp. 16-25.
41. Trezek, G. J., and Jewett, D. L., "Thermal Modeling of Cylindrical Source Transient Temperature Field in Brain," Proceedings of the Twenty-First Annual Conference on Engineering in Medicine and Biology, Houston, Texas, 1967, p. 53.4.
42. Trezek, G. J., and Cooper, T. E., "Analytical Determination of Cylindrical Source Temperature Fields and Their Relation to Thermal Diffusivity of Brain Tissue," Thermal Problems in Biotechnology, ASME Symposium Series, 1968, pp. 1-15.
43. Trezek, G. J., "Thermal and Electrical Modeling for Brain Surgical Probes," ASME Paper No. 69-WA/HT-40, 1969.
44. Cooper, T. E., "Bio-Heat Transfer Studies," University of California at Berkeley, Ph.D. Thesis, 1970.
45. Priebe, L., and Betz, E., "Wärmetransport in Homogen und Isotrop Durchbluteten Gewebe," Arzliche Forschung, Vol. 10, 1969, pp. 18-30.
46. Keller, K. H., and Seiler, L., Jr., "An Analysis of Peripheral Heat Transfer in Humans," Simulation Council Meeting, Chicago, Illinois, March 9-10, 1970.
47. Nunneley, S. A., "Water Cooled Garments: A Review," to appear in Space Life Sciences.
48. Webb, P., editor, Bioastronautics Data Book, NASA Scientific and Technical Information Division, Washington, D.C., 1964.
49. Chato, J. C., "A Survey of Thermal Conductivity and Diffusivity Data on Biological Materials," ASME Paper No. 66-WA/HT-37, 1966.
50. Chato, J. C., "Heat Transfer in Bioengineering," in Advanced Heat Transfer, B. T. Chao, editor, University of Illinois Press, 1969, pp. 359-403.
51. Pond, J. B., "A Study of the Biological Action of Focused Mechanical Waves (Focused Ultrasound)," University of London, Ph.D. Thesis, 1968.

52. Cooper, T. E., and Trezek, G. J., "Thermal Properties of Human Organs via the Needle Probe Technique," Proceedings of the Twenty-Third Annual Conference on Engineering in Medicine and Biology, Washington, D.C., 1970, p.155.
53. Chato, J. C., Shitzer, A., and Fry, F. J., "Measurement of Thermal Properties of Living Tissue," Proceedings of the Twenty-Third Annual Conference on Engineering in Medicine and Biology, Washington, D.C., 1970, p. 156.
54. Ganong, W. F., Review of Medical Physiology, Third Edition, Lange Medical Publications, Los Altos, California, 1967, p. 450.
55. Bazett, H. C., "The Regulation of Body Temperatures," in Physiology of Heat Regulation and the Science of Clothing, L. H. Newburgh, editor, Hafner Publishing Co., New York, 1968, pp. 109-192.
56. Grollman, S., The Human Body--Its Structure and Physiology, Second Edition, The Macmillan Co., London, England, 1969, p. 166.
57. Nielsen, M., "Die Regulation der Körpertemperature bei Muskelarbeit," Skand. Arch. Physiol., Vol. 79, 1938, pp. 193-230.
58. Shitzer, A., and Chato, J. C., "Analytical Modeling of the Thermal Behavior of Living Human Tissue," Proceedings of the Fourth International Heat Transfer Conference, Versailles, France, 1970, pp. Cu-3.9.
59. Brad, P., Medical Physiology, The C. V. Mosby Co., St. Louis, Mo., 1956, p. 221.
60. Sokolnikoff, I. S., and Redheffer, R. M., Mathematics of Physics and Modern Engineering, McGraw-Hill Book Co., Second Edition, New York, 1966, p. 251.
61. Abramowitz, M., and Stegun, I. A., editors, Handbook of Mathematical Functions, Dover Publications, New York, 1965.
62. Chato, J. C., Hertig, B. A., Gammon, N. A., Streckert, J. H., and Lechner, P., "Physiological and Engineering Study of Advanced Thermoregulatory Systems for Extravehicular Space Suits," Semi-Annual Status Report No. 2, NASA Contract No. NGR 14-005-103, June, 1968.
63. Carslaw, H. S., and Jaeger, J. C., Conduction of Heat in Solids, Second Edition, Oxford University Press, London, England, 1959, pp. 30-32.
64. McLachlan, N. W., Bessel Functions for Engineers, Second Edition, Oxford University Press, London, England, 1941.

65. Chato, J. C., and Shitzer, A., "On The Dimensionless Parameters Associated with Heat Transport within Living Tissue," Aerospace Medicine, Vol. 41, 1970, pp. 390-393.
66. Johnson, R. E. Robbins, F., Schilke, R., Mole, P., Harris, J., and Wakat, D., "A Versatile System for Measuring Oxygen Consumption in Man," Journal of Applied Physiology, Vol. 22, 1967, pp. 377-379.
67. Molnar, S., "The Relationship between Cardiac Time Components, Maximal Oxygen Consumption and Endurance Performance," University of Illinois at Urbana-Champaign, Ph.D. Thesis, 1970.
68. Consolazio, F. C., Johnson, R. E., and Pecora, L. J., Physiological Measurements of Metabolic Functions in Man, McGraw-Hill Book Co., New York, 1963.
69. Dubois, D., and Dubois, E. F., "A Formula to Estimate the Approximate Surface Area if Height and Weight be Known," Archiv. International of Medicine, Vol. 17, 1916, pp. 863-871.
70. Carpenter, T. M., Tables, Factors and Formulas for Computing Respiratory Exchange and Biological Transformation of Energy, Third Edition, Carnegie Institute of Washington, Washington, D.C., 1939.
71. Webb, P., and Annis, J. F., "Bio-Thermal Responses to Varied Work Programs in Men Kept Thermally Neutral by Water Cooled Clothing," NASA Report No. CR-739, 1967.
72. Nunneley, S. A., "Head Cooling in Work and Heat Stress," Ohio State University, Master's Thesis, 1970.
73. Shvartz, E., "Effect of Cooling Hood on Physiological Responses to Work in a Hot Environment," Journal of Applied Physiology, Vol. 29, 1970, pp. 36-39.
74. Hatch, T., "Assessment of Heat Stress," in Temperature, Its Measurement and Control in Science and Industry, J. D. Hardy, editor, Vol. 3, Part 3, Reinhold, New York, 1963, pp. 307-318.
75. Craig, F. N., Medical Division Research Report No. 5, Chemical Corps Army Chemical Center, 1950.
76. Hall, J. F., and Polte, J. W., "Physiological Index of Strain and Body Heat Storage in Hyperthermia," Journal of Applied Physiology, Vol. 15, 1960, pp. 1027-1030.
77. Gold, A. J., and Zornitzer, A., "Effect of Partial Body Cooling on Man Exercising in a Hot, Dry, Environment," Aerospace Medicine, Vol. 39, 1968, pp. 944-946.

78. Hardy, J. D., "The 'Set-Point' Concept in Physiological Temperature Regulation," in Physiological Controls and Regulations, W. S. Yamamoto and J. R. Brobeck, editors, Saunders, Philadelphia, 1965, pp. 98-116.
79. Nagayama, T. H., Eisenman, J. S., and Hardy, J. D., "Single Unit Activity of Anterior Hypothalamus during Local Heating," Science, Vol. 134, 1961, pp. 560-561.
80. Hardy, J. D., Hellon, R. F., and Sutherland, K., "Temperature Sensitive Neurons in the Dog's Hypothalamus," Journal of Physiology, Vol. 175, 1964, pp. 242-253.
81. Robinson, S., Meyer, F. R., Newton, J. L., Ts'ao, C. H., and Holgersen, L. O., "Relations Between Sweating, Cutaneous Blood Flow and Body Temperature in Work," Journal of Applied Physiology, Vol. 20, 1965, pp. 575-582.
82. Thauer, R., "Der Nervose Mechanismus der Chemischen Temperaturregulation des Warmbluters," Naturwissenschaften, Vol. 51, 1964, pp. 73-80.
83. Bligh, J., "Localization of the Thermal Stimulus to Polypnoea," Journal of Physiology, Vol. 135, 1957, pp. 48p-49p.
84. Stoll, A. M., and Chianta, M. A., "Application of Biophysical Heat Transfer Studies in Protection Systems," Aerospace Research Department, NADC-MR-6722, 1967.
85. Chato, J. C., and Shitzer, A., "Thermal Modeling of the Human Body-- Further Solutions of the Steady-State Heat Equation," to appear in AIAA Journal.

STEADY STATE AND TRANSIENT TEMPERATURE  
DISTRIBUTIONS IN THE HUMAN THIGH  
COVERED WITH A COOLING PAD

R. J. Leo  
A. Shitzer  
J. C. Chato  
B. A. Hertig

Technical Report No. ME-TR-286

June 1971

DEPARTMENT OF MECHANICAL AND INDUSTRIAL ENGINEERING  
LABORATORY FOR ERGONOMICS RESEARCH  
ENGINEERING EXPERIMENT STATION  
UNIVERSITY OF ILLINOIS AT URBANA - CHAMPAIGN  
URBANA, ILLINOIS 61801



# **STEADY STATE AND TRANSIENT TEMPERATURE DISTRIBUTIONS IN THE HUMAN THIGH COVERED WITH A COOLING PAD**

by

R. J. LEO  
A. SHITZER  
J. C. CHATO  
B. A. HERTIG

Technical Report No. ME-TR-286

June 1971

Supported by  
National Aeronautics and Space Administration  
under

Grant No. NGR-14-005-103

*I*  
340<

i

STEADY STATE AND TRANSIENT TEMPERATURE  
DISTRIBUTIONS IN THE HUMAN THIGH COVERED  
WITH A COOLING PAD

by

R. J. Leo  
A. Shitzer  
J. C. Chato  
B. A. Hertig

Technical Report No. ME-TR-286

June 1971

Supported by

National Aeronautics and Space Administration

under

Grant No. NGR 14-005-103

## ABSTRACT

An analytical and experimental study was done on the performance of cooling pads attached to a human thigh. Each cooling pad consisted of a long, water cooled tube formed into a serpentine shape with uniform spacing between the parallel sections.

The analytical work developed a cylindrical model for the human thigh. The transient times predicted by this model ranged from 25 to 80 minutes, which is reasonably close to the experimental results. Calculated and measured steady state temperature profiles were in fair agreement.

Three cooling pads with different cooling tube sizes and spacings were constructed and tested. These pads were equipped with thermocouples to measure the temperature profiles between adjacent tubes on the skin surface of a thigh of a male subject while he was performing various activity schedules. The pad with the highest tube density removed the greatest amounts of heat with the least temperature variations on the skin. Also, the transient times for this pad were the shortest.

The transient times associated with a change from a high metabolic rate of 1800 Btu/hr (528 w) to a low level of 300 Btu/hr (88 w), were found to be about 120 minutes. A change from 900 Btu/hr (264 w) to 300 Btu/hr (88 w) resulted in 90 to 100 minute transients. However, the transient times for a change in metabolic rate in the opposite direction from 300 Btu/hr (88 w) to 1800 Btu/hr (528 w) were 40 to 60 minutes. When an intermediate step of 900 Btu/hr (264 w) was introduced between the last two metabolic rates, the transient times associated with the individual steps varied from 40 to 80 minutes. However, the overall transient times for each double step were approximately the same in either direction.

## NOMENCLATURE†

a	half distance between cooling tubes, [L]
A	total skin surface area, [L <sup>2</sup> ]
b	depth of tissue layer, [L]
c <sub>b</sub>	specific heat of blood, [L <sup>2</sup> θ <sup>-2</sup> T <sup>-1</sup> ] or [QM <sup>-1</sup> T <sup>-1</sup> ]
c <sub>p</sub>	specific heat of tissue, [L <sup>2</sup> θ <sup>-2</sup> T <sup>-1</sup> ] or [QM <sup>-1</sup> T <sup>-1</sup> ]
f	heat flux, [Mθ <sup>-3</sup> ] or [QL <sup>-2</sup> θ <sup>-1</sup> ]
F, F <sub>o</sub>	uniform heat flux, [Mθ <sup>-3</sup> ] or [QL <sup>-2</sup> θ <sup>-1</sup> ]
h	height, [L]
I <sub>i</sub>	modified Bessel function of the first kind of order i
J <sub>i</sub>	Bessel function of the first kind of order i
k	thermal conductivity, [MLθ <sup>-3</sup> T <sup>-1</sup> ] or [QL <sup>-1</sup> θ <sup>-1</sup> T <sup>-1</sup> ]
K <sub>i</sub>	modified Bessel function of the second kind of order i
q <sub>b</sub>	rate of heat transported by blood, defined by Eq. (2.1), [ML <sup>-1</sup> θ <sup>-3</sup> ] or [QL <sup>-3</sup> θ <sup>-1</sup> ]
Q <sub>i</sub>	defined by Eq. (2.13), [L <sup>-2</sup> T]
q <sub>m</sub> , $\dot{Q}_i$	internal heat generation rate per unit volume, [ML <sup>-1</sup> θ <sup>-3</sup> ] or [QL <sup>-3</sup> θ <sup>-1</sup> ]
Q <sub>m</sub>	total metabolic rate, [ML <sup>2</sup> θ <sup>-3</sup> ] or [Qθ <sup>-1</sup> ]
r	radial coordinate, [L]
R <sub>1</sub>	radius of inner core in cylindrical model, [L]
R <sub>12</sub>	radius of interface between skeletal muscle and skin layer in cylindrical model, [L]
R <sub>2</sub>	radius of the skin surface in cylindrical model, [L]

---

†Units in brackets are: M, mass; L, length; θ, time; T, temperature; Q, heat [ML<sup>2</sup>θ<sup>-2</sup>].

$t$	time, $[\theta]$
$t^*$	characteristic time, $[\theta]$
$T$	tissue temperature, $[T]$
$T_a$	arterial blood temperature, $[T]$
$T_1$	constant temperature at inner core, $[T]$
$V$	volume, $[L^3]$
$w_b$	blood perfusion rate per unit volume, $[ML^{-3}\theta^{-1}]$
$w_i$	defined by Eq. (2.12), $[L^{-1}]$
$W$	weight, $[ML\theta^{-2}]$
$Y_i$	Bessel function of the second kind of order $i$
$z$	coordinate, parallel to the axis of the cylinder, $[L]$
$\alpha$	thermal diffusivity, $[L^2\theta^{-1}]$
$\alpha_{n,i}$	defined by Eq. (2.17), $[L^{-1}T]$
$\beta$	ratio of width of cooling tube to cooling tube spacing
$\epsilon_i$	defined by Eq. (2.22), $[L^{-1}]$
$\zeta_i$	defined by Eq. (2.15), $[L^{-1}]$
$\eta$	ratio of heat fluxes of the uncontacted to the contacted skin
$\theta$	defined by Eq. (2.11), $[T]$
$\lambda_n$	defined by Eq. (2.16), $[L^{-1}]$
$\xi$	dummy variable of integration, $[L]$
$\mu_n$	defined by Eq. (2.21), $[L^{-1}]$
$\rho$	specific density of tissue, $[ML^{-3}]$
$\sigma_n$	defined by Eq. (2.20)
$\phi$	angular coordinate
$\chi_n$	defined by Eq. (2.19)
$\psi_{k\ell}^j(\zeta_i, r)$	combination of modified Bessel functions, defined by Eq. (2.10)

## Subscripts

- 1            pertaining to skin layer or initial state
- 2            pertaining to skeletal muscle or final state
- b            blood
- $i, j, k, l, n$  integer
- m            metabolic

## LIST OF FIGURES

- Figure 2.1 Representative section of the cylindrical model with the cooling tubes on the skin running perpendicular to the axis of the cylinder.
- Figure 2.2 Geometry and boundary conditions for the cylindrical model with the cooling tubes on the skin running perpendicular to the axis of the cylinder. Skin layer and skeletal muscle are considered as a combined region.
- Figure 2.3 Temperature distributions in the tissue for the one-dimensional, cylindrical model. Step change is from low (290 Btu/hr, 85 w) to high (2600 Btu/hr, 760 w) activity level. Constant temperature of 99.7°F (37.7°C) at the inner core,  $R_1 = 0.15$  ft (4.6 cm), A and b are constant.
- Figure 2.4 Temperature distributions in the tissue for the one-dimensional, cylindrical model. Step change is from high (2600 Btu/hr, 760 w) to low (290 Btu/hr, 85 w) activity level. Constant temperature of 99.7°F (37.7°C) at the inner core,  $R_1 = 0.15$  ft (4.6 cm), A and b are constant.
- Figure 2.5 Temperature distributions on the skin surface for the two-dimensional, cylindrical model. Step change is from low (290 Btu/hr, 85 w) to high (2600 Btu/hr, 760 w) activity level.  $\beta = 0.1$ , constant temperature of 99.7°F, (37.7°C) at the inner core,  $R_1 = 0.15$  ft (4.6 cm), A and b are constant.
- Figure 3.1(a) Schematic diagram of cooling pad and water supply system with temperature measuring points indicated.
- Figure 3.1(b) Cross section A-A showing details of thermocouple placement.
- Figure 3.2 View of one of the individual pads.
- Figure 3.3 A view of the Tele-Thermometer and system for collecting samples for determining metabolic rates.
- Figure 3.4 Work program for each experiment.
- Figure 3.5 General view of the set-up used for the experiments with the individual cooling pads. A test subject is shown pedalling the bicycle ergometer.
- Figure 4.1 Results of experiments 1, 2, and 3 using cooling pad No. 2 with constant experimental conditions and varying work load.

- Figure 4.2 Results of experiments 4, 5, and 6 with constant experimental conditions and constant metabolic rate 900 Btu/hr (264 w).
- Figure 4.3 Steady state temperature distribution for pads 2 and 3 under constant experimental conditions and constant metabolic rate at 300 Btu/hr (88 w).
- Figure 4.4 Steady state temperature distribution for pads 1, 2, and 3 under constant experimental conditions and constant metabolic rate at 900 Btu/hr (264 w).
- Figure 4.5 Steady state temperature distribution for pads 2 and 3 under constant experimental conditions and constant metabolic rate at 1800 Btu/hr (528 w).
- Figure 4.6 Comparison of analysis with experimental results for cooling pad No. 2. Metabolic rate 1800 Btu/hr (528 w).
- Figure 4.7 Comparison of analysis with experimental results for cooling pad No. 3. Metabolic rate 1800 Btu/hr (528 w).
- Figure 4.8 Results of experiments 7 and 8.
- Figure 4.9 Development of temperature profile on the skin for pad No. 2 resulting from an increase in metabolic rate from 300 to 1800 Btu/hr (88 to 528 w).
- Figure 4.10 Development of temperature profile on the skin for pad No. 2 resulting from a decrease in metabolic rate from 1800 to 300 Btu/hr (528 to 88 w).
- Figure 4.11 Development of temperature profile on the skin for pad No. 3 resulting from an increase in metabolic rate from 300 to 1800 Btu/hr (88 to 528 w).
- Figure 4.12 Development of temperature profile on the skin for pad No. 3 resulting from a decrease in metabolic rate from 1800 to 300 Btu/hr (528 to 88 w).
- Figure 4.13 Results of experiments 9 and 10.
- Figure 4.14 Development of temperature profile on the skin for pad No. 2 resulting from increases in metabolic rates from 300 to 900 Btu/hr (88 to 264 w) and from 900 to 1800 Btu/hr (264 to 528 w).
- Figure 4.15 Development of temperature profile on the skin for pad No. 2 resulting from decreases in metabolic rates from 1800 to 900 Btu/hr (528 to 264 w) and from 900 to 300 Btu/hr (264 to 88 w).

Figure 4.16 Development of temperature profile on the skin for pad No. 3 resulting from increases in metabolic rates from 300 to 900 Btu/hr (88 to 264 w) and from 900 to 1800 Btu/hr (264 to 528 w).

Figure 4.17 Development of temperature profile on the skin for pad No. 3 resulting from decreases in metabolic rates from 1800 to 900 Btu/hr (528 to 264 w) and from 900 to 300 Btu/hr (264 to 88 w).

## TABLE OF CONTENTS

	Page
NOMENCLATURE . . . . .	v
1. INTRODUCTION . . . . .	1
1.1 BACKGROUND . . . . .	1
1.2 REVIEW OF RELATED STUDIES . . . . .	2
1.3 SPECIFIC STATEMENT OF THE PROBLEM . . . . .	5
1.4 SCOPE OF THE STUDY AND LIMITATIONS . . . . .	6
2. THEORETICAL ANALYSIS . . . . .	8
2.1 THE BIOTHERMAL MODEL WITH DEVELOPMENT OF THE GOVERNING PARTIAL DIFFERENTIAL EQUATION . . . . .	8
2.2 GEOMETRY, BOUNDARY AND INITIAL CONDITIONS . . . . .	9
3. EXPERIMENTS . . . . .	22
3.1 OBJECTIVES . . . . .	22
3.2 EXPERIMENTAL APPARATUS . . . . .	22
3.3 EXPERIMENTAL PROCEDURE AND TEST SCHEDULES . . . . .	29
3.4 THE TEST SUBJECT . . . . .	31
3.5 RECORDED AND CALCULATED QUANTITIES . . . . .	33
4. RESULTS AND DISCUSSION . . . . .	35
4.1 GENERAL RESULTS . . . . .	35
4.2 TEMPERATURE DISTRIBUTIONS FOR SITTING, STANDING AND MILD WORK . . . . .	38
4.3 COMPARISON OF THE SURFACE TEMPERATURE TRANSIENTS FOR THE THREE PADS . . . . .	42
4.4 COMPARISON OF THE STEADY STATE SURFACE TEMPERATURE DISTRIBUTIONS FOR THE THREE PADS . . . . .	45
4.5 COMPARISON OF THE EXPERIMENTAL STEADY STATE TEMPERATURE DISTRIBUTION WITH ANALYTICAL RESULTS . . . . .	49
4.6 RESULTS OF TRANSIENT EXPERIMENTS . . . . .	54
5. SUMMARY AND CONCLUSIONS . . . . .	70
REFERENCES . . . . .	72

## 1. INTRODUCTION

### 1.1 BACKGROUND

There are many instances in which it may be desirable to regulate the micro-climate of an individual who is exposed to a thermally hostile environment. One may consider, as examples, the necessity to protect the fire fighter from high temperatures or the need to protect the deep sea diver from low temperatures. Both require some sort of thermal assistance to be able to perform efficiently in their respective environments. In the case of space travel, the astronaut must be protected from a hostile environment for reasons other than strictly thermal ones. Here too, the thermal micro-climate of the astronaut must be controlled in response primarily to his metabolic heat generation rate, a variable which changes with his activity level.

Several attempts have been made at solving the problem of regulating the micro-climate of an individual. One method that has been developed to regulate the thermal micro-climate of the human body is to provide for removal or addition of heat by means of liquid filled cooling or heating tubes in contact with the skin surface. So-called thermal suits have been designed [1]\* which consist of individual cooling pads. These cooling pads contact the skin surface of the various major parts of the body, e.g., legs, arms and trunk. Each individual cooling pad consists of tubes held in some geometric pattern.

In general, it is not practical to provide an individual with such a cooling or heating suit if, in doing so, his ability to

---

\*Numbers in brackets refer to entries in REFERENCES.

function efficiently is seriously hindered. Therefore, for most applications, the weight and size of the suit become critical factors. One of the design objectives then would be to minimize the weight and bulk of the suit while maintaining an adequate cooling capacity. When considering the parameters of weight and size as variables governing the efficiency of a man wearing such a suit, weight seems to be most significant. With respect to weight, there will be some optimum combination of cooling tube size and spacing that will provide an adequate cooling or heating capacity.

To date little work has been done on the problem of defining an optimum relationship between cooling capacity, tube size and spacing. A potential contribution to the solution of this problem would be to develop an analytical model of human tissue in contact with a network of cooling tubes. Such a model should facilitate the prediction of heat fluxes and temperature distributions in the tissue. The validity of such a model could be verified by experimental methods.

The purpose of this work was to obtain a solution for such a model [1] and then to compare the calculated results with experimental data.

## 1.2 REVIEW OF RELATED STUDIES

For the past few decades studies have been conducted dealing with the problem of analytical modeling of the human thermal system and with the measurement of thermophysical properties of human tissue. The results of some comprehensive work done in the area of analytical modeling is presented in a report by Shitzer, Chato and Hertig [1]. In their work, the authors develop the so-called

biothermal model for various geometries.

Some experimental work has been done in an attempt to provide a thermally controllable micro-climate for an individual. The concept of a water cooled suit was first suggested in 1958 by Billingham [2] and a prototype suit was constructed at the Royal Aircraft Establishment in 1964 by Burton and Collier [3]. Their primary interest was protection of crewmembers in hot environments such as sunlit aircraft cockpits, but it was realized that practical personal cooling would have many possible applications. In general, the suit was thought of as a form-fitting heat exchanger in which water absorbed heat from the pilot's body as it passed through tubes over the skin. The heat was then dissipated by an external heat sink. By analogy with the circulation, the process is generally called convective cooling [3] although other investigators refer to it as "conductive cooling" [4,5].

A prototype water cooled garment (WCG) was built [3] of 40 PVC tubes sewn to a suit of cotton underwear. Water was piped to the ankles and wrists where manifolds distributed it to smaller tubes which ran back over the limbs to the outlet manifolds at the mid-thorax. The head and neck were not cooled. Preliminary tests indicated excellent thermal coupling between the skin and water stream [3]. The suit was comfortable even when high heat loads necessitated low water temperatures and despite the existence of wide differences in skin temperatures when comparing sites directly beneath the cooling tubes with sites lying between the tubes [6,7].

Following a demonstration of the British WCG at Houston [3], development of similar garments in the United States was undertaken

for the National Aeronautics and Space Administration (NASA), [8,9]. A series of suits was designed with the distribution of tubing proportional to body mass and with water flow from the extremities toward the torso. Experiments demonstrated the practicality of the WCG as a sole heat sink for men working at metabolic rates up to 2000 Btu/hr, which was the expected activity level rate for lunar surface activity. Cooling virtually eliminated sweating, and for any given work rate subjective comfort included a surprisingly wide envelope of water flow and temperature combinations. Other results showed that heat output rose sharply over working muscle groups, e.g., leg versus arm work [8], and that the interposition of any material between skin and tubing caused significant reduction in cooling efficiency [9].

Direct comparison of air and water cooling in pressure suits showed the latter to be far more effective in reducing signs of heat stress such as sweat rate and rectal temperature rise. Subjective comfort was also much improved by the WCG. These findings applied whether the heat stress was due to a hot environment [10, 11] or high work rates [12,13].

The Apollo water cooled garment is a system of clear plastic tubes sewn inside a suit of stretch underwear with an added nylon slip layer between tubing and skin [4,5,9]. Cooling is provided for the torso and legs but excludes the head and neck. Water flows through 40 tubes in a loop pattern which begins and ends in manifolds located at mid-torso. Flow rate is fixed at 237.6 lb/hr (1.8 liters/min) with manual operation of a diverter valve to

produce water inlet temperatures of 44.1°F (6.7°C), 59.9°F (15.5°C), or 71.6°F (22°C). The external heat sink is located in the back pack where water from a separate supply is sublimated to space. It is designed to handle continuous loads of 1600 Btu/hr (469 w) with peaks to 2000 Btu/hr (586 w). Plans for lunar extra vehicular-activity (EVA) have been tailored to this limit. Lunar surface activities on Apollo 11 and 12 averaged 800 to 1200 Btu/hr (234 to 352 w) [4]. In the case of Apollo 14, actual levels of 2500 Btu/hr (720 w) were attained, exceeding the design limit. The resulting heat storage caused noticeable signs of heat strain and much discomfort [14].

At least one group of researchers [7] has considered the problem of an optimum relationship between cooling tube size and spacing. In this study experiments were performed in which the tube spacing was considered as the only variable. The experimental work indicated that the temperature differences on the skin were of the order of 8°F (4.45°C) with 1-in. spacing of 1/8-in. O.D. cooling tubes and 3.5°F (1.94°C) with 0.5-in. spacing of the same tubes. The temperature profile on the skin was found to develop approximately three times as fast with the closer spacing.

### 1.3 SPECIFIC STATEMENT OF THE PROBLEM

Consideration of the biothermal model of human tissue in contact with a network of parallel cooling tubes [1] led to the following three basic objectives of this study:

1. To obtain the solution of the biothermal model for the steady state and transient cases in cylindrical coordinates.
2. To construct three different cooling pads and to perform experiments with them. It is hoped that the results may be

used to gain some insight into the validity of the biothermal model and its solution, and

3. To compare experimental data for the three cooling pads, each pad having a different combination of cooling tube size and spacing.

The solution of the biothermal model should predict the temperature profile on the skin surface between adjacent cooling tubes. The objective of the experimental scheme, then, was to construct a cooling pad and to measure the temperature distribution between the tubes corresponding to various activity levels. Three different cooling pad configurations were tested. The corresponding measured results were then compared to each other and related to the analytical predictions.

#### 1.4 SCOPE OF THE STUDY AND LIMITATIONS

Experimental measurement of the temperature distribution between cooling tubes were limited to data taken on the skin surface of the human thigh. Measurements were taken for three different cooling pads at four metabolic activity levels. In general, the four activity categories and associated metabolic rates were:

1. Standing, 300 Btu/hr (88 w);
2. Mild work, 600 Btu/hr (176 w);
3. Moderate work, 900 Btu/hr (264 w); and
4. Heavy work, 1800 Btu/hr (528 w).

The metabolic levels associated with mild, moderate and heavy work were attained by the subject as he rode on a variable load bicycle ergometer. During the individual experiments the transient temperature

distribution was also measured as the subject's metabolic rate changed from one level to another.

Since the experimental measurements of the temperature distribution was limited to the thigh only, the solution to the biothermal model was obtained in cylindrical coordinates. Engineering judgment, as applied to thermal systems, suggested the modeling of the leg as a cylinder of finite length. There were, however, a number of assumptions and limitations to be considered when modeling the human body. The thermophysical properties of human tissue and their detailed relationship to the formulation of the analytical model will be discussed later.

## 2. THEORETICAL ANALYSIS

### 2.1 THE BIOTHERMAL MODEL WITH DEVELOPMENT OF THE GOVERNING PARTIAL DIFFERENTIAL EQUATION

The problem of developing an analytical expression to describe the thermal behavior of living human tissue is indeed very complex. At this time, even the most basic of the mechanisms that govern heat transfer in living tissue remain unexplained, i.e., the exact nature of blood perfusion and metabolic heat generation rates have yet to be described and measured in detail. The problem is further complicated by the lack of accurate data on the thermophysical properties of living tissue. Thus, several assumptions had to be made before an analytical model could be developed.

1. The thermophysical properties of the tissue were assumed to be constant in time and space and the tissue to be homogeneous and isotropic.
2. The temperature of the blood leaving the tissue was assumed to equal the temperature of the tissue.
3. The temperature of the blood flowing into the tissue was assumed constant and equal to the temperature of the artery.
4. Blood perfusion rates and metabolic heat generation rates were assumed uniform and constant throughout the entire layer of tissue [15].

The values associated with these rates were considered as average values.

The storage, conduction and production of heat within the tissue could be represented by well known expressions in heat transfer. An additional term was needed to represent the heat

transported by the blood stream. It was assumed that the amount of heat gained by the tissue due to blood perfusion was [1]

$$q_b = w_b c_b (T_a - T) \quad (2.1)$$

Equation (2.1), when substituted into the heat equation, yields the general form which describes the biothermal model:

$$\rho c_p \frac{\partial T}{\partial t} = k \nabla^2 T + w_b c_b (T_a - T) + q_m \quad (2.2)$$

Equation (2.2) is a mathematical statement of the first law of thermodynamics describing the "in vivo" relationship between the various modes of heat transfer, storage, and production within biological tissue. It was referred to as the "bio-heat" equation [1]. Similar forms have been obtained by Pennes [16], Hertzman [17], Wissler [18], Perl [19], Chato [20], Trezek [21] and Keller and Seiler [22].

## 2.2 GEOMETRY, BOUNDARY AND INITIAL CONDITIONS

### 2.2.1 Geometry

The experimental phase of this study was concerned with the removal of metabolic heat produced in the thigh muscles as the human subject engaged in various levels of activity. The experimental cooling pads have been designed such that the cooling tubes were in direct contact with the skin surface. The cooling pad was placed around the thigh with the axis of the tubes perpendicular to the axis of the leg, as illustrated in Fig. 2.1. Consequently, the geometry of the thigh was approximated by a circular cylinder.

The living tissue that composes the thigh can be divided into

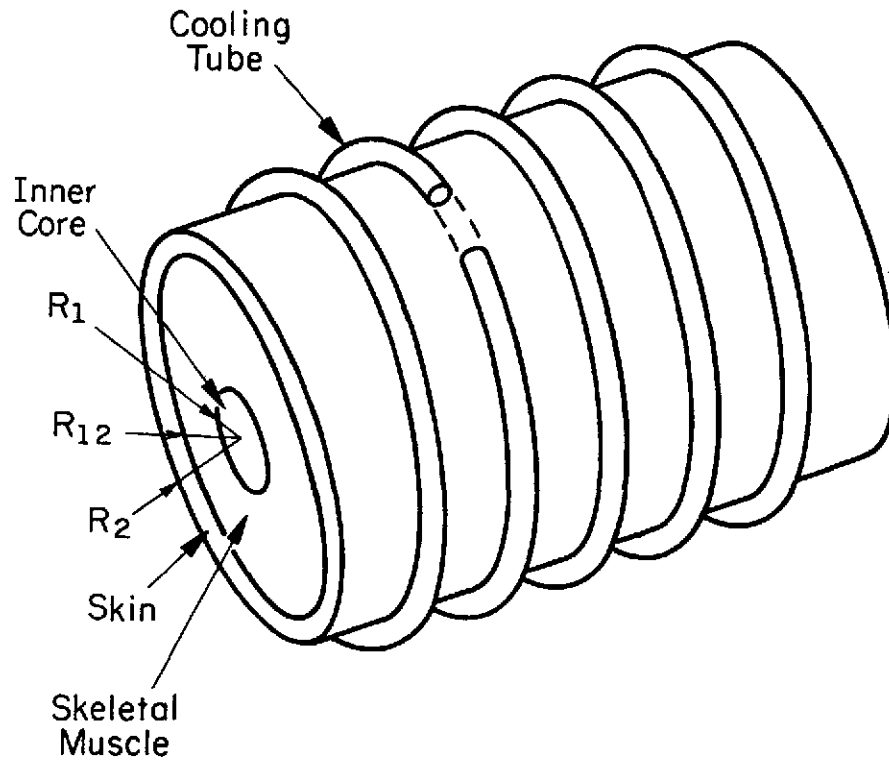


Figure 2.1 Representative section of the cylindrical model with the cooling tubes on the skin running perpendicular to the axis of the cylinder.

three layers:

1. A skin layer composed of epidermis, dermis, and subcutaneous fat. The total thickness of these layers varies from 1 to 6 mm [23]. In the model all excess metabolic heat was assumed to be removed at the contact areas between the epidermis and cooling tubes,
2. A layer of skeletal muscle, and
3. An inner core layer consisting of bone and all the internal members. At steady state this layer was assumed to be at a constant temperature.

For steady state conditions the first two layers were treated separately [1], but for the transient cases it was assumed that these layers could be approximated by a single, combined layer with averaged properties.

#### 2.2.2 Boundary and Initial Conditions

The temperature of the interface between the skeletal muscle and the inner core was assumed constant and uniform and equal to that of the inner core. At the skin surface, a heat flux corresponding to the amount of heat removed by the cooling tubes was assumed. No heat was considered to be removed from the remaining areas of the skin which were not in contact with the cooling tubes. A representation of the leg as a cylinder covered with equally spaced cooling tubes running perpendicular to the axis of the cylinder, Fig. 2.1, rendered the problem geometrically symmetrical. Consequently, the lines of symmetry running through the tubes and one-half the distance between the two adjacent tubes could be considered as adiabatic planes.

Gradients along the cooling tubes were assumed to be negligibly

small when compared to those occurring in a direction perpendicular to the tubes. In mathematical terms

$$\frac{\partial}{\partial \phi} = 0 \quad (2.3)$$

and the problem becomes two-dimensional in  $r$  and  $z$ .

The steady state temperature distribution in the tissue at a given metabolic rate was assumed to be the initial condition for the transient state. The geometry and associated boundary conditions for this problem are shown in Fig. 2.2. In the analysis presented below, the skin and skeletal muscle were considered to constitute a combined region. The problem as formulated then becomes

$$\frac{1}{\alpha} \frac{\partial \theta}{\partial t} = \frac{1}{r} \frac{\partial}{\partial r} \left( r \frac{\partial \theta}{\partial r} \right) + \frac{\partial^2 \theta}{\partial z^2} - w_2^2 \theta + Q_2 \quad (2.4)$$

such that

$$R_1 \leq r \leq R_2, \quad 0 \leq z \leq a; \quad t \geq 0$$

with the boundary and initial conditions:

at

$$r = R_1, \quad \theta = 0 \quad (2.5)$$

at

$$r = R_2, \quad \left\{ \begin{array}{l} \frac{\partial \theta}{\partial r} = \frac{f_2(z)}{k}, \quad 0 \leq z < \beta a \\ \frac{\partial \theta}{\partial r} = 0, \quad \beta a < z \leq a \end{array} \right\} \quad (2.6)$$

at

$$z = 0, \quad \frac{\partial \theta}{\partial z} = 0 \quad (2.7)$$

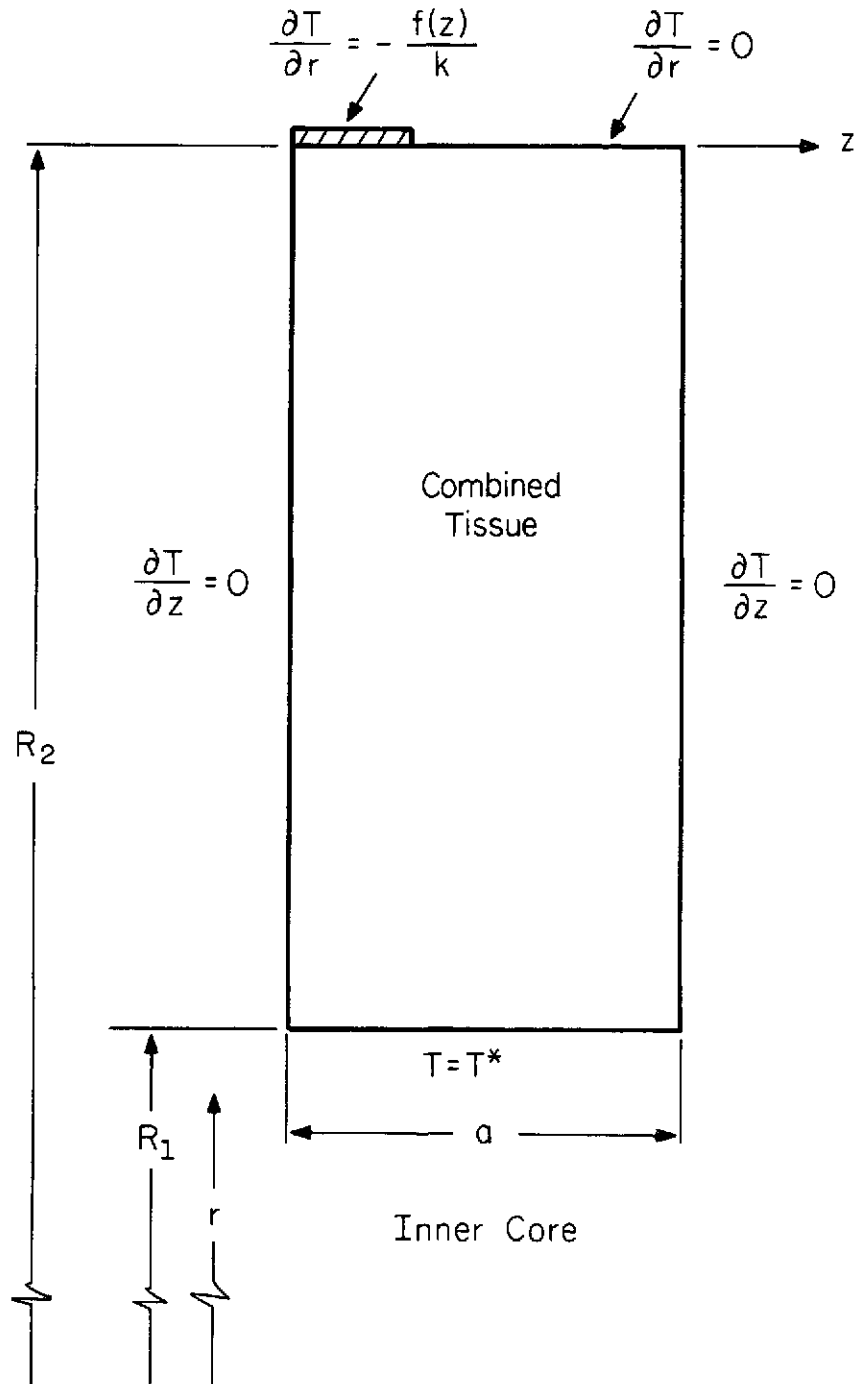


Figure 2.2 Geometry and boundary conditions for the cylindrical model with the cooling tubes on the skin running perpendicular to the axis of the cylinder. Skin layer and skeletal muscle are considered as a combined region.

at

$$z = a, \quad \frac{\partial \theta}{\partial z} = 0 \quad (2.8)$$

at

$$t < 0, \quad \theta = \frac{Q_1}{w_1} \left[ 1 - \frac{\psi_{01}^2(w_1 r)}{\psi_{01}^2(w_1 R_1)} \right] - \frac{\beta f_{a,1} \psi_{00}^1(w_1 r)}{k w_1 \psi_{01}^2(w_1 R_1)} - \sum_{n=1}^{\infty} \frac{\alpha_{n,1} \psi_{00}^1(\zeta_1 r)}{\zeta_1 \psi_{01}^2(\zeta_1 R_1)} \cos(\lambda_n z) \quad (2.9)$$

where

$$\psi_{k\ell}^j(\zeta_1 r) \equiv I_k(\zeta_1 r) K_\ell(\zeta_1 R_1) - (-1)^{k+\ell} I_\ell(\zeta_1 R_1) K_k(\zeta_1 r) \quad (2.10)$$

$I_i$  and  $K_i$  are the modified Bessel functions of the first and second kind, respectively, of order  $i$ . The other parameters appearing in Eq. (2.9) are defined by

$$\theta = T(r, z) - T_1 \quad (2.11)$$

$$w_i^2 = \frac{w_{b,i} c_b}{k} \quad (2.12)$$

$$Q_i = \frac{\dot{Q}_i + w_{b,i} c_b (T_a - T_1)}{k} \quad (2.13)$$

$$f_{a,i} = \frac{1}{\beta a} \int_0^{\beta a} f_i(\xi) d\xi \quad (2.14)$$

$$\zeta_i^2 = w_i^2 + \lambda_n^2 \quad (2.15)$$

$$\lambda_n \equiv \frac{n\pi}{a} \quad (2.16)$$

$$\alpha_{n,i} = \frac{2}{a} \int_0^{\beta a} \frac{f_i(\xi)}{k} \cos(\lambda_n \xi) d\xi \quad (2.17)$$

The special function  $\psi_{k\ell}^i(\zeta_i, r)$  was defined to simplify the mathematical derivation of Eq. (2.9) [1]. It is a combination of modified Bessel functions of the first and second kinds which was found to recur in the solution many times.

Solution to the above set of equations and boundary and initial conditions was obtained by employing the technique of separating the variables to yield

$$\begin{aligned} T(r,z,t) = & T_1 + \frac{Q_2}{w_2^2} \left[ 1 - \frac{\psi_{01}^2(w_2 r)}{\psi_{01}^2(w_2 R_1)} \right] - \frac{\beta f_{a,2} \psi_{00}^1(w_2 r)}{k w_2 \psi_{01}^2(w_2 R_1)} \\ & - \sum_{n=1}^{\infty} \frac{\alpha_{n,2} \psi_{00}^1(\zeta_2 r)}{\zeta_2 \psi_{01}^2(\zeta_2 R_1)} \cos(\lambda_n z) \\ & + \frac{2\pi}{k} \sum_{n=1}^{\infty} \frac{2 \left[ \frac{\dot{Q}_2}{\epsilon_2^2} - \frac{\dot{Q}_1}{\epsilon_1^2} \right] + \beta \mu_n \sigma_n(\mu_n R_2) \left[ \frac{f_{a,2}}{\epsilon_2^2} - \frac{f_{a,1}}{\epsilon_1^2} \right]}{\sigma_n^2(\mu_n R_2) - 4} \\ & \cdot \chi_n(\mu_n r) \exp[-\alpha \epsilon_2^2 t] \\ & + 2\pi \sum_{m=1}^{\infty} \sum_{n=1}^{\infty} \left[ \frac{\alpha_{m,2}}{\epsilon_2^2 + \lambda_m^2} - \frac{\alpha_{m,1}}{\epsilon_1^2 + \lambda_m^2} \right] \frac{\mu_n \sigma_n(\mu_n R_2)}{\sigma_n^2(\mu_n R_2) - 4} \\ & \cdot \chi_n(\mu_n r) \cos(\lambda_m z) \exp\{-\alpha[\epsilon_2^2 + \lambda_m^2]t\} \end{aligned} \quad (2.18)$$

where

$$\chi_n(\mu_n r) = J_0(\mu_n r)Y_0(\mu_n R_1) - J_0(\mu_n R_1)Y_0(\mu_n r) \quad (2.19)$$

$J_0$  and  $Y_0$  are the Bessel functions of the first and second kind, respectively, of order zero.

$$\sigma_n(\mu_n R_2) = \pi(\mu_n R_2)\chi_n(\mu_n R_2) \quad (2.20)$$

$\mu_n$ 's are the roots of

$$J_0(\mu_n R_1)Y_1(\mu_n R_2) - J_1(\mu_n R_2)Y_0(\mu_n R_1) = 0 \quad (2.21)$$

and

$$\epsilon_i^2 = \mu_n^2 + w_i^2 \quad (2.22)$$

The first fifteen eigenvalues,  $\mu_n$ , were computed using Newton-Raphson's method. Results are present in TABLE 2.1. As the ratio  $R_2/R_1$  approaches unity (rectangular model), or as  $n$  increases, the eigenvalues approach those of the rectangular model,  $\mu_n \rightarrow [(2n - 1)\pi]/2b$ , as is to be expected.

Numerical values of transient temperature distributions in the tissue and on the skin surface were obtained with the aid of a digital computer.

Figures 2.3 and 2.4 show results obtained for a one-dimensional model (uniform cooling of the skin). Step changes in activity level were assumed from low (290 Btu/hr, 85 w) to high (2600 Btu/hr, 760 w) and reversed, respectively. The substantial changes in the

TABLE 2.1

FIRST 15 ROOTS OF EQ. (2.21) AS A FUNCTION OF THE RATIO OF THE OUTER TO INNER RADII OF THE CYLINDRICAL MODEL,  $R_2/R_1$ . THE RIGHTMOST COLUMN GIVES THE ASYMPTOTIC VALUES,  $[(2n - 1)\pi/2b]$ , AS  $R_1 \rightarrow \infty$  AND  $R_2/R_1 \rightarrow 1$  (RECTANGULAR MODEL)

$R_2/R_1$	2.46	1.73	1.37	1.24	1.19	1.15	1.00
$R_1$ (ft)	0.05	0.10	0.20	0.30	0.40	0.50	$\rightarrow \infty$
n							
1	17.827850	19.184982	20.156525	20.550354	20.764221	20.898514	21.48830
2	63.293686	63.736526	64.037781	64.161377	64.229202	64.272369	64.46491
3	106.737122	107.005951	107.186890	107.258667	107.301025	107.326599	107.44152
4	149.914780	150.107346	150.236740	150.285004	150.316589	150.336288	150.41813
5	193.003647	193.153290	193.244324	193.295212	193.316849	193.331406	193.39473
6	236.050980	236.173935	236.252670	236.290054	236.304901	236.319809	236.37134
7	279.075439	279.179932	279.249756	279.279053	279.293457	279.304688	279.34795
8	322.091553	322.179932	322.240234	322.263428	322.278320	322.287598	322.32455
9	365.093994	365.173584	365.227051	365.244385	365.258789	365.268799	365.30116
10	408.092285	408.152588	408.201416	408.232178	408.241211	408.249512	408.27777
11	451.093018	451.151367	451.190430	451.213135	451.250000	451.229492	451.25438
12	494.078369	494.135498	494.175537	494.193115	494.200439	494.210205	494.23098
13	537.066895	537.121094	537.157959	537.171143	537.180664	537.189453	537.20759
14	580.054199	580.104248	580.114258	580.147217	580.156982	580.167480	580.18420
15	623.040283	623.073730	623.105957	623.132324	623.138916	623.145508	623.16080

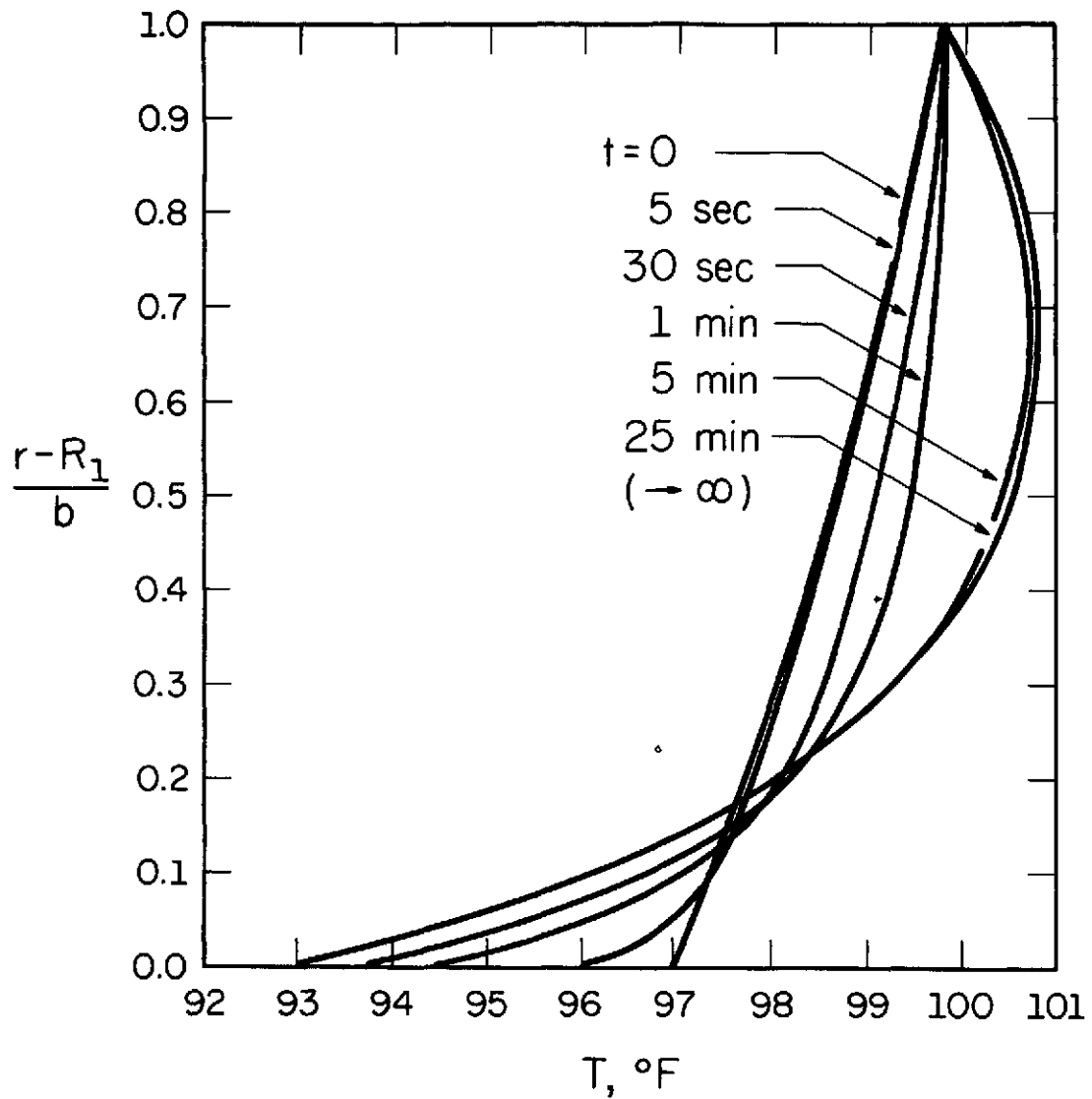


Figure 2.3 Temperature distributions in the tissue for the one-dimensional, cylindrical model. Step change is from low (290 Btu/hr, 85 w) to high (2600 Btu/hr, 760 w) activity level. Constant temperature of  $99.7^\circ\text{F}$  ( $37.7^\circ\text{C}$ ) at the inner core,  $R_1 = 0.15$  ft (4.6 cm),  $A$  and  $b$  are constant.

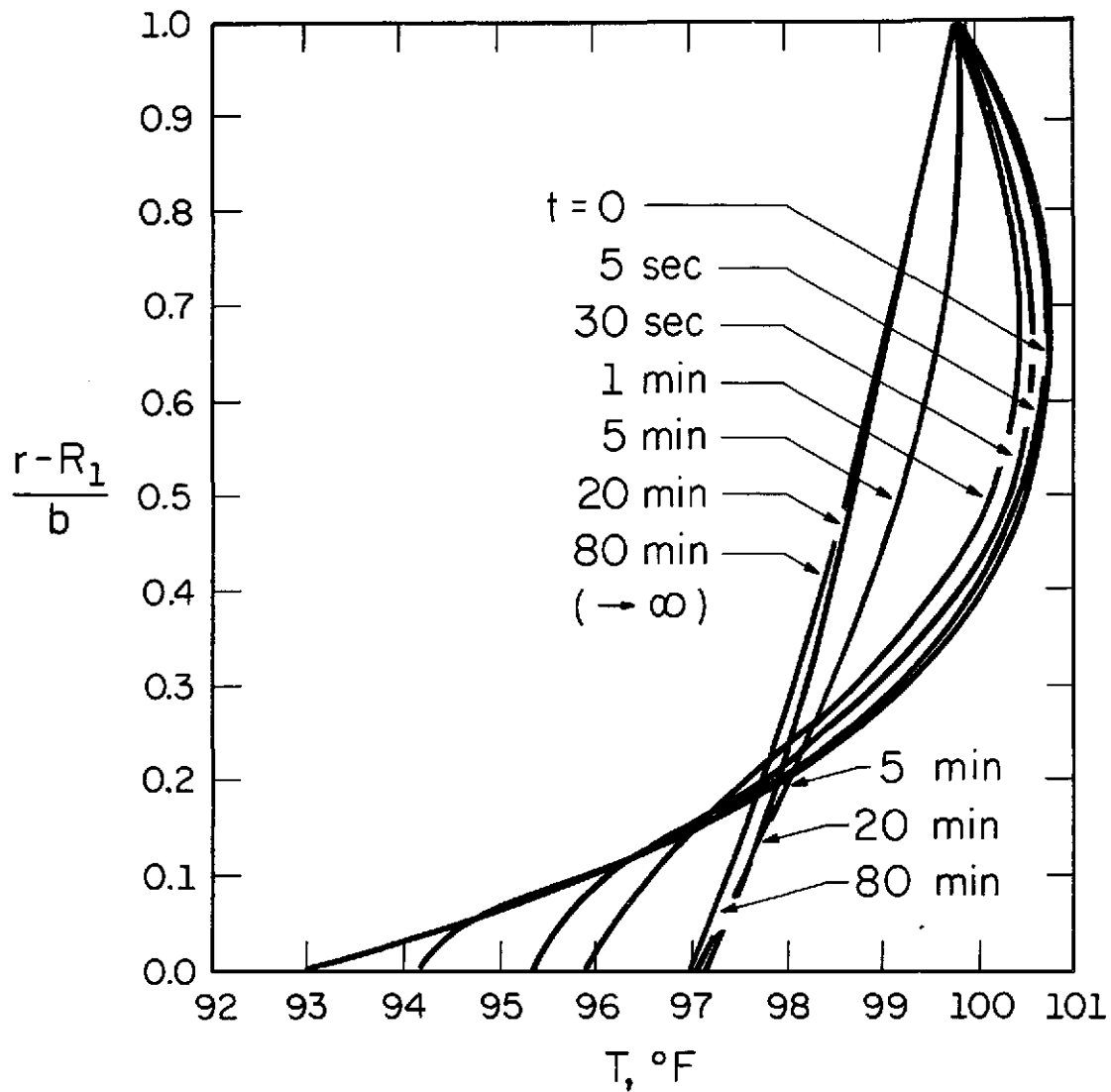


Figure 2.4 Temperature distributions in the tissue for the one-dimensional, cylindrical model. Step change is from high (2600 Btu/hr, 760 w) to low (290 Btu/hr, 85 w) activity level. Constant temperature of  $99.7^\circ\text{F}$  ( $37.7^\circ\text{C}$ ) at the inner core,  $R_1 = 0.15$  ft (4.6 cm),  $A$  and  $b$  are constant.

temperature of the tissue were found to occur during the first 5 minutes from the onset of the change from low to high activity level. When the change is reversed, substantial temperature variations occur during the first 25 minutes, approximately. The final steady state temperature profile is attained after 25 (low to high) and 80 (high to low) minutes. The ratio of these time constants was supported by the experimental results.

In Fig. 2.5 temperature variations on the skin of the cylindrical model are shown. Time constants associated with this two-dimensional geometry were found to be identical to those obtained for one-dimensional configurations [1].

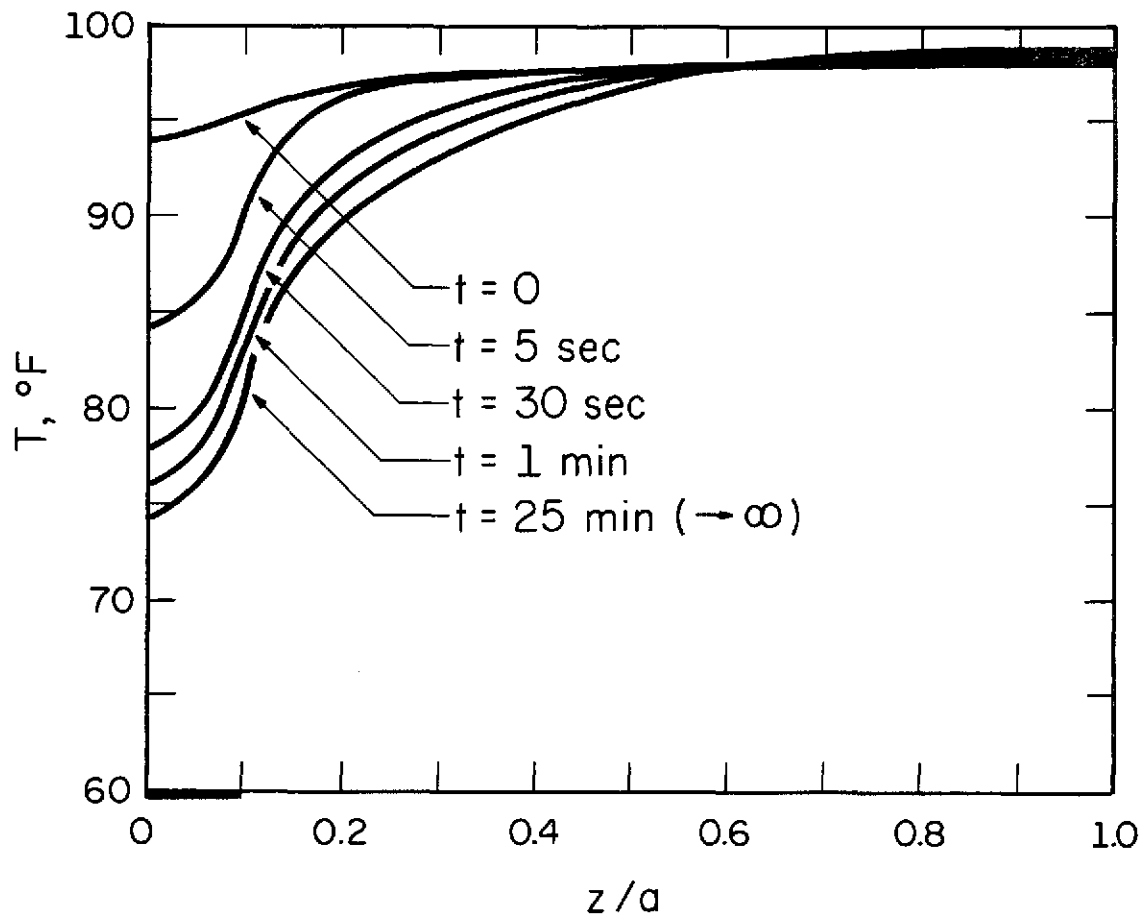


Figure 2.5 Temperature distributions on the skin surface for the two-dimensional, cylindrical model. Step change is from low (290 Btu/hr, 85 w) to high (2600 Btu/hr, 760 w) activity level.  $\beta = 0.1$ , constant temperature of 99.7°F, (37.7°C) at the inner core,  $R_1 = 0.15$  ft (4.6 cm), A and b are constant.

### 3. EXPERIMENTS

#### 3.1 OBJECTIVES

The basic objective of the experimental phase of the study was to measure the temperature distribution on the skin surface between adjacent tubes of cooling pads placed around a human thigh. This temperature distribution was measured during activity levels corresponding to low, mild, moderate and high metabolic rates. Also, the temperature distribution was monitored during the transient periods between those activity levels. A secondary objective was to evaluate the effect that various cooling tube sizes and spacings have on the temperature distribution and the overall cooling efficiency. Three cooling pads with different tube size and spacing were tested on a human subject while performing various experimental activity schedules. Figure 3.1 is a schematic diagram of the experimental setup showing the water supply, cooling pad and temperature measuring equipment.

#### 3.2 EXPERIMENTAL APPARATUS

##### 3.2.1 The Individual Pads

Three different cooling pads were built and tested. These pads were specifically designed to fit over the right thigh of the test subject. All three pads were constructed of a flexible, elastic sheet of 1/8-in. gum rubber. Tygon tubes were affixed in a parallel configuration to one side of the pads using Eastman Kodak 910 adhesive. The diameter and spacing of tubes were constant for each individual pad, but varied from pad to pad. TABLE 3.1 gives the pertinent data on the individual pads. Figure 3.2 shows a view

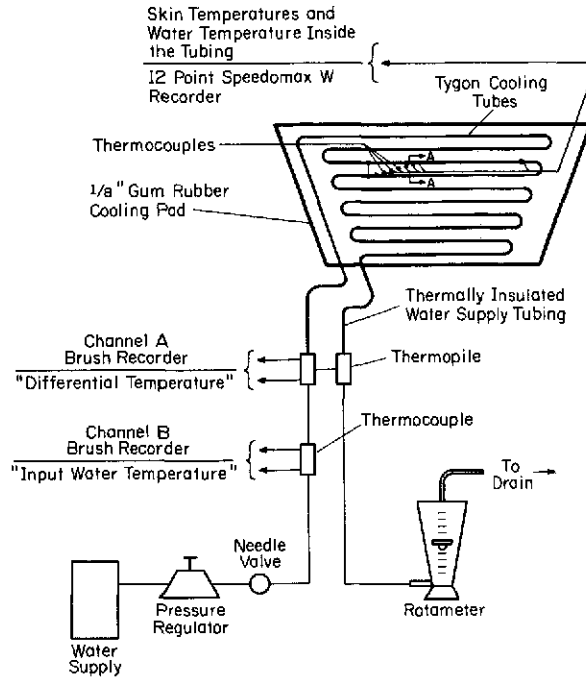


Figure 3.1(a) Schematic diagram of cooling pad and water supply system with temperature measuring points indicated.

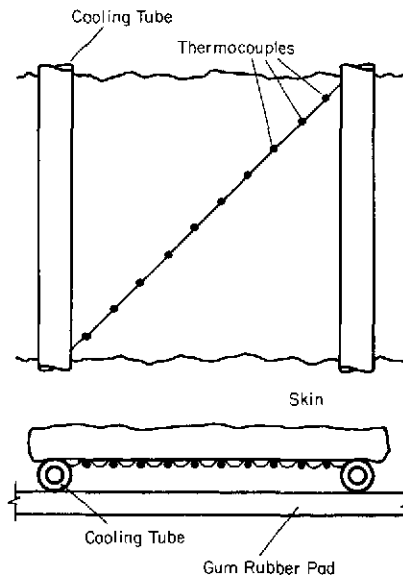


Figure 3.1(b) Cross section A-A showing details of thermocouple placement.

TABLE 3.1

## Data On the Individual Cooling Pads

	Outside Diameter of Tubes		Spacing of Tubes		Number of Rows of Tubes	Total Length of Tubes		Area Covered by Pad		Approximate Contact Area with the Skin		Percent of Area in Contact with Tubes
	in.	cm	in.	cm		in.	cm	in. <sup>2</sup>	cm <sup>2</sup>	in. <sup>2</sup>	cm <sup>2</sup>	
Pad No. 1	5/32	0.397	1	2.54	10	163	414	140	910	22.9	148	16.4
Pad No. 2	5/32	0.397	5/8	1.59	14	228	580	132	852	32.1	207	24.3
Pad No. 3	7/32	0.556	1	2.54	10	163	414	145	937	28.5	184	19.7

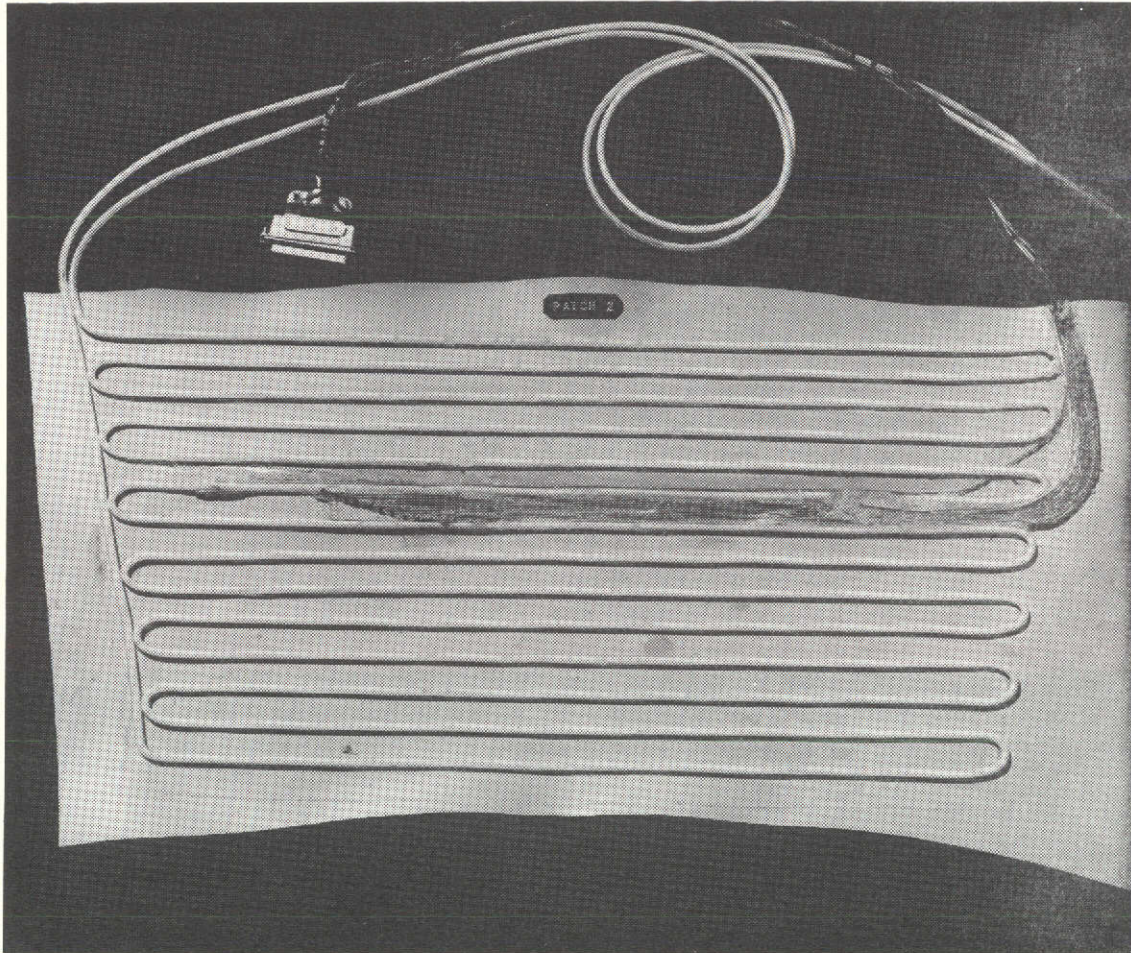


Figure 3.2 View of one of the individual pads.

of one of the individual cooling pads.

Number 30-gauge copper-constantan thermocouples were used to measure cooling water temperatures and skin temperatures between the two adjacent tubes. The thermocouples were equally spaced on a 30 degree diagonal between adjacent cooling tubes. The thermocouples were also located such that they were pressed against the skin surface to insure good thermal contact when the pad was fastened to the thigh. Figure 3.2 illustrates one of the cooling pads and thermocouples.

A Leeds and Northrup Speedomax W, 12-point potentiometer-recorder was used for continuous monitoring and recording of the temperature of the cooling water and the skin temperatures between adjacent tubes. The water supply temperature and the difference between the water outlet and inlet temperatures were continuously recorded by a Brush Mark 280 recorder. Thermopiles consisting of five copper-constantan thermocouples connected in series and a Brush pre-amplifier were used to increase the sensitivity of the reading of the differential water temperature for the pad. The water supply lines leading to the pad were thermally insulated with rubber tubing which provided an air-gap type of thermal barrier.

### 3.2.2 The Water Supply

The source for the water supply was the cold water line in the laboratory. Before each experiment the cold water was run continuously until an equilibrium temperature was reached and the inlet water temperature became constant at 54.5°F (12.5°C). Figure 3.1 shows the water supply system along with the instrumentation used to record

the experimental data.

The flow rate was maintained constant by a pressure regulator and controlled by a needle valve. The flow rate was measured by a Fischer and Porter Rotameter. All flow rates were maintained constant at 40.5 lb/hr (18.4 kg/hr).

### 3.2.3 The Metabolic Measurements

For metabolic measurements, expired air samples were taken with a collecting apparatus and stored in metalized Douglas bags [24]. These bags were placed inside a sealed Plexiglas chamber whose pressure was maintained at -5 mm Hg. [25]. Air was inhaled and exhaled through a mouth piece while the nostrils were blocked with a noseclip. Two sets of one-way rubber flap valves insured separation of the two streams. The expired air was directed through a 1-in. I.D. rubber hose into a mixing chamber. One minute sampling was achieved by opening a one-way stopcock valve thus exposing a previously evacuated metalized bag to the exhaled air. The vacuum in the Plexiglas chamber facilitated the filling of the Douglas bags as positive exhaled air pressure existed at the inlet to the bag, and negative chamber pressure surrounded the bag structure.

Air volumetric flow rates were measured by means of a Parkinson-Cowan dry gas meter. Inlet and outlet air temperatures were measured by a Yellow Springs Instrument, Co. Tele-Thermometer and two No. 401 interchangeable, multipurpose thermistors. Figure 3.3 shows the system used to collect air samples.

Once collected in the individual Douglas bags, the air samples were analyzed for  $\text{CO}_2$  and  $\text{O}_2$  content. A Godart-Mijnhardt  $\text{CO}_2$  thermal-

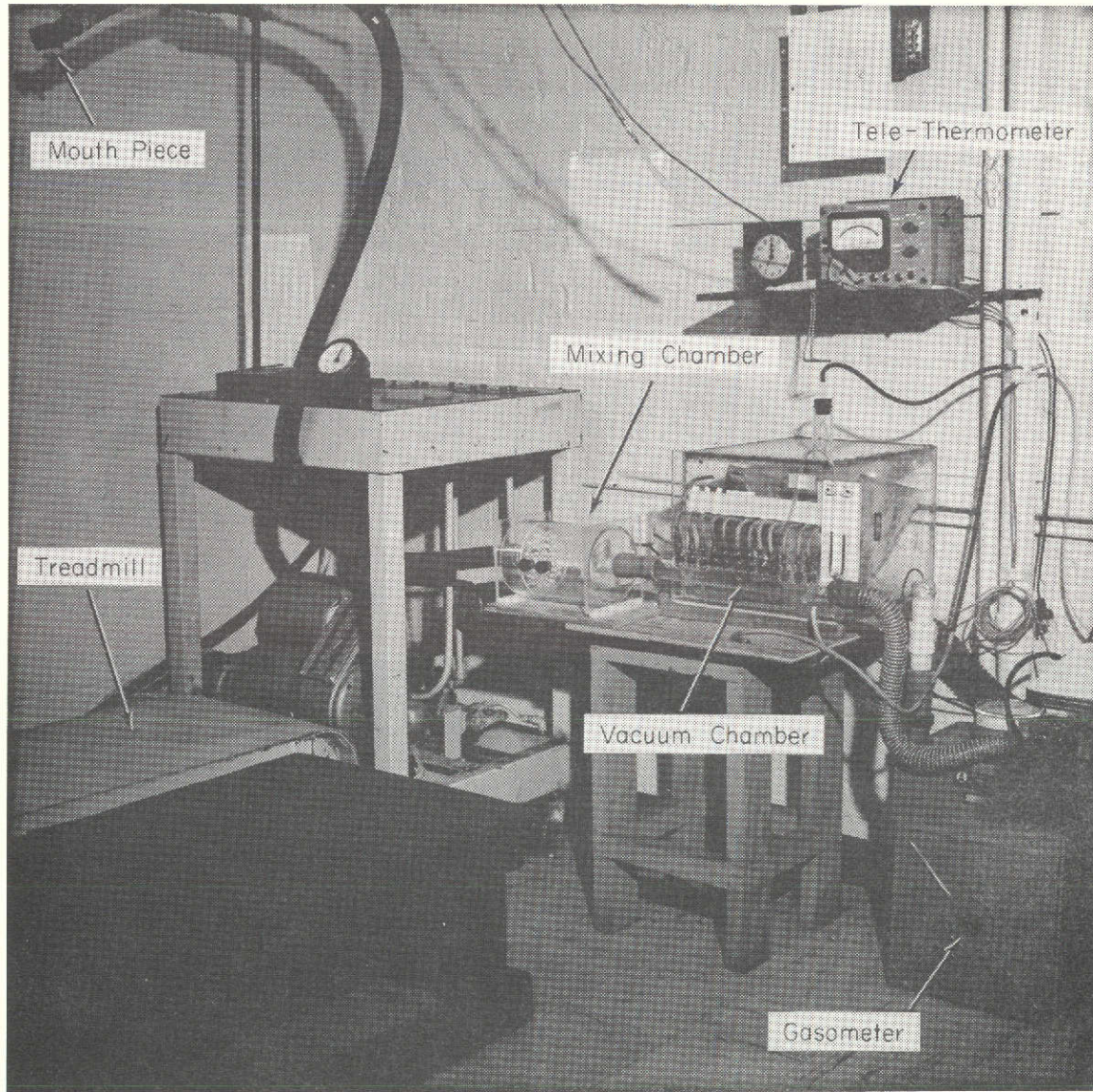


Figure 3.3 A view of the Tele-Thermometer and system for collecting samples for determining metabolic rates.

conductivity meter, Pulmo Analyser Type 44-A-2 and a Beckman Paramagnetic O<sub>2</sub> analyzer, Model C2 were used. The results of this analysis were combined with other data to calculate the metabolic heat generation rate of the subject [26] which is a measure of the energy expenditure. Various levels of energy expenditure were obtained by the subject pedalling a Monark bicycle ergometer at a constant pre-set speed and load.

### 3.3 EXPERIMENTAL PROCEDURE AND TEST SCHEDULES

At the beginning of each experiment the ambient temperature, pressure and humidity were recorded. The test subject was weighed and his blood pressure and oral temperature were recorded. During the experiments the test subject wore a sweat shirt, track shorts and tennis shoes. The ear canal temperature was continuously monitored and recorded throughout the duration of the experiment. At the end of the experiment the subject's weight, blood pressure and oral temperature were again measured and recorded.

Figure 3.4 shows the work programs for the experiments. In experiments 1, 2, and 3 the temperature distribution on the skin surface was measured using pad No. 2. Temperature distributions were recorded for these experiments corresponding to activity levels of sitting, standing and mild work, respectively.

Experiments 4, 5, and 6 were conducted using pads No. 1, 2, and 3, respectively. In these experiments the steady state temperature distribution was recorded for a moderate work activity level of 900 Btu/hr (264 w). In experiments 4, 5, and 6 the work load, inlet water temperature and flow rate were maintained at an equal

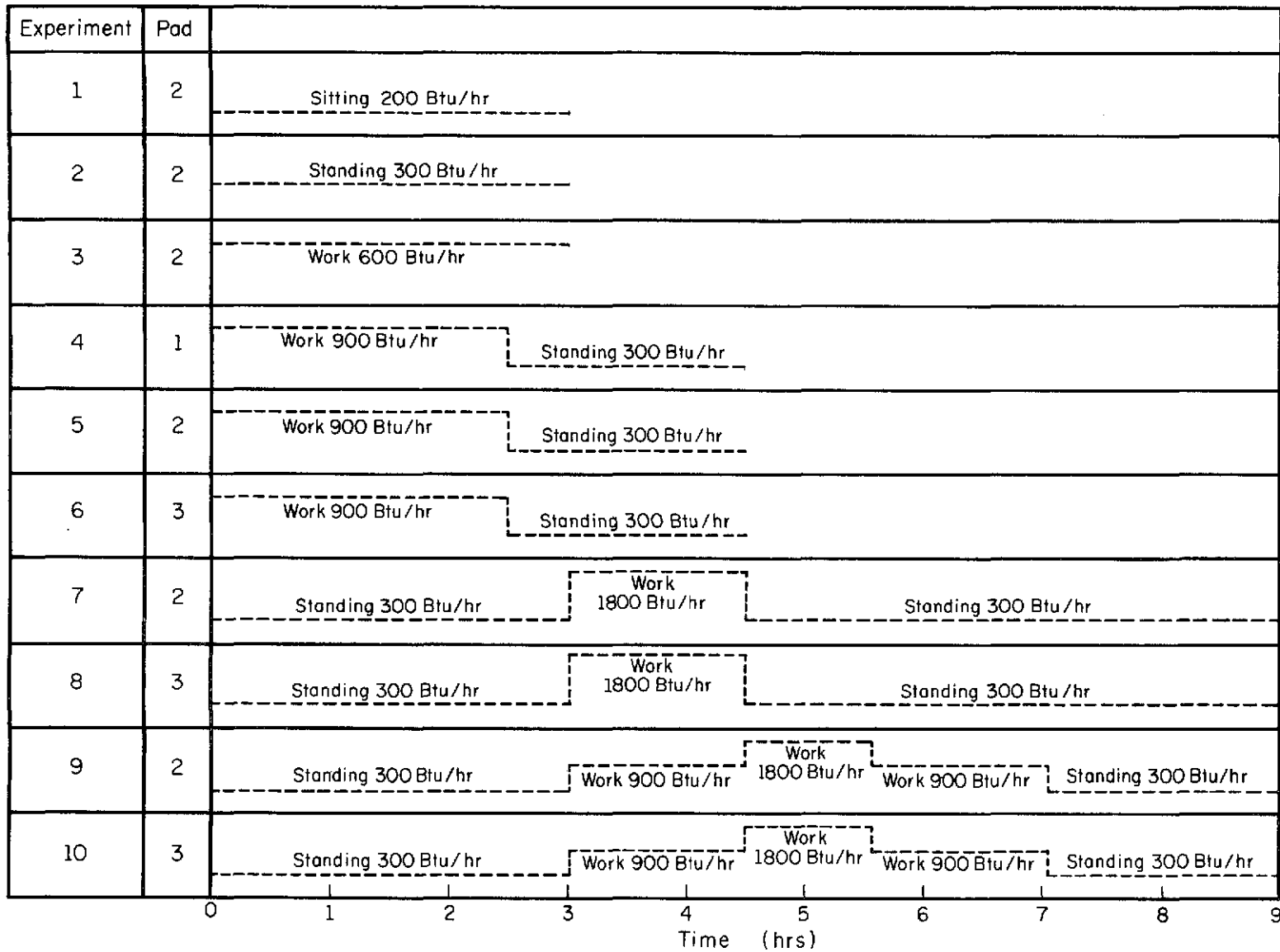


Figure 3.4 Work program for each experiment.

329

level and held constant for each experiment.

In experiments 7 and 8, cooling pads No. 2 and 3 were used to measure the course of change of the skin temperature distribution resulting from a change in activity level. The temperature distribution was recorded for a change from a steady state level at 300 Btu/hr (88 w) to an elevated level at 1800 Btu/hr (528 w). The change in activity levels during experiments 8, 9 and 10 was achieved by varying the load on the bicycle ergometer. Figure 3.5 shows the test subject pedaling the bicycle ergometer. The test subject continued work at the 1800 Btu/hr (528 w) level until a steady state skin temperature was achieved. At this point the subject stopped working and the resulting transient temperature profile was monitored as he returned to the 300 Btu/hr (88 w) level.

Experiments 9 and 10 were also run with pads No. 2 and 3. Here a similar approach was taken: The temperature distribution was monitored for changes from 300 Btu/hr (88 w) to 900 Btu/hr (264 w) and from 900 Btu/hr (264 w) to 1800 Btu/hr (528 w). The skin temperature profile was recorded again as the test subject decreased activity from 1800 to 900 Btu/hr and finally from 900 to 300 Btu/hr (528, 264, and 88 w, respectively).

#### 3.4 THE TEST SUBJECT

The test subject was a caucasian male student of the University of Illinois at Urbana-Champaign. The subject was in excellent physical condition. TABLE 3.2 illustrates his personal characteristics.

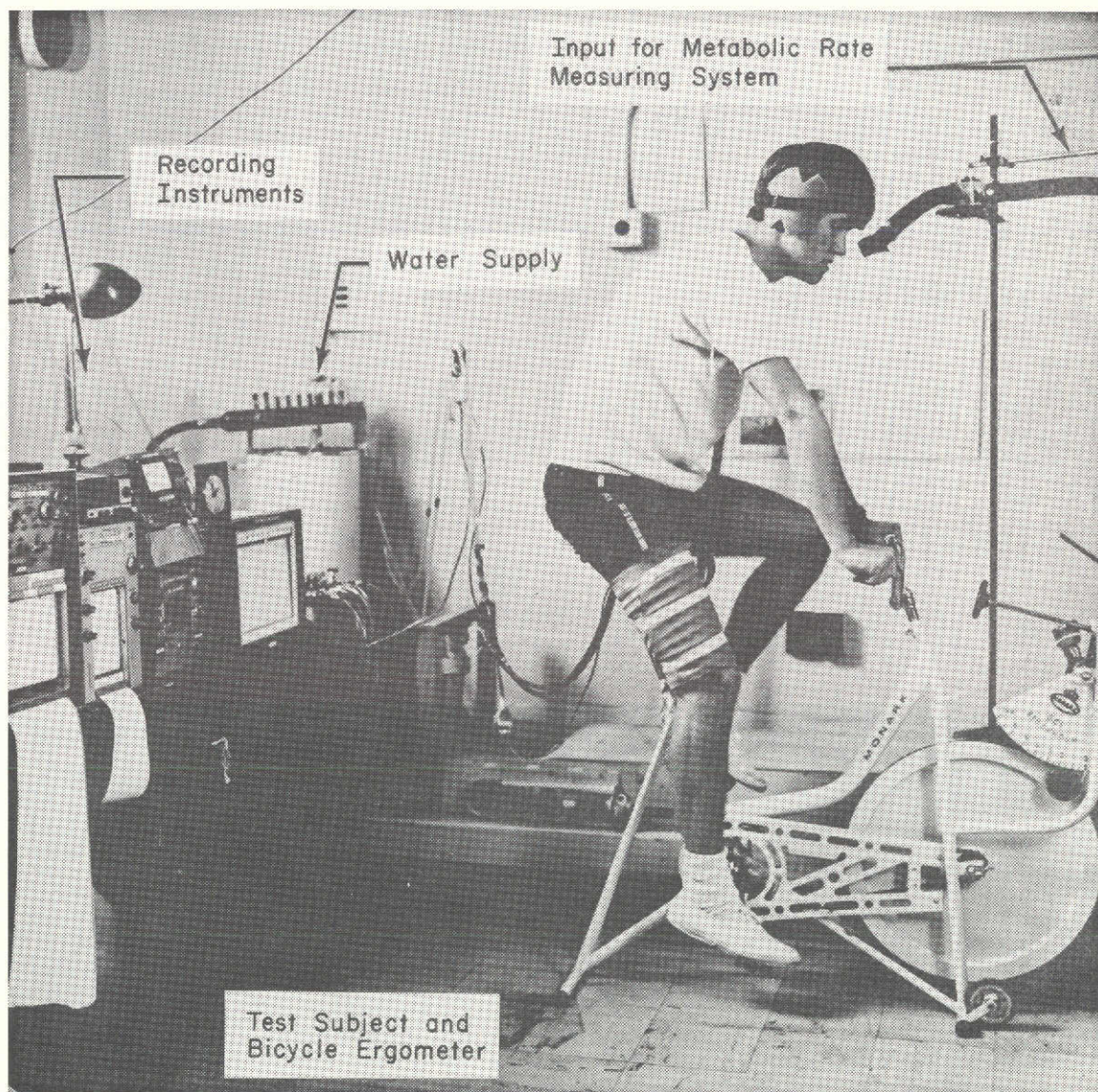


Figure 3.5 General view of the set-up used for the experiments with the individual cooling pads. A test subject is shown pedalling the bicycle ergometer.

TABLE 3.2 CHARACTERISTICS OF SUBJECT TEK

Subject	Age	Height		Weight		Surface Area	
		cm	in.	kg.	lb.	m <sup>2</sup>	ft <sup>2</sup>
TEK	19	189	74.5	79.7	175.5	2.02	21.7

### 3.5 RECORDED AND CALCULATED QUANTITIES

#### 3.5.1 Recorded Quantities

During the course of the experiments the following quantities were recorded using the corresponding instrumentation:

1. Temperature distribution on the skin surface between adjacent tubes was measured with No. 30 copper-constantan thermocouples with ice water reference junction and a Leeds and Northrup Speedomax W Potentiometer Recorder.
2. Differential temperature measurement for cooling pad ( $T_{inlet} - T_{outlet}$ ) was made by thermopiles constructed of five copper-constantan thermocouples in series mounted in special plexiglas connectors and a Brush Mark 280 strip chart recorder with high sensitivity Brush Pre-Amplifier.
3. Inlet water supply temperature was taken with one copper-constantan thermocouple with ice reference junction and a Brush Mark 280 strip chart recorder with a high sensitivity Brush Pre-Amplifier.
4. Ear canal temperature was measured with an ear thermistor No. 510 and Yellow Springs Instrument Co. Tele-Thermometer with a Brush Mark 220 recorder.
5. Flow rate was measured with a Fischer-Porter No. 48 Rotameter type flow meter.
6. Expired air flow rate was measured with a Parkinson-Cowan

dry gas meter. This flow was measured and collected continuously during transient conditions and periodically during steady state conditions.

7. Oxygen content in expired air was obtained by a Beckman Paramagnetic O<sub>2</sub> analyzer, model C2.
8. CO<sub>2</sub> content in expired air was analyzed with a Godart-Mijnhardt CO<sub>2</sub> thermal conductivity type pulmo analyzer.

### 3.5.2 Calculated Quantities

1. Total metabolic rate was calculated from the volumetric flow rate of the expired air and the oxygen and CO<sub>2</sub> content obtained from the analysis of this air. The caloric value of oxygen was assumed at 5.0 Kcal/lit [27]. This value, although slightly high, was confirmed by Shitzer, et al., [1] with respiratory quotients found in their experiments. Maximum deviation from the actual caloric value was assumed to be at about 4 percent.
2. The rate of heat removed by each pad was taken as the product of the difference between inlet and outlet temperatures and the coolant flow rate. The specific heat of water was assumed at 1 Btu/lb-°F or 1 Kcal/kg-°C.
3. For the determination of the rate of heat loss by respiration; flow rate, temperature and enthalpy of expired air, assuming it to be saturated, were used.

#### 4. RESULTS AND DISCUSSION

##### 4.1 GENERAL RESULTS

The equipment functioned well throughout the research and the test subject, although overstressed in experiments 9 and 10, was able to complete all of the pre-designed test schedules. TABLE 4.1 outlines the experimental data pertaining to the test subject, the environmental conditions, and each of the variations in the ten experiments. As TABLE 4.1 indicates, the experiments were performed in an environment with the following average conditions:

Pressure	29.35 Hg.
Relative humidity	42 percent
Temperature	71.5°F

Throughout the duration of the ten experiments (approximately six weeks) the test subject maintained an average weight of 176 lb (79.9 kg) although a weight reduction of 1.5 to 3 pounds (0.68 to 1.36 kg) were observed during each of the ten experiments due to loss of body fluid. The test subject's blood pressure and oral temperature remained normal before and after each of the experiments.

The test subject's thigh was cooled with a constant flow (40.5 lb/hr, 18.4 kg/hr) of water at 54.5°F (12.5°C) during all experiments. TABLE 4.2 shows the performance of each test pad for the various experimental conditions. The test subject's metabolic rate shown is the maximum steady state work load that was achieved for each of the experiments. The heat removed by the cooling pad given in the table corresponds to the maximum heat removed from the thigh at the highest steady state work load. The steady state condition was assumed to exist when the temperature profile on the skin surface between the

TABLE 4.1

## Experimental Conditions and Measured Data

(Water flow rates and inlet temperatures were identical for all experiments at 40.5 lb/hr and 54.5°F (12.5°C))

Experiment No.	Pad No.	Weight, lb		Blood Pressure		Oral Temp, °F		Pressure in. Hg.	Relative Humidity	Temperature °F
		Before	After	Before	After	Before	After			
1	2	176.83	175.25	120/80	120/80	98.5	97.6	29.38	42	72
2	2	177.66	177.52	120/80	120/90	98.2	98.4	29.32	41	72
3	2	176.40	175.60	125/80	125/80	98.4	98.2	29.38	43	71
4	1	179.68	177.34	120/65	120/90	97.6	98.0	29.32	40	73
5	2	178.36	176.60	120/80	120/80	97.8	98.2	29.30	41	72
6	3	176.06	175.12	120/80	120/80	97.8	98.4	29.50	43	73
7	2	175.71	174.12	115/60	120/70	97.7	98.6	29.52	40	72
8	3	176.54	174.09	120/80	120/80	97.6	98.2	29.44	42	70
9	2	173.36	170.39	110/80	120/80	98.3	98.5	29.30	43	73
10	3	175.92	172.50	110/80	110/80	98.4	98.0	29.41	43	72

TABLE 4.2

Heat Removed by Cooling Pads During Maximum Steady State Metabolic Rates						
Experiment	Pad	Maximum Steady State Total Metabolic Rate of Subject		Heat Removed by Pad During Steady State		Percent of Total Removed by Pad
		Btu/hr	w	Btu/hr	w	
1	2	200	59	-- *	*	-- *
2	2	320	94	148	44	46**
3	2	600	176	183	54	30
4	1	900	264	185	54	20
5	2	900	264	190	56	21
6	3	900	264	208	61	23
7	2	1800	528	290	85	16
8	3	1800	528	300	88	17
9	2	1800	528	290	85	16
10	3	1800	528	300	88	17

\*Steady state temperature profile was not attained.

\*\*Questionable value.

cooling tubes was fully developed and did not change as a function of time.

#### 4.2 TEMPERATURE DISTRIBUTIONS FOR SITTING, STANDING AND MILD WORK

Cooling pad No. 2 was used for experiments 1, 2, and 3. The objective of these experiments was to investigate the nature of the human thigh's response to cooling by a pad with a constant water temperature and flow rate but for three activity levels. Figure 4.1 illustrates the results of experiments 1, 2, and 3. For each experiment there is one set of data consisting of two lines. These approximately parallel lines represent the highest and lowest temperatures which occurred on the skin surface between two adjacent cooling tubes. The higher temperature line represents a point on the skin surface equidistant between the cooling tubes, and the lower temperature line represents a point on the skin surface immediately adjacent to the cooling tube. The difference between the input water temperature and the temperature of the water that leaves the pad is also plotted.

TABLE 4.3 summarizes the information which is presented in Fig. 4.1. As illustrated, a steady state condition was never achieved in experiment No. 1. After three hours the temperature on the skin surface of the thigh was still decreasing at a fairly steady rate of  $1.35^{\circ}\text{F}$  ( $0.75^{\circ}\text{C}$ ) per hour. The metabolic rate of the sitting test subject remained constant at 200 Btu/hr (59 w). It should be noted that this measured value of 200 Btu/hr (59 w) is about 75 to 100 Btu/hr below average for a sitting individual.

In experiment No. 2 all of the experimental parameters remained

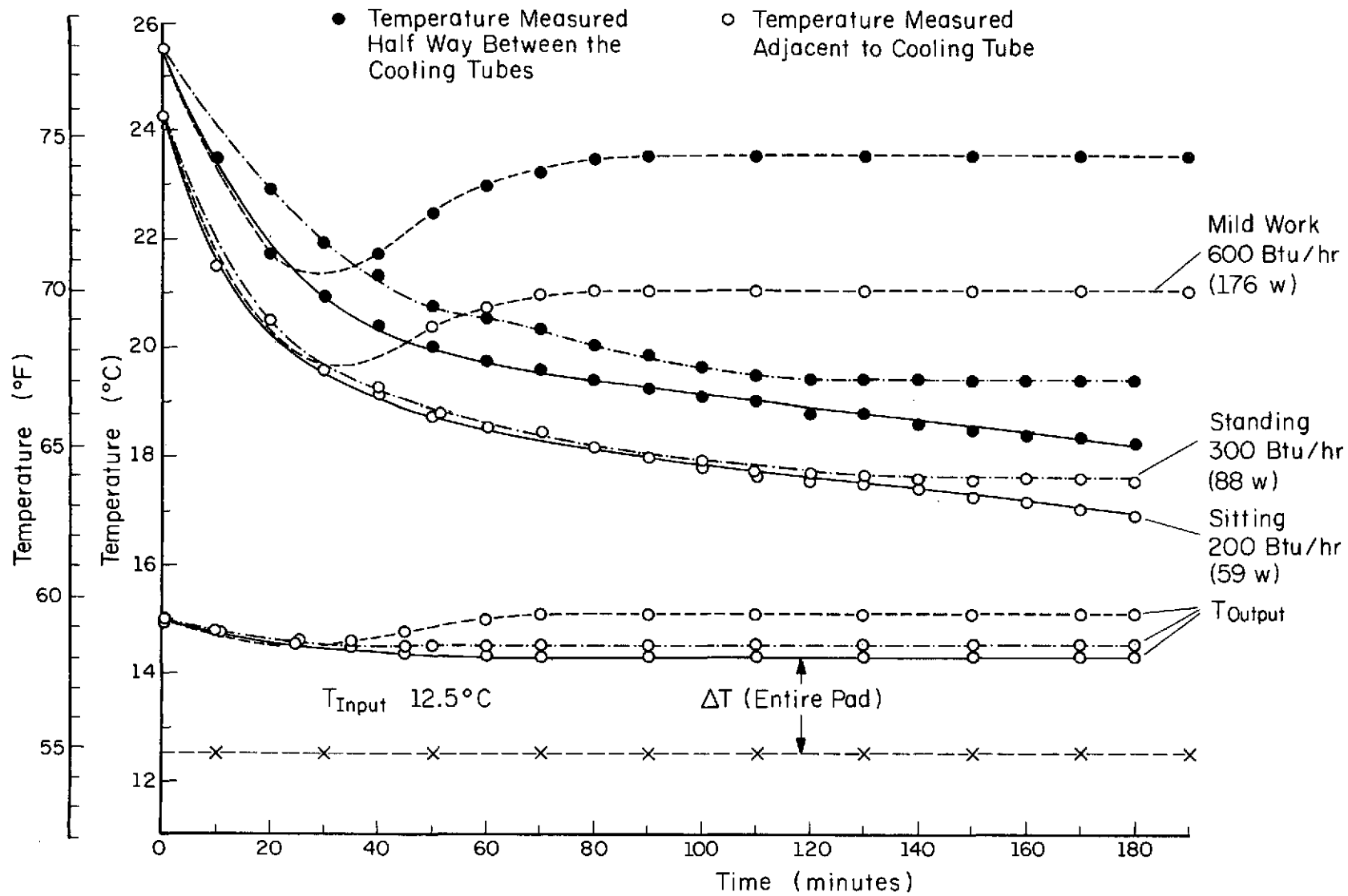


Figure 4.1 Results of experiments 1, 2, and 3 using cooling pad No. 2 with constant experimental conditions and varying work load.

TABLE 4.3

Summary of the Results of Experiments 1, 2, and 3 with Pad No. 2

Experiment Number	Highest Metabolic Rate Reached by Subject During Steady State Conditions		Approximate Time to Reach Steady State Temperature Profile, min.	Difference Between Highest and Lowest Temperatures at Steady State		Temperature Rise Across Pad, $T_{in} - T_{out}$ at Steady State		Heat Removed by Pad at Steady State	
	Btu/hr	w		°F	°C	°F	°C	Btu/hr	w
1	200*	59	>180	---	---	---	---	---	---
2	320	94	130	3.40	1.89	3.6	2.00	142	41**
3	600	176	90	4.50	2.50	4.7	2.61	185	54

\*Steady state profile was not attained.

\*\*Questionable value.

the same as in experiment No. 1 with the exception of the test subject's metabolic rate. The standing position was employed and the resulting metabolic rate was 320 Btu/hr (94 w), 120 Btu/hr (35 w) higher than in the case of sitting. This time the temperature distribution on the surface of the thigh did reach a steady state in approximately 130 minutes. During the steady state condition a maximum temperature difference of 3.4°F (1.9°C) was observed on the skin surface. At the same time a total temperature rise of 3.6°F (2.0°C) was recorded for the water supply. At a work load of 320 Btu/hr (94 w) this temperature difference corresponded to a heat removal rate of 142 Btu/hr (41 w).

An assumption was made that a mild work activity level would correspond to twice the metabolic rate of standing. This mild work was simulated by an activity level of 600 Btu/hr (176 w). During experiment No. 3 the test subject reached a steady state temperature distribution in 90 minutes while working at 600 Btu/hr (176 w). The maximum temperature difference on the skin surface during steady state was 4.5°F (2.5°C). At steady state the heat removed from the thigh by the cooling pad was 185 Btu/hr (54 w) corresponding to a water temperature rise of 4.7°F (2.6°C). It should be noted that the highest temperature recorded between adjacent tubes rose from 67.1°F (19.5°C) at 320 Btu/hr (94 w) in experiment No. 2 to 74.3°F (23.5°C) at 600 Btu/hr (176 w) in experiment No. 3.

At the beginning of experiments 1, 2, and 3 the cooling pad was strapped on the subject's thigh while cooling water was flowing through the pad. In later experiments the pad was placed on the thigh and the subject was then allowed to rest for 30 minutes.

During this time the thigh came to equilibrium with no flow in the cooling pad. Cooling fluid was introduced only after the thigh had reached a steady state without cooling. This procedure was instituted in order to gain some additional insight as to the course of change of the skin temperature on the surface of the thigh during the onset of cooling.

#### 4.3 COMPARISON OF THE SURFACE TEMPERATURE TRANSIENTS FOR THE THREE PADS

During experiments 4, 5, and 6, cooling pads 1, 2, and 3 were tested, respectively. During each of these experiments the inlet water temperature was maintained constant at 54.5°F (12.5°C); the flow rate was maintained constant at 40.5 lb/hr (18.4kg/hr) and the activity level of the test subject was monitored and regulated at 900 Btu/hr (264 w).

Figure 4.2 illustrates the result of experiments 4, 5, and 6 and these results are also summarized in TABLE 4.4. As is shown, the cooling pad was placed on the test subject at  $t = 0$ . He was allowed to rest for the first 30 minutes after which the cooling fluid was introduced. The temperature profile on the skin surface decreased afterward. The transient times to reach steady state were 90 minutes for pad No. 2 and 100 minutes for pads No. 1 and 3. It is interesting to note that at steady state the temperature distributions for pads No. 1 and 3 almost coincide while the temperature profile for pad No. 2 is noticeably lower by about 3.5°F (2°C). This observation can be accounted for by the fact that pad No. 2 has a higher cooling tube density than pads No. 1 and 3. This high tube density is also reflected in a skin temperature differential of

392  
265

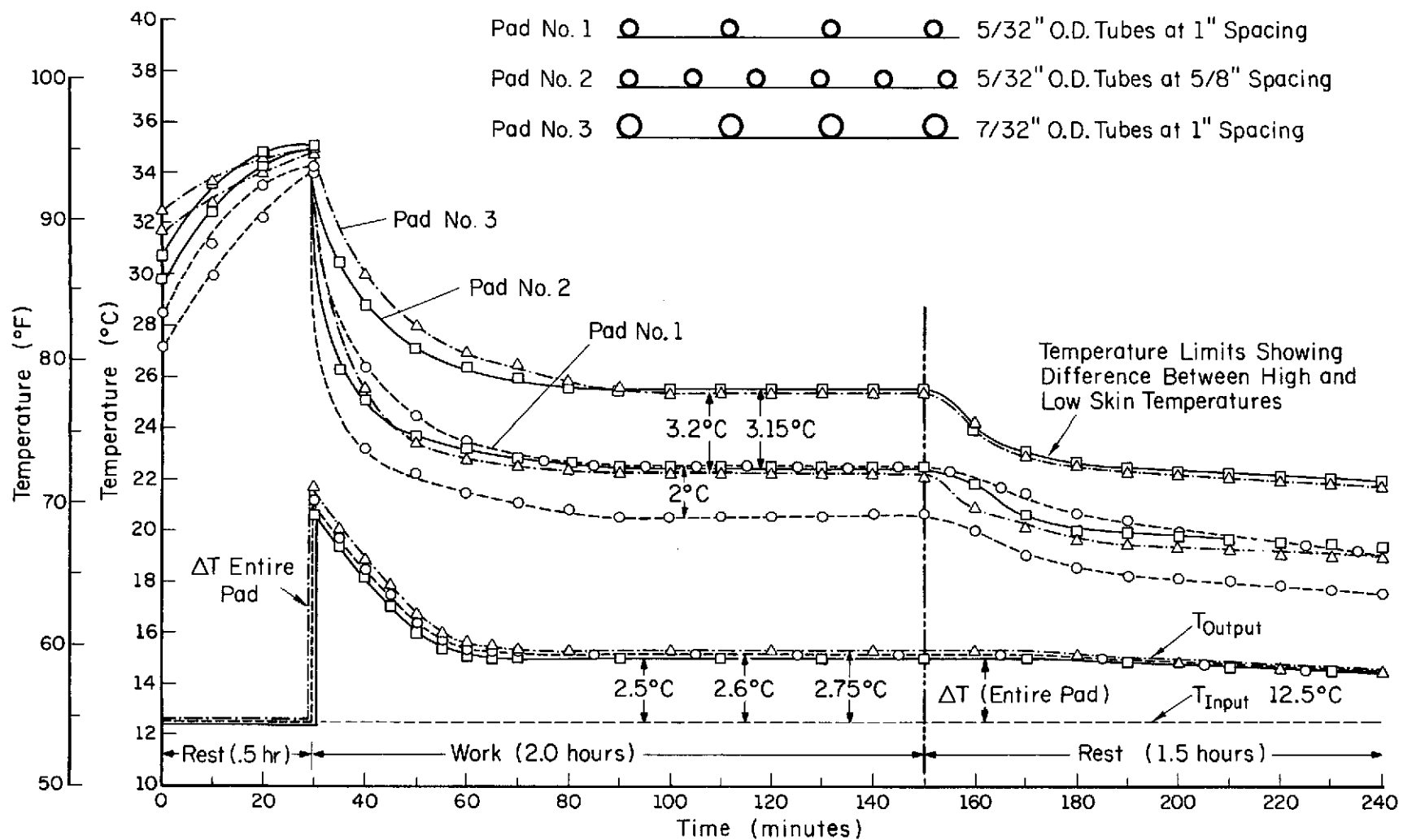


Figure 4.2 Results of experiments 4, 5, and 6 with constant experimental conditions and constant metabolic rate 900 Btu/hr (264 w).

TABLE 4.4

Results of Experiments 4, 5, and 6 with Constant Metabolic Rate of 900 Btu/hr (257 w) Using Pads 1, 2, and 3

Experiment	Pad	Highest Metabolic Rate at Steady State		Time to Develop Steady State Temperature Profile, min.	Highest Skin Temperature		Lowest Skin Temperature		$T_h - T_{low}$		$\Delta T$ Pad		Heat Removed by Pad	
		Btu/hr	w		°F	°C	°F	°C	°F	°C	°F	°C	Btu/hr	w
4	1	900	264	100	78.1	25.6	70.61	21.4	10.2	5.67	4.5	2.5	185	54
5	2	900	264	90	72.3	22.4	68.7	20.4	6.5	3.6	4.7	2.6	190	56
6	3	900	264	100	77.7	25.4	71.9	22.2	10.3	5.7	4.95	2.75	208	61

t/t

only 3.6°F (2°C) for pad No. 2 while the differences between the high and low skin temperatures for pads No. 1 and 3 are 5.67°F (3.15°C) and 5.76°F (3.2°C), respectively. Consequently, while pad No. 2 provided a lower skin temperature in general, it also provided a more uniform skin temperature profile between the tubes. With a work load of 900 Btu/hr (264 w), pad No. 3 removed the highest amount of heat; i.e., 208 Btu/hr (61 w) corresponding to a cooling fluid temperature difference of 4.95°F (2.75°C).

#### 4.4 COMPARISON OF THE STEADY STATE SKIN SURFACE TEMPERATURE DISTRIBUTIONS FOR THE THREE PADS

Steady state temperature distributions on the skin corresponding to activity levels of 300 Btu/hr (88 w), 900 Btu/hr (264 w), and 1800 Btu/hr (528 w) are shown in Figs. 4.3, 4.4, and 4.5, respectively. The results for pad No. 1 are shown in Fig. 4.4 alone since this pad was used during experiment No. 4 only (mild work, 900 Btu/hr, TABLE 4.2).

All profiles shown in these figures resemble bell-shaped curves. The same qualitative results have been obtained by Chato and co-workers [7]. In general, the profiles obtained from pad No. 2 were the flattest and also lowest in temperatures. These results are due to the higher tube density of pad No. 2 as compared to the other two pads.

Temperatures immediately underneath the cooling tubes could not be accurately obtained with the present measuring technique. Thus, only measured skin temperatures in the region not in contact with the cooling tubes, i.e.,  $\beta < z/a < (2 - \beta)$ , are shown in Figs. 4.3,

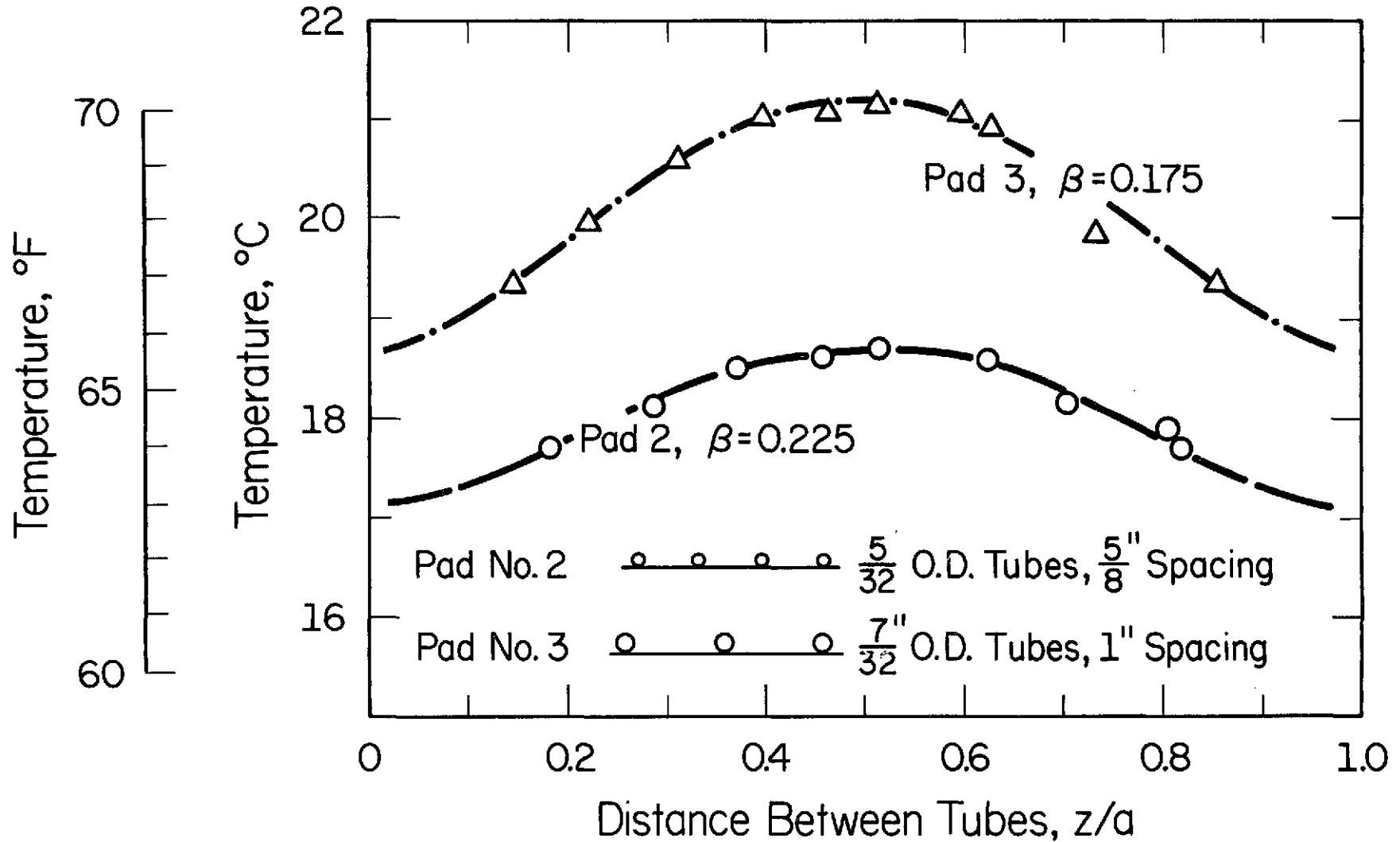


Figure 4.3 Steady state temperature distribution for pads 2 and 3 under constant experimental conditions and constant metabolic rate at 300 Btu/hr (88 w).

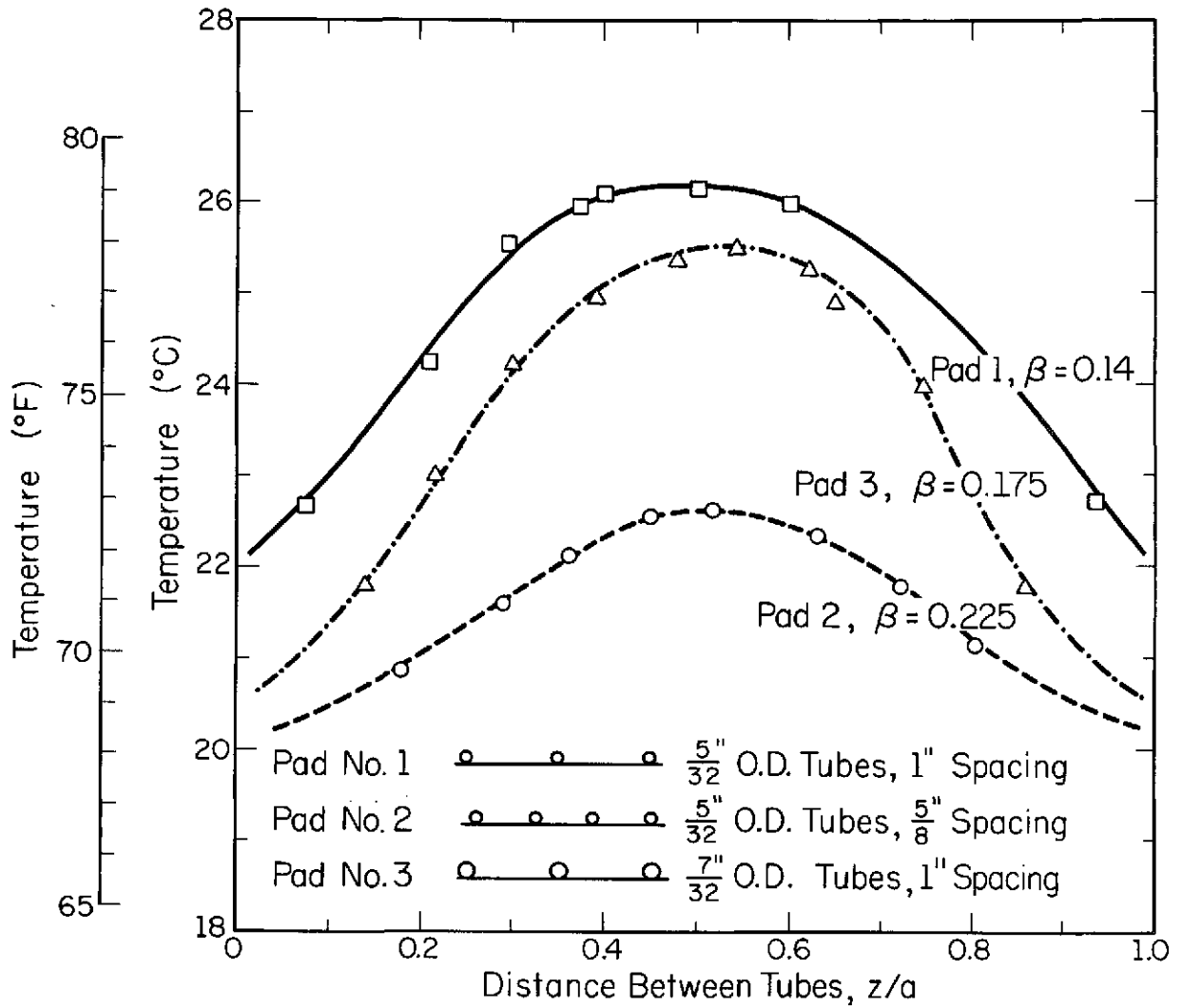


Figure 4.4 Steady state temperature distribution for pads 1, 2, and 3 under constant experimental conditions and constant metabolic rate at 900 Btu/hr (264 w).

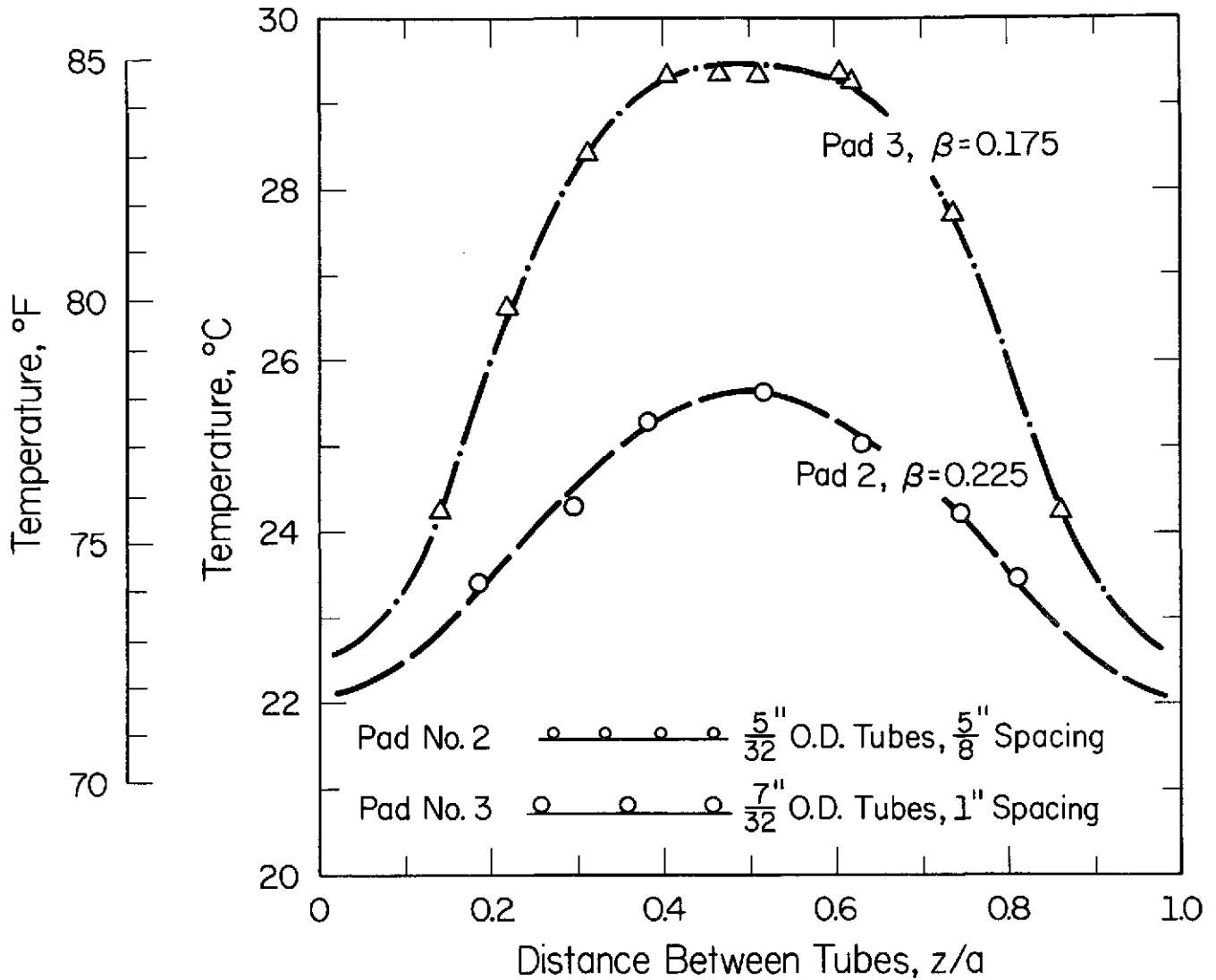


Figure 4.5 Steady state temperature distribution for pads 2 and 3 under constant experimental conditions and constant metabolic rate at 1800 Btu/hr (528 w).

4.4, and 4.5. The profiles in these figures were extrapolated into the areas covered by the cooling strips, too. The extrapolated values could not be verified and should be treated as estimates only.

#### 4.5 COMPARISON OF THE STEADY STATE SURFACE TEMPERATURE DISTRIBUTIONS WITH ANALYTICAL RESULTS

Analytical expressions for the steady state temperature distribution on the skin surface between adjacent cooling tubes for the tissue modeled as a rectangular slab or a cylindrical shell are given in Ref. [1] by Eqs. (5.1) and (E.2) (with  $r = R_2$ ), respectively.

Following is a list of parameters appearing in those equations that affect the temperature distribution:

- (1) Temperature of the inner core and the arterial blood,  $T_1 = T_a$ ,
- (2) Specific heat of blood,  $c_b$ ,
- (3) Thermal conductivity of the tissue,  $k$ ,
- (4) Ratio of cooling tube width to cooling tube spacing,  $\beta$ ,
- (5) Cooling tube spacing,  $2a$ ,
- (6) Average heat flux at skin surface,  $f_a$ ,
- (7) Number of terms used in the series computation,  $n$ ,
- (8) Depth of tissue,  $b$ ,
- (9) Shape of the flux function,  $f(z)$ ,
- (10) Average rate of heat generated per unit volume of tissue,  $q_m$ ,
- (11) Average blood perfusion rate per unit volume of tissue,  $w_b$ , and, in the cylindrical model only due to the additional degree of freedom,
- (12) Radius of cylindrical shell,  $R_1$  or  $R_2$ .

The first eight of these parameters and the radius of the cylindrical shell could either be measured or estimated with a fair degree of accuracy. The remaining three, i.e.,  $f(z)$ ,  $q_m$ , and  $w_b$ , were not measured in the present work and were left to be estimated by the method of fitting theoretical curves to the experimental data. Curve fitting was done with the aid of a digital computer. Equations (5.1) and (E.2) of Ref. [1] were programmed and temperature profiles were computed for various combinations of the above three parameters. The computer output was then analyzed to determine that combination of parameters which yielded curves fitting closest with the experimental data. Simultaneously, the parameters and the corresponding temperature profiles were checked against the following criteria:

- (1) The lowest temperature on the skin (immediately underneath the cooling tube) should not be below the temperature of the cooling water; in all experiments coolant temperature was maintained at 54.5°F (12.5°C).
- (2) Blood perfusion and heat generation rates per unit volume of tissue should not exceed values found in the literature.
- (3) Only temperatures measured on the skin away from the cooling tubes were considered for the comparison.

In addition, the following two assumptions were made:

- (1) An estimated 25 to 30 Btu/hr (7.3 to 8.7 w) of the total heat removed by the cooling pads were gained from the environment.

- (2) Some heat was removed through the air gap along the areas not in contact with the cooling tubes. A parameter,  $\eta$ , denoting the ratio of heat fluxes at the uncontacted to that at the contacted areas was introduced. This ratio was usually assumed at about 10 percent.

A large number of combinations of the above parameters over a wide range were considered. Results for pads No. 2 and 3 at the high metabolic rate of 1800 Btu/hr (528 w) are shown in Figs. 4.6 and 4.7, respectively. In these figures comparison is made between the experimental results and both the cylindrical and rectangular models. The agreement between experimental and theoretical results is quite good, particularly for pad No. 2. Also, as can be observed, no significant differences exist between the cylindrical and rectangular models. It should, however, be noted that the curves presented in Figs. 4.6 and 4.7 are not unique; nor are the parameters that yielded those curves to be regarded as representing the true physiological values. The only objective that we had in mind while attempting the fitting of analytical curves to measured data was to explore whether a reasonable correspondence could be obtained. Anything beyond this specific objective is not implied. Improved techniques for measuring the unknown parameters and skin temperatures are required to render the comparison between measured and analytically predicted results more meaningful.

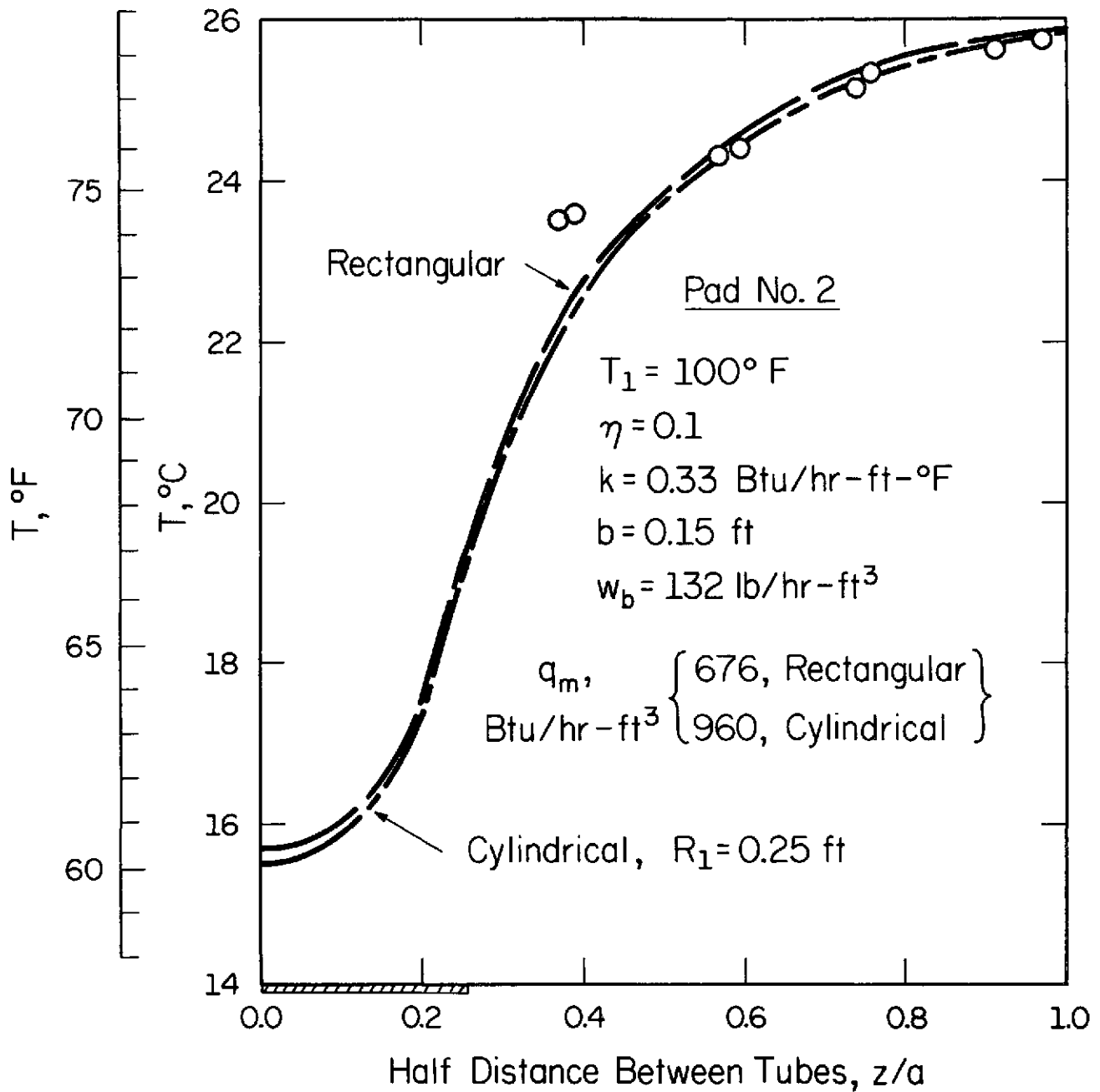


Figure 4.6 Comparison of analysis with experimental results for cooling pad No. 2. Metabolic rate 1800 Btu/hr (528 w).

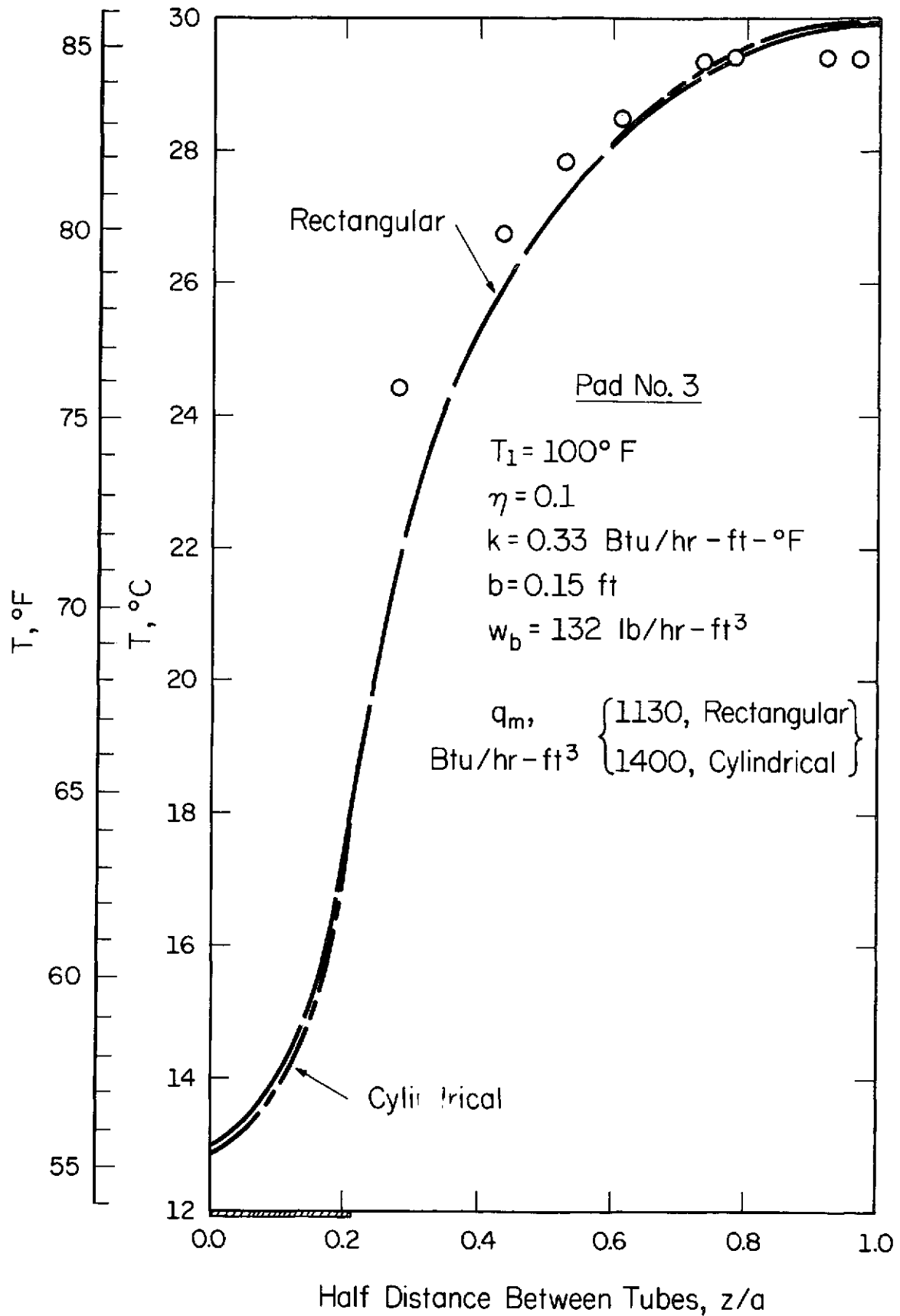


Figure 4.7 Comparison of analysis with experimental results for cooling pad No. 3. Metabolic rate 1800 Btu/hr (528 w).

#### 4.6 RESULTS OF TRANSIENT EXPERIMENTS

In experiments 7 and 8 the transient response due to a large and sudden increase in metabolic rate was studied. As shown in Fig. 4.8, the test subject stood for about three hours in order to reach a steady state temperature distribution on the skin surface. With the flow rate and input water temperature held constant, the metabolic heat generation rate was then raised from 300 Btu/hr (88 w) to 1800 Btu/hr (528 w). As can be seen, the transition in metabolic rate from low to high activity level occurred in about five minutes. The test subject maintained the 1800 Btu/hr (528 w) activity level for 90 minutes. At this time he was allowed to rest and his metabolic rate returned to 300 Btu/hr (88 w) in about ten minutes.

The transient response of the skin surface temperature profile corresponding to sudden change in the total metabolic rate was recorded for pads No. 2 and 3 in experiments 7 and 8, respectively. Figures 4.9 and 4.10 show the results of experiment 7. Figure 4.9 shows the course of change of the temperature profile on the skin surface between adjacent cooling tubes. The lowest curve at  $t = 0$  represents the fully developed temperature profile at 300 Btu/hr (88 w) and the highest curve at  $t = 40$  min represents the fully developed profile corresponding to an activity level of 1800 Btu/hr (528 w). The curves at  $t = 10$  min and  $t = 20$  min are plotted at the intermediate stages and show the nature of the development of the temperature profile.

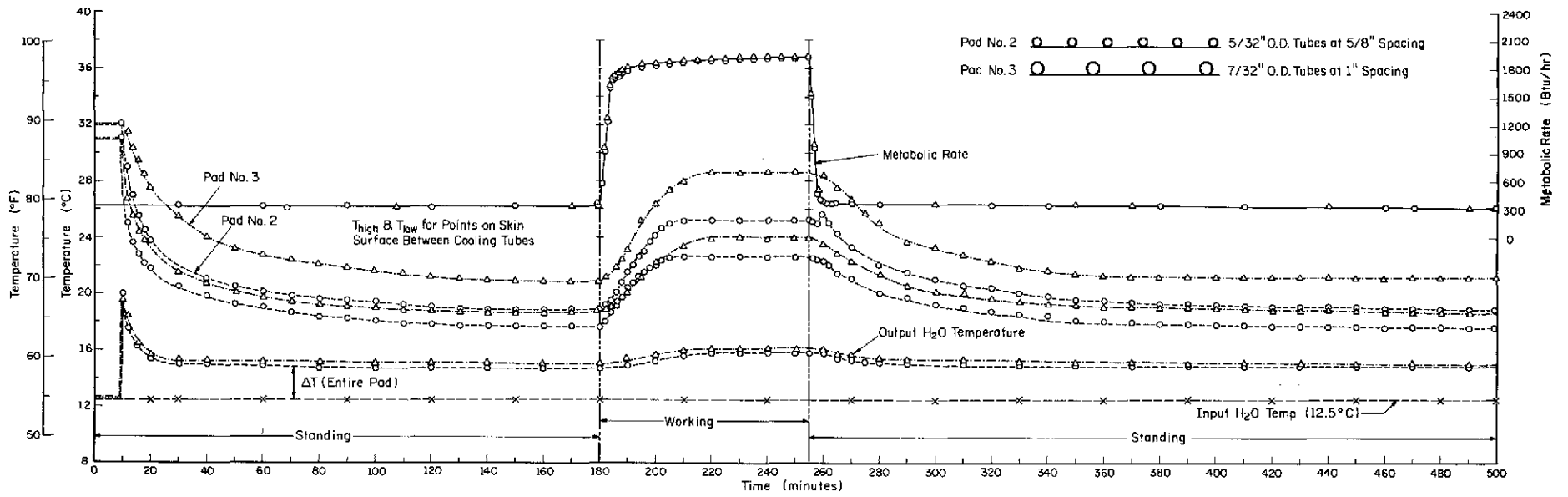


Figure 4.8 Results of experiments 7 and 8.

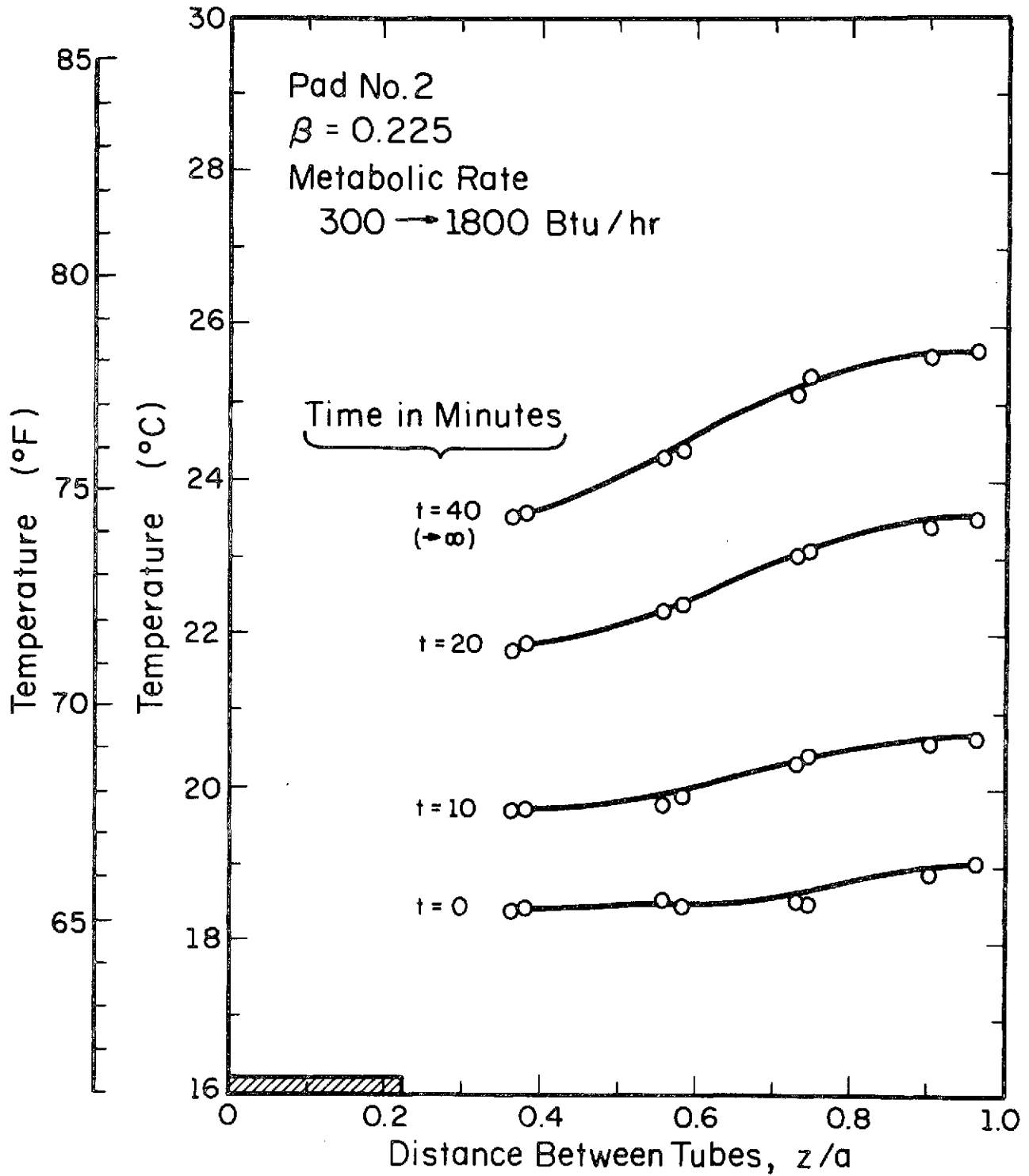


Figure 4.9 Development of temperature profile on the skin for pad No. 2 resulting from an increase in metabolic rate from 300 to 1800 Btu/hr (88 to 528 w).

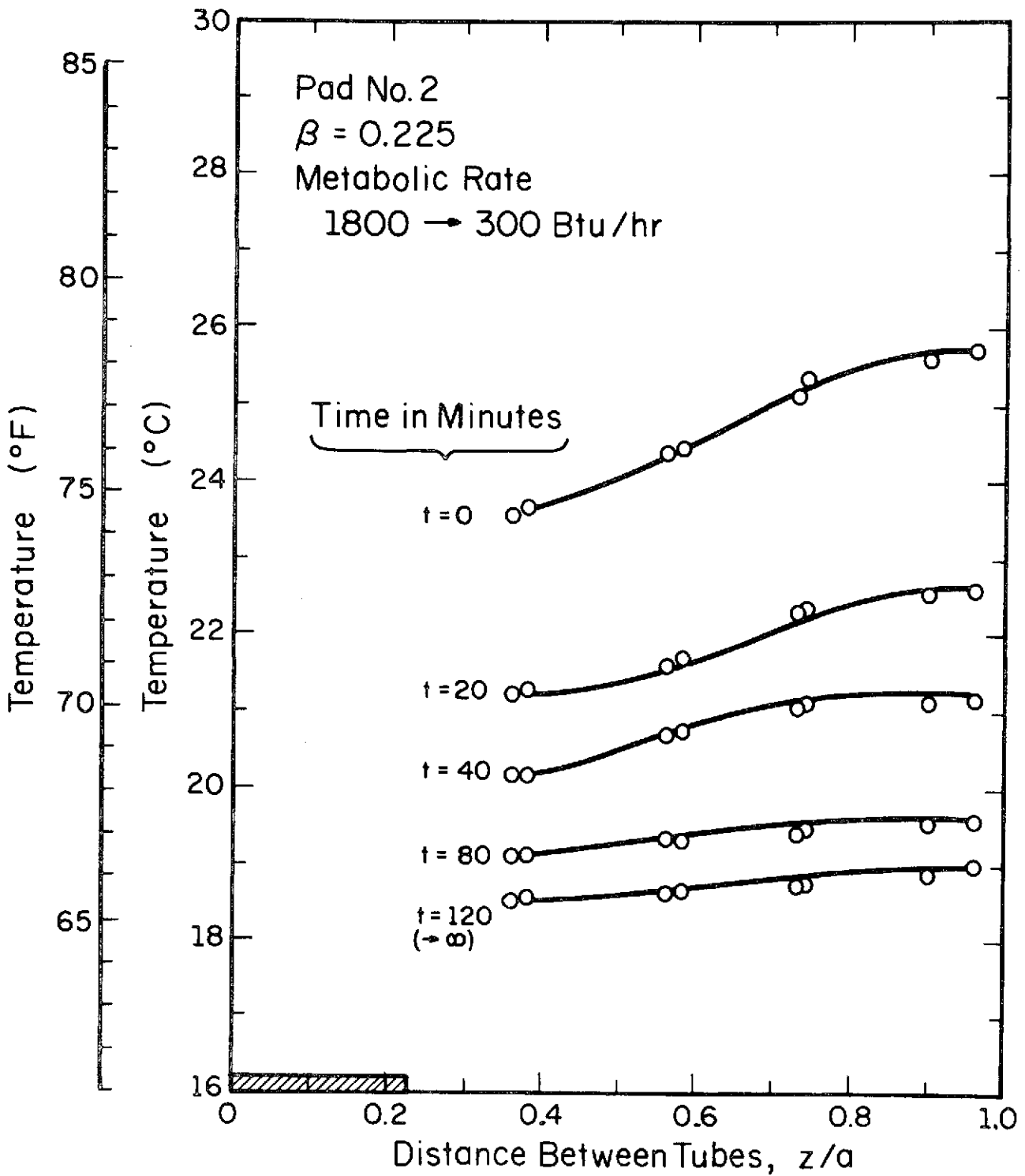


Figure 4.10 Development of temperature profile on the skin for pad No. 2 resulting from a decrease in metabolic rate from 1800 to 300 Btu/hr (528 to 88 w).

Figure 4.10 shows the course of change of the temperature profile as it changed with a decrease in metabolic rate from 1800 Btu/hr (528 w) to 300 Btu/hr (88 w). In this case the highest curve at  $t = 0$  represents the fully developed temperature profile at 1800 Btu/hr (528 w). The lower curve at  $t = 120$  represents the temperature profile at steady state corresponding to a metabolic activity rate of 300 Btu/hr (88 w). The intermediate values at  $t = 20, 40, 60$  and 80 minutes show the nature of the development of the lower temperature profile.

In the case of the increasing metabolic rate the temperature distribution reaches a steady state in 40 minutes for pad No. 2. However, a decrease in the total metabolic rate over the same range results in a transient time of 120 minutes to reach steady state for the same pad. Thus, it takes about three times as long to reach steady state when changing from a high to a low metabolic rate as compared to changing from a lower to a higher rate for pad No. 2.

The results of experiment 8 (using pad No. 3) are shown in Figs. 4.11 and 4.12. In these figures the same scheme was used to present the data as in Figs. 4.9 and 4.10. Figure 4.11 represents the change in the temperature profile for an increasing metabolic rate and Fig. 4.12 represents the change for a decreasing metabolic rate. Again, the metabolic rates ranged from 300 Btu/hr (88 w) at the low end to 1800 Btu/hr (528 w) at the high end. TABLE 4.5 summarizes the results of experiments 7 and 8 and can be used to compare the performance of pads No. 2 and 3.

The temperature profile develops slightly faster for pad No. 2 at 40 minutes as compared with a time of 60 minutes for pad No. 3

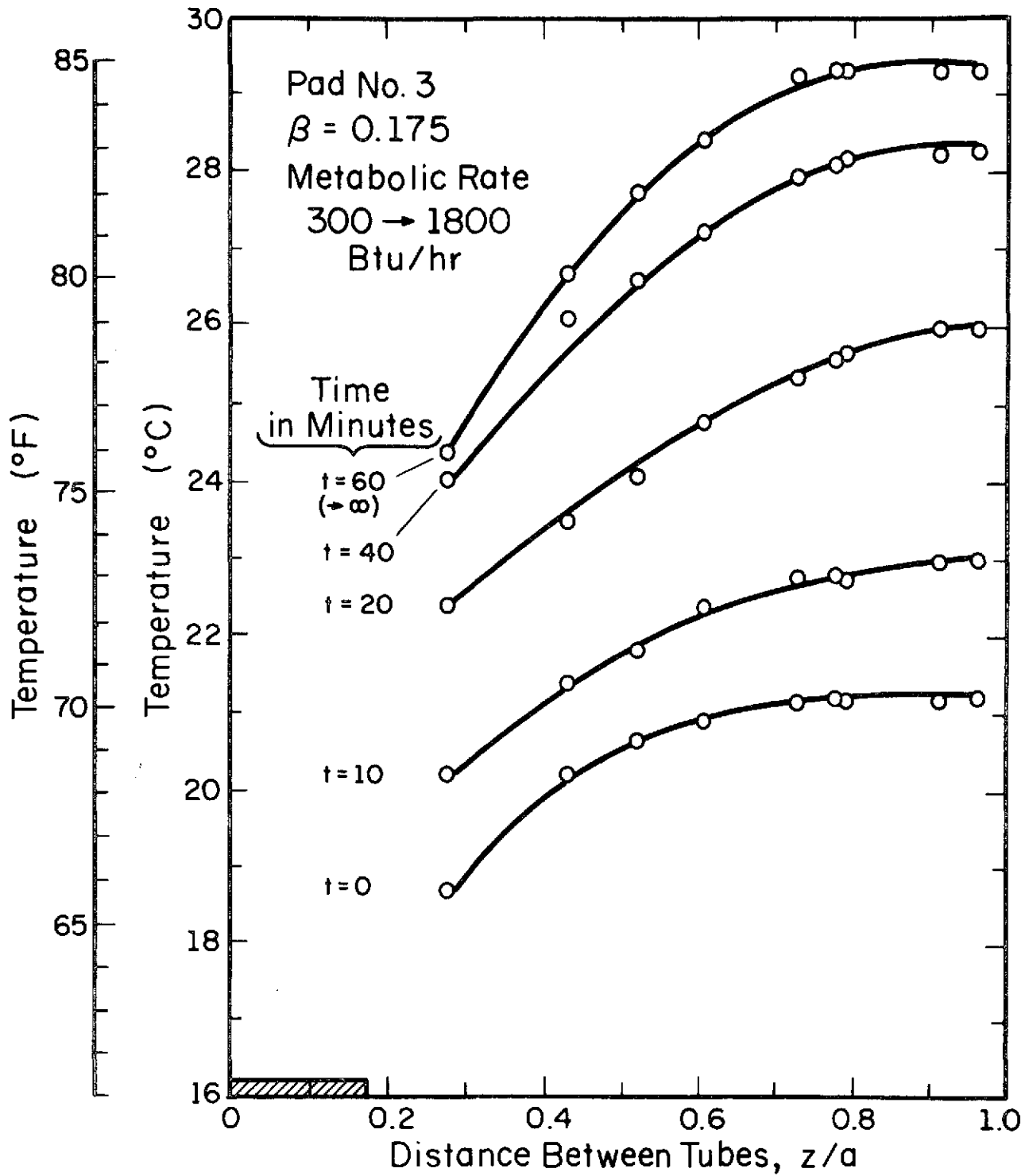


Figure 4.11 Development of temperature profile on the skin for pad No. 3 resulting from an increase in metabolic rate from 300 to 1800 Btu/hr (88 to 528 w).

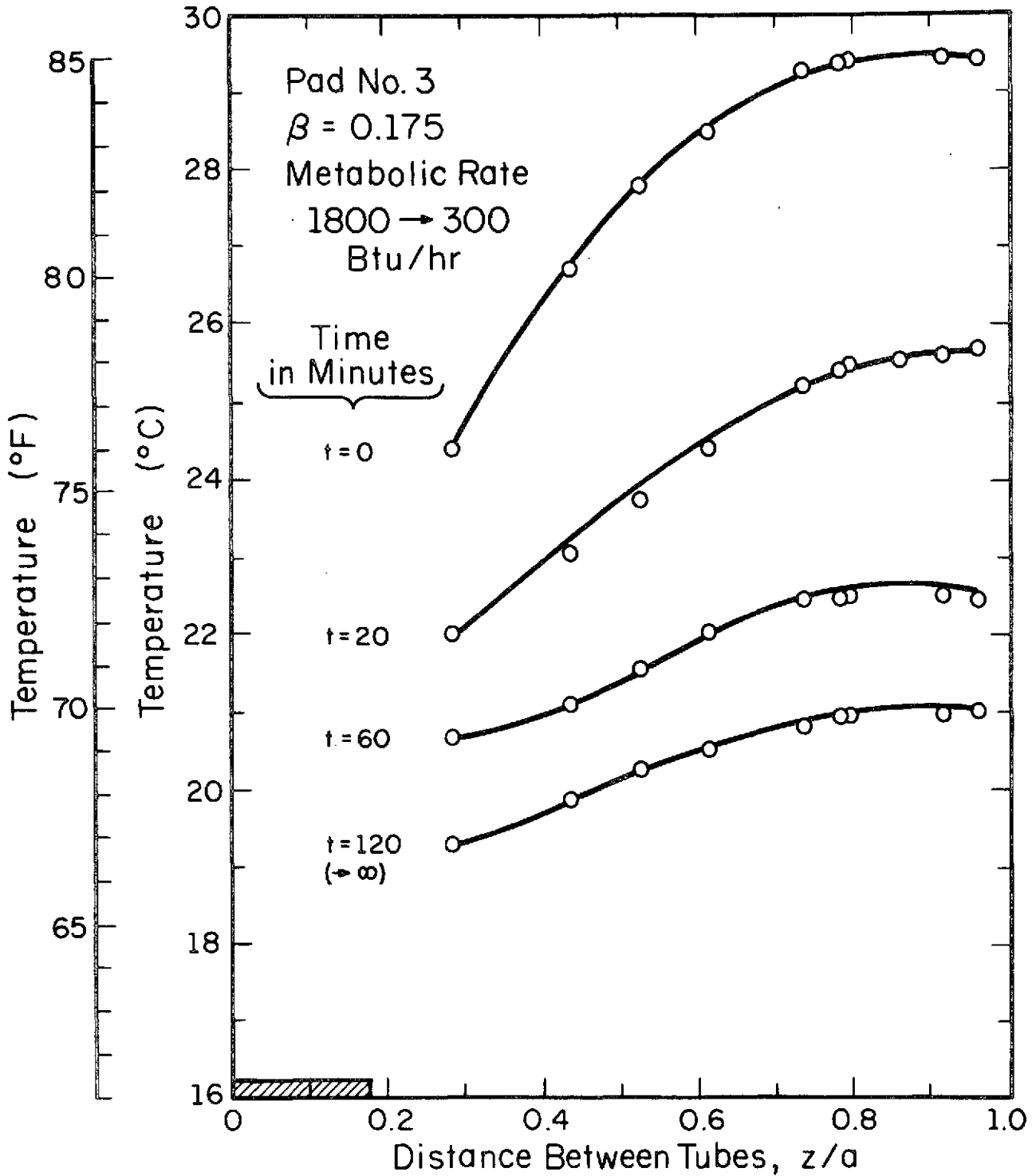


Figure 4.12 Development of temperature profile on the skin for pad No. 3 resulting from a decrease in metabolic rate from 1800 to 300 Btu/hr (528 to 88 w).

TABLE 4.5

## Results of Experiments 7 and 8

(Flow rate and water temperature remained constant)

Experiment	Pad	Change in Metabolic Rate Btu/hr	Change in Metabolic Rate w	Time to Reach Steady State Profile, Min.
7	2	300 → 1800	88 → 528	40
8	3	300 → 1800	88 → 528	60
7	2	1800 → 300	528 → 88	120
8	3	1800 → 300	528 → 88	120

for an increasing metabolic rate. The time for the temperature profile development was equal for both pads in the case of a decreasing metabolic rate. Comparison of Figs. 4.9 and 4.11 reveals that the temperature profile is both lower and flatter for pad No. 2 as compared with pad No. 3. Also, the profile was shifted about 12.5°F (7°C) for pad No. 2 compared with a 16°F (9°C) shift for pad No. 3, for the case of increasing and decreasing metabolic rates.

In general then, pad No. 2 provided a lower, more uniform temperature distribution. This temperature distribution also proved to be more stable and did not shift as much as in the case of pad No. 3 under identical conditions of change. This probably is the major factor in accounting for a smaller time constant for pad No. 2 as compared with pad No. 3.

The results for experiments 9 and 10 are shown in Fig. 4.13. As illustrated in Fig. 4.13, the skin temperatures were monitored

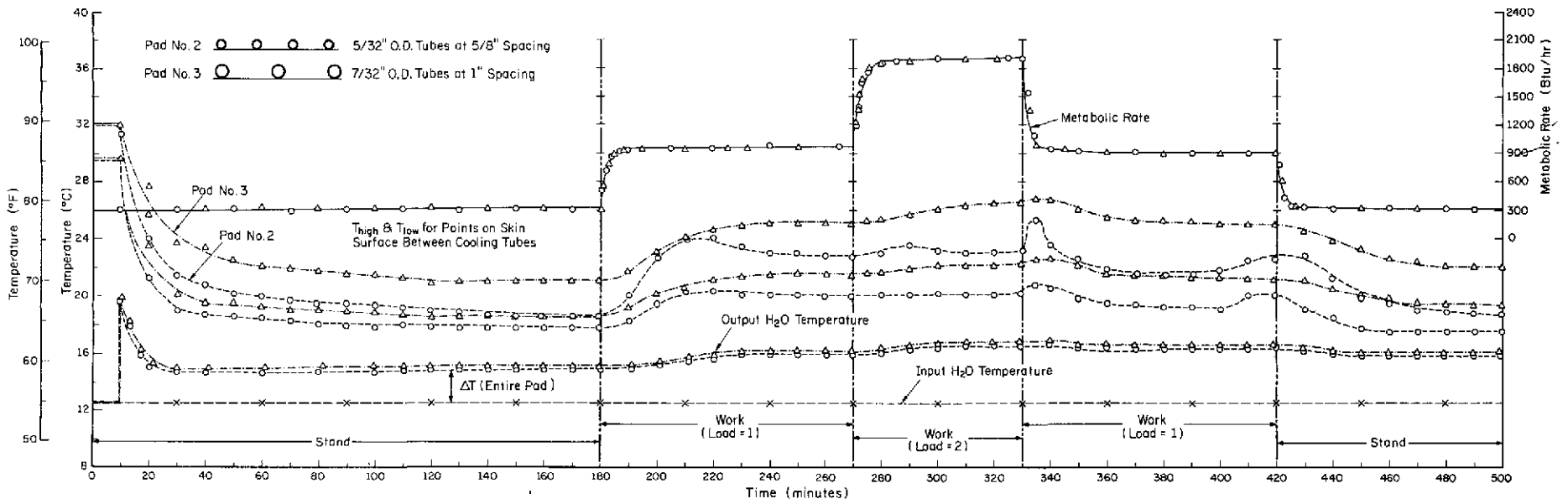


Figure 4.13 Results of experiments 9 and 10.

for pads No. 2 and 3 for several transient metabolic conditions.

The transient intervals analyzed were as follows: increasing metabolic rates for pads No. 2 and 3 from:

1. 300 Btu/hr (88 w) to 900 Btu/hr (264 w),
2. 900 Btu/hr (264 w) to 1800 Btu/hr (528 w)

and reversed sequence of decreasing metabolic rates for pads No. 2 and 3 from:

3. 1800 Btu/hr (528 w) to 900 Btu/hr (264 w)
4. 900 Btu/hr (264 w) to 300 Btu/hr (88 w).

Again, it can be noted that the test subject required very little time to reach a steady metabolic rate for each new activity. This fact supports the initial assumption that changes in metabolic rates can be regarded as step functions as compared to changes in temperature.

There are relatively short duration increases in temperature occurring at the beginning of some of the work loads, particularly after a reduction in metabolic rate. The rapidity of this change indicates a physiological response of some kind, such as a sudden reduction in blood flow.

Figure 4.14 shows the course of change for the temperature profile reacting to changes from low to moderate and to high metabolic activity levels for pad No. 2. Figure 4.15 shows the nature of the temperature distributions as the metabolic rate decreases from high to low.

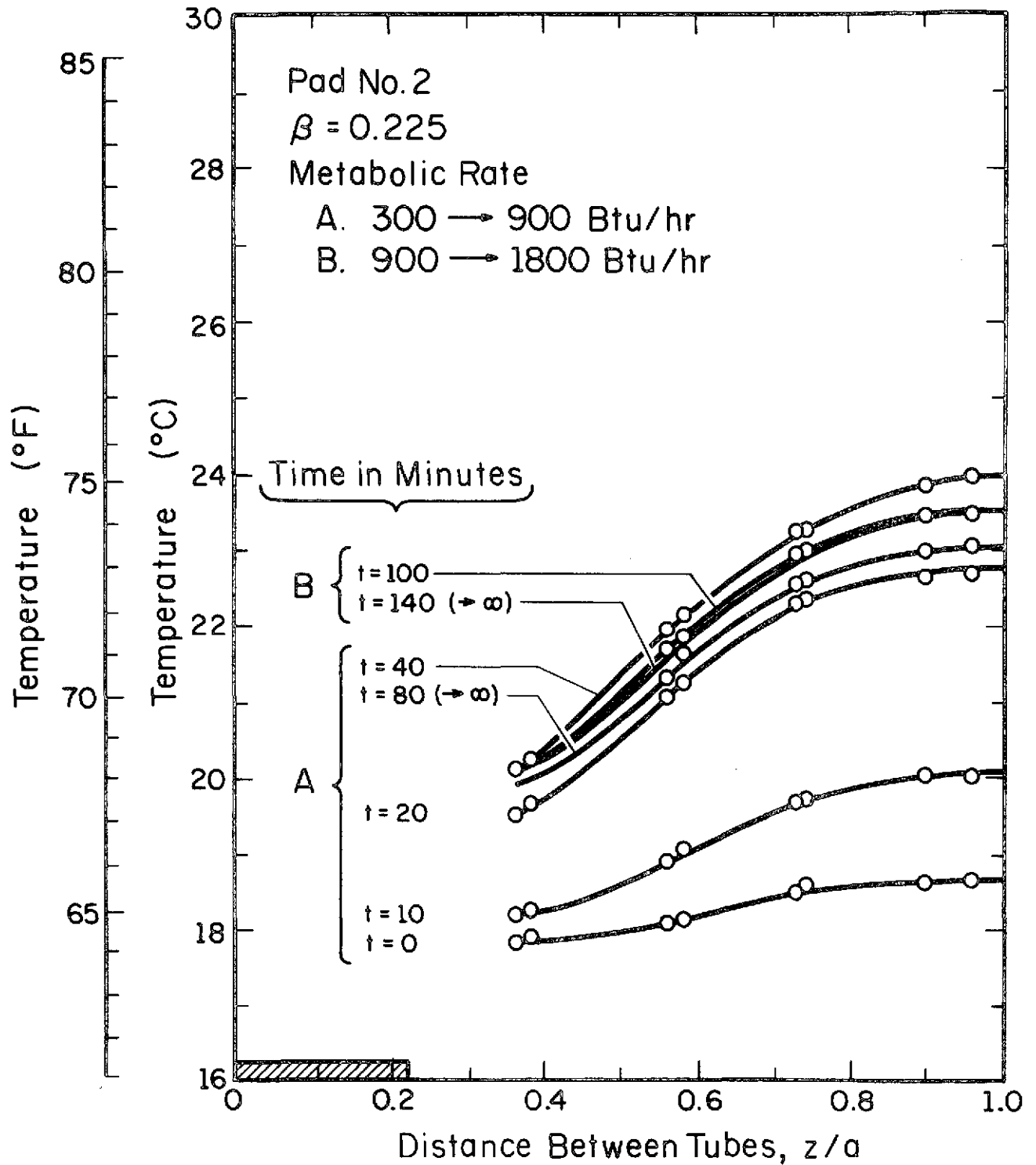


Figure 4.14 Development of temperature profile on the skin for pad No. 2 resulting from increases in metabolic rates from 300 to 900 Btu/hr (88 to 264 w) and from 900 to 1800 Btu/hr (264 to 528 w).

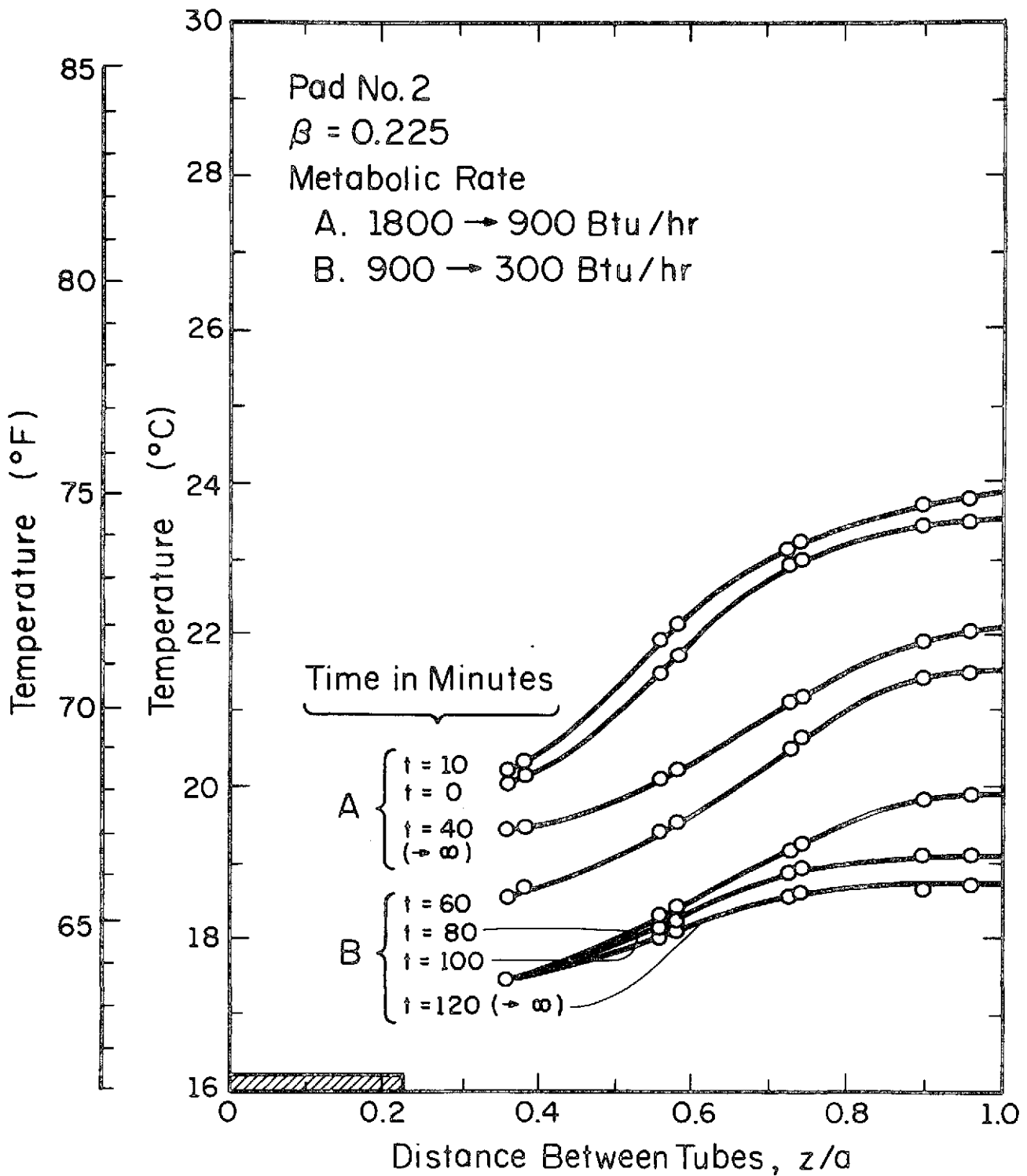


Figure 4.15 Development of temperature profile on the skin for pad No. 2 resulting from decreases in metabolic rates from 1800 to 900 Btu/hr (528 to 264 w) and from 900 to 300 Btu/hr (264 to 88 w).

The results of experiment 10 are shown in Figs. 4.16 and 4.17. In this case pad No. 3 was tested and the temperature distributions were measured in accordance with changes in metabolic activity from low to high and from high to low. The results of experiments 9 and 10 are presented in summary form in TABLE 4.6. It can be seen that both pads No. 2 and 3 required a time of 80 minutes to reach a steady state temperature distribution in accordance with an increase in metabolic activity from 300 to 900 Btu/hr (88 w to 264 w). Similarly, pads No. 2 and 3 also required an additional time of sixty minutes to reach steady state with an increase in metabolic rate from 900 Btu/hr to 1800 Btu/hr (264 w to 528 w).

TABLE 4.6

Results of Experiments 9 and 10

(Flow rates and input water temperatures held constant)

Experiment	Pad	Change in Metabolic Rate Btu/hr	Change in Metabolic Rate w	Time to Reach Steady State Profile, min.
9	2	300 → 900	88 → 264	80
10	3	300 → 900	88 → 264	80
9	2	900 → 1800	264 → 528	60
10	3	900 → 1800	264 → 528	60
9	2	1800 → 900	528 → 264	40
10	3	1800 → 900	528 → 264	80
9	2	900 → 300	264 → 88	80
10	3	900 → 300	264 → 88	60

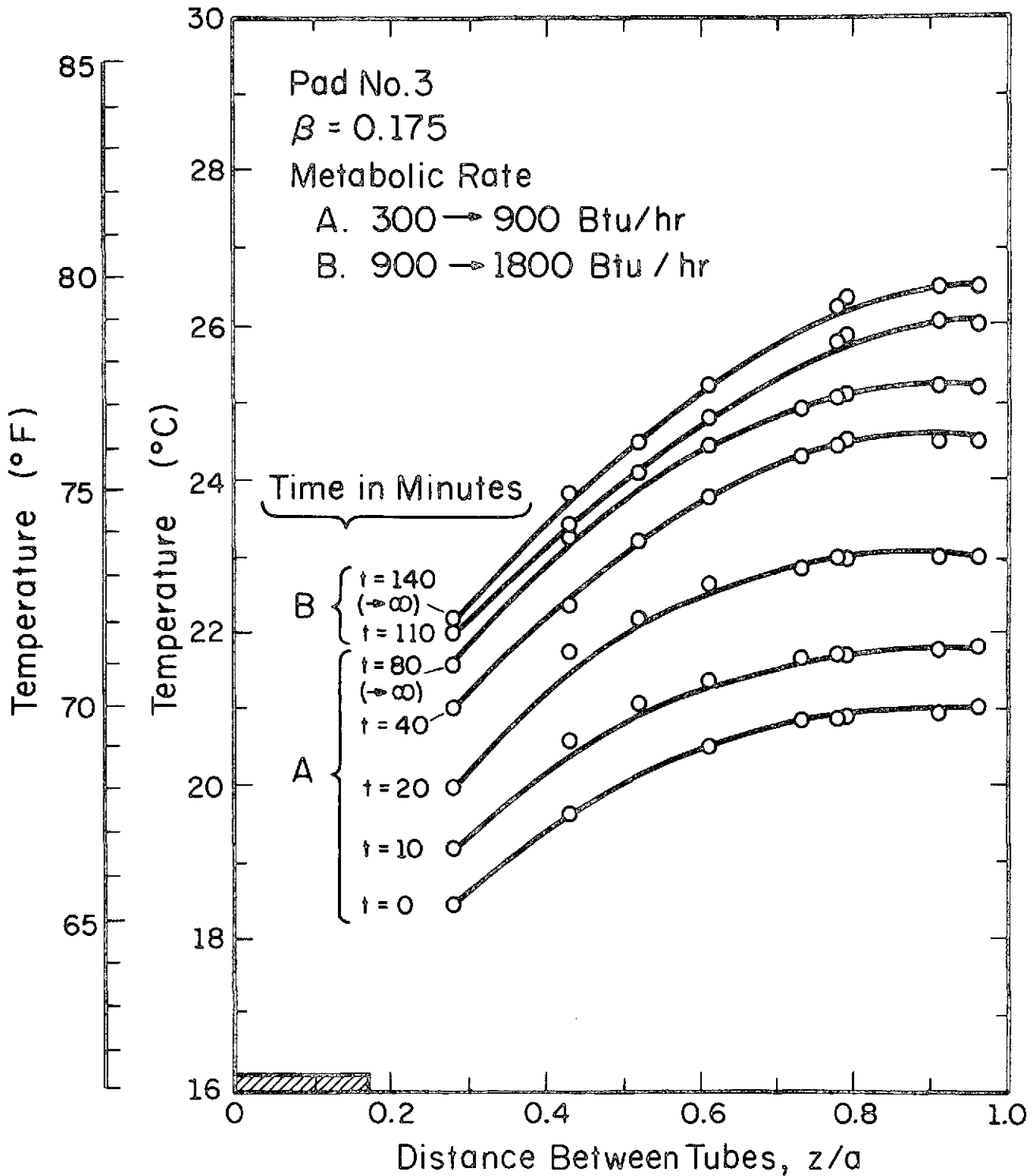


Figure 4.16 Development of temperature profile on the skin for pad No. 3 resulting from increases in metabolic rates from 300 to 900 Btu/hr (88 to 264 w) and from 900 to 1800 Btu/hr (264 to 528 w).

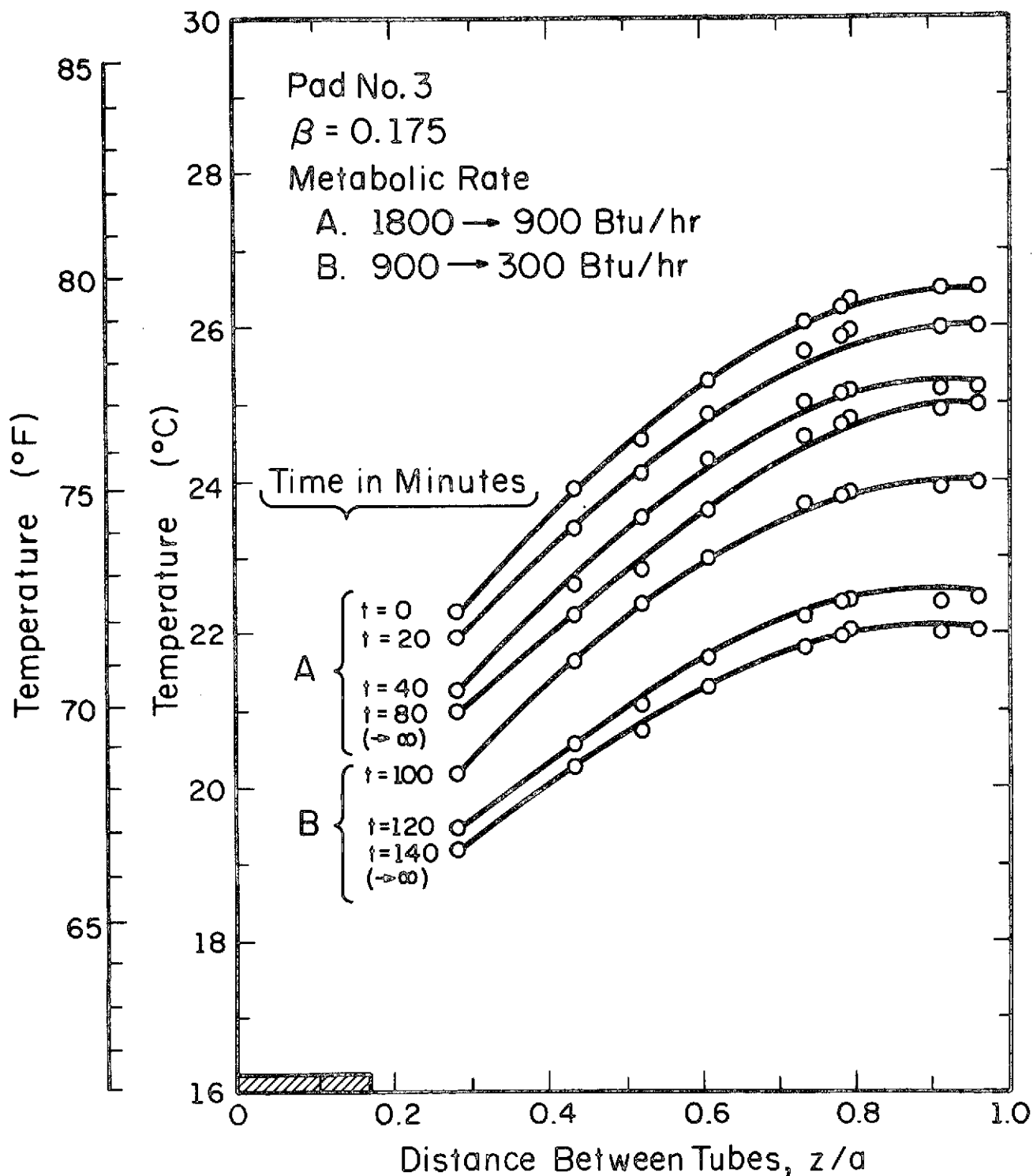


Figure 4.17 Development of temperature profile on the skin for pad No. 3 resulting from decreases in metabolic rates from 1800 to 900 Btu/hr (528 to 264 w) and from 900 to 300 Btu/hr (264 to 88 w).

In response to a decrease in metabolic activity, it was noted that pad No. 3 required 80 minutes to reach steady state, whereas pad No. 2 required only 40 minutes to reach the same level.

For the transition from 900 Btu/hr (264 w) to 300 Btu/hr (88 w), it can be seen that pad No. 3 required less time (60 minutes) than did pad No. 2 which required 80 minutes to reach steady state. It should be noted, however (see Fig. 4.15), that, in the case of pad No. 2, the lowest temperature was reached in approximately 40 minutes. During the remaining 40 minutes of the development of the steady state temperature profile, only the middle or warmer portion of the distribution was affected.

Again, some general comments can be made with respect to pad No. 2 in that it provided a lower, more uniform temperature distribution than did pad No. 3. Also, there was less of a range of temperature variation in the case of pad No. 2 as compared with pad No. 3. All of these observations can be accounted for by the higher tube density of pad No. 2 and the corresponding increase in cooling effectiveness.

## 5. SUMMARY AND CONCLUSIONS

Three separate cooling pads with different cooling tube sizes and spacings were constructed and tested. These pads were equipped with thermocouples and were used to measure the temperature profiles on the skin surface of the right thigh between adjacent cooling tubes. All pads were tested under the same experimental conditions with equal coolant flow rate and temperature. Pad No. 2 which consisted of 5/32 in. tubes spaced at 5/8 in. intervals provided the best cooling capacity. Pad No. 2 removed 15 percent of the total heat generated at high metabolic rates and much higher percentages at low metabolic rates. Pad No. 2 provided the lowest and most uniform skin temperature profiles throughout the tests. Also, the temperature profiles on the skin did not shift as much with changes in metabolic rate for pad No. 2 than with pads No. 1 and 3. The time constants for surface temperatures associated with changes in metabolic rate were also smallest for pad No. 2. In general, it can be concluded that pad No. 2 provided a lower, much more uniform and stable temperature distribution on the skin surface than was attainable with pads No. 1 and 3.

Times required for reaching a steady state from the onset of a change in activity level were also recorded. When an increase in metabolic rate was introduced, the times involved were found to be between 40 to 60 minutes, the shorter periods pertaining to pad No. 2 with the higher density of tubes. When the change in activity level was reversed, i.e., high (1800 Btu/hr, 528 w) to low (300 Btu/hr, 88 w), times for reaching a steady state temperature profile were about equal for pads No. 2 and 3 at 120 minutes. Thus, a ratio of

about 2-3 was found between the lengths of time required for the development of temperature profiles for extreme, opposite changes in levels of activity. When intermediate changes were used (experiments 9 and 10), the ratios of transient times were found to be of the order of 1-1.5. Overall transient times for these double-step changes were of the same order ( $\sim 140$  min) for both increasing and decreasing metabolic rates.

It is clear that both tube size and spacing have a noticeable effect on overall cooling efficiency. In order to optimize the relationship between these two parameters then, a definition of maximum metabolic rate should be secured. Once obtained, a cooling pad can be designed that will remove heat from the body at any predetermined rate.

A time dependent analytical solution has been obtained for the biothermal model in cylindrical coordinates. Equation (2.18) is the solution as a function of  $r$ ,  $z$ , and  $t$  and was used to predict the transient temperature distributions on the skin surface between adjacent cooling tubes and for the one-dimensional geometry (uniform cooling of the skin).

A comparison between steady state measured and analytical results was attempted. The comparison was made with both the cylindrical and rectangular models of Ref. [1]. Agreement between measured and predicted results was found to be fair, particularly for pad No. 2. Improved techniques for measuring skin temperatures and physiological quantities, e.g., blood perfusion and metabolic heat generation rates, are required to render the comparison more meaningful and reliable.

## REFERENCES

1. Shitzer, A., Chato, J. C. and Hertig, B. A., "A Study of the Thermal Behavior of Living Biological Tissue with Application to Thermal Control of Protective Suits," University of Illinois Technical Report, No. ME-TR-207, January 1971.
2. Nunneley, S. A., "Water Cooled Garments: A Review," Space Life Sciences, 2, 1970, pp. 335-360.
3. Burton, D. R. and Collier, L., "The Development of Water Conditioned Suits," Technical Note ME-400, Royal Aircraft Establishment, Farnborough, England, 1964.
4. Chambers, A. B., "Controlling Thermal Comfort in the EVA Space Suit," ASHRAE J., March 1970, pp. 33-38.
5. Waligora, J. S. and Michel, E. L., "Application of Conductive Cooling for Working Men in a Thermally Isolated Environment," Aerospace Medicine, 39, pp. 485-487, 1968.
6. Allen, J. R., "The Liquid Conditioned Suit, a Physiological Assessment," Memo 234, Flying Personnel Research Committee, Royal Air Force Institute of Aviation Medicine, Farnborough, England, 1966.
7. Chato, J. C., Hertig, B. A., et al., "Physiological and Engineering Study of Advanced Thermoregulatory Systems for Extra Vehicular Space Suits," Semiannual Report No. 2, NASA Grant No. NGR 14-005-103, June 1968.
8. Crocker, J. F., Webb, P. and Jennings, D. C., "Metabolic Heat Balances in Working Men Wearing Liquid Cooled Sealed Clothing," AIAA-NASA Third Manned Spacecraft Meeting, AIAA Publication CP-10, 1964, pp. 111-117.
9. Jennings, D. C., "Water Cooled Space Suit," J. Spacecraft, August 1966, pp. 1251-1256.
10. Allen, J. R., "Protection of Air Crews Against Heat," paper presented to Ergonomics Research Society Annual Conference, 1970.
11. Veghte, J. H., "Efficiency of Pressure Suit Cooling Systems in Hot Environments," Aerospace Medicine, 36, 1965, pp. 964-967.
12. Santa Maria, L.J., "Physiological Effects of Water Cooling under Different Environmental Conditions," Portable Life Support Systems, NASA SP-234, 1970, pp. 211- 220.
13. Webb, P. and Annis, J. R., "Cooling Required to Suppress Sweating During Work," J. Applied Physiology, 25, 1968, pp. 489-493.

14. Champaign-Urbana Courier, an Associated Press News Article, March 2, 1971.
15. Chato, J. C., and Shitzer, A., "Thermal Modeling of the Human Body--Further Solutions of the Steady-State Heat Equation," AIAA Journal, Vol. 9, 1971, pp. 865-869.
16. Pennes, H. H., "Analysis of Tissue and Arterial Blood Temperature in the Resting Human Forearm," J. of Applied Physiology, Vol. 1, 1948, pp. 93-122.
17. Hertzman, A. B., "Some Relations between Skin Temperature and Blood Flow," American Journal of Physical Medicine, Vol. 32, 1953, pp. 233-251.
18. Wissler, E. H., "Steady State Temperature Distribution in Man," J. of Applied Physiology, Vol. 16, 1961, pp. 734-740.
19. Perl, W., "Heat and Matter Distribution in Body Tissues and the Determination of Tissue Blood Flow by Local Clearance Methods," J. of Theoretical Biology, Vol. 2, 1962, pp. 201-235.
20. Chato, J. C., "A Method for the Measurement of Thermal Properties of Biological Materials," Thermal Problems in Biotechnology, ASME Symposium Series, 1968, pp. 16-25.
21. Trezek, G. J. and Cooper, T. E., "Analytical Determination of Cylindrical Source Temperature Fields and Their Relation to Thermal Diffusivity of Brain Tissue," Thermal Problems in Biotechnology, ASME Symposium Series, 1968, pp. 1-15.
22. Keller, K. H. and Seiler, L., "An Analysis of Peripheral Heat Transfer in Humans," Simulation Council Meeting, Chicago, Ill., March 9-10, 1970.
23. Grollman, S., The Human Body--Its Structure and Physiology, Second Edition, The Macmillan Co., London, England, 1969, p. 166.
24. Johnson, R. E., Robbins, F., Schilke, R., Mole, P., Harris, J. and Wakat, D., "A Versatile System for the Measurement of Oxygen Consumption in a Man," J. of Applied Physiology, Vol. 22, 1967, pp. 377-379.
25. Molnar, S., "The Relationship between Cardiac Time Components, Maximal Oxygen Consumption and Endurance Performance," University of Illinois at Urbana-Champaign, Ph.D. Thesis, 1970.
26. Consolazio, F. C., Johnson, R. E. and Pecora, L. J., Physiological Measurements of Metabolic Functions in Man, McGraw-Hill Book Co., New York, 1963.
27. Carpenter, T. M., Tables, Factors and Formulas for Computing Respiratory Exchange and Biological Transformation of Energy, Third Edition, Carnegie Institute of Washington, Washington, D.C., 1939.

A LINEAR COMBINATION OF MODIFIED BESSEL FUNCTIONS

A. Shitzer

J. C. Chato

Technical Note No. ME-TN-310

November 1971

DEPARTMENT OF MECHANICAL AND INDUSTRIAL ENGINEERING  
LABORATORY FOR ERGONOMICS RESEARCH  
ENGINEERING EXPERIMENT STATION  
UNIVERSITY OF ILLINOIS AT URBANA - CHAMPAIGN  
URBANA, ILLINOIS 61801



# A LINEAR COMBINATION OF MODIFIED BESSEL FUNCTIONS

by

A. SHITZER  
J. C. CHATO

Technical Note No. ME - TN - 310  
November 1971

Supported by  
National Aeronautics and Space Administration  
under  
Grant No. NGR-14-005-103

*I* 424<

A LINEAR COMBINATION OF MODIFIED BESSEL FUNCTIONS

by

A. Shitzer

J.C. Chato

Research Supported by  
National Aeronautics and Space Administration  
under  
Grant No. NGR-14-005-103

Technical Note No. ME-TN-310

November 1971

Department of Mechanical and Industrial Engineering  
Laboratory for Ergonomics Research  
Engineering Experiment Station  
University of Illinois at Urbana-Champaign  
Urbana, Illinois 61801

/

## ABSTRACT

A linear combination of modified Bessel functions is defined, discussed briefly, and tabulated; namely,

$$\Psi_{k\ell}^1(\lambda x) \equiv I_k(\lambda x) K_\ell(\lambda x_1) - (-1)^{k+\ell} I_\ell(\lambda x_1) K_k(\lambda x)$$

This combination was found to recur in the analysis of various heat transfer problems and in the analysis of the thermal behavior of living tissue when modeled by cylindrical shells.

## 1. INTRODUCTION

Many physics and engineering problems are amenable to solutions in terms of Bessel functions. These functions have been extensively studied and tabulated. A hitherto undefined linear combination of modified Bessel functions was found to recur in the analysis of numerous engineering problems dealing with diffusion phenomena. Some examples in heat transfer are: steady heat flow in thin rods, tapering fins and thin fins around cylinders, electrical transmission lines, Laplace transforms applied to flow of heat in cylinders, and the modeling of living tissue by the "bio-heat" equation. This combination of Bessel functions is defined, discussed, and tabulated in this paper.

## 2. ANALYSIS

Consideration of a steady state energy balance in a heat generating material whose heat source is linearly dependent on the temperature leads to the following equation:

$$\nabla^2 T - \lambda^2 T = 0 \quad (1)$$

where  $T$  is the temperature of the medium and  $\lambda^2$  is the ratio of the strength of the source per unit time, degree and unit volume to the conductivity of the medium. In many cases, and for cylindrical geometries in particular, Eq. (1) may yield the following equation [1,2]\*

$$Y'' + \frac{1}{x} Y' - (\lambda^2 + \nu^2/x) Y = 0 \quad (2)$$

Equation (2) is referred to as the modified Bessel equation of order  $\nu$ .

If  $\nu$  is an integer, the following linear combination of modified Bessel functions is found to recur in the solution of Eq. (2):

$$\Psi_{k\ell}^1(\lambda x) \equiv I_k(\lambda x) K_\ell(\lambda x_1) - (-1)^{k+\ell} I_\ell(\lambda x_1) K_k(\lambda x) \quad (3a)$$

or

$$\Psi_{k\ell}^1(\lambda x) \equiv \begin{vmatrix} I_k(\lambda x) & (-1)^{k+\ell} K_k(\lambda x) \\ I_\ell(\lambda x_1) & K_\ell(\lambda x_1) \end{vmatrix} \quad (3b)$$

This shorthand definition of the linear combination of modified Bessel functions simplifies the analysis of the problems considerably. Furthermore, it was observed that the function defined in Eqs. (3a) or (3b)

---

\*Numbers in brackets refer to entries in REFERENCES.

exhibits a few interesting characteristics that render the above definition even more useful. These characteristics are:

- (a) By definition, the function  $\Psi_{k\ell}^1(\lambda x)$  satisfies the modified Bessel equation of order  $k$ ,

$$\frac{1}{x} \frac{d}{dx} \left[ x \frac{d\Psi_{k\ell}^1(\lambda x)}{dx} \right] - \left( \lambda^2 - \frac{k^2}{x^2} \right) \Psi_{k\ell}^1(\lambda x) = 0 \quad (4)$$

- (b) This function obeys the same differentiation rule as does the modified Bessel function of the first kind.

$$x \frac{d}{dx} \left[ \Psi_{k\ell}^1(\lambda x) \right] = k \Psi_{k\ell}^1(\lambda x) + \lambda x \Psi_{(k+1)\ell}^1(\lambda x) \quad (5)$$

Therefore, it is not a so-called cylinder function.

- (c) For two consecutive indices the following identity is obtained [3 (p. 375)].

$$\Psi_{k(k+1)}^1(\lambda x_1) \equiv \frac{1}{\lambda x_1} \quad (6)$$

- (d) When the indices are reversed in order, the following expression is obtained:

$$\Psi_{k\ell}^1(\lambda x_j) = (-1)^{k+\ell+1} \Psi_{\ell k}^j(\lambda x_i) \quad (7)$$

- (e) For identical indices the following result is obtained

$$\Psi_{kk}^1(\lambda x_1) \equiv 0 \quad (8)$$

The above list of characteristics is not an exhaustive one.

When plotted on semi-log coordinates, the function  $\Psi_{k(k+1)}^1(\lambda x)$  appears to behave as two straight lines as shown in Figs. 1 and 2. Also, the absolute magnitudes of the slopes of these lines seem to be identical. These characteristics suggest the approximation of the function by an exponential expression of the kind

$$\Psi_{k(k+1)}^1(\lambda x) \approx \exp U(\lambda x_1) + S\lambda x \quad (9)$$

for

$$\lambda x < X_2$$

and

$$\lambda x > X_3$$

where  $X_2 < \lambda x_1$  and  $X_3 > \lambda x_1$ . The branches are symmetrical with respect to  $\lambda x = \lambda x_1$  with slopes of  $S \approx -0.43$  and  $S \approx 0.43$ , respectively. For the right-hand branch, *i.e.*,  $\lambda x > X_3$ ,  $U$  is about  $-0.5\lambda x_1$ , whereas for the left-hand branch  $U$  is of the order of  $0.4\lambda x_1$ .

Figures 3 and 4 show the function for repeated subscripts 0 and 1.

A simple computer program was written for the purpose of computing the function  $\Psi_{k\ell}^1(\lambda x) = \Psi_{k\ell}^1(X)$ . Results for the first four combinations of indices are given in the tables. Values of the arguments,  $X$  as well as  $X_1$ , in the tables are for the range 0.01 to 100.

### 3. ACKNOWLEDGMENT

Numerical computations were carried out on the IBM 360/75 computer at the Computer Science Laboratory of the University of Illinois at Urbana-Champaign.

### REFERENCES

1. McLachlan, N. W., Bessel Functions for Engineers, Oxford University Press, London, 1948.
2. Shitzer, A., "A Study of the Thermal Behavior of Living Biological Tissue with Application to Thermal Control of Protective Suits," Ph.D. Thesis, University of Illinois at Urbana-Champaign, 1971. Also Technical Report No. ME-TR-207, Department of Mechanical and Industrial Engineering, University of Illinois at Urbana-Champaign, 1971.
3. Abramovitz, M. and Stegun, I. A., Handbook of Mathematical Functions, Dover Publications, New York, 1965.

### LIST OF FIGURES

- Figure 1 The function  $\Psi_{01}^1(\lambda x)$  drawn on semi-log coordinates.
- Figure 2 The function  $\Psi_{12}^1(\lambda x)$  drawn on semi-log coordinates
- Figure 3 The function  $\Psi_{00}^1(\lambda x)$
- Figure 4 The function  $\Psi_{11}^1(\lambda x)$

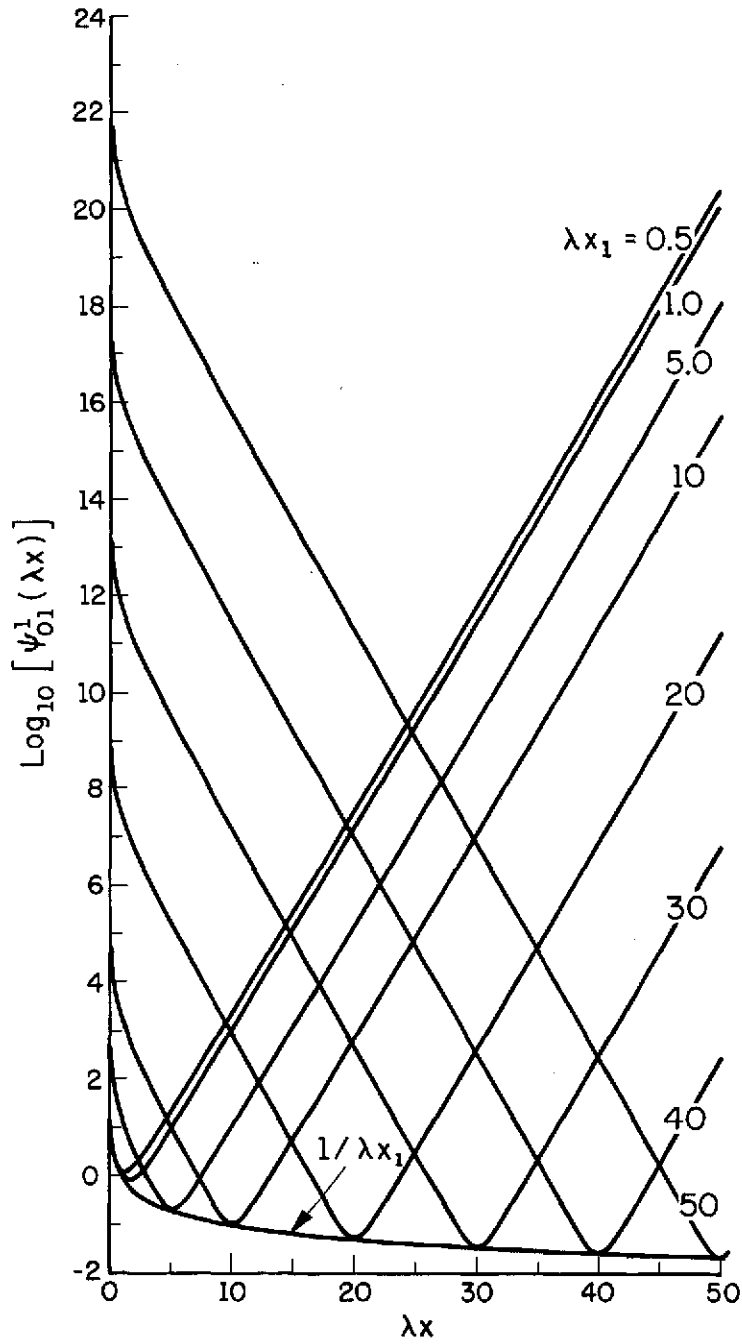


Figure 1 The function  $\psi_{01}^1(\lambda x)$  drawn on semi-log coordinates

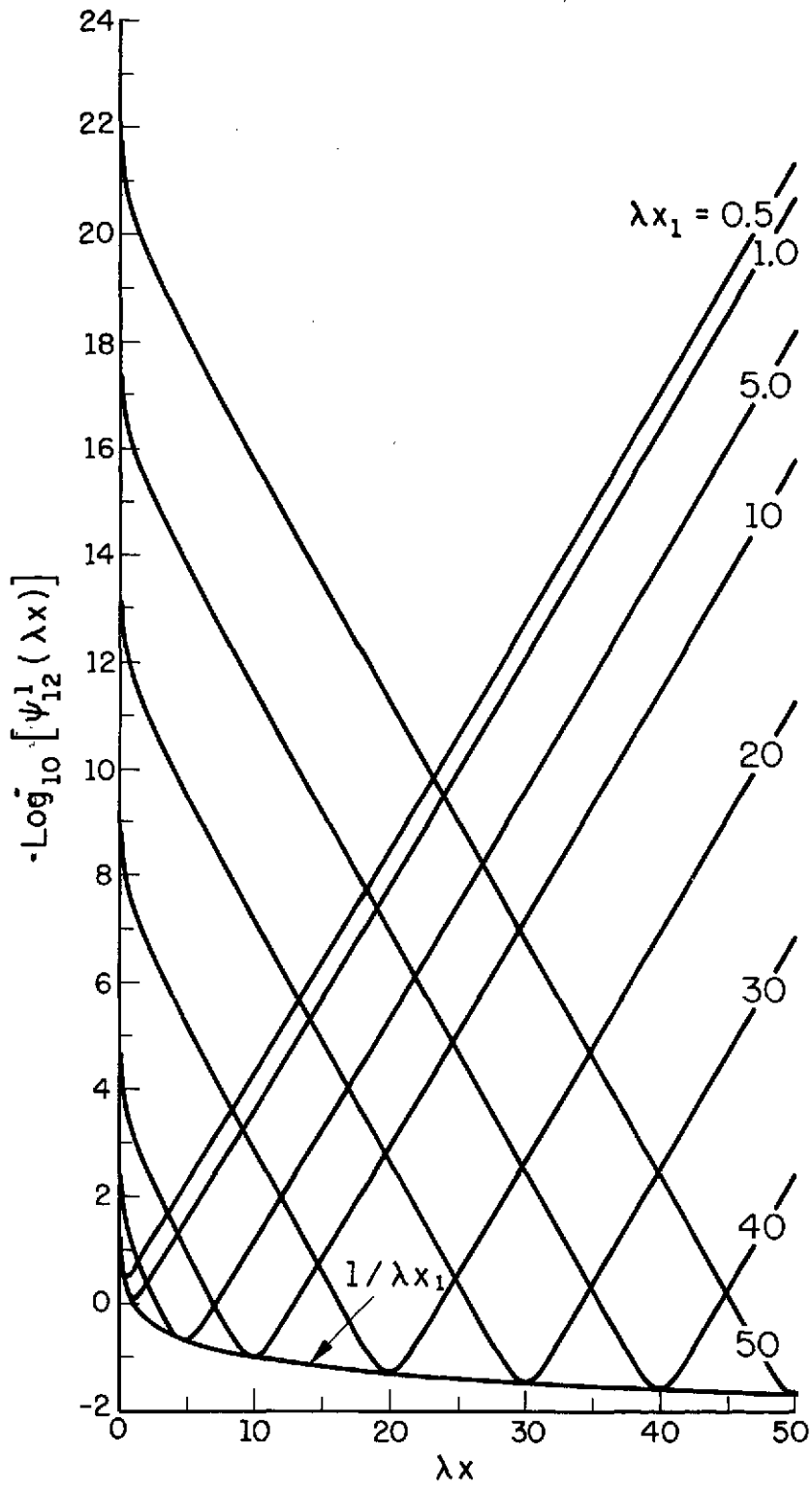


Figure 2 The function  $\psi_{12}^1(\lambda x)$  drawn on semi-log coordinates

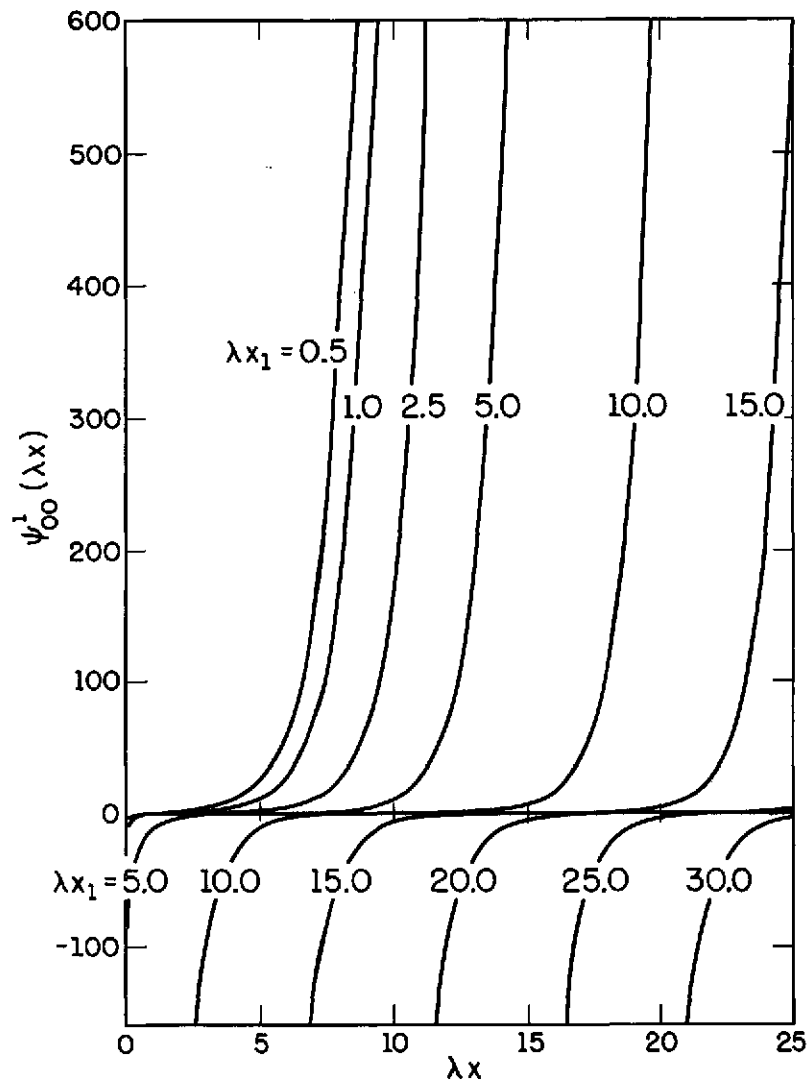


Figure 3 The function  $\psi_{00}^1(\lambda x)$

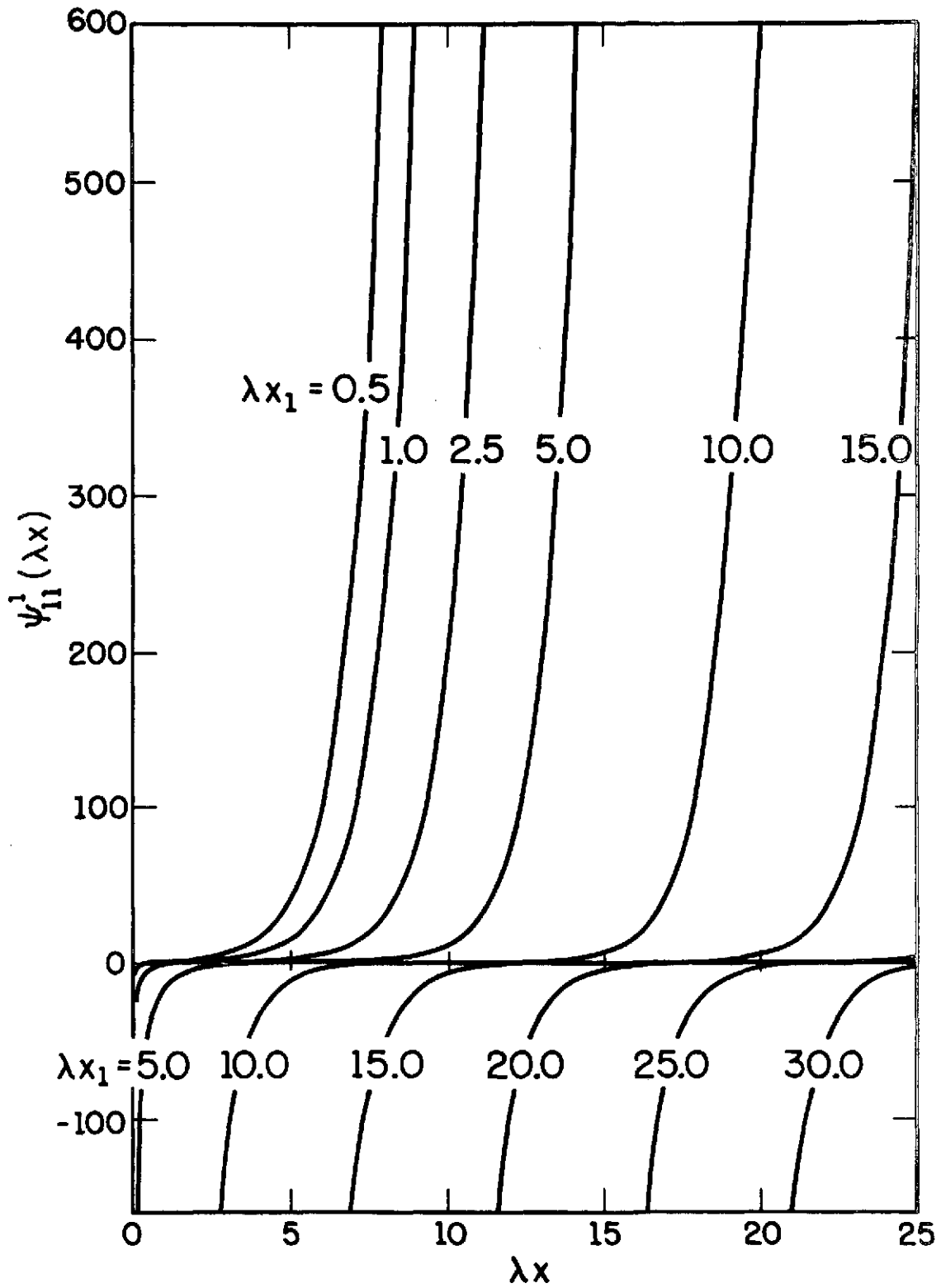


Figure 4 The function  $\psi_{11}^1(\lambda x)$

TABLES OF THE FUNCTION

$$\psi_{KL}^1(x) \equiv I_K(x) K_L(x_1) - (-1)^{K+L} I_L(x_1) K_K(x)$$

X1= 0.01

X1= 0.05

X	K=0,L=0	K=0,L=1	K=1,L=1	K=1,L=2	K=0,L=0	K=0,L=1	K=1,L=1	K=1,L=2
0.01	0.0	0.100000E 03	0.0	0.999999E 02	-0.160988E 01	0.200282E 02	-0.240058E 01	0.402879E 01
0.05	0.100988E 01	0.100052E 03	0.240058E 01	0.500144E 03	0.0	0.200000E 02	0.0	0.200000E 02
0.10	0.230592E 01	0.100236E 03	0.495567E 01	0.100123E 04	0.693436E 00	0.200201E 02	0.750304E 00	0.400280E 02
0.20	0.301582E 01	0.100985E 03	0.100236E 02	0.200996E 04	0.139165E 01	0.201530E 02	0.188150E 01	0.803518E 02
0.30	0.345557E 01	0.102243E 03	0.151501E 02	0.303380E 04	0.181138E 01	0.203944E 02	0.294374E 01	0.121280E 03
0.40	0.379743E 01	0.104018E 03	0.203864E 02	0.408043E 04	0.212482E 01	0.207419E 02	0.400747E 01	0.163120E 03
0.50	0.409651E 01	0.106325E 03	0.257744E 02	0.515775E 04	0.238693E 01	0.211967E 02	0.509316E 01	0.206187E 03
0.60	0.437826E 01	0.109180E 03	0.313557E 02	0.627392E 04	0.262287E 01	0.217616E 02	0.621315E 01	0.250807E 03
0.70	0.465700E 01	0.112604E 03	0.371736E 02	0.743740E 04	0.284663E 01	0.224408E 02	0.737772E 01	0.297318E 03
0.80	0.494203E 01	0.116624E 03	0.432708E 02	0.865707E 04	0.306709E 01	0.232390E 02	0.859663E 01	0.346075E 03
0.90	0.522905E 01	0.121269E 03	0.496960E 02	0.994227E 04	0.329048E 01	0.241622E 02	0.987969E 01	0.397452E 03
1.00	0.552637E 01	0.126576E 03	0.564981E 02	0.113029E 05	0.352153E 01	0.252175E 02	0.112371E 02	0.451844E 03
2.00	0.106486E 02	0.227899E 03	0.159021E 03	0.318119E 05	0.698519E 01	0.453885E 02	0.316655E 02	0.127171E 04
3.00	0.230087E 02	0.487952E 03	0.395233E 03	0.790654E 05	0.151652E 02	0.971757E 02	0.787092E 02	0.316072E 04
4.00	0.533479E 02	0.112990E 04	0.975691E 03	0.195184E 06	0.351856E 02	0.225018E 03	0.194307E 03	0.780269E 04
5.00	0.128602E 03	0.272327E 04	0.243292E 04	0.486700E 06	0.848274E 02	0.542335E 03	0.484513E 03	0.194563E 05
6.00	0.317428E 03	0.672168E 04	0.613259E 04	0.122681E 07	0.209382E 03	0.133861E 04	0.122129E 04	0.490428E 05
7.00	0.795472E 03	0.168550E 05	0.155998E 05	0.312070E 07	0.525040E 03	0.335664E 04	0.310668E 04	0.124753E 06
8.00	0.201803E 04	0.427452E 05	0.399767E 05	0.799724E 07	0.133153E 04	0.851263E 04	0.796131E 04	0.319698E 06
9.00	0.516309E 04	0.109330E 06	0.103064E 06	0.206177E 08	0.340568E 04	0.217729E 05	0.205251E 05	0.824215E 06
10.00	0.132937E 05	0.281498E 06	0.267029E 06	0.534184E 08	0.876879E 04	0.560599E 05	0.531784E 05	0.213545E 07
20.00	0.205049E 09	0.435468E 10	0.424439E 10	0.849078E 12	0.135650E 09	0.867228E 09	0.845264E 09	0.339428E 11
30.00	0.369040E 13	0.781467E 14	0.768331E 14	0.153703E 17	0.243430E 13	0.155628E 14	0.153012E 14	0.614441E 15
40.00	0.705218E 17	0.148909E 19	0.147035E 19	0.294141E 21	0.463857E 17	0.296549E 18	0.292819E 18	0.117586E 20
50.00	0.138453E 22	0.293178E 23	0.290232E 23	0.580601E 25	0.913264E 21	0.583860E 22	0.577992E 22	0.232101E 24
60.00	0.270273E 26	0.584253E 27	0.584322E 27	0.116892E 30	0.183555E 26	0.117349E 27	0.116367E 27	0.467288E 28
70.00	0.567299E 30	0.120127E 32	0.119266E 32	0.238569E 34	0.374202E 30	0.239232E 31	0.237517E 31	0.953783E 32
80.00	0.110859E 33	0.247453E 36	0.245902E 36	0.491920E 38	0.770828E 34	0.492799E 35	0.489710E 35	0.196650E 37
90.00	0.242036E 39	0.513789E 40	0.510927E 40	0.102210E 43	0.160048E 39	0.102320E 40	0.101750E 40	0.408593E 41
100.00	0.500944E 43	0.107347E 45	0.106809E 45	0.213669E 47	0.334391E 43	0.213780E 44	0.212709E 44	0.854161E 45

437  
11

X1= 0.10

X1= 0.20

X	K=0,L=0	K=0,L=1	K=1,L=1	K=1,L=2	K=0,L=0	K=0,L=1	K=1,L=1	K=1,L=2
0.01	-0.230592E 01	0.100904E 02	-0.495567E 01	0.112260E 01	-0.301582E 01	0.525058E 01	-0.100236E 02	0.749102E 00
0.05	-0.693436E 00	0.100159E 02	-0.750304E 00	0.501406E 01	-0.139165E 01	0.509194E 01	-0.188150E 01	0.133808E 01
0.10	0.0	0.999999E 01	0.0	0.100000E 02	-0.694311E 00	0.503184E 01	-0.751221E 00	0.252815E 01
0.20	0.694311E 00	0.100404E 02	0.751221E 00	0.200562E 02	0.0	0.500000E 01	0.0	0.499999E 01
0.30	0.110609E 01	0.101455E 02	0.134177E 01	0.302673E 02	0.406141E 00	0.502196E 01	0.417356E 00	0.752605E 01
0.40	0.140781E 01	0.103077E 02	0.190109E 01	0.407068E 02	0.697813E 00	0.508093E 01	0.754897E 00	0.101128E 02
0.50	0.165441E 01	0.105257E 02	0.245832E 01	0.514530E 02	0.930281E 00	0.517206E 01	0.106522E 01	0.127773E 02
0.60	0.187100E 01	0.107998E 02	0.302596E 01	0.625868E 02	0.112871E 01	0.529371E 01	0.136730E 01	0.155388E 02
0.70	0.207144E 01	0.111315E 02	0.361186E 01	0.741927E 02	0.130693E 01	0.544556E 01	0.167053E 01	0.184179E 02
0.80	0.226445E 01	0.115229E 02	0.422224E 01	0.863593E 02	0.147354E 01	0.562805E 01	0.198074E 01	0.214365E 02
0.90	0.245604E 01	0.119769E 02	0.486273E 01	0.991795E 02	0.163439E 01	0.584209E 01	0.230225E 01	0.246175E 02
1.00	0.265075E 01	0.124967E 02	0.553886E 01	0.112752E 03	0.179379E 01	0.608901E 01	0.263869E 01	0.279854E 02
2.00	0.541853E 01	0.224684E 02	0.156669E 02	0.317338E 03	0.388040E 01	0.108987E 02	0.758277E 01	0.787569E 02
3.00	0.118112E 02	0.480963E 02	0.389539E 02	0.788713E 03	0.851949E 01	0.233140E 02	0.188771E 02	0.195741E 03
4.00	0.274193E 02	0.111368E 03	0.961676E 02	0.194705E 04	0.197976E 02	0.539788E 02	0.466097E 02	0.483215E 03
5.00	0.661092E 02	0.268417E 03	0.239799E 03	0.485504E 04	0.477396E 02	0.130097E 03	0.116226E 03	0.120491E 04
6.00	0.163181E 03	0.662517E 03	0.604453E 03	0.122379E 05	0.117841E 03	0.321109E 03	0.292967E 03	0.303719E 04
7.00	0.409188E 03	0.166130E 04	0.153758E 04	0.311304E 05	0.295494E 03	0.805199E 03	0.745237E 03	0.772586E 04
8.00	0.103772E 04	0.421314E 04	0.394028E 04	0.797760E 05	0.749391E 03	0.204203E 04	0.190978E 04	0.197986E 05
9.00	0.265421E 04	0.107760E 05	0.101585E 05	0.205671E 06	0.191673E 04	0.522294E 04	0.492361E 04	0.510430E 05
10.00	0.683393E 04	0.277456E 05	0.263195E 05	0.532872E 06	0.493511E 04	0.134478E 05	0.127565E 05	0.132247E 06
20.00	0.105719E 09	0.429215E 09	0.418345E 09	0.846993E 10	0.763445E 08	0.208033E 09	0.202764E 09	0.210205E 10
30.00	0.189717E 13	0.770246E 13	0.757300E 13	0.153325E 15	0.137004E 13	0.373324E 13	0.367049E 13	0.380519E 14
40.00	0.361506E 17	0.146771E 18	0.144924E 18	0.293418E 19	0.261061E 17	0.711369E 17	0.702421E 17	0.728199E 18
50.00	0.711749E 21	0.288969E 22	0.286065E 22	0.579176E 23	0.513989E 21	0.140058E 22	0.138650E 22	0.143738E 23
60.00	0.145053E 26	0.580792E 26	0.575932E 26	0.116605E 28	0.103305E 26	0.281499E 26	0.279144E 26	0.289388E 27
70.00	0.291633E 30	0.118403E 31	0.117554E 31	0.238003E 32	0.210603E 30	0.573875E 30	0.569761E 30	0.590670E 31
80.00	0.600742E 34	0.243900E 35	0.242371E 35	0.490712E 36	0.433825E 34	0.118214E 35	0.117473E 35	0.121784E 36
90.00	0.124733E 39	0.506412E 39	0.503591E 39	0.101959E 41	0.900755E 38	0.245449E 39	0.244081E 39	0.253039E 40
100.00	0.260606E 43	0.105806E 44	0.105275E 44	0.213144E 45	0.188196E 43	0.512820E 43	0.510250E 43	0.528976E 44

438  
12

X1= 0.30

X1= 0.40

X	K=C,L=0	K=0,L=1	K=1,L=1	K=1,L=2	K=C,L=0	K=0,L=1	K=1,L=1	K=1,L=2
0.01	-0.345557E 01	0.377225E 01	-0.151501E 02	0.124189E 01	-0.379743E 01	0.314766E 01	-0.203864E 02	0.208645E 01
0.05	-0.181138E 01	0.353031E 01	-0.294374E 01	0.769481E 00	-0.212482E 01	0.282110E 01	-0.400747E 01	0.704530E 00
0.10	-0.110609E 01	0.343180E 01	-0.134177E 01	0.120033E 01	-0.140781E 01	0.268500E 01	-0.190109E 01	0.802284E 00
0.20	-0.406141E 00	0.335250E 01	-0.417356E 00	0.223959E 01	-0.697813E 00	0.256384E 01	-0.754897E 00	0.130645E 01
0.30	0.0	0.333333E 01	0.0	0.333333E 01	-0.288163E 00	0.251379E 01	-0.292151E 00	0.188777E 01
0.40	0.288163E 00	0.334852E 01	0.292151E 00	0.446146E 01	0.0	0.249999E 01	0.0	0.249999E 01
0.50	0.514251E 00	0.339022E 01	0.536851E 00	0.562687E 01	0.223513E 00	0.251162E 01	0.225374E 00	0.313766E 01
0.60	0.705072E 00	0.345522E 01	0.761045E 00	0.683648E 01	0.408179E 00	0.254404E 01	0.419427E 00	0.380224E 01
0.70	0.870339E 00	0.354216E 01	0.977139E 00	0.809869E 01	0.568088E 00	0.259500E 01	0.598030E 00	0.449734E 01
0.80	0.102285E 01	0.365061E 01	0.119210E 01	0.942272E 01	0.711923E 00	0.266342E 01	0.769702E 00	0.522755E 01
0.90	0.110703E 01	0.378070E 01	0.141052E 01	0.108185E 02	0.845508E 00	0.274889E 01	0.939706E 00	0.599808E 01
1.00	0.130707E 01	0.393295E 01	0.163582E 01	0.122966E 02	0.973031E 00	0.285143E 01	0.111170E 01	0.681462E 01
2.00	0.301217E 01	0.698367E 01	0.483975E 01	0.345911E 02	0.242216E 01	0.500265E 01	0.344597E 01	0.191482E 02
3.00	0.666316E 01	0.149209E 02	0.120754E 02	0.859693E 02	0.540363E 01	0.106685E 02	0.862735E 01	0.475847E 02
4.00	0.155000E 02	0.345403E 02	0.298229E 02	0.212227E 03	0.125847E 02	0.246896E 02	0.213156E 02	0.117468E 03
5.00	0.373818E 02	0.832452E 02	0.743687E 02	0.529195E 03	0.303557E 02	0.595021E 02	0.531566E 02	0.292910E 03
6.00	0.922751E 02	0.205468E 03	0.187460E 03	0.133392E 04	0.749333E 02	0.146864E 03	0.133992E 03	0.738329E 03
7.00	0.231388E 03	0.515221E 03	0.476853E 03	0.339318E 04	0.187902E 03	0.368268E 03	0.340844E 03	0.187813E 04
8.00	0.586813E 03	0.130663E 04	0.122200E 04	0.869550E 04	0.476531E 03	0.933948E 03	0.873460E 03	0.481297E 04
9.00	0.150090E 04	0.334199E 04	0.315046E 04	0.224180E 05	0.121883E 04	0.238878E 04	0.225188E 04	0.124084E 05
10.00	0.306445E 04	0.860480E 04	0.816250E 04	0.580825E 05	0.313819E 04	0.615051E 04	0.583437E 04	0.321487E 05
20.00	0.597818E 08	0.133113E 09	0.129742E 09	0.923214E 09	0.485468E 08	0.951464E 08	0.927366E 08	0.511000E 09
30.00	0.107281E 13	0.238878E 13	0.234863E 13	0.167123E 14	0.871194E 12	0.170744E 13	0.167874E 13	0.925027E 13
40.00	0.204424E 17	0.455182E 17	0.449457E 17	0.319623E 18	0.166006E 17	0.325354E 17	0.321261E 17	0.177022E 18
50.00	0.402480E 21	0.896185E 21	0.887178E 21	0.631295E 22	0.326841E 21	0.640572E 21	0.634134E 21	0.349423E 22
60.00	0.808937E 25	0.180122E 26	0.178615E 26	0.127098E 27	0.656910E 25	0.128747E 26	0.127670E 26	0.703491E 26
70.00	0.164913E 30	0.367204E 30	0.364572E 30	0.259421E 31	0.133920E 30	0.262469E 30	0.260588E 30	0.143590E 31
80.00	0.339708E 34	0.756412E 34	0.751670E 34	0.534871E 35	0.275865E 34	0.540665E 34	0.537276E 34	0.296052E 35
90.00	0.703339E 38	0.157055E 39	0.156180E 39	0.111134E 40	0.572782E 38	0.112259E 39	0.111634E 39	0.615128E 39
100.00	0.147365E 43	0.326137E 43	0.326493E 43	0.232325E 44	0.119672E 43	0.234545E 43	0.233369E 43	0.128592E 44

439  
13

X1= 0.50

X1= 0.60

X	K=0,L=0	K=0,L=1	K=1,L=1	K=1,L=2	K=0,L=0	K=0,L=1	K=1,L=1	K=1,L=2
0.01	-0.409651E 01	0.287406E 01	-0.257744E 02	0.322753E 01	-0.437826E 01	0.278394E 01	-0.313557E 02	0.466091E 01
0.05	-0.238693E 01	0.246062E 01	-0.509316E 01	0.824053E 00	-0.262287E 01	0.228059E 01	-0.621315E 01	0.105116E 01
0.10	-0.165441E 01	0.228651E 01	-0.245832E 01	0.692379E 00	-0.187100E 01	0.206747E 01	-0.302596E 01	0.713211E 00
0.20	-0.930281E 00	0.212505E 01	-0.106522E 01	0.911181E 00	-0.112871E 01	0.186572E 01	-0.136730E 01	0.736033E 00
0.30	-0.514251E 00	0.204786E 01	-0.536851E 00	0.124282E 01	-0.703672E 00	0.176286E 01	-0.761045E 00	0.918410E 00
0.40	-0.223513E 00	0.201079E 01	-0.225374E 00	0.101013E 01	-0.408179E 00	0.170510E 01	-0.419427E 00	0.114596E 01
0.50	0.0	0.199999E 01	0.0	0.200000E 01	-0.182625E 00	0.167553E 01	-0.183638E 00	0.139730E 01
0.60	0.182625E 00	0.200942E 01	0.183638E 00	0.241009E 01	0.0	0.166666E 01	0.0	0.166666E 01
0.70	0.338723E 00	0.203599E 01	0.345134E 00	0.284127E 01	0.154407E 00	0.167459E 01	0.155020E 00	0.195283E 01
0.80	0.477110E 00	0.207806E 01	0.494766E 00	0.329570E 01	0.289606E 00	0.169712E 01	0.293607E 00	0.225635E 01
0.90	0.603675E 00	0.213476E 01	0.638670E 00	0.377625E 01	0.411590E 00	0.173300E 01	0.422894E 00	0.257866E 01
1.00	0.722622E 00	0.220574E 01	0.780924E 00	0.428626E 01	0.524616E 00	0.178155E 01	0.547488E 00	0.292169E 01
2.00	0.198617E 01	0.380537E 01	0.259872E 01	0.120140E 02	0.164805E 01	0.300565E 01	0.202846E 01	0.815102E 01
3.00	0.447495E 01	0.809370E 01	0.653816E 01	0.298499E 02	0.375698E 01	0.636976E 01	0.513799E 01	0.202443E 02
4.00	0.104358E 02	0.187238E 02	0.161627E 02	0.736861E 02	0.877530E 01	0.147280E 02	0.127110E 02	0.499720E 02
5.00	0.251771E 02	0.451221E 02	0.403094E 02	0.183738E 03	0.211755E 02	0.354901E 02	0.317039E 02	0.124606E 03
6.00	0.621514E 02	0.111370E 03	0.101609E 03	0.463142E 03	0.522748E 02	0.875956E 02	0.799179E 02	0.314089E 03
7.00	0.155851E 03	0.279265E 03	0.258469E 03	0.117812E 04	0.131085E 03	0.219650E 03	0.203293E 03	0.798967E 03
8.00	0.395247E 03	0.708233E 03	0.662363E 03	0.301910E 04	0.332439E 03	0.557044E 03	0.520967E 03	0.204747E 04
9.00	0.101093E 04	0.181146E 04	0.170765E 04	0.778358E 04	0.850287E 03	0.142476E 04	0.134311E 04	0.527859E 04
10.00	0.260290E 04	0.460406E 04	0.442432E 04	0.201664E 05	0.218928E 04	0.366841E 04	0.347985E 04	0.136763E 05
20.00	0.402660E 08	0.721515E 08	0.703241E 08	0.320542E 09	0.338674E 08	0.567491E 08	0.553118E 08	0.217382E 09
30.00	0.722594E 12	0.129479E 13	0.127303E 13	0.580255E 13	0.607766E 12	0.101839E 13	0.100127E 13	0.393512E 13
40.00	0.137690E 17	0.246723E 17	0.243619E 17	0.111043E 18	0.115810E 17	0.194054E 17	0.191613E 17	0.753063E 17
50.00	0.271690E 21	0.485759E 21	0.480877E 21	0.219188E 22	0.228012E 21	0.382063E 21	0.378223E 21	0.148646E 22
60.00	0.544459E 25	0.976317E 25	0.968148E 25	0.441289E 26	0.458276E 25	0.767899E 25	0.761474E 25	0.299269E 26
70.00	0.111077E 30	0.199036E 30	0.197609E 30	0.900717E 30	0.934260E 29	0.156547E 30	0.155425E 30	0.610839E 30
80.00	0.226810E 34	0.409998E 34	0.407428E 34	0.185709E 35	0.192450E 34	0.322475E 34	0.320453E 34	0.125942E 35
90.00	0.475081E 38	0.851233E 38	0.846541E 38	0.385860E 39	0.399587E 38	0.669557E 38	0.665827E 38	0.261679E 39
100.00	0.992595E 42	0.177800E 43	0.176969E 43	0.806638E 43	0.834864E 42	0.139892E 43	0.139191E 43	0.547038E 43

14 920<

X1= 0.70

X1= 0.80

X	K=0,L=0	K=0,L=1	K=1,L=1	K=1,L=2	K=0,L=0	K=0,L=1	K=1,L=1	K=1,L=2
0.01	-0.465700E 01	0.280604E 01	-0.371730E 02	0.639559E 01	-0.494203E 01	0.290546E 01	-0.432708E 02	0.844667E 01
0.05	-0.284663E 01	0.220905E 01	-0.737772E 01	0.136159E 01	-0.306709E 01	0.221036E 01	-0.859663E 01	0.174745E 01
0.10	-0.207144E 01	0.195548E 01	-0.361186E 01	0.811867E 00	-0.226445E 01	0.191453E 01	-0.422224E 01	0.967359E 00
0.20	-0.130693E 01	0.171260E 01	-0.167053E 01	0.672622E 00	-0.147354E 01	0.162910E 01	-0.198074E 01	0.676208E 00
0.30	-0.870339E 00	0.158443E 01	-0.977139E 00	0.750340E 00	-0.102285E 01	0.147537E 01	-0.119210E 01	0.670358E 00
0.40	-0.968068E 00	0.150718E 01	-0.598030E 00	0.886346E 00	-0.711923E 00	0.137904E 01	-0.769702E 00	0.739168E 00
0.50	-0.338723E 00	0.146073E 01	-0.345134E 00	0.104999E 01	-0.477110E 00	0.131664E 01	-0.494766E 00	0.841146E 00
0.60	-0.154407E 00	0.143610E 01	-0.155020E 00	0.123168E 01	-0.289606E 00	0.127766E 01	-0.293607E 00	0.963110E 00
0.70	0.0	0.142857E 01	0.0	0.142857E 01	-0.133754E 00	0.125654E 01	-0.134151E 00	0.110003E 01
0.80	0.133754E 00	0.143541E 01	0.134151E 00	0.163983E 01	0.0	0.125000E 01	0.0	0.125000E 01
0.90	0.252994E 00	0.145498E 01	0.255658E 00	0.186585E 01	0.117979E 00	0.125601E 01	0.118252E 00	0.141252E 01
1.00	0.362060E 00	0.148629E 01	0.365739E 00	0.210762E 01	0.224636E 00	0.127332E 01	0.226499E 00	0.158789E 01
2.00	0.137743E 01	0.243656E 01	0.161860E 01	0.583275E 01	0.115590E 01	0.201380E 01	0.131024E 01	0.433801E 01
3.00	0.318473E 01	0.513912E 01	0.413722E 01	0.144771E 02	0.271882E 01	0.422121E 01	0.338956E 01	0.107558E 02
4.00	0.745257E 01	0.118743E 02	0.102455E 02	0.357333E 02	0.637649E 01	0.974462E 01	0.840512E 01	0.265448E 02
5.00	0.179883E 02	0.286108E 02	0.255577E 02	0.891007E 02	0.153956E 02	0.234764E 02	0.209702E 02	0.661883E 02
6.00	0.444082E 02	0.706155E 02	0.644257E 02	0.224593E 03	0.380093E 02	0.579419E 02	0.528627E 02	0.166838E 03
7.00	0.111359E 03	0.177071E 03	0.163885E 03	0.571309E 03	0.953135E 02	0.145291E 03	0.134471E 03	0.424395E 03
8.00	0.282413E 03	0.449062E 03	0.419978E 03	0.146406E 04	0.241721E 03	0.368466E 03	0.344602E 03	0.108757E 04
9.00	0.722335E 03	0.114857E 04	0.108275E 04	0.377451E 04	0.618256E 03	0.942433E 03	0.888422E 03	0.280388E 04
10.00	0.185983E 04	0.295729E 04	0.280529E 04	0.977934E 04	0.159186E 04	0.242653E 04	0.230180E 04	0.726454E 04
20.00	0.287710E 08	0.457483E 08	0.445897E 08	0.155441E 09	0.246255E 08	0.375376E 08	0.365869E 08	0.115469E 09
30.00	0.516309E 12	0.820974E 12	0.807175E 12	0.281384E 13	0.441915E 12	0.673629E 12	0.662307E 12	0.209025E 13
40.00	0.983827E 16	0.156437E 17	0.154469E 17	0.538485E 17	0.842070E 16	0.128360E 17	0.126746E 17	0.400012E 17
50.00	0.193701E 21	0.308000E 21	0.304905E 21	0.106291E 22	0.165791E 21	0.252722E 21	0.250182E 21	0.789579E 21
60.00	0.389314E 25	0.619043E 25	0.613863E 25	0.213995E 26	0.333219E 25	0.507940E 25	0.503690E 25	0.158966E 26
70.00	0.793671E 29	0.126201E 30	0.125296E 30	0.436786E 30	0.679314E 29	0.103551E 30	0.102808E 30	0.324465E 30
80.00	0.163490E 34	0.259963E 34	0.258334E 34	0.900561E 34	0.139933E 34	0.213306E 34	0.211969E 34	0.668978E 34
90.00	0.339456E 38	0.539764E 38	0.536758E 38	0.187116E 39	0.290545E 38	0.442890E 38	0.440423E 36	0.138998E 39
100.00	0.709233E 42	0.112774E 43	0.112209E 43	0.391165E 43	0.607042E 42	0.925338E 42	0.920701E 42	0.290575E 43

15 441 <

X1= 0.90

X1= 1.00

X	K=0,L=0	K=0,L=1	K=1,L=1	K=1,L=2	K=0,L=0	K=0,L=1	K=1,L=1	K=1,L=2
0.01	-0.524005E 01	0.306360E 01	-0.496960E 02	0.108335E 02	-0.555637E 01	0.327017E 01	-0.564981E 02	0.135793E 02
0.05	-0.329048E 01	0.226515E 01	-0.987969E 01	0.220740E 01	-0.352153E 01	0.236232E 01	-0.112371E 02	0.274332E 01
0.10	-0.245604E 01	0.192488E 01	-0.486273E 01	0.117385E 01	-0.265075E 01	0.197509E 01	-0.553886E 01	0.141898E 01
0.20	-0.163439E 01	0.159503E 01	-0.230225E 01	0.725988E 00	-0.179379E 01	0.159850E 01	-0.263869E 01	0.811624E 00
0.30	-0.116703E 01	0.141503E 01	-0.141052E 01	0.646215E 00	-0.130707E 01	0.139118E 01	-0.163582E 01	0.661321E 00
0.40	-0.845508E 00	0.129954E 01	-0.939706E 00	0.660653E 00	-0.973031E 00	0.125611E 01	-0.111170E 01	0.628030E 00
0.50	-0.603675E 00	0.122157E 01	-0.638670E 00	0.715493E 00	-0.722622E 00	0.116256E 01	-0.780924E 00	0.643894E 00
0.60	-0.411590E 00	0.116901E 01	-0.422894E 00	0.793242E 00	-0.524616E 00	0.109673E 01	-0.547488E 00	0.686574E 00
0.70	-0.252494E 00	0.113539E 01	-0.255658E 00	0.836849E 00	-0.362060E 00	0.105123E 01	-0.369739E 00	0.746817E 00
0.80	-0.117979E 00	0.111689E 01	-0.118252E 00	0.993232E 00	-0.224636E 00	0.102164E 01	-0.226499E 00	0.820319E 00
0.90	0.0	0.111111E 01	0.0	0.111111E 01	-0.105537E 00	0.100518E 01	-0.105731E 00	0.905017E 00
1.00	0.105537E 00	0.111648E 01	0.105731E 00	0.124014E 01	0.0	0.100000E 01	0.0	0.999999E 00
2.00	0.971392E 00	0.169002E 01	0.107021E 01	0.332211E 01	0.815563E 00	0.143646E 01	0.878368E 00	0.260351E 01
3.00	0.233349E 01	0.351452E 01	0.281276E 01	0.822349E 01	0.201095E 01	0.295742E 01	0.235686E 01	0.642903E 01
4.00	0.548745E 01	0.810375E 01	0.698677E 01	0.202915E 02	0.474425E 01	0.680901E 01	0.586723E 01	0.158592E 02
5.00	0.132540E 02	0.195201E 02	0.174352E 02	0.505947E 02	0.114640E 02	0.163979E 02	0.146455E 02	0.395419E 02
6.00	0.327235E 02	0.481763E 02	0.439528E 02	0.127531E 03	0.283057E 02	0.404695E 02	0.369213E 02	0.996708E 02
7.00	0.820592E 02	0.120803E 03	0.111807E 03	0.324408E 03	0.709815E 02	0.101478E 03	0.939207E 02	0.253538E 03
8.00	0.206108E 03	0.306363E 03	0.286521E 03	0.831343E 03	0.180014E 03	0.257353E 03	0.240686E 03	0.649727E 03
9.00	0.532282E 03	0.783591E 03	0.738683E 03	0.214329E 04	0.460426E 03	0.658238E 03	0.620514E 03	0.167507E 04
10.00	0.137049E 04	0.201755E 04	0.191385E 04	0.555304E 04	0.118548E 04	0.169480E 04	0.160768E 04	0.433991E 04
20.00	0.212011E 08	0.312109E 08	0.304204E 08	0.882649E 08	0.183390E 08	0.262180E 08	0.255540E 08	0.689824E 08
30.00	0.380463E 12	0.560093E 12	0.550679E 12	0.159780E 13	0.329102E 12	0.470493E 12	0.462585E 12	0.124874E 13
40.00	0.724973E 16	0.106726E 17	0.105383E 17	0.305770E 17	0.627105E 16	0.896525E 16	0.885248E 16	0.238971E 17
50.00	0.142736E 21	0.210127E 21	0.208015E 21	0.603557E 21	0.123467E 21	0.176512E 21	0.174738E 21	0.471703E 21
60.00	0.260882E 25	0.422329E 25	0.418796E 25	0.121514E 26	0.248155E 25	0.354768E 25	0.351800E 25	0.949677E 25
70.00	0.584349E 29	0.860977E 29	0.854805E 29	0.248022E 30	0.505898E 29	0.723244E 29	0.718060E 29	0.193839E 30
80.00	0.120474E 34	0.177355E 34	0.176243E 34	0.511369E 34	0.104211E 34	0.148983E 34	0.148049E 34	0.399655E 34
90.00	0.250142E 38	0.368243E 38	0.366192E 38	0.106251E 39	0.216374E 38	0.309334E 38	0.307611E 38	0.830391E 38
100.00	0.522627E 42	0.769378E 42	0.765522E 42	0.222117E 43	0.452075E 42	0.646298E 42	0.643059E 42	0.173593E 43

16 442 <

X1= 2.00

X1= 3.00

X	K=0,L=0	K=0,L=1	K=1,L=1	K=1,L=2	K=0,L=0	K=0,L=1	K=1,L=1	K=1,L=2
0.01	-0.106486E 02	0.764965E 01	-0.159021E 03	0.688781E 02	-0.230087E 02	0.187050E 02	-0.395233E 03	0.224463E 03
0.05	-0.698519E 01	0.509356E 01	-0.316655E 02	0.137231E 02	-0.151652E 02	0.123519E 02	-0.787092E 02	0.447029E 02
0.10	-0.541853E 01	0.400079E 01	-0.156669E 02	0.680149E 01	-0.118112E 02	0.963535E 01	-0.389539E 02	0.221270E 02
0.20	-0.388040E 01	0.292918E 01	-0.758277E 01	0.331590E 01	-0.851949E 01	0.696964E 01	-0.188771E 02	0.107292E 02
0.30	-0.301217E 01	0.232611E 01	-0.483975E 01	0.214391E 01	-0.666316E 01	0.546690E 01	-0.120754E 02	0.687067E 01
0.40	-0.2+2216E 01	0.191832E 01	-0.344597E 01	0.155668E 01	-0.540363E 01	0.444792E 01	-0.862735E 01	0.491688E 01
0.50	-0.196617E 01	0.161916E 01	-0.259872E 01	0.120664E 01	-0.447495E 01	0.369727E 01	-0.653816E 01	0.373492E 01
0.60	-0.164805E 01	0.138949E 01	-0.202846E 01	0.577191E 00	-0.375698E 01	0.311768E 01	-0.513799E 01	0.294443E 01
0.70	-0.137743E 01	0.120818E 01	-0.161860E 01	0.817957E 00	-0.318473E 01	0.265650E 01	-0.413722E 01	0.238098E 01
0.80	-0.115590E 01	0.106242E 01	-0.131024E 01	0.703566E 00	-0.271882E 01	0.228187E 01	-0.338956E 01	0.196151E 01
0.90	-0.971392E 00	0.943865E 00	-0.107021E 01	0.619805E 00	-0.233349E 01	0.197293E 01	-0.281276E 01	0.163934E 01
1.00	-0.815563E 00	0.846775E 00	-0.878368E 00	0.558097E 00	-0.201095E 01	0.171530E 01	-0.235686E 01	0.138617E 01
2.00	0.0	0.499999E 00	0.0	0.499999E 00	-0.476700E 00	0.541804E 00	-0.489067E 00	0.411869E 00
3.00	0.476700E 00	0.737914E 00	0.489067E 00	0.103087E 01	0.0	0.333333E 00	0.0	0.333333E 00
4.00	0.126178E 01	0.159850E 01	0.134516E 01	0.248516E 01	0.338155E 00	0.497963E 00	0.342553E 00	0.628337E 00
5.00	0.309403E 01	0.381579E 01	0.339728E 01	0.617817E 01	0.928282E 00	0.110845E 01	0.961240E 00	0.150597E 01
6.00	0.765474E 01	0.940577E 01	0.857749E 01	0.155670E 02	0.232962E 01	0.270481E 01	0.245796E 01	0.377618E 01
7.00	0.192008E 02	0.235812E 02	0.218238E 02	0.395967E 02	0.585479E 01	0.677180E 01	0.626417E 01	0.959904E 01
8.00	0.486965E 02	0.598017E 02	0.559281E 02	0.101471E 03	0.148526E 02	0.171700E 02	0.160568E 02	0.245966E 02
9.00	0.124553E 03	0.152955E 03	0.144189E 03	0.261604E 03	0.379904E 02	0.439147E 02	0.413976E 02	0.634120E 02
10.00	0.326692E 03	0.393822E 03	0.373579E 03	0.677788E 03	0.978164E 02	0.113069E 03	0.107257E 03	0.164293E 03
20.00	0.496101E 07	0.609230E 07	0.593800E 07	0.107734E 08	0.151319E 07	0.174914E 07	0.170484E 07	0.261142E 07
30.00	0.890274E 11	0.109329E 12	0.107491E 12	0.195022E 12	0.271548E 11	0.313891E 11	0.308615E 11	0.472727E 11
40.00	0.169642E 16	0.208327E 16	0.205706E 16	0.373214E 16	0.517436E 15	0.598120E 15	0.590596E 15	0.904658E 15
50.00	0.335999E 20	0.410163E 20	0.406041E 20	0.736684E 20	0.101875E 20	0.117761E 20	0.116577E 20	0.178570E 20
60.00	0.671294E 24	0.824379E 24	0.817481E 24	0.148316E 25	0.204757E 24	0.236685E 24	0.234704E 24	0.359513E 24
70.00	0.136853E 29	0.168061E 29	0.166856E 29	0.302729E 29	0.417425E 28	0.482515E 28	0.479056E 28	0.733803E 28
80.00	0.261907E 33	0.346192E 33	0.344022E 33	0.624162E 33	0.859864E 32	0.993943E 32	0.987712E 32	0.151295E 33
90.00	0.565327E 37	0.718803E 37	0.714799E 37	0.129687E 38	0.178534E 37	0.206373E 37	0.205224E 37	0.314356E 37
100.00	0.122293E 42	0.150181E 42	0.149428E 42	0.271109E 42	0.373015E 41	0.431180E 41	0.429019E 41	0.657159E 41

17

443

X1= 4.00

X1= 5.00

X	K=0,L=0	K=0,L=1	K=1,L=1	K=1,L=2	K=0,L=0	K=0,L=1	K=1,L=1	K=1,L=2
0.01	-0.533479E 02	0.460893E 02	-0.975691E 03	0.642051E 03	-0.128602E 03	0.114898E 03	-0.243292E 04	0.175010E 04
0.05	-0.351856E 02	0.304057E 02	-0.194307E 03	0.127864E 03	-0.848274E 02	0.757907E 02	-0.484513E 03	0.348529E 03
0.10	-0.274193E 02	0.236994E 02	-0.961676E 02	0.632841E 02	-0.661092E 02	0.590682E 02	-0.239799E 03	0.172497E 03
0.20	-0.197976E 02	0.171180E 02	-0.466097E 02	0.306739E 02	-0.477396E 02	0.426571E 02	-0.116226E 03	0.836065E 02
0.30	-0.155006E 02	0.134072E 02	-0.298229E 02	0.196288E 02	-0.373818E 02	0.334037E 02	-0.743687E 02	0.534976E 02
0.40	-0.125847E 02	0.108902E 02	-0.213156E 02	0.140319E 02	-0.303557E 02	0.271269E 02	-0.531566E 02	0.382393E 02
0.50	-0.104358E 02	0.903510E 01	-0.161627E 02	0.106424E 02	-0.251771E 02	0.225005E 02	-0.403094E 02	0.289982E 02
0.60	-0.877530E 01	0.760183E 01	-0.127110E 02	0.837250E 01	-0.211755E 02	0.189258E 02	-0.317039E 02	0.228085E 02
0.70	-0.745257E 01	0.646037E 01	-0.102455E 02	0.675157E 01	-0.179883E 02	0.160787E 02	-0.255577E 02	0.183877E 02
0.80	-0.637649E 01	0.553205E 01	-0.840512E 01	0.554205E 01	-0.153956E 02	0.137628E 02	-0.209702E 02	0.150882E 02
0.90	-0.548745E 01	0.476537E 01	-0.698677E 01	0.461036E 01	-0.132540E 02	0.118498E 02	-0.174352E 02	0.125459E 02
1.00	-0.474425E 01	0.412478E 01	-0.586723E 01	0.387539E 01	-0.114640E 02	0.102510E 02	-0.146455E 02	0.105397E 02
2.00	-0.126178E 01	0.114000E 01	-0.134516E 01	0.925923E 00	-0.309403E 01	0.278089E 01	-0.339728E 01	0.245687E 01
3.00	-0.338155E 00	0.399968E 00	-0.342553E 00	0.326686E 00	-0.928282E 00	0.865147E 00	-0.961240E 00	0.723948E 00
4.00	0.0	0.250000E 00	0.0	0.250000E 00	-0.262271E 00	0.317289E 00	-0.264320E 00	0.270343E 00
5.00	0.262271E 00	0.376071E 00	0.264320E 00	0.449449E 00	0.0	0.200000E 00	0.0	0.199999E 00
6.00	0.736254E 00	0.851461E 00	0.752645E 00	0.107607E 01	0.214282E 00	0.302210E 00	0.215399E 00	0.349186E 00
7.00	0.187665E 01	0.210878E 01	0.194348E 01	0.271821E 01	0.610725E 00	0.692234E 00	0.620064E 00	0.836352E 00
8.00	0.476931E 01	0.533891E 01	0.499028E 01	0.695933E 01	0.157419E 01	0.173289E 01	0.161354E 01	0.212561E 01
9.00	0.122635E 02	0.136523E 02	0.128689E 02	0.179397E 02	0.403515E 01	0.442437E 01	0.416834E 01	0.547399E 01
10.00	0.314222E 02	0.351501E 02	0.333430E 02	0.464790E 02	0.103926E 02	0.113889E 02	0.108026E 02	0.141804E 02
20.00	0.460995E 06	0.543758E 06	0.529987E 06	0.738777E 06	0.160778E 06	0.176176E 06	0.171714E 06	0.225391E 06
30.00	0.872519E 10	0.975798E 10	0.959396E 10	0.133735E 11	0.288522E 10	0.316155E 10	0.310841E 10	0.408009E 10
40.00	0.166221E 15	0.185939E 15	0.183600E 15	0.255930E 15	0.549780E 14	0.602435E 14	0.594857E 14	0.780807E 14
50.00	0.327263E 19	0.366085E 19	0.362406E 19	0.505177E 19	0.108243E 19	0.118610E 19	0.117418E 19	0.154123E 19
60.00	0.657759E 23	0.735786E 23	0.729629E 23	0.101707E 24	0.217556E 23	0.238392E 23	0.236397E 23	0.310294E 23
70.00	0.134693E 28	0.150000E 28	0.148925E 28	0.207594E 28	0.443518E 27	0.485995E 27	0.482511E 27	0.633343E 27
80.00	0.276222E 32	0.308988E 32	0.307051E 32	0.428016E 32	0.913612E 31	0.100111E 32	0.994837E 31	0.130582E 32
90.00	0.573522E 36	0.641556E 36	0.637982E 36	0.889318E 36	0.189694E 36	0.207862E 36	0.206704E 36	0.271319E 36
100.00	0.119627E 41	0.134042E 41	0.133370E 41	0.185911E 41	0.396332E 40	0.434290E 40	0.432114E 40	0.567191E 40

18

444

X1= 6.00

X1= 7.00

X	K=0,L=0	K=0,L=1	K=1,L=1	K=1,L=2	K=0,L=0	K=0,L=1	K=1,L=1	K=1,L=2
0.01	-0.317428E 03	0.289611E 03	-0.613259E 04	0.467748E 04	-0.795972E 03	0.736698E 03	-0.155998E 05	0.123979E 05
0.05	-0.209382E 03	0.191034E 03	-0.122129E 04	0.931513E 03	-0.525040E 03	0.485941E 03	-0.310668E 04	0.246902E 04
0.10	-0.163181E 03	0.148832E 03	-0.604453E 03	0.461032E 03	-0.409188E 03	0.378717E 03	-0.153758E 04	0.122199E 04
0.20	-0.117841E 03	0.107515E 03	-0.292967E 03	0.223454E 03	-0.295494E 03	0.273490E 03	-0.745237E 03	0.592274E 03
0.30	-0.922751E 02	0.841906E 02	-0.187460E 03	0.142981E 03	-0.231388E 03	0.214158E 03	-0.476853E 03	0.378977E 03
0.40	-0.749333E 02	0.683686E 02	-0.133992E 03	0.102200E 03	-0.187902E 03	0.173910E 03	-0.340844E 03	0.270884E 03
0.50	-0.621514E 02	0.567070E 02	-0.101609E 03	0.775003E 02	-0.155851E 03	0.144246E 03	-0.258469E 03	0.205417E 03
0.60	-0.522748E 02	0.476961E 02	-0.799179E 02	0.609563E 02	-0.131085E 03	0.121324E 03	-0.203293E 03	0.161566E 03
0.70	-0.444082E 02	0.405190E 02	-0.644257E 02	0.491402E 02	-0.111359E 03	0.103067E 03	-0.163885E 03	0.130247E 03
0.80	-0.360093E 02	0.346810E 02	-0.528627E 02	0.403209E 02	-0.953135E 02	0.882167E 02	-0.134471E 03	0.106871E 03
0.90	-0.327235E 02	0.298586E 02	-0.439528E 02	0.335253E 02	-0.820592E 02	0.759494E 02	-0.111807E 03	0.888584E 02
1.00	-0.263057E 02	0.258281E 02	-0.369213E 02	0.281624E 02	-0.709815E 02	0.656967E 02	-0.939207E 02	0.746435E 02
2.00	-0.765474E 01	0.698952E 01	-0.857749E 01	0.654660E 01	-0.192008E 02	0.177729E 02	-0.218238E 02	0.173458E 02
3.00	-0.232962E 01	0.213754E 01	-0.245796E 01	0.188549E 01	-0.585479E 01	0.542293E 01	-0.626417E 01	0.498204E 01
4.00	-0.736254E 00	0.699744E 00	-0.752645E 00	0.600573E 00	-0.187665E 01	0.174648E 01	-0.194348E 01	0.155350E 01
5.00	-0.214282E 00	0.263027E 00	-0.215399E 00	0.230410E 00	-0.610725E 00	0.588327E 00	-0.620064E 00	0.515072E 00
6.00	0.0	0.166666E 00	0.0	0.166666E 00	-0.181169E 00	0.224648E 00	-0.181843E 00	0.200679E 00
7.00	0.181169E 00	0.252634E 00	0.181843E 00	0.285263E 00	0.0	0.142857E 00	0.0	0.142857E 00
8.00	0.322038E 00	0.583595E 00	0.527865E 00	0.683839E 00	0.156933E 00	0.217047E 00	0.157371E 00	0.241021E 00
9.00	0.135699E 01	0.147281E 01	0.138217E 01	0.174678E 01	0.455973E 00	0.504627E 00	0.459853E 00	0.578357E 00
10.00	0.350154E 01	0.378518E 01	0.358844E 01	0.452009E 01	0.119310E 01	0.128162E 01	0.121020E 01	0.148354E 01
20.00	0.541861E 05	0.585387E 05	0.570561E 05	0.718324E 05	0.185033E 05	0.197833E 05	0.192823E 05	0.235439E 05
30.00	0.972394E 09	0.105050E 10	0.103285E 10	0.130033E 10	0.332050E 09	0.355021E 09	0.349053E 09	0.426199E 09
40.00	0.162290E 14	0.200173E 14	0.197655E 14	0.248844E 14	0.632722E 13	0.676493E 13	0.667984E 13	0.815616E 13
50.00	0.384807E 18	0.394111E 18	0.390150E 18	0.491191E 18	0.124573E 18	0.133191E 18	0.131853E 18	0.160994E 18
60.00	0.735218E 22	0.792115E 22	0.785487E 22	0.988912E 22	0.250377E 22	0.267698E 22	0.265458E 22	0.324127E 22
70.00	0.149477E 27	0.161484E 27	0.160326E 27	0.201847E 27	0.510429E 26	0.545740E 26	0.541828E 26	0.661578E 26
80.00	0.307911E 31	0.332644E 31	0.330559E 31	0.416166E 31	0.105144E 31	0.112418E 31	0.111713E 31	0.136403E 31
90.00	0.639318E 35	0.690672E 35	0.686824E 35	0.864698E 35	0.218312E 35	0.233415E 35	0.232115E 35	0.283415E 35
100.00	0.133574E 40	0.144303E 40	0.143580E 40	0.180765E 40	0.456124E 39	0.487678E 39	0.485234E 39	0.592477E 39

X1= 8.00

X1= 9.00

X	K=0,L=0	K=0,L=1	K=1,L=1	K=1,L=2	K=0,L=0	K=0,L=1	K=1,L=1	K=1,L=2
0.01	-0.201863E 04	0.188789E 04	-0.399767E 05	0.327509E 05	-0.516309E 04	0.486719E 04	-0.103064E 06	0.864269E 05
0.05	-0.133153E 04	0.124529E 04	-0.796131E 04	0.652229E 04	-0.340568E 04	0.321050E 04	-0.205251E 05	0.172118E 05
0.10	-0.103772E 04	0.970516E 03	-0.354028E 04	0.322806E 04	-0.265421E 04	0.250210E 04	-0.101585E 05	0.851859E 04
0.20	-0.749391E 03	0.700656E 03	-0.190978E 04	0.156458E 04	-0.191673E 04	0.180688E 04	-0.492361E 04	0.412880E 04
0.30	-0.580013E 03	0.548808E 03	-0.122200E 04	0.100113E 04	-0.150090E 04	0.141489E 04	-0.315046E 04	0.264189E 04
0.40	-0.470531E 03	0.445608E 03	-0.873460E 03	0.715581E 03	-0.121883E 04	0.114898E 04	-0.225188E 04	0.188836E 04
0.50	-0.395247E 03	0.369649E 03	-0.662363E 03	0.542040E 03	-0.101093E 04	0.952995E 03	-0.170765E 04	0.143198E 04
0.60	-0.332439E 03	0.310909E 03	-0.520967E 03	0.426801E 03	-0.850287E 03	0.801557E 03	-0.134311E 04	0.112629E 04
0.70	-0.282413E 03	0.264123E 03	-0.419978E 03	0.344066E 03	-0.722335E 03	0.680938E 03	-0.108275E 04	0.907962E 03
0.80	-0.241721E 03	0.226007E 03	-0.344602E 03	0.282314E 03	-0.618256E 03	0.582824E 03	-0.888422E 03	0.745005E 03
0.90	-0.208108E 03	0.196030E 03	-0.286521E 03	0.234732E 03	-0.532282E 03	0.501777E 03	-0.738683E 03	0.619439E 03
1.00	-0.180014E 03	0.160350E 03	-0.240686E 03	0.197181E 03	-0.460426E 03	0.434039E 03	-0.620514E 03	0.520345E 03
2.00	-0.480905E 02	0.455433E 02	-0.559281E 02	0.458195E 02	-0.124553E 03	0.117415E 03	-0.144189E 03	0.120913E 03
3.00	-0.148520E 02	0.138921E 02	-0.160568E 02	0.131557E 02	-0.379904E 02	0.358137E 02	-0.413976E 02	0.347152E 02
4.00	-0.476981E 01	0.446419E 01	-0.499028E 01	0.409133E 01	-0.122035E 02	0.115053E 02	-0.128689E 02	0.107925E 02
5.00	-0.157419E 01	0.148020E 01	-0.161354E 01	0.132950E 01	-0.403515E 01	0.380666E 01	-0.416834E 01	0.349807E 01
6.00	-0.522038E 00	0.507884E 00	-0.527865E 00	0.451628E 00	-0.135699E 01	0.128606E 01	-0.138217E 01	0.116566E 01
7.00	-0.150933E 00	0.196058E 00	-0.157371E 00	0.177703E 00	-0.455973E 00	0.446970E 00	-0.459853E 00	0.402437E 00
8.00	0.0	0.125000E 00	0.0	0.124999E 00	-0.138423E 00	0.173932E 00	-0.138724E 00	0.159428E 00
9.00	0.130423E 00	0.190256E 00	0.138724E 00	0.208613E 00	0.0	0.111111E 00	0.0	0.111111E 00
10.00	0.464018E 00	0.444585E 00	0.407532E 00	0.501077E 00	0.123823E 00	0.169356E 00	0.124038E 00	0.183861E 00
20.00	0.330000E 04	0.676760E 04	0.659620E 04	0.786746E 04	0.221530E 04	0.233633E 04	0.227716E 04	0.266620E 04
30.00	0.114492E 09	0.121448E 09	0.119406E 09	0.142419E 09	0.397724E 08	0.419265E 08	0.412217E 08	0.482643E 08
40.00	0.210164E 13	0.231414E 13	0.228508E 13	0.272547E 13	0.757604E 12	0.798910E 12	0.788861E 12	0.923633E 12
50.00	0.429335E 17	0.455628E 17	0.451049E 17	0.537978E 17	0.149212E 17	0.157293E 17	0.155712E 17	0.182315E 17
60.00	0.805308E 21	0.915757E 21	0.908094E 21	0.108311E 22	0.299398E 21	0.316140E 21	0.313495E 21	0.367054E 21
70.00	0.175997E 26	0.186690E 26	0.185351E 26	0.221074E 26	0.611383E 25	0.644496E 25	0.639875E 25	0.749195E 25
80.00	0.302541E 30	0.384566E 30	0.382156E 30	0.455807E 30	0.125940E 30	0.132761E 30	0.131929E 30	0.154468E 30
90.00	0.752747E 34	0.798479E 34	0.794031E 34	0.947062E 34	0.261491E 34	0.275653E 34	0.274118E 34	0.320949E 34
100.00	0.157273E 39	0.166828E 39	0.165992E 39	0.197983E 39	0.546338E 38	0.575927E 38	0.573041E 38	0.670943E 38

20

446<

x1= 10.00

x1= 20.00

X	K=0,L=0	K=0,L=1	K=1,L=1	K=1,L=2	K=0,L=0	K=0,L=1	K=1,L=1	K=1,L=2
0.01	-0.132937E 05	0.126104E 05	-0.267029E 06	0.228092E 06	-0.205649E 09	0.200440E 09	-0.424439E 10	0.393025E 10
0.05	-0.876879E 04	0.831806E 04	-0.531784E 05	0.454242E 05	-0.135650E 09	0.132215E 09	-0.845264E 09	0.782703E 09
0.10	-0.663393E 04	0.648266E 04	-0.263195E 05	0.224817E 05	-0.105719E 09	0.103041E 09	-0.418345E 09	0.387382E 09
0.20	-0.493511E 04	0.468144E 04	-0.127565E 05	0.108965E 05	-0.763445E 08	0.744109E 08	-0.202764E 09	0.187757E 09
0.30	-0.366445E 04	0.366532E 04	-0.816250E 04	0.697229E 04	-0.597818E 08	0.582677E 08	-0.129742E 09	0.120140E 09
0.40	-0.313619E 04	0.297639E 04	-0.583437E 04	0.498363E 04	-0.485468E 08	0.473172E 08	-0.927366E 08	0.858729E 08
0.50	-0.260290E 04	0.246911E 04	-0.442432E 04	0.377919E 04	-0.402660E 08	0.392462E 08	-0.703241E 08	0.651192E 08
0.60	-0.218928E 04	0.207675E 04	-0.347985E 04	0.297244E 04	-0.338674E 08	0.330097E 08	-0.553118E 08	0.512180E 08
0.70	-0.185983E 04	0.176424E 04	-0.280529E 04	0.239623E 04	-0.287710E 08	0.280423E 08	-0.445897E 08	0.412895E 08
0.80	-0.159186E 04	0.151003E 04	-0.230180E 04	0.196617E 04	-0.246255E 08	0.240018E 08	-0.365869E 08	0.338790E 08
0.90	-0.137049E 04	0.130005E 04	-0.191385E 04	0.163478E 04	-0.212011E 08	0.206641E 08	-0.304204E 08	0.281689E 08
1.00	-0.116548E 04	0.112455E 04	-0.160768E 04	0.137326E 04	-0.183390E 08	0.178746E 08	-0.255540E 08	0.236626E 08
2.00	-0.320692E 03	0.304208E 03	-0.373579E 03	0.319106E 03	-0.496101E 07	0.483536E 07	-0.593800E 07	0.549851E 07
3.00	-0.976164E 02	0.927887E 02	-0.107257E 03	0.916176E 02	-0.151319E 07	0.147486E 07	-0.170484E 07	0.157866E 07
4.00	-0.314222E 02	0.298075E 02	-0.333430E 02	0.284815E 02	-0.486095E 06	0.473784E 06	-0.529987E 06	0.490761E 06
5.00	-0.103926E 02	0.985937E 01	-0.108026E 02	0.922836E 01	-0.160778E 06	0.156705E 06	-0.171714E 06	0.159005E 06
6.00	-0.356154E 01	0.332394E 01	-0.358844E 01	0.306749E 01	-0.541861E 05	0.528137E 05	-0.570561E 05	0.528332E 05
7.00	-0.119310E 01	0.113776E 01	-0.121020E 01	0.103958E 01	-0.185033E 05	0.180347E 05	-0.192823E 05	0.178552E 05
8.00	-0.404818E 00	0.399194E 00	-0.407532E 00	0.363078E 00	-0.636000E 04	0.621841E 04	-0.659620E 04	0.610799E 04
9.00	-0.123623E 00	0.156297E 00	-0.124038E 00	0.144548E 00	-0.221630E 04	0.216016E 04	-0.227716E 04	0.210862E 04
10.00	0.0	0.999998E-01	0.0	0.999997E-01	-0.774467E 03	0.754852E 03	-0.791732E 03	0.733134E 03
20.00	0.774467E 03	0.812306E 03	0.791732E 03	0.913198E 03	0.0	0.499999E-01	0.0	0.500000E-01
30.00	0.136981E 08	0.145772E 08	0.143322E 08	0.165310E 08	0.448776E 03	0.459861E 03	0.452132E 03	0.486445E 03
40.00	0.264629E 12	0.277769E 12	0.274275E 12	0.316353E 12	0.855143E 07	0.876267E 07	0.865244E 07	0.930911E 07
50.00	0.521409E 16	0.546884E 16	0.541388E 16	0.624446E 16	0.168365E 12	0.172524E 12	0.170790E 12	0.183751E 12
60.00	0.104797E 21	0.109917E 21	0.108997E 21	0.125719E 21	0.338392E 16	0.346751E 16	0.343850E 16	0.369946E 16
70.00	0.213643E 25	0.224081E 25	0.222475E 25	0.256606E 25	0.689860E 20	0.706901E 20	0.701833E 20	0.755098E 20
80.00	0.440088E 29	0.461590E 29	0.458696E 29	0.529068E 29	0.142106E 25	0.145616E 25	0.144703E 25	0.155685E 25
90.00	0.913759E 33	0.958404E 33	0.953065E 33	0.109928E 34	0.295056E 29	0.302344E 29	0.300660E 29	0.323478E 29
100.00	0.190913E 38	0.200241E 38	0.199238E 38	0.229804E 38	0.616465E 33	0.631693E 33	0.628528E 33	0.676229E 33

X1= 30.00

X1= 40.00

X	K=0,L=0	K=0,L=1	K=1,L=1	K=1,L=2	K=0,L=0	K=0,L=1	K=1,L=1	K=1,L=2
0.01	-0.369046E 13	0.362843E 13	-0.760331E 14	0.730246E 14	-0.703218E 17	0.694372E 17	+0.147035E 19	0.141557E 19
0.05	-0.243430E 13	0.239339E 13	-0.153012E 14	0.145427E 14	-0.463857E 17	0.458022E 17	-0.292819E 18	0.281909E 18
0.10	-0.189717E 13	0.186528E 13	-0.757300E 13	0.719761E 13	-0.361506E 17	0.356958E 17	-0.144924E 18	0.139525E 18
0.20	-0.137004E 13	0.134701E 13	-0.367049E 13	0.348855E 13	-0.261061E 17	0.257777E 17	-0.702421E 17	0.676249E 17
0.30	-0.107281E 13	0.105478E 13	-0.234863E 13	0.223221E 13	-0.204424E 17	0.201853E 17	-0.449457E 17	0.432710E 17
0.40	-0.871194E 12	0.856550E 12	-0.167874E 13	0.159553E 13	-0.166006E 17	0.163918E 17	-0.321261E 17	0.309291E 17
0.50	-0.722591E 12	0.710445E 12	-0.127303E 13	0.120992E 13	-0.137690E 17	0.135958E 17	-0.243619E 17	0.234542E 17
0.60	-0.607766E 12	0.597550E 12	-0.100127E 13	0.951638E 12	-0.115810E 17	0.114353E 17	-0.191613E 17	0.184474E 17
0.70	-0.510309E 12	0.507630E 12	-0.807175E 12	0.767164E 12	-0.983827E 16	0.971451E 16	-0.154469E 17	0.148714E 17
0.80	-0.441915E 12	0.434487E 12	-0.662307E 12	0.629477E 12	-0.842070E 16	0.831478E 16	-0.126746E 17	0.122023E 17
0.90	-0.380463E 12	0.374068E 12	-0.550679E 12	0.523382E 12	-0.724973E 16	0.715853E 16	-0.105383E 17	0.101457E 17
1.00	-0.329102E 12	0.323571E 12	-0.462585E 12	0.439655E 12	-0.627105E 16	0.619217E 16	-0.885248E 16	0.852264E 16
2.00	-0.890274E 11	0.875310E 11	-0.107491E 12	0.102163E 12	-0.169642E 16	0.167508E 16	-0.205706E 16	0.198042E 16
3.00	-0.271548E 11	0.266984E 11	-0.308615E 11	0.293317E 11	-0.517436E 15	0.510927E 15	-0.590596E 15	0.568591E 15
4.00	-0.872319E 10	0.857657E 10	-0.959396E 10	0.911840E 10	-0.166221E 15	0.164130E 15	-0.183600E 15	0.176759E 15
5.00	-0.288522E 10	0.283673E 10	-0.310841E 10	0.295433E 10	-0.549780E 14	0.542864E 14	-0.594857E 14	0.572692E 14
6.00	-0.972394E 09	0.956049E 09	-0.103285E 10	0.981648E 09	-0.185290E 14	0.182959E 14	-0.197655E 14	0.190291E 14
7.00	-0.332050E 09	0.326469E 09	-0.349053E 09	0.331751E 09	-0.632722E 13	0.624763E 13	-0.667984E 13	0.643095E 13
8.00	-0.114492E 09	0.112567E 09	-0.119406E 09	0.113487E 09	-0.218164E 13	0.215420E 13	-0.228508E 13	0.219993E 13
9.00	-0.397724E 08	0.391039E 08	-0.412217E 08	0.391784E 08	-0.757864E 12	0.748331E 12	-0.788861E 12	0.759468E 12
10.00	-0.136981E 08	0.136645E 08	-0.143322E 08	0.136217E 08	-0.264829E 12	0.261498E 12	-0.274275E 12	0.264055E 12
20.00	-0.448776E 03	0.441232E 03	-0.452132E 03	0.429720E 03	-0.855143E 07	0.844386E 07	-0.865244E 07	0.833005E 07
30.00	0.0	0.333333E-01	0.0	0.333333E-01	-0.317627E 03	0.313632E 03	-0.318817E 03	0.306938E 03
40.00	0.317627E 03	0.322878E 03	0.318817E 03	0.334886E 03	0.0	0.250000E-01	0.0	0.250000E-01
50.00	0.625300E 07	0.635098E 07	0.629310E 07	0.661029E 07	0.246125E 03	0.249183E 03	0.246678E 03	0.259985E 03
60.00	0.125090E 12	0.127768E 12	0.126699E 12	0.133085E 12	0.494681E 07	0.500827E 07	0.496636E 07	0.515373E 07
70.00	0.250236E 16	0.260472E 16	0.258605E 16	0.271639E 16	0.100848E 12	0.102100E 12	0.101369E 12	0.105193E 12
80.00	0.527820E 20	0.536552E 20	0.533189E 20	0.560063E 20	0.207738E 16	0.210319E 16	0.209001E 16	0.216886E 16
90.00	0.109593E 25	0.111405E 25	0.110784E 25	0.116368E 25	0.431329E 20	0.436688E 20	0.434255E 20	0.450639E 20
100.00	0.228975E 29	0.232760E 29	0.231594E 29	0.243267E 29	0.901184E 24	0.912380E 24	0.907808E 24	0.942057E 24

X1= 50.00

X1= 60.00

X	K=0,L=0	K=0,L=1	K=1,L=1	K=1,L=2	K=0,L=0	K=0,L=1	K=1,L=1	K=1,L=2
0.01	-0.138453E 22	0.137061E 22	-0.290232E 23	0.281570E 23	-0.278273E 26	0.275945E 26	-0.584322E 27	0.569776E 27
0.05	-0.913264E 21	0.904086E 21	-0.577992E 22	0.560741E 22	-0.183555E 26	0.182019E 26	-0.116367E 27	0.113470E 27
0.10	-0.711749E 21	0.704597E 21	-0.286065E 22	0.277527E 22	-0.143053E 26	0.141856E 26	-0.575932E 26	0.561595E 26
0.20	-0.515989E 21	0.508823E 21	-0.138650E 22	0.134512E 22	-0.103305E 26	0.102441E 26	-0.279144E 26	0.272195E 26
0.30	-0.402480E 21	0.398435E 21	-0.887178E 21	0.860699E 21	-0.808937E 25	0.802168E 25	-0.178615E 26	0.174169E 26
0.40	-0.320841E 21	0.323556E 21	-0.634134E 21	0.615207E 21	-0.656910E 25	0.651413E 25	-0.127670E 26	0.124492E 26
0.50	-0.271090E 21	0.268366E 21	-0.480877E 21	0.466525E 21	-0.544859E 25	0.540300E 25	-0.968148E 25	0.944046E 25
0.60	-0.220012E 21	0.225721E 21	-0.378223E 21	0.366934E 21	-0.458276E 25	0.454442E 25	-0.761474E 25	0.742518E 25
0.70	-0.193701E 21	0.191754E 21	-0.304905E 21	0.295804E 21	-0.389314E 25	0.386057E 25	-0.613863E 25	0.598582E 25
0.80	-0.165791E 21	0.164125E 21	-0.250182E 21	0.242715E 21	-0.333219E 25	0.330431E 25	-0.503690E 25	0.491151E 25
0.90	-0.142730E 21	0.141302E 21	-0.208015E 21	0.201807E 21	-0.286882E 25	0.284482E 25	-0.418796E 25	0.408370E 25
1.00	-0.123467E 21	0.122227E 21	-0.174738E 21	0.169523E 21	-0.248155E 25	0.246078E 25	-0.351800E 25	0.343042E 25
2.00	-0.335999E 20	0.330842E 20	-0.406041E 20	0.393922E 20	-0.671298E 24	0.665681E 24	-0.817481E 24	0.797130E 24
3.00	-0.101875E 20	0.100851E 20	-0.116577E 20	0.113098E 20	-0.204757E 24	0.203044E 24	-0.234704E 24	0.228861E 24
4.00	-0.327203E 19	0.323974E 19	-0.362406E 19	0.351589E 19	-0.657759E 23	0.652255E 23	-0.729629E 23	0.711466E 23
5.00	-0.108243E 19	0.107155E 19	-0.117418E 19	0.113914E 19	-0.217556E 23	0.215735E 23	-0.236397E 23	0.230512E 23
6.00	-0.304807E 18	0.361141E 18	-0.390150E 18	0.378506E 18	-0.733218E 22	0.727083E 22	-0.785487E 22	0.765933E 22
7.00	-0.124573E 18	0.123321E 18	-0.131853E 18	0.127917E 18	-0.250377E 22	0.248282E 22	-0.265458E 22	0.258850E 22
8.00	-0.425533E 17	0.425216E 17	-0.451049E 17	0.437587E 17	-0.863308E 21	0.856084E 21	-0.908094E 21	0.885488E 21
9.00	-0.149212E 17	0.147712E 17	-0.155712E 17	0.151065E 17	-0.299898E 21	0.297388E 21	-0.313495E 21	0.305691E 21
10.00	-0.521409E 16	0.516109E 16	-0.541388E 16	0.525229E 16	-0.104797E 21	0.103920E 21	-0.108997E 21	0.106284E 21
20.00	-0.165805E 12	0.165873E 12	-0.170790E 12	0.165892E 12	-0.338392E 16	0.335561E 16	-0.343850E 16	0.335290E 16
30.00	-0.625300E 07	0.619075E 07	-0.629310E 07	0.610527E 07	-0.125690E 12	0.124638E 12	-0.126699E 12	0.123544E 12
40.00	-0.240125E 03	0.243651E 03	-0.246678E 03	0.239316E 03	-0.494681E 07	0.490542E 07	-0.496636E 07	0.484273E 07
50.00	0.0	0.200000E-01	0.0	0.200000E-01	-0.200998E 03	0.199316E 03	-0.201299E 03	0.196288E 03
60.00	0.200998E 03	0.202498E 03	0.201299E 03	0.207368E 03	0.0	0.166666E-01	0.0	0.166667E-01
70.00	0.409782E 07	0.413839E 07	0.410872E 07	0.423259E 07	0.169892E 03	0.171302E 03	0.170074E 03	0.174343E 03
80.00	0.849077E 11	0.852476E 11	0.847132E 11	0.872670E 11	0.349965E 07	0.352869E 07	0.350657E 07	0.359459E 07
90.00	0.175257E 16	0.176015E 16	0.176015E 16	0.181321E 16	0.726635E 11	0.732666E 11	0.728584E 11	0.746873E 11
100.00	0.360167E 20	0.369810E 20	0.367957E 20	0.379050E 20	0.151817E 16	0.153077E 16	0.152310E 16	0.156133E 16

23

449

X1= 70.00

X1= 80.00

X	K=0,L=0	K=0,L=1	K=1,L=1	K=1,L=2	K=0,L=0	K=0,L=1	K=1,L=1	K=1,L=2
0.01	-0.507299E 30	0.563232E 30	-0.119266E 32	0.116720E 32	-0.116859E 35	0.116127E 35	-0.245902E 36	0.241306E 36
0.05	-0.374202E 30	0.371520E 30	-0.237517E 31	0.232446E 31	-0.770828E 34	0.765995E 34	-0.489710E 35	0.480557E 35
0.10	-0.291633E 30	0.289543E 30	-0.117554E 31	0.115044E 31	-0.600742E 34	0.596976E 34	-0.242371E 35	0.237841E 35
0.20	-0.210603E 30	0.209093E 30	-0.569761E 30	0.557596E 30	-0.433825E 34	0.431105E 34	-0.117473E 35	0.115277E 35
0.30	-0.164913E 30	0.163731E 30	-0.364572E 30	0.356788E 30	-0.339708E 34	0.337578E 34	-0.751670E 34	0.737621E 34
0.40	-0.133920E 30	0.132960E 30	-0.260588E 30	0.255024E 30	-0.275865E 34	0.274136E 34	-0.537276E 34	0.527234E 34
0.50	-0.111077E 30	0.110281E 30	-0.197609E 30	0.193390E 30	-0.228810E 34	0.227376E 34	-0.407428E 34	0.399813E 34
0.60	-0.934260E 29	0.927563E 29	-0.155425E 30	0.152106E 30	-0.192450E 34	0.191244E 34	-0.320453E 34	0.314464E 34
0.70	-0.793671E 29	0.787982E 29	-0.125296E 30	0.122621E 30	-0.163490E 34	0.162465E 34	-0.258334E 34	0.253505E 34
0.80	-0.679314E 29	0.674444E 29	-0.102808E 30	0.100613E 30	-0.139933E 34	0.139056E 34	-0.211969E 34	0.208007E 34
0.90	-0.584849E 29	0.580657E 29	-0.854805E 29	0.836555E 29	-0.120474E 34	0.119719E 34	-0.176243E 34	0.172949E 34
1.00	-0.505898E 29	0.502271E 29	-0.718060E 29	0.702729E 29	-0.104211E 34	0.103558E 34	-0.148049E 34	0.145282E 34
2.00	-0.136853E 29	0.135872E 29	-0.160856E 29	0.163294E 29	-0.281907E 33	0.280140E 33	-0.344022E 33	0.337592E 33
3.00	-0.417425E 28	0.414433E 28	-0.479056E 28	0.468828E 28	-0.859864E 32	0.854474E 32	-0.987712E 32	0.969251E 32
4.00	-0.134093E 28	0.133132E 28	-0.148925E 28	0.145745E 28	-0.276222E 32	0.274490E 32	-0.307051E 32	0.301312E 32
5.00	-0.443518E 27	0.440338E 27	-0.482511E 27	0.472209E 27	-0.913612E 31	0.907885E 31	-0.994837E 31	0.976243E 31
6.00	-0.149477E 27	0.148405E 27	-0.160326E 27	0.156903E 27	-0.307911E 31	0.305980E 31	-0.330559E 31	0.326380E 31
7.00	-0.510429E 26	0.506770E 26	-0.541828E 26	0.530259E 26	-0.105144E 31	0.104485E 31	-0.111713E 31	0.109625E 31
8.00	-0.175997E 26	0.174736E 26	-0.185351E 26	0.181594E 26	-0.362541E 30	0.360268E 30	-0.382156E 30	0.375013E 30
9.00	-0.611383E 25	0.607001E 25	-0.639875E 25	0.626214E 25	-0.125940E 30	0.125151E 30	-0.131929E 30	0.129463E 30
10.00	-0.215643E 25	0.212111E 25	-0.222475E 25	0.217725E 25	-0.440088E 29	0.437329E 29	-0.458696E 29	0.450123E 29
20.00	-0.689360E 20	0.684914E 20	-0.701833E 20	0.686849E 20	-0.142106E 25	0.141215E 25	-0.144703E 25	0.141999E 25
30.00	-0.256236E 16	0.254399E 16	-0.258605E 16	0.253083E 16	-0.527826E 20	0.524517E 20	-0.533189E 20	0.523223E 20
40.00	-0.100848E 12	0.100129E 12	-0.101369E 12	0.992043E 11	-0.207738E 16	0.206436E 16	-0.209001E 16	0.205094E 16
50.00	-0.409762E 07	0.406824E 07	-0.410872E 07	0.402100E 07	-0.844077E 11	0.838785E 11	-0.847132E 11	0.831299E 11
60.00	-0.169692E 03	0.166674E 03	-0.170074E 03	0.166443E 03	-0.349965E 07	0.347771E 07	-0.350657E 07	0.344103E 07
70.00	0.0	0.142857E-01	0.0	0.142857E-01	-0.147141E 03	0.146218E 03	-0.147259E 03	0.144507E 03
80.00	0.147141E 03	0.148188E 03	0.147259E 03	0.150426E 03	0.0	0.125000E-01	0.0	0.125000E-01
90.00	0.305910E 07	0.307685E 07	0.305971E 07	0.312550E 07	0.129772E 03	0.130580E 03	0.129853E 03	0.132295E 03
100.00	0.636308E 11	0.642851E 11	0.639630E 11	0.653384E 11	0.271135E 07	0.272824E 07	0.271457E 07	0.276562E 07

24

450<

X1= 90.00

X1=100.00

X	K=0,L=0	K=0,L=1	K=1,L=1	K=1,L=2	K=0,L=0	K=0,L=1	K=1,L=1	K=1,L=2
0.01	-0.242636E 39	0.241284E 39	-0.510927E 40	0.502436E 40	-0.506944E 43	0.504403E 43	-0.106809E 45	0.105211E 45
0.05	-0.160048E 39	0.159156E 39	-0.1C1750E 40	0.100059E 40	-0.334391E 43	0.332715E 43	-0.212709E 44	0.209526E 44
0.10	-0.124733E 39	0.124038E 39	-0.503591E 39	0.495222E 39	-0.260606E 43	0.259300E 43	-0.105275E 44	0.103700E 44
0.20	-0.900755E 38	0.895738E 38	-0.244081E 39	0.240025E 39	-0.188196E 43	0.187253E 43	-0.510250E 43	0.502616E 43
0.30	-0.705339E 38	0.701410E 38	-0.156180E 39	0.153584E 39	-0.147366E 43	0.146629E 43	-0.326493E 43	0.321608E 43
0.40	-0.572782E 38	0.569591E 38	-0.111634E 39	0.109778E 39	-0.119672E 43	0.119073E 43	-0.233369E 43	0.229878E 43
0.50	-0.475081E 38	0.472434E 38	-0.846541E 38	0.832472E 38	-0.992595E 42	0.987621E 42	-0.176969E 43	0.174321E 43
0.60	-0.399587E 38	0.397361E 38	-0.665827E 38	0.654762E 38	-0.834864E 42	0.830680E 42	-0.139191E 43	0.137108E 43
0.70	-0.339456E 38	0.337565E 38	-0.536758E 38	0.527837E 38	-0.709233E 42	0.705678E 42	-0.112209E 43	0.110530E 43
0.80	-0.290545E 38	0.288927E 38	-0.440423E 38	0.433163E 38	-0.607042E 42	0.604000E 42	-0.920701E 42	0.906926E 42
0.90	-0.250142E 38	0.248749E 38	-0.366192E 38	0.360106E 38	-0.522627E 42	0.520008E 42	-0.765522E 42	0.754068E 42
1.00	-0.216574E 38	0.215169E 38	-0.307611E 38	0.302499E 38	-0.452075E 42	0.449810E 42	-0.643059E 42	0.633438E 42
2.00	-0.585327E 37	0.582066E 37	-0.714799E 37	0.702919E 37	-0.122293E 42	0.121681E 42	-0.149428E 42	0.147193E 42
3.00	-0.178534E 37	0.177540E 37	-0.205224E 37	0.201813E 37	-0.373015E 41	0.371146E 41	-0.429019E 41	0.422600E 41
4.00	-0.573522E 36	0.570327E 36	-0.637982E 36	0.627379E 36	-0.119827E 41	0.119227E 41	-0.133370E 41	0.131374E 41
5.00	-0.189694E 36	0.188638E 36	-0.206704E 36	0.203269E 36	-0.396332E 40	0.394346E 40	-0.432114E 40	0.425649E 40
6.00	-0.639318E 35	0.635757E 35	-0.686824E 35	0.675410E 35	-0.133574E 40	0.132904E 40	-0.143580E 40	0.141432E 40
7.00	-0.218312E 35	0.217096E 35	-0.232115E 35	0.228257E 35	-0.456124E 39	0.453839E 39	-0.485234E 39	0.477974E 39
8.00	-0.752747E 34	0.748554E 34	-0.794031E 34	0.780834E 34	-0.157273E 39	0.156485E 39	-0.165992E 39	0.163508E 39
9.00	-0.261491E 34	0.260034E 34	-0.274118E 34	0.269562E 34	-0.544338E 38	0.543600E 38	-0.573041E 38	0.564467E 38
10.00	-0.913759E 33	0.908669E 33	-0.953065E 33	0.937225E 33	-0.190913E 38	0.189957E 38	-0.199238E 38	0.196257E 38
20.00	-0.295056E 29	0.293412E 29	-0.300660E 29	0.295663E 29	-0.616465E 33	0.613376E 33	-0.628528E 33	0.619124E 33
30.00	-0.109593E 25	0.108983E 25	-0.110784E 25	0.108943E 25	-0.228975E 29	0.227827E 29	-0.231594E 29	0.228129E 29
40.00	-0.431329E 20	0.428926E 20	-0.434255E 20	0.427038E 20	-0.901184E 24	0.896668E 24	-0.907808E 24	0.894225E 24
50.00	-0.175257E 16	0.174280E 16	-0.176015E 16	0.173089E 16	-0.366167E 20	0.364332E 20	-0.367957E 20	0.362452E 20
60.00	-0.726635E 11	0.722587E 11	-0.728584E 11	0.716475E 11	-0.151817E 16	0.151056E 16	-0.152310E 16	0.150031E 16
70.00	-0.305510E 07	0.303808E 07	-0.305971E 07	0.300885E 07	-0.638308E 11	0.635109E 11	-0.639630E 11	0.630060E 11
80.00	-0.129772E 03	0.129049E 03	-0.129853E 03	0.127695E 03	-0.271135E 07	0.269776E 07	-0.271457E 07	0.267395E 07
90.00	0.0	0.111111E-01	0.0	0.111111E-01	-0.116075E 03	0.115493E 03	-0.116133E 03	0.114396E 03
100.00	0.116075E 03	0.116718E 03	0.116133E 03	0.118074E 03	0.0	0.999998E-02	0.0	0.999999E-02

ANALYTICAL PREDICTION OF THE HEAT TRANSFER  
FROM A BLOOD VESSEL NEAR THE SKIN SURFACE  
WHEN COOLED BY A SYMMETRICAL COOLING STRIP

J. C. Chato

A. Shitzer

Technical Report No. ME-TR-344

December 1971

452<

DEPARTMENT OF MECHANICAL AND INDUSTRIAL ENGINEERING  
LABORATORY FOR ERGONOMICS RESEARCH  
ENGINEERING EXPERIMENT STATION  
UNIVERSITY OF ILLINOIS AT URBANA - CHAMPAIGN  
URBANA, ILLINOIS 61801



# **ANALYTICAL PREDICTION OF THE HEAT TRANSFER FROM A BLOOD VESSEL NEAR THE SKIN SURFACE WHEN COOLED BY A SYMMETRICAL COOLING STRIP**

by

J. C. CHATO

A. SHITZER

Technical Report No. ME-TR-344

December 1971

Supported by

National Aeronautics and Space Administration

under Special Supplement to

Grant No. NGR-14-005-103

*I*

453<

/

ANALYTICAL PREDICTION OF THE HEAT TRANSFER FROM A  
BLOOD VESSEL NEAR THE SKIN SURFACE COOLED  
BY A SYMMETRICAL COOLING STRIP

J. C. Chato

A. Shitzer

Technical Report No. ME-TR-344

December 1971

Supported by

National Aeronautics and Space Administration

under special supplement to

Grant No. NGR 14-005-103

## ABSTRACT

An analytical method has been developed to estimate the amount of heat extracted from an artery running close to the skin surface which is cooled in a symmetrical fashion by a cooling strip.

The results indicate that the optimum width of a cooling strip is approximately three times the depth to the centerline of the artery. The heat extracted from an artery with such a strip is about  $0.9 \text{ w/m-}^\circ\text{C}$  which is too small to affect significantly the temperature of the blood flow through a main blood vessel, such as the carotid artery.

The method is applicable to veins as well.

## NOMENCLATURE

A through H	locations in Fig. 1
a	width of tissue, (L)*
2a <sub>n</sub>	cooled width of skin, (L)
b	depth to centerline of artery, (L)
c <sub>b</sub>	specific heat of blood, (E/M - T)
c <sub>p</sub>	specific heat of tissue, (E/M - T)
d	depth to body core, (L)
F <sub>1</sub> , F <sub>2</sub> , F <sub>3</sub>	constant heat fluxes, (E/L <sup>2</sup> t)
k	thermal conductivity of tissue, (E/t - L - T)
L	length of cooled section, (L)
q	local volumetric heat generation rate, (E/t - L <sup>3</sup> )
q <sub>a</sub>	heat loss from 1/2 artery per unit length, (E/t - L)
q <sub>1</sub>	heat extracted by cooling strip per unit length, (E/t - L)
Q	q/k, (T/L <sup>2</sup> )
R	radius of artery, (L)
t	time, (t)
T	temperature, (T)
T <sub>1</sub>	temperature of cooled skin, (T)
T <sub>2</sub>	temperature of uncooled skin, (T)
T <sub>a</sub>	arterial temperature, (T)
T <sub>m</sub>	mean temperature, (T)
w	(w <sub>b</sub> c <sub>b</sub> / k) <sup>1/2</sup> , (L <sup>-1</sup> )
w <sub>b</sub>	blood perfusion rate, (M/t - L <sup>3</sup> )
x	coordinate perpendicular to centerline of artery, parallel to skin surface, (L)

\*Units in parentheses are: E, energy; M, mass; L, length; T, temperature; t, time.

$y$	coordinate perpendicular to centerline of artery, perpendicular to skin surface, (L)
$\beta$	length ratio AA'/AF, approaching zero in the limit
$\gamma$	length ratio AG/AF
$\zeta_n$	$(w^2 + \lambda_n^2)^{1/2}$ , (L <sup>-1</sup> )
$\eta$	length ratio CD/CE
$\theta$	$(T - T_1)/\theta_o$
$\theta'$	$T - T_a$ , (T)
$\theta_o = -\theta_1$	$T_a - T_1$ , (T)
$\theta_1 = -\theta_o$	$T_1 - T_a$ , (T)
$\theta_2$	$T_2 - T_a$ , (T)
$\lambda_n$	$n\pi/a$ , (L <sup>-1</sup> )
$\rho$	density of tissue, (M/L <sup>3</sup> )

## SUBSCRIPTS

$a$	arterial
$o$	reference condition

TABLE OF CONTENTS

	Page
INTRODUCTION . . . . .	1
ANALYSIS . . . . .	2
DISCUSSION . . . . .	10
CONCLUSIONS AND RECOMMENDATIONS . . . . .	17
ACKNOWLEDGEMENTS . . . . .	18
REFERENCES . . . . .	19

## INTRODUCTION

Experiments on localized cooling of the neck skin above the carotid artery indicated a significant effect of this cooling on the thermal comfort sensation of the individual [1]\*. An analytical study of the thermal interaction between an artery near the skin and a cooling patch on the skin surface was undertaken to estimate the amount of heat that can be extracted from a blood vessel transcutaneously. The results should help to determine if the effect on the thermal comfort is due to indirect hypothalamic cooling by a reduction of the arterial blood supply temperature or due to some other influence such as that of a local cold receptor.

It is to be understood that the method is applicable to veins as well even though the term "artery" is used throughout this work.

## ANALYSIS

The analysis depends on the solution of the "bio-heat" equation [2,3]:

$$\rho c_p \frac{\partial T}{\partial t} = k \nabla^2 T + w_b c_b (T_a - T) + q \quad (1)$$

The following assumptions were made in developing this equation [3]:

1. The thermophysical properties of the tissue are constant and the tissue is homogeneous and isotropic.
2. Blood enters the tissue at a constant arterial temperature,  $T_a$ , and leaves at the local temperature of the tissue,  $T$ . (This last assumption is based on the almost perfect heat exchange occurring in the capillary bed.)
3. Blood perfusion,  $w_b$ , and metabolic heat production rates,  $q$ , are uniform and constant everywhere in the tissue.

The boundary conditions depend on the assumed geometry as well as on considerations which make the solutions easier to obtain while retaining a reasonable similarity with the physical situation.

Figure 1 depicts the basic tissue geometry considered. It is assumed that the cooling patch runs parallel and symmetrically to the artery. If the temperature gradients along the artery are neglected in comparison to those perpendicular to the artery, the problem becomes two dimensional as shown.

The line of symmetry, through the centerline of the artery A-C, must be adiabatic. Along the skin surface, C-D and D-E, temperatures or heat fluxes can be specified. Since the temperature measurements are much more reliable than flux measurements at the skin surface,

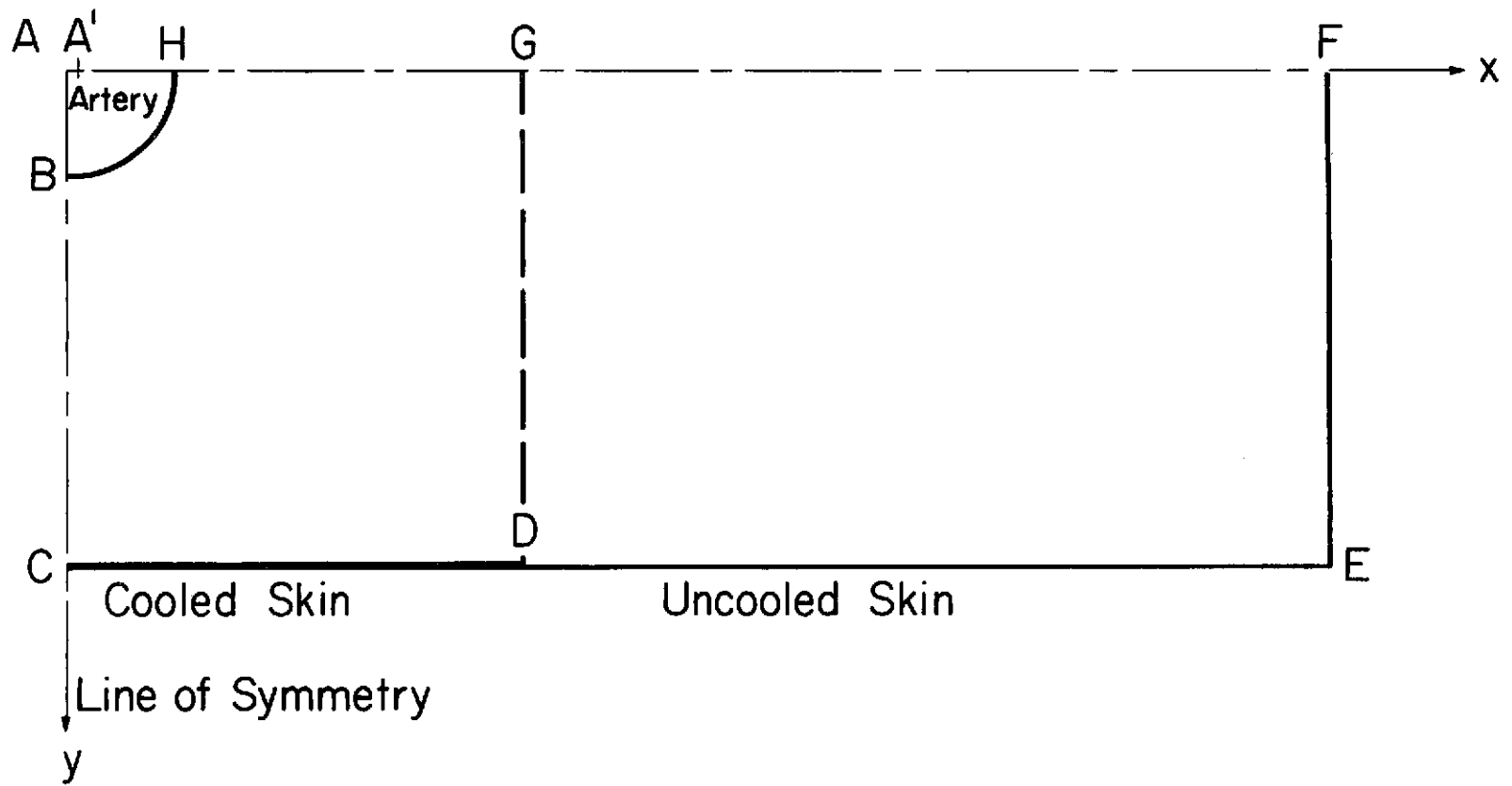


Figure 1 Geometrical configuration of the cooling strip and blood vessel.

temperatures are selected as boundary conditions. If the boundary, E-F, is far enough away from the artery as described below, it may be considered adiabatic. This assumption is equivalent to saying that at long distances from the artery and from the cooling patch, the heat flow is one dimensional, corresponding to a temperature difference between the uncooled skin and the body core located at some fixed distance under the skin. By numerical computations it was found that these two conditions are essentially identical if  $\eta = CD/CE < 1/3$ . For all calculations  $\eta = 0.25$  was used thereafter. At the surface of the artery, B-H, the temperature should be  $T_a$ . Since it is difficult to solve a basically rectangular problem with conditions specified along a curved boundary, an approximation was developed which depended on the specification of the heat flux along the inner boundary, A-F. The approximation is based on the well established fact that the two-dimensional isotherms (constant temperature lines) around a point heat source are circular, (cf. [4]). Consequently, specifying a heat flux of some appropriate intensity at the centerline of the artery, A, will produce circular temperature lines, one of which can be made to coincide as nearly as possible with the surface of the artery. Near the other end of the inner boundary, F, a uniform heat flux can be specified corresponding to a temperature difference between the uncooled skin and the body core. Between A and F, the flux can be somewhat arbitrary, but it must be zero near A to keep the isotherms circular. As will be seen later, the flux distribution is expressed in terms of Fourier series which become more involved as the flux function becomes more complicated.

It has been found, however, that the most important single result, i.e., the total heat lost from the artery, is rather insensitive to the exact shape of the flux function. Therefore, in addition to the heat source at A, zero flux is assumed along A-G and an appropriate, uniform flux is assumed along G-F. G is arbitrarily located under the outer edge of the cooling strip, D. Finally, deep body temperature is assumed to be equal to  $T_a$ .

If the origin of the coordinate system is located at the center of the artery, the problem in mathematical terms becomes as follows:

$$\nabla^2 \theta' - w^2 \theta' = -Q \quad (2)$$

where

$$\theta' = T - T_a \quad (3)$$

$$Q = \frac{q}{k} \quad (4)$$

$$w^2 = \frac{w_b c_b}{k} \quad (5)$$

The boundary conditions are

$$\frac{\partial \theta'}{\partial x} = 0 \text{ at } x = 0 \quad (6a)$$

$$\frac{\partial \theta'}{\partial x} = 0 \text{ at } x = a \quad (6b)$$

$$\frac{\partial \theta'}{\partial y} = -\frac{F_1}{k} \text{ at } 0 < x < \beta a, y = 0 \quad (6c)$$

where

$$\beta = \frac{AA'}{AF} \rightarrow 0$$

$$\frac{\partial \theta'}{\partial y} = 0 \text{ at } \beta a < x < \gamma a, y = 0 \quad (6d)$$

$$\frac{\partial \theta'}{\partial y} = -\frac{F_2}{k} \text{ at } \gamma a < x < a, y = 0 \quad (6e)$$

where  $\gamma = \frac{AG}{AF}$

$$\theta' = \theta_1 \text{ at } 0 < x < \eta a, y = b \quad (6f)$$

$$\theta' = \theta_2 \text{ at } \eta a < x < a, y = b \quad (6g)$$

where  $\eta = \frac{CD}{CE}$ , and

$$\theta_1 = T_1 - T_a \quad (7)$$

$$\theta_2 = T_2 - T_a \quad (8)$$

To non-dimensionalize the problem and to utilize the fact that  $T_1$  is the lowest temperature in the system, define

$$\theta_o = -\theta_1 = T_a - T_1 > 0 \quad (9)$$

$$\theta = \frac{T - T_1}{\theta_o} = 1 - \frac{\theta'}{\theta_1} \quad (10)$$

The solution can be obtained by appropriate transformations of the variables and by Fourier series expansion of the temperature and flux functions [3]. The result is:

$$\begin{aligned} \theta = & 1 - \left[ \frac{Q}{w^2 \theta_o} + \left( 1 - \frac{\theta_2}{\theta_1} \right) + \frac{\theta_2}{\theta_1} \right] \frac{\cosh (wy)}{\cosh (wb)} + \frac{Q}{w^2 \theta_o} \\ & + \frac{F_1 \beta + F_2 (1 - \gamma)}{kw \theta_o} \left[ \frac{\sinh [w(b - y)]}{\cosh (wb)} \right] \\ & + 2 \sum_{n=1}^{\infty} \left\{ \frac{F_1 \beta}{k \theta_o \zeta_n} \sinh [\zeta_n (b - y)] - \frac{F_2}{k \theta_o \zeta_n} \right. \\ & \left. \cdot \frac{\sin (n\pi\gamma)}{n\pi} \sinh [\zeta_n (b - y)] - \frac{\left( 1 - \frac{\theta_2}{\theta_1} \right) \sin (n\pi\eta) \cosh (\zeta_n y)}{n\pi} \right\} \\ & \cdot \frac{\cos (\lambda_n x)}{\cosh (\zeta_n b)} \quad (11) \end{aligned}$$

where

$$\lambda_n = \frac{n\pi}{a} \quad (12)$$

$$\zeta_n^2 = w^2 + \lambda_n^2 \quad (13)$$

$F_2$  can be evaluated from the one-dimensional temperature distribution [3,5] calculated for a depth,  $d$ , from the skin surface to the body core and a temperature difference of  $(T_1 - T_2)$ .

$$\frac{F_2}{kw\theta_o} = \frac{F_3}{kw\theta_o} \frac{\cosh [w(d-b)]}{\cosh (wd)} - \frac{Q}{w^2\theta_o} \frac{\sinh (wb)}{\cosh (wd)} \quad (14)$$

where

$$\frac{F_3}{kw\theta_o} = \frac{\frac{\theta_2}{\theta_1} + \frac{Q}{w^2\theta_o} \left[ 1 - \frac{1}{\cosh (wd)} \right]}{\tanh (wd)} \quad (15)$$

$F_1$  must be selected to provide  $\theta = 1$  at the circumference of the artery at a distance  $R$  from the center. Mathematically, this condition can be satisfied only at one point, which was arbitrarily chosen to be

$$\theta = 1 \text{ at } x = R, y = 0 \quad (16)$$

Thus, from Eq. (11)

$$\begin{aligned} \frac{F_1\beta}{kw\theta_o} = & \left\{ \left[ \frac{Q}{w^2\theta_o} + \left( 1 - \frac{\theta_2}{\theta_1} \right) \eta + \frac{\theta_2}{\theta_1} \right] \frac{1}{\cosh (wb)} - \frac{Q}{w^2\theta_o} \right. \\ & - \frac{F_2(1-\gamma)\tanh (wb)}{kw\theta_o} \\ & + 2 \sum_{n=1}^{\infty} \left[ \frac{F_2}{k\theta_o\zeta_n} \frac{\sin (n\pi\gamma)}{n\pi} \tanh (\zeta_n b) + \frac{\left( 1 - \frac{\theta_2}{\theta_1} \right) \sin (n\pi\eta)}{n \cosh (\zeta_n b)} \right] \\ & \left. \cdot \cos (\lambda_n R) \right\} / \left\{ \tanh (wb) + 2w \sum_{n=1}^{\infty} \frac{\tanh (\zeta_n b)}{\zeta_n} \cos (\lambda_n R) \right\} \quad (17a) \end{aligned}$$

An alternate selection was

$$\theta = 1 \text{ at } x = 0, y = R$$

Then, from Eq. (11)

$$\begin{aligned} \frac{F_1 \beta}{kw\theta_0} = & \left\{ \left[ \frac{Q}{w^2\theta_0} + \left( 1 - \frac{\theta_2}{\theta_1} \right) \eta + \frac{\theta_2}{\theta_1} \right] \frac{\cosh(wR)}{\cosh(wb)} - \frac{Q}{w^2\theta_0} \right. \\ & - \frac{F_2(1-\gamma)}{kw\theta_0} \frac{\sinh[w(b-R)]}{\cosh(wb)} \\ & + 2 \sum_{n=1}^{\infty} \left[ \frac{F_2}{k\theta_0 \zeta_n} \frac{\sin(n\pi\gamma)}{n\pi} \sinh[\zeta_n(b-R)] \right. \\ & \left. \left. + \frac{\left( 1 - \frac{\theta_2}{\theta_1} \right) \sin(n\pi\eta) \cosh(\zeta_n R)}{n\pi} \right] \frac{1}{\cosh(\zeta_n b)} \right\} / \\ & \left\{ \frac{\sinh[w(b-R)]}{\cosh(wb)} + 2w \sum_{n=1}^{\infty} \frac{\sinh[\zeta_n(b-R)]}{\zeta_n \cosh(\zeta_n b)} \right\} \quad (17b) \end{aligned}$$

The two alternatives, Eqs. (17a) and (17b), gave similar results as long as the  $\theta = 1$  isotherm was nearly circular, i.e., as long as a constant arterial surface temperature was closely approximated. Equation (17) generally gave slightly higher heat extraction rates from the artery due to the slightly higher temperature gradients occurring between B and C (see Fig. 1) with this equation.

For evaluating all the series on a digital computer, at least 30 terms were used to obtain good convergence.

The heat lost per unit length from the quarter artery shown in Fig. 1 is equal to

$$\frac{q_a}{2} = F \beta a + \frac{q\pi R^2}{4} + \frac{w_b c_b (T_a - T_m) \pi R^2}{4} \quad (18)$$

where  $q_a$  is the heat loss per unit time per unit length of the skin-side half of the artery.

The first term on the right-hand side is the heat produced by the source at the centerline. The second term is the heat generated within the quarter circle. The third term represents an approximation of the heat supplied by the assumed "blood flow" within the quarter circle. The mean tissue temperature,  $T_m$ , was calculated as the average of 12 temperatures representing 12 equal areas within the quarter circle. This last term was usually negative. The heat removed from the deeper half of the artery must be less than  $q_a$ ; it was estimated to be generally less than 15 percent of  $q_a$ . Because of the uncertainties in establishing the boundary conditions for the other half of the artery, only  $q_a$  was considered for all numerical work and comparisons.

The heat extracted by the cooling strip per unit length can be found by integrating the heat flux at  $y = b$  from  $x = 0$  to  $x = \eta a$  and doubling the result. In dimensionless form this expression becomes

$$\begin{aligned} \frac{q_1 b}{k\theta_0 a} = & 2wb \left\{ \left[ \frac{Q}{w^2\theta_0} + \left( 1 - \frac{\theta_2}{\theta_1} \right) \eta + \frac{\theta_2}{\theta_1} \right] \tanh (wb) \right. \\ & \left. + \frac{F_1 \beta + F_2 (1 - \gamma)}{kw\theta_0 \cosh (wb)} \right\} \eta + 4wb \sum_{n=1}^{\infty} \left\{ \frac{F_1 \beta}{kw\theta_0} - \frac{F_2}{kw\theta_0} \frac{\sin (n\pi\gamma)}{n\pi} \right. \\ & \left. + \frac{\left( 1 - \frac{\theta_2}{\theta_1} \right) \sin (n\pi\eta) \zeta_n \sinh (\zeta_n b)}{wn\pi} \right\} \frac{\sin (n\pi\eta)}{n\pi \cosh (\zeta_n b)} \end{aligned} \quad (19)$$

## DISCUSSION

Although the heat lost from the artery is the most significant result, it is worth while to investigate other aspects of the problem as well. Examination of the analytical results indicates that the following dimensionless parameters occur:

$$\theta, \frac{Q}{w^2 \theta_o}, \frac{\theta_2}{\theta_1}, \gamma, \eta, wb, wd$$

In addition, other geometrical parameters such as  $b_o/2na$ ,  $b/b_o$ , and  $R_o/R$  can be considered.

The influence of  $\eta$  was discussed earlier. It was always taken as 0.25. Variations of  $\gamma$  and  $wd$  were found to affect the heat lost from the artery only minimally. Therefore,  $\gamma$  was made equal to  $\eta$  and  $d$  was set equal to  $b$ .

For the sake of comparisons, the following additional quantities were selected for "normal" or "reference" conditions [3,6]:

Width of cooling strip . . . . .	$2na = 0.0264 \text{ m}$
Depth to centerline of artery . . . . .	$b_o = 0.01 \text{ m} = 1 \text{ cm}$
Radius of artery . . . . .	$R_o = 0.0025 \text{ m} = 0.25 \text{ cm}$
Temperature ratio . . . . .	$\theta_2/\theta_1 = 0.3 \text{ and } 0.15$
Blood heat capacity rate . . . . .	$w_b c_b = 1746 \text{ w/m}^3 \text{ }^\circ\text{C}$
Heat generation rate . . . . .	$q = 660 \text{ w/m}^3$
Thermal conductivity of tissue . . . . .	$k = 0.54 \text{ w/m}^\circ\text{C}$

Figure 2 shows the dimensionless temperature distribution in the vicinity of the artery under the assumed "normal" conditions. The  $\theta = 1.0$  line is virtually circular, as is required for good modeling of the arterial wall temperature. The effect of the temperature

Normal Conditions

$$\theta = \frac{T - T_{\text{cooled skin}}}{T_{\text{artery}} - T_{\text{cooled skin}}}$$

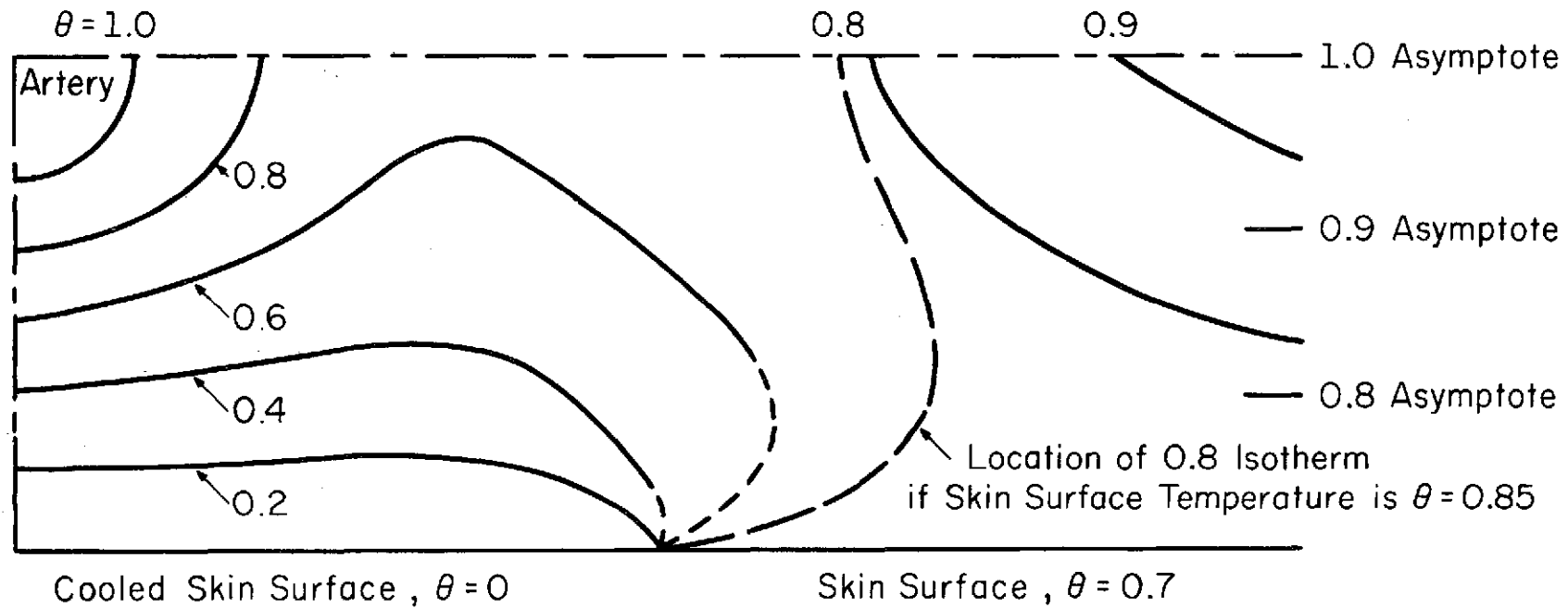


Figure 2 Dimensionless temperature distribution in the vicinity of a cooled artery under the assumed "normal" conditions.

ratio,  $\theta_2/\theta_1$ , is significant only in the relatively unimportant area, DEFG (see Fig. 1), as is demonstrated by the  $\theta = 0.8$  isotherm. The heat loss from the artery changed little for the two temperature ratios used because all this heat was extracted through the cooled portion of the skin as calculated from Eqs. (18) and (19).

Figure 3 should be compared with Fig. 2 to realize the effects of blood perfusion and internal heat generation rates on the temperature distributions. Increasing both of these variables shifts the isotherms toward the skin surface. The effects of the high heat generation rate are relatively small, whereas the increased blood perfusion rate changes the temperature field very significantly, as shown most dramatically by the  $\theta = 0.8$  isotherm.

Figure 4 shows the heat extraction rate from an artery per unit length and unit temperature difference,  $\theta_0 = 1$ , as a function of five dimensionless parameters, all of which have significant influence. One of the curves, showing the effect of  $b_0/2\eta a$ , behaves anomalously below  $b_0/2\eta a = 0.36$ . Physical considerations suggest an asymptotic leveling off of the curve as this parameter approaches zero, i.e., as the width of the cooling strip becomes very wide compared to the depth of the artery. Instead, the calculations show a decrease of heat extraction rates. Investigation of the temperature profiles, however, revealed that in this regime ( $b_0/2\eta a < 0.36$ ) the  $\theta = 1$  isotherm ceased to be circular (it flattened out) the deviation becoming more pronounced as the parameter decreased. In some instances, indications of a possible numerical instability in this regime also occurred. Thus, the model presented here should be considered inappropriate in this region. Instead, it should be assumed that the curve asymptotically

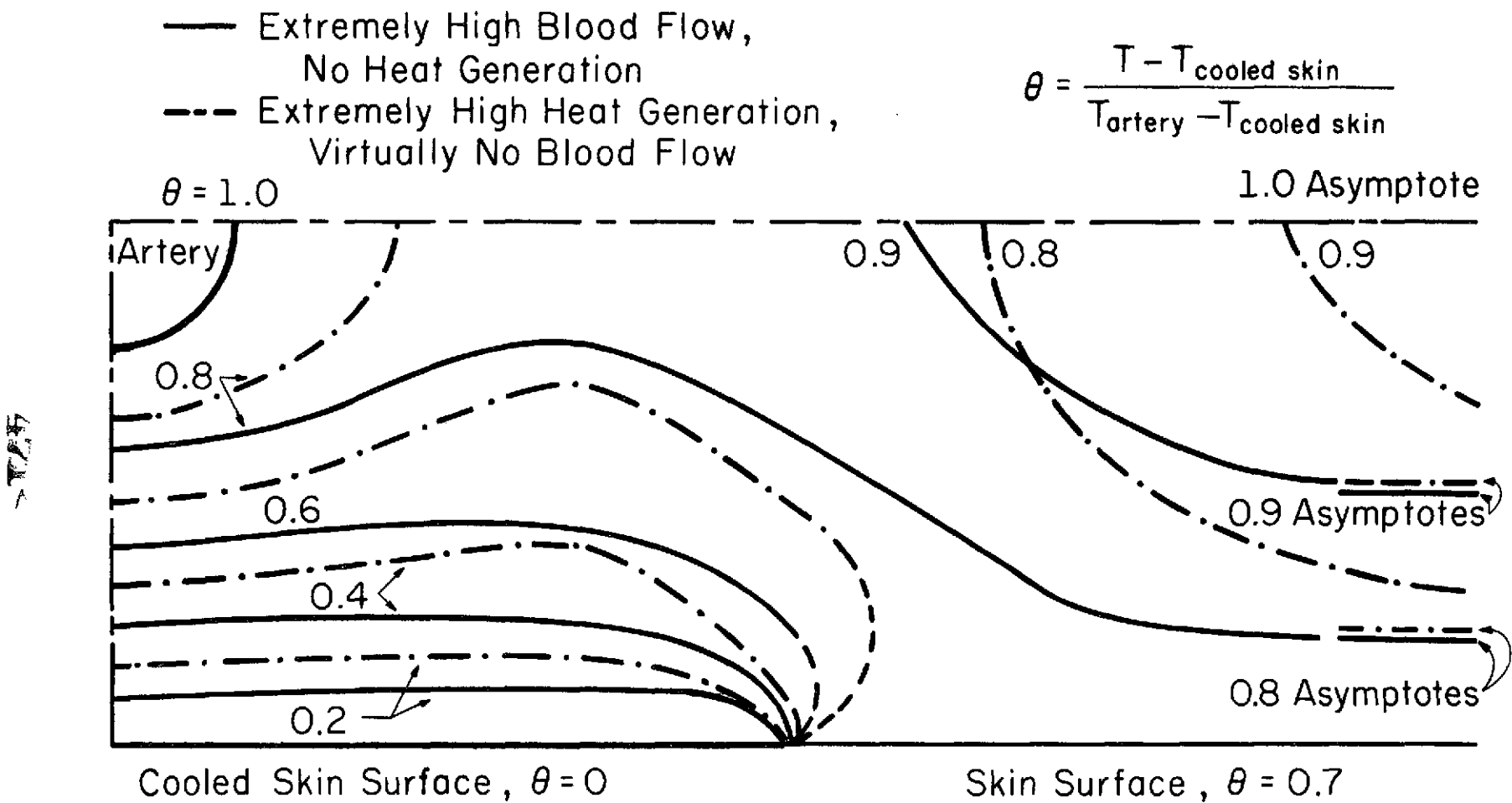


Figure 3 Dimensionless temperature distributions in the vicinity of a cooled artery with extremely high blood perfusion rate ( $wb = 2$ ) and with extremely high internal heat generation rate ( $Q/w^2\theta_0 = 250$ ) within the tissue.

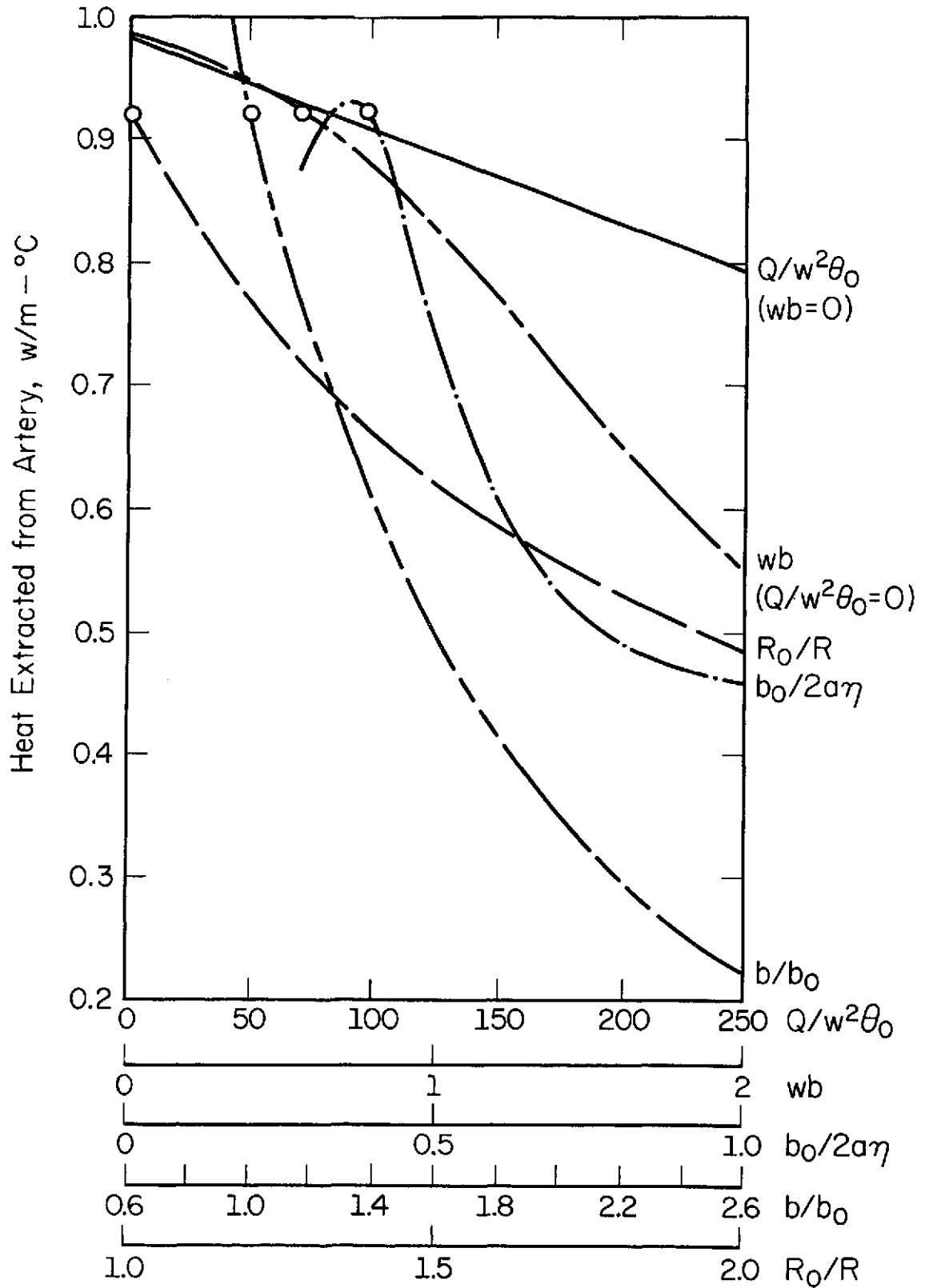


Figure 4 Heat extraction rates per unit length of artery, per unit temperature difference between artery and cooled skin.  $\theta_2/\theta_1 = 0.15$ . Circles indicate "normal" conditions.

reaches a maximum as  $b_0/2\eta a$  approaches zero. This maximum should be just slightly higher than the maximum of the curve shown. Thus, the "normal" conditions are close to optimal as far as the width of the cooling strip is concerned. The optimum, i.e., minimum width for close to maximum heat extraction rate, is around a cooling width to arterial depth ratio of 3.

The remaining curves indicate that the heat extraction rate increases with decreasing internal heat generation rate ( $Q/w^2\theta_0$ ), with decreasing blood flow rate ( $wb$ ), with decreasing arterial depth ( $b/b_0$ ), and with increasing arterial radius (i.e., decreasing  $R_0/R$ ). These are, however, physiological parameters which usually cannot be controlled arbitrarily. It is to be noted, however, that if the cooling strip temperature could be lowered enough to cause local vasoconstriction, then the heat extraction rate from the artery would increase not only because of the increased temperature difference, but also as a result of decreased blood perfusion of the tissue.

The results indicate that under the "normal" conditions a square cooling patch with an area of  $7 \text{ cm}^2$  (sides,  $2\eta a = 2.64 \text{ cm}$ ) will extract about 0.025 watts from the artery for each  $1^\circ\text{C}$  difference between the artery and the cooled skin surface. On the other hand, the blood requires about 0.06 watts to change its temperature by  $1^\circ\text{C}$  for each cc/min of flow. Thus, if  $\theta_0 = 20^\circ\text{C}$  and the arterial blood flow is 200 cc/min, the arterial blood temperature is expected to decrease only about  $0.04^\circ\text{C}$ . Even if allowance is made for additional heat loss from the deep side of the artery, this is indeed a very small temperature change. The temperature drop is too small to have any effect on the hypothalamic temperature regulator; consequently, the

pronounced effects on thermal comfort found by Williams and Chambers [1] were probably due to some local thermal receptor action rather than to reduced arterial temperatures reaching the hypothalamus.

To check the magnitude of these results, the maximum possible heat extraction rate from the artery can be calculated by assuming an equivalent one-dimensional conduction problem from an area equal to that of the skin-side surface of the artery,  $2\pi RL$ , across a distance equal to the depth of the point on the artery closest to the skin,  $b - R$ .

$$\frac{q_a}{\theta_1} = \frac{2\pi Rk}{b - R} \quad (20)$$

Substituting the values for the "normal" condition yields a value of 1.13 w/m°C, which corresponds to about 0.03 w/°C for a patch with an area of 7 cm<sup>2</sup>. Thus, the previously estimated value of 0.025 w/°C is quite reasonable.

## CONCLUSIONS AND RECOMMENDATIONS

An analytical method has been developed to estimate the amount of heat extracted from an artery running near and parallel to the skin surface, such as the carotid artery in the neck, when the skin surface is cooled in a symmetrical fashion above the artery.

The results indicate that the optimum width of the cooling strip is approximately three times the depth to the centerline of the artery. However, even at the optimum size the amount of heat removed from a main artery with reasonable skin temperatures is too small to affect the temperature of the blood significantly.

A three-dimensional, finite difference method could be attempted to obtain a more accurate model of the actual, circular cooling patch used in the work reported on in [1]. However, the results presented in this report indicate that the additional accuracy is not going to change the values sufficiently to alter the conclusions drawn.

## ACKNOWLEDGEMENTS

This work was supported in part by a Supplemental Grant from the National Aeronautics and Space Administration to Grant No. NGR 14-005-103. Thanks are due to Drs. B. A. Williams and A. B. Chambers of the Biotechnology Division, NASA Ames Research Center, Moffett Field, California, for their help and support. The able staff of the Publications Office of the Department of Mechanical and Industrial Engineering handled final preparation of the report. Some of the numerical computations were performed at the Digital Computer Laboratory of the University of Illinois at Urbana-Champaign.

## REFERENCES

1. Williams, B. A. and Chambers, A. B., "The Effect of Neck Warming and Cooling on Thermal Comfort," 42nd Annual Sci. Meeting, Aerospace Med. Assoc., Houston, Texas, April 26-29, 1971. Also, Second Conference on Life Support Systems, NASA Ames Research Center, Moffett Field, Cal., May 1972.
2. Pennes, H. H., "Analysis of Tissue and Arterial Blood Temperature in the Resting Human Forearm," J. Appl. Physiol., 1, 1948, pp. 93-122.
3. Shitzer, A., Chato, J. C., and Hertig, B. A., "A Study of the Thermal Behavior of Living Biological Tissue with Application to Thermal Control of Protective Suits," Tech. Rep. No. ME-TR-207, Department of Mechanical and Industrial Engineering, University of Illinois at Urbana-Champaign, Urbana, Illinois, January 1971.
4. Carslaw, H. S. and Jaeger, J. G., Conduction of Heat in Solids, Second Edition, Oxford University Press, London, 1959.
5. Chato, J. C. and Shitzer, A., "On the Dimensionless Parameters Associated with the Heat Transport within Living Tissue," Aerospace Med., 41, 1970, pp. 390-393.
6. Williams, B. A., NASA Ames Research Center, Moffett Field, Cal., personal communication.

Part III  
LIST OF PUBLICATIONS

## PUBLICATIONS

1. Chato, J. C., Hertig, B. A., et al., "Physiological and Engineering Study of Advanced Thermoregulatory Systems for Extravehicular Space Suits," Semiannual Status Reports on NASA Grant No. 14-005-103, published between December 1967 and December 1970.
2. Chato, J. C., "A Method for the Measurement of Thermal Properties of Biological Materials," Thermal Problems in Biotechnology, ASME Symposium, 1968, pp. 16-25. Also, abstracts in Proc. Thermal Cond. Conference, West Lafayette, Indiana, 1968, and Proc. 21st ACEMB, Houston, Texas, 1968.
3. Streckert, J. H. and Chato, J. C., "Development of a Versatile System for Detailed Studies on the Performance of Heat Pipes," Technical Report No. ME-TR-64, Department of Mechanical and Industrial Engineering, University of Illinois at Urbana-Champaign, Urbana, Ill., 1968, 45 pp.
4. Chato, J. C., "Heat Transfer in Bioengineering," Advanced Heat Transfer, B. T. Chao, Editor, University of Illinois Press, Champaign, Ill., 1969, pp. 395-414.
5. Chato, J. C., "Combined Free and Forced Convection Flows in Channels," Advanced Heat Transfer, B. T. Chao, Editor, University of Illinois Press, Champaign, Ill., 1969, pp. 439-459.
6. Chato, J. C. and Hertig, B. A., "Regulation of Thermal Sweating in EVA Space Suits," Proc. Symp. on Individual Cooling, Kansas State University, Manhattan, Kansas, 1969, pp. 78-91.
7. Chato, J. C., Hertig, B. A., et al., "On Feasibility of Metabolic Heat Removal without Sweating by Direct Cooling of the Skin," Proc. 21st ACEMB, Houston, Texas, 1968.
8. Chato, J. C. and Streckert, J. H., "Performance of a Wick-Limited Heat Pipe," ASME Paper No. 69-HT-20, ASME-AIChE Heat Transfer Conference, Minneapolis, Minnesota, 1969.
9. Shitzer, A. and Chato, J. C., "Analytical Modeling of the Thermal Behavior of Living Human Tissue," Proc. Fourth International Heat Transfer Conf., 1970, Cu 3.9, pp. 1-10.
10. Chato, J. C. and Shitzer, A., "On the Dimensionless Parameters Associated with Heat Transport within Living Tissue," Aerospace Med., 41, 1970, pp. 390-393.
11. Chato, J. C. and Hertig, B. A., "Thermal Behavior of Biological Media," AIAA Paper No. 70-813, 1970.
12. Chato, J. C., Shitzer, A., and Fry, F. J., "Measurement of Thermal Properties of Living Tissue," Proc. 23rd ACEMB, Washington, D.C., 1970, p. 156.
13. Hunsberger, D. L. and Chato, J. C., "Experimental Investigation of the Performance of Various Wick Configurations in Single- and Two-Fluid Heat Pipes Operating in the Gravitational Field," Technical Report No. ME-TR-187, Department of Mechanical and Industrial Engineering, University of Illinois at Urbana-Champaign, 1970, 42 pp.

14. Shitzer, A., Chato, J. C., and Hertig, B. A., "A Study of the Thermal Behavior of Living Biological Tissue with Application to Thermal Control of Protective Suits," Technical Report No. ME-TR-207, Department of Mechanical and Industrial Engineering, University of Illinois at Urbana-Champaign, 1971, 200 pp.
15. Chato, J. C. and Shitzer, A., "Thermal Modeling of the Human Body-- Further Solutions of the Steady-State Heat Equation," AIAA J., 9, 1971, pp. 865-869.
16. Shitzer, A., Chato, J. C., and Hertig, B. A., "The Removal of Metabolic Heat from Man Working in a Protective Suit," Second Conf. on Life Support Systems, NASA-Ames Research Center, Moffett Field, Cal., May 1971, NASA SP-302, 1972.
17. Leo, R. J., Shitzer, A., Chato, J. C., and Hertig, B. A., "Steady-State and Transient Temperature Distribution in the Human Thigh Covered with a Cooling Pad," Technical Report No. ME-TR-286, Department of Mechanical and Industrial Engineering, University of Illinois at Urbana-Champaign, 1971, 72 pp.
18. Shitzer, A. and Chato, J. C., "Effect of Variable Blood Supply Temperature on the Temperature Distribution in Biological Tissue," Proc. 25th ACEMB, Las Vegas, Nevada, 1971, p. 57.
19. Shitzer, A. and Chato, J. C., "Further Studies on the Dimensionless Parameters Associated with the 'In Vivo' Transport of Heat within Biological Tissue," Aerospace Medicine, 42, No. 12, 1971, pp. 1279-1283.
20. Shitzer, A. and Chato, J. C., "Steady-State Temperature Distribution in Living Tissue Modeled as Cylindrical Shells," ASME Paper No. 71-WA/HT-34, 1971, 12 pp.
21. Shitzer, A. and Chato, J. C., "Analytical Solutions to the Problem of Transient Heat Transfer in Living Tissue," ASME Paper No. 71-WA/HT-36, 1971, 11 pp.
22. Shitzer, A. and Chato, J. C., "A Linear Combination of Modified Bessel Functions," Report No. ME-TN-310, Department of Mechanical and Industrial Engineering, University of Illinois at Urbana-Champaign, 1971, 25 pp.
23. Chato, J. C. and Shitzer, A., "Analytical Prediction of the Heat Transfer from a Blood Vessel near the Skin Surface Cooled by a Symmetrical Cooling Strip," Report No. ME-TR-344, Department of Mechanical and Industrial Engineering, University of Illinois at Urbana-Champaign, 1971, 20 pp.
24. Shitzer, A., Chato, J. C., and Hertig, B. A., "Thermal Protective Garment using Independent Regional Control of Coolant Temperature," Aerospace Medicine, to be published.
25. Leo, R. J., Shitzer, A., Chato, J. C., and Hertig, B. A., "Steady State and Transient Temperature Distributions on the Skin of the Human Thigh covered with a Cooling Pad," ASHRAE Paper No. 754, Trans. ASHRAE, to be published.

## THESES

1. Streckert, J. H., "Development of a Versatile System for Detailed Studies on the Performance of Heat Pipes," M.S. Thesis, Department of Mechanical and Industrial Engineering, University of Illinois at Urbana-Champaign, Urbana, Ill., December 1968.
2. Hunsberger, D. L., "Experimental Investigation of the Performance of Various Wick Configurations in Single- and Two-Fluid Heat Pipes Operating in the Gravitational Field," M.S. Thesis, Department of Mechanical and Industrial Engineering, University of Illinois at Urbana-Champaign, Urbana, Ill., October 1970.
3. Shitzer, A., "A Study of the Thermal Behavior of Living Biological Tissue with Application to Thermal Control of Protective Suits," Ph.D. Thesis, University of Illinois at Urbana-Champaign, Urbana, Ill., February 1971.
4. Leo, R. J., "Steady State and Transient Temperature Distributions on the Skin of the Human Thigh Covered with a Cooling Pad," M.S. Thesis, Department of Mechanical and Industrial Engineering, University of Illinois at Urbana-Champaign, Urbana, Ill., August 1971.